Representation of a multipurpose reservoir system and vulnerability of water management under global change : Application to the Neste water system

Peng Huang

Communauté
UNIVERSITÉ Grenoble Alpes

THÈSE

Pour obtenir le grade de

DOCTEUR DE L'UNIVERSITÉ GRENOBLE ALPES

Spécialité : **Océan, Atmosphère, Hydrologie**

Arrêtée ministériel : 25 mai 2016

Présentée par

Peng HUANG

Thèse dirigée par **Eric SAUQUET, Directeur de recherche, INRAE**
et co-encadrée par **Jean-Philippe VIDAL, Chargé de recherche, INRAE**

préparée au sein de **l'unité de recherche RiverLy à INRAE centre de Lyon-Genoble, France**
dans **l'École Doctorale Sciences de la Terre, de l'Environnement et des Planètes**

Representation of a multipurpose reservoir system and vulnerability of water management under global change

Application to the Neste water system

Thèse soutenu publiquement le **17 mai 2022**,
devant le jury composé de :

M. Eric SAUQUET
DIRECTEUR DE RECHERCHE, INRAE, Directeur de thèse
M. Santiago BEGUERÍA
DOCTEUR EN SCIENCES, CSIC, Rapporteur
Mme. Anne-Catherine FAVRE-PUGIN
PROFESSEUR DES UNIVERSITES, UGA, Examinatrice
M. Benoît HINGRAY
CHARGE DE RECHERCHE HDR, CNRS, Examinateur
Mme. Agnès DUCHARNE
DIRECTRICE DE RECHERCHE, CNRS, Rapporteure et Présidente
M. Simon GASCOIN
CHARGE DE RECHERCHE HDR, CNRS, Examinateur
M. Jean-Philippe VIDAL
CHARGE DE RECHERCHE HDR, INRAE, Invité
Mme. Natacha DA RIBA
INGENIEURE, ENGIE, Invitée

CONTENTS

Acknowledgements v

Résumé vii

Abstract ix

List of Figures xi

List of Tables xxii

1 General context 1
- 1.1 Human and water . . . 2
  - 1.1.1 Water management in the ancient time: the legacy . . . 2
  - 1.1.2 Water management challenges nowadays: the Anthropocene . . . 3
- 1.2 Scientific problems and research objectives . . . 8
- 1.3 Structure of the dissertation . . . 10

2 Literature review 12
- Abstract . . . 13
- 2.1 Introduction . . . 14
- 2.2 Impact of global change on reservoir performance . . . 17
  - 2.2.1 Hydropower reservoirs . . . 17
  - 2.2.2 Irrigation reservoirs . . . 20
  - 2.2.3 Multi-purpose reservoirs . . . 21
  - 2.2.4 Summary . . . 22
- 2.3 Adaptation of reservoir system under global change . . . 24
  - 2.3.1 Actions in reservoir planning . . . 24
  - 2.3.2 Actions in reservoir management . . . 25
  - 2.3.3 Adaptation paradigms of reservoir water system . . . 28
- 2.4 Challenge of adaptation under global change . . . 31
  - 2.4.1 Challenges in the assessment approaches . . . 31
  - 2.4.2 Challenges in the design and appraisal of adaptation . . . 34
  - 2.4.3 Challenges in the participation of stakeholders and managers . . . 37
- 2.5 Conclusion . . . 39

3 Materials **42**
3.1 General conditions of the Neste water system 44
3.1.1 Topography and climatology 44
3.1.2 Water infrastructures in the Neste water system 46
3.1.3 Water management in the Neste water system: the Aure Valley . . 48
3.1.4 Water management in the Neste water system: the Neste Canal and the Gascogne region 55
3.2 Data collection 59
3.2.1 Climatic drivers 59
3.2.2 Naturalized inflow 63
3.2.3 Water management records of SHEM 71
3.2.4 Water management records of CACG 74
3.2.5 Population projections 78
3.3 Summary 80

4 Water resources estimation **84**
4.1 Implementation of models for water resources estimation 86
4.1.1 Introdution 86
4.1.2 The hydrological model GR6J-CEMANEIGE 86
4.1.3 Performance assessment of GR6J-CEMANEIGE 89
4.1.4 Simulation results 92
4.2 Water resources model for the Aure Valley 100
4.2.1 The implementation and performance of the model 100
4.2.2 Water accounting for the Aure Valley 102

5 Water demand and management modelling **106**
5.1 Water demand modelling 108
5.1.1 Introduction 108
5.1.2 Water demand for hydropower from SHEM 108
5.1.3 Water demand for drinking water from CACG 113
5.1.4 Water demand for industrial use from CACG 115
5.1.5 Water demand for irrigation from CACG 115
5.1.6 Water demand for environment from CACG 124
5.2 Water management modelling 128
5.2.1 Introduction 128
5.2.2 Water management model of SHEM 128
5.2.3 Water management model of CACG 135
5.3 Summary 141

6 Vulnerability assessment **143**
Abstract 145
6.1 Introduction 146
6.2 Study area 149
6.3 Data and methods 152
6.3.1 Climatic drivers 152
6.3.2 Naturalized inflow 154
6.3.3 Hydrological modelling 154
6.3.4 The SN framework for water management 155

6.4 Results . . . 159
6.4.1 Hydrological model performance . . . 159
6.4.2 Water management sensitivity analysis . . . 161
6.4.3 Water management vulnerability assessment . . . 165
6.5 Discussion . . . 169
6.5.1 The contribution to the Pyrenean studies . . . 169
6.5.2 Potential mitigation and adaptation actions . . . 170
6.5.3 Limitations and future works . . . 170
6.6 Conclusion . . . 172

7 Impact assessment under global change 175
7.1 Introduction . . . 177
7.2 Climate change impact on natural water resources . . . 184
7.2.1 The Aure Valley (SB1-4) . . . 184
7.2.2 The Gascogne region (SB5) . . . 191
7.3 Global change impact on water demand . . . 194
7.3.1 Hydropower demand changes . . . 194
7.3.2 Drinking water demand changes . . . 197
7.3.3 Industrial water demand changes . . . 198
7.3.4 Irrigation water demand changes . . . 198
7.3.5 Environmental water demand changes in SB5 . . . 201
7.3.6 Summary . . . 202
7.4 Global change impact on water management . . . 206
7.4.1 Water management in the Aure Valley . . . 206
7.4.2 Summary . . . 230

8 Conclusion and perspectives 233
8.1 Conclusion . . . 234
8.2 Perspectives . . . 236

Bibliography 238

A Sensitivity analysis between Safran reanalyses and the two sets of the hydrological model GR6J-CEMANEIGE 276
A.1 Model validation . . . 277
A.1.1 A better model set . . . 277
A.1.2 A better forcing data . . . 277

ACKNOWLEDGEMENTS

I would like to express my sincere gratitude to my supervisors, Dr. Eric Sauquet and Dr. Jean-Philippe Vidal, for offering me an opportunity to continue my study at the laboratory INRAE. Over the last three years, they continuously encourage and support me on various aspects of the PhD project. I enjoy their thought and creativity, their insight and advice, and their attitude and patience. At the same time, I very much appreciate for their useful discussion on data analysis and model development, and valuable suggestions for the improvement of the PhD project. I have gained a lot from their vast knowledge and skills, not only in terms of water management and climate change, but also in terms of research methodologies.

Many thanks to A./Prof. Baptiste François from the University of Massachusetts in the USA for serving as my committee member and for stimulating and interesting discussions on my papers. I am amazed by his academic attitude during his correcting papers, which will benefit my future career development. I am equally grateful to other committee members Dr. Sabine Sauvage, Dr. Pere Quintana Seguí, David Dorchies, Natacha Da Riba, and Ludovic Lhuissier for their very generous help to improve my PhD project.

I would also like to thank my colleagues in the RiverLy group for their invaluable discussions and suggestions and for their friendships and conversations over the last three years.

This PhD was funded by the Interreg-PIRAGUA project. The project has allowed me to communicate with the water managers and stakeholders of the Neste water system in French Pyrenees. I would like to thank Bertran Loock, Charles-Eric Husum, Romain Radulesco from ENGIE, Damien Lilas, Marie Lefrancq, Pascal Chisné from CACG, and Cyrille Flourette from SHEM for sharing their their knowledge and experience on water management, which has greatly deepened my understanding of the PhD project.

And finally, I would like to thank my mother Xu Yinlan and my father Huang Wei for their unconditional support and love during my candidature. I have also my thanks to say to all of my friends (Sheng, Shijun, Junjian, Yihan, Emeric, David...) for their continuous encouragement and support.

Thank you.

RÉSUMÉ

La compréhension de la vulnérabilité de la gestion de l'eau dans le contexte du changement global est la condition préalable à la conception de mesures d'adaptation. Une évaluation complète de la vulnérabilité des modes de gestion de l'eau aux changements futurs repose sur de nouveaux outils capables de représenter l'impact humain sur les ressources en eau et sur des cadres innovants capables de générer de nouvelles idées pour informer la conception de l'adaptation. Par conséquent, cette thèse vise à (1) développer et améliorer des modèles pour représenter les ressources en eau, la demande en eau et la gestion de l'eau de manière intégrée ; (2) appliquer un cadre bottom-up "scenario-neutral" et un cadre top-down "scenario-led" pour identifier et étudier la vulnérabilité et l'impact plausibles dans le cadre du changement global. Ces développements et applications ont concerné le système Neste dans les Pyrénées françaises.

Pour le premier objectif, cette recherche (1.1) inclut des informations sur la neige qui sont essentielles pour l'estimation des ressources en eau dans la zone d'étude située en montagne ; (1.2) améliore et applique des méthodes et des modèles basés sur des observations pour représenter la demande locale en eau ; (1.3) développe un outil de gestion de l'eau flexible qui est capable de s'adapter à différents scénarios de changement global et à différents contextes de gestion. La chaîne de modélisation est donc transférable et applicable à d'autres études de cas sous réserve de connaître les principaux facteurs de contrôle.

Pour le deuxième objectif, cette recherche utilise les modèles développés pour évaluer la vulnérabilité de la gestion de l'eau au changement global en appliquant deux cadres : (2.1) un cadre bottom-up "scenario-neutral" pour répondre à la question "Comment et quand la performance du système de l'eau passe-t-elle d'acceptable à inacceptable ?"; (2.2) un cadre top-down "scenario-led" pour répondre à la question "Quel est l'impact et la vulnérabilité potentiels de la gestion de l'eau sous changement global ?". Les résultats sont cohérents dans les deux cadres, et plus important encore, ils sont complémentaires pour informer la conception de l'adaptation.

La conclusion générale en termes de vulnérabilité de la gestion de l'eau peut se résumer ainsi : étant donné les contrats d'eau contraignants actuels et les restrictions environnementales, le système va être fortement impacté par le changement climatique avec des réductions notables de la ressource en eau; tous les usages seront affectés avec des risques de non garantie des demandes; et, compte tenu des modalités actuelles, l'usage hydroélectricité est la plus vulnérable au changement global annoncé. Une stratégie d'adaptation impliquant les acteurs est indispensable sur ce territoire.

ABSTRACT

Understanding the vulnerability of water management under global change is the premise for designing adaptation actions. A comprehensive assessment of current water management vulnerability to future changes hinges on new tools that are able to represent human impact on water resources and innovative frameworks that are able to generate new insights to inform adaptation designing. Therefore, this dissertation sets out to (1) develop and improve models to represent water resources, water demand, and water management in an integrated hydrological modelling framework; (2) apply a "scenario-neutral" bottom-up framework and a "scenario-led" top-down framework to identify and investigate plausible vulnerability and impact under global change. These developments and applications are demonstrated by taking the Neste water system in French Pyrenees as a case study.

For the first aim, this research (1.1) includes snow information that is critical for the water resources estimation in the mountainous study area; (1.2) improves and applies data-driven methods and models to represent local water demand; (1.3) develops a flexible water management tool that is capable to adapt to different global change scenarios and different management contexts. The modelling chain is thus transferable and applicable to other case studies as long as the principal controlling factors are known.

For the second aim, this research uses the developed models to assess the vulnerability of water management to global change by applying two frameworks: (2.1) a "scenario-neutral" bottom-up framework to answer the question "How and when the performance of the water system shifts from acceptable to unacceptable?"; (2.2) a "scenario-led" top-down framework to answer the question "What is the potential impact and vulnerability in the water management under global change?". The results are consistent within the two frameworks, and more importantly complimentary to inform adaption designing.

The general conclusion in terms of water management vulnerability is summarized as follow: given the current binding water contract and environmental restrictions, the system will be strongly impacted by climate change with significant reductions in water resources availability; all water uses will be affected with increasing risks of failing to meet the demand; and, given the current arrangements, hydropower production is the most vulnerable to global change. An adaptation strategy involving the stakeholders is essential in this area.

LIST OF FIGURES

1.1 Simplified diagrams of ancient water management techniques and their locations. . . . 3
1.2 Spatial changes and temporal trends of global streamflow under climate change scenarios. . . . 4
1.3 Total 35 climatic impact-drivers (CIDs) of 7 types (heat and cold, wet and dry, wind, snow and ice, coastal, open ocean, and other) are projected to increase or decrease with high/medieu confidence in the how many land&coastal regions (a) and open-ocean regions (b). These regions can be explored in the WGI Interactive Atlas. . . . 5
1.4 The trends of global socio-economic development from 1750 to 2010 for 12 indicators: population, real Gross Domestic Product (GDP), foreign direct investment, urban population, primary energy use, fertilizer consumption, large dams, water use (annual water consumption for irrigation, domestic, livestock, and industrial uses), paper production, transportation (global production of new automobiles), telecommunications (total subscribers to fixed landlines and mobile phones), and international tourism (annual number of international arrivals). . . . 7

2.1 (a) The increasing trend of the number of large dams (large: a minimum of 15 m height above foundation) from 1900 to 2010 in three categories of the world countries: the OECD countries (members in 2010); the emerging economies defined as the BRICS countries including Brazil, Russia, India, China (China mainland with Macau, Hong Kong and Taiwan where applicable), and South Africa; and the rest countries. (b) The drainage area of georeferenced large dams in the three categories of the world countries . . . 15
2.2 The flow charts of adaptation to climate change in the top-down approach (a) and bottom-up approach (b). . . . 32

3.1 A simplified schema of the Neste water system and the associated abbreviations used in this chapter. . . . 43
3.2 The location of the Neste water system. . . . 44
3.3 The topographic map and the hypsometry curve for the Aure Valley (a) and the Gascogne region (b). . . . 44
3.4 The monthly regime of precipitation and temperature for the Aure Valley and the Gascogne region. . . . 45
3.5 The overview of the Neste water system: the reservoirs in the upstream Aure Valley, the Neste Canal, and the reservoirs in the downstream Gascogne region. . . . 47

3.6 The drainage area of the Oule, Orédon, Caillaouas, and Pouchergues reservoirs. . . . 49
3.7 The water management system for hydropower production in the Aure Valley. . . . 50
3.8 Mean monthly and annual water share in the Gascogne region. . . . 56
3.9 Water management in the Neste Canal. . . . 57
3.10 The Neste system area overlaid with Safran-France (a) and Safran-PIRAGUA (b) girds. . . . 60
3.11 The 5 equi-surface elevation bands of the Aure Valley overlaid with grid center points of the gap-filled MODIS snow product. . . . 61
3.12 Climate change projections of the 6 GCMs in Table 3.4 in terms of annual precipitation (P), potential evapotranspiration (PET), and temperature (T) under historical (1961-2005), RCP 4.5 (2006-2100), and RCP 8.5 (2006-2100) scenarios for the Aure Valley (a) and SB5 (b). . . . 62
3.13 (a) The annual regime of France daily temperature compared with the annual regime of the local daily temperature (the daily temperature of the Neste water system area) over the period from 09/1979 to 08/2014; (b) The linear relationship between the local temperature of the Neste water system area and the France temperature. The local temperature is calculated with the SAFRAN-PIRAGUA dataset and the France temperature is calculated with the SAFRAN-France dataset over the period from 09/1979 to 08/2014. . . . 64
3.14 The comparison between the simulated and observed France temperature over the period from 09/1979 to 08/2014. . . . 64
3.15 The mean annual simulated France temperature projections under historical (1961-2005), RCP 4.5 (2006-2100), and RCP 8.5 (2006-2100) scenarios. The fine lines represent the mean annual changes and the thick lines represent the rends with loess smoothing method. . . . 65
3.16 Comparison between the naturalized inflow (Q_{nat1}) and the influenced outflow (Q_{inf1}) of SB1 for the period from 01/2001 to 12/2018. . . . 66
3.17 Comparison between the naturalized inflow (Q_{nat2}) for the period from 07/2014 to 12/2018 and the transferred outflow ($Tran_1$) of SB2 for the period from 01/2001 to 12/2018. . . . 67
3.18 Comparison between the naturalized inflow (Q_{nat3}) and the influenced outflow (Q_{inf3}) of SB3 for the period from 01/2001 to 12/2018. . . . 68
3.19 Naturalized inflow of SB4 for the period from 01/2001 to 12/2018. . . . 69
3.20 The drainage area of SB5 is the total drainage area of the sub-basins upstream the ten discharge control points: Beaumarchès, Roquebrune, Nérac, Montestruc, Saint-Antoine, Castelferrus, Larra, Fousseret, Laffite, and Lavet. . . . 69
3.21 Comparison between the naturalized inflow (Qnat) and the influenced outflow (Qinf) of SB5 for the period from 01/2013 to 12/2019. . . . 70
3.22 Daily water release from the Eget and Louron groups in comparison with CACG regulartory demand for the period from 01/2001 to 12/2018. . . . 71
3.23 Operation information in the Eget hydropower group . . . 72
3.24 Operation information in the Louron hydropower group . . . 73

3.25 Annual groundwater and surface water extraction of SB5 from the dataset BNPE for drinking water, industrial and irrigation uses from year 2003 to 2017. . . . 74
3.26 Mean annual groundwater and surface water extraction of SB5 from the dataset BNPE for drinking water, industrial and irrigation uses from year 2003 to 2017 for the ten sub-basins upstream the discharge control points: : Beaumarchès, Roquebrune, Nérac, Montestruc, Saint-Antoine, Castelferrus, Larra, Fousseret, Laffite, and Lavet. . . . 75
3.27 Comparison between BNPE extraction and CACG release records in terms of drinking water, industiral, and irrigation uses for period for year 2004 to 2017. . . . 76
3.28 Regime of water extraction (Q_{canal}) by the Neste Canal to feed SB5 in comparison with river flows downstream Sarrancolin (Q_{ds}) and at Sarrancolin (Q_{infs}) for the period from 01/1992 to 09/2019. . . . 77
3.29 Regime of volume and release of the 15 reservoirs in SB5 for the period from 01/2013 to 12/2019. . . . 78
3.30 The population information in terms of the observation by INSEE from 2006 to 2017, the projection by INSEE from 2013 to 2050, and the simulation from 1961 to 2100. . . . 79

4.1 A simplified schema of the Neste water system and the associated abbreviations used in this chapter. . . . 85
4.2 Schematic representation of the GR6J hydrological model (a) coupled with a snow module CEMANEIGE (b). . . . 87
4.3 (a) Simulated $\sqrt{Q}$ regime compared with naturalized $\sqrt{Q}$ regime for SB1; (b) simulated SCA regimes compared with observed SCA regimes for the five elevation bands of SB1. . . . 95
4.4 As in Figure 4.3 but for SB2. . . . 96
4.5 As in Figure 4.3 but for SB3. . . . 97
4.6 As in Figure 4.3 but for SB4. . . . 98
4.7 Simulated $\sqrt{Q}$ regime compared with naturalized $\sqrt{Q}$ regime for SB5. . . . 99
4.8 The regimes of observed influenced flow (Q_{obss}), calculated influenced flow (Q_{infs}), and calculated natural flow (Q_{sims}) at Sarrancolin in comparison with releases for energy production and releases for CACG demand over the period from 01/2002 to 08/2014. . . . 101
4.9 Monthly hydrological regimes for SB1-4 and the Aure Valley. . . . 104

5.1 A simplified schema of the Neste water system and the associated abbreviations used in this chapter. . . . 107
5.2 Regimes of energy demand indexes HDD and CDD in France calculated from Safran-France over the period from 08/1958 to 07/2018. . . . 109
5.3 Water release (top) and corresponding energy production (bottom) in weekdays and holidays for the Eget and Louron power systems in cold months (November to March) over the period from 01/2002 to 03/2018. . . . 110
5.4 Historical hydropower production for low and high demand periods in linear relation to HDD of France over the period from 01/2002 to 03/2018. 111

5.5 ECDF of the 10 trials of the low demand model (and high demand model) simulated with the HDD of France over the period from 01/2002 to 03/2018 as input compared with the low hydropower demand set A_1 (and high hydropower demand set A_2). 113
5.6 Annual water extraction for drinking water (a), population information (b), and calculated DWI (c) in SB5 from 2006 to 2017. 114
5.7 A typical practice of maize cropping and irrigation in the Sourthern France. 116
5.8 The calculated Id values for year from 1995 to 2019. 120
5.9 (a) The simulated weekly irrigation water demand compared with the observed CACG registration for each year in 1995-2019; (b) The regime of the simulated weekly irrigation water demand compared with the observed release regime for year 1995-2019. 121
5.10 The simulated sowing date (a), maize growth duration (b), and irrigation duration (c) in SB5. Maize growth duration is the time interval between sowing date and the stage of maturity. Irrigation duration is the time interval between the stage of flowering and the stage of 50% grain moisture content. Last irrigation activity in a year is after the stage of 50% grain moisture content. 122
5.11 The regime of the simulated daily environmental water demand in SB5 compared with the calculated observed daily water release regime for the environment of SB5 over the period from 01/2003 to 12/2019. 126
5.12 ECDF of the 10 trials of the environmental water demand (simulated with naturalized river discharge Q_{nat5} in SB5, observed canal water extraction, and observed daily request from SHEM reservoirs by CACG) compared with the observed environmental water release from the CACG reservoirs for four seasons over the period from 01/2003 to 12/2019. 127
5.13 The simplification of the Eget-Louron system for the optimization process. 129
5.14 The simulated regimes of water volume in the Oule, Orédon and Lassoula reservoirs compared with the observed water volume regimes over the period from 07/2002 to 06/2014. The observed water volume of the Orédon reservoir is from 07/2014 to 12/2018. 133
5.15 The regime of simulated water transfer from the Orédon to Oule reservoir compared with the observed water transfer regime over the period from 07/2002 to 06/2014. 134
5.16 The simulated monthly water release for hydropower production of the Eget-Louron system compared with the observed water release for hydropower. 134
5.17 The process of maintaining DOE requirement when extracting water via the Neste Canal at Sarrancolin. 137
5.18 (a) ECDF of the 10 trials of the canal extraction model simulated with the observed river flow at Sarrancolin and the observed water demand in SB5 over the period from 01/2013 to 09/2019 as inputs compared with the observed water extraction from the Neste Canal; (b) The regime of the simulated water extraction from the Neste Canal compared with the regime of the observations over the period from 01/2013 to 09/2019. . . . 138
5.19 Linear relation between CACG request to release water from the SHEM reservoirs and the total water demand of SB5. The two variables are in the period from 01/2013 to 09/2019. 138

5.20 (a) ECDF of the 10 trials of the CACG demand model simulated with the observed water demand in SB5 over the period from 01/2013 to 09/2019 as input compared with the observed CACG demand; (b) The regime of the simulated CACG demand compared with the regime of the observed CACG demand over the period from 01/2013 to 09/2019. 139

5.21 The simulated volume of CACG reservoirs compared with the observed volume of CACG reservoirs over the period from 01/2001 to 09/2019. . . 140

6.1 A simplified schema of the Neste water system and this chapter investigates the vulnerability of water management in the Aure Valley (SB1-4) under climate change scenarios with a bottom-up framework. 144

6.2 (a) The topographic map of the Aure Valley with the five sub-basins. (b) The water management system of the Valley. 151

6.3 The Scenario Neutral framework is applied to assessing the vulnerability of water management in the study area. The inputs and outputs are labelled in blue and red, respectively. 152

6.4 The perturbation of precipitation (P) in (a) and temperature (T) in (b) at monthly time step. 157

6.5 Observed (red) and simulated (blue) median Q (left) and SCA (right) regimes for SB1(a), SB2(b), SB3(c), and SB4(d). The ribbon area in Q regime represents the percentile range of 25% and 75%. The SCA regimes are displayed for the five elevation bands. The observed/simulated period for SB1, SB3, and SB4 is from 01/2001 to 08/2014 while the observed/simulated period for SB2 is from 07/2014 to 07/2018. 160

6.6 Response surfaces of water management metrics to climate change for QA(a), DOE and tDOE(b), NSA(c), and tNSA(d) with their associated study area. Note the difference in x (precipitation changes) and y (temperature changes) axes with each response surface. The metrics under current climate condition (ref) are also provided (see Table 6.5 for corresponding values). 164

6.7 The vulnerability of annual hydropower production under climate change for the Eget and Lassoula systems. The vulnerability is assessed by combining the sensitivity domain of QA, the current hydropower cost-effectiveness thresholds, and the climate change trajectories under RCP 4.5 and 8.5, respectively. The black lines are the isolines that represent the cost-effectiveness thresholds for the management metric QA. 166

6.8 As in figure 6.7 but for the environmental management metrics DOE and tDOE of the Sarrancolin catchment. 166

6.9 As in figure 6.7 but for the reservoir refill management metrics NSA and tNSA of the Eget and Lassoula systems. 167

7.1 A simplified schema of the Neste water system, and this chapter uses a top-down framework to investigate the natural water resources changes in the Neste water system (SB1-5), the water demand changes in the Neste water system (SB1-5), and the water management changes in the Aure Valley (SB1-4) under global change scenarios. 176

7.2 The schema of the modelling chain that represents the Neste water system under global change. Different colors represent different inputs and models: the color green represents climate change projections based on GCMs; the color gray the changes in socio-economic drivers; the color blue the hydrological models in the Neste water system (SB1-5); the color yellow the water demand models; and the color red the water management models by the SHEM and CACG. 177

7.3 Mean monthly potential evapotranspiration (PET), mean monthly precipitation (T) and mean monthly temperature (T) changes of the Aure Valley under 6 GCMs (bcc-csm1-1, CNRM-CM5, inmcm4, MIROC-ESM, MPI-ESM-MR, MRI-CGCM3) for the near-term (2021-2040), medium-term (2041-2060), and long-term (2081-2100) phases under two RCP scenarios (RCPs 4.8 and 8.5). The changes over historical period (1961-2005) of the 6 GCMs, along with the reanalysis Safran-PIRAGUA (1979-2014), are illustrated to compare with the changes under climate change scenarios. The three sub-figures in the column "HISTORICAL" are identical to visually help the comparison. 180

7.4 As in Figure 7.3 but for the Gascogne region. 182

7.5 Climate change impact on the median discharge (Q) and median snow cover area (SCA for the averaged 5 elevation bands) of SB1 under 6 GCMs (bcc-csm1-1, CNRM-CM5, inmcm4, MIROC-ESM, MPI-ESM-MR, MRI-CGCM3) for the near-term (2021-2040), medium-term (2041-2060), and long-term (2081-2100) phases under two RCP scenarios (RCPs 4.8 and 8.5). The simulations over historical period (1961-2005) of the 6 GCMs, along with the simulations from Safran-PIRAGUA (1979-2014), are illustrated to compare with the simulations under climate change scenarios. The three sub-figures in the column "HISTORICAL" are identical to visually help the comparison. 185

7.6 As in Figure 7.5 but for SB2. 186

7.7 As in Figure 7.5 but for SB3. 187

7.8 As in Figure 7.5 but for SB4. 188

7.9 As in Figure 7.5 but for median Q of SB5. 192

7.10 The number of days when there is energy demand for heating in the market within a year (HDD days), and the number of days when there is energy demand for cooling in the market within a year (CDD days) under 6 GCMs (bcc-csm1-1, CNRM-CM5, inmcm4, MIROC-ESM, MPI-ESM-MR, MRI-CGCM3) from 1961 to 2100 for two RCP scenarios (RCPs 4.8 and 8.5). The historical (1961-2005), near-term (2021-2040), medium-term (2041-2060), and long-term (2081-2100) phases are labelled in gray ribbons from left to right. The simulations from Safran-France (1958-2018) are also plotted to compare with the simulations under climate change scenarios. 195

7.11 The impact of temperature increase on the mean daily HDD and CDD values under 6 GCMs (bcc-csm1-1, CNRM-CM5, inmcm4, MIROC-ESM, MPI-ESM-MR, MRI-CGCM3) for the near-term (2021-2040), medium-term (2041-2060), and long-term (2081-2100) phases under two RCP scenarios (RCPs 4.8 and 8.5). The simulations over historical period (1961-2005) of the 6 GCMs, along with the simulations from Safran-France (1958-2018), are illustrated to compare with the simulations under climate change scenarios. The three sub-figures in the column "HISTORICAL" are identical to visually help the comparison. 196
7.12 As in Figure 7.11 but for mean daily hydropower demand for the SHEM. 197
7.13 The increase of drinking water demand in the Gascogne region from 1961 to 2100. The historical (1961-2005), near-term (2021-2040), medium-term (2041-2060), and long-term (2081-2100) periods are labelled in gray ribbons from left to right. 198
7.14 The distribution of sowing date in the 6 GCMs (bcc-csm1-1, CNRM-CM5, inmcm4, MIROC-ESM, MPI-ESM-MR, MRI-CGCM3) for the near-term (2021-2040), medium-term (2041-2060), and long-term (2081-2100) phases under two RCP scenarios (RCPs 4.8 and 8.5). The simulations over historical period (1961-2005) of the 6 GCMs, along with the simulations from Safran-PIRAGUA (1979-2014), are illustrated to compare with the simulations under climate change scenarios. The three sub-figures in the column "HISTORICAL" are identical to visually help the comparison. 199
7.15 As in Figure 7.14 but for maize growth duration (a) and irrigation duration (b). 200
7.16 As in Figure 7.14 but for the regime of daily maize irrigation water demand. 202
7.17 As in Figure 7.14 but for the regime of mean daily environmental water demand in SB5. 203
7.18 As in Figure 7.14 but for the regime of total water demand in SB5. 204
7.19 As in Figure 7.14 but for the regime of mean daily CACG request from the SHEM. 205
7.20 As in Figure 7.14 but for the annual CACG request for the SHEM. The red line is the current limit of the CACG request (48 Mm^3). 205
7.21 The coupling process to represent the current management of SHEM and CACG at Sarrancolin. The color blue represents the hydrological models associated in the coupling process; the color yellow the water demand; and the color red water management models by SHEM and CACG. 209
7.22 As in Figure 7.21 but under a different management context that CACG can request as much as the CACG wants. 210
7.23 The regime of mean daily water release for CACG under 6 GCMs (bcc-csm1-1, CNRM-CM5, inmcm4, MIROC-ESM, MPI-ESM-MR, MRI-CGCM3) for the near-term (2021-2040), medium-term (2041-2060), and long-term (2081-2100) phases under two RCP scenarios (RCPs 4.8 and 8.5) and the two management contexts ((a) the current management context that the CACG can only request 48 Mm^3; (b) the changed management context that there is no limit on the CACG request). The three sub-figures in the column "HISTORICAL" are identical to visually help the comparison. . 217

7.24 The annual water release for CACG under 6 GCMs (bcc-csm1-1, CNRM-CM5, inmcm4, MIROC-ESM, MPI-ESM-MR, MRI-CGCM3) for the near-term (2021-2040), medium-term (2041-2060), and long-term (2081-2100) phases under two RCP scenarios (RCPs 4.8 and 8.5) and the two management contexts ((a) the current management context that the CACG can only request 48 Mm^3; (b) the changed management context that there is no limit on the CACG request). The three sub-figures in the column "HISTORICAL" are identical to visually help the comparison. The red line is the quota (48 Mm^3) that the CACG can request under the current management context. 218

7.25 The annual water release for hydropower production by the SHEM under 6 GCMs (bcc-csm1-1, CNRM-CM5, inmcm4, MIROC-ESM, MPI-ESM-MR, MRI-CGCM3) for the near-term (2021-2040), medium-term (2041-2060), and long-term (2081-2100) phases under two RCP scenarios (RCPs 4.8 and 8.5) and the two management contexts ((a) the current management context that the CACG can only request 48 Mm^3; (b) the changed management context that there is no limit on the CACG request). The three sub-figures in the column "HISTORICAL" are identical to visually help the comparison. The red line is the threshold of the cost-effectiveness metric (69.8 Mm^3). 220

7.26 The regime of mean daily water release for hydropower production by the SHEM under 6 GCMs (bcc-csm1-1, CNRM-CM5, inmcm4, MIROC-ESM, MPI-ESM-MR, MRI-CGCM3) for the near-term (2021-2040), medium-term (2041-2060), and long-term (2081-2100) phases under two RCP scenarios (RCPs 4.8 and 8.5) and the two management contexts ((a) the current management context that the CACG can only request 48 Mm^3; (b) the changed management context that there is no limit on the CACG request). The three sub-figures in the column "HISTORICAL" are identical to visually help the comparison. 221

7.27 The annual number of days for hydropower production by the SHEM under 6 GCMs (bcc-csm1-1, CNRM-CM5, inmcm4, MIROC-ESM, MPI-ESM-MR, MRI-CGCM3) for the near-term (2021-2040), medium-term (2041-2060), and long-term (2081-2100) phases under two RCP scenarios (RCPs 4.8 and 8.5) and the two management contexts ((a) the current management context that the CACG can only request 48 Mm^3; (b) the changed management context that there is no limit on the CACG request). The three sub-figures in the column "HISTORICAL" are identical to visually help the comparison. 222

7.28 The regime of mean daily volume of the Oule reservoir under 6 GCMs (bcc-csm1-1, CNRM-CM5, inmcm4, MIROC-ESM, MPI-ESM-MR, MRI-CGCM3) for the near-term (2021-2040), medium-term (2041-2060), and long-term (2081-2100) phases under two RCP scenarios (RCPs 4.8 and 8.5) and the two management contexts ((a) the current management context that the CACG can only request 48 Mm^3; (b) the changed management context that there is no limit on the CACG request). The three sub-figures in the column "HISTORICAL" are identical to visually help the comparison. 224

7.29 The regime of mean daily volume of the Orédon reservoir under 6 GCMs (bcc-csm1-1, CNRM-CM5, inmcm4, MIROC-ESM, MPI-ESM-MR, MRI-CGCM3) for the near-term (2021-2040), medium-term (2041-2060), and long-term (2081-2100) phases under two RCP scenarios (RCPs 4.8 and 8.5) and the two management contexts ((a) the current management context that the CACG can only request 48 Mm^3; (b) the changed management context that there is no limit on the CACG request). The three sub-figures in the column "HISTORICAL" are identical to visually help the comparison. 225

7.30 The regime of mean daily volume of the Lassoula reservoir under 6 GCMs (bcc-csm1-1, CNRM-CM5, inmcm4, MIROC-ESM, MPI-ESM-MR, MRI-CGCM3) for the near-term (2021-2040), medium-term (2041-2060), and long-term (2081-2100) phases under two RCP scenarios (RCPs 4.8 and 8.5) and the two management contexts ((a) the current management context that the CACG can only request 48 Mm^3; (b) the changed management context that there is no limit on the CACG request). The three sub-figures in the column "HISTORICAL" are identical to visually help the comparison. 226

7.31 The regime of mean daily influenced river flow at Sarrancolin under 6 GCMs (bcc-csm1-1, CNRM-CM5, inmcm4, MIROC-ESM, MPI-ESM-MR, MRI-CGCM3) for the near-term (2021-2040), medium-term (2041-2060), and long-term (2081-2100) phases under two RCP scenarios (RCPs 4.8 and 8.5) and the two management contexts ((a) the current management context that the CACG can only request 48 Mm^3; (b) the changed management context that there is no limit on the CACG request). The three sub-figures in the column "HISTORICAL" are identical to visually help the comparison. The red line is the DOE requirement at Sarrancolin (4 m^3/s) 228

7.32 The regime of mean daily canal extraction under 6 GCMs (bcc-csm1-1, CNRM-CM5, inmcm4, MIROC-ESM, MPI-ESM-MR, MRI-CGCM3) for the near-term (2021-2040), medium-term (2041-2060), and long-term (2081-2100) phases under two RCP scenarios (RCPs 4.8 and 8.5) and the two management contexts ((a) the current management context that the CACG can only request 48 Mm^3; (b) the changed management context that there is no limit on the CACG request). The three sub-figures in the column "HISTORICAL" are identical to visually help the comparison. . 229

A.1 KGE criterion results on two model sets with the Safran-France input data are presented on two different calibration-validation procedure A.1a and A.1b: the 10-parameter model set (with a consideration of SCA-SWE hysteresis) are histograms labeled "calibrated with snow and Q" and the 8-parameter model set (without a consideration of SCA-SWE hysteresis) are labeled "calibrated with only Q". 278

A.2 KGE criterion results on two model sets with the Safran-PIRAGUA input data are presented on two different calibration-validation procedure A.1a and A.1b: the 10-parameter model set (with a consideration of SCA-SWE hysteresis) are histograms labeled "calibrated with snow and Q" and the 8-parameter model set (without a consideration of SCA-SWE hysteresis) are labeled "calibrated with only Q". 279
A.3 KGE criterion results on the 10-parameter-GR6J-CEMANEIGE model with two different input data Safran-France and Safran-PIRAGUA. 280
A.4 The performance of the 8-parameter-GR6J-CEMANEIGE model with two different input data Saran-France and Safran-PIRAGUA. 281

LIST OF TABLES

2.1 Selected impact studies of hydropower potential and production under various drivers in three example regions: Asia, Western Europe, and North America . . . 18
2.2 Advantages and limitations of the top-down and bottom-up approaches for adaptation development . . . 33
2.3 Examples of studies that applied the bottom-up approach on reservoir water system . . . 35

3.1 TMain characteristics of the 19 major reservoirs in the Neste water system 48
3.2 Physiographic and environmental flow information of the reservoirs and the associated sub-basins in the Aure Valley . . . 52
3.3 Characteristics of hydropower plants . . . 53
3.4 List of selected CMIP5 GCMs. . . . 61
3.5 DOE information of the ten stations. . . . 77
3.6 A summary of data collection. . . . 82

4.1 Parameters of the hydrological model GR6J coupled with the CEMANEIGE snow module . . . 88
4.2 A summary of the calibration elements of the GR6J-CEMANEIGE hydrological model for all the sub-basins in the Neste water system. . . . 89
4.3 GR6J-CEMANEIGE performance (KGE values) for for SB1, SB2, and SB4 in the split-sample tests. . . . 92
4.4 GR6J-CEMANEIGE performance (KGE values) for SB1-5 over the whole period of data length. . . . 92
4.5 Parameters of the GR6J-CEMANEIGE model obtained in the calibration over the whole period of data length. . . . 93
4.6 Water accounting for the Aure Valley . . . 103

5.1 The performance (R^1 values) of the hydropower demand model for 25%, 50%, and 75% quantile regression lines as examples. . . . 112
5.2 The inputs, outputs, initial conditions, and parameters of the ADEAUMIS model. . . . 116
5.3 The necessary thermal time for the major five stages of maize growth. . . . 117
5.4 Decision rules for irrigation in the ADEAUMIS model. . . . 118
5.5 Coefficient of determination R^2 between water release of the environmental flow from the CACG reservoirs R^{env}_{obs} and natural discharge in SB5 (or reservoir storage in SB5, or both) for four seasons. . . . 125
5.6 The seasonal extraction rules of the Neste Canal. . . . 135

5.7 The summary of the hydrological model, water demand models, and water management models with inputs and outputs. 141

6.1 Physiographic and hydro-climatic (precipitation P, temperature T, and naturalized inflow Q) information of the reservoirs and the sub-basins in the Aure Valley 150
6.2 List of selected CMIP5 GCMs. 154
6.3 GR6J-CEMANEIGE performance (KGE values) 159
6.4 The simulation results (sim and sim*) of water management metrics by the GR6J-CEMANEIGE model compared with observations (obs) in terms of QA for SB1-3, DOE and tDOE for the Sarrancolin catchment, and NSA and tNSA for SB1-3 162
6.5 The current management reference values for the water systems in the Aure Valley 163

7.1 Socio-economic drivers of the Neste water system in the near-term (2021-2040), medium-term (2041-2060), and long-term (2081-2100). 183
7.2 Four management modes of the SHEM management model to satisfy the CACG request under global change 207
7.3 The utilization frequency of the four management modes in the SHEM management optimization in the 6 GCMs (bcc-csm1-1, CNRM-CM5, inmcm4, MIROC-ESM, MPI-ESM-MR, MRI-CGCM3) for the near-term (2021-2040), medium-term (2041-2060), and long-term (2081-2100) phases under RCP 4.5 and the current management context. 212
7.4 As in Table 7.3 but under RCP 8.5 and the current management context (CACG can request 48 Mm^3). 213
7.5 As in Table 7.3 but under RCP 4.5 and the changed management context (no limit on CACG request). 214
7.6 As in Table 7.3 but under RCP 8.5 and the changed management context (no limit on CACG request). 215

1 General context

This chapter introduces the general context of water resources planning and management, and the objectives of the work undertaken.

Contents

1.1 Human and water **2**

1.1.1 Water management in the ancient time: the legacy 2

1.1.2 Water management challenges nowadays: the Anthropocene . . 3

1.2 Scientific problems and research objectives **8**

1.3 Structure of the dissertation **10**

1.1 Human and water

Water is the lifeblood of the planet and one of the most important basic necessities for humankind. Abundant water resource covers 70 to 75 % of the earth's surface while finite freshwater accounting for only 1 % of the earth's surface is available for human use (Gleick, 1993). While the global supply of freshwater is sufficient to fulfill all present and foreseeable water needs, the spatio-temporal distribution characteristic of freshwater resource make it inadequate or excessive for some regions of the world or for some periods of the year. Drought and flood events, the two major natural disasters that manifest through water, are reported to have the most devastating consequences among all the disasters that have stricken to human community (e.g., Ritchie and Roser, 2014; WHO, 2007).

Humankind, on the other hand, has been seeking ambitiously ways for efficient control and movement of water resources in order to minimize damage and maximize utilization. These activities of planning, developing, distributing and managing natural water resources through engineering (e.g., reservoirs, canals, and dikes) and non-structural (e.g., reducing water demand and distribution regulations) measures are defined as water resources planning and management (Loucks and van Beek, 2017). Water resources planning and management is a broad term and is rarely simple. Multiple disciplines and various associations that deal with water issues have described sophisticated relations between climate, water cycle and human community (including demographic, governmental, legal, and socio-economical aspects) (e.g., Bates et al., 2008; Biswas, 2004; Perrone and Hornberger, 2014). Besides, in terms of its functions and purposes, water can be planned and managed for food production (agricultural irrigation, fishery and animal husbandry), energy production (hydroelectricity and cooling for thermal and nuclear power stations), transport (navigation), industrial uses (e.g., chemical products), environmental protection (e.g., ecosystem preservation), and recreation (e.g., water sports).

1.1.1 Water management in the ancient time: the legacy

The ability to harness and to utilize water's power in the ancient time supports the development of agriculture and the rise of earliest urban areas (Berking et al., 2018). So crucial was water planning and management to early human societies that historians and archaeologists refer to them as "River Valley Civilizations" or "Irrigation Civilizations" (e.g., Mithen, 2010). However, coping with unwelcome changes (e.g., climate change, aridification) has been a frequent theme in human community throughout history, particularly in the water sector. For this purpose, early societies have developed complex techniques and accompanying management rules for using water (Angelakis and Zheng, 2015).

Figure 1.1 illustrates ten examples of water management techniques in the ancient time and some of them are located in some of what are now considered as the water-stressed regions in the world (e.g., the Mediterranean region). "Lessons from the past" or variations thereupon (e.g. Di Baldassarre et al., 2021, 2018; Holt, 2017; Kaptijn, 2017; Koutsoyiannis et al., 2008) is becoming more popular as water management experiences from the past can inform nowadays. In another word, understanding how water management efforts in the past were able to remain sustainable in the face of changes (e.g., climate change and increased demographic pressure), or why they failed to do so, can bring valuable information for water stakeholders and managers nowadays. For example, a project of promoting the ancient chinampas technique for agriculture development (a technique

that raises crops in lakes, see 5 in Figure 1.1) in Mexico during the late 1970s was reported to fail due to the negligence of indigenous knowledge and the inefficient communication among stakeholders (Kaptijn, 2017). Other examples such as qanat irrigation and oasis agriculture (see 8 and 9 in Figure 1.1) in the semi-arid and arid regions (West Asia and North Africa) are known as global agricultural heritage systems and proved to be resilient to changes (Koohafkan and Altieri, 2010). Their longevity and sustainability in managing water may serve as inspirations for addressing the challenges of agricultural production and water resource management under changes.

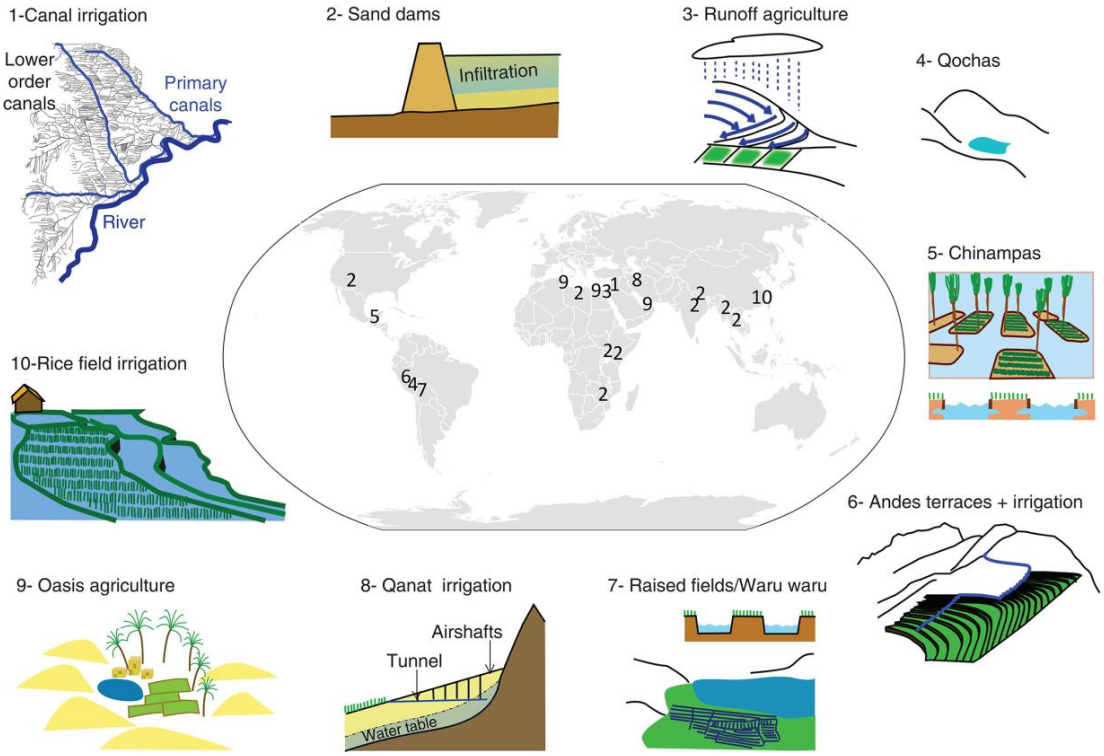

Figure 1.1 – Simplified diagrams of ancient water management techniques and their locations. Source from Kaptijn (2017).

To summarize, the lessons from the past can also inform the implementation of water management for the future. Furthermore, in the era of global change, these retrospective experiences are fundamental to the future adaptation design, particularly in the bottom-up frameworks which focuses on the vulnerability of water management (Benito et al., 2015; Mendoza et al., 2018).

1.1.2 Water management challenges nowadays: the Anthropocene

The "Anthropocene" was initially proposed by Paul J. Crutzen as the term for the current geological epoch during a meeting of the International Geosphere-Biosphere Programme (IGBP, 1999-2003) (Crutzen and Stoermer, 2000). As described by Carruthers (2019):

> *"On that occasion, Paul J. Crutzen, the Dutch, Nobel Prize-winning atmospheric chemist, and then Vice-Chair of the IGBP, had become increasingly impatient with his colleagues' repetitive use of the word 'Holocene' and exclaimed, 'Stop using the word Holocene. We're not in the Holocene any*

more. We're in the... the... the... [searching for the right word]... the Anthropocene!'"

Since then, albeit some debates on formalizing it (e.g., the beginning time), the Anthropocene signifies human impact on the Earth, including but not limited to anthropogenic climate change (e.g., Ruddiman, 2018; Steffen et al., 2015a; Zalasiewicz et al., 2019). Water is becoming a major concern in this human-induced era. It was characterized by the nonstationarity on both water supply and demand sides that challenges the efficiency and the sustainability of current water management (Cosgrove and Loucks, 2015).

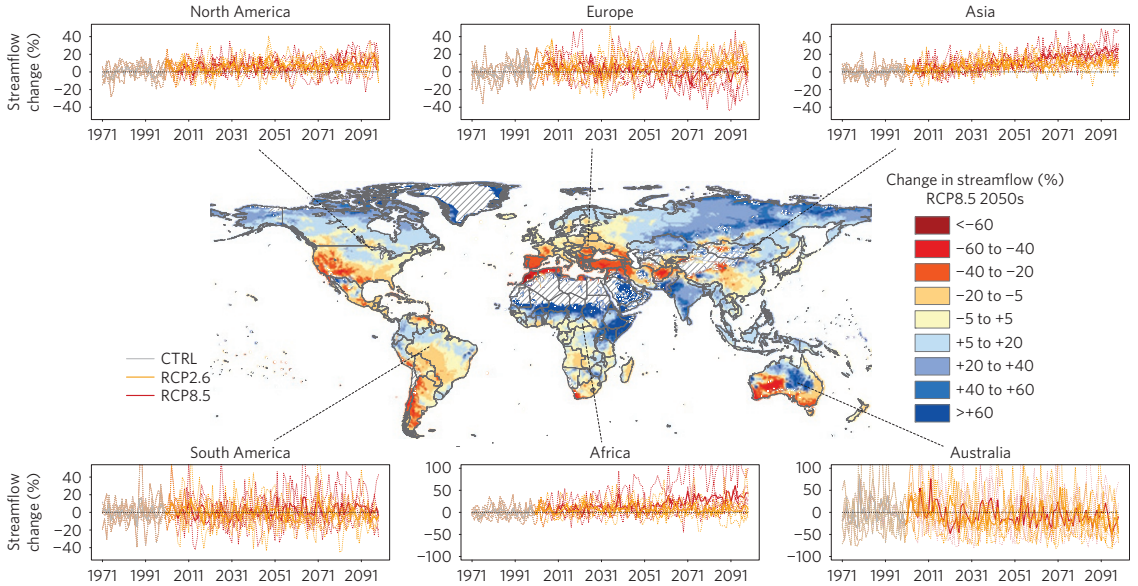

Figure 1.2 – Spatial changes of streamflow are presented under RCP 8.5 for the period from 2040 to 2069 (2050s) in comparison with the control period from 1971 to 2000. Temporal trends of streamflow are presented for the continents of North America, Europe, Asia, South America, Africa, and Australia for the period from 1971 to 2100 with the thick lines representing mean changes (gray for the control period, orange for RCP 2.6, and red for RCP 8.5) and thin dotted lines representing the five individual GCM results. Source from Van Vliet et al. (2016b)

On the water supply side, climate change associated with global warming induced by the increase of greenhouse gases (e.g., CO_2 and CH_4) in the atmosphere by human activities is one of the major drivers that redistributes spatially and temporally water resources towards an uncertain future (IPCC, 2014). Figure 1.2 illustrates the spatial changes and temporal trends of global streamflow under climate change scenarios. There is a remarkable reduction of streamflow in the Mediterranean-climate regions worldwide. Besides, climate change deeply alters the climatic impact-drivers (CIDs), known as the physical climate characteristics (e.g., means, occurrences, and extremes) that affect an element of societies or ecosystems (IPCC, 2021). Figure 1.3 shows that the disasters such as extreme heat, flood, storm, and drought events are projected to increase with high confidence in a large number of regions in the world. The general increase in the frequency and magnitude of global flood and drought events can lead to severe consequences on environment and economy (e.g., Arnell and Gosling, 2014; Dai, 2013; Hirabayashi et al., 2013; Trenberth et al., 2013). Global crop production could lower by 9-10%, which would worsen

the stability of global food security (Lesk et al., 2016). The increasing risks of these events cannot been seen as purely natural hazards anymore (Cai et al., 2014; Tabari, 2020). In addition, glaciers are significantly impacted by global warming as the Figure 1.3 shows. Glacier retreat from 1961 to 2016 results in sea-level rise of 27 ± 22 millimetres that accounts for 25-30% of the total observed rise, which massively reduces freshwater resource on the land (Zemp et al., 2019). Other non-climatic drivers (e.g., land use and land cover changes) can also alter hydrological regime and eventually impact water availability (Arheimer et al., 2017).

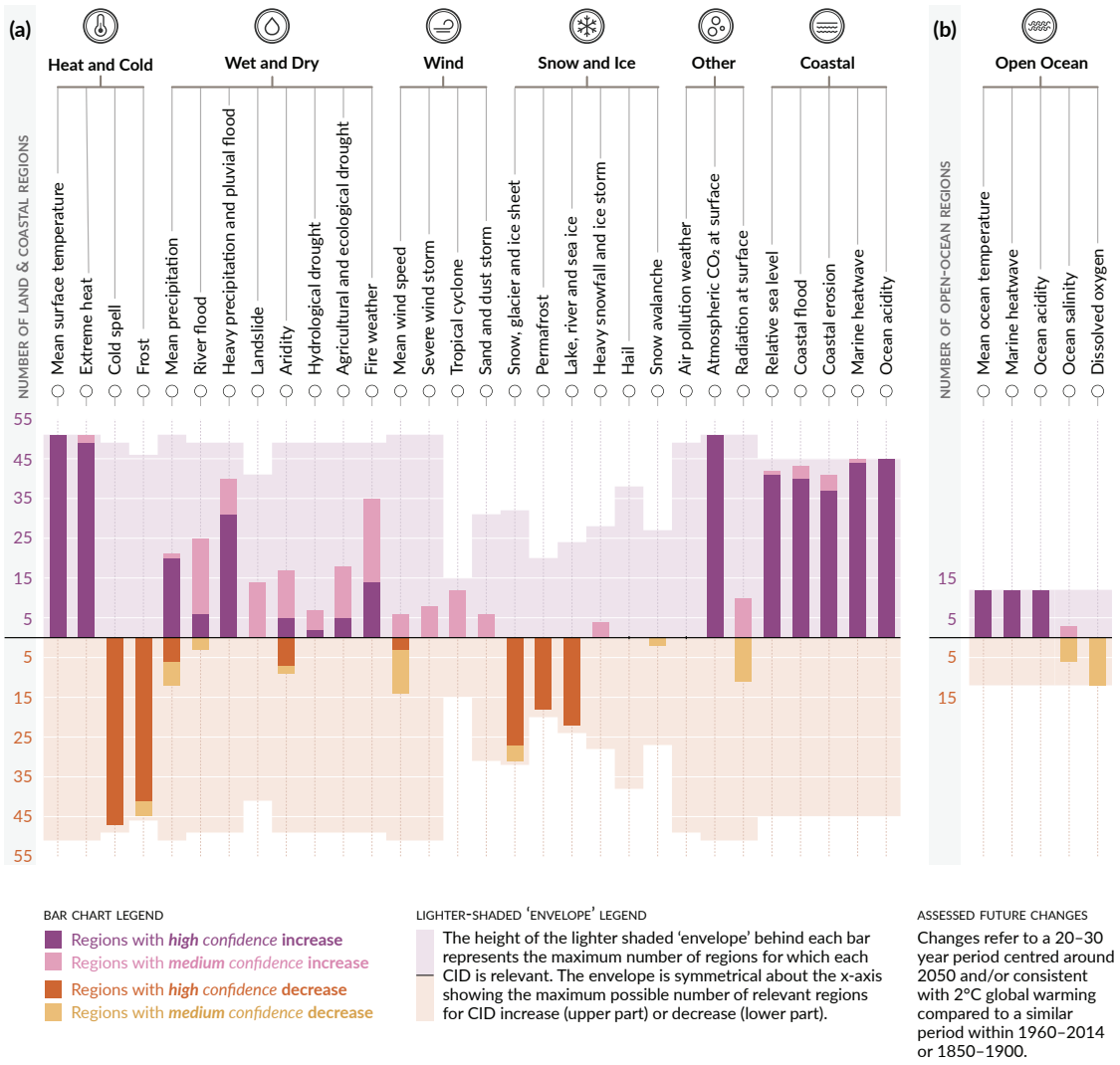

Figure 1.3 – Total 35 climatic impact-drivers (CIDs) of 7 types (heat and cold, wet and dry, wind, snow and ice, coastal, open ocean, and other) are projected to increase or decrease with high/medieu confidence in the how many land&coastal regions (a) and open-ocean regions (b). These regions can be explored in the WGI Interactive Atlas. Source from (IPCC, 2021).

On the water demand side, rapid socio-economic development in the Anthropocene, and particularly in the Great Acceleration since 1950, boosts current world water consumption as Figure 1.4 shows. Moreover, irrigation dominates all the water use sectors ($\approx$ 70%) (Gleick, 1993). Kummu et al. (2016) also concluded that global water use increased fourfold over the 20th century and the population under water shortage grew from

0.24 billion (14% of global population) to 3.8 billion (58% of global population). Future water consumption would continuously increase with the socio-economic development (e.g., Wada et al., 2016). Besides, other drivers, such as climate change, would induce more agricultural water consumption and shift energy demand pattern (e.g., from heating in winter to cooling summer) within the Water-Energy-Food nexus (e.g., Huang et al., 2019; Spinoni et al., 2017b). In addition to human uses, a call upon the natural environment is gaining increasing attention (e.g., Poff et al., 2015).

Furthermore, water scarcity could arise from not only changes in quantity-based supply and demand sides but also quality-based pollution (i.e., inadequate water for various uses due to different water quality requirements). Water quality is affected through complicated series of natural and anthropogenic mechanisms (e.g., sediment load, industrial chemicals and heavy medal release, and pesticide overuse). The combined effect from both quantity and quality aggravates water scarcity and augments water treatment cost (e.g., Ma et al., 2020; Tang et al., 2021; Yu et al., 2019).

Indeed, untangling water management issues will always be challenging under global change and will unavoidably necessitate the mixing of methodological frameworks because human and water systems cannot be regarded separately in this Anthropocene epoch but rather in a co-evolved view with climate. It is thus essential to acknowledging the "planetary boundary" within which human societies can operate safely and sustainably (Steffen et al., 2015b). A first step forward is to deepen the understanding of human role in mitigating and adapting to global change (Van Loon et al., 2016). Information collected from such frameworks improves practical mitigation and adaptation agendas.

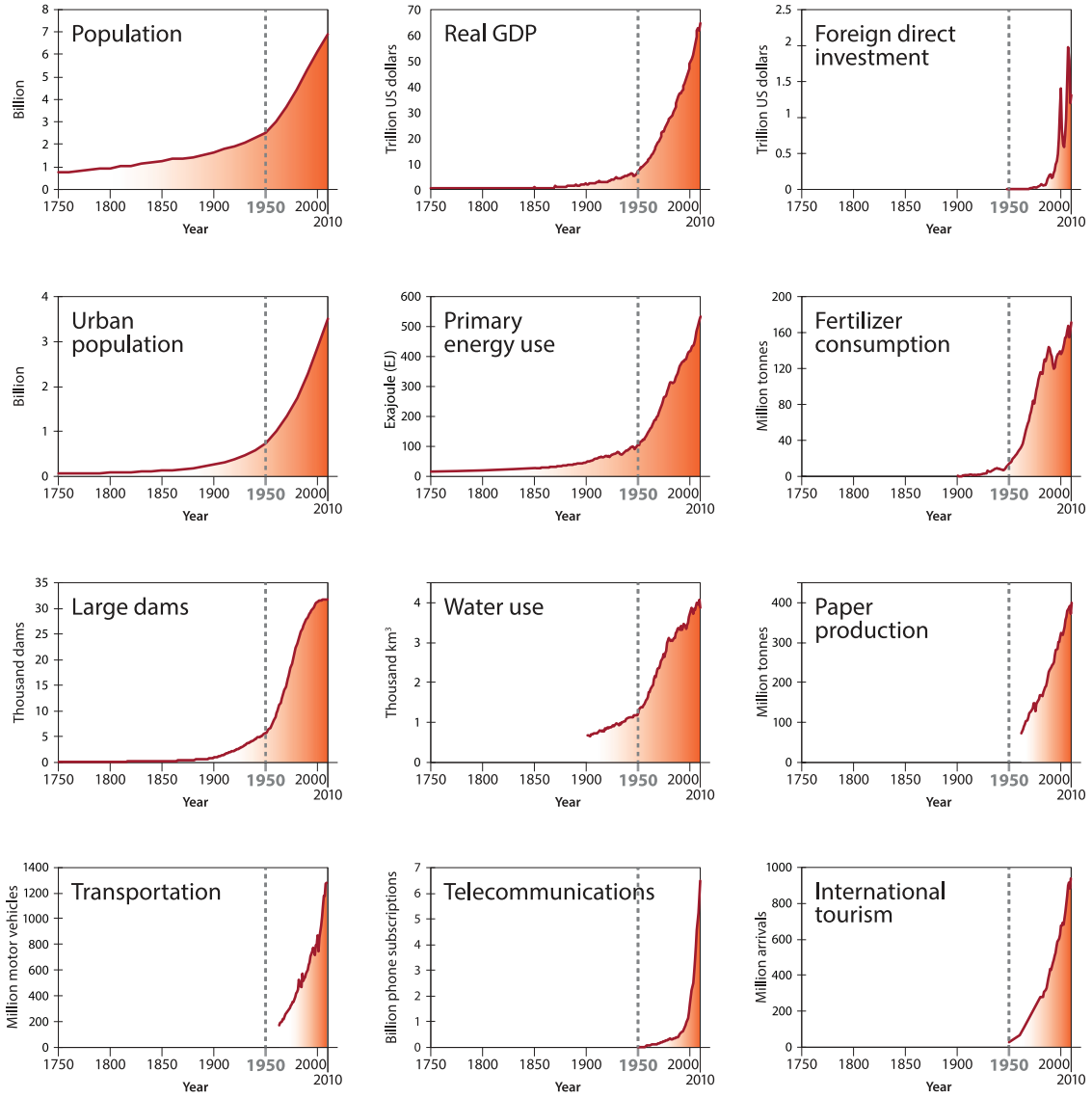

Figure 1.4 – The trends of global socio-economic development from 1750 to 2010 for 12 indicators: population, real Gross Domestic Product (GDP), foreign direct investment, urban population, primary energy use, fertilizer consumption, large dams, water use (annual water consumption for irrigation, domestic, livestock, and industrial uses), paper production, transportation (global production of new automobiles), telecommunications (total subscribers to fixed landlines and mobile phones), and international tourism (annual number of international arrivals). The gray vertical dotted lines represent the year 1950, which is the start of the "Great Acceleration" as the characteristics of contemporary world. Source from Steffen et al. (2015a)

1.2 Scientific problems and research objectives

Modelling the natural component of the water cycle has long been a focus of hydrologists; to go beyond that, the hydrological community, the PANTA RHEI initiative of the International Association of Hydrological Sciences, is currently encouraging the integration of the human interactions with water resources within hydrological modelling (Montanari et al., 2013). As such, the questions related to sustainable water management necessitate the development of new tools capable of representing human influence on water resources and of innovative frameworks to evaluate the vulnerability of current management rules in an evolving context. These advancements are essential for examining global change impact on water management (e.g., water resource availability and water use satisfaction under climatic and socio-economic changes) and eventually for outlining plausible adaptation strategies.

Research is required to uncover the continually evolving link between hydrology, management rules and water demand. Particularly, the analytical framework tailored to the management and allocation issues of water systems and to the outlook of future changes is of great importance for characterizing the global change impact on this human-water link. This implies identifying the facets of global change to which each user is the most sensitive and the degree of tolerance of each user to disturbances of current state or to extreme events. Thereafter vulnerability can be assessed based on the likelihood of critical changes for different future time slices (beginning, middle and end of the 21st century).

The European project PIRAGUA [1], in line with the strategy of crossboarder cooperation of the OPCC [2] (Pyrenean Climate Change Observatory), aims ultimately at improving the adaptation of Pyrenean territories to climate change. This thesis is a scientific contribution to the project and new developments are illustrated on the Neste water system, a complex multiobjective reservoir water system located in the French Pyrenees. The sustainability of the current water management rules employed for upstream hydropower production, downstream water consumption (including irrigation, domestic, industrial uses), and environmental regulations will be investigated under global change scenarios. This work was carried out in close collaboration with local water stakeholders and managers (the SHEM [3] and the CACG [4]), and with other research partners in the PIRAGUA consortium (e.g., CLIMPY[5]).

Among the many components of water resource systems, reservoirs are a long-standing method for reducing the spatio-temporal variability of natural water supply, and they are constructed worldwide. However, global change questions the sustainability of reservoir water management. In this work, we take the example of the Neste water system to investigate the vulnerability of reservoir water management under global change. The two main objectives of the thesis are:

1. **Developing and improving water demand and management models as pieces**

[1] https://www.opcc-ctp.org/en/piragua

[2] https://www.opcc-ctp.org/en/

[3] Société Hydro-Electrique du Midi (www.shem.fr) is a French electricity producing company, a subsiniary of ENGIE group.

[4] Compagnie d'Aménagement des Coteaux de Gascogne (www.cacg.fr) is a water management and distribution company for the Gascogne region in Southern France.

[5] https://www.opcc-ctp.org/en/climpy

of an integrated hydrological modelling framework:

The thesis is an opportunity to implement models that may reproduce water management rules of multipurpose reservoirs. An analysis should be firstly carried out to identify the drivers and regulatory aspects that control water release and storage actions. The challenges are then to explore the realistic representation of the current management, but simple enough to be applied to global change scenarios and to be transferred to other case studies.

The modelling chain is therefore expected to represent the modules of water resources, water demand, and water management that could run in present and future scenarios. Finally, the outputs of these models will be used to diagnose the sustainability of the management in its current configuration, and to test new adaptation methods under a modified context.

2. **Characterizing the vulnerability of the management mode of the Neste water system:**

   There is a growing concern on the sustainability of reservoirs to cope with altered water supply and demand regimes by global change. The thesis will investigate their vulnerability based on the bottom-up approach adopted by Sauquet et al. (2019) that is based on three components: "sensitivity" (how does the system respond to external disturbances?), "exposure" (what is the probability of occurrence of disturbances in the future?), and "threshold" (where are the boundaries within which the system performs acceptably?).

   The challenges of this method remain for characterizing the water management failures (e.g., storage objectives, capacity to meet high peak demands for energy and irrigation), correlating the intensity or frequency of failures to those of hydrometeorological hazards (e.g., unanticipated flooding or severe low flow), and identifying management metrics (e.g., the performance and the associated critical thresholds for reservoir management mode).

1.3 Structure of the dissertation

This dissertation is organised in eight chapters and is structured around two articles (one under review and the other submitted):

1. The first chapter aims to introduce the general context and the objectives of the work undertaken.
2. The second chapter is a literature review, allowing in particular to explore the challenges of reservoir water management under global change and the potential adaptation strategies.
3. The third chapter presents the study case, the Neste water system, and its current management modes, as well as the dataset used in the following work.
4. The fourth chapter presents the estimation of water resources in the study area.
5. The fifth chapter proposes water demand and management models applied to the Neste water system.
6. The sixth chapter, based on an article, presents the results of vulnerability assessment of the study area under climate change. This assessment has identified the key climatic drivers for water management of the Neste water system.
7. The seventh chapter uses a top-down approach to assess the potential impact of global change on the study area.

Finally, a general conclusion summarises the main results obtained and lists some perspectives associated with these results.

2 Literature review

This chapter is a literature review article submitted to WIREs water, entitled "Challenges of reservoir planning and management under global change: impact and adaptation", and currently under review.

Contents

Abstract **13**

2.1 Introduction **14**

2.2 Impact of global change on reservoir performance **17**

2.2.1 Hydropower reservoirs 17

2.2.2 Irrigation reservoirs 20

2.2.3 Multi-purpose reservoirs 21

2.2.4 Summary 22

2.3 Adaptation of reservoir system under global change **24**

2.3.1 Actions in reservoir planning 24

2.3.2 Actions in reservoir management 25

2.3.3 Adaptation paradigms of reservoir water system 28

2.4 Challenge of adaptation under global change **31**

2.4.1 Challenges in the assessment approaches 31

2.4.2 Challenges in the design and appraisal of adaptation 34

2.4.3 Challenges in the participation of stakeholders and managers . . 37

2.5 Conclusion **39**

CHALLENGES OF RESERVOIR PLANNING AND MANAGEMENT UNDER GLOBAL CHANGE: IMPACT AND ADAPTATION

PENG HUANG[1], ERIC SAUQUET[1], BAPTISTE FRANÇOIS[2], JEAN-PHILIPPE VIDAL[1]

[1]UR RiverLy, INRAE, Villeurbanne, France
[2]University of Massachusetts, Amherst Center, MA, United-States

Abstract

The potential impact of global change on water infrastructure planning and management highlights the need for adaptation. Reservoirs are among the most powerful infrastructures in resolving water problems and exploiting water uses. Here, we reviewed (1) the potential implication of global change on hydropower, agricultural, and multi-purpose reservoir water systems; (2) the plausible adaptation strategies dedicated to reservoir water planning and management; (3) the challenges in adaptation procedures in terms of impact assessment, adaptation design and appraisal, and adaptation implementation. We found that the performance of reservoir systems is broadly degraded by both climatic and socio-economic changes that alter water supply and demand. Adaptation of reservoir water systems relies on embracing the non-stationary practice on the premise of comprehensive impact assessment, and should be implemented from water supply and demand sides. The bottom-up assessment approach combined with top-down impact approach provides complementary information for adaptation, which is promising to design effective strategies. Still, challenges remain in the appraisal and implementation of adaptation, which needs deeper cooperation among scientific community, stakeholders and water managers.

2.1 Introduction

Water infrastructure provides essential services for human society, including but not limited to hydropower generation, agricultural irrigation, drinking water supply, and flood control. Global change, which encompasses changes in climate, socio-economic development, demography, land-use and land-cover, among others (Steffen et al., 2015a), brings new challenges for planning and management of water infrastructure (Montanari et al., 2013; Viviroli et al., 2011). Compared with natural river basins, those regulated by water infrastructures could suffer from more severe water pressure in the future (Nilsson et al., 2005; Palmer et al., 2008; Vogel et al., 2011). River regulation reduces the natural capacity of rivers to conform themselves to disturbances (Arheimer et al., 2017; Vörösmarty et al., 2010). Further, potential water supply alterations with large variation and demand increases induced by global change complicate water planning and management. Therefore, these challenges highlight the need for innovative analysis frameworks and effective adaptation strategies to mitigate the adverse impact on water systems (Brown et al., 2015; Ceola et al., 2016).

Reservoir systems are considered among the most efficient infrastructures in resolving water problems and exploiting water resource by redistributing water spatially and temporally. In general, reservoir functionalities can be achieved by regulating natural flows depending on the magnitude of inflows and water demand at a specific time. Concerning the purposes of reservoirs, they can be divided into single-purpose and multi-purpose reservoirs. According to ICOLD (2019), almost half of reservoirs registered in the database are single-purpose ones. Among these single-purpose reservoirs, 47% are constructed for irrigation supporting and 22% are solely for hydropower generation. As for multi-purpose reservoirs, the leading objectives are irrigation, flood control, water supply, and hydropower generation, which cover 80% of all multi-purpose reservoirs registered. Given these benefits, reservoir systems are world-widely constructed despite their intensive investment (see Figure 2.1b). On the other hand, reservoir constructions show a decreasing trend from the late 20th century (see Figure 2.1a) probably because global major river systems are getting saturated with reservoirs, and the environmental and social acceptance is now against reservoir constructions (Nilsson et al., 2005; Poff et al., 2007; Renöfält et al., 2010). However, since 2014, around 3,700 hydropower dams are either planned (83%) or under construction (17%) to secure future energy supply, especially in developing countries (Zarfl et al., 2015). To date, the number of large reservoirs registered is more than 58,000 with their aggregated impoundment approximately 15,000 km^3 (ICOLD, 2019). Large reservoirs significantly impact terrestrial water system at the global scale (Chao et al., 2008; Zhou et al., 2016). In addition, the cumulative effect of medium or small reservoirs also plays an important role in changes of downstream river flow regime (Habets et al., 2018; Morán-Tejeda et al., 2012b). As such, reservoir systems are of great importance for integrated water resource management (Biswas, 2004) and water security within the food-energy-water (FEW) nexus (Perrone and Hornberger, 2014).

Water resource planning and management is a broad concept with different definitions suggested by numerous associations and individuals (Loucks and van Beek, 2017). The review here focuses on reservoir water planning and management. Reservoir planning means that on the basis of the current knowledge of the evolution of water supply and demand, together with the expected change in operational constraints (e.g., change in environmental regulations), the best development plan and corresponding engineer-

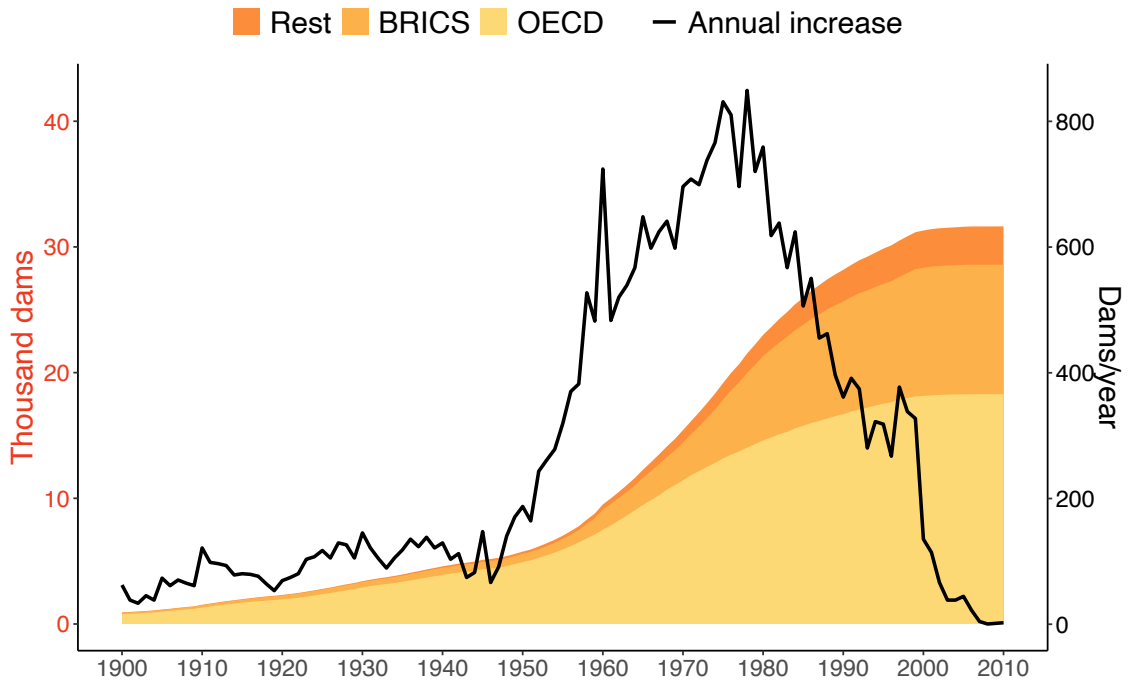

(a)

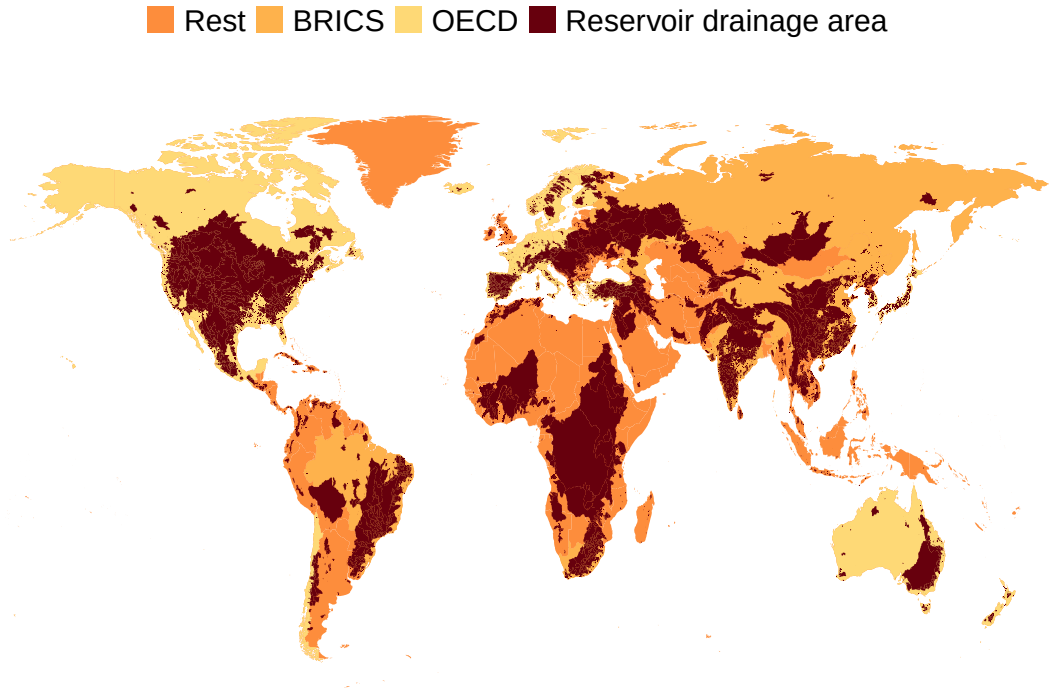

(b)

Figure 2.1 – (a) The increasing trend of the number of large dams (large: a minimum of 15 m height above foundation) from 1900 to 2010 in three categories of the world countries: the OECD countries (members in 2010); the emerging economies defined as the BRICS countries including Brazil, Russia, India, China (China mainland with Macau, Hong Kong and Taiwan where applicable), and South Africa; and the rest countries. The data source is from Steffen et al. (2015a). (b) The drainage area of georeferenced large dams in the three categories of the world countries. The data source is from the GOODD dataset (Mulligan et al., 2020).

ing measures (including reservoir sizing and supporting facilities design) are formulated. Reservoir management is a set of rules or guidelines during an operation period (single-year or multi-year) serving reservoir purposes. Historically, reservoir systems have been planned and managed assuming that water supply and demand were both stationary and, as such, the available historical records were adequate to represent, statistically, the future supply and demand distributions (National Research Council, 2011). Nevertheless, the recent AR6 report of IPCC (2021) reaffirmed that the increasing GHG (GreenHouse Gas) concentration in the atmosphere has raised global temperature, referred as global warming. Climate is changing in ways that cannot just be attributed by natural variability with more occurring extreme events (AghaKouchak et al., 2020; Hari et al., 2020; IPCC, 2014; Lins and Cohn, 2011). Severe droughts in Europe (representative years of 2003 and 2015, see Laaha et al. 2017), Australia (Millennium Drought, see Van Dijk et al. 2013), and Western United States (Griffin and Anchukaitis, 2014) have questioned the ability to face extreme and unexpected events. Remarkably, the most severe drought events in California from 2012 to 2015 surpassed historical observations and resulted in less water availability in the reservoirs than usual, which increased electricity cost of 2 billion dollars by meeting the demand with other energy sources instead of hydropower (Gleick, 2016; Swain et al., 2014). The unanticipated and unusual drought events would worsen water scarcity, making reservoir planning and management more problematic. Zhou et al. (2015) concluded that a primary concern for hydropower was precipitation changes. Regarding water demand, global economic and demographic growth boosts freshwater consumption that is water withdrawals for agricultural, industrial and municipal uses (Boretti and Rosa, 2019). Global water demand has faced a six-fold increase over the last century and BRICS countries (the emerging economies including Brazil, Russia, India, China, and South Africa) have consumed the largest share at about 45% (Ritchie, 2017). Therefore, changes in both water availability and water demand due to global change pose many challenges for reservoir planning and management.

Assessing the impacts of water systems to global change is a central premise in designing mitigation and adaptation actions (Bates et al., 2008). Over the last decades, the issues of implications of global change on water resource have received considerable attention and has been well documented (e.g., Alcamo et al., 2007; Arnell, 2004; Vörösmarty et al., 2000). Recent concentration shifts towards a continuous concern that current water infrastructure and management are not prepared to handle future uncertainty (Brown et al., 2020, 2015), and how water systems can be adapt to climate change are discussed (e.g., Dittrich et al., 2016; Herman et al., 2020; Schaefli, 2015). Guidelines for stating robust adaptation strategies - those proposing a system that can operate properly under a wide range of future conditions (Herman et al., 2015) - are still expected. Thus, this paper aims to review the impact and adaptation induced by global change from the perspective of reservoir systems. The analysis of the review is based on a large selection of published papers on reservoir water planning and management from global, regional, and local aspects. In section 2.2 we explore the implications of global change on reservoir purposes. We then proceed to summarize the possible adaptation strategies to global change (section 2.3). Section 2.4 analyzes the remaining challenges in the procedure of adaptation. A set of conclusions is finally drawn.

2.2 Impact of global change on reservoir performance

The performance of water systems could be impacted from water supply and demand changes. On the water supply side, precipitation change, and Land Use and Land Cover (LULC) are the leading drivers that result in potential changes in reservoir performance. While on the water demand side, population growth, climate-induced change in irrigation (e.g., shortened crop growth period), and human activities (e.g., water market response, policy, and cropping pattern) are the main drivers. Here, reservoir performance is discussed based on a reduced set of drivers from both supply and demand sides of reservoir water resource.

2.2.1 Hydropower reservoirs

As reported by World Energy Council (2013), approximately 15% of the world electricity production is generated by hydropower installations (including run-of-the-river facilities), which accounts for about 78% of total renewable energy production. Hydropower is also a major energy source holding over 50% of annual electricity generation for countries like Brazil, Canada, Norway, and Switzerland (World Energy Council, 2013). Hydropower and climate change are double-side: hydropower itself, as a clean and renewable energy source, contributes to reducing GHG emissions by replacing fossil energy while climate change can alter streamflow regime and variability, affecting hydropower potential and production (Berga, 2016; Wasti et al., 2022).

Hydropower potential refers to the amount of energy that can be exploited from water resource. *Gross* hydropower potential (GHP) and *developed* hydropower potential (DHP) are the two aspects mostly investigated in the literature: the former corresponds to the total energy to natural runoff over the entire elevation of the study area without any energy losses; the latter the energy that can be maximized from the existing power plants. Hydropower production (HPP) is the actual electricity generation through the existing installations and operation rules. Turner and Voisin (2022) summarized methods employed in the simulation of GHP, DHP and HPP at subcontinental to global scales. Most studies attempted to examine the influence of global change on hydropower potential and production from a regional or local perspective and the general approach is model-based. Hydropower potential and production depend directly on changes in water availability of discharge. Besides, changes in energy market and policy can strongly impact hydropower production and revenue (Anghileri et al., 2018; Gaudard et al., 2013). Table 2.1 lists recent impact studies on hydropower for three example regions: Asia, Western Europe, and North America.

The major cause for changes in water availability is climate change, which propagates to hydropower potential and production by altering river flow regime in terms of discharge range and seasonality. Several global-scale assessments showed regional variations of hydropower potential (e.g., Gernaat et al., 2017; Van Vliet et al., 2016a,b; Zhang et al., 2018) and highlighted substantial uncertainty in projected changes in HPP (e.g., Hamududu and Killingtveit, 2012; Turner et al., 2017a,b; Yalew et al., 2020; Zhou et al., 2018). Uncertainty in the sign of the changes is illustrated in the Alps: Hänggi and Weingartner (2012) concluded that the overall warming and increased winter precipitation is a potential prominent advantage for the HPP in the Swiss Alps while the studies in table 2.1 (the row of the HPP of the Alps under the driver of climate change) suggested the opposite. The warming effect and precipitation variability significantly alter snow

Table 2.1 – Selected impact studies of hydropower potential and production under various drivers in three example regions: Asia, Western Europe, and North America

References	Targets	Drivers	Impacts
	Asia		
Liu et al. (2016)	GHP and DHP of China	CC	GHP tended to increase by 6% while DHP tended to decrease by 4% by the end of the 21st century
Wang et al. (2017)	HPP of south-western China	MC	Hydro-wind-solar system significantly fluctuated HPP
Qin et al. (2020a)	HPP of south-western China	CC+MC	The concurrent effect of CC and MC increases the mismatch between HPP and demand
Hecht et al. (2019); Li et al. (2017); Shrestha et al. (2017)	HPP of Vietnam	HA	Upstream damming and LULC reduces HPP of the lower Mekong River basin
	Western Europe		
Anghileri et al. (2018); Majone et al. (2016); Maran et al. (2014)	DHP and HPP of the Alps	CC+PC	Compared with CC, PC may have more significant impact on hydropower revenue
Finger et al. (2012); Schaefli et al. (2007); Wagner et al. (2016)	HPP of the Alps	CC	HPP was estimated to decrease due to temperature increase and changes in precipitation
Gaudard et al. (2013, 2014); Puspitarini et al. (2020); Savelsberg et al. (2018); Stanton et al. (2016)	HPP of the Alps	CC+MC	In addition to CC, seasonal consumption shift and the complementarity with other renewable energy sources impacted HPP
Hendrickx and Sauquet (2013)	HPP of the French Pyrenees	CC	Reduced annual inflow and modified seasonal runoff distribution decreased HPP
	North America		
Craig et al. (2018); Hamlet et al. (2010); Markoff and Cullen (2008); Turner et al. (2019); Vicuna et al. (2008)	HPP of the Pacific Northwest	CC+MC	Seasonal supply/demand mismatch (more for cooling, less for heating) and population growth impacted the performance of HPP
Kern and Characklis (2017); Kern et al. (2014a,b); Su et al. (2017)	HPP of the USA	MC	The integration with other renewable energy sources influenced HPP revenue
Haguma et al. (2014); Jabbari and Nazemi (2019); Minville et al. (2009, 2010); Oni et al. (2012)	HPP of Canada	CC	HPP was projected to increase while the efficiency did not necessarily improve

Note: CC, MC, PC, and HA represent climate change, energy market change, policy change, and human activities, respectively.

accumulation and melt patterns, and eventually the seasonal flow patterns (Barnett et al., 2005; Fayad et al., 2017; Viviroli et al., 2011). The discordant results in different regions of the Alps could be attributed to the transition characteristics of the Alps in terms of precipitation shifting from an increase in North to a decrease in South (Frei et al., 2018; Gobiet et al., 2014; Smiatek et al., 2016). Moreover, spatial heterogeneity in the Alps can yield different hydrological regimes and thus different sensitivity to climate change (Maran et al., 2014). Elsewhere, in the Southern Europe, the hydropower potential and production converge towards a decreasing tendency due to projected drier climate and increased water competition by socio-economic development (e.g., irrigation and industry demand) (e.g., Bonjean Stanton et al., 2016; Lehner et al., 2005; Turner et al., 2017b; Wagner et al., 2019).

Another primary cause for changes in water availability for reservoirs is human activities, such as damming and LULC. Examples in the Mekong River basin (MRB) are illustrated in table 2.1. Damming in the upper MRB, especially the Xiaowan and Nuozhadu dams that boost the total active storage capacity of the upper MRB from 0.72km^3 to 32.1km^3, significantly attenuate the HPP in the lower MRB (Hecht et al., 2019). Li et al. (2017) further concluded that damming and dam regulations in the upper MRB had stronger influence on annual streamflow of the lower MRB than climate change. Besides, the rapid transition of LULC (e.g., deforestation for farmland and urban area expansion) significantly impacted the performance of hydropower generation in the lower MRB (MRC, 2018). Shrestha et al. (2017) examined the implications of deforestation on the three most important tributaries (the Sesan, Srepok, and Sekong Rivers) of the lower MRB. The results showed that deforestation reduced peak flows in all scenarios, and thus the HPP during wet season. The contradiction to common sense that deforestation increases runoff could be attributed to the increased evapotranspiration due to the transition from low-density forest to intensive agriculture (Shrestha et al., 2017).

Assessment on HPP from the perspective of energy consumption in market is also important (Gaudard and Romerio, 2014). Climate change may alter the electricity consumption pattern by increasing demand for cooling and decreasing demand for heating, which could lead to modification of the price schemes (Gaudard et al., 2013; Golombek et al., 2011; Mideksa and Kallbekken, 2010; Yalew et al., 2020). Hydropower in the Pacific Northwest is an important component in the energy supply system but vulnerable to climatic changes (see Table 2.1). In addition to reduced water resource, the seasonal mismatch between hydropower supply and energy demand impaired the performance of HPP, and thus reduced the revenue (e.g., Markoff and Cullen, 2008; Turner et al., 2019; Vicuna et al., 2008). Auffhammer et al. (2017) showed that the peak load of energy consumption under climate change could be higher and more frequent than business-as-usual situation, meaning additional energy cost by increasing energy capacity to meet the peak demand. Furthermore, the population growth in the Pacific Northwest could unduly burden the hydropower system for summer cooling demand (Hamlet, 2011).

Increasing penetration of other renewable technologies in energy market as an influence on hydropower should not be neglected (e.g., Danso et al., 2021; François et al., 2017). Hydropower itself as a renewable energy source without direct emission of CO_2 is playing an important role in the electricity grid of many countries. For instance, the energy market liberalization from the 2000s in Europe enhanced the role of hydropower in the energy market (e.g., hydropower-dominant Switzerland and Norway, nuclear-hydropower-mixed France, and fossil-hydropower-mixed Italy) (Gaudard et al., 2014). Due to their operational flexibility, hydropower reservoirs are optimal candidates to complement the

variability of intermittent energy generation (e.g., wind and solar) (François et al., 2014a). Run-of-the-river hydropower plants have also been shown to ease integration of solar and wind energy sources (François et al., 2016). However, the integrated development of hydropower with other renewable energy sources could fluctuate the hydropower revenue and hydrological regime downstream (e.g., Kern and Characklis, 2017; Kern et al., 2014a,b; Su et al., 2017; Wang et al., 2017).

2.2.2 Irrigation reservoirs

Irrigation water demand is the quantity of water, in addition to precipitation, that is needed to ensure crop development and to maintain an acceptable soil moisture content. The global water supply for irrigation has been significantly improved through the construction of reservoirs (Biemans et al., 2011). Around 30-40% of the 271 million hectares of agricultural lands in the world are supported by irrigation reservoirs (World Commission on Dams, 2000). Global food security highly relies on irrigation reservoirs, which has contributed 12-16% of world food production and has benefited 1 billion people (World Commission on Dams, 2000). However, the performance of irrigation-purpose reservoirs is constrained by the changes in potential water availability and water demand resulting from climatic and socio-economic changes.

Irrigation reservoir management is sensitive to inflow changes. Irrigation water availability is generally reported to reduce due to global warming and changes in precipitation pattern (e.g., Mehta et al., 2013; Qin et al., 2020b; Ronco et al., 2017; Vano, 2020; Varela-Ortega et al., 2014). Sufficient irrigation water supply in the future might not be maintained without constructing new reservoirs (Yoshikawa et al., 2014). For instance, the largest irrigation system in Europe located in Spanish Pyrenees would experience water scarcity induced by climate change in the future especially in summer when agricultural water demand is at peak (Haro-Monteagudo et al., 2020). Supposing that annual irrigation water demand and land use remain constant, the agriculture sustainability in this area is threatened under climate change and the use of the current management strategy. However, the assumptions of business-as-usual irrigation requirements and land use are optimistic to analyze the performance of irrigation reservoir management.

Yet, when it comes to the comprehensive assessment of irrigation water system, the incorporation of irrigation water demand is essential because crops are directly exposed to climate and changes in climate variables (temperature, CO_2 concentration) will alter water demand pattern (e.g., Ashofteh et al., 2017; Qin et al., 2020b; Stöckle et al., 2010; Vano et al., 2010). Irrigation water demand has been studied at global scale with an increasing trend in the future (e.g., Wada et al., 2013). By contrast, a slight decrease in global crop water deficits was reported, which could be attributed to increased precipitation in many rainfed croplands (e.g., in Africa, China, and South America) and reduced diurnal temperature variation (Zhang and Cai, 2013). At the regional scale, Vidal et al. (2012) projected more severe and frequent agricultural droughts in France over the 21st century. In southern India, an increased irrigation water demand in the future was simulated due to changes in other meteorological variables offsetting the precipitation increase (Rehana and Mujumdar, 2012). Besides, water scarcity for irrigation can be aggravated by increasing population for food and changes in agricultural land use (e.g., Konzmann et al., 2013; Mehta et al., 2013; Vörösmarty et al., 2000).

Changes in supply and demand sides challenge the performance of irrigation-purpose reservoirs. Particularly, the drought events in the Mediterranean region render the man-

agement of irrigation reservoirs vulnerable to changes (e.g., Fayad et al., 2017; Folton et al., 2019; García-Ruiz et al., 2011; Spinoni et al., 2017b; Tramblay et al., 2020). For example, Nunes et al. (2017) concluded that the dry Mediterranean region of southern Portugal could experience a moderate degradation of irrigation water scarcity in the future under both climate change and socio-economic scenarios. The simulation results indicated that water scarcity resulted from decreased water availability due to climate change and increased water demand due to combined climate and socio-economic changes. Additionally, water quality would decrease through the increase of sediment and phosphorus inflows into the reservoir, which was attributed to the land use evolution in the socio-economic scenarios. Similar irrigation water stress in the Mediterranean region was reported (e.g., Dono et al., 2013; Gorguner and Kavvas, 2020; Okkan and Kirdemir, 2018; Rocha et al., 2020).

2.2.3 Multi-purpose reservoirs

Compared with single-purpose reservoirs, multi-purpose reservoirs are designed to satisfy two or more functions in a regulation period. Apart from changes in water availability and water demand, conflicts and tradeoffs arise among various objectives, which drastically complicate the management of multi-purpose reservoirs. Thus, this section highlights the inherent conflicts and tradeoffs of multi-purpose reservoirs under global change. They can be classified as (1) volumetric tradeoffs (given the limited reservoir storage, these occur when reservoir managers hesitate on how much storage to be allocated for each objective, such as flood control and water conservation) and (2) temporal tradeoffs (these occur when the reservoir objectives show different patterns of water use in time, such as irrigation in summer and hydropower in winter for heating in France, see François et al. 2015, 2014b, and in Spain see Pereira-Cardenal et al. 2014).

Volumetric tradeoffs

Volumetric tradeoffs are usually associated with the objective of flood control. Flood control requires that the reservoir water level is maintained at a certain level to absorb flood inflows. This conflicts with the water conservation purpose which requires storing water as much as possible for future use. Given the global flood risk projections, there is a widespread concern whether the current reservoir capacity and the flood management policy are resilient to future flood risks (e.g., Fluixá-Sanmartín et al., 2018; François et al., 2019; Kundzewicz et al., 2010). The revenue of hydropower production and the reliability of water supply could be improved when reservoir inflows increased. However, flood risks are also prone to increase by more extreme flood events, which endangers the reservoir safety if current management rules remain unchanged (Bates et al., 2008; Bhadoriya et al., 2020; Park and Kim, 2014). While in regions with generally reduced reservoir water availability, the volumetric tradeoffs would be more intense under global change (Alam et al., 2019; Kim et al., 2009; Mehta et al., 2013; Raje and Mujumdar, 2010). The current flood management threshold might be comparatively oversized for the future climate in these regions where flood risks are projected to decrease.

Temporal tradeoffs

Temporal tradeoffs arise when the demand seasonality of objectives is mismatched, especially for multi-purpose reservoirs serving consumptive purposes and hydropower production (Gonzalez et al., 2020; Mereu et al., 2016). Water for consumptive purposes (such as irrigation, drinking water, and environmental regulations) is allocated by water share rights or binding contracts in many countries. However, warming climate and population growth induce a boost in water demand for irrigation and drinking water (Vörösmarty et al., 2000). Hydropower production is expected to increase owing to its renewable characteristics and its role in balancing intermittent energy production (see section 2.1) (Berga, 2016; François et al., 2014a; Zarfl et al., 2015). Zeng et al. (2017) concluded that over half of the global installed hydropower capacity competes with irrigation while only 8% complements irrigation. Tilmant et al. (2020) also reported that food safety might be much more sensitive to hydroclimatic changes and allocation policies under the irrigation-hydropower tradeoffs. Besides, environmental regulations refer to the minimum flow requirement out of the reservoirs and are also found to compete with hydropower (e.g., Giuliani and Castelletti, 2013) and irrigation (e.g., Grafton et al., 2011) water uses. Moreover, many regions are arguing for increased environmental flows (e.g., Palmer et al., 2008; Poff et al., 2015; Poff and Zimmerman, 2010; Renöfält et al., 2010), which drastically compromises the other water uses.

Temporal tradeoffs among the key functions of multi-purpose reservoirs introduce further complexity in reservoir water management. Lower water availability will stimulate more conservative management policies to store more water for summer irrigation, which requires tradeoffs from other sectors. Besides, climate change and human activities (e.g., deforestation and mining) could yield more frequent flood events and thus increase the sedimentation in reservoirs, which reduces their storage capacity and increases operational costs (e.g., Bangash et al., 2013; Fraga-Santiago et al., 2019; Mendes et al., 2015).

2.2.4 Summary

On the basis of the impact studies of global change from above, the possible changes either climatic or socio-economic will not only be adverse to the performance of water systems but will also be costly to cope with, both economically and socially. Note that global change does not always imply negative influence on water resource planning and management. Global change may create favorable conditions for hydropower generation (e.g., potential increase under climate change, see Minville et al. 2009, 2010; Oni et al. 2012) or agricultural irrigation (e.g., less irrigation pressure under climate change and LULC, see Seung-Hwan et al. 2013). These improvements can not be achieved spontaneously unless actions are made to exploit the potential benefits and to maintain the sustainability of water system.

Furthermore, a comprehensive impact assessment on water systems relies on the precise estimation from both water supply and demand sides. However, water supply studies under climate change dominate in the literature. In addition to climate change, other drivers such as policy changes (e.g., Anghileri et al., 2018; Majone et al., 2016), LULC (e.g., Hecht et al., 2019; Li et al., 2017), and population growth (e.g., Hamlet, 2011; Vörösmarty et al., 2000) are worth considering in impact research. In particular, assessing multi-purpose reservoirs under global change are more challenging due to their inherent tradeoffs. In summary, stationary management and traditional planning based on histori-

cal experience are no longer reliable and valid to deal with future changes (Brown, 2010; Brown et al., 2020; François et al., 2019). Actions are thus needed to adapt or mitigate the impacts of global change.

2.3 Adaptation of reservoir system under global change

Adaptation or mitigation strategies are designed and implemented on the premise of the assessment of global change impacts. Adaptation can be adopted from two sides: water supply and water demand sides, independently or jointly (Bates et al., 2008). The key aspect in the supply side is to increase or maintain the water availability and to reduce the water loss from the reservoir system, such as increasing storage capacity and leakage control (Palmer et al., 2008). Correspondingly, actions on the demand side aim at reducing water use, such as improving irrigation methods and increasing wastewater reuse (Grafton et al., 2018; Ronco et al., 2017). Based on the characteristics of adaptation practices, they can be distinguished into soft measures and hard measures (Sovacool, 2011). Hard measures refer to increasing the capacity of reservoir water systems to satisfy demand (e.g., increasing storage capacity, increasing the number of supply sources such as groundwater wells and/or connection to neighbors systems), which normally corresponds to water planning. It is argued that hard measures are economically expensive, inflexible, and usually constrained by local communities due to the concern for the environment (Maran et al., 2014). In contrast to hard measures, soft measures place particular emphasis on efficient management (e.g., adaptive reservoir operation rules), which is more flexible but requires balancing the tradeoffs among stakeholders. However, the hard measures are reported to be more competent in offsetting the vulnerabilities induced by future changes (e.g., Ehsani et al., 2017). The combined strategy involving hard measures and soft measures is also appreciated in dealing with global change (e.g., Du et al., 2020).

2.3.1 Actions in reservoir planning

Changes in reservoir system infrastructure

Hard measures like changes in reservoir system infrastructure are long-standing strategies to offset the impact of global change. Increasing the total efficiency of hydropower generation by 10% is able to counteract the future water limit conditions and to maintain the future energy security for most regions of the world (Van Vliet et al., 2016b). In addition, converting non-powered dams into pump hydro-storage not only increases the water use efficiency but also provides an opportunity to cooperate with other renewable energy sources (Emmanouil et al., 2021; François et al., 2014a; Gaudard et al., 2013; Liu et al., 2016; Patsialis et al., 2016).

Increasing reservoir storage or constructing new reservoirs is promising in mitigating the future risks where precipitation is prone to increase and/or water demand is expected to increase (e.g., Bertoni et al., 2019; Eum and Simonovic, 2010; Finger et al., 2012; Fletcher et al., 2019; Haguma et al., 2017; Hui et al., 2018; Jeuland and Whittington, 2014; Raje and Mujumdar, 2010). Sufficient reservoir storage in these areas is competent to stock enough water to compensate for the water loss (Ehsani et al., 2017). For example, in the regions dominated by the monsoon climate, increasing storage of reservoirs can maintain (or even improve) the original flood control standard and concurrently store more water for future use (e.g., Raje and Mujumdar, 2010). Note that this case has a very high ratio of annual inflow to reservoir volume and spills occur every year during the rainy season. Notwithstanding some adverse arguments among local communities for the concern of environment (Maran et al., 2014) and the intensive investment (Zarfl et al., 2015), this option is commonly recommended as an efficient adaptation to global change

for these regions in the literature.

Changes in reservoir infrastructure should be made under the full investigation of climate change, LULC, and water demand to avoid maladaptation (IPCC, 2014). In the northeastern Portugal mountainous catchment, a new reservoir was planned and built to cooperate with an existing reservoir to secure agricultural water supply (Carvalho-Santos et al., 2017). The two-reservoir system was designed to better solve the water shortage problem than a single reservoir under current climate conditions. However, the reliability of this solution is projected to decrease under future scenarios due to the small drainage area of this catchment and the expected drying conditions. Another example is located in the upper Aragon river basin and the current project is to enlarge the reservoir volume from 476 hm^3 to 1059 hm^3 (López-Moreno et al., 2014). The water supply including irrigation and environmental targets can thus be maintained. However, the basin is projected to have lower water availability as a result of climate change and forest regeneration. Consequently, the enlargement of the reservoir could be oversized and reservoir storage would rarely reach half of the expected capacity. Thus, the lessons from the two over-designing examples highlight the importance of considering future nonstationarity.

Changes in environmental planning

Poff and Zimmerman (2010) reviewed 165 papers and summarized that flow alteration degraded ecological performance. Environmental regulation flows are thus essential for reservoir downstream biota and their abiotic environment. Research has been promoting a sustainable mitigation planning that is to make environmental regulation flows similar to natural regimes while assuring human water needs and involving small tradeoffs from other water use sectors (e.g., Morán-Tejeda et al., 2012b; Poff et al., 2015; Renöfält et al., 2010). However, improving environmental conditions without large losses from hydropower or irrigation remains challenging. Actions in environmental planning are proposed in the literature and are often context specific. Renöfält et al. (2010) reported that warming climate made electricity demand and hydrological regimes similar in Sweden with more winter flows and lower spring flood, which means less reservoir conservation and restoration efforts to benefit freshwater species and ecosystems. While in dry western United States, watershed restoration planning is encouraged with structural measures (e.g., fish pathways) to mitigate the river flow alterations (Reclamation, 2021). In particular, the method that designs overbank flows to mimic natural flow pulses in major river reaches is proposed to support the spawning of fish species facing extinction and to reduce trade-offs from irrigation (Reclamation, 2021).

2.3.2 Actions in reservoir management

Changes in operation rules

Maximum utilization of water resource has always been a research hotspot. There is a large body of literature regarding mathematical optimization methods that are promising in reservoir water management (see reviews: Dobson et al. 2019; Fayaed et al. 2013; Labadie 2004; Rani and Moreira 2009). Additionally, the scientific community has drawn attention to the optimization methods based on metaheuristic algorithms (e.g., genetic or evolutionary algorithms) to solve complex reservoir water problems and their critical tradeoffs (see reviews: Maier et al. 2014; Nicklow et al. 2010; Reed et al. 2013). These methods are proved powerful in tackling water management under current conditions.

However, all the changes cannot be anticipated in practice and global change is deepening the uncertainty in the management issues.

In general, changing the current operating policies to adapt to the future changes (i.e., adaptive operations) is low-cost and reversible compared with changes in infrastructure. Most studies claimed the necessity of adaptive operations by comparing the original operation rules and the adaptive operation strategies under global change scenarios. Examples are hydropower reservoirs (see Haguma et al. 2015; Jahandideh-Tehrani et al. 2014; Minville et al. 2010), irrigation reservoirs (see Ashofteh et al. 2015, 2013), and multi-purpose reservoirs (see Ahmadi et al. 2014; Giuliani et al. 2016a; Quinn et al. 2017, 2018).

Some studies attempted to derive adaptive operation strategies by testing some changes on the original operation rules based on future changes. Concerning the snow-dominated basins, earlier reservoir refill is commonly proposed to buffer the earlier spring flood and future water shortage under global warming (Hendrickx and Sauquet, 2013; Payne et al., 2004). Besides, flood policy needs to be reconsidered in climate change conditions. Relaxing flood control could be a move to prevent water loss in regions with frequent drought events, such as California (VanRheenen et al., 2004). The incorporation of forecasting information should be accompanied to manage flood risk (Huaringa-Alvarez et al., 2014; Steinschneider and Brown, 2012). Given the intensified competition for water between hydropower and irrigation under global change, one possible solution is to shift the hydro-electricity production from winter (for heating) to summer (for cooling) to align both water use (Pereira-Cardenal et al., 2014). Note that these adaptive strategies should be revised with caution as the managers are conservative in changes (Raje and Mujumdar, 2010). Furthermore, the adaptive operation rules should be adopted with a consideration of environment protection (e.g., Poff et al., 2015; Suen, 2010; Yin et al., 2011).

Changes in conjunctive water use

Reservoir water management should not be limited to a narrow reservoir-scale but extended to a greater sense, such as integrated water resource management (Biswas, 2004). Since reservoir water problems are becoming increasingly interrelated and interlinked (e.g., food, energy, and water nexus, see Perrone and Hornberger 2014), changes in conjunctive water use are needed to adapt to global change. Tilmant et al. (2009) proposed a dynamic water transfer process to reduce water competition among agricultural and hydroelectric sectors by compensating farmers with hydropower benefits. Besides, interbasin water conveyance is a practical manner that can settle the unequal distribution of regional water resource (Liu et al., 2016). Especially in the agricultural sector, water transfer among reservoirs is a useful method to deal with drought events (Nunes et al., 2017). In addition to this, allowing water to move among water users with different water rights can reduce the overall agricultural loss caused by climate change (Vano et al., 2010). As such, water market should play an important role in allocating water resource and managing drought risks in agricultural and urban water users (Loch et al., 2013).

While in the basin scale, groundwater resource plays an important role in complementing irrigation water use. Drying and warming climate would decrease water resource into reservoirs and increase the water demand for irrigation (e.g., Vicuña et al., 2012). As a result, groundwater would be excessively extracted to fulfill the irrigation water deficit and the drop of underground water level would degrade the environment of the basin, such as salinization. Thus, integrated management of reservoir water and groundwater

should be highlighted for increasing the resilience of reservoir water supply in face of a changing climate and more importantly for environment protection. Artificial recharge of groundwater from the reservoir during wet years is a plausible alternative to improve the dynamics of aquifers (Bangash et al., 2013).

All these changes require a more integrated and cooperative manner of water resource management (e.g., Zeff et al., 2016). As supported by Dono et al. (2013), improvements in water use towards a collective way can better succeed in climate change adaptation. Madani (2010) summarized methods in resolving water resource conflict and proposed applying game theory in water resource management. Maran et al. (2014) also suggested that implementing such integrated water resource management should be enhanced with water governance, which requires professional, institutional, and political participation.

Changes in water demand

Given the complexity of socio-economic changes, a comprehensive representation of water demand is rarely considered roundly. However, demand reduction always stands as a "no-regret" strategy (Hallegatte, 2009; Walsh et al., 2016). For example, in the Pacific Northwest, reducing electricity consumption is a necessary and prudent measure for the hydropower system to adapt to climate change (Markoff and Cullen, 2008). Instead of managing to increase the water availability for hydropower or to raise the efficiency of hydropower facilities, measures to reduce consumption, such as water market design and price strategies in the management level (Gaudard and Romerio, 2014), are more prominent in alleviating water stress in such populated regions. Besides, raising public awareness is also critical.

As for the irrigation reservoirs or irrigation-incorporated multi-purpose reservoirs, the key aspect is to guarantee sufficient water supply during dry spells. Possible adaptation actions are changes in practice such as drainage and flood management, modernisation of irrigation infrastructure, crop selection, and changes in crop calendars. Promoting crop types with less water requirement is useful in adapting to climate change (e.g., Okkan and Kirdemir, 2018). However, this option is deficient for regions focusing on a single crop like paddy rice or wheat in eastern Asia and other options are needed (see, Nam et al. 2015; Seung-Hwan et al. 2013). Else, increasing irrigation efficiency by water saving technologies (e.g., dripping or sprinkler irrigation system) is effective to reduce water loss. For instance, in the Sacramento Valley, water savings are sufficient to counterbalance the negative impact of climate change without adapting the current water management (Purkey et al., 2007). Methods in reducing water demand can be combined when one option is not sufficient to adapt to climate change. This was the case for the irrigation reservoir in the Aidoghmoush River basin of northern Iran, for which a decrease in natural inflows together with an increase in irrigation demand are projected (Ashofteh et al., 2015, 2013). Ashofteh et al. (2017) tested three measures on the water demand side to mitigate future water shortage, including delaying planting, deficit irrigation stress strategy, and improving irrigation efficiency. The results showed that the deficit irrigation stress outperformed the other two measures in reducing water use. However, crop yield would decrease, and thus increasing irrigation efficiency is needed to keep the same level of crop productivity. Note that increasing irrigation efficiency does not mean reducing water consumption but water loss and improvements in irrigation technology must be accompanied by a method like water accounting to avoid misunderstanding (Grafton et al., 2018; Lecina et al., 2010).

2.3.3 Adaptation paradigms of reservoir water system

Adaptation of water resource system to climatic and socio-economic changes has become a key spotlight in scientific community (McMillan et al., 2016; Montanari et al., 2013; Wasti et al., 2022). The success of adaptation depends on acknowledging the deep uncertainty stemming from these changes and on a robust assessment that is favorable for the designing of efficient adaptation options (Wilby and Dessai, 2010). "No-regret" strategies that generate benefits regardless of these changes are commonly proposed to bypass the difficulty in dealing with future uncertainty (Hallegatte, 2009). How water system is adapted to global change should be supported in practical cases to share experiences, both negative and positive. As such, we present three case studies to illustrate considerations of adaptation strategies based on the SECURE Water Act project reports (Reclamation, 2016, 2021) and scientific research: Columbia River basin, Colorado River basin, and Sacramento-San Joaquin River basin.

Columbia River Basin

The impact of climate change in the Columbia River basin has been extensively examined (Cohen et al., 2000; Hamlet et al., 2013; Hamlet and Lettenmaier, 1999; Payne et al., 2004; Vano et al., 2015). Winter runoff is increased and earlier as a result of snow melting from warming climate, thus reducing the summer water availability. The multipurpose reservoir system is faced with reduced reliability to meet objectives including flood control, hydropower, fisheries habitat protection, irrigation, and recreation (Cohen et al., 2000; Payne et al., 2004). Under current operation policies, the altered hydrology regime would cause: 1) a decrease in future flood risks; 2) a decrease in hydropower production and revenue; 3) difficulties to achieve fisheries protection goal; 4) a decrease in agricultural water supply reliability; 5) a high impact on sustained storage level in summer for recreation due to the lower resulting storage.

Payne et al. (2004) tested four mitigation operational strategies to reduce exacerbated tradeoffs, including lower flood evacuation with earlier reservoir refill, reallocating winter energy demand, increasing storage for fishes, and a combination of the three mentioned. Each mitigation option can be effective to some extent but tradeoffs still exist between fishery flow targets and hydropower. Generally, the current flood control policy is recommended to be reconsidered to reduce the overall losses in fisheries and hydropower production given the future warmer climate. Population growth in this region is expected to expand, especially in Washington State (US), by a double value in the late 21st century according to the GMA assessments [1]. Thus, energy demand for heating is expected to increase 50% in the late 21st century while the demand for cooling can be doubled in the early 21st century under both warming climate and population growth (Hamlet et al., 2010). The SECURE Water Act project (Reclamation, 2016) is planning to improve the hydroelectric facilities at the Coulee Dam, the Palisades Dam, the Hungry Horse Dam, and the Black Canyon Dam to increase power generation efficiency and delivery. Other energy sources like solar are recommended to satisfy the demand in summer and conjoint management strategies with other regions are also appreciated (Hamlet et al., 2010). Irrigation water demand in the Columbia River basin would increase slightly while the crop mix had a positive response to climate change, which makes the agriculture sector less

[1] GMA: the Washington State Growth Management Act, see http://www.ofm.wa.gov/pop/gma/

vulnerable (Rajagopalan et al., 2018). The rehabilitation efforts such as providing habitat access, increasing fish passage, and enhancing instream flows can mitigate the impact of climate change on fishery protection (Reclamation, 2016, 2021). Hamlet (2011) proposed that the success of adaptation strategies in the Columbia River basin hinged on the collaboration of stakeholders, the efficient communication of water agencies, and the federal participation.

Colorado River basin

The Colorado River basin is one of the over-allocated regions in the world, where twelve major reservoirs are cooperated to meet the objectives of agriculture, municipal water demand, flood control, and hydropower production (Castle et al., 2014; Christensen et al., 2004; Fleck and Udall, 2021). There is a consensus on the reduced water availability in the Colorado River basin with an increase in temperature, an earlier snowmelting, and a probable decrease in precipitation (e.g., Clow, 2010; Dawadi and Ahmad, 2012; McCabe and Wolock, 2007; Vano et al., 2014). The reduced water availability degrades the management of the Colorado water system, leading to hydropower decreases and contract violations (Christensen and Lettenmaier, 2007; Christensen et al., 2004). Besides, the past poor planning of the reservoirs (over-estimated storage requirement) also contributes to the degradation of Colorado reservoir system performance. Water shortage due to frequent drought events stimulates groundwater consumption and groundwater extraction will probably not be balanced by recharge, which further aggravates the over-allocation of water resource in the basin (Castle et al., 2014).

Given the already large storage of Colorado water resource system to annual average flow ratio (four times based on historical data), it is unlikely that changes in operating strategies can sufficiently buffer the influence of climate, nor the changes in reservoir capacity (Christensen and Lettenmaier, 2007; Christensen et al., 2004; Fleck and Udall, 2021). However, Rajagopalan et al. (2009) reported that flexible operation policies could mitigate some of the adverse effects of reduced water resource in the Colorado River basin. While the management of the Colorado River basin is very complicated with a set of agreements and contracts over the last 100 years, the rapid adjustment of policy will not be a simple task (Udall and Overpeck, 2017). Thus, water deliveries can be maintained in a sustainable way when the average supply can be reduced to 0-20% compared with the current state (Barnett and Pierce, 2009). The SECURE Water Act project (Reclamation, 2016) proposed a set of portfolios for agricultural (e.g., irrigation with buried pipes or sprinkler systems to reduce loss, and application of advanced flow meter and automated valves/gates to increase efficiency) and municipal/industrial water conservation (e.g., installation of water meters to monitor usage, wastewater reuse, and construction of recharge basins to maintain groundwater storage). Besides, ocean water desalination, rainwater harvesting, and importation from other river basins (e.g., Missouri River and Columbia River basins) increase the water supply capacity of the Colorado River basin (Reclamation, 2016, 2021). Given the lower water levels of the Hoover Dam and the Lake Mead, some of the existing hydroelectric turbines are replaced with wide-head turbines to increase hydropower efficiency (Reclamation, 2016). Also, the SECURE Water Act project (Reclamation, 2021) actively contributes to enhancing environmental flows of the Colorado River basin, such as the coordination of reservoir operations and the promotion of fish recovery program.

Sacramento-San Joaquin River basin

The Sacramento-San Joaquin river basin consists of two major projects: Central Valley Project and State Water Project. They are aimed at water deliveries, fish/environment conservation, hydropower, and flood control. Numerous studies reported a marked warming effect (Anderson et al., 2007), and a probable increasing trend of precipitation with large inter-annual variability in California (Brekke et al., 2009, 2004; Georgakakos et al., 2012b; VanRheenen et al., 2004). In general, the influence of climate change would result in a seasonal shift of snowing melting, increased winter-spring flood risk, and decreased water availability during summer (Georgakakos et al., 2012b; Pagán et al., 2016; Vicuna et al., 2007). As a result, the performance of the two projects is vulnerable to climate change (Ray et al., 2020). Besides, water competition in the basin will exacerbate the overuse of groundwater due to reduced water supply from the reservoir system (Alam et al., 2019; Mehta et al., 2013).

VanRheenen et al. (2004) examined three adaptation actions including earlier reservoir refill, adaptive flood control curves, and a combination of the two. The simulation results showed that the combination of the two outperformed the other actions while the tradeoffs between hydropower production and fish/environment requirements still exist. To reduce these tradeoffs, increasing reservoir storage and updating hydroelectric infrastructures can be effective (Madani and Lund, 2009; VanRheenen et al., 2004). Tanaka et al. (2006), Groves et al. (2008), Purkey et al. (2007), and Georgakakos et al. (2012a) suggested that integrated regional water management and sustainable groundwater management can be useful to deal with the challenges of warming climate, population growth, and lifestyle changes. The SECURE Water Act project reported that increasing agricultural, municipal, and industrial water use efficiency improves the system performance at minimum cost (Reclamation, 2016). The method of transferring to an improved irrigation technology (e.g., drip and micro-sprinkler) should be accompanied by crop diversification to reduce the agricultural vulnerabilities to climate change (Mehta et al., 2013). New plannings to reduce winter-spring flood risk are also needed, such as constructing flood bypasses and improving levees (Andrew and Sauquet, 2017). To ensure the implementation of these adaptive strategies, government participation to enhance the communication among stakeholders and institutional reform to improve the local authority cooperation are also essential from a political perspective (Andrew and Sauquet, 2017; Hanak and Lund, 2011).

2.4 Challenge of adaptation under global change

How reservoir systems can be adapted to future changes requires not only a far-sighted view of possible changes in water supply and water demand but also a thorough understanding of the socio-hydrology relationship (Di Baldassarre et al., 2018; Kellner, 2021; Sivapalan and Blöschl, 2015). Adapting to global change must reject stationary practice that hinges on historical conditions, and embrace non-stationary planning and management. Given the deep uncertainty, adaptation of reservoir systems to global change is challenging. In general, the process of adaptation to global change involves three basic steps: first, a comprehensive assessment of the system to change; second, adaptive strategies design and adaptation options appraisal in a decision-making framework; third, adaptation implementation. Challenges remain in each step.

2.4.1 Challenges in the assessment approaches

As the basis for developing adaptation strategies, there are two main frameworks to conduct an investigation of global change on water systems: top-down approach (scenario-based) and bottom-up approach (vulnerability-based). Figure 2.2 shows the flow chart of the two approaches.

Top-down approach Initially, IPCC groups project future climate conditions based on climate models through a sequence of consequences under different scenarios of GHG emissions. Following this philosophy to investigate the potential implications of climate change on a specific system (e.g., hydrological, ecological, or socio-economical systems), the projections of impacts are extended through a succession of models that represent the system as presented in Figure 2.2a. This method produces the possible alterations of the system for different future time slices given by scenarios, which can then be compared with historical system conditions. In the case of reservoir systems, the top-down approach is implemented as follows. First, future climate conditions are projected from GCMs with given GHG scenarios as input. Whereas, the coarse estimates, which typically have a spatial resolution of 2 degrees, do not match with the regional or local impact assessment (Tapiador et al., 2020). Second, these outputs from GCMs are downscaled by statistical method, or RCMs (see reviews, Ekström et al. 2015; Wilby and Wigley 1997), and thereafter bias correction. Third, the downscaled climatic variables are propagated through a modelling chain (e.g., hydrological model, a water demand model, and a water system model) that represents the reservoir system. Finally, a "snap-shot" of future time slices of reservoir water management can be derived and then compared to current situations to estimate system performance in the future. Socio-economic features can also be included in this impact assessment procedure.

Bottom-up approach Contrary to the scenario-led top-down approach, the bottom-up approach shifts attention to the vulnerability analysis of an existing system to climatic (and non-climatic) attributes as presented in Figure 2.2b. The bottom-up approach launches by establishing a plausible range (upper and lower bounds) of the driving climate variables to the system, which can be wider than the limits of climate change projections (Guo et al., 2017). This plausible range frames the "exposure space" as described in Culley et al. (2016). Climate change scenarios in the "exposure space" are then generated through the perturbations of historical climate variables either by parametric method (i.e., simple scaling factor, see Prudhomme et al. 2013a,b, 2015; Weiß 2011) or by stochastic method (i.e., weather generator, see Culley et al. 2019; Guo et al. 2017; Steinschneider

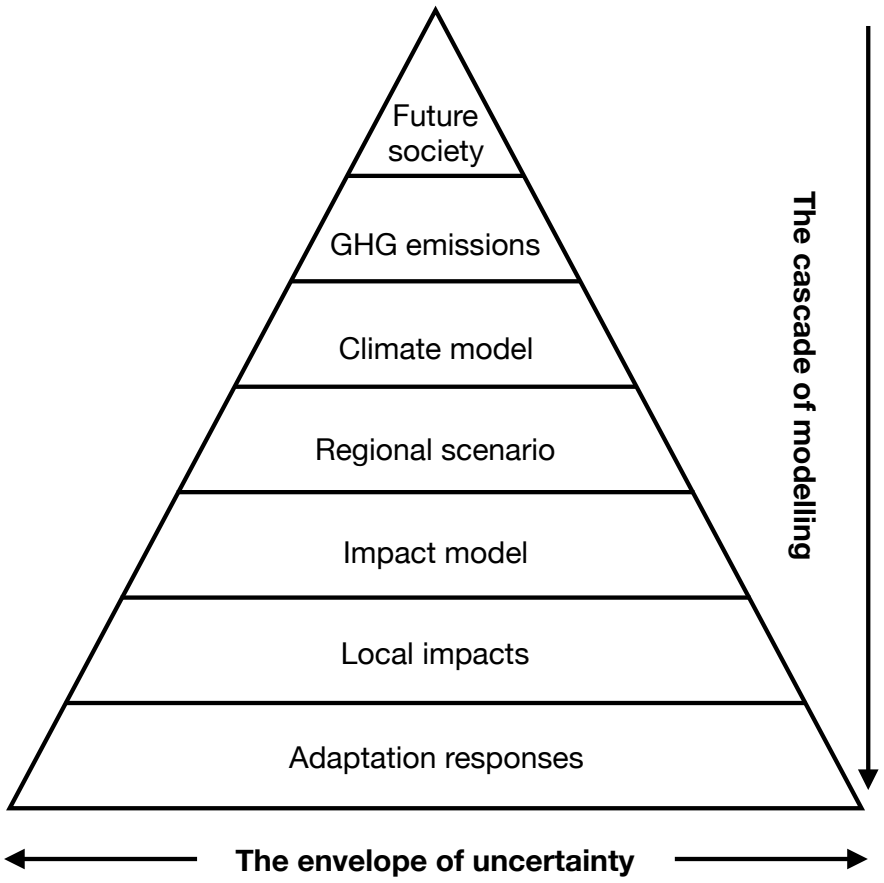

(a)

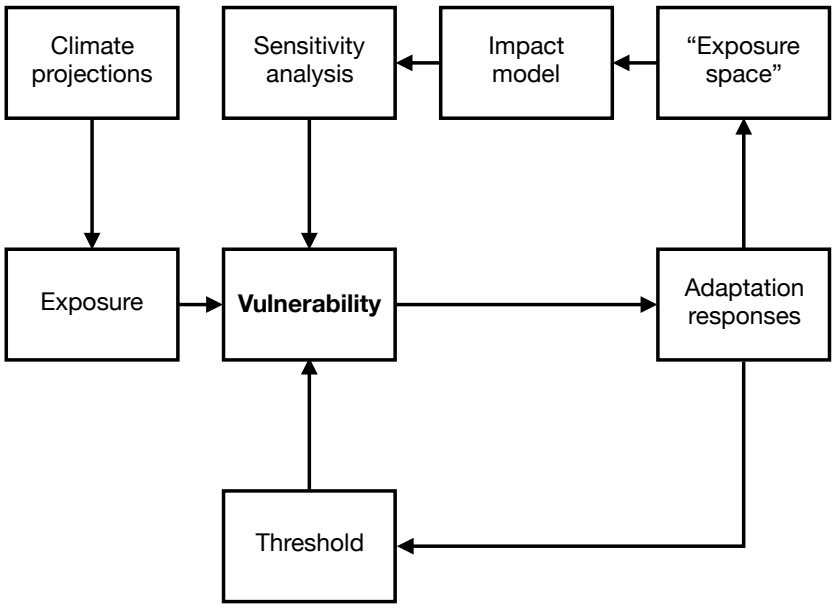

(b)

Figure 2.2 – Adaptation to climate change in the top-down approach (a) and bottom-up approach (b). The figure of top-down approach is modified from the Figure 1 in Wilby and Dessai (2010). The figure of bottom-up approach is based on the "scenario-neutral" concept in Prudhomme et al. (2010).

and Brown 2013; Steinschneider et al. 2019). The succeeding step involves the sensitivity analysis (or stress test) to assess the response of the system's performance indicators to the spectrum of perturbed climate scenarios. Exposure is climate change projections to which the system could be exposed. Threshold is the limit beyond which the system performs unsatisfactorily. As such, potential changes can thus be assessed by the sensitivity and exposure of the system (Prudhomme et al., 2013b). The vulnerability of the system can thus be perceived by comparing the potential changes to the predefined threshold (a summary of thresholds in Sauquet et al. 2019). In practice, the "response surface" tool (see Prudhomme et al. 2010; Sauquet et al. 2019) is employed to illustrate the results of the bottom-up approach.

Among the two frameworks, the top-down approach dominates in the literature while the bottom-up approach has emerged as an alternative to bypass the shortcomings of the top-down assessment (Brown and Wilby, 2012a; Wilby and Dessai, 2010). Table 2.2 summarizes the advantages and the limitations of the top-down and the bottom-up approaches for the development of adaptation strategies. The bottom-up approach is flexible in that the "exposure space" is not constrained to climatic variables (e.g., hydrological variables such as mean flow in Poff et al. 2015 and glacier coverage in Puspitarini et al. 2020; socio-economic variables such as water demand/supply in Foti et al. 2014, LULC changes in see Singh et al. 2014, and financial issues in Ray et al. 2018).

Table 2.2 – Advantages and limitations of the top-down and bottom-up approaches for adaptation development

	Advantages	**Limitations**
Top-down	An entire timeline of climate change with respect to history (Köplin et al., 2012)	A cascade of uncertainty propagating through the modelling chain (Figure 2.2a)
	Identification and quantification of sources of uncertainty in models (Vidal et al., 2016)	A lower bound of the full range of uncertainty (Hallegatte, 2009; Stainforth et al., 2007)
		Not favorable for decision-making (Prudhomme et al., 2013a)
Bottom-up	Flexible and versatile structure (Prudhomme et al., 2010)	Lacking generalized tools to produce non-stationary climate variables (Steinschneider and Brown, 2013; Vormoor et al., 2017)
	A consideration of extreme events in the sensitivity analysis (Broderick et al., 2019)	Challenges in defining the system thredhold (Sauquet et al., 2019)
	Easier identification of system vulnerability under changes to refine management (Ghile et al., 2013; Guo et al., 2017)	

However, when it comes to water planning and management under global change, managers seek the risk-relevant explanation of future situations (Lempert et al., 2004). The determination of risk in water planning and management involves two aspects that are the occurrence probability of an adverse event and its associated consequences (Jones,

2001). Even though attempts have been made in the top-down approach with ensemble-based projections to quantify uncertainty (e.g., Harris et al., 2010; Konzmann et al., 2013; Terray and Boé, 2013a; Vidal et al., 2016; Wada et al., 2013), the realistic (or "true" as described in Brown et al. 2012) range of uncertainty of climate change implications is unknown (Stainforth et al., 2007). Rather than a manner of prediction, approaches have been proposed to first concentrate on understanding the vulnerability of the system to changes by placing the top-down projections at a later stage to inform risks, instead of driving risks (e.g., Brown et al., 2012; Brown and Wilby, 2012a; Jones, 2001; Lempert et al., 2006; Prudhomme et al., 2015, 2010; Sauquet et al., 2019). Through probabilistic projections of hazards (e.g., Brekke et al., 2009), termed as relative or subjective probability (Brown et al., 2012), the bottom-up and top-down approaches are linked.

The combined approach that integrates the results from the top-down and bottom-up approaches provides complementary insights into the system under changes. This approach takes a step forward in supporting adaptation planning and management decisions by closely connecting scientists, water managers, and stakeholders (Conway et al., 2019; Mastrandrea et al., 2010). The results of this combined approach can be immediately updated to inform risks when new projection information is available, which is cost-efficient (Prudhomme et al., 2010). However, the generated probability information is relative (or subjective), which should be explained with caution to avoid the pitfalls that managers take the relative probability as the true occurrence of future events (Brown et al., 2012; Lempert et al., 2004). A critical challenge remains in defining system performance metrics and associated thresholds, which requires deep cooperation with managers and stakeholders (Sauquet et al., 2019). Besides, the generation of plausible and realistic climate scenarios requires the effort of the scientific community (e.g., Culley et al., 2019; Guo et al., 2018; Whateley et al., 2016).

2.4.2 Challenges in the design and appraisal of adaptation

Impact assessment under global change is essential to provide reliable and robust information for the design of adaptation options. Section 4.1 illustrated that the bottom-up approach is highlighted to bring necessary information to support adaptation (Conway et al., 2019). Table 2.3 lists the selected studies that applied the bottom-up approach on reservoir water systems for the design of adaptation strategies.

Concerning the design of adaptation, the "predict-then-act" framework (i.e., top-down framework in Figure 2.2a) is significantly deficient in dealing with projection uncertainty (Lempert et al., 2004, 2006). Some explored the potential for narrowing projection uncertainty (e.g., Hawkins and Sutton, 2009, 2010). An alternative is the bottom-up approach by understanding how the system responds to plausible changes and minimizing "regret". As such, practical adaptation options can thus be made to reduce vulnerability. For example, Schlef et al. (2018) demonstrated that a water supply system in the southeastern United States was more sensitive to changes in precipitation than temperature. This implies that the design of adaptation should be capable of withstanding precipitation changes and that reducing the uncertainty of future precipitation projection should be attached more importance to better inform risks. However, most studies are limited in testing climatic stresses (i.e., changes in precipitation and temperature from Table 2.3). Socio-economic stress variables, such as water demand, land use change, and population growth, and ecological requirements (e.g., environmental regulation flow) should be further investigated to refine the adaptation design.

Table 2.3 – Examples of studies that applied the bottom-up approach on reservoir water system

Reference	Reservoir system	Perturbation	Driving variables	Performance metrics	Climate projections	Vulnerabilities and adaptations
Vicuña et al. (2012)	Agricultural reservoir system of the Limari Basin (Chile)	Parametric	T and P	Irrigation supply and demand	Exposure	Propositions of adding reservoir storage and enhancing management are made to mitigate climate change
Whateley et al. (2014)	Water supply reservoir of the Westfield Basin (USA)	Stochastic	T and P	Supply reliability	Risk information	Optimal operations compensate for a 10% of precipitation loss
Turner et al. (2014)	Water supply reservoir of Melbourne (Australia)	Stochastic	T and P	System yield	Risk information	Increasing system capacity and reducing demand are promising to increase water supply robustness
Poff et al. (2015)	The Coralville Dam on the Iowa River (USA)	Stochastic	Deviation of mean flow and P variability	Annual cost, inundation area, and flow recession rate	Risk information	Re-operation and raising levees are favorable to reduce risks of climate change
Steinschneider et al. (2015)	The Belton Lake (USA)	Stochastic	P and water demand	Robustness index	Risk information	Increasing conservation pool is proposed to adapt to changes
Culley et al. (2016)	Lake Como system (Italy)	Parametric	T and P	Operational failure	Exposure	Flexible management policies are proposed to reduce the vulnerability to climate change
Taner et al. (2017)	Hydropower of north Rumphi River and south Rukuru River (Malawi)	Stochastic	T and P	Levelized cost of energy	Risk information	The system is sensitive to climate change; No adaptions recommended

(To be continued)

Reference	Reservoir system	Perturbation	Driving variables	Performance metrics	Climate projections	Vulnerabilities and adaptations
Ray et al. (2018)	Hydropower on the Arun River (Nepal)	Stochastic	T, P, and financial variables	Net present value	Risk information	Climate change is not critical future uncertainty; No adaptation recommended
Schlef et al. (2018)	Water supply system in the southeastern of USA	Stochastic	T and P	Reliability, vulnerability, and effective life metrics	Risk information	The system is more sensitive to precipitation than temperature; Water reuse and leakage control are proposed
Kim et al. (2019)	The Yangak reservoir (South Korea)	Stochastic	T and P	Water scarcity index	Exposure	Increasing storage capacity makes the reservoir sensitive to climatic stresses
Nazemi et al. (2020)	Water supply system of the Saskatchewan river Basin (Canada)	Stochastic	T and streamflow	Net benefit, surface water coverage, and water supply	NA	Water supply is sensitive to annual inflow; No adaptations recommended
Ray et al. (2020)	Central Valley water system in California (USA)	Parametric	T and P	Water system's storage, outflow, and deliveries	Risk information	The system is more vulnerable in dry years; No adaptations recommended

Note: T and P stand for temperature and precipitation, respectively.

Section 3.1 presents possible actions that can be implemented for reservoir water systems to mitigate and adapt to global change. The consequent questions for water resource managers are how to choose efficient adaptation measures and to what extent these measures should be planned. In addition to traditional "cost-benefit" analysis, frameworks such as "Info-gap" (e.g., Hipel and Ben-Haim, 1999), "Robust Decision Making (RDM)" (e.g., Lempert et al., 2004) (including advanced RDM frameworks, such as Many-Objective RDM, see Kasprzyk et al. 2013, and Hadjimichael et al. 2020 for a dedicated tool), "Decision Scaling" (e.g., Brown et al., 2012), and "Borg Multiobjective Evolutionary Algorithm (MOEA)" (e.g., Hadka and Reed, 2013) are proposed to improve decision-making under uncertainty. In particular, the "Many-Objective RDM" and "Borg MOEA" frameworks are powerful tools to deal with the tradeoffs in reservoir water planning and management (e.g., Giuliani et al., 2016b, 2014; Herman et al., 2014). Walker et al. (2013) further suggested that adaptation decisions could be implemented in a dynamic process by monitoring vulnerability changes and updating adaptation actions when these monitored changes reach the predefined trigger points. To this end, the framework "Dynamic Adaptive Policy Pathways" is proposed by Haasnoot et al. (2013) to guide the implementation of future adaptation actions. Several studies (e.g., Dias et al., 2020; Kingsborough et al., 2016; Zandvoort et al., 2017) applied this framework to water system adaptation under global change. Efficient adaptation strategies hinge on connecting short-term actions with long-term planning in a dynamic way (Walker et al., 2013). However, the functioning of this dynamic adaptation approach could be challenged by intensive monitoring demand (Metzger et al., 2021).

Adaptation metrics has become a central issue in the appraisal of adaptation options. Traditionally, RRV (Reliability, Resilience, and Vulnerability) metrics are used to evaluate the performance of water systems in terms of the frequency, duration, and severity of their failure (Hashimoto et al., 1982b). For instance, Haro-Monteagudo et al. (2020) applied RRV metrics to evaluate the performance of the irrigation system in northern Spain under climate change. Further, the concept of "robustness" was proposed in the literature to guide how to decide in the decision-making framework under deep uncertainty (e.g., Hashimoto et al., 1982a; Maier et al., 2016; Wilby and Dessai, 2010) and there are multiple definitions for robustness metrics (see review Herman et al. 2015). An informed robustness definition, such as climate-informed robustness index, is supportive in making decisions under the deep uncertainty of climate change (Whateley et al., 2014). Generally, robustness is stated when a system performs acceptably to a broad range of plausible futures (Metzger et al., 2021). However, different definitions of robustness metrics could lead to different decision-making consequences (Giuliani and Castelletti, 2016). Herman et al. (2015) also suggested a multivariate mechanism of robustness metrics that is useful for stakeholders to explore potential decision consequences and to capture their interest. In brief, a careful formulation of robustness metrics prevents from maladaptation to global change (Ekström et al., 2018).

2.4.3 Challenges in the participation of stakeholders and managers

Robust adaptation to global change requires active engagements of scientists, stakeholders, and managers not only in the adaptation designing but also in the practical implementation. The adaptation implementation could be impeded by conflicting interests among stakeholders. A particular example is the long-lasting debate on whether to construct reservoirs to mitigate water crisis (e.g., Ansar et al., 2014; Berga, 2016; Poff et al., 2015;

Zarfl et al., 2015). In addition, how to motivate water managers to positively participate in adapting to global change is rather challenging. Firstly, changing their attitude from stationary-based practice to uncertainty-based management is difficult (Bates et al., 2008). Secondly, managers are conservative in changes for fear of the losses or the risks brought by changing (see the case described in Raje and Mujumdar 2010). Thirdly, reservoir managers are reluctant to share data, making it problematic to model reservoir systems for impact assessment (Schaefli, 2015).

Efficient communication is thus crucial due to gaps in knowledge and professional backgrounds. A "common language" mechanism should be established to bridge these gaps (Viviroli et al., 2011), which necessitates the deeper comprehension of the coupled hydrology-society system (Ceola et al., 2016; Montanari et al., 2013). Multidisciplinary scientific cooperation and integration between research and management promote provoking and innovative perspectives for decision-makers (Ceola et al., 2016). For example, the expertise of economists supports the appropriate decision or policy in adaptation selection and implementation (Hallegatte, 2009). Although proactive adaptation is more advantageous to reduce long-term global change risk than reactive adaptation (see the example in Palmer et al. 2008), the uncertainty regarding the future, the inflexible institution that increases decision-making time, economic constraints, and other barriers hamper decision-makers to generate adaptive programs in time. Enhancing institutional capacity and governance could be essential (Amundsen et al., 2010; Metzger et al., 2021).

2.5 Conclusion

The previous sections have argued that global change is altering the performance of reservoir water systems and that adaptation strategies are necessary to reduce the associated risks. It is broadly accepted that deep uncertainty on future changes not only climatic but also socio-economic renders the adaptation challenging. The International Association of Hydrological Sciences (IAHS) stated a flexible and resilience assessment framework is fundamental to appraise the future risks and design adaptive measures from the perspective of general water resource system (Ceola et al., 2016). Reservoirs, as major components in water systems, are worth discussing in detail to contribute to the adaptation of the whole water systems. Therefore, this review contributes to firstly explore the potential implication of global change on hydropower, agricultural, and multi-purpose reservoirs, secondly summarize the plausible adaptation strategies dedicated to reservoir systems with three cases, and thirdly analyze the challenges in adaptation procedures.

Given the global change impact on reservoir water management, the risks raise with the spatial and temporal changes in water availability, alteration of demand pattern, and the tradeoffs among reservoir functions. At the global scale, an agreement is found in the literature that water inflows are likely to increase in high-latitude reservoirs (e.g., Canada), and to decrease in mid-latitude reservoirs (e.g., Mediterranean region). Regional and local heterogeneity require refined evaluation on reservoir system cases (e.g., the transition characteristics of the Alps). On the other hand, socio-economic changes such as population growth, land use change, and policies introduce endogenous uncertainty in the assessment, which is seldom addressed in the literature. Going forward, integration of the socio-economic drivers is thus essential in thoroughly examining the impact of global change on reservoir water planning and management by coupling human-natural systems (Kellner, 2021).

In general, adaptation of large hydropower reservoirs can be realized through increasing hydropower production efficiency and integrated management programs (e.g., Van Vliet et al., 2016a,b). Adaptively changing the current operating policies is the most cost-efficient way for a medium or small-size hydropower reservoir system. As for reservoirs involved with irrigation purpose, the key aspect is secure water supply during the water shortage period. The adaptation strategies should be made from two sides: increasing water supply ability (e.g., building new infrastructure, reasonable use of underground water) and decreasing water consumption (e.g., water right strategy, crops with less water demand). Given the inherent tradeoffs of multi-purpose reservoirs, the possible ways to alleviate water competition from a management perspective are aligning several water uses (e.g., hydropower and irrigation), compromising flood standards for some drying areas, and integrated water resource management. However, Di Baldassarre et al. (2018) argued that enhancing water supply by building reservoirs could increase the dependency on reservoirs and thus in turn increase the vulnerability when severe drought events occurs. The characteristics of reservoir systems (e.g., storage capacity and operating policy) might delay the timely observation of management problems (Garcia et al., 2020). Efficient monitoring and feedback mechanisms are thus essential after adaptation (Metzger et al., 2021).

In all, robust adaptation hinges on the accuracy and reliability of impact evaluation on future changes. The scenario-led approach dominates in the literature in outlining adaptive measures to global change. Despite the benefits in framing the storyline of future changes and in quantifying uncertainty sources in modelling chain, this approach

is flawed in making decisions in the context of adaptation. Flexible vulnerability-based approach is in favor of designing robust adaptation strategies to improve reservoir water planning and management under global change. Finally, unless scientists, reservoir managers, and stakeholders are actively engaged in participation and communication, the success of adapting reservoir water systems to global change will not be attained.

3 Materials

This chapter presents the study case, the Neste water system, and its current management modes, as well as the dataset used in the following work.

Contents

3.1 General conditions of the Neste water system 44

3.1.1 Topography and climatology 44

3.1.2 Water infrastructures in the Neste water system 46

3.1.3 Water management in the Neste water system: the Aure Valley . 48

3.1.4 Water management in the Neste water system: the Neste Canal and the Gascogne region 55

3.2 Data collection 59

3.2.1 Climatic drivers 59

3.2.2 Naturalized inflow 63

3.2.3 Water management records of SHEM 71

3.2.4 Water management records of CACG 74

3.2.5 Population projections 78

3.3 Summary 80

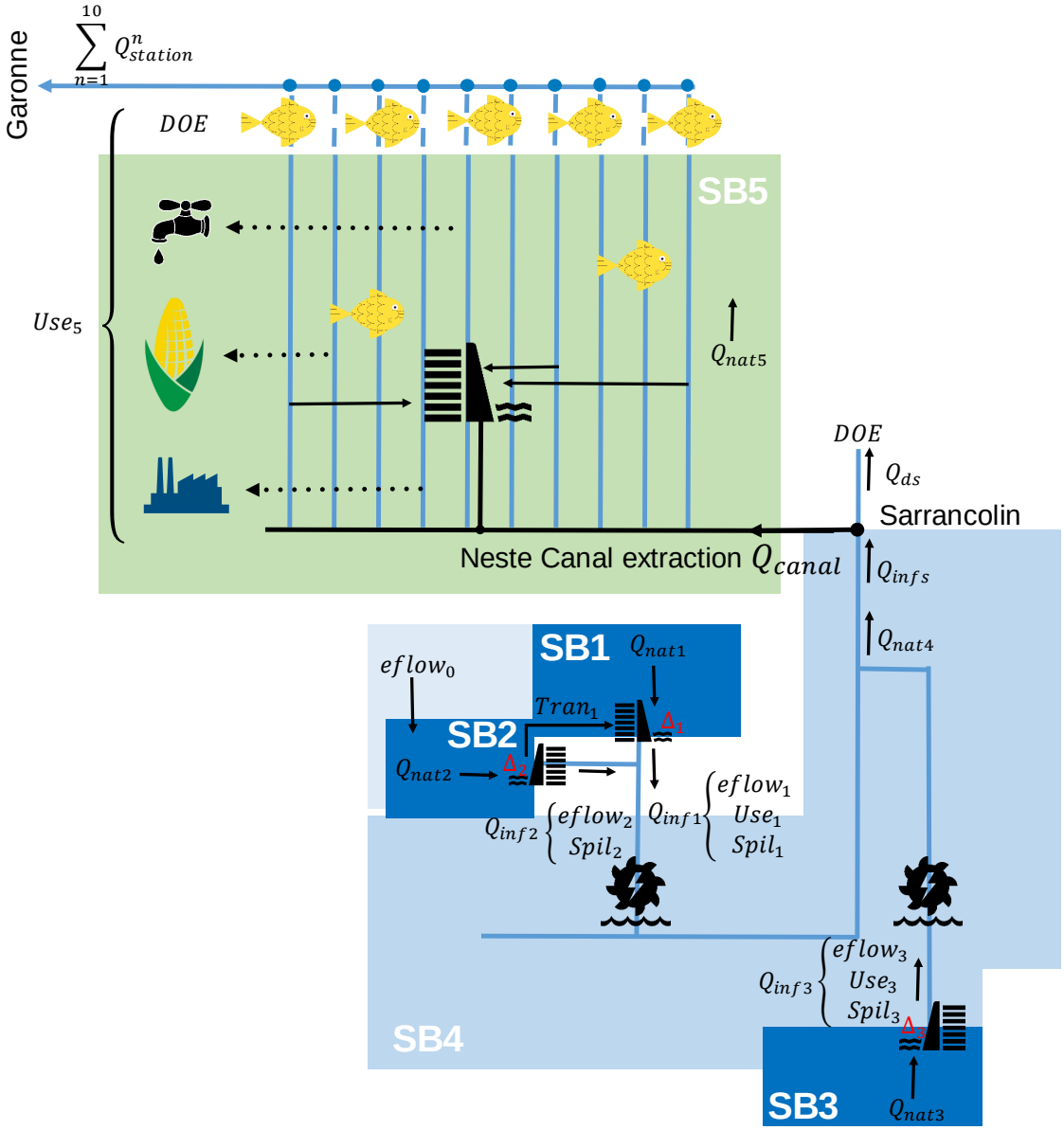

Figure 3.1 – A simplified schema of the Neste water system and the associated abbreviations used in this chapter.

3.1 General conditions of the Neste water system

3.1.1 Topography and climatology

The Pyrenees is an east-west mountain range as the border between Andorra, France, and Spain, providing important water resources for local regions. This work targets the Neste water system in the French Pyrenees and Figure 3.2 shows the location of the system. The Neste water system is divided into two parts: the upstream Aure Valley and the downstream Gascogne region. Figure 3.3 details the topographic and hypsometric overview for the upstream Aure Valley and the downstream Gascogne region.

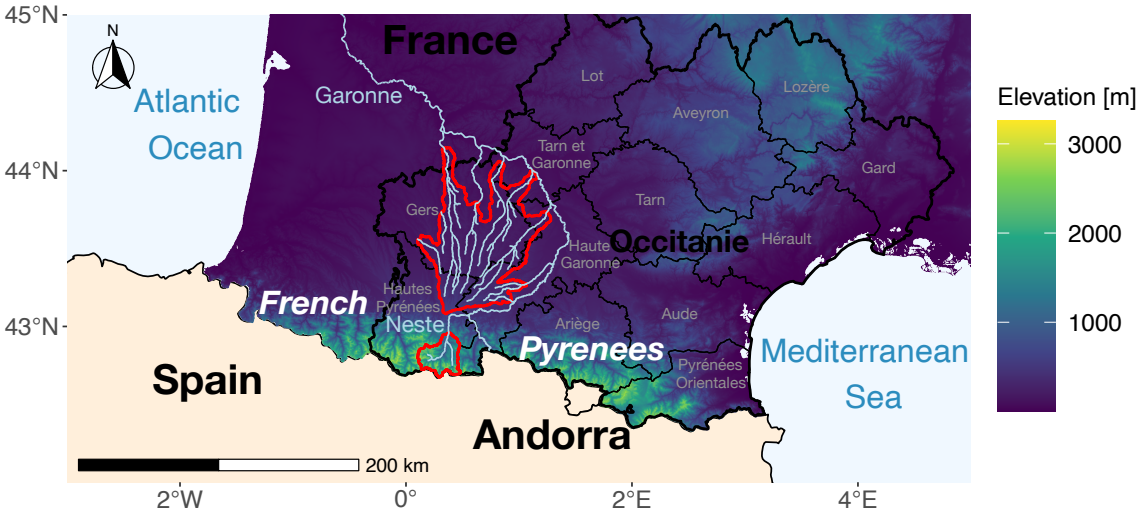

Figure 3.2 – The location of the Neste water system as marked in red polygons.

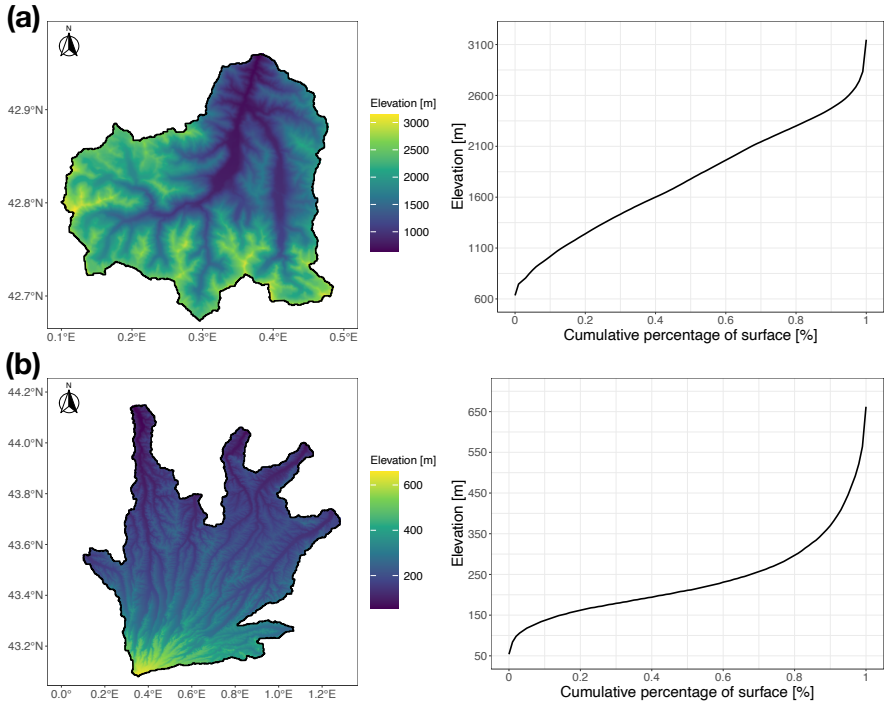

Figure 3.3 – The topographic map and the hypsometry curve for the Aure Valley (a) and the Gascogne region (b).

The Aure Valley is located in the Hautes-Pyrénées department of the Occitanie administrative region of France. It is characterized as a typical mountainous area with the summit of 3147 m. The Aure Valley forms the westernmost part of the Garonne Basin and contributes to the Garonne River through the Neste River.

The Gascogne region, located in the western Occitanie, includes the majority of the Gers administrative department as well as portions of the surrounding departments. Besides, it is also located in the Lannemezan plateau area downstream the central Pyrenees, a large fluvio-glacial alluvial cone, with around 80% of plain land. The Gascogne region was built by the Neste River during the ancient Quaternary after which the course of this river was diverted to the east during the Quaternary (Icole, 1969; Patin, 1967). The rivers in the Gascogne region contributes to the middle of the Garonne River.

Figure 3.4 shows the monthly regime of precipitation and temperature for the Aure Valley and the Gascogne region, respectively. The climate of the Neste water system is characterized by wet and cold winter, and dry and hot summer.

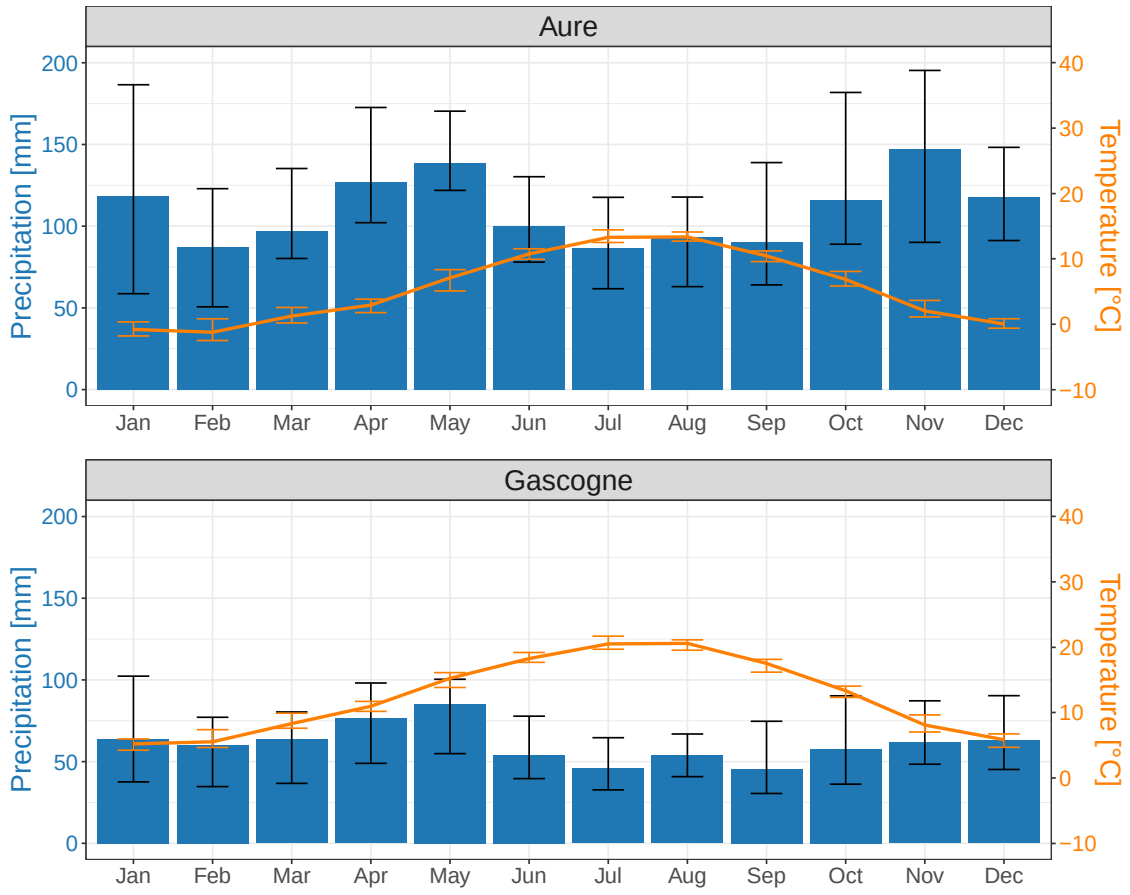

Figure 3.4 – The monthly median precipitation and temperature for the Aure Valley and the Gascogne region during the period from 1979-09-01 to 2014-08-31. The error bars are defined by 25% and 75% quantiles with black for precipitation and orange for temperature. These values are calculated based on the Safran-PIRAGUA reanalysis data.

The climate in the Pyrenees is influenced by the Atlantic Ocean in the west and the Mediterranean Sea in the east whose effects are demonstrated into temperate marine climate (mild summer and cool winter; high annual precipitation) and Mediterranean-style climate (hot and dry summer; mild and wet winter), respectively. As a central valley of

the Pyrenees, the Aure Valley has more relatively drought events than the western part, with a moderate rainfall. The influence of westerly winds, which carry moist air from the Atlantic Ocean, is less effective here due to the block of the Arbizon massif (Ingrand, 1961). The mean annual precipitation in the Aure Valley is 1438 mm calculated from the Safran-PIRAGUA reanalysis (Quintana-Seguí et al., 2016, 2017; Vidal et al., 2010) and most water resource is stored as snow during winter period. In addition, southern heat penetrates through the border ridge, affecting the upper valley particularly, and snow melt dominates the spring flows.

Concerning the climate in the Gascogne region, its geographical position determines the confluence of air masses coming down from the Pyrenees and those coming from the Atlantic Ocean and, to a lesser extent, Mediterranean influences. The mean annual precipitation in the Gascogne region is 786 mm calculated from the Safran-PIRAGUA reanalysis, which is less efficient than that of the Aure Valley. Besides, the mean daily temperature in the Gascogne region is 12.5 °C, which is higher than that of the Aure Valley 5.5 °C, due to the higher elevation of the Gascogne region.

3.1.2 Water infrastructures in the Neste water system

The Gascogne region, crossed by fan-shaped valleys, presents an important rural area with a very wide diversity of landscapes and soil types, which is advantageous for agriculture development (Icole, 1969). The economy in the area of the Neste water system is based mainly on agriculture, poultry and livestock. Taking the Gers department as an example, the agricultural sector represented 12.1% of employment in 2014, three times more than that of the Occitanie administrative region (Insee, 2014).

Concerning the crop cultivation, maize, wheat, rapeseed, soybean, and sunflower are the main crops in the Gascogne region. Besides, the crops, mostly maize and soybean, are irrigated through travelling gun sprinklers (Maton et al., 2005). Particularly, maize cultivation in the Gers department accounts for around 73% of total irrigated area surface and 77% of total irrigated water volume from 2000 to 2005 (Teyssier, 2006). As such, maize cultivation in the Gascogne region is an important source of animal feed and starch industries for local uses and France (Caubel et al., 2018; Leenhardt et al., 2004a).

The agriculture-based economy structure of the Gascogne region determines its high water consumption characteristics. However, water resources in the Gascogne region is naturally inadequate compared with water demand patterns, especially in summer when agriculture water demand is high and precipitation is low. Besides, as mentioned before, the Neste River diverts towards east without contributing to the northern Gascogne region (see Figure 3.2). Therefore, the Gascogne region is separated from the Pyrenees and does not benefit from Pyrenean snowmelt (Leenhardt et al., 2004a,b).

In order to compensate for this inadequacy of natural water resource in the Gascogne region, the water distribution system that depends on the Neste Canal was constructed from 1848 to 1862 to artificially divert abundant water resource from the Neste River and upstream reservoirs into downstream rivers and reservoirs in the Gascogne region. Figure 3.5 illustrates the Neste water system that includes the reservoirs in the upstream Aure Valley, the Neste Canal, and the reservoirs in the downstream Gascogne region. The Neste Canal, 28.6 km long, transfers water with a maximum capacity of 14 m^3/s from the Neste River at Sarrancolin. It then distributes it to 17 downstream rivers (e.g., Bouès, Baïs, Baïsole, Gers, Gimone, Save, Louge) via a network of 90 km of channels. Besides, reservoirs in the Neste water system store and redistribute water resource to ensure

the necessary water demand throughout the year (hydropower production, agricultural irrigation, environmental support, drinking water supply, and industrial uses). Table 3.1 summarizes the general information of the 15 major reservoirs in the Neste water system.

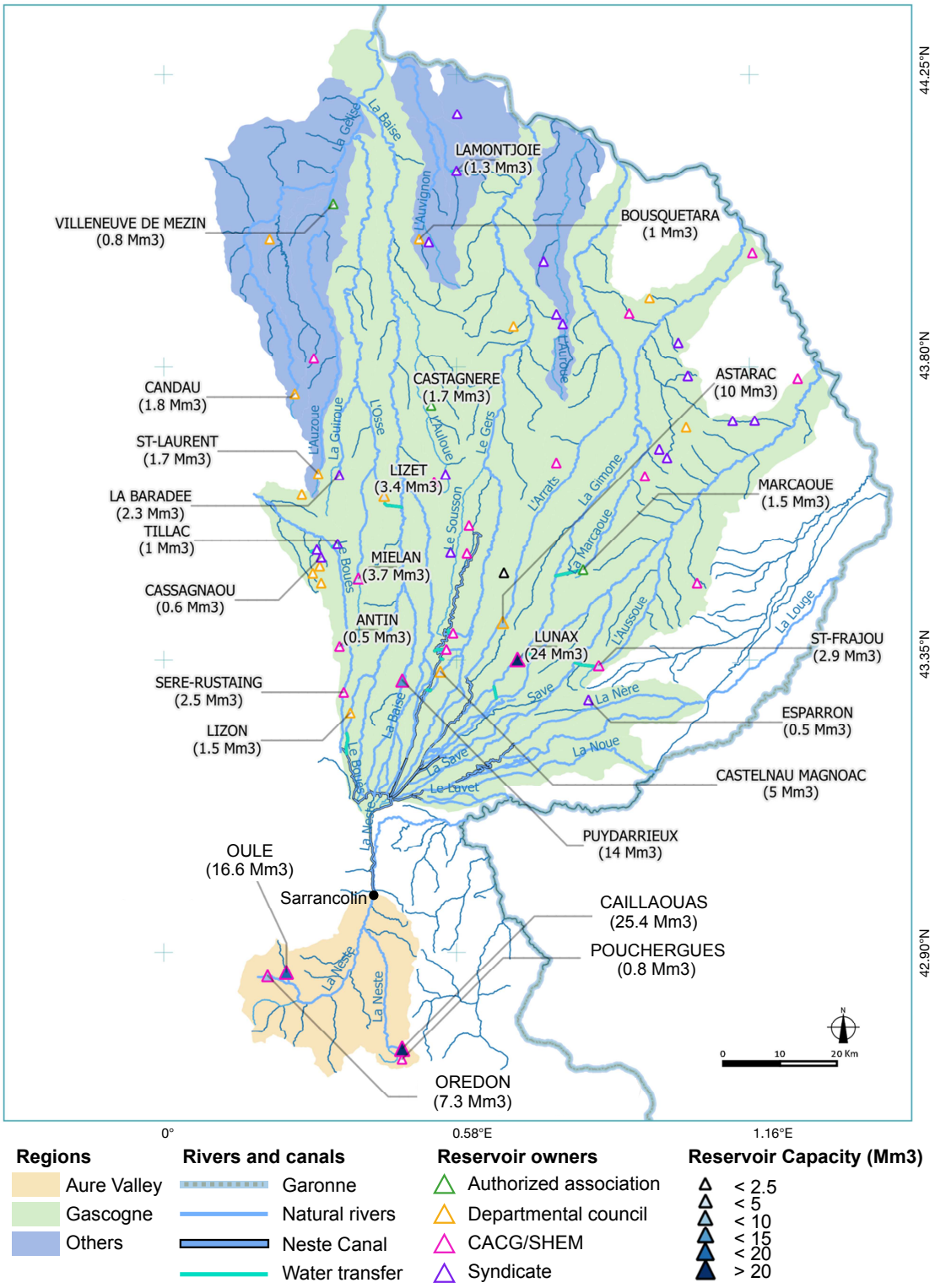

Figure 3.5 – The overview of the Neste water system: the reservoirs in the upstream Aure Valley, the Neste Canal, and the reservoirs in the downstream Gascogne region. Modified from CACG (2019).

Table 3.1 – Main characteristics of the 19 major reservoirs in the Neste water system

Name	**River**	**Owner**	**Department**	**Max volume [Mm^3]**
The Aure Valley				50.1
Oule	Neste	SHEM	65	16.6
Orédon	Neste	SHEM	65	7.27
Caillaouas	Neste	SHEM	65	25.4
Pouchergues	Neste	SHEM	65	0.83
The Gascogne region				73.3
Antin	Bouès	CACG	65	0.47
Astarac	Arrats	Department council	32	10.0
Baradée	Guiroue	Syndicate	32	2.30
Cassagnaou	Bouès	Syndicate	32	0.60
Esparron	Nère	Syndicate	31	0.50
Gimone	Gimone	CACG	31 & 32	24.0
Lizet	Osse	Department council	32	3.40
Lizon	Baïse	Department council	65	1.45
Magnoac	Gers	Department council	65	4.95
Miélan	Osse	CACG	32	3.72
Puydarrieux	Baïsole	CACG	65	14.0
Sère Rustaing	Bouès	CACG	65	2.50
Tillac	Bouès	Syndicate	32	1.00
Saint-Frajou	Aussoue	CACG	31	2.93
Marcaoué	Marcaoué	Authorized association	32	1.50

Note: the department codes 31, 32, and 65 correspond to Haute Garonne, Gers, and Hautes Pyrénées, respectively. The source is from CACG (2019).

In summary, the water infrastructures of the Neste water system have a pivotal role in managing water resources of the Aure Valley and the Gascogne region. They are managed in a coordinated manner to address the issue of water scarcity and water conflicts related to multipurpose uses of the study area. The current water management for the Aure Valley and the Gascogne region is presented in the next sub-sections.

3.1.3 Water management in the Neste water system: the Aure Valley

Despite the slight insufficiency of precipitation to the western part of the Pyrenees, the abrupt topography of the Aure Valley (see Figure 3.3) compensates for this shortage and

allows the intensive exploitation of hydropower (Ingrand, 1961). Figure 3.6 shows the location of reservoirs (Oule, Orédon, Caillaouas, and Pouchergues) in the Aure Valley, including the four corresponding sub-basins located in Figure 3.1: the sub-basins (SB1-3) upstream the reservoirs and the intermediate catchment (SB4) between the outlets of the reservoirs and Sarrancolin.

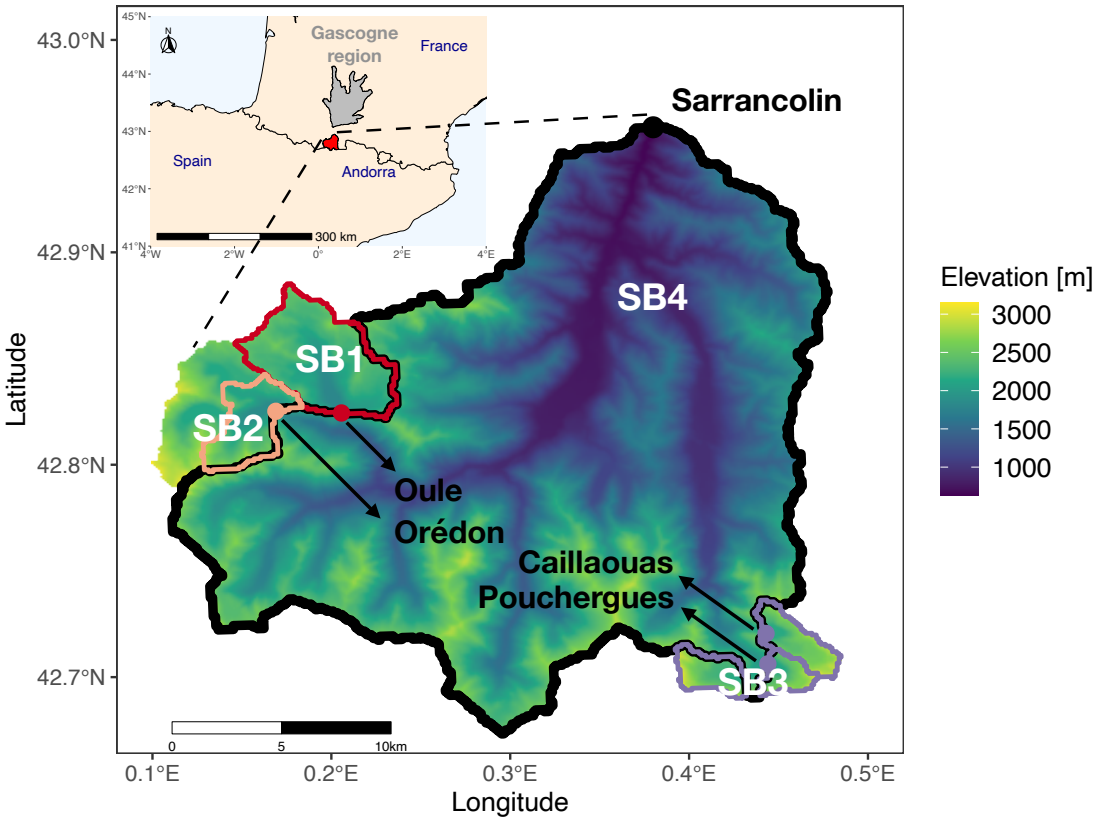

Figure 3.6 – The drainage area of the Oule, Orédon, Caillaouas, and Pouchergues reservoirs.

Figure 3.7 illustrates the sketch of the water system dedicated to hydropower production in the Aure Valley. Two main hydroelectricity producers in the valley are the SHEM company that manages the several reservoirs (in orange in Figure 3.7) of the valley and EDF[1] that manages the westernmost part of the valley (including the Cap de Long, Aubert, and Aumar reservoirs in Figure 3.7). Natural water flow to the Aure Valley is partly diverted: the westernmost part is transferred outside the Aure Valley (into the western neighbour Gavarnie Valley for the Pragnères hydropower plant[2]) and is thus not considered in this study.

Water in the Oule and Orédon reservoirs generates hydropower in the Eget plant while water in Caillaouas and Pouchergues reservoirs generates hydropower through a cascade of plants, the Louron system. The two hydropower groups are presented individually as follows.

[1] Electricité de France (www.edf.fr) is a French electric utility company

[2] https://www.edf.fr/sites/default/files/Hydraulique/Sud-Ouest/documents/plaquette_edf_hydro_pragneres_2018.pdf

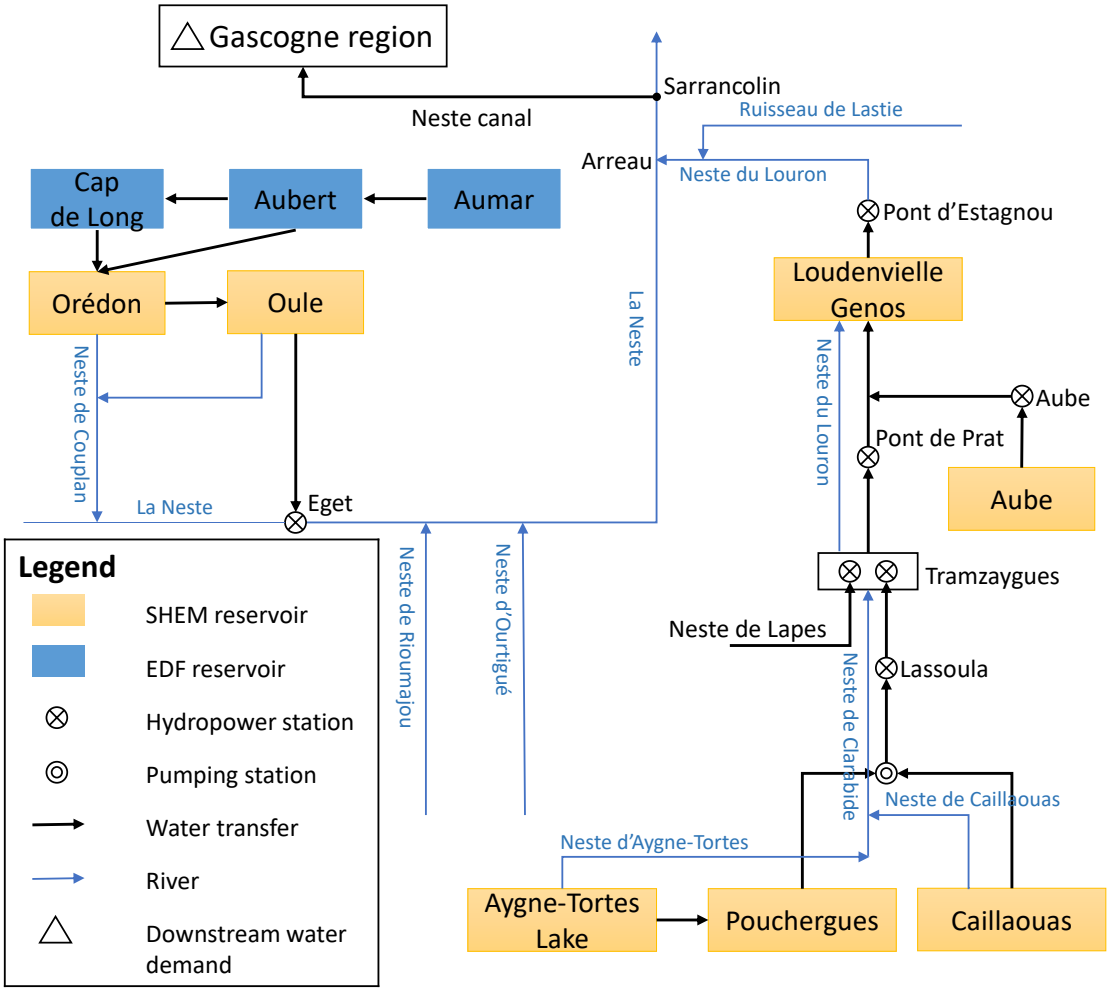

Figure 3.7 – The water management system for hydropower production in the Aure Valley.

Eget hydropower group The Oule reservoir is located at the outlet of SB1 with an altitude of 1800 m. Its normal pool level is 1816.5 m and the minimum pool level is 1777.0 m. It receives, in addition to the water volume of SB1, the water transfer from the Orédon reservoir via an underground pressure pipeline. This Orédon reservoir stores water from SB2, and also environmental flows from upstream reservoirs, Cap de Long and Aubert. Besides, the normal pool level of the Orédon reservoir is 1849.4 m and minimum pool level 1825.0 m. Water stored in the Oule reservoir will be forced to the hydropower plant with a water fall of 728 m, and then be dropped into the riverway.

Louron hydropower group The two main reservoirs, the Caillaouas and Pouchergues, compose the Louron hydropower group. The Caillaouas reservoir, located at the foot of the glacier Gourgs-Blancs, stores the melted snow water from this glacier. The normal pool level of the Caillaouas is 2172.5 m and the minimum pool level 2112.0 m. The Pouchergues reservoir receives water from the same glacier, as well as, by artificial adduction, the water volume from the Aygues-Tortes Lake. Note that, in Figure 3.6, the drainage area upstream the Pouchergues reservoir includes two parts and water in the left part (water intake from the Aygne-Tortes Lake) is transferred into the Pouchergues reservoir in the right part. The normal pool level

of the Pouchergues is 2111.0 m and the minimum pool level 2105.0 m.

The water storage in the Pouchergues can be transferred into the Caillaouas by gravity or by pumping station and can also be delivered directly to downstream cascade power plants. The Lassoula plant exclusively generates electricity with the water releases by the two reservoirs without any intermediate water adduction. The downstream Tramezaygues plant does not only use water from Lassoula but also receives complementary adduction from the upstream rivers (the Neste de Caillaouas, the Neste de Clarabide, the Neste de Lapes). All these along with water from the Aube basin will be released into the Loudenvielle-Genos reservoir to produce energy at the Pont d'Estagnou plant. The discharge out of the Pont d'Estagnou plant goes directly into the Neste River.

In summary, the favorable condition in the Aure Valley allows full use of hydropower. Besides, it is required that reservoirs should provide environmental flows (eflows) to support the downstream riverine ecosystem. Table 3.2 summarizes the physiographic characteristics and environmental flows for the four reservoirs and the corresponding four sub-basins. Table 3.3 summarizes the main characteristics of the hydropower plants exploited for the two hydropwer groups.

In addition to hydropower generation, the water storage in the four reservoirs (Oule, Orédon, Caillaouas, and Pouchergues) is oriented to provide at most 48 Mm^3 of water for uses (irrigation, drinking water, industrial use, and ecological flows) in the Gascogne region that is managed by CACG. This 48 Mm^3 amount of water can only be required by CACG during the period from 15 June to 1 March of the next year. As such, the management of the four reservoirs can be expressed in a rational way as: how to achieve the maximum profit of the hydropower generation under the major constraint of downstream water demand, as well as the reserve for the support of the environment downstream the reservoirs.

To simplify the study case, the two hypotheses are: (1) SB4 is seen as near-natural due to the comparatively small regulation storage of the reservoirs in this sub-basin as shown in Table 3.2; (2) the Caillaouas and the Pouchergues reservoirs can be considered as a single one because they are jointly managed.

Current management rules of SHEM

Since the liberalisation of European electric markets that is legislatively acknowledged at the European Union level in 1996, hydropower has jumped to an important position in the existing energy grids because it is a low-carbon source of renewable energy (Jamasb and Pollitt, 2005; Schittekatte et al., 2021). Hydropower is flexible enough to cooperate with other green energies (e.g., wind and solar resources). Therefore, reservoir water managers are faced with increasing tradeoffs and conflicts. How to keep the high productivity of hydropower while the needs of different stakeholders are well satisfied is challenging.

Currently, SHEM optimizes the hydropower groups by forcing the predicted inflows into the reservoirs, the estimated CACG demand and the predicted electricity price to the optimization procedure, with some restraint parameters (e.g., eflows and non-availability of hydropower plants). The outcome of this procedure is water value in unit €/m^3 for each reservoir storage, which guides the management of SHEM. The four reservoirs are managed together in a single-year pattern to meet multiple purposes. This annual operation process starts from the beginning of April to the end of March of the next year.

Table 3.2 – Physiographic and environmental flow information of the reservoirs and the associated sub-basins in the Aure Valley

Reservoir	Dam type	Upstream basin	Hydropower group	Elevation range [m]	Normal pool level [m]	Minimum pool level [m]	Reservoir storage [Mm^3]	Drainage surface [km^2]	Environmental flow [m^3/s]
Oule	Gravity	SB1	Eget	1771-2693	1816.5	1777.0	16.6	28.4	0.030/0.055
Orédon	Embankment	SB2	Eget	1820-2929	1849.4	1825.0	7.27	11.3	0.051
Caillaouas	Gravity	SB3	Louron	2161-3064	2172.5	2112.0	25.4	6.7	0.004
Poucherges	Gravity	SB3	Louron	2100-3146	2111.0	2105.0	0.83	9.9	0.021

Note: the environmental flow donwstream the Oule reservoir was 0.030 m^3/s before 2014-05-01 and 0.055 m^3/s after.

Table 3.3 – Characteristics of hydropower plants

Hydropower group	Hydropower plant	Installed power $[MW]$	Installed discharge $[m^3/s]$	Water fall $[m]$	Water-energy transition coefficient $[kwh/m^3]$
Eget	Eget	32.6	5.10	728	1.730
Louron	Lassoula-Caillaouas	20.3	5.42	434	variable from 0.900 to 1.155
Louron	Lassoula-Pouchergues	13.0	3.93	434	0.920
Louron	Tramezaygues-Clarabide	19.0	5.17	415	1.020
Louron	Tramezaygues-Lapes	4.80	2.67	245	0.500
Louron	Pont de Prat	0.60	4.50	16.0	0.037
Louron	Aube	2.50	1.24	250	0.560
Louron	Pont d'Estagnou	0.43	4.78	16.4	0.025

The reservoirs are emptied out every end of March so that they can be able to contain the capacity of snow melt. In this work, we assume that the reservoir management remains identical since the liberalization of European electric markets.

The electricity produced by SHEM can be purchased in the electric markets while some can still be redeemed of what has been promised if not profitable due to unusual circumstances (unexpected heat in some months causing less energy consumption). The estimation of electricity price in the markets fluctuates depending on current meteorological conditions and other external factors such as gas price.

In addition to hydropower production and regulatory eflows, as said above, SHEM is committed to provide at most 48 Mm^3 of water to CACG for water uses in the Gascogne region and environmental requirement at Sarrancolin. This 48 Mm^3 is more than any of the storage capacity of the reservoirs in the Aure Valley. As such, the water release from the four reservoirs is conducted based on the current availability (water value) of water in each group, the forecast of of natural inflow to come and the CACG water demand derived from historical information.

Current optimization procedure of SHEM

The procedure plans executed by SHEM are the result of an economic optimization at a daily time step subject to various constraints based on current and known information, which are:

1. compliance with the regulatory demand of CACG for water uses in the Gascogne region and to maintain the good ecological status at Sarrancolin;
2. non-availability known in advance, such as maintenance of turbines;
3. non-spillage of the reservoirs.

The optimization procedure chooses the best hours to operate based on the "water value" (expressed in $€/m^3$). When the "water value" in the reservoirs is higher than the market price over a given time period, water is kept in the reservoirs. Otherwise, water is released to turbines. Given the same volume of water release, the Louron hydropower group produces more hydropower than the Eget group because of the cascade power plants in the Louron group as shown in Table 3.3.

As mentioned before, the CACG has the right to request at most 48 Mm^3 of water for each management year and this draw of water is considered as the maximum in the optimization procedure. Overall, the procedure tries to respect the releases by prioritizing the water with the lowest value. In another word, the procedure tries to minimize the cost of non-optimization and this draw of water is placed on hours that are the least interesting for SHEM to produce energy. It is considered that turbine work is cost-effective when the release water exceed the eflows and the regulatory flow requested by CACG. Normally, the cost-effective flows correspond to the peaks placed during hours of high market prices.

The market price, also called spot price, is the price set at midday of one day for an electricity delivery on the 24 hours of the next day. The forecasts of the market price are the result of an assimilation of historical data coupled with macroeconomic models that try to find the balance point in supply and demand.

As for the non-availability of the turbines, this event is usually unforeseen for the most part, however sometimes it is know well in advance due to regular maintenance of the machines or even the draining of the reservoirs for clearing away sediments. There is another

issue that may cause the non-availability of the turbines: during the winter it is important to ensure that the water stays in motion to prevent frost from clogging damage or exploding the pipe lines. The obligation to operate regularly for the reservoirs represents a cost of non-optimization, which is not taken into account in this optimization procedure. The current optimization procedure in SHEM is deterministic and does not take into consideration of the damage either. The procedure can empty a reservoir completely (typically Oule) without foreseeing a damage on the machines of the other reservoirs.

Typical operation periods of SHEM

A typical management year executed by SHEM for hydropower production is presented as follow.

April-June: The market prices are low and the water levels of the reservoirs are low. In May, snowmelt causes intensive contributions of inflow in all reservoirs, which might risk the overflow for the reservoirs at the same time. The optimization procedure begins the turbine work of the Eget group well in advance in anticipation of the non-availability period. At the beginning of June, the Oule reservoir goes to its maximum storage. For the reservoirs in the Louron group, the situation is less complicated and the risk of overflow is less important as the capacity of the Caillaouas and Pouchergues reservoirs is around 26 Mm^3 compared to the 16 Mm^3 of the Oule reservoir. The Caillaouas and Pouchergues reservoirs reach its maximum storage in late July due to its higher altitude.

July-September: Water release increases to a maximum discharge of 8 m^3/s for the four reservoirs in the middle August, in compliance with the CACG regulatory. The draw of water goes down to 2 m^3/s in November. In order to meet the demand of CACG, the procedure tends to draw water in the Eget group by start and then completes with the Louron group when the demand is larger than the water outflow capacity of the Eget group. In September, the water stock in the Eget group is almost emptied and the Louron group is at 50% on average of its water reservation.

October-March: The market prices are high of the year and SHEM exploits to gain a maximum economic benefit. The energy demand is intensive in this period in exception of Christmas holidays due to the lower industrial activities. The water releases are roughly stabilized around 2 m^3/s. The energy supply is insured by the Eget group on weekends when the market prices are the lowest in the weekly schedule and by the Louron group on the weekday period. In this optimization procedure, the weekdays from October to April are the most profitable period.

3.1.4 Water management in the Neste water system: the Neste Canal and the Gascogne region

The CACG is in charge of water management of the Neste Canal, the reservoirs in the Gascogne region, and 48 Mm^3 of storage in the Oule, Orédon, Caillaouas and Pouchergues reservoirs.

CACG is required to manage the tradeoff between two competing water demand in the Gascogne region (SB5). One is the consumptive water demand that includes agricultural irrigation, drinking water supply, and industrial uses; the other is the environmental quality that requires river flows in the SB5 no lower than a minimum target (DOE). The DOE requirement is assessed at several points most of which are near the confluence to the Garonne River. These control points are monitored by CACG, particularly to ensure

sufficient river flows in SB5 during the dry spells in summer. As mentioned before, irrigation water is mostly contributed to the maize cropping. Drinking water is supplied to local residents with a population of around 180 thousands. Most industrial water is provided for the Arkéma[3]. Note that water releases for the environment of SB5 are conducted daily to remain a good ecological status, which causes water conflicts with storage for future consumptive water demand. Figure 3.8 illustrates the water volume distribution by reservoirs managed by SHEM and CACG for the four types of water demand according historical experience of CACG. Nearly total water volume are distributed for the daily environment and summer irrigation uses. Details on water uses will be detailed later in chapter 5.

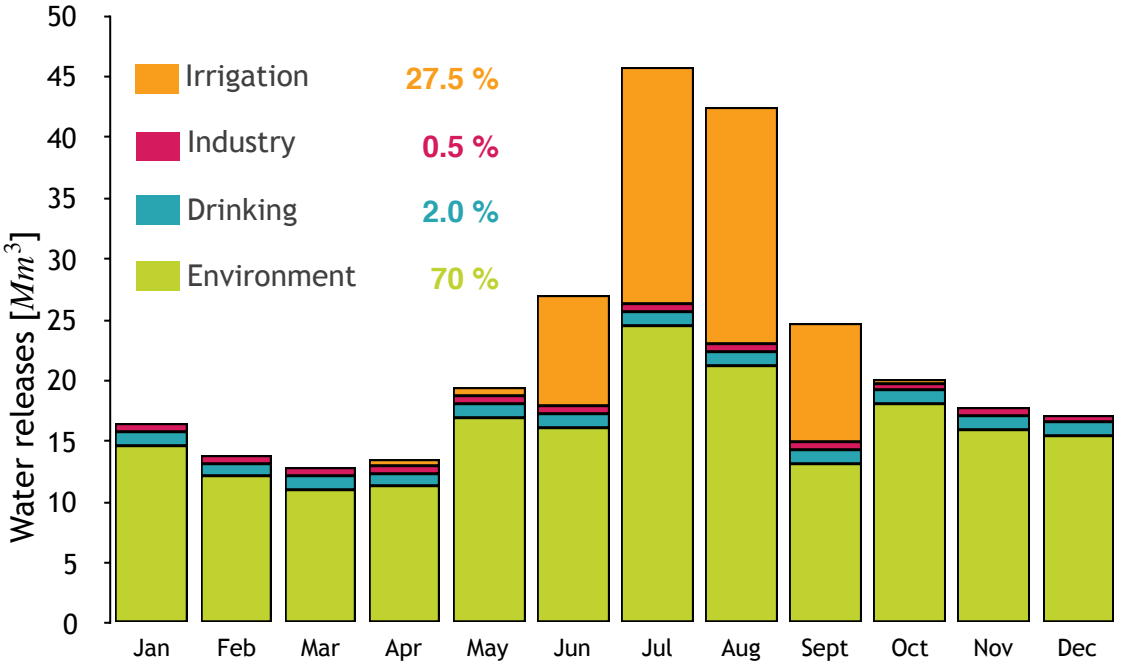

Figure 3.8 – Mean monthly and annual water share in the Gascogne region. Source from CACG.

Concerning the management of the Neste Canal, the canal extracts water at Sarrancolin to feed the reservoirs and rivers in SB5 as shown in Figure 3.5. The volume of water extraction is mainly based on the water availability at Sarrancolin and the water demand of SB5. Besides, the mandatory environmental legislation furthermore requires that the river flow at and downstream Sarrancolin should be larger than 4 m^3/s (DOE at Sarrancolin). If not maintained, either more water out of the reservoirs in the Aure Valley (accounted in the 48 Mm^3) or less water abstraction at Sarrancolin for the SB5 uses will be conducted. However, it is possible to derogate from the 4 m^3/s by lowering the constraint to 3 m^3/s up to 90 days in one year.

Current management rules of CACG

The available water volume that can be mobilized by CACG is composed of the storage in the 15 reservoirs in SB5 with a capacity of 73.3 Mm^3 as displayed in Table 3.1 and

[3] A specialty chemicals and advanced materials company (https://www.arkema.com/)

the contract of 48 Mm^3 in the reservoirs managed by SHEM. In general, there are three management rules for CACG when demanding water from the reservoirs of SHEM: (1) CACG should save water as much as possible for SHEM and the 15 reservoirs in SB5 should be released first to meet the four types of water needs; (2) CACG can only demand water from 15 June to 1 March of the next year as mentioned before; (3) CACG need to respect DOE at Sarrancolin when extracting water through the Neste Canal to feed the rivers and reservoirs in SB5. Given the complexity of the management of the Neste system, there is no formalized water management optimization process by CACG.

However, the system is equipped with a dense network of sensors of river discharge and a decision supporting system (RIO) that allow real-time water management in coordination with meteorological information and water demand from local stakeholders (e.g., farmers). Figure 3.9 shows that the Neste Canal transfers water resources from the Aure Valley to SB5 with the help of water gates and discharge measure sensors. The RIO system is a multifunction procedure for the strategic management of the Neste system by CACG, which aims at first anticipating future irrigation requirements at a weekly time step and second improving decision making for managing water resource. A detailed description of the RIO system can be found in Leenhardt et al. (2004b).

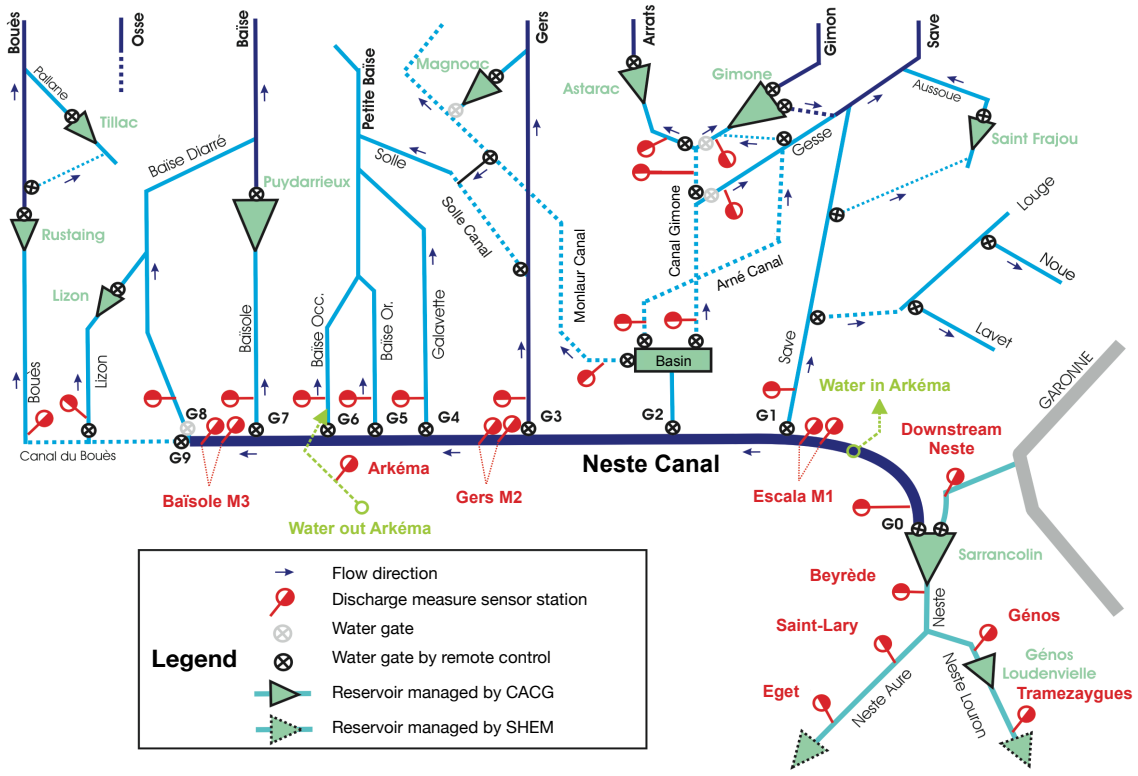

Figure 3.9 – Water management in the Neste Canal. Source from CACG.

Water management in terms of agricultural irrigation and environment uses in SB5 is complex. This is because both water uses consume most water storage of the reservoirs and cause water competition in summer. In most cases, the irrigation management procedures of CACG can be divided into three levels based on temporal scales (annual, weekly, and daily) (Leenhardt et al., 2004a). The progressive management levels are presented as follow.

1. The water volume that may be assigned to agricultural irrigation is determined each

year based on the existing amount of water storage in the reservoirs of SB5, the regulatory 48 Mm^3 in the four reservoirs of the Aure Valley, and estimated information of natural water resources. After that, irrigation users are assigned with water volume quotas depending on the demand. The irrigation users will be charged for the water volume requested.

2. Weekly decisions are made in the irrigation season concerning the tradeoffs how much water to release for environment purposes or to store to ensure irrigation satisfaction.

3. CACG managers make decisions on how much water to release for which purpose from which reservoir(s) every day.

In summary, the current management of the Neste system by CACG mainly involves distributing the overall available water, a total storage of 121.3 Mm^3 (73.3 Mm^3 reservoir storage in the Gascogne region and 48 Mm^3 quota from the reservoirs in the Aure Valley), for the four types of water demand. During drought events, a successful management is: (1) to satisfy all consumptive water demand and (2) to keep downstream river flows, as well as the Neste Canal extraction location Sarrancolin, always no lower than DOE requirement. However, when the Neste system is in severe water scarcity, the CACG managers additionally check whether the weekly volume allocated to irrigation is overestimated. If so, they will consider lower the water quota for irrigation.

3.2 Data collection

3.2.1 Climatic drivers

Baseline climate: Safran reanalyses

The near-surface meteorological reanalysis Safran-PIRAGUA that focuses on the Pyrenees is used in this study for driving the hydrological modelling. This dataset is a high resolution (2.5 km $\times$ 2.5 km) surface reanalysis based on the Safran algorithm obtained by merging the Safran-France reanlysis product (Vidal et al., 2010) and the Safran-Spain reanalysis product (Quintana-Seguí et al., 2016, 2017). It provides daily climate information of air temperature and precipitation. The potential evapotranspiration information is calculated from the Penman-Monteith equation (Allen et al., 1998). Catchment-scale climatic data of the study area is computed with a weighted mean of all cells intersected by the catchment surface. The Safran-PIRAGUA dataset is available from 09/1979 to 08/2014.

Besides, the Safran-France reanalysis dataset (resolution 8 km $\times$ 8 km) is also used when the calibration period of hydrological modelling is not overlapped with the Safran-PIRAGUA dataset. The Safran-France dataset is available from 08/1958 onwards. Figure 3.10 shows the Safran-France and the Safran-PIRAGUA grid center points in the study area. Compared with Safran-France reanalysis data, Safran-PIRAGUA data can provide a more detailed information of climate due to its high spatial resolution that allows representing abundant climate variability.

Snow product: the gap-filled MODIS

The MODIS[4] is an important instrument embedded in the Terra and Aqua satellites to measure the dynamics in Earth's processes, such as snow cover, vegetation index, and land-surface temperature. Daily snow cover products are adopted in this study to calibrate the hydrological model. However, the missing snow cover observations from satellites due to the coverage of clouds makes it difficult to acquire a full temporal description on the study area. Gascoin et al. (2015) developed a cloud-free snow cover product in the Pyrenees based on the MODIS products and a gap-filling algorithm. The accuracy of the gap-filled MODIS products was validated against in situ snow observations and Landsat data in the Pyrenees range. The spatial resolution of this gap-filled snow product is consistent with the original MODIS snow product (0.5 km $\times$ 0.5 km). The dynamics of catchment-scale snow cover can thus be computed with a weighted mean of all contributive cells to the catchment surface. Time series of snow cover area (SCA) were derived from the MODIS data over the period from 09/2000 to 04/2018.

Water resources in the Aure Valley is dominated by snow accumulation in winter and snow melt in spring while SB5 is not. As such, only the SCA time series of the Aure Valley (SB1-4) are extracted from the MODIS snow product. Figure 3.11 shows the MODIS grid center points in the 5 elevation bands of the Aure Valley. The decomposition of the Aure Valley (SB1-4) into 5 equi-surface bands will be used for calibrating the snow module CEMANEIGE (see next chapter) in the hydrological modelling.

[4]Moderate Resolution Imaging Spectroradiometer (https://modis.gsfc.nasa.gov/)

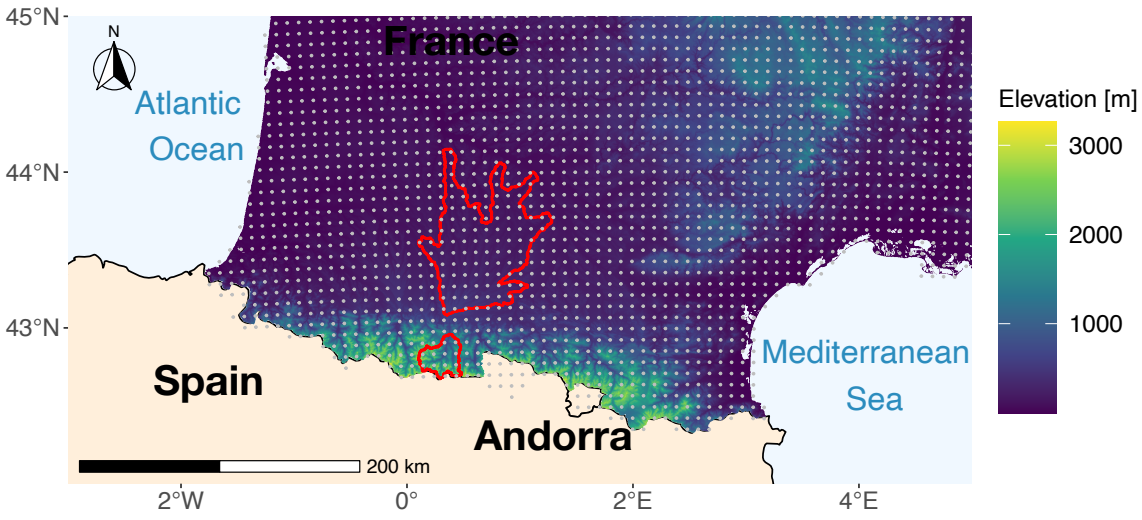

(a)

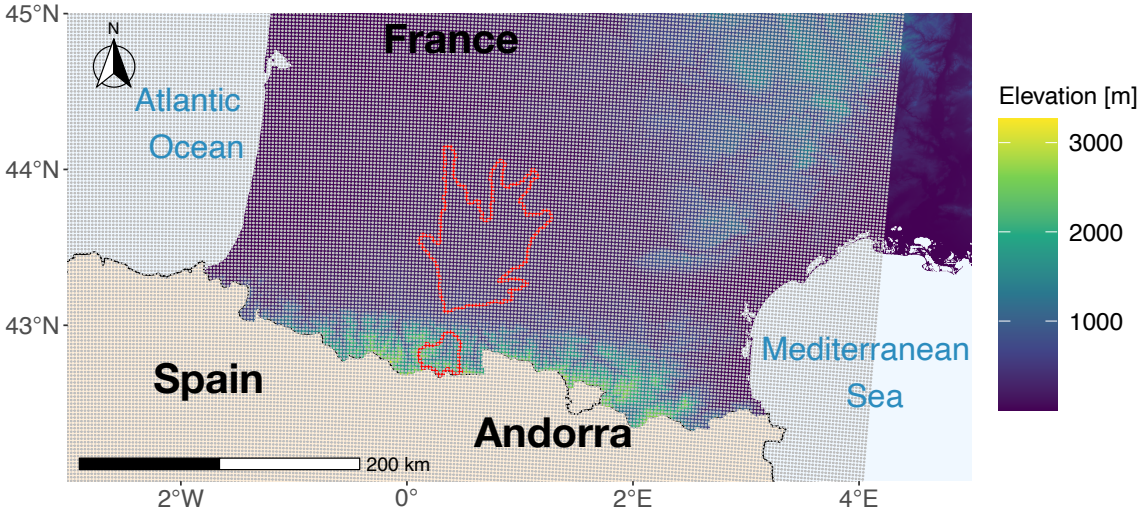

(b)

Figure 3.10 – The Neste system area overlaid with Safran-France (a) and Safran-PIRAGUA (b) gird center points.

Climate change projections

Representative Concentration Pathways (RCPs) 4.5 and 8.5 are moderate and high GHG concentration trajectories by the IPCC to describe climate futures (IPCC, 2014). Climate projections considered here originate from a subset of 6 CMIP5 GCMs as shown in Table 3.4 and previously selected for assessing future water resource in Spain run under RCP 4.5 and RCP 8.5 (CEDEX/MAPAMA, 2017). These projections have been previously downscaled with an analogue downscaling method to generate daily total precipitation (Ptot), maximum temperature (Tx), and minimum temperature (Tn) over a 5 km $\times$ 5 km grid for Spain and the Pyrenees within the CLIMPY project (Amblar-Francés et al., 2020; Amblar Francés et al., 2017). The CLIMPY projections have been here further refined in order to match both the higher spatial resolution and the multiple variables of the Safran-PIRAGUA surface reanalysis. To this aim a multi-site and multi-variable analogue resampling method has been set-up following the approach proposed by Clemins et al. (2019) and applied to the Pyrenean area within the PIRAGUA project (Vidal, personnal commu-

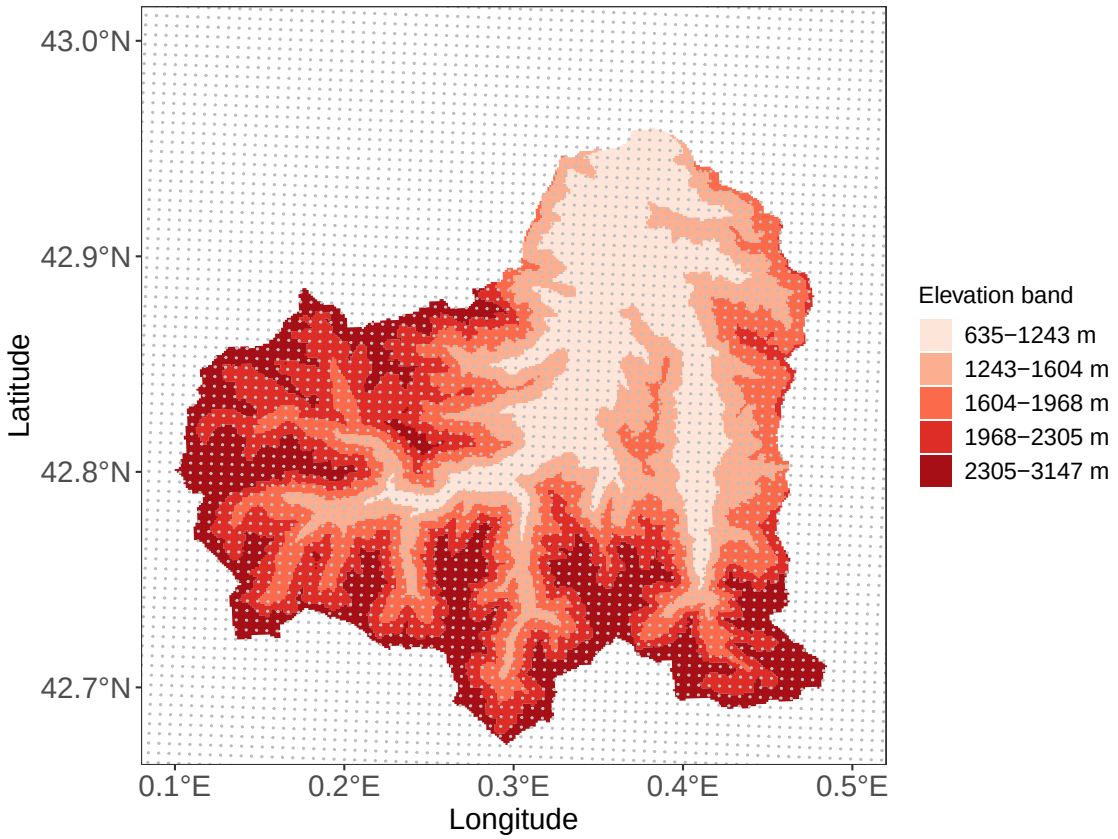

Figure 3.11 – The 5 equi-surface elevation bands of the Aure Valley overlaid with grid center points of the gap-filled MODIS snow product.

nication).

Table 3.4 – List of selected CMIP5 GCMs.

Acronym	Institute	Reference
CNRM-CM5	CNRM, France	(Voldoire et al., 2013)
MRI-CGM3	MRI, Japan	(Yukimoto et al., 2012)
MPI-ESM-MR	MPI, Germany	(Giorgetta et al., 2013)
MIROC-ESM	AORI NIES JAMSTEC, Japan	(Watanabe et al., 2011)
inmcm4	INM, Russia	(Volodin et al., 2010)
bcc-csm1.1	BCC, China	(Wu et al., 2013)

In short, for a target day in a given CLIMPY projection, an analogue date in the 1961-2005 Safran-PIRAGUA surface reanalysis is selected, based on the best possible match of Ptot, Tn, and Tx over the whole Pyrenean mountain range. This analogue re-sampling is made on monthly anomalies with respect to a baseline climatology, in both Safran-PIRAGUA and CLIMPY projections. For Tn and Tx CLIMPY projections, the baseline climatology is considered as linearly transient from 2006 onwards, in order to find relevant analogue dates even with temperatures higher than any experienced in the

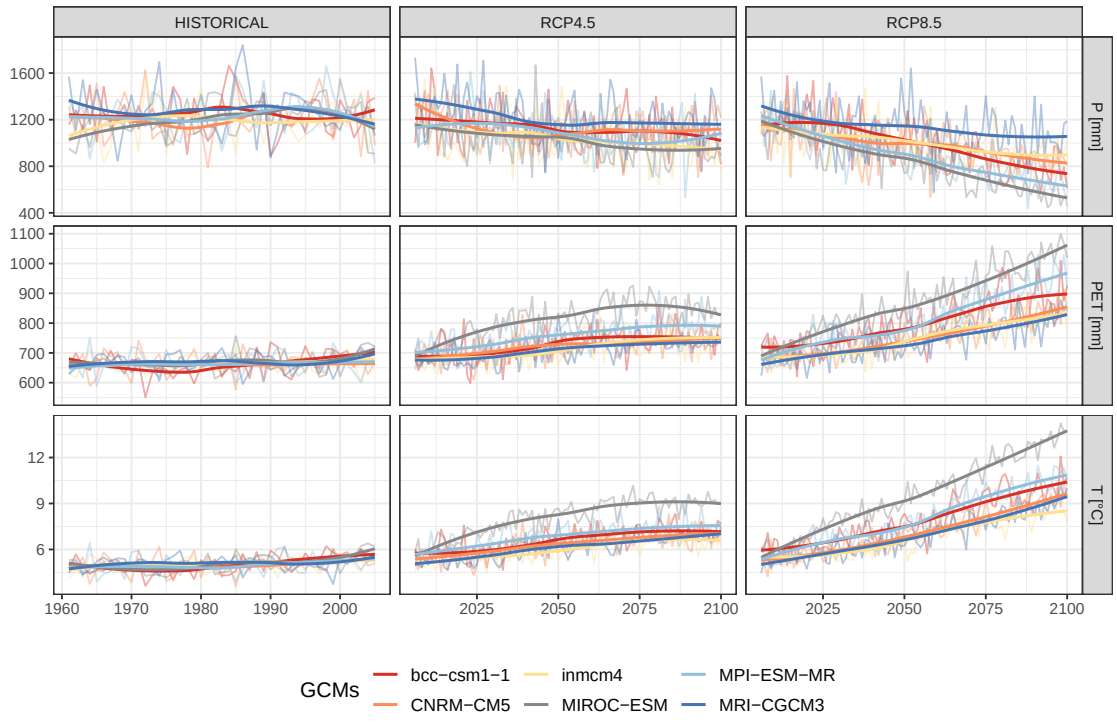

(a)

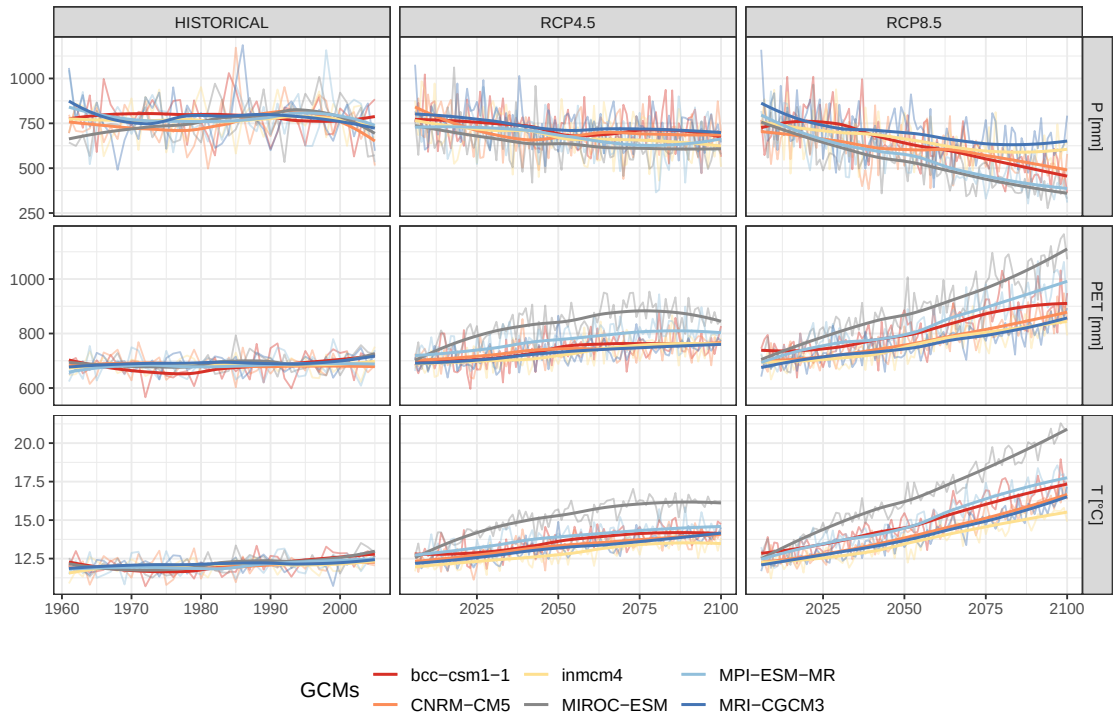

(b)

Figure 3.12 – Climate change projections of the 6 GCMs in Table 3.4 in terms of annual precipitation (P), potential evapotranspiration (PET), and temperature (T) under historical (1961-2005), RCP 4.5 (2006-2100), and RCP 8.5 (2006-2100) scenarios for the Aure Valley (a) and SB5 (b). The fine lines represent the mean annual changes and the thick lines represent the trends with loess smoothing method.

Safran-PIRAGUA 1961-2005 archive. All variables from the analogue dates are used as values for the target date considered. Results are therefore daily gridded projections over the Safran-PIRAGUA grid, with all corresponding variables – including precipitation and temperature required for the hydrological models – for 6 GCMs run under both RCP 4.5 and RCP 8.5 emissions scenarios, for the whole 1961-2100 period. Figure 3.12 shows the climate change projections of evapotranspiration, precipitation, and temperature under different scenarios of 6 GCMs in Table 3.4. Climate in the Aure Valley and SB5 is projected to be warmer and drier under the two RCPs. Especially, climate projections under RCP 8.5 are much more warmer and drier than RCP 4.5.

In addition to regional climate change projections, France temperature projections are necessary in this study for energy demand simulation (see section 5.1.2). However, the future temperature projections in France are not available in the CLIMPY project. In order to be in line with the regional projections of the Neste water system, we apply a linear interpolation method to calculate the future France temperature based on the regional temperature projections. Figure 3.13 shows the comparison between the temperature of the Neste water system (SB1-5) and the France temperature over the period from 09/1979 to 08/2014. The annual temperature regimes show the same pattern with the maximum values located in summer and the minimum values located in winter while there is a vertical distance between the two regimes due to the lower latitude of the Neste water system area (higher temperature in the Neste water system area). The regression line (the red line in the Figure 3.13) between the France temperature and the local temperature is calculated as follow.

$$\mathrm{T(France)} = \mathrm{T(Local)} \times 0.945 - 0.359 \tag{3.1}$$

The determinant coefficient R^2 is 0.94.

In order to validate the method, we calculate the France temperature over the period from 09/1979 to 08/2014 based on the local temperature by applying this linear regression line. Figure 3.14 illustrates the annual regimes of the simulated and the observed France temperature. The simulated France temperature over the period from 09/1979 to 08/2014 well follows the observations. As such, we apply this regression method to calculate the France temperature projections based on the local temperature projections. The results are shown in Figure 3.15 and the future France temperature shows a warmer trend similar to the local temperature projections.

3.2.2 Naturalized inflow

Compared with SB5, river flows in the Aure Valley is highly influenced due to the intensive developement of hydropower (Décamps, 1967; Ingrand, 1961). A study was conducted by Falgon (2014) to reconstruct natural inflows upstream the reservoirs (SB1-3) in the Aure Valley applying a water balance approach. The principle of this approach is to sum up all exports for water use and to subtract all imports from other basins. It can be expressed as the following equation.

$$Q_{natural} = Exports\ for\ water\ use - Imports\ from\ basins + \Delta Storage$$

SB4 is considered as a near-natural sub-basin, and the naturalized inflow of SB4 is the observed river discharge at Sarrancolin minus the regulated outflows upstream the reservoirs. The naturalized inflow of SB5 is estimated by CACG, and it is the observed river

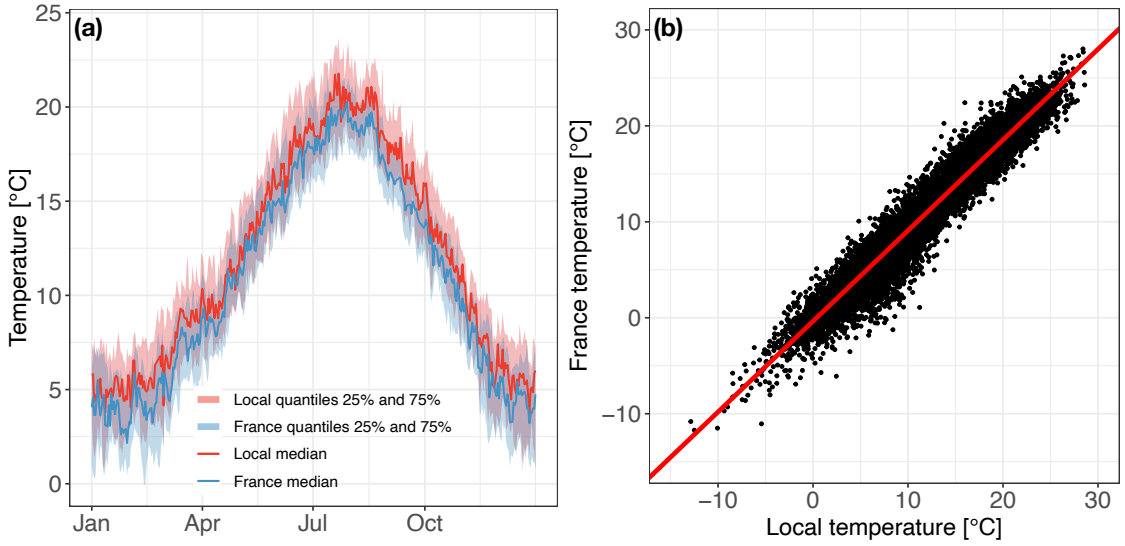

Figure 3.13 – (a) The annual regime of France daily temperature compared with the annual regime of the local daily temperature (the daily temperature of the Neste water system area) over the period from 09/1979 to 08/2014; (b) The linear relationship between the local temperature of the Neste water system area as shown in Figure 3.2 and the France temperature. The local temperature is calculated with the SAFRAN-PIRAGUA dataset and the France temperature is calculated with the SAFRAN-France dataset over the period from 09/1979 to 08/2014.

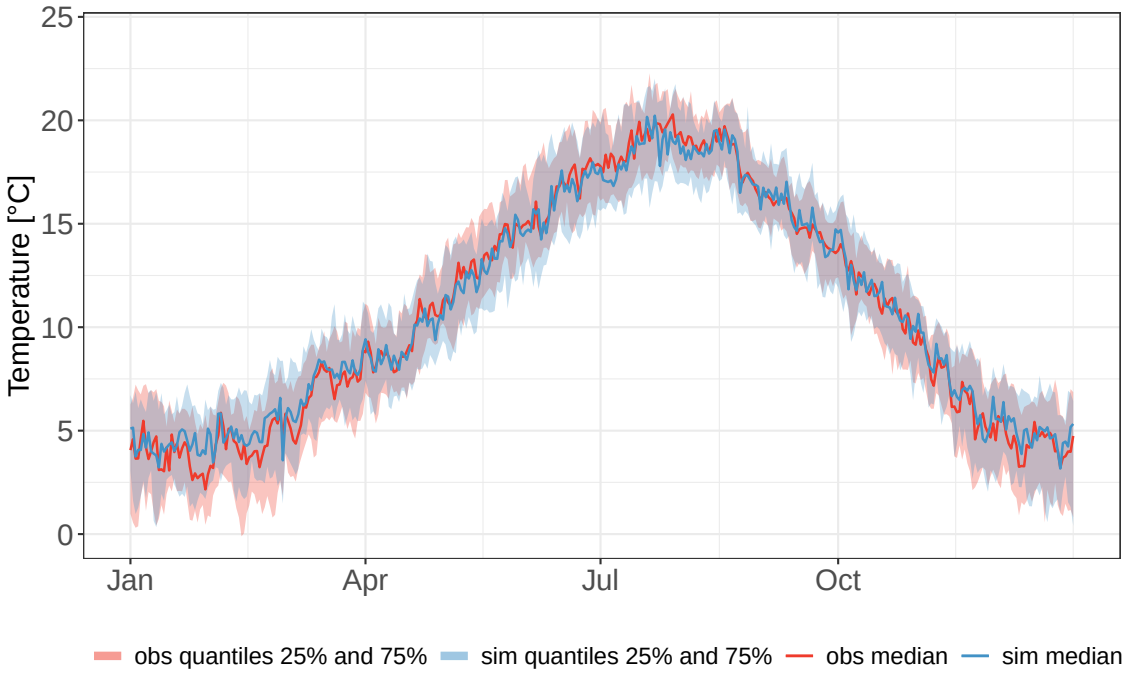

Figure 3.14 – The comparison between the simulated and observed France temperature over the period from 09/1979 to 08/2014.

discharge minus the sum of the water intake from the Neste Canal and the water releases from the reservoirs. The naturalized inflows of SB1-5 are at daily time step. The natural-

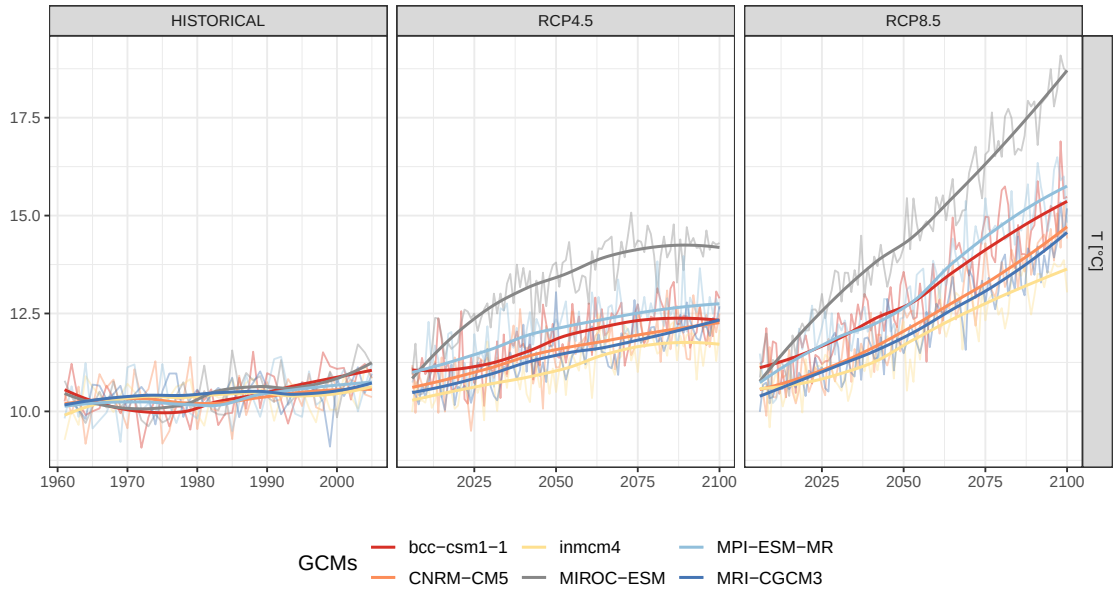

Figure 3.15 – The mean annual simulated France temperature projections under historical (1961-2005), RCP 4.5 (2006-2100), and RCP 8.5 (2006-2100) scenarios. The fine lines represent the mean annual changes and the thick lines represent the rends with loess smoothing method.

ization processes for SB1-5 are presented in detail as follow.

Naturalized inflow of SB1

The formula for reconstructing the daily natural flows upstream the Oule reservoir is derived as:

$$Q_{nat1} = eflow_1 + Use_1 + \Delta_1 + Spil_1 - Tran_1 \tag{3.2}$$

where

- $eflow_1$ is the daily reserved flow for the environment for the downstream of the Oule reservoir (see Table 3.2);
- Use_1, daily flows out of the Oule reservoir for water uses;
- Δ_1, daily variation of the volume of the Oule reservoir;
- $Spil_1$, daily overflow from the Oule reservoir;
- $Tran_1$, daily water transfer from the Orédon reservoir into the Oule reservoir.

The naturalized inflow into the Oule reservoir is calculated from 01/2001 to 12/2018 at daily time step. Figure 3.16 shows the naturalized flow of SB1 compared with the influenced flow out of the Oule reservoir. The flow regime of SB1 is deeply modified as the flow peak shift from spring to summer due to CACG water demand (mainly for irrigation) and winter flow shows an evident increase due to hydropower generation. The lowest flows in spring is due to reservoir storage purpose in this period.

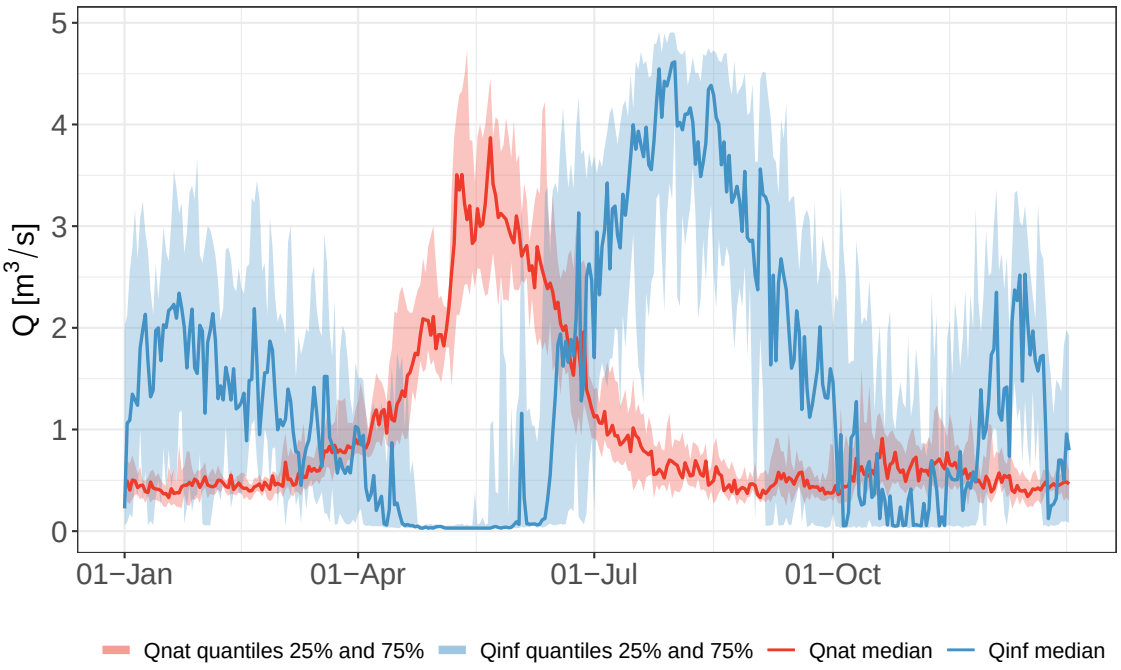

Figure 3.16 – Comparison between the naturalized inflow (Q_{nat1}) and the influenced outflow (Q_{inf1}) of SB1 for the period from 01/2001 to 12/2018.

Naturalized inflow of SB2

The formula for reconstructing the daily natural flows upstream the Orédon reservoir is derived as:

$$Q_{nat2} = eflow_2 + Tran_1 + \Delta_2 + Spil_2 - eflow_0 \tag{3.3}$$

where

- $eflow_2$ is the daily reserved flow for the environment for the downstream of the Orédon reservoir (see Table 3.2);
- Δ_2, daily variation of the volume of the Orédon reservoir;
- $Spil_2$, daily overflow from the Orédon reservoir;
- $eflow_0$, the daily reserved flow for the environment for the downstream of the Cap de Long reservoir (0.05 m^3/s, see section 3.1.3).

The data length of naturalized inflow for SB2 is from 07/2014 to 12/2018 and the data quality is relatively low. Figure 3.17 shows the naturalized flow of SB2 compared with the transferred flow out of the Orédon reservoir. Water use of the Orédon reservoir is realized through transferring water into the Oule reservoir by a underground pressure pipeline. Note that the eflow for the downstream of the Orédon reservoir is released directly from the Orédon reservoir. The transfer period is mainly in the summer to meet the CACG demand. The rest water volume will be emptied by transferring to the Oule reservoir for hydropower production in winter. There is no water transfer in spring due to reservoir refill. Here, due to the lack of data, we consider the water releases from the Cap de Long and Aubert into the Orédon are environmental flows $eflow_0$ with a total value of 0.05 m^3/s.

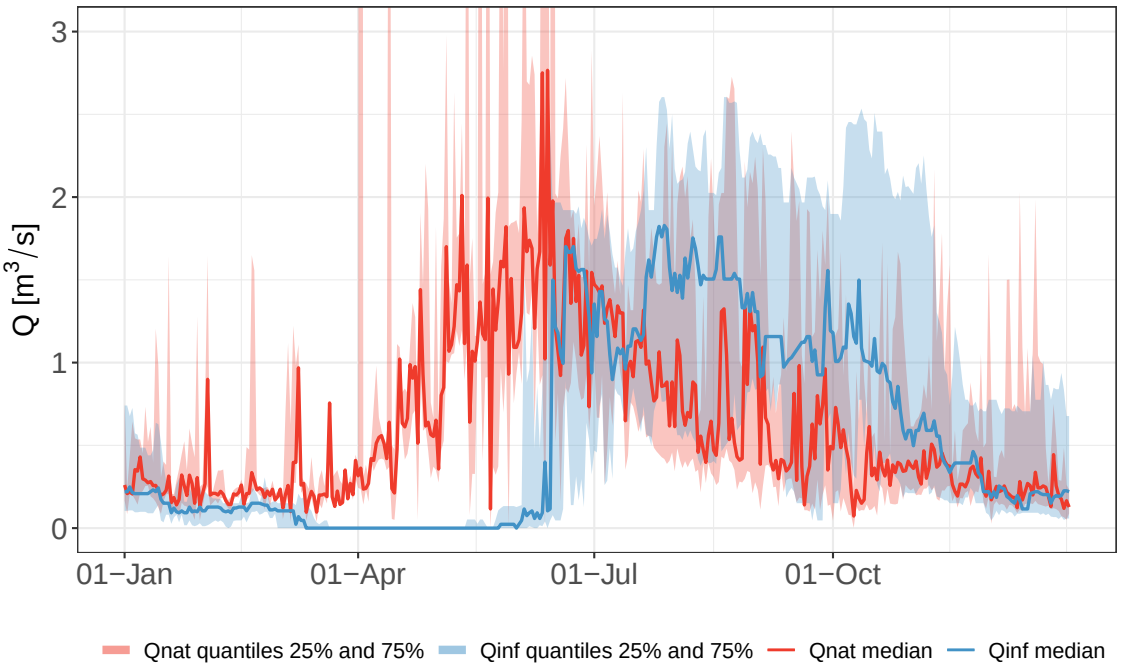

Figure 3.17 – Comparison between the naturalized inflow (Q_{nat2}) for the period from 07/2014 to 12/2018 and the transferred outflow ($Tran_1$) of SB2 for the period from 01/2001 to 12/2018.

Naturalized inflow of SB3

SB3 is composed of two reservoirs, the Caillaouas and Pouchergues. The choice was made to consider the catchments upstream the reservoirs as one. Using a global formula for SB3, including the Caillaouas and the Pouchergues reservoirs, makes it possible to get rid of the gravity or pumping water transfer between the two reservoirs (the two information, water move by gravity and pumping water transfer, is poorly known). As such, the sub-basins upstream the Caillaouas and the Pouchergues reservoirs can be considered as a single one (SB3) to reduce these uncertainties.

The formula for reconstructing the daily natural flows of SB3 is derived as:

$$Q_{nat3} = eflow_3 + Use_3 + \Delta_3 + Spil_3 \tag{3.4}$$

where

- $eflow_3$ is the sum of daily reserved flow for the environment of the downstream of the Caillaouas and Pouchergues reservoirs (see Table 3.2);
- Use_3, daily flows out of the Caillaouas and Pouchergues reservoirs for water uses;
- Δ_3, daily variation of the volume of the Caillaouas and Pouchergues reservoir;
- $Spil_3$, daily overflows from the Caillaouas and Pouchergues reservoir.

The naturalized inflow of SB3 is calculated from 01/2001 to 12/2018 at daily time step. Figure 3.18 shows the naturalized flow of SB3 compared with the influenced flow. The peak of naturalized flow of SB3 is in spring due to snowmelt. The peaks of influenced flow are in summer and winter period for CACG demand and energy production, repectively. The lowest outflow from SB3 is in spring as a result of reservoir refill purpose.

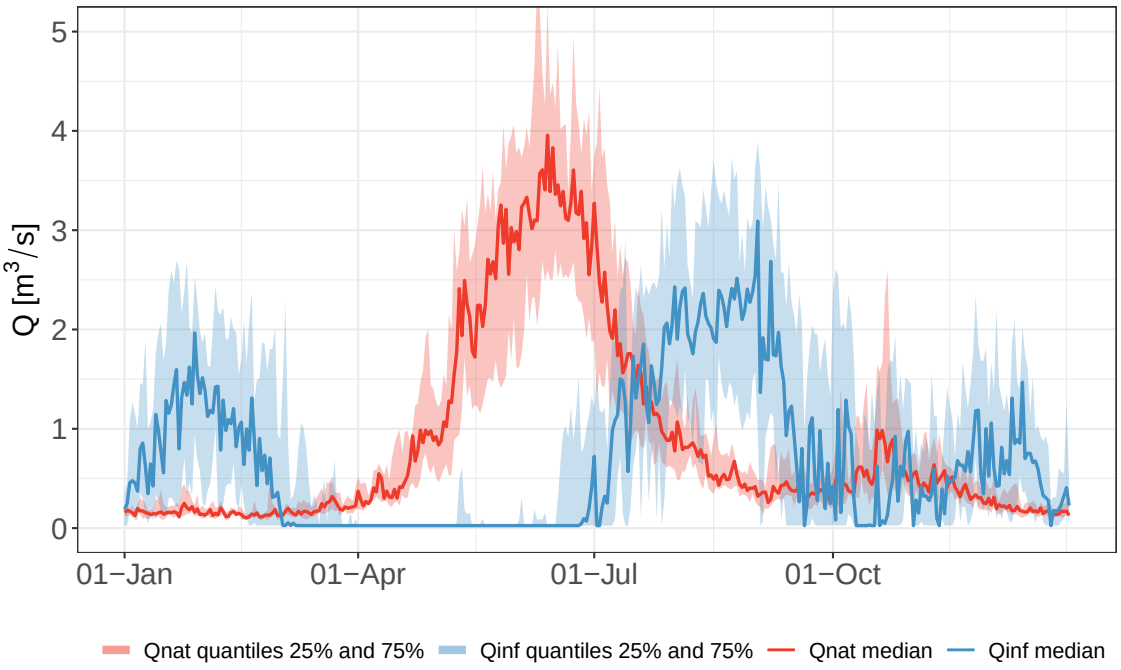

Figure 3.18 – Comparison between the naturalized inflow (Q_{nat3}) and the influenced outflow (Q_{inf3}) of SB3 for the period from 01/2001 to 12/2018.

Naturalized inflow of SB4

SB4 is the sub-basin of the Aure Valley excluding SB1-3 and the drainage area upstream the Cap de Long, Aubert, and Aumar reservoirs. CACG measures river flow at Sarrancolin, including that extracted by the Neste Canal and that downstream Sarrancolin (see Figure 3.9). The formula for reconstructing the daily natural of SB4 is derived as:

$$Q_{nat4} = Q_{canal} + Q_{ds} - Q_{inf1} - Q_{inf2} - Q_{inf3} \tag{3.5}$$

where

- Q_{canal} is the daily water flow extracted by CACG into the Neste Canal;
- Q_{ds}, the daily river flow downstream Sarrancolin;
- Q_{inf1}, daily flows out of SB1;
- Q_{inf2}, daily flows out of SB2;
- Q_{inf3}, daily flows out of SB3.

Note that the premise of this formula is that SB4 is a near-natural sub-basin. Figure 3.19 shows the regime of the naturalized inflow of SB4 with distinct peak in spring.

Naturalized inflow of SB5

The drainage area of SB5 is the sub-basins upstream the ten control discharge measure points as shown in Figure 3.20. The red dots in the figure are the control points where discharge is compared to DOE requirement. The surface of SB5 is 5433 km^2.

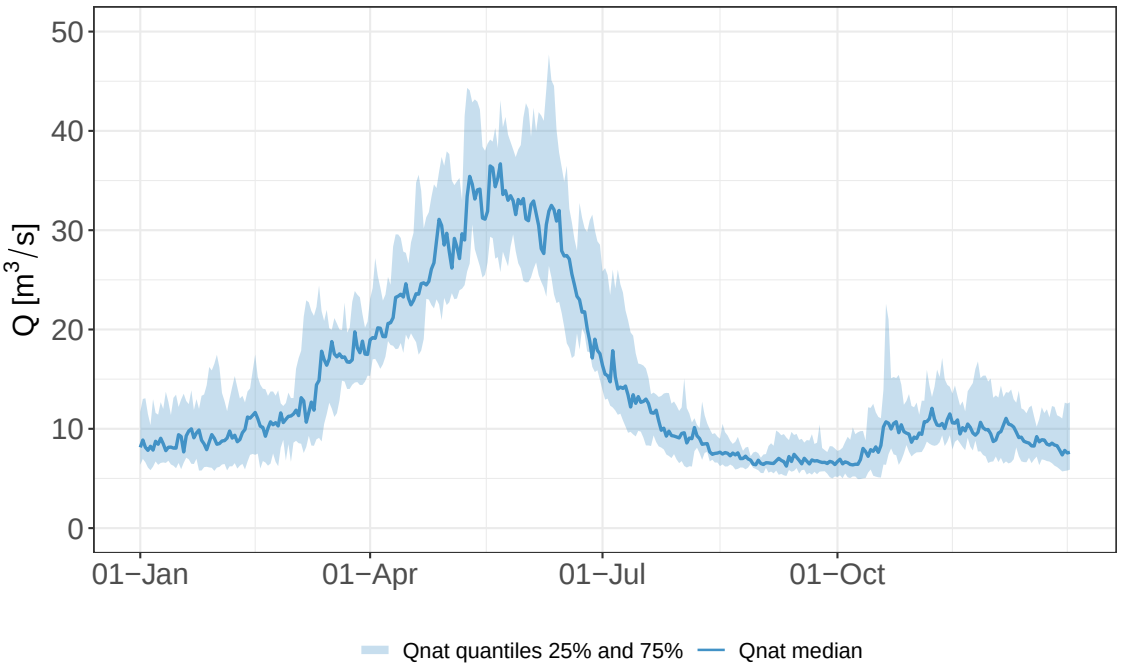

Figure 3.19 – Naturalized inflow of SB4 (Q_{nat4}) for the period from 01/2001 to 12/2018.

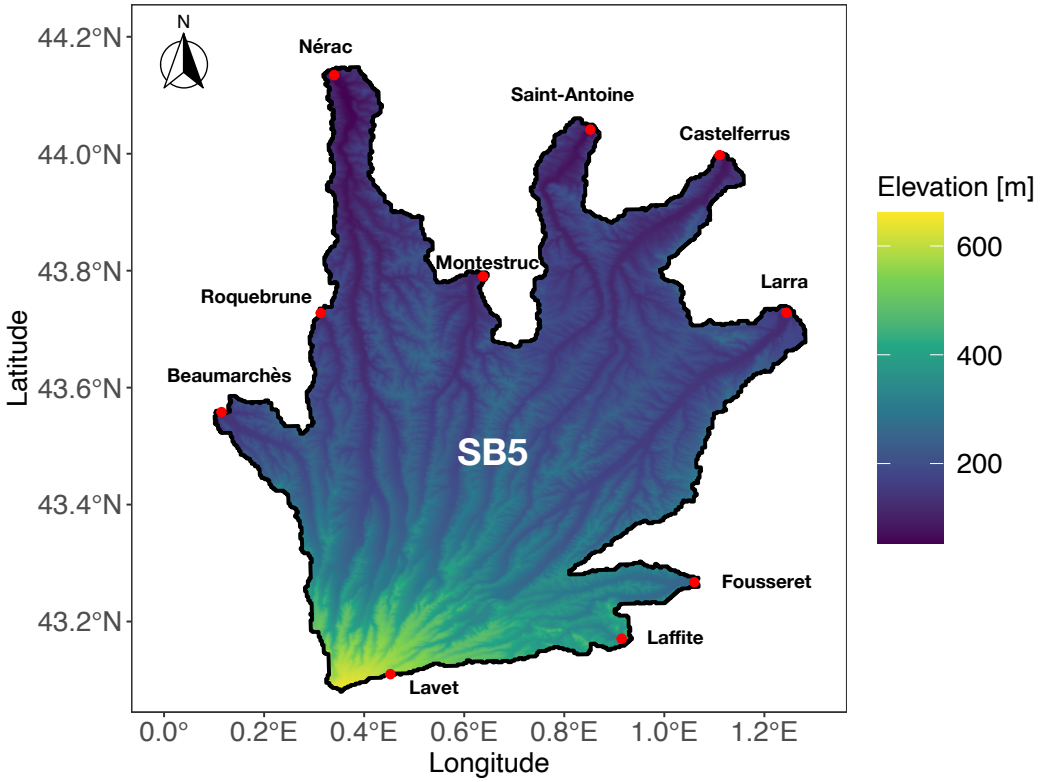

Figure 3.20 – The drainage area of SB5 is the total drainage area of the sub-basins upstream the ten discharge control points: Beaumarchès, Roquebrune, Nérac, Montestruc, Saint-Antoine, Castelferrus, Larra, Fousseret, Laffite, and Lavet.

The naturalized inflow of SB5 is estimated by aggregating the 10 stations into one. The formula for reconstructing the daily natural of SB4 is derived as:

$$Q_{nat5} = \sum_{n=1}^{10} Q^{n}_{station} - Q_{canal} - Use_5 \tag{3.6}$$

where

- $\sum_{n=1}^{10} Q^{n}_{station}$, represents the sum of daily flows at the ten stations (source from the Banque Hydro[5]): Beaumarchès, Roquebrune, Nérac, Montestruc, Saint-Antoine, Castelferrus, Larra, Fousseret, Laffite, and Lavet;

- Use_5, daily flows out of the 15 reservoirs in SB5 (see Table 3.1) for water uses.

The inflow of SB5 is naturalized in a global formula, allowing reducing the error of water transfer among the reservoirs in SB5. The naturalized inflow of SB5 is available from 01/2013 to 12/2019. Figure 3.21 shows the naturalized flow of SB5 compared with the influenced flow. The naturalized flow peak is in February and March. Note that the influenced flow in SB5 is larger the naturalized flow, especially in summer, mainly due to DOE requirement. A detailed description of DOE requirement in SB5 will be given in the section 3.2.4.

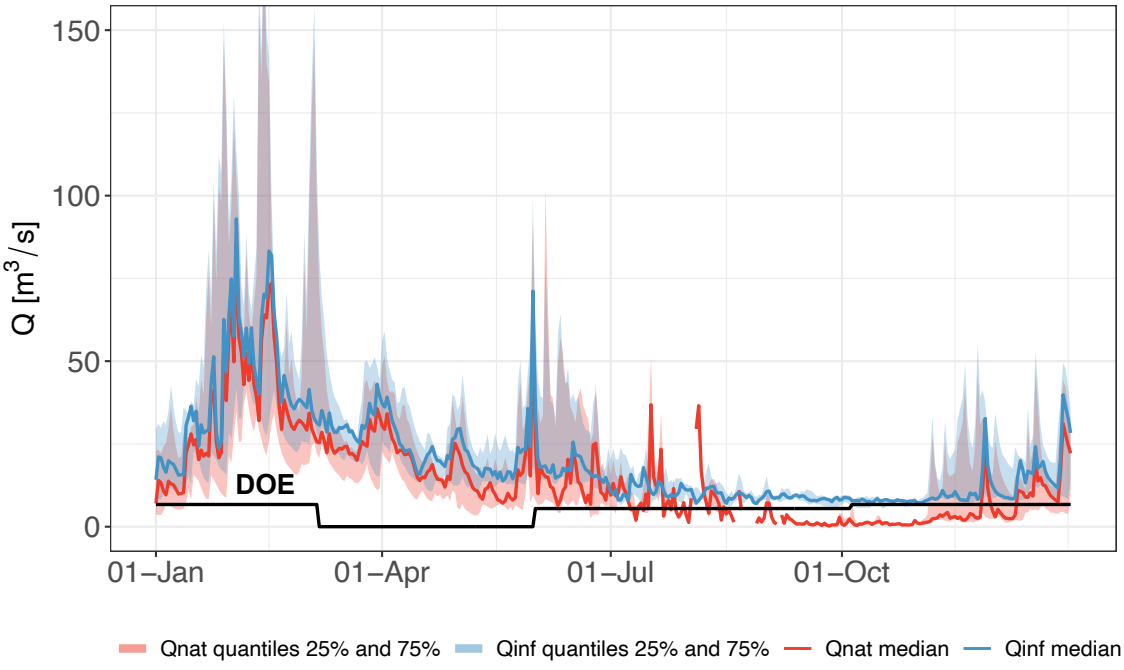

Figure 3.21 – Comparison between the naturalized inflow (Qnat) and the influenced outflow (Qinf) of SB5 for the period from 01/2013 to 12/2019.

[5]Hydrometric data are processed and collected within a single platform managed by the SCHAPI (central service for hydrometeorology and flood forecasting support) (see the platform: http://www.hydro.eaufrance.fr/).

3.2.3 Water management records of SHEM

Water releases for CACG demand are registered and SHEM releases water via turbines to gain a marginal profit. The data of water releases for CACG demand is available from 01/2002 to 12/2018.

Figure 3.22 shows the total water release from the Eget and Louron groups in comparison with the CACG water demand. As observed from this figure, water demand from CACG is mostly satisfied, except for year 2015 due to an accident on the pipe line of the Lassoula plant (non-availability of the Louron group). However, it is obliged to satisfy the CACG water demand and in this year water out of the Pouchergues reservoir is delivered to CACG, which is still not enough. As for year 2013 and 2014, there is not much water demand from CACG during summer time. In year 2013, the snowpack is double thick than usual time and snow melts late so that this melting snow water is exploited for hydropower. In year 2014, CACG water demand starts at late summer due to the rainfall in June and July. Thus, the stored water in the system is used to produce electricity for the industrial program.

In summary, CACG demand is concentrated in summer mainly for irrigation and environmental purposes in SB5. However, water releases for CACG shows specific patterns each year, which indicates a high variability of actual management.

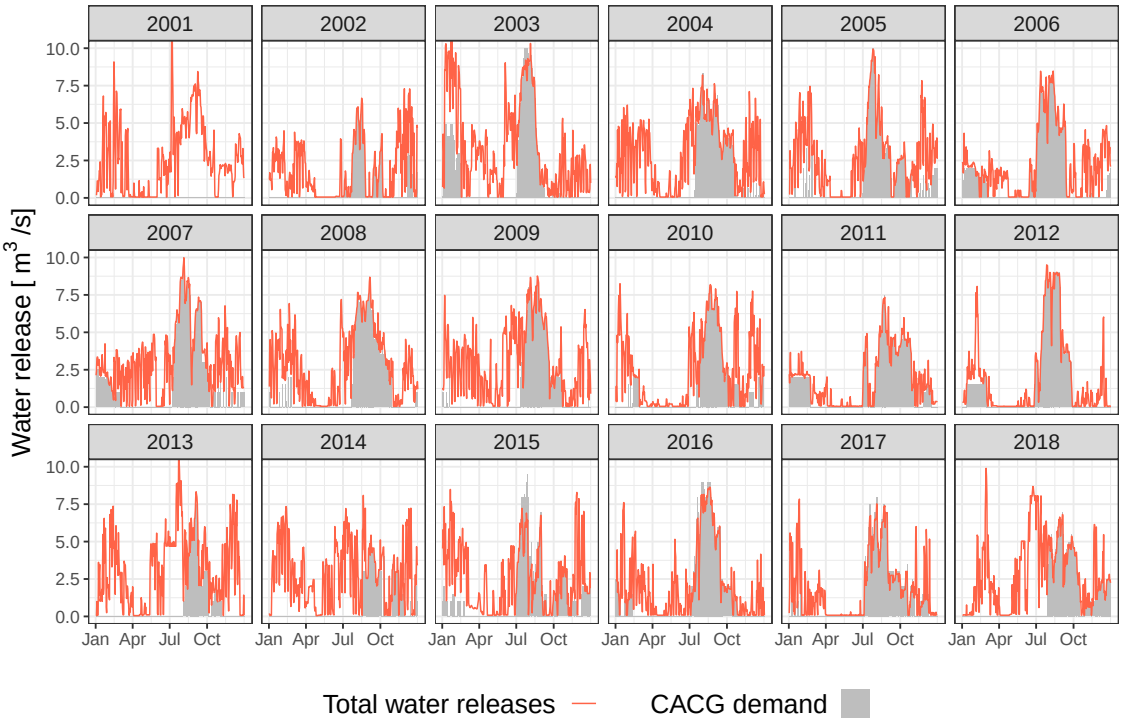

Figure 3.22 – Daily water release from the Eget and Louron groups in comparison with CACG regulartory demand for the period from 01/2001 to 12/2018.

Besides, SHEM provides daily operation information on water level of reservoirs, water transfer among reservoirs. The operation information is from 01/2001 to 12/2018. Figures 3.23 and 3.24 shows the management information of the Eget and Louron hydropower groups for the extracted period from 01/2015 to 12/2017.

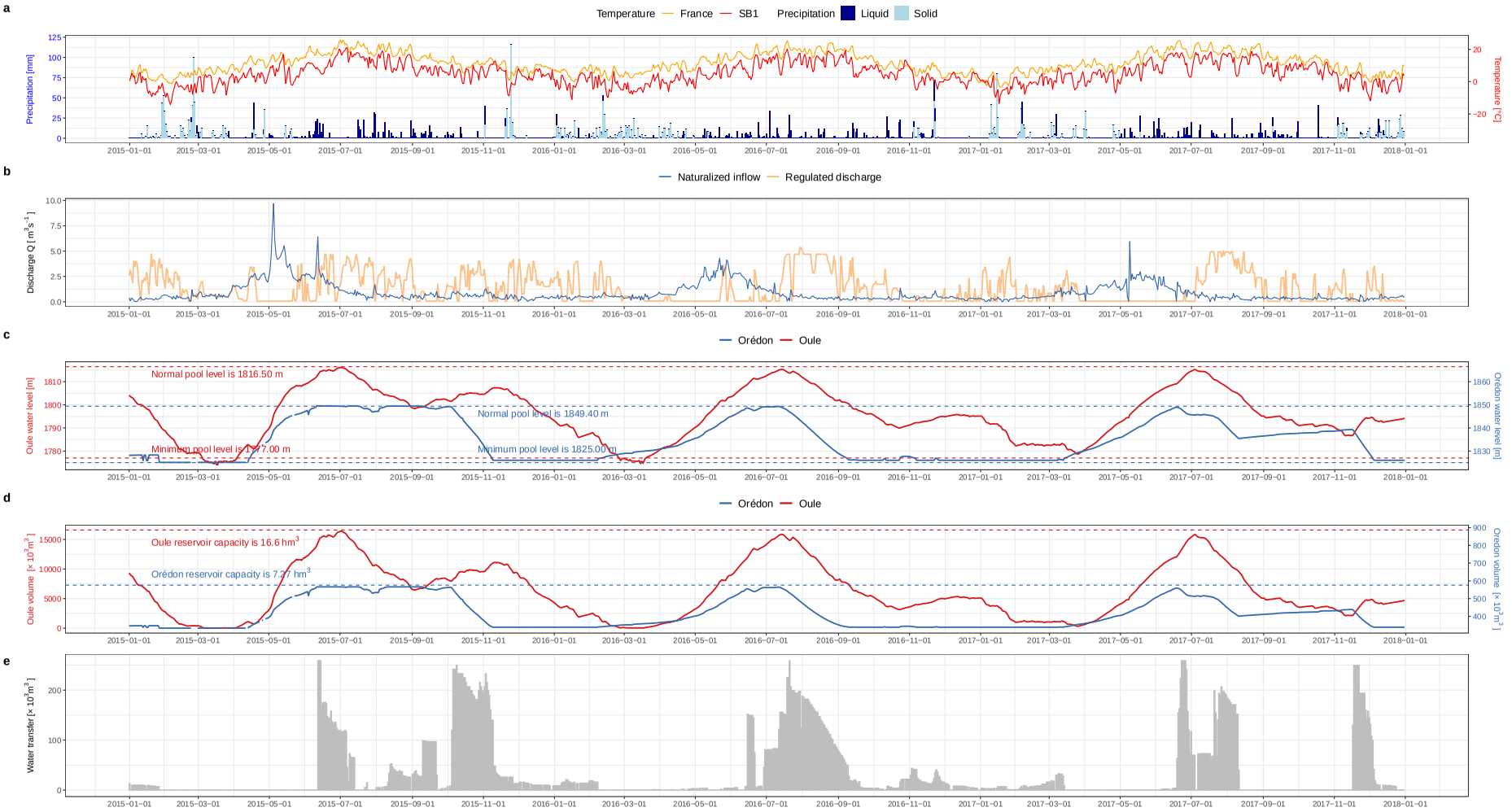

Figure 3.23 – An overview of the operation information in the Eget group for period from 01/2015 to 12/2017: climatic information is extracted from Safran-France (a); the naturalized inflow is compared with the influenced outflow for SB1 (b); water level (c) and water volume (d) for the reservoirs in the Eget group; water transfer from the Orédon reservoir to the Oule reservoir (e).

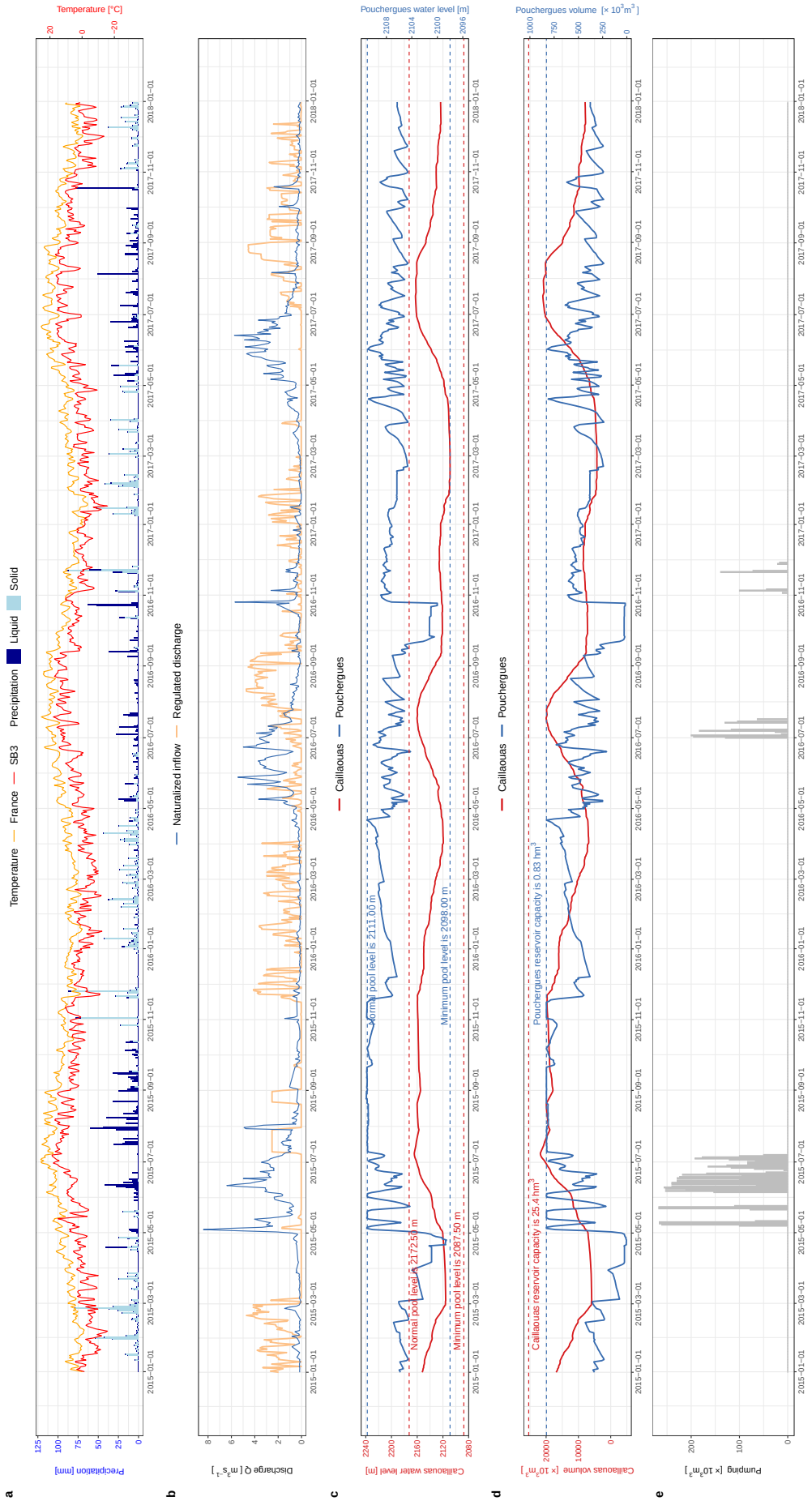

Figure 3.24 – An overview of the operation information in the Louron group for period from 01/2015 to 12/2017: climatic information is extracted from Safran-France (a); the naturalized inflow is compared with the influenced outflow for SB3 (b); water level (c) and water volume (d) for the reservoirs in the Louron group; water pumping from the Pouchergues reservoir to the Caillaouas reservoir (e).

3.2.4 Water management records of CACG

Records for irrigation, drinking, industrial water uses

Water extraction information in SB5 can be extracted from the BNPE[6] in terms of agricultural irrigation, drinking water, and industrial uses. The objective of the BNPE is to record the annual volumes directly withdrawn from the water resource. These volumes are distinguished by location (administrative commune scale), nature (surface water or groundwater) and category of water use. The data availability is from year 2003 to 2017. Figure 3.25 shows the annual water extraction of SB5 based on the BNPE dataset. Surface water is the major water source in SB5 and surface water extraction for irrigation dominates the total water use in SB5. Concerning the spatial distribution of water use, Figure 3.26 shows that drinking water and irrigation extraction from surface water are almost homogeneous for all the sub-basins of SB5 while industrial water extraction is concentrated on two sub-basins of SB5.

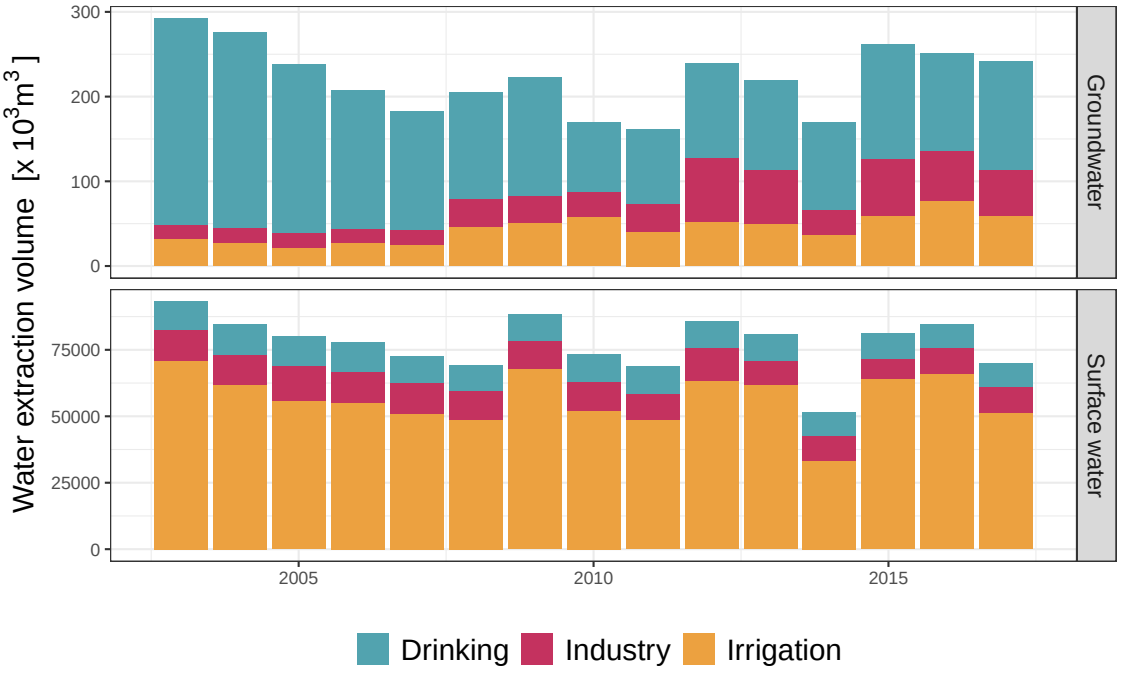

Figure 3.25 – Annual groundwater and surface water extraction of SB5 from the dataset BNPE for drinking water, industrial and irrigation uses from year 2003 to 2017.

In addition, CACG also provides registration of annual drinking water, annual industrial water, and weekly irrigation water releases for the period (CACG, 2019). The annual drinking water and industrial water releases are in period from 2004 to 2018. The weekly irrigation water releases are in period from 1995 to 2020. Figure 3.27 compares water uses for drinking water, industry, and irrigation for the common period 2004-2017 beween BNPE and CACG records. The determinant coefficient (R^2) for the drinking water, industrial, irrigation, and total uses between the two sources of data are 0.24, 0.05, 0.56,

[6]The Banque Nationale des Prélèvements quantitatifs en Eau (BNPE) is the national tool dedicated to the distribution of water abstractions for metropolitan France and the overseas departments (see https://www.bnpe.eaufrance.fr).

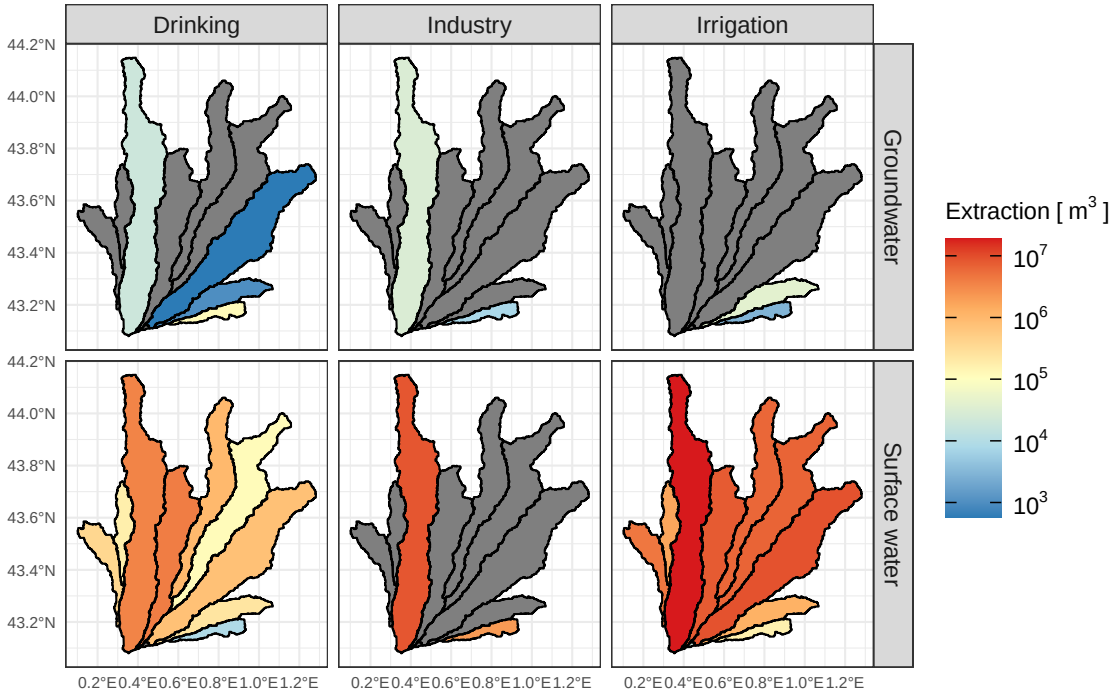

Figure 3.26 – Mean annual groundwater and surface water extraction of SB5 from the dataset BNPE for drinking water, industrial and irrigation uses from year 2003 to 2017 for the ten sub-basins upstream the discharge control points: Beaumarchès, Roquebrune, Nérac, Montestruc, Saint-Antoine, Castelferrus, Larra, Fousseret, Laffite, and Lavet (see Figure 3.20). The color gray means no water extraction.

and 0.67, respectively. Besides, the magnitude of water use volume are similar between the two source of data. As such, the registration of CACG water releases is validated.

In this study, we prefer local information registered by CACG compared to the BNPE extraction data. Water releases from the local water manager (CACG) are considered more reliable to represent the local water demand.

Environmental water management in SB5

CACG manages to maintain a good environmental and ecological status in SB5. The locations of the ten control hydrological stations are illustrated in Figure 3.20. Table 3.5 details the DOE requirement for each hydrological station in SB5. As shown by Figure 3.21, the DOE requirement is maintained in the historical management from 2013 to 2019.

Water extraction and releases

CACG management records in terms of the water extraction by the Neste Canal at Sarrancolin and water releases from the reservoirs in SB5 are provided.

The data availability of water extraction by the Neste Canal is from 10/1961 to 09/2019. The river flow downstream Sarrancolin is measured from 01/1992 to 12/2019. River flow at Sarrancolin can thus be calculated by summing the two series of data. Figure 3.28 shows the regime of water extraction by the Neste Canal at Sarrancolin in comparison with river flows downstream Sarrancolin and at Sarrancolin for the period from 01/1992 to 09/2019. The Neste Canal extracts water in a seasonal pattern with the peak in summer

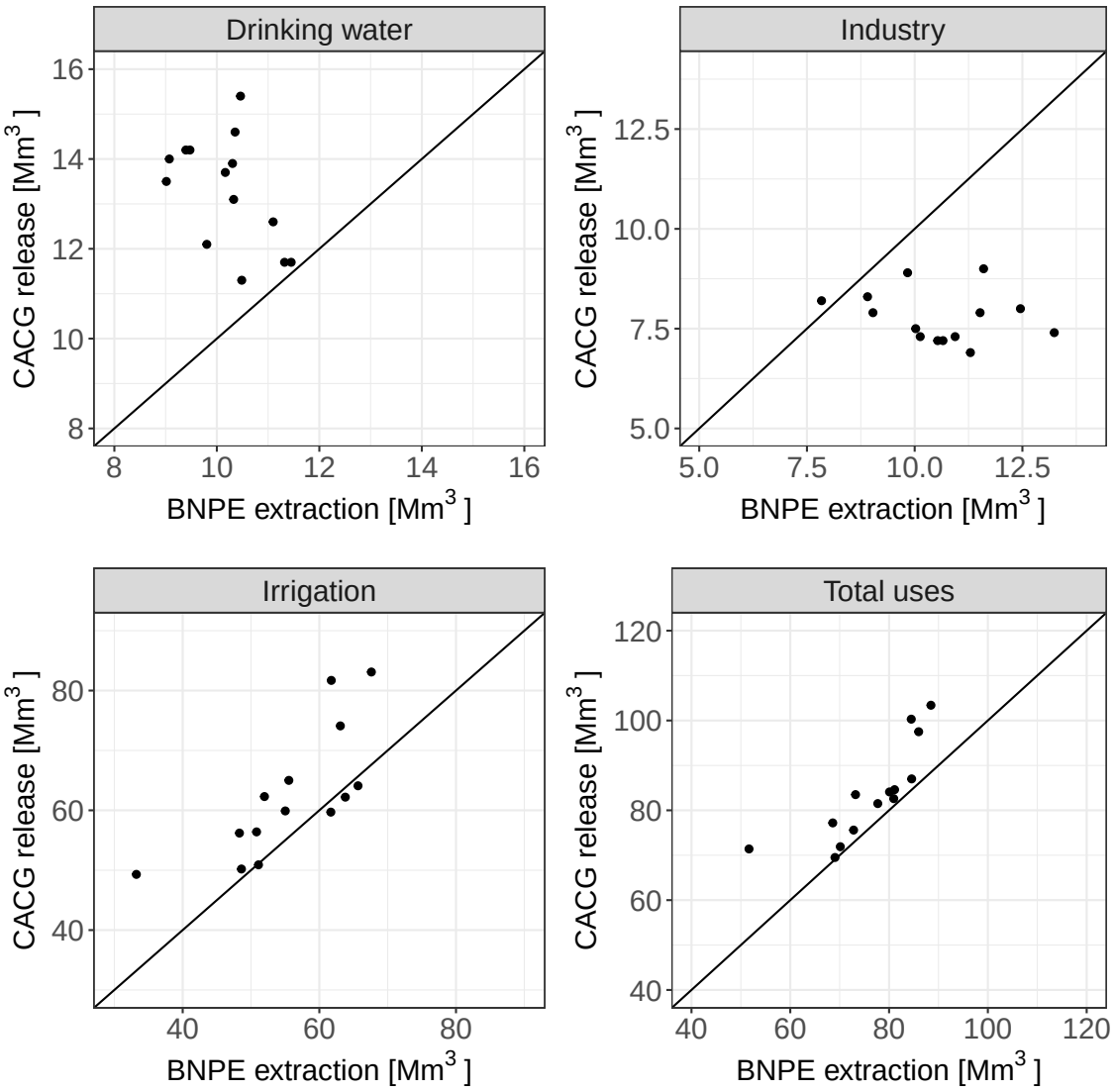

Figure 3.27 – Comparison between BNPE extraction and CACG release records in terms of drinking water, industiral, and irrigation uses for period for year 2004 to 2017.

period due to the request of releasing the 48 Mm^3 volume in the reservoirs managed by SHEM (see Figure 3.22). Diverted volumes are limited by the capacity of the channel (14 m^3/s). A drop of water extraction in spring is the result of the regular maintenance of the Neste Canal. As mentioned before, river flow downstream Sarrancolin should be kept above 4 m^3/s (the DOE value at Sarrancolin) after the extraction by the Neste Canal. As Figure 3.28 shown, the DOE rule at Sarrancolin is well followed.

The storage change data of the 11 reservoirs (Astarac, Baradée, Esparron, Gimone, Lizet, Lizon, Magnoac, Miélan, Puydarrieux, Saint-Frajou, Marcaoué, see Table 3.1) at daily time step are available from 10/2012 to 12/2019. The time series of the 11 reservoir volume changes is validated by the internal calculation of CACG. The total volume of these 11 reservoirs is 68.7 Mm^3 close to the 73.3 Mm^3 of the total 15 reservoirs. The simplification is that the management of the 15 reservoirs in SB5 is considered as one reservoir. As such, a coefficient of 1.07 will be multiplied to the time series of the sum of the 11 reservoir volume to extend to the 15 reservoir volume change in SB5.

Table 3.5 – DOE information of the ten stations.

River	Station	Banque Hydro code	DOE in summer $[m^3/s]$	DOE in winter $[m^3/s]$
Bouès	Beaumarchès	Q0664020	0.20	0.30
Osse	Roquebrune	O6834620	0.37	0.55
Baïse	Nérac	O6692920	1.11	1.35
Gers	Montestruc	O6312520	2.12	2.12
Arrats	Saint-Antoine	O6094010	0.27	0.41
Gimone	Castelferrus	O2883310	0.40	0.48
Save	Larra	O2552910	0.67	1.01
Louge	Fousseret	O0964030	0.19	0.29
Noue	Laffitte	O0295310	0.10	0.15
Lavet	Lavet	-	0.05	0.05
Total	-	-	5.48	6.71

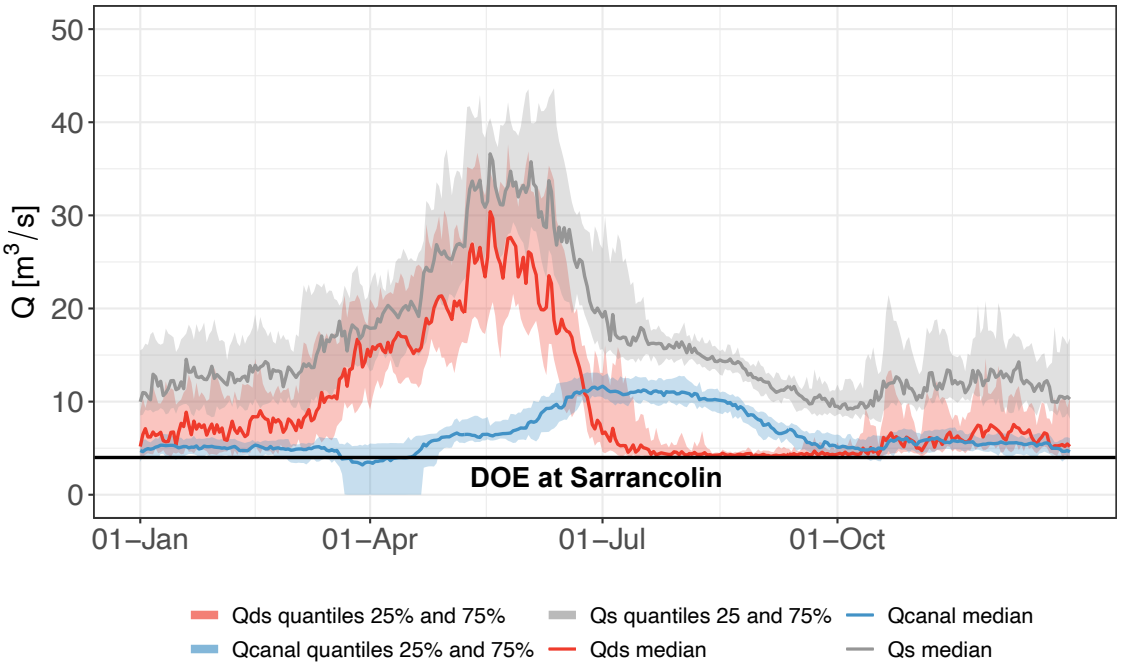

Figure 3.28 – Regime of water extraction (Q_{canal}) by the Neste Canal to feed SB5 in comparison with river flows downstream Sarrancolin (Q_{ds}) and at Sarrancolin (Q_{infs}) for the period from 01/1992 to 09/2019.

Besides, the data availability of water release information from the 15 reservoirs is from 01/2013 to 12/2019. This data is the daily release volume without specifying the purpose of water use. Figure 3.29 shows the regime of volume and release of the 15

reservoirs in SB5 for the period from 01/2013 to 12/2019. Water storage reaches the maximum value of 73.3 Mm^3 at the end of spring. Water release peaks are placed in summer mainly for maize irrigation and for environmental DOE requirement in SB5.

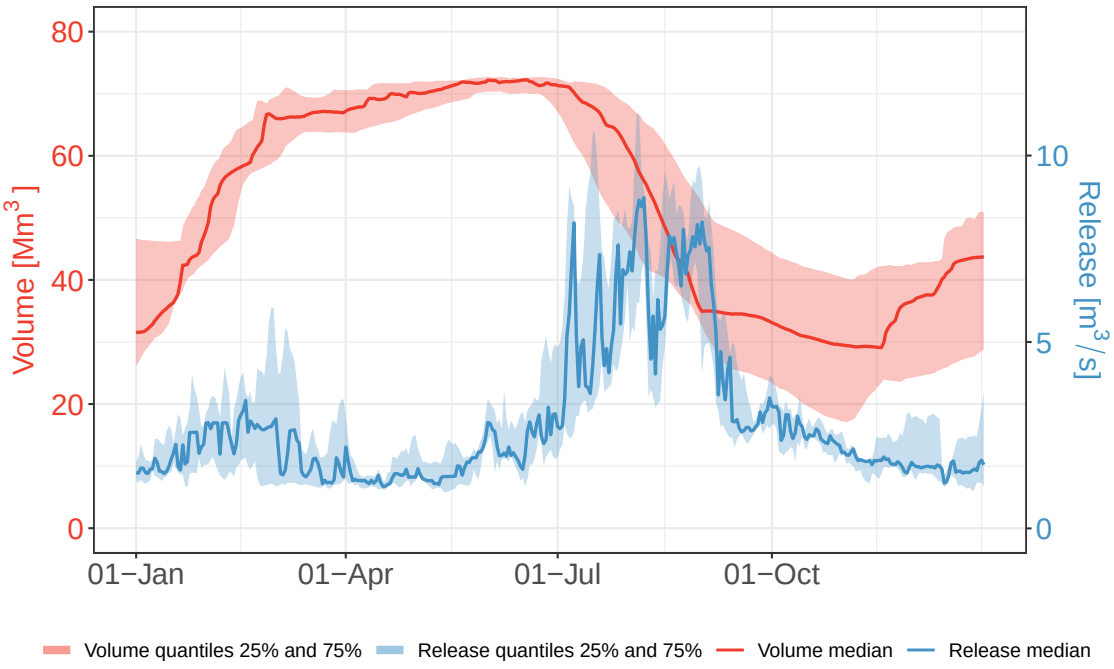

Figure 3.29 – Regime of volume and release of the 15 reservoirs in SB5 for the period from 01/2013 to 12/2019.

3.2.5 Population projections

Historical population and future projection information in the study area is provided by the INSEE [7]. The historical population is provided at the commune scale, which allows an accurate estimation of the number of inhabitants in the study area. However, the future population is projected by the INSEE at the departmental scale over the period from 2013 to 2050. Here, we choose the Gers department to represent the future population in the study area. Figure 3.30 shows the historical and future projected population in the study area.

In order to have a longer record of population to be in line with the period of climate change projections (1961-2100), the INSEE projection is interpolated from 2050 to 1961. As for the period from 2051 to 2100, INSEE declares that there might be a slight decrease of national population between 2040 (69.3 millions) and 2070 (68.1 millions) depending more on the assumptions [8]. This slight decrease downscaled to the Gers department could be considered as a near stable state of population. As such, we consider that the population from 2051 to 2100 remains the same as 2050. The simulated population change over the period from 1961 to 2100 is shown as red line in Figure 3.30.

[7] National Institute of Statistics and Economic Studies, see https://www.insee.fr/en/.
[8] see https://www.insee.fr/fr/statistiques/5893969/

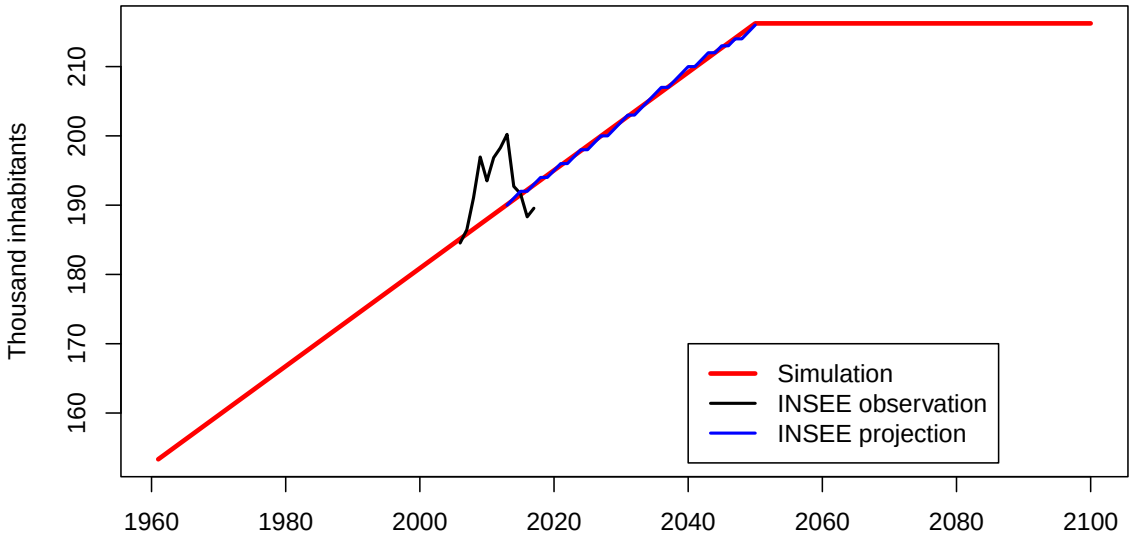

Figure 3.30 – The population information in terms of the observation by INSEE from 2006 to 2017, the projection by INSEE from 2013 to 2050, and the simulation from 1961 to 2100.

3.3 Summary

In summary, the Neste water system relies on the Neste Canal at Sarrancolin that connects the upstream Aure Valley managed by SHEM and the downstream Gascogne region managed by CACG. Water management of the Neste water system is multipurpose with the Aure Valley focusing on the hydropower production and the Gascogne region focusing on the water consumptive demand (drinking water supply, industrial uses, and agricultural irrigation) and the environmental demand. In particular, if the Neste River at Sarracolin is not able to naturally supply necessary water resource for the Gascogne region, CACG demands extra water release from the reservoirs managed by SHEM with an annual quota. The management of the Neste water system is operated on annual basis and the behavior of water managers (i.e., SHEM and CACG) is highly seasonal.

Given the complexity of the Neste system, the next modelling and analysis work in terms of the water resource estimation, demand, and management requires a number of hypotheses:

1. The preferred reference period should start from the beginning of the 21st century considering the current management configuration (e.g., maximum extraction capacity by the Neste Canal, strategies for energy production, water share quota for CACG in the reservoirs managed by SHEM)

2. The management of the reservoirs supplying the Pragnères plant will not be considered and the regulatory obligations of the reserved flow for the environment will be assumed to be respected.

3. The reservoirs in the Aure Valley will be examined at a certain level of aggregation sufficient to answer the questions of adaptation and consistent in terms of management. The Caillaouas and Pouchergues reservoirs will form a single reservoir because they are jointly managed and it is indeed difficult to assess the exchanges between the two reservoirs.

4. Water resource estimation in the Gascogne region will be conducted on a global scale (i.e., the ten sub-basins upstream the hydrological control stations will be aggregated into one sub-basin). Similarly, water demand and reservoir water management managed by the CACG will also be modelled on a global scale. Besides, environmental quality will be examined by the sum of minimum flow requirement in the ten rivers of the Gascogne region (Bouès, Osse, Baïse, Gers, Arrats, Gimone, Save, Louge, Noue, and Lavet).

Table 3.6 presents the data collected and the application of the data. SB1-5 represent the sub-basin upstream the Oule reservoir, the sub-basin upstream the Orédon reservoir, the sub-basin upstream the Caillaouas-Pouchergues reservoirs, the sub-basin between Sarrancolin and the outlets of the four reservoirs above, and the Gascogne region, respectively.

The complexity of the Neste water system is characterized by numerous water infrastructures managed by different water managers with different management rules for various water uses, which causes numerous data sources from different water managers. Therefore, the uncertainties on the time series and the period of their availability are heterogeneous that makes the analysis and thereafter the modelling difficult.

Generally, the common period of water management for all the data in the Aure Valley is from 01/2002 to 08/2014. The common period of water management for all the data in the Gascogne region is from 01/2013 to 07/2018. The naturalized flow for SB1-5 will be used to calibrate the hydrological model to estimate the water resources availability. Water release registrations, water extraction information, and water management operation data will be used to construct water demand and management models of the Neste water system. Climatic drivers are the forcing data into the developed models above.

Table 3.6 – A summary of data collection.

Data type	Data length	Data use
Climatic drivers		
Safran-France	08/1958-07/2018	Hydrological modelling, irrigation water demand, energy demand modelling
Safran-PIRAGUA	09/1979-08/2014	Hydrological modelling
MODIS	09/2000-04/2018	Hydrological modelling
Climate projections	01/1961-12/2100	Impact assessment
Water resource estimation		
Naturalized Q of SB1, SB3, SB4	01/2001-12/2018	Hydrological modelling
Naturalized Q of SB2	07/2014-12/2018	Hydrological modelling
Naturalized Q of SB5	01/2013-12/2019	Hydrological modelling
Observed Q downstream Sarrancolin	01/1992-12/2019	Hydrological modelling and water management modelling
Water demand and management		
BNPE	2003-2017	Drinking water, industrial, and irrigation demand modelling
CACG registration for drinking water and industrial uses	2004-2018	Drinking water and industrial demand modelling
CACG weekly registration for irrigation	1995-2020	Irrigation demand modelling
DOE requirement	-	Environmental management
SHEM releases for CACG demand	01/2002-12/2018	CACG demand and water management modelling
SHEM reservoir operation	01/2001-12/2018	Energy demand modelling, Water management modelling
Canal extraction by CACG	10/1961-09/2019	Hydrological modelling and water management modelling
CACG reservoir operation	01/2013-12/2019	Drinking water, industrial, irrigation, environmental demand and management modelling
Population information		
Population	1961-2100	Drinking water demand modelling

4

Water resources estimation

This chapter presents the hydrological modelling employed for this work that contributes to estimate water resources availability of the Neste system.

Contents

4.1 Implementation of models for water resources estimation 86

4.1.1 Introdution 86

4.1.2 The hydrological model GR6J-CEMANEIGE 86

4.1.3 Performance assessment of GR6J-CEMANEIGE 89

4.1.4 Simulation results 92

4.2 Water resources model for the Aure Valley 100

4.2.1 The implementation and performance of the model 100

4.2.2 Water accounting for the Aure Valley 102

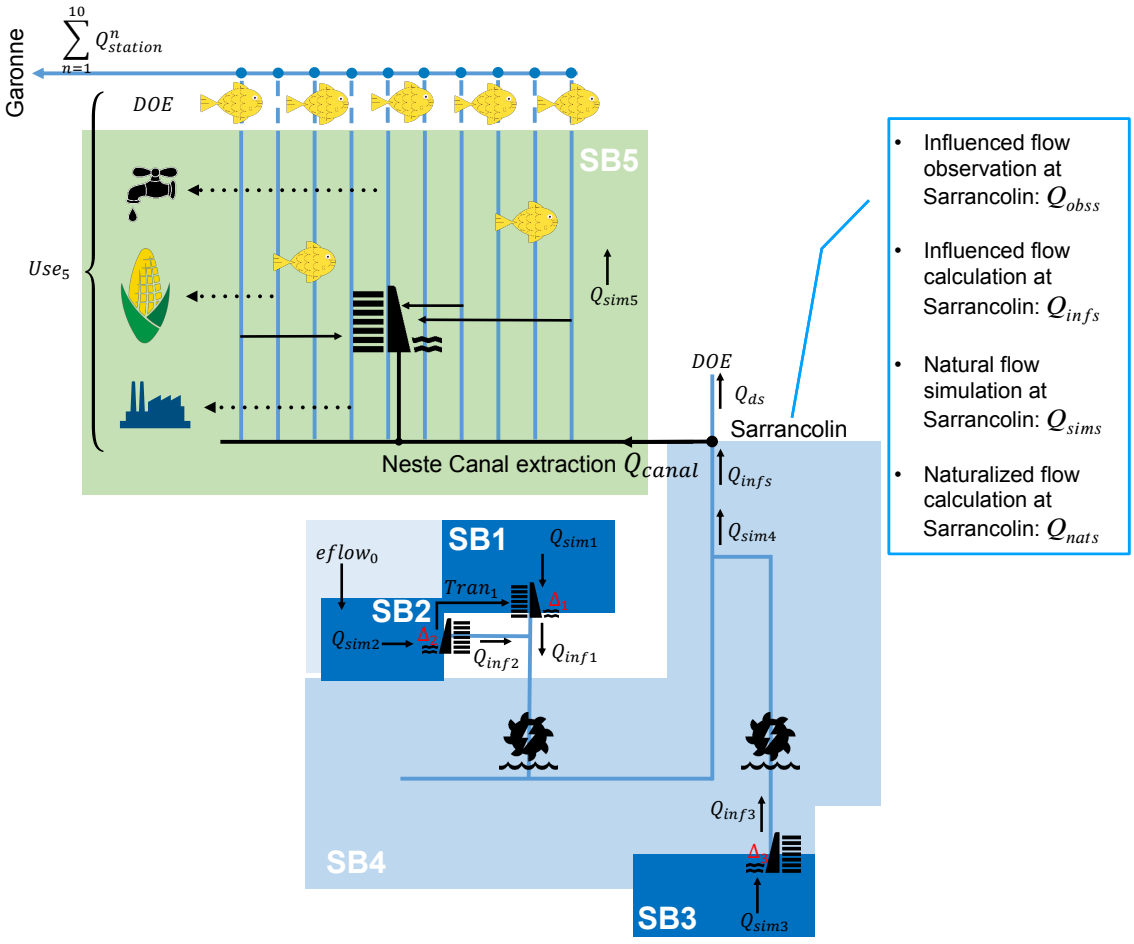

Figure 4.1 – A simplified schema of the Neste water system and the associated abbreviations used in this chapter.

4.1 Implementation of models for water resources estimation

4.1.1 Introdution

In order to estimate water resources of the Neste water system, hydrological models can be implemented to understand and to simulate the hydrological processes. Hydrological models are the simplifications of hydrological processes in reality, transforming meteorological information into runoff with the consideration of physical characteristics of the study area. In this work, water resources of the sub-basins SB1-5 in the Neste water system are simulated to represent the inflows into the reservoirs and the environmental components of water management.

4.1.2 The hydrological model GR6J-CEMANEIGE

The hydrolgocal model employed to estimate water resources in SB1-5 is the GR6J model (Pushpalatha et al., 2011), a six parameter lumped model at daily time step developed by the Catchment Hydrology research group of INRAE[1]. This conceptual lumped rainfall-runoff model was developed to improve low-flow simulation based on the extensively used GR4J hydrological model (Perrin et al., 2003) for French basins.

Since the hydrological processes in the Aure Valley (SB1-4) is dominated by spring snowmelt, a model that can represent snow information is necessary. A four parameter semi-distributed degree-day snow module CEMANEIGE can be coupled with the GR6J model (Riboust et al., 2018; Valéry et al., 2014a,b). The initial version of the CEMANEIGE module can generally be adjusted on ungauged catchments in France where the influence of snow is mild, as it has an acceptable performance with default parameter values (Valéry et al., 2014a,b). The recent work by Riboust et al. (2018) has used the snow cover area (SCA) observations from MODIS to improve the performance of CEMANEIGE in representing snow content. It takes into account the snow accumulation and melt hysteresis between SCA and snow water equivalent (SWE), which is the dynamic lag between the two states of snow. In the real world, SCA increases rapidly and remains stable whereas SWE increases more slowly during the accumulation period. The situation is opposite in the snowmelt process. This hysteresis results in different patterns of snow state, which is essential for reservoir refill management in the Aure Valley.

Figure 4.2 shows the structure of the coupled GR6J-CEMANEIGE hydrological model. Table 4.1 shows the parameters to be calibrated in the GR6J-CEMANEIGE model. Three time series are needed as the meteorological inputs of the model: (i) potential evapotranspiration, (ii) precipitation, and (iii) air temperature time series. Two time series are simulated as the outputs of the model: (i) catchment runoff and (ii) SCA time series. As such, the coupled GR6J-CEMANEIGE hydrological model should be calibrated not only with discharge observations but also with the observed SCA of catchment. The description of model structure and functionality is given below.

We describe how the CEMANEIGE works and be coupled with the GR6J hydrological model. The first step of CEMANEIGE is to divide the catchment into five equi-surface

[1]National Research Institute for Agriculture, Food and Environment (see https://webgr.inrae.fr/)

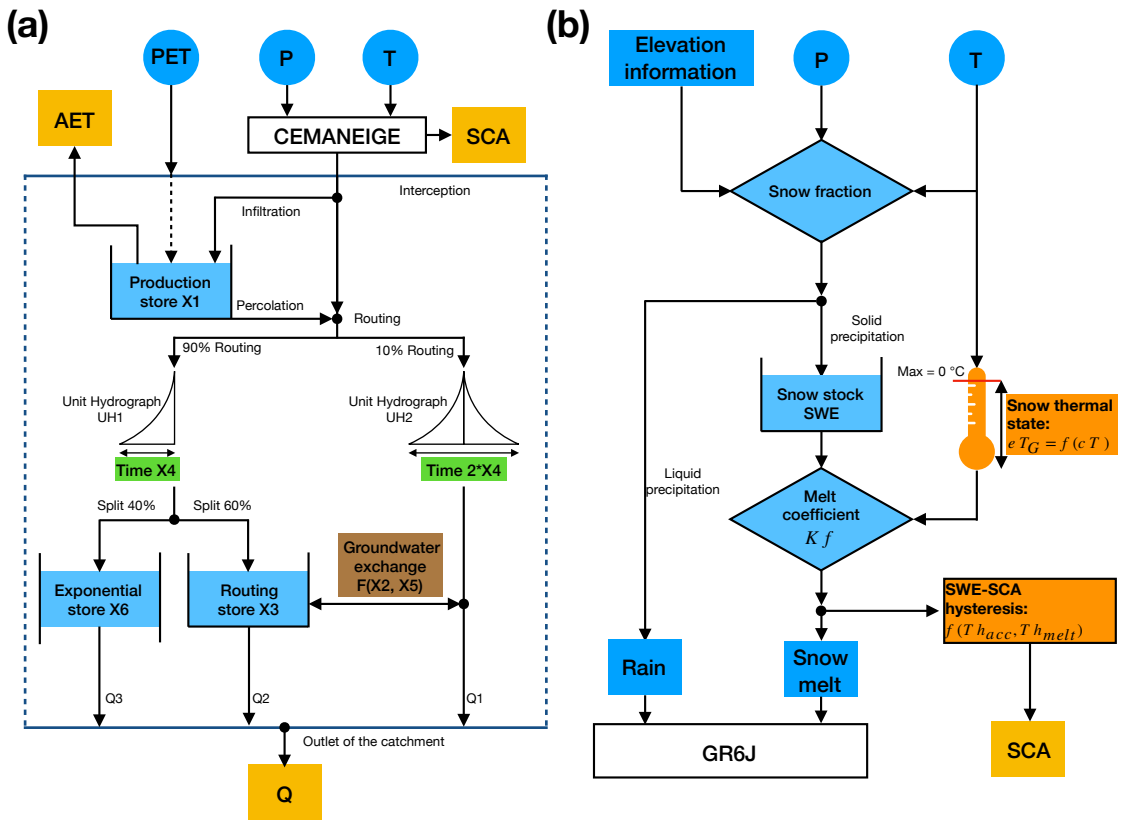

Figure 4.2 – Schematic representation of the GR6J hydrological model (a) (modified from (Pushpalatha et al., 2011)) coupled with a snow module CEMANEIGE (b) (modified from (Riboust et al., 2018)). The meteorological inputs of the model are labelled as blue circles: potential evapotranspiration (PET), precipitation (P), and temperature (T). The outputs of the model are labelled as yellow squares: actual evapotranspiration (AET), runoff (Q), and snow cover area (SCA).

elevation bands based on the hypsometric information of the catchment. The snow content is calculated for each equi-surface elevation band as follow:

1. The representative precipitation and temperature are extrapolated from the precipitation and temperature of inputs. The snow fraction of precipitation is calculated based on temperature, which allows dividing precipitation into liquid-precipitation (rain) and solid-precipitation stored in the snow stock reservoir (snow accumulation process expressed as SWE). The cold content of the snowpack in the reservoir (eT_G, the snowpack thermal inertia in unit °C) is modulated by a weighting coefficient cT that links the eT_G value of previous day and current air temperature. The maximum eT_G value is set to be 0 °C.

2. When the current eT_G value is 0 °C and current air temperature is larger than 0 °C, snow has a potential to melt. A degree-day coefficient Kf is involved in this process to determine how much water can be melted as a maximum limit. The actual snow melt is calculated by the current SCA value. The more the SCA decreases, the more snowpack is melted.

3. In order to take account snow hysteresis, the SCA value is calculated in two ways based on whether snow is accumulated (ΔSWE > 0) or melted (ΔSWE < 0). If

Table 4.1 – Parameters of the hydrological model GR6J coupled with the CEMANEIGE snow module

GR6J	
X1[mm]	Capacity of the production reservoir
X2[mm/d]	Coefficient of the underground exchange
X3[mm]	Capacity of the routing reservoir
X4[d]	Base time of unit hydrograph
X5[-]	Change sign threshold of the underground exchange
X6[mm]	Control of the recession slope
CEMANEIGE	
cT[-]	Weighting coefficient for snowpack thermal state
Kf[°C/d]	Degree-day melt coefficient
Th_{acc} [mm]	SWE-SCA threshold in snow accumulation
Th_{melt} [mm]	SWE-SCA threshold in snowmelt

Note: cT and Kf are the two parameters need to be calibrated for the CEMANEIGE module without considering SWE-SCA hysteresis; cT, Kf, Th_{acc}, and Th_{melt} are the four parameters need to be calibrated for the CEMANEIGE module with considering SWE-SCA hysteresis.

snow is accumulated, current SCA changes is calculated with ΔSWE divided by the parameter Th_{acc}. The current SCA value is thus the sum of the SCA value of precious day and the SCA change with the maximum limit of 1 and minimum limit of 0. If snow is melted, Riboust et al. (2018) proposed a linear melting curve whose slope, the parameter Th_{melt}, is determined by the mean annual precipitation of the elevation band considered. The current SCA value is thus the current SWE in the snow stock reservoir divided by the parameter Th_{melt} with a maximum limit of 1. The melting curve is more gradual than the accumulation curve as snowmelt process takes more time than snow accumulation process.

The steps 1-2 above are the simulation processes employed by the initial version of the CEMANEIGE module as in Valéry et al. (2014a,b). The steps 1-3 are the simulation processes employed by the CEMANEIGE module with consideration of SWE-SCA hysteresis as in Riboust et al. (2018). After the above steps for each equi-surface elevation band, the sum of the initially determined liquid fraction and the snowmelt are then forced into the GR6J hydrological model as precipitation. The interception process determines the net precipitation and net evapotranspiration at the catchment scale. If the net precipitation is not 0, part of it infiltrates to the production reservoir X1. However, if the net evapotranspiration is not 0, the actual evapotranspiration is subtracted from the content of the production reservoir. Then, the percolation from the production reservoir and the amount of water not infiltrated are fed into the routing part of the model. 90% of routing flow is routed, via a first unit hydrograph (UH1), to the routing reservoir X3 and the exponential reservoir X6. 10% of routing flow is routed, via a second unit hydrograph (UH2), to the outlet of the catchment. The groundwater exchange process and an addi-

tional exponential routing reservoir X6 contribute to low-flow simulations. Finally, the sum of the flows from direct routing and routing reservoirs are transferred to the outlet of the catchment as the daily discharge.

4.1.3 Performance assessment of GR6J-CEMANEIGE

Data and model configuration

As shown in Table 4.1, the GR6J-CEMANEIGE hydrological model with considering the SWE-SCA hysteresis has ten parameters to calibrate while that without considering the SWE-SCA hysteresis has eight parameters to calibrate. Table 4.2 summarizes the version of model (ten or eight calibration parameters), meteorological forcing, calibration benchmark, and simulation length applied to all the sub-basins of the Neste water system. The choice of the parameters and forcings is based on both a performance assessment and a sensitivity analysis for the two sets of GR6J-CEMANEIGE model and two Safran reanalyses are presented in Appendix A.

The hydrological calibration and simulation of SB1-4 is conducted with the GR6J-CEMANEIGE model with 10 parameters while those of SB5 is conducted with the model of 8 parameters. This is because SB1-4 are dominated by snow process while SB5 has a low influence by snow process. As illustrated in Figure 3.4, the winter temperature in SB5 is mostly larger than 0 °C. As such, the two parameters of the CEMANEIGE module for SB5 are fixed with default values with cT = 0.17 and Kf = 6.80 °C/d, respectively (Valéry et al., 2014a,b). The meteorological forcing for the water resources simulation of SB2 and SB5 is Safran-France data due to the limited length of naturalized inflows.

Table 4.2 – A summary of the calibration elements of the GR6J-CEMANEIGE hydrological model for all the sub-basins in the Neste water system.

Area	Model parameters	Meteorological forcing	Benchmark	Simulation length
SB1	10	PET, P, and T from Safran-PIRAGUA	Q and SCA	01/2001-08/2014
SB2	10	PET, P, and T from Safran-France	Q and SCA	07/2014-07/2018
SB3	10	PET, P, and T from Safran-PIRAGUA	Q and SCA	01/2001-08/2014
SB4	10	PET, P, and T from Safran-PIRAGUA	Q and SCA	01/2001-08/2014
SB5	8	PET, P, and T from Safran-France	Q	01/2013-07/2018

Note: Q and SCA are the naturalized inflow and the snow cover area extracted from the gap-filled MODIS snow product, repectively. The information on Q and SCA is presented in the previous section.

Model calibration

Three steps in the calibration process is presented. First, a transformation on target values of hydrological simulation is often used in calibration process to better focus on high or low value simulation performance (Garcia et al., 2017). For example, log(Q) is a log-transformed discharge to focus on low flows (Santos et al., 2018). This study has no tendency to focus on high or lows flows but the total water resources instead. A root-square transformation on Q, which does not favor high or low flow, is thus used to calibrate model (Garcia et al., 2017). No transformation has been applied on SCA.

Second, the KGE criterion is current commonly used criterion for the assessment of hydrlogical model performance (Gupta et al., 2009; Kling et al., 2012). KGE in Gupta et al. (2009) is improved to a modified version in Kling et al. (2012) and the new version has a better ability to evaluate variability error. The formulation of the improved KGE criterion is presented bellow:

$$KGE = 1 - \sqrt{(r-1)^2 + (\beta-1)^2 + (\gamma-1)^2} \tag{4.1}$$

where

- r, the Pearson correlation coefficient, evaluates the error in shape and timing between observed values and simulated values:

  $$r = \frac{cov(obs, sim)}{{\sigma_{obs}}^2 {\sigma_{sim}}^2}$$

  where the numerator is the covariance between observed and simulated values; ${\sigma_{obs}}^2$ and ${\sigma_{sim}}^2$ represent the standard deviation of observed and simulated values, respectively.

- β, evaluates the bias between observed and simulated values:

  $$\beta = \frac{m_{sim}}{m_{obs}}$$

  where m_{sim} and m_{obs} represent the mean of observed and simulated values, respectively.

- γ, the ratio between the observed and simulated coefficients of variation, evaluates the variability error:

  $$\gamma = \frac{m_{obs}\sigma_{sim}}{m_{sim}\sigma_{obs}}$$

The KGE criterion varies from $-\infty$ to 1. The larger the KGE, the better the model performance. In the calibration process, the most suitable parameters are obtained when the criterion KGE reaches the highest value in the optimization.

Third, two objective functions for two model configurations in Table 4.2 should be formulated and optimized. In the model set of the hydrological GR6J-CEMANEIGE with hysteresis (10 parameters), there are two benchmark observations: naturalized inflow Q and SCA observations from MODIS. An objective function involved discharge Q and SCA should be established. The work in Riboust et al. (2018) tested several combinations of both Q and SCA as the objective functions and concluded that a combination of 75% weighting on Q and 5% on each elevation band is the most advantageous compromise for

model performance evaluation. If the function has a larger weight on Q, the model gives more focus on discharge to calibrate and the situation is the same to SCA. As such, the formulation of the objective function for this model set is:

$$\begin{cases} f = a \times KGE(\sqrt{Q}) + \sum_{i=1}^{5} b_i \times KGE(SCA_i) & (4.2) \\ a + \sum_{i=1}^{5} b_i = 1 & (4.3) \end{cases}$$

where a is the weighting coefficient for runoff Q calibration, b_i the weighting coefficient for SCA_i calibration of elevation zone i. The value of a is 75% and b 5%.

As for the model set of the GR6J-CEMANEIGE without hysteresis (8 parameters), only one benchmark observations, naturalized inflow Q, should be calibrated. The objective function is thus formulated:

$$f = KGE(\sqrt{Q}) \tag{4.4}$$

Model performance

In order to test the calibration robustness (parameter transferability, see Heuvelmans et al. (2004)) of the GR6J-CEMANEIGE model, split-sample tests are conducted. SB1, SB3, and SB4 are chosen as examples to test the hydrological model parameter transferability because their simulation length is longer (see Table 4.2). The common period for all the data is from 01/2001 to 08/2014. This almost 14-year period is divided in half for model calibration and validation, separately. Meteorological forcing and benchmarks are from 01/2001 to 08/2007 are used to calibrate the hydrological model. The rest period from 09/2007 to 08/2014 is used for validation assessment with the parameters obtained in the calibration. Then, the process is turned around with the period from 09/2007 to 08/2014 for calibration and the period from 01/2001 to 08/2007 for validation assessment. Note that in each evaluation, the beginning two years are chosen to "warm-up" the model.

Table 4.3 shows the KGE values for SB1, SB3, and SB4 in the split-sample tests. However, SB2 and SB5 are not able to use the split-sample tests due to their short data length (the limitation of naturalized inflows). The KGE values of Q indicate that the model generally performs satisfactorily in simulating Q with the KGE values in validation period close to the those in calibration period. However, SB1 shows a lower performance for the validation period from 01/2001 to 08/2007, which could be attributed to the uncertainties of naturalized inflows. Besides, the high KGE values of SCA in 5 elevation bands indicate that the model can well reproduce the snow cover changes with all KGE values above 0.70, which is highly related to the implementation of the SWE-SCA hysteresis.

As such, the parameter transferability of the GR6J-CEMANEIGE model for SB1, SB3, and SB4 are justified by the overall good KGE performance. Here, we investigate the model performance for the whole data length period for SB1-5. Table 4.4 shows the KGE performance for SB1-5 over this period. The results indicate the satisfied model simulation in reproducing natural water inflows and snow cover changes. The calibrated parameters over the whole period are presented in Table 4.5. Note that the value of X1 for SB3 departs from those obtained by other catchments. The reason is probably due to the major land cover of bare rocks in SB3 that is characterized by low soil water content and low evapotranspiration processes. By contrast, other catchments (SB1, SB2, SB4, and

Table 4.3 – GR6J-CEMANEIGE performance (KGE values) for for SB1, SB2, and SB4 in the split-sample tests.

	$\sqrt{Q}$	SCA_1	SCA_2	SCA_3	SCA_4	SCA_5	$\sqrt{Q}$	SCA_1	SCA_2	SCA_3	SCA_4	SCA_5
	Calibration (01/2001-08/2007)						Validation (09/2007-08/2014)					
SB1	0.79	0.79	0.91	0.91	0.93	0.93	0.70	0.76	0.89	0.92	0.95	0.94
SB3	0.83	0.83	0.90	0.92	0.92	0.87	0.84	0.84	0.93	0.93	0.92	0.83
SB4	0.87	0.74	0.74	0.72	0.87	0.92	0.86	0.75	0.75	0.73	0.87	0.92
	Calibration (09/2007-08/2014)						Validation (01/2001-08/2007)					
SB1	0.81	0.78	0.89	0.92	0.94	0.93	0.65	0.81	0.90	0.91	0.92	0.91
SB3	0.90	0.79	0.90	0.93	0.93	0.90	0.79	0.79	0.87	0.88	0.90	0.90
SB4	0.86	0.78	0.80	0.80	0.91	0.90	0.85	0.74	0.77	0.77	0.90	0.90

Notes: SCA_{1-5} represent the snow cover area from the lower to the higher elevation band, respectively.

SB5) are covered by forest and meadow. Thus, the values of X1 for these catchments are larger than that of SB3 due to larger soil water content and more active evapotranspiration processes.

Table 4.4 – GR6J-CEMANEIGE performance (KGE values) for SB1-5 over the whole period of data length.

	Calibration period	$\sqrt{Q}$	SCA_1	SCA_2	SCA_3	SCA_4	SCA_5
SB1	01/2001-08/2014	0.80	0.80	0.90	0.92	0.93	0.92
SB2	07/2014-07/2018	0.72	0.80	0.92	0.96	0.95	0.88
SB3	01/2001-08/2014	0.83	0.81	0.90	0.92	0.93	0.89
SB4	01/2001-08/2014	0.86	0.75	0.77	0.76	0.89	0.91
SB5	01/2013-07/2018	0.95	-	-	-	-	-

4.1.4 Simulation results

Figures 4.3, 4.4, 4.5, and 4.6 show the simulation results of $\sqrt{Q}$ and SCA regimes over the whole data length period (see Table 4.4) for SB1-4 by applying the GR6J-CEMANEIGE model with a consideration of SWE-SCA hysteresis (10 parameters). Figure 4.7 shows the simulation results of $\sqrt{Q}$ regime over the whole data length period (see Table 4.4) for SB5 by appling the GR6J-CEMANEIGE model without considering SWE-SCA hysteresis (8 parameters). The discharge Q is transferred to $\sqrt{Q}$ so as to illustrate the performance of high and low flow simulations in figures.

The GR6J-CEMANEIGE model is efficient in simulating the hydrological regime as the simulated Q follows the variability of the naturalized inflow and can capture the high peaks and low flow spells. We can observe that the recession limbs for SB1-4 during

Table 4.5 – Parameters of the GR6J-CEMANEIGE model obtained in the calibration over the whole period of data length.

	GR6J					
	X1 [mm]	X2 [mm/d]	X3 [mm]	X4 [d]	X5 [-]	X6 [mm]
SB1	256.55	0.51	61.01	1.12	-0.03	18.91
SB2	14.30	0.53	38.86	1.19	-0.03	11.25
SB3	0.01	1.63	30.29	1.17	0.39	7.77
SB4	306.61	0.84	51.82	1.39	0.38	20.91
SB5	160.74	-0.52	13.11	2.22	0.17	10.04
	CEMANEIGE					
	cT [-]	Kf [°C/d]	Th_{acc} [mm]	Th_{melt} [mm]		
SB1	0.91	3.75	8.45	0.24		
SB2	0.89	3.90	21.40	0.58		
SB3	0.95	3.09	9.32	0.20		
SB4	0.88	3.40	7.30	0.38		
SB5	0.17	6.80	-	-		

summer period are well fitted. However, the spring flow is underestimated and the winter flow is overestimated for SB1-4. The low quality of the naturalized inflow of SB2 results in lower performance of Q simulation. Besides, as for SB5, high flows in winter and spring are well simulated while the recession limb during summer and low spells during autumn have a lower performance. This is probably due to the quality of naturalized inflows of SB5 in different seasons. The reasons are: (1) note that SB5 is not really a catchment but a combination of catchments (see Figure 3.5) and a consideration of SB5 as a whole by the hydrological model might increase the bias of river flow estimation for each catchment in SB5; (2) there are many gaps in the naturalized inflows depending on the problems of measurement (many gauging stations), no major influence in winter, and high uncertainties in summer due to many sources of perturbation. Water management in SB5 is intense in summer and autumn mainly for irrigation and DOE requirement. The observed low flows in the ten stations in this period could amplify the calculation or data registration errors.

From the SCA changes for SB1-4, the module CEMANEIGE can well reproduce the seasonality of snow cover changes in the five elevation bands, as well as the accumulation phase of snow and relatively tardy melting processes. Besides, higher attitudinal elevation band shows longer snow cover duration as expected. However, the snow melting process simulation is less efficient than the snow accumulation process given the simple characteristics of the empirical degree-day model in representing snow thermal state changes (Riboust et al., 2018). SCA variations for SB1-4 are well simulated with a high performance in high elevation bands and a moderate performance in medium elevation bands. This can be attributed to the high variability of snow cover in moderate elevation bands

which is difficult to represent in the model.

In summary, from the evaluation of the GR6J-CEMANEIGE hydrological model above considering the water resources aspects of Q and SCA, this model shows an overall good performance in representing water resources of the sub-basins in the Neste water system. Indeed, the snow component of the sub-basins, especially SB1-4, has a dominant influence on the hydrology (and snow processes are particularly difficult to model). In this study, we concentrate on the SCA changes instead of SWE changes because SCA data is richer thanks to satellite images. Moreover, the quality of naturalized inflows plays an important role in hydrological modelling. As such, water accounting in these highly anthropogenic catchments is thus essential.

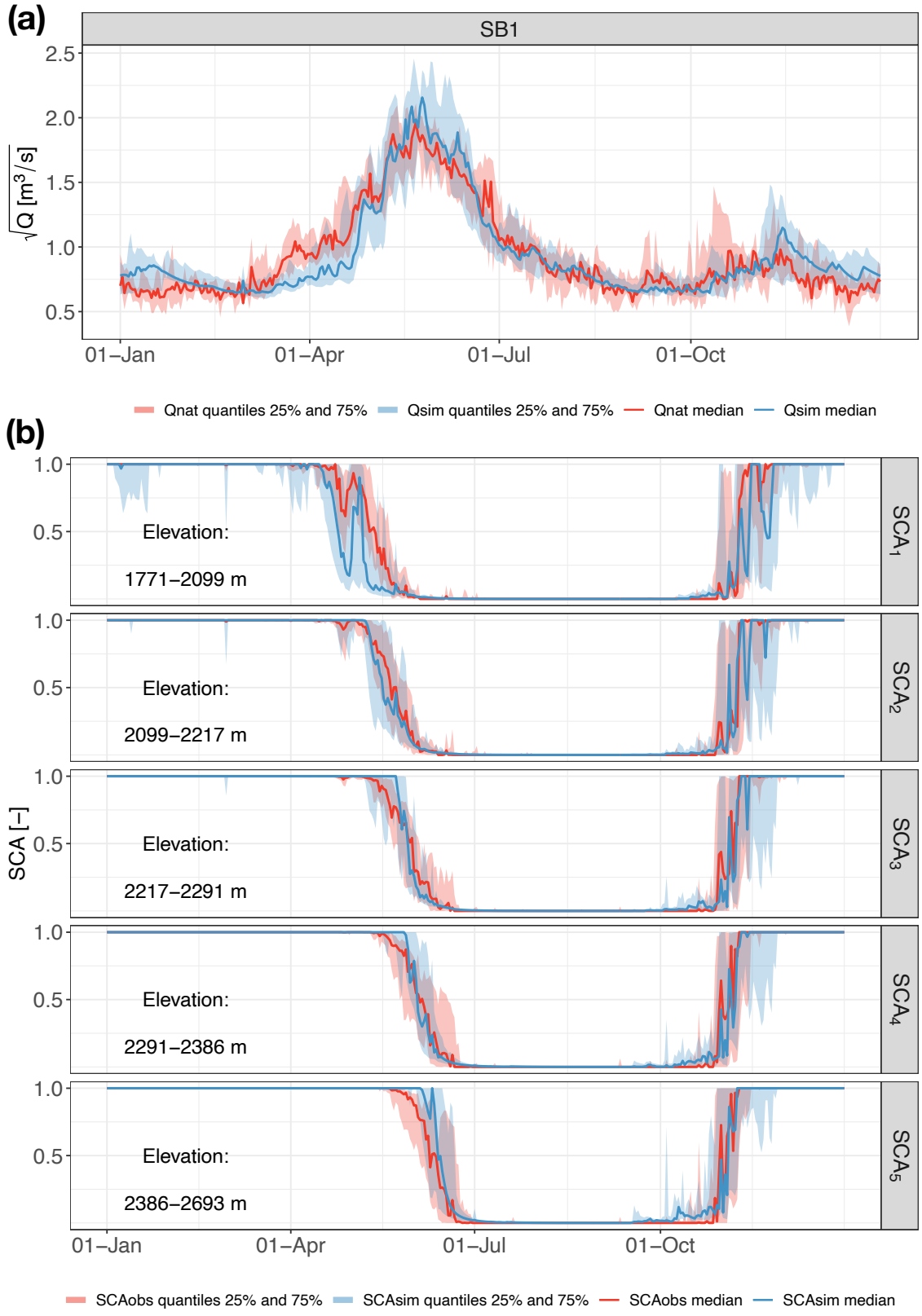

Figure 4.3 – (a) Simulated $\sqrt{Q}$ regime compared with naturalized $\sqrt{Q}$ regime for SB1; (b) simulated SCA regimes compared with observed SCA regimes for the five elevation bands of SB1.

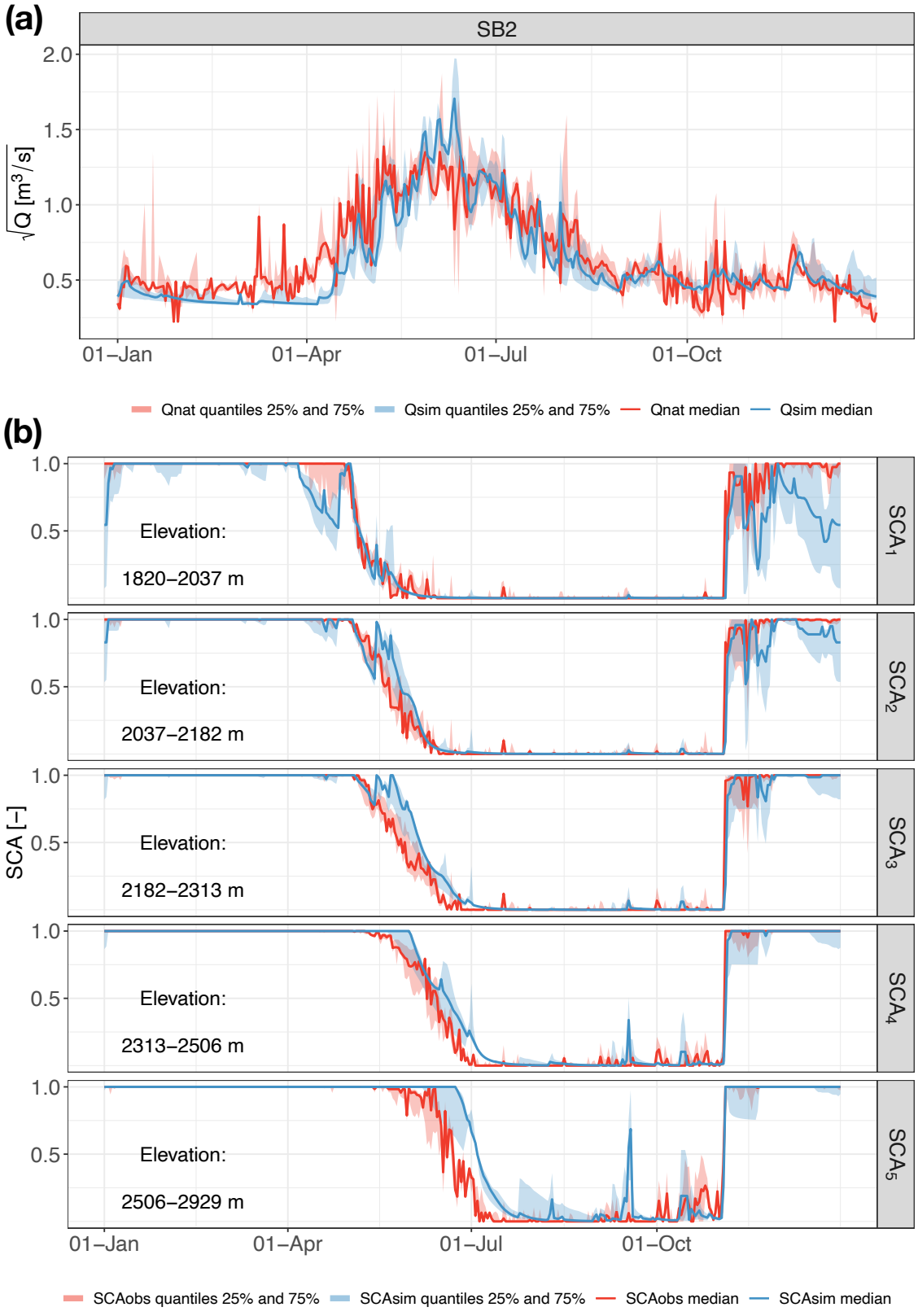

Figure 4.4 – As in Figure 4.3 but for SB2.

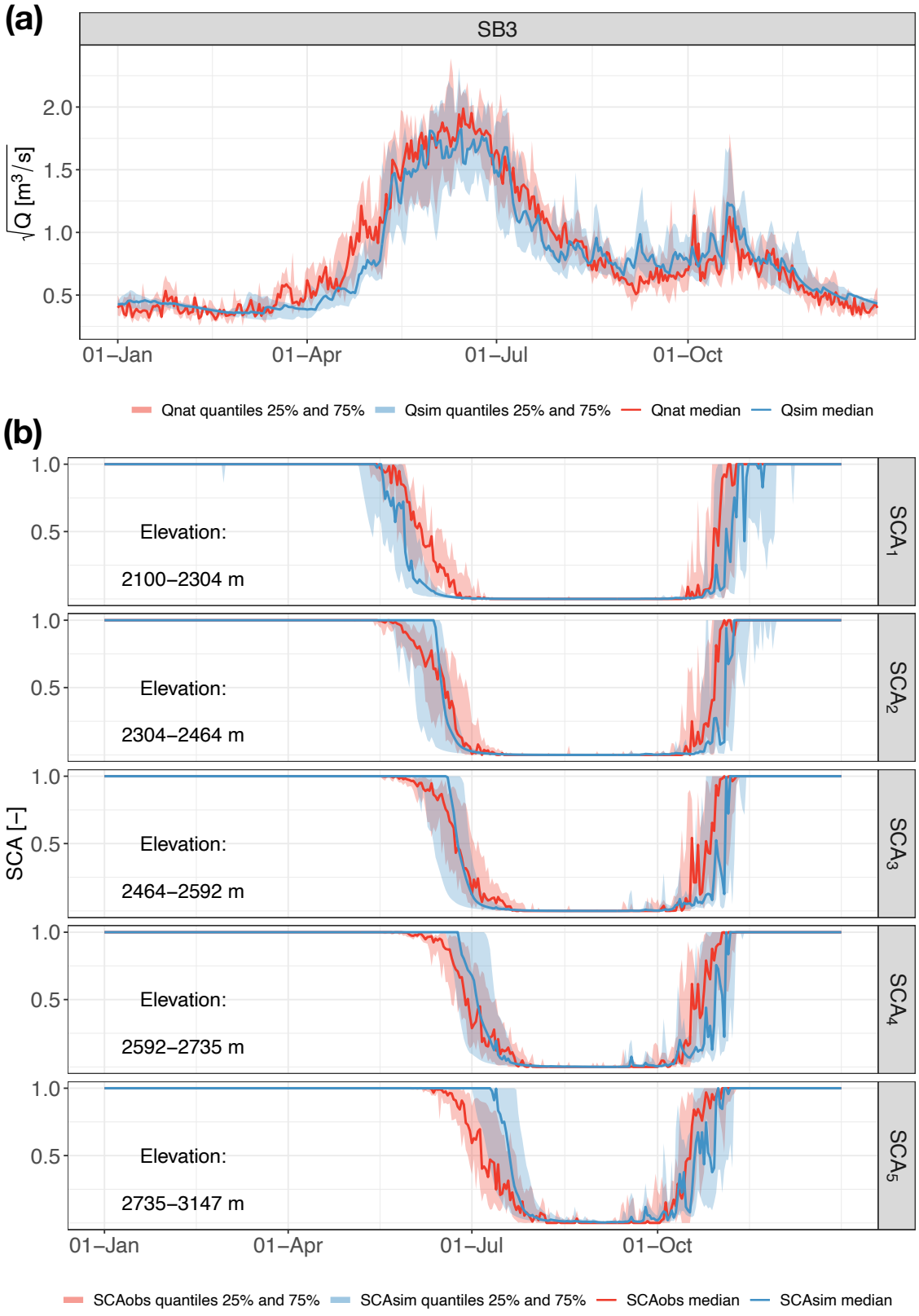

Figure 4.5 – As in Figure 4.3 but for SB3.

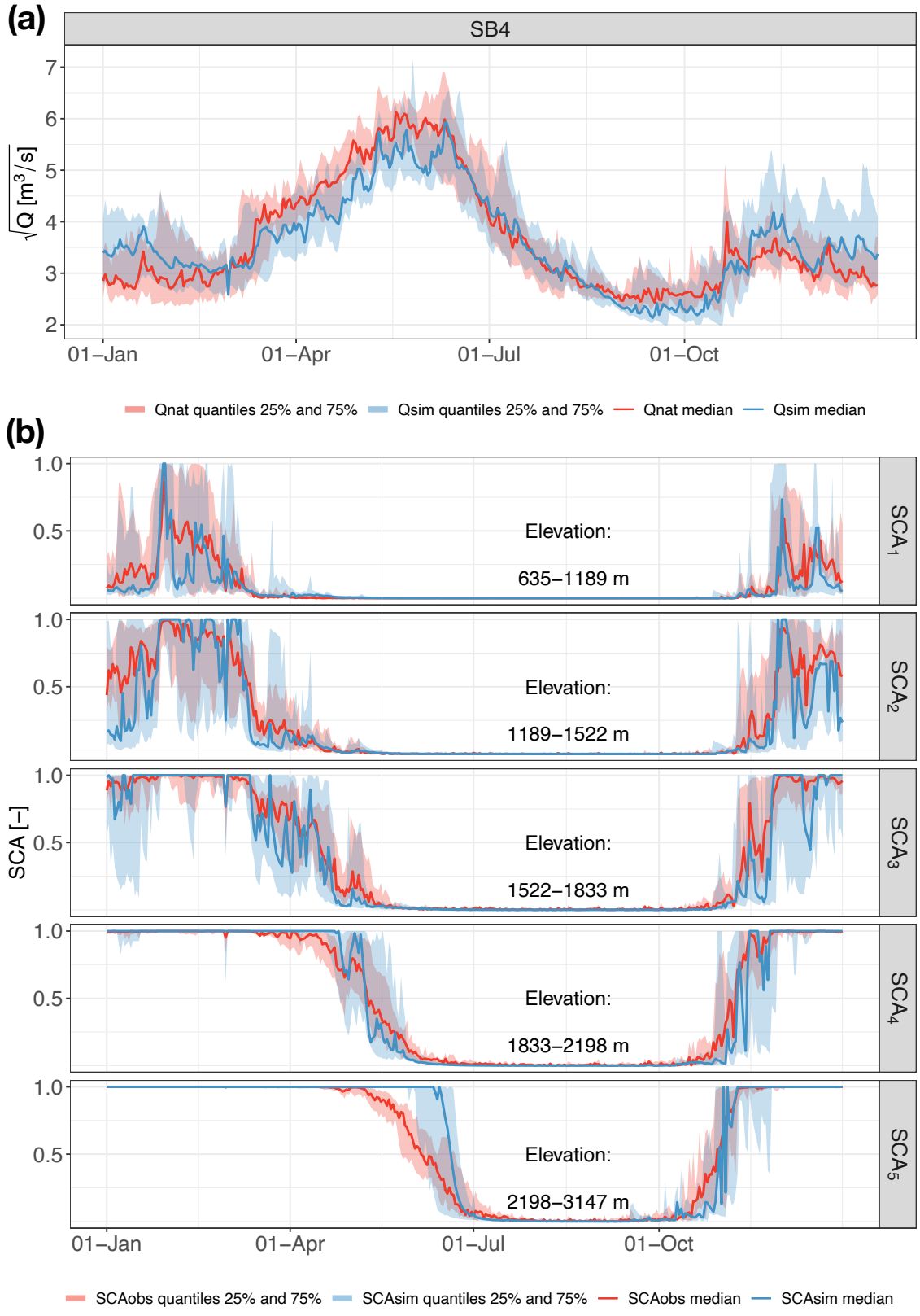

Figure 4.6 – As in Figure 4.3 but for SB4.

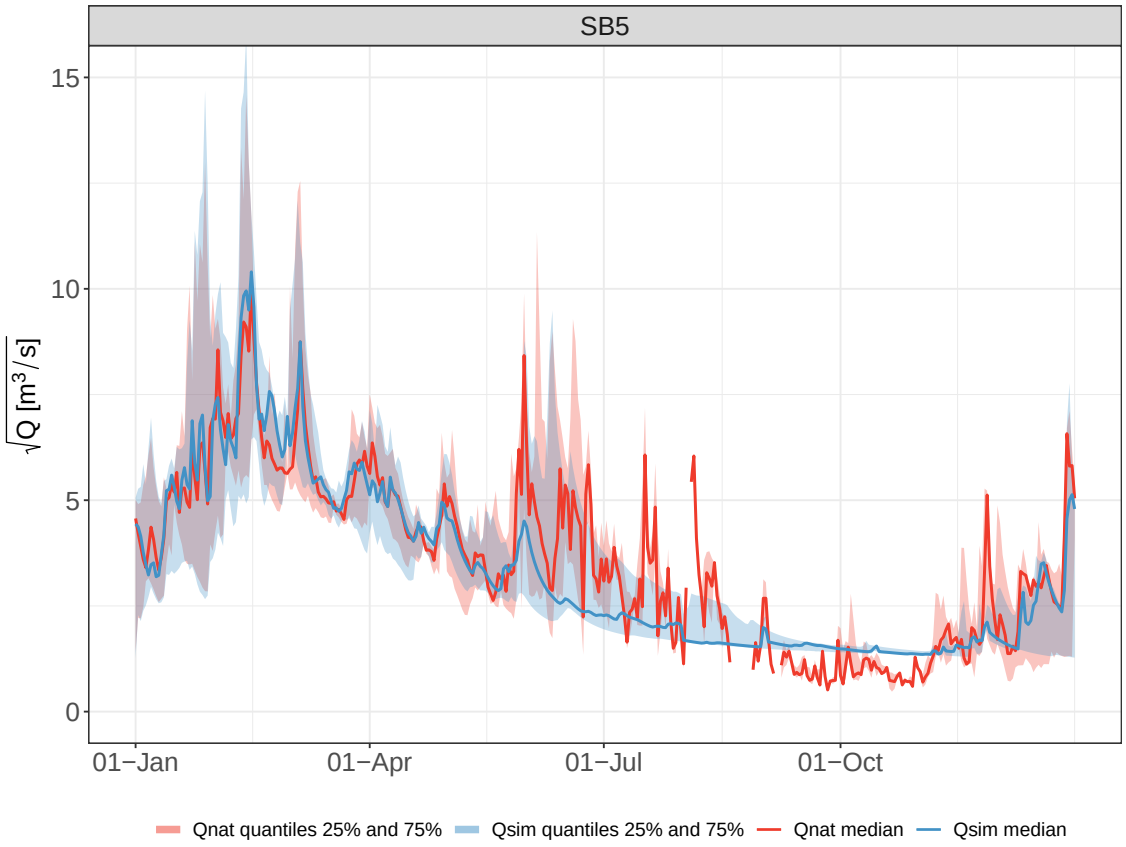

Figure 4.7 – Simulated $\sqrt{Q}$ regime compared with naturalized $\sqrt{Q}$ regime for SB5.

4.2 Water resources model for the Aure Valley

4.2.1 The implementation and performance of the model

A robust estimation of the Neste river flow at Sarrancolin is important to model the CACG water management and to frame the integrated water system of the Neste. Here, we established a water resources model of the catchment Sarrancolin based on the results obtained from the hydrological model GR6J-CEMANEIGE. Figure 4.1 shows the simplified sketch of the Neste water system. Note that the reservoir Cap de Long contributes a small part of water resource to SB2, and eventually the Neste water system, by reserved flow for the environment ($eflow_0$).

SB1-4 directly contribute to river flow at Sarrancolin. As such, the calculation of the influenced flow at Sarrancolin Q_{infs} is based on the formula as follow.

$$Q_{infs} = Q_{inf1} + Q_{inf2} + Q_{inf3} + Q_{nat4} \tag{4.5}$$

where

- Q_{inf1} is the daily outflow from the Oule reservoir that contributes to Sarrancolin ($Q_{inf1} = eflow_1 + Use_1 + Spil_1$);
- Q_{inf2}, daily outflow from the Orédon reservoir that contributes to Sarrancolin ($Q_{inf2} = eflow_2 + Spil_2$);
- Q_{inf3}, daily outflows from the Caillaouas and Pouchergues reservoirs that contribute to Sarrancolin ($Q_{inf3} = eflow_3 + Use_3 + Spil_3$);
- Q_{nat4}, daily naturalized outflow from SB4.

Note that a large amount of water in the Orédon reservoir is transferred into the Oule reservoir and there is barely overflow from the Orédon reservoir. Thus, the Orédon reservoir contributes to Sarrancolin through eflow. Based on the equations 3.2, 3.3, and 3.4, the formula to calculate the influenced flow at Sarrancolin can be obtained:

$$Q_{infs} = Q_{nat1} + Tran_1 - \Delta_1 + eflow_2 + Q_{nat3} - \Delta_3 + Q_{nat4} \tag{4.6}$$

In order to calculate the influenced flow at Sarrancolin within an integrated hydrological modelling framework, the naturalized inflows (Q_{nat1}, Q_{nat3}, and Q_{nat4}) in equation 4.6 can be replaced with the simulated Q by the GR6J-CEMANEIGE model. Besides, the simulated naturalized flow at Sarrancolin (Q_{sims}) can also be calculated by the simulated Q for SB1-4. Therefore, the equations to calculate Q_{infs} and Q_{sims} are formulated as follows.

$$\begin{cases} Q_{infs} = Q_{sim1} + Tran_1 - \Delta_1 + eflow_2 + Q_{sim3} - \Delta_3 + Q_{sim4} & (4.7) \\ Q_{sims} = Q_{sim1} + Q_{sim2} + Q_{sim3} + Q_{sim4} & (4.8) \end{cases}$$

where Q_{sim1}, Q_{sim2}, Q_{sim3}, and Q_{sim4} are the simulated Q by the GR6J-CEMANEIGE model for SB1-4, respectively.

Here, we use the registered data of water management by SHEM ($Tran_1$, Δ_1, and Δ_3) to calculate the equation 4.7 to validate the water resource model for the Aure Valley. The three water management aspects ($Tran_1$, Δ_1, and Δ_3) will be replaced by the water management models (next section) to formalize the final framework of available water

resource at Sarrancolin of the Aure Valley. Figure 4.8 shows the hydrological regimes of the observed influenced flow, calculated influenced flow, and calculated natural flow at Sarrancolin in comparison with releases for energy production and releases for CACG demand over the period from 01/2002 to 08/2014. The observed influenced flow at Sarrancolin (Q_{obss}) is the sum of the water extraction by the Neste Canal (Q_{canal}) and river flow downstream Sarrancolin (Q_{ds}) from the CACG registration data. The releases for energy production and CACG demand are sourced from the SHEM management registration data.

The KGE value between observed influenced flow and calculated natural flow at Sarrancolin is 0.69 while the KGE coefficient between observed influenced flow and calculated influenced flow at Sarrancolin is 0.79. This indicates that the calculated influenced flow (Q_{infs}, red line) shows a better fit to the observed influenced flow at Sarrancolin (Q_{obss}, black line) than the calculated natural flow (Q_{sims}, blue line).

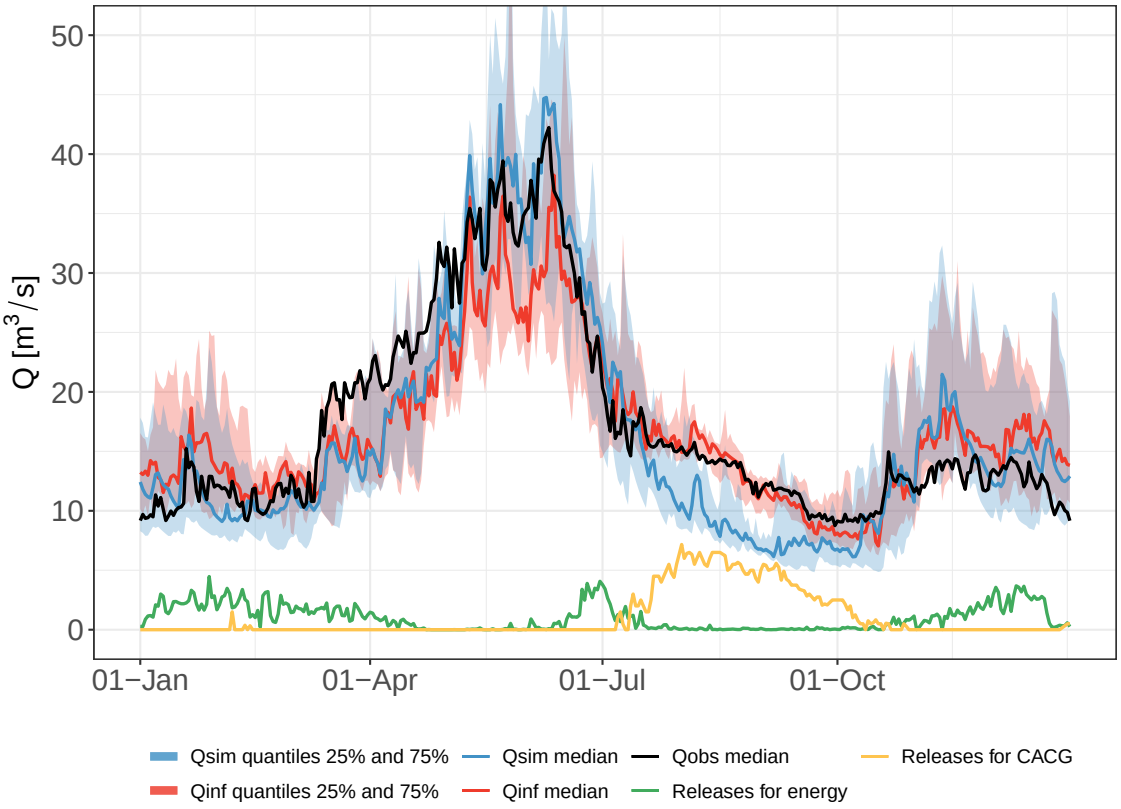

Figure 4.8 – The regimes of observed influenced flow (Q_{obss}), calculated influenced flow (Q_{infs}), and calculated natural flow (Q_{sims}) at Sarrancolin in comparison with releases for energy production and releases for CACG demand over the period from 01/2002 to 08/2014.

If we compare the calculated influenced flow (Q_{infs}, red line) with the observed influenced data from CACG (Q_{obss}, black line) at Sarrancolin, we can conclude that the calculating framework can well represent the flow at Sarrancolin. Especially in summer, the calculated influenced flow is consistent with the observed data. However, the calculated influenced flow is underestimated in spring and overestimated in winter, which can be attributed to the uncertainties of the hydrological model GR6J-CEMANEIGE (the same behavior for SB1-4). If we compare the calculated influenced flow (Q_{infs}, red line)

with the calculated natural flow at Sarrancolin (Q_{sims}, blue line), we can observe that the calculated influenced flow is smaller than the calculated natural flow for spring due to the refill of upstream reservoirs. The calculated influenced flow is greater than the calculated natural flow for winter and summer due to the reservoir regulation for hydropower production and CACG demand, respectively.

4.2.2 Water accounting for the Aure Valley

Table 4.6 summarizes the mean monthly and annual water accounting for the Aure Valley. The simulated natural Q (Q_{sim}), the naturalized Q (Q_{nat}), and the influenced outflow Q (Q_{inf}) are illustrated for SB1-4, respectively. Given the assumption that SB4 is a near-natural sub-basin, Q_{nat4} and Q_{inf4} are the same. As for river flow at Sarrancolin, the simulated natural Q (Q_{sims}), the naturalized Q (Q_{nats}), and the observed Q (Q_{obss}) are also illustrated. Note that Q_{nats} is the sum of the naturalized Q for SB1-4 over a common period from 07/2014 to 12/2018 (see Table 3.6).

To validate the water balance within the Aure Valley, influenced outflows from SB1-4 can be compared with the observed flow at Sarrancolin. Here, mean annual Q_{inf4} is used to frame the water balance criterion. The relative error (δ) between the mean annual Q_{inf4} and that based on the calculation from the observed data (see also equation 3.5) can be derived as follow.

$$\delta = \left| \frac{(Q_{obss}^{Annual} - Q_{inf1}^{Annual} - Q_{inf2}^{Annual} - Q_{inf3}^{Annual}) - Q_{inf4}^{Annual}}{Q_{inf4}^{Annual}} \right| \tag{4.9}$$

The calculated relative error is 1.9%, which validates the water balance within the sub-basins of the Aure Valley.

Besides, we evaluate the performance of the GR6J-CEMANEIGE model in reproducing seasonal hydrological regime over the whole length of dataset Safran-PIRAGUA and Safran-France for SB1-4 and the Aure Valley. Time series of Q_{sim} for SB1-4 and the Aure Valley are compared with available Q_{nat} and Q_{inf} (or Q_{obs}). Figure 4.9 shows the monthly hydrological regimes for SB1-4 and the Aure Valley based on the Table 4.6. Generally, the GR6J-CEMANEIGE model well simulates the seasonal flow variations with high peaks in spring and low spells in summer. In contrast, the difference betweeen the influenced outflow and the naturalized inflow for SB1-3 are remarkable. SB1 and SB3 shift high peaks in summer and winter due to energy and downstream demand. Water in SB2 is transferred to the Oule reservoir and the outflow is the eflow. River flow at Sarrancolin is also changed: lower spring flow due to water storage from the upstream reservoirs, higher summer flow due to reservoir releases for downstream demand, and higher winter flow due to energy production.

Table 4.6 – Water accounting for the Aure Valley. The monthly water volume is in unit $10^3 m^3$.

	Jan	Feb	Mar	Apr	May	Jun	Jul	Aug	Sep	Oct	Nev	Dec	Annual
SB1 (28.4 km^2)													
Q_{sim1} (09/1979-08/2014)	1644	1276	1588	2722	8108	7938	3062	1814	1701	2353	2778	2070	37053
Q_{nat1} (01/2001-08/2014)	1474	1219	2296	4111	8392	6861	2722	1985	1814	2580	2466	1474	37394
Q_{inf1} (01/2001-12/2018)	4820	4224	3487	1616	1644	4253	8448	9185	5216	2948	2693	4139	52674
SB2 (11.3 km^2)													
Q_{sim2} (08/1958-07/2018)	383	326	405	686	2925	4478	2655	1204	979	1080	866	518	16504
Q_{nat2} (07/2014-07/2018)	585	371	540	1643	3949	3994	2014	1429	821	765	754	439	17303
Q_{inf2} (01/2001-12/2018)	135	124	135	135	135	135	135	135	135	135	135	135	1609
SB3 (16.6 km^2)													
Q_{sim3} (09/1979-08/2014)	512	347	446	875	4488	7722	4703	2492	2459	2855	1931	842	29667
Q_{nat3} (01/2001-08/2014)	594	363	627	1799	6023	8993	5165	2013	1386	2673	1601	677	31911
Q_{inf3} (01/2001-12/2018)	3234	3036	1155	330	545	1122	3894	5907	3812	2426	2046	2211	29717
SB4 (541.0 km^2)													
Q_{sim4} (09/1979-08/2014)	35709	28134	33544	43283	71958	74664	45447	26511	22183	33544	42201	39496	496675
Q_{nat4} (01/2001-08/2014)	29757	24347	43824	62220	88731	81156	42742	22724	21101	28675	35709	28675	509660
Q_{inf4} (01/2001-12/2014)	29757	24347	43824	62220	88731	81156	42742	22724	21101	28675	35709	28675	509660
The Aure Valley upstream Sarrancolin (597.3 km^2)													
Q_{sims} (09/1979-08/2014)	38217	30454	35828	47771	87182	94348	55534	31648	27468	40008	48368	42994	579823
Q_{nats} (07/2014-12/2018)	22094	22094	32246	66283	111665	96737	37620	27468	17317	24483	27468	25677	511152
Q_{obss} (01/1992-12/2019)	38814	32843	44188	57325	88377	81211	53145	40008	31648	37620	40606	38217	584003

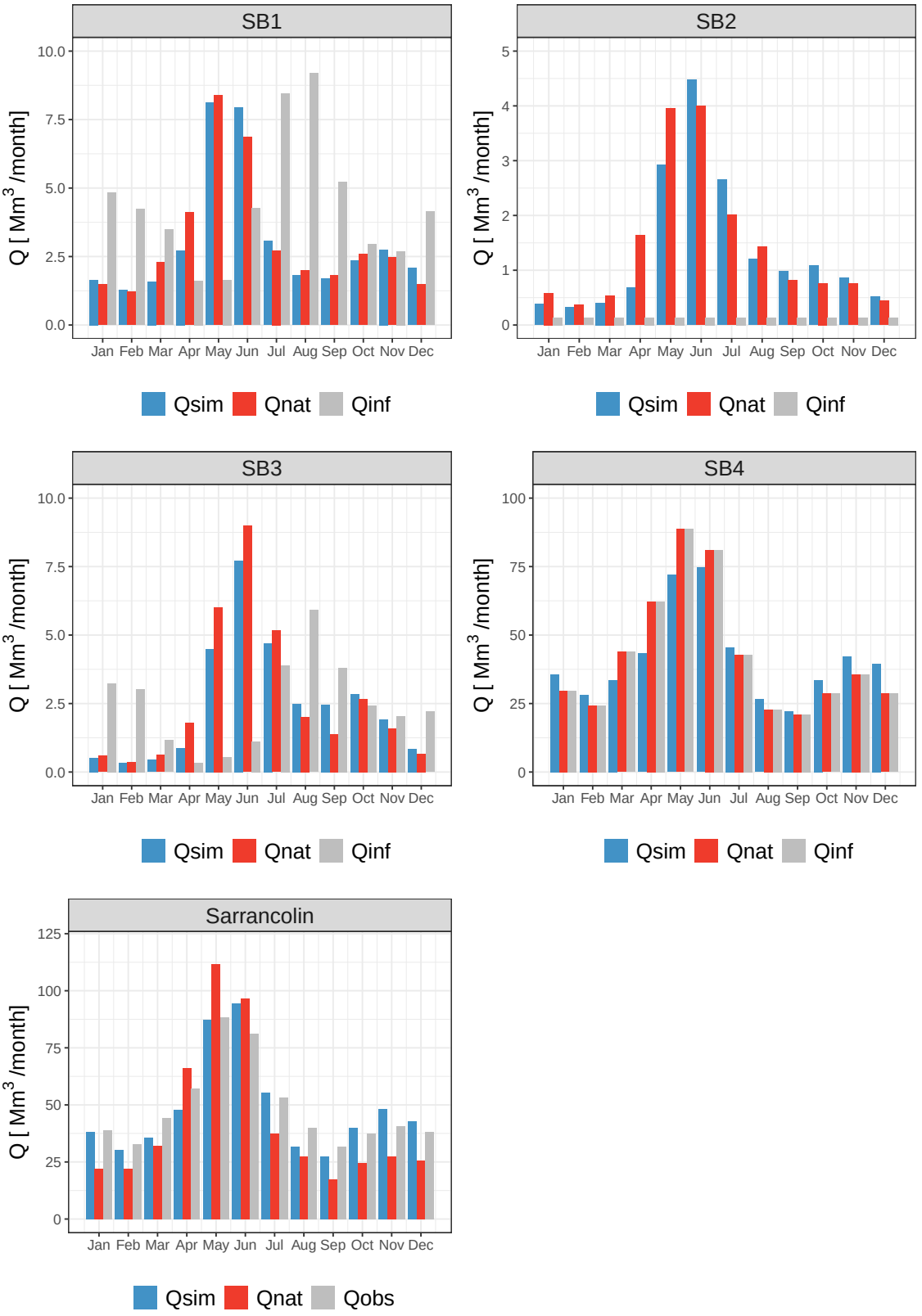

Figure 4.9 – Monthly hydrological regimes for SB1-4 and the Aure Valley. The values are extracted from Table 4.6.

5

Water demand and management modelling

This chapter presents the water demand models in terms of hydropower demand, drinking water demand, industrial water demand, irrigation demand, and environmental demand in the Neste water system. The management behaviors of the two water managers within the Neste water system, SHEM and CACG, are simulated.

Contents

5.1 Water demand modelling 108
5.1.1 Introduction 108
5.1.2 Water demand for hydropower from SHEM 108
5.1.3 Water demand for drinking water from CACG 113
5.1.4 Water demand for industrial use from CACG 115
5.1.5 Water demand for irrigation from CACG 115
5.1.6 Water demand for environment from CACG 124
5.2 Water management modelling 128
5.2.1 Introduction 128
5.2.2 Water management model of SHEM 128
5.2.3 Water management model of CACG 135
5.3 Summary 141

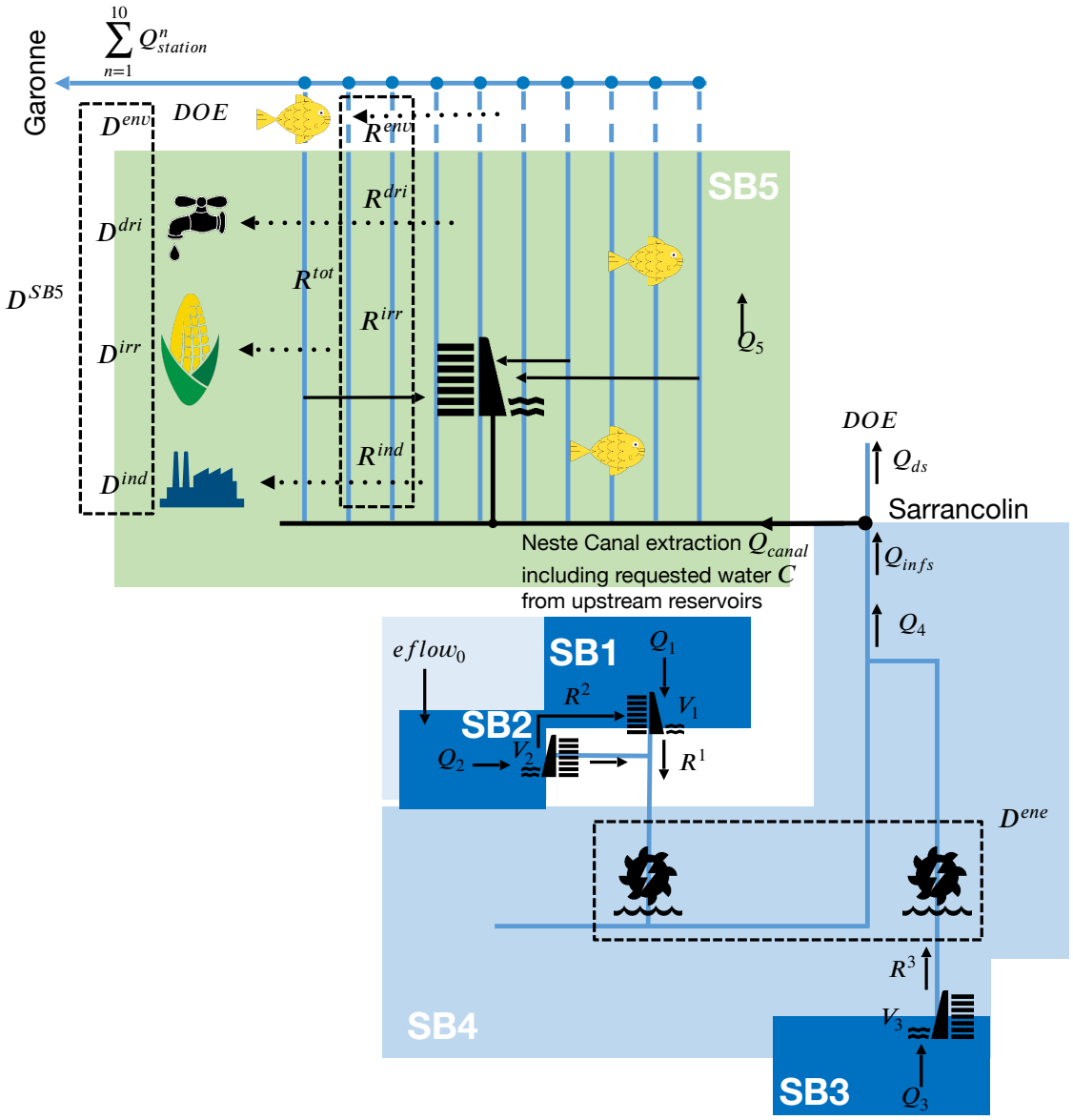

Figure 5.1 – A simplified schema of the Neste water system and the associated abbreviations used in this chapter.

5.1 Water demand modelling

5.1.1 Introduction

The impact of global change (e.g., global warming and population growth) induces increases in water demand (e.g., Boretti and Rosa, 2019; IPCC, 2014). The development of water demand models of the Neste water system thus should consider global change components (e.g., climatic drivers and population growth). As mentioned in chapter 3, there are two principal water managers involved in the Neste water system, the SHEM and the CACG. Water resource in the Aure Valley (SB1-4) is exploited by the SHEM for intensive hydropower production and water demand from the CACG. Water resource in the Gascogne region (SB5) is managed by the CACG to provide reliable water supply for local drinking water, industrial use, irrigation, and environment. As such, five water demand models are developed as follows.

5.1.2 Water demand for hydropower from SHEM

Model development

The widely used indexes Heating Degree Day (HDD) and Cooling Degree Day (CDD) are the technical indicators based on air temperature to describe the energy demand for heating and cooling, respectively (Spinoni et al., 2014). There are different methods and equations to calculate the HDD and CDD indexes (see the summary in Spinoni et al. (2017a)). In general, HDD and CDD are expressed as the difference values of daily air temperature to the base temperature values. The larger the HDD (or CDD) values the more need for energy for heating (or cooling). The base temperature values of HDD and CDD are determined by a number of factors of regional characteristics (e.g., buildings, market strategy, and energy demand behavior). The concept of linking energy demand to air temperature for water management is performed in other similar studies and shows efficient to reproduce energy demand (e.g., François et al., 2014b; Gaudard et al., 2013; Hendrickx and Sauquet, 2013).

In this study, we applied the method from JRC[1] to calculate daily HDD and CDD values of France. The equations to calculate daily HDD and CDD values are derived as follows:

$$\begin{cases} HDD_t = max(\tau_H - T_t, 0) & (5.1) \\ CDD_t = max(T_t - \tau_C, 0) & (5.2) \end{cases}$$

where T_t (°C) is the air temperature of day t over France, τ_H (°C) the base temperature of HDD (15°C for France), τ_C (°C) the base temperature of CDD (24°C for France). The HDD and CDD values for France are sourced from Eurostat[2].

Figure 5.2 shows the general energy demand pattern in a national scale of France generated from equations 5.1 and 5.2. In France, energy is mostly needed in winter for heating while there is barely no demand for summer cooling. However, the CDD value of year 2003 is calculated larger than 0 due to the severe heat wave. In order to meet the demand

[1]The Jointly Research Centre is the European Commission's science and knowledge service (https://joint-research-centre.ec.europa.eu/).

[2]Eurostat is the statistical office of the European Union (see https://ec.europa.eu/eurostat/statistics-explained/).

for winter energy consumption, the energy structure of France is nuclear-hydropower mixed: the base load of energy is provided by nuclear stations while hydropower production from reservoirs or dams mostly concentrates on peak periods of electricity markets. Hydropower allows to respond to quick fluctuations in the markets that nuclear production with lower flexibility are unable to do so.

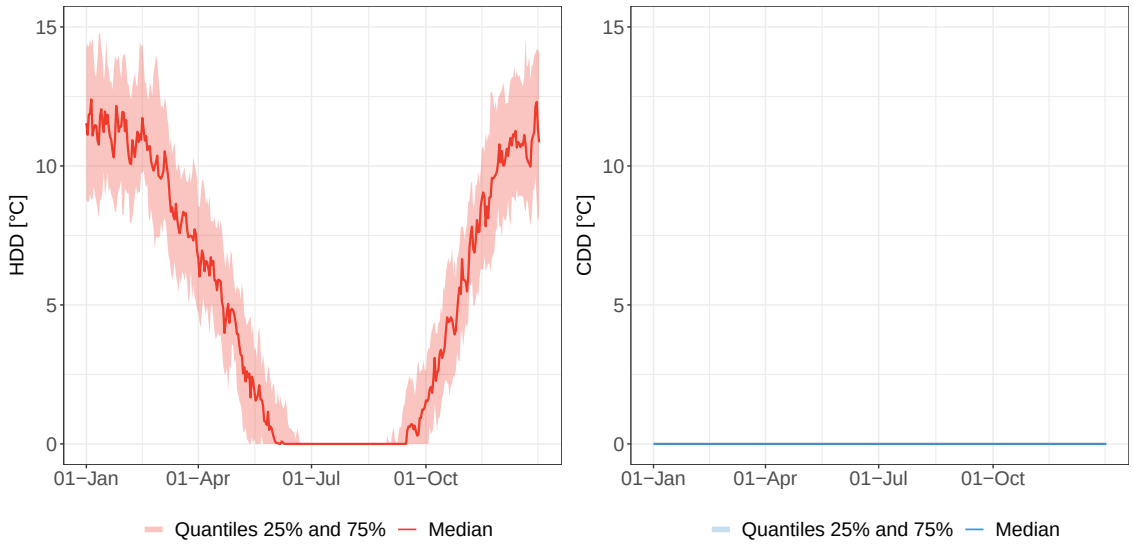

Figure 5.2 – Regimes of energy demand indexes HDD (left) and CDD (right) in France calculated from Safran-France over the period from 08/1958 to 07/2018.

The link between the national energy demand and hydropower production in the Neste water system is presented. The operation of the reservoirs in the Aure Valley for water use is highly seasonal. Currently, water is released by SHEM for hydropower production normally in winter due to high demand for heating (high HDD values) and high market prices in this period. However, hydropower production in summer for cooling is not considered as the current objective of SHEM.

Therefore, the philosophy of hydropower demand model is that when HDD values of France are high, SHEM shows an interest in producing energy as the HDD values represents a high demand and thus a potentially high profit. A hydropower demand model can thus be designed from the historical information provided by SHEM operation data. The hydropower demand model in this study is simplified as a linear relation to the HDD values of France without considering other influence factors in the energy market (e.g., energy policy, energy price fluctuation). However, a deterministic model between hydropower demand and the HDD value can not represent the variability of hydropower demand. Deterministic modelling should be combined with a stochastic model when the deterministic model gives too poor results and where information is not available to build an adapted model. Thus, the quantile regression method (Koenker and Bassett, 1978), a stochastic method to reproduce the variability, is used to link hydropower demand with the HDD value.

Moreover, hydropower production in winter by SHEM is divided into two demand periods: high demand period in weekdays and low demand period in holidays (here refers to weekends and Christmas vacations from 23/Dec to 01/Jan). Figure 5.3 shows the total water release and the corresponding produced energy of the two hydropower systems for weekdays and holidays in the winter season from 01/2002 to 03/2018. What stands out in

this figure is that SHEM releases much more water (produces more energy) in weekdays than in the holidays for both systems.

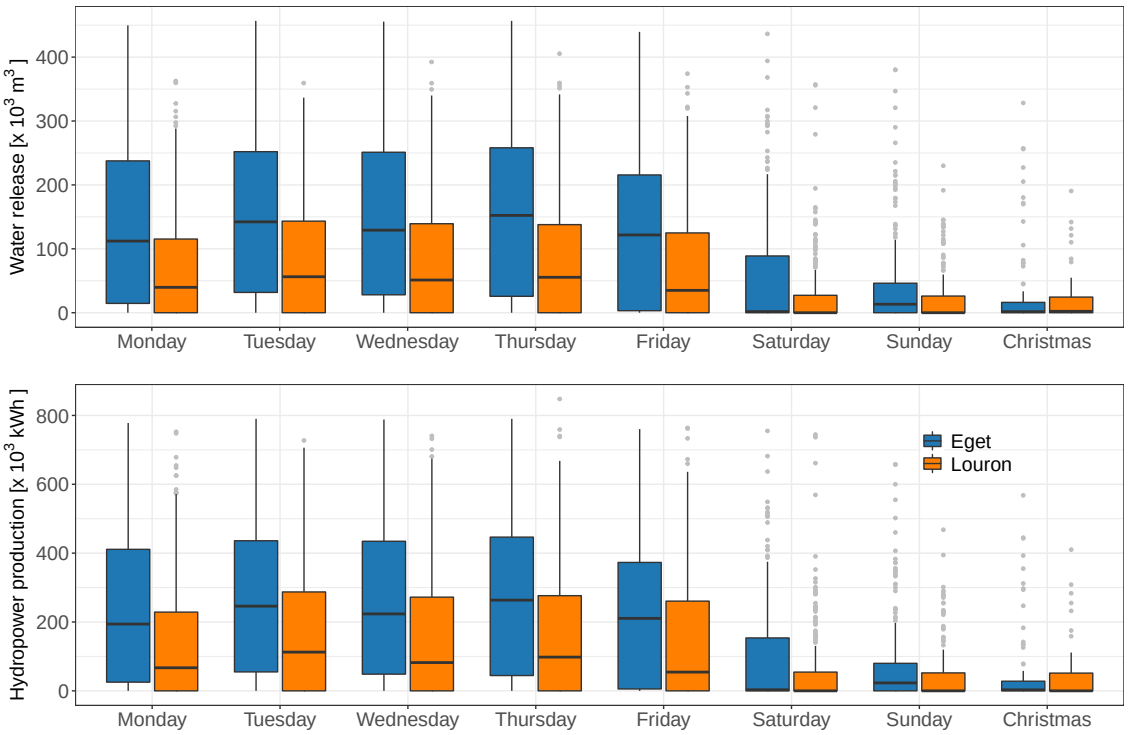

Figure 5.3 – Water release (top) and corresponding energy production (bottom) in weekdays and holidays for the Eget and Louron power systems in cold months (November to March) over the period from 01/2002 to 03/2018.

The formulation of hydropower demand can be derived as:

$$D_t^{ene} = \begin{cases} max\big(min(HDD_t \times a_1|A_1 + b_1|A_1, D_{max}^{ene}), D_{min}^{ene}\big) \\ \text{if } t \text{ in low demand period} \\ \\ max\big(min(HDD_t \times a_2|A_2 + b_2|A_2, D_{max}^{ene}), D_{min}^{ene}\big) \\ \text{if } t \text{ in high demand period} \end{cases} \tag{5.3}$$

where

- D_t^{ene} (kWh), is the market demand from SHEM of day t;
- HDD_t (°C), the HDD value of day t;
- D_{min}^{ene} (kWh), minimum hydropower demand, set to be 0;
- D_{max}^{ene}, maximum hydropower demand defined as DHP in chapter 2, 1.75×10^6 kWh calculated from the Table 3.3;
- A_1 (or A_2), a set of historical energy production linking to historical HDD values in low(high) demand period from 01/2002 to 03/2018;

- a_1 (or a_2) (kWh/°C), the slope of quantile regression line calculated from the set A_1 (or A_2);
- b_1 (or b_2) (kWh), the intercept of quantile regression line calculated from the set A_1 (or A_2);

Given the variations in the management behaviors of SHEM mentioned before, the values of a_1 and b_1 (or a_2 and b_2) is calculated in a stochastic manner with the uniform distribution to randomly select a quantile regression line (Hendrickx and Sauquet, 2013). The sets A_1 and A_2 are thus divided into 101 quantile lines from the quantile line 0% to the quantile line 100%. Figure 5.4 displays the historical energy production sets A_1 and A_2 in quantile linear relation to HDD values. The 25%, 50%, and 75% quantile regression lines are calculated and presented in the figure. Energy production of SHEM is driven by HDD values. The higher the HDD values, the more hydropower demand will be provided by SHEM.

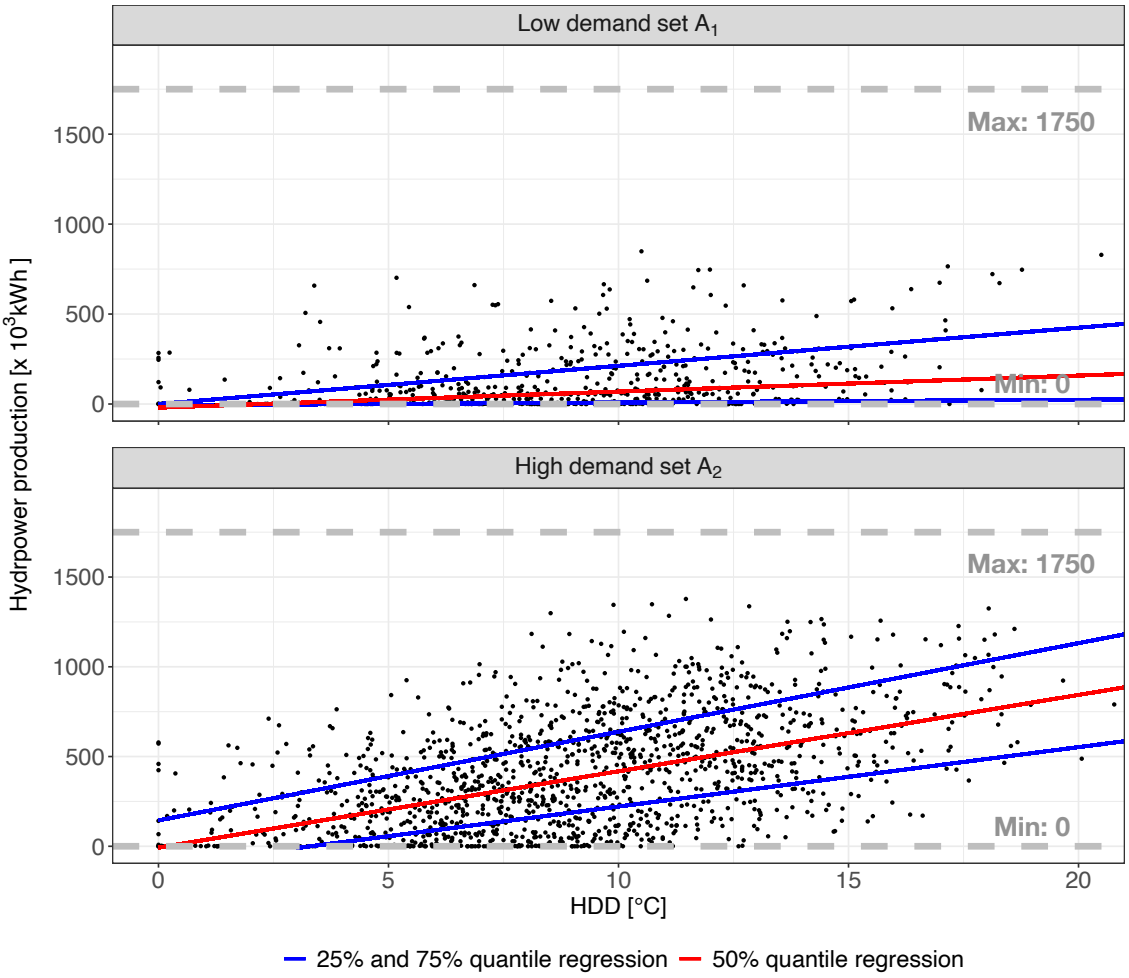

Figure 5.4 – Historical hydropower production for low and high demand periods in linear relation to HDD values of France over the period from 01/2002 to 03/2018.

In practice, the developed hydropower demand model is forced with daily France temperature series and their associated dates. As such, the hydropower demand model can be applied to current and future conditions. The model firstly calculates the daily HDD and CDD values based on the equations 5.2 and 5.3. Since the current hydropower

production is focused on heating demand, the calculated HDD values are used and the associated date information distinguishes them into high and low demand. Secondly, one quantile regression line is uniformly chosen among the 101 quantile regression lines for each demand set (each regression line has the same probability to be chosen). The hydropower demand can thus be calculated based on the chosen quantile regression line and the calculated HDD values.

Model assessment

Koenker and Machado (1999) introduced a coefficient R^1, a local measure of goodness of fit for a particular quantile regression model. This coefficient is analogous to the conventional coefficient of determination R^2 that varies from 0 to 1, where 1 would correspond to a perfect fit. The formulation of the coefficient R^1 is presented bellow:

$$R^1 = 1 - \frac{\hat{V}(\tau)}{\tilde{V}(\tau)} \tag{5.4}$$

where τ is the quantile value, $\hat{V}(\tau)$ the sum of absolute deviations of the fully parameterized model at a particular quantile τ, and $\tilde{V}(\tau)$ the sum of absolute deviations in the null (non-conditional) model at a particular quantile τ. The calculation of V terms are given in Koenker and Machado (1999). Note that R^1 values will always be smaller than R^2 values because R^1 is calculated with absolute deviations while R^2 is calculated with the variance of squared deviations.

The R^2 values between historical hydropower production and associated HDD of France for low demand set A_1 and high demand set A_2 are 0.10 and 0.26, respectively. Table 5.1 shows the goodness of fit of R^1 for the 25%, 50%, and 75% quantile regression lines between historical hydropower production and associated HDD of France for the two demand sets. Indeed, the various incentives of SHEM reservoir managers, such as whether to release water and how much water to be released for hydropower production, cannot be fully interpreted by daily HDD values of France. This can be attributed to the real water management practiced by SHEM that chooses the best hours of a day with the most interesting price in the market to produce energy for the highest profitability and benefits.

Table 5.1 – The performance (R^1 values) of the hydropower demand model for 25%, 50%, and 75% quantile regression lines as examples.

Quantile regression values	25%	50%	75%
Low demand set A_1	0.02	0.05	0.09
High demand set A_2	0.15	0.15	0.14

Empirical cumulative distribution functions (ECDF) between simulations and observations are suitable for statistical significance testing and analysis of hydropower demand model performance. Figure 5.5 compares the ECDF of 10 simulations of the hydropower demand model with that of the observed SHEM operations. The ECDF of simulations follows with the observations, which indicates that the hydropower demand model is capable of representing the probability distribution of observed hydropower production. As such, the hydropower demand model gives acceptable results.

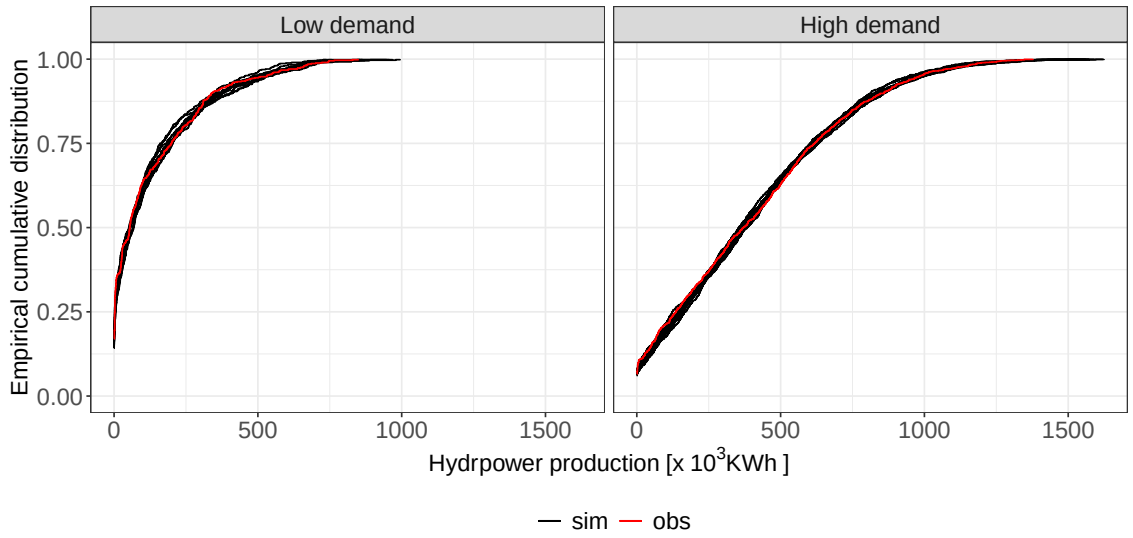

Figure 5.5 – ECDF of the 10 trials of the low demand model (and high demand model) simulated with the HDD of France over the period from 01/2002 to 03/2018 as input compared with the low hydropower demand set A_1 (and high hydropower demand set A_2).

In summary, the energy market is a tremendously complicated and massively coupled system. The electricity consumption and price are influenced by socio-economic development, but they are also susceptible to seasonal and weather-related fluctuations. This study sets out to simplify the hydropower demand from the electricity markets by only considering the weather-related change represented by a temperature-based index (HDD of France). As such, the development of hydropower demand model is not aimed at producing accurate hydropower demand from the markets but realizing a general demand trend. The hydropower demand model generates daily demand in unit kWh with daily HDD values of France as input and with historical hydropower production practice as base to calculate linear coefficients.

5.1.3 Water demand for drinking water from CACG

Figure 3.26 displays that drinking water extraction is generally homogeneous in the scale of SB5. Water demand for drinking water in SB5 can be calculated based on the concept of drinking water index (DWI), an indicator of the necessary water consumption per local inhabitant. The water extraction data from BNPE for 2003-2017 is used to calculate DWI because the BNPE data is downscaled to administrative commune scale. The population information in each commune is extracted from INSEE over the period from 2006 to 2017. As such, the detailed water extraction and population information for 2006-2017 of the communes in SB5 allows a good estimate of DWI.

Besides, current network efficiency of transferring water is taken into account. Dequesne and Portela (2019) reported that the value of network efficiency within the major administrative department associated with SB5 is 70-75% for Gers. Here, we consider that the network efficiency in SB5 is approximately around 75%.

Thus, the calculation of current annual DWI can be formulated as follow.

$$\mathrm{DWI} = \frac{\text{Extraction} \times 75\%}{\text{Population}} \tag{5.5}$$

Figure 5.6 shows the calculated annual DWI values from 2006 to 2017. Therefore, the mean annual value $\overline{\mathrm{DWI}}$ in SB5 is 39.4 m^3 per inhabitant.

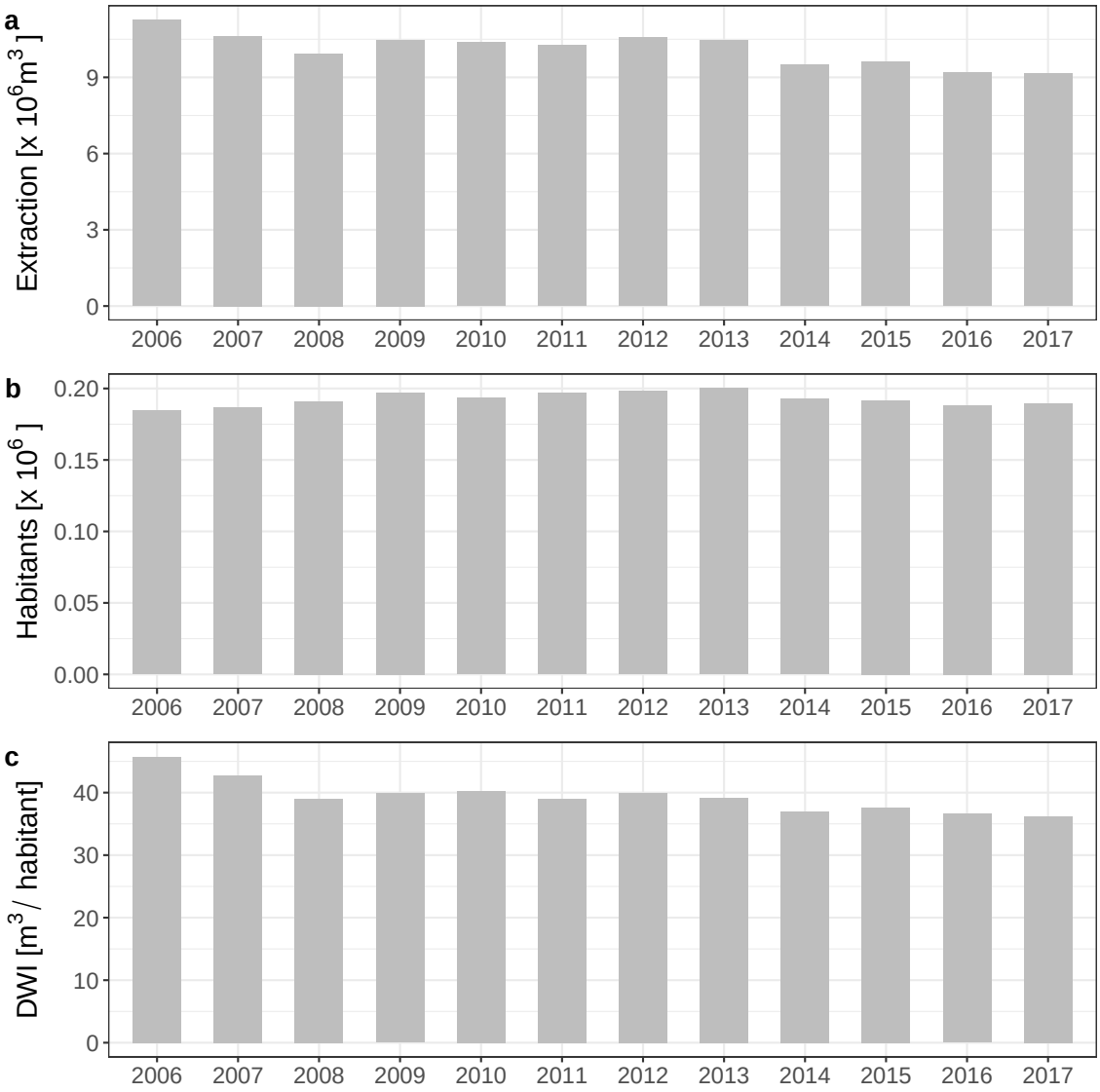

Figure 5.6 – Annual water extraction for drinking water (a), population information (b), and calculated DWI (c) in SB5 from 2006 to 2017.

The $\overline{\mathrm{DWI}}$ value is then used to calculate the daily release for drinking water demand from the 15 reservoirs managed by CACG. The daily drinking water demand from the CACG reservoirs can thus be derived as:

$$D_t^{dri} = \frac{\frac{\overline{DWI}}{365} \times Popu_t}{e_t} \tag{5.6}$$

where D_t^{dri} (m^3/s) is the drinking water demand for the CACG reservoirs of day t, $Popu_t$ population in SB5 of day t, and e_t network efficiency of day t. To apply in the current and

future conditions, the drinking water demand model is forced with projected population information and the water transfer network efficiency of both conditions.

5.1.4 Water demand for industrial use from CACG

Industrial water use in SB5 is simplified as a constant since CACG mainly provides water for Arkéma as mentioned in Chapter 3. Water transfer efficiency is not considered here. As such, daily water demand for industrial use is calculated with historical CACG registration information from 2004 to 2018. The daily industrial water demand from the CACG storage can be derived as:

$$D_t^{ind} = 0.338 \tag{5.7}$$

where D_t^{ind} (m^3/s) is the industrial water demand of day t from CACG reservoirs.

5.1.5 Water demand for irrigation from CACG

The ADEAUMIS model

From a technical point of view, irrigation water demand is mainly dependant on a few principles: understanding the growth stages of the crop, knowing the water and temperature requirement to satisfy each growth stage, climatic conditions that influence the evapotranspiration of the crop, and estimating irrigation intervals. When natural water supply (e.g., rainfall and soil water content) is not sufficient for crop growth, irrigation practices are needed.

In this study, the ADEAUMIS model developed by Leenhardt et al. (2004a,b) that dynamically simulate crop growth and water demand in each growth step is employed to represent irrigation water consumption in SB5. This model has shown a good performance in simulating irrigation water demand in the Baïse sub-basin of SB5 (Leenhardt et al., 2004b). In the framework of PIRAGUA project, the ADEAUMIS model is coded, adapted, and calibrated by Dr. Clotaire Catalogne from ICARE[2][3]. This model is modified from the original version to adapt to the irrigation activities of SB5 under climate change conditions. The irrigation activities in SB5 is simplified for maize since maize cultivation consumes the most irrigation water and covers the most irrigation surface. Maize is an annual crop. Figure 5.7 shows a typical maize cropping and irrigation in the Southern France with sowing in spring, irrigation in summer, and harvesting in autumn. Water requirement for irrigation should be adjusted according to the maize growth stage that varies from one stage to another.

The ADEAUMIS model is a bio-decisional model at daily time step composed of two sub-models: a sub-model of crop growth coupled with a sub-model of decision rules. Table 5.2 summarizes the general configuration information of the ADEAUMIS model. The inputs of the ADEAUMIS model are climatic variables including potential evapotranspiration (PET), temperature (T), and precipitation (P). The simulation of the ADEAUMIS model is divided into three steps: (1) determination of sowing date, (2) determination of crop growth, and (3) determination of irrigation water volume. Each simulation step is presented as follows.

[3] An engineer consulting company for agriculture, water, and environment. The communication information of Dr. Clotaire Catalogne is provided: clotaire.catalogne@icare2.fr

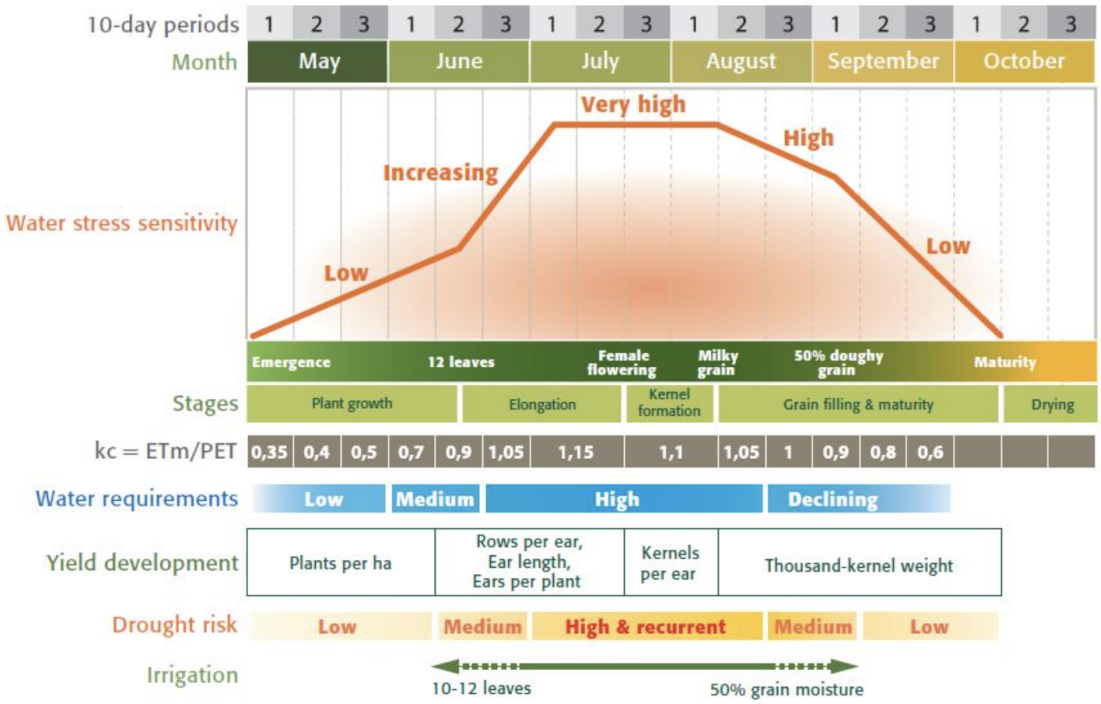

Figure 5.7 – A typical practice of maize cropping and irrigation in the Sourthern France. Source from https://www.maizeinfrance.com/.

Table 5.2 – The inputs, outputs, initial conditions, and parameters of the ADEAUMIS model modified from Leenhardt et al. (2004a).

Inputs	PET, P, and T
Initial conditions	Sowing period
Model parameters	Accumulation of temperature for each crop stage, and threshold values for irrigation decision-making
Outputs	Sowing date, duration of crop growth, duration of irrigation, and irrigation water volume required

(1) Determination of sowing date The sowing date is variant due to soil moisture and weather conditions. The ADEAUMIS model considers the precipitation as the driver to determine the sowing date. In order to correspond to the maize sowing in spring of SB5, the potential sowing period is predefined based on the historical experience of maize cropping in SB5. Here, the beginning date of sowing period is 07/April and the end is 31/May.

The sowing dates is decided based on the rules of precipitation conditions:

$$\begin{cases} \sum_{i=t-4}^{i=t-2} P(i) < 9 \text{ mm} & (5.8) \\ P(t-1) < 5 \text{ mm} & (5.9) \end{cases}$$

where P(t) (mm) is the precipitation of day t. The dates that fit the rules are the potential

and suitable days for sowing. The median value of these dates is thus the representative sowing date (i.e., the starting point of maize growth).

(2) Determination of crop growth duration The duration of maize growth stage is then determined based on the thermal time (the accumulation of daily temperature for maize development). To be more specific, the maize is considered to grow in a specific temperature interval above and below which the crop stops to grow. This temperature intervals is variant among different maize types. Based on historical maize cropping experience in SB5, Leenhardt et al. (2004a) summarized that the majority of maize types are late growing varieties. As such, the temperature intervals of maize growth in SB5 is from 6 °C to 27.5 °C. This indicates that maize grows when and only when daily temperature is in this interval. Daily temperature less than 6 °C or larger than 27.5 °C stops maize growth. Besides, Table 5.3 summarizes the parameters of thermal time for the five major stages of maize: 10-12 leaves stage, flowering stage, early grain filling stage, 50% grain moisture content, and maturity. The accumulation of daily temperature reaches each parameter of the five stages of maize growth, indicating the development of maize to each stage. As such, the days to reach each parameter of the five stages are thus the duration of each stage for maize growth.

Table 5.3 – The necessary thermal time for the major five stages of maize growth. The parameters are from Leenhardt et al. (2004a).

Maize growth stage	Thermal time [°C day]
10-12 leaves stage	650
Flowering stage	910
Early grain filling stage	1495
50% grain moisture content	1630
Maturity	1990

(3) Determination of irrigation water volume Except in rare circumstances where irrigation is required to facilitate emergence, maize irrigation is ineffective prior to the appearance of 10-12 leaves. The maize plants use very little water before that stage. The decision rules for irrigation of the ADEAUMIS model is based on the surveys from the 20 farmers in the Baïse sub-basin (Leenhardt et al., 2004a). These rules are considered representative for the irrigation practices of SB5. On this basis, the decision rules are modified to adapt to the global SB5 irrigation activities and to climate change from the expertise in the PIRAGUA project framework. Table 5.4 summarizes the decision rules for irrigation in the ADEAUMIS model. The major change is the rule of "Returning (without rain)": the irrigation volume is calculated from the arbitrary formula

$$2 \times \left[\sum_{i=t-4}^{i=t} PET(i) - \sum_{i=t-4}^{i=t} P(i) \right]$$

and the coefficient 2 is confirmed by experts and water managers in SB5.

Table 5.4 – Decision rules for irrigation in the ADEAUMIS model. The rules are modified based on Leenhardt et al. (2004a).

Rule	If	Condition			Then	Action	Irrigation volume
		Indicator	Operator	Threshold value			
Starting		Julian day	$\geqslant$	15/June		Irrigation	20 mm
	And	Crop stage	$\geqslant$	10-12 leaves			
	And	$\sum_{t-4}^{t} P(t)$	$<$	10 mm			
	And	$\sum_{t-4}^{t} PET(t)$	$>$	15 mm			
Returning (without rain)		Last irrigation	$\geqslant$	10 days before		Irrigation	$2 \times \left[\sum_{t-4}^{t} PET(t) - \sum_{t-4}^{t} P(t)\right]$
Delaying (in case of rain)		$\sum_{t-4}^{t} P^*(t)$	$\geqslant$	16 mm		No irrigation before $min\left(7, \frac{1}{5}\sum_{t-4}^{t} P^*(t)\right)$ days	0
Ending		Crop stage	$\geqslant$	50% grain moisture content stage		Ending irrigation	0
	And	$\sum_{t-6}^{t} P(t)$	$>$	20 mm			
	And	$\sum_{t-6}^{t} PET(t)$	$<$	25 mm			
	Else					Last irrigation	20 mm

$P^*(t)$ is the adjusted precipitation of day t and $P^*(t) = max(P(t) - 2, 0)$

Through the three steps above, the outputs are sowing date, the duration of crop growth stage and associated irrigation duration, and the necessary irrigation water to satisfy each crop growth stage. Although the decisional model works at daily time step, the results of irrigation date and volume is at weekly time step (maximum 10-day interval beween the two irrigation activities). Besides, the results of irrigation volume is in unit mm/week.

The assessment of the ADEAUMIS model

In order to validate the ADEAUMIS model, the information of the maize irrigation area and the irrigation efficiency in SB5 is necessary. Particularly, the irrigation area of maize cultivation in SB5 varies from year to year (Teyssier, 2006). These information should be multiplied with the results from the ADEAUMIS model and then compare with the weekly irrigation water release registration from CACG. However, this validation of the ADEAUMIS model is difficult because these information is barely known.

In this study, a concept of "derived irrigation area" (Id) was introduced to link the simulated irrigation water demand with the release registration of CACG for irrigation (Clotaire, personnal communication).

The formulations are presented as:

$$\begin{cases} Id_t = \dfrac{Ia_t}{Ie_t} & (5.10) \\ R^{irr}_{obs,t} = D^{irr}_t \times Id_t & (5.11) \end{cases}$$

where Ia_t (km^2) is the irrigation area of day t, Ie_t the irrigation efficiency, $R^{irr}_{obs,t}$ (m^3/s) the observed CACG water release for irrigation in SB5 (total release form CACG reservoirs and the 48 Mm^3 storage in the Aure Valley), and D^{irr}_t (m^3/s/km^2) irrigation water demand simulated from the ADEAUMIS model. Since the two information Ia_t and Ie_t is unknown, they are aggregated into one variable Id_t to reduce the difficulty of validation.

Leenhardt et al. (2004a) stated that the simulated irrigation water extraction demonstrated great sensitivity to the estimation of irrigation surface while the dynamics of water extraction are well simulated. In another word, the estimation of Id_t dominates the annual irrigation release and the simulation results D^{irr}_t dominates the seasonal irrigation demand pattern. As such, the performance of the ADEAUMIS model was assessed by investigating the seasonal dynamics.

The observed irrigation water release at weekly time step from CACG registration is from 1995 to 2019 (year 1996 is missing). Thus, the irrigation water demand D^{irr}_t in SB5 is simulated by the ADEAUMIS model with the PET, P, and T variables of each Safran-France grid in SB5 as inputs over the period from 1995 to 2019. A total 126 grids are simulated to represent the irrigation activities in SB5.

The Id values for each year from 1995 to 2019 can be calculated by the observed annual release divided by the simulated annual aggregation of D^{irr}_t from equation 5.11. Therefore, the calculated Id values for each year in Figure 5.8 can be seen as the observed "derived irrigation area".

The calculated Id values for each year are then used to multiply the simulated irrigation demand D^{irr}_t, which can be compared with the observed irrigation release $R^{irr}_{obs,t}$. Figure 5.9 shows the comparison between the simulated irrigation water demand (mean simulated irrigation demand of 126 Safran-France grids multiplied by the Id values of

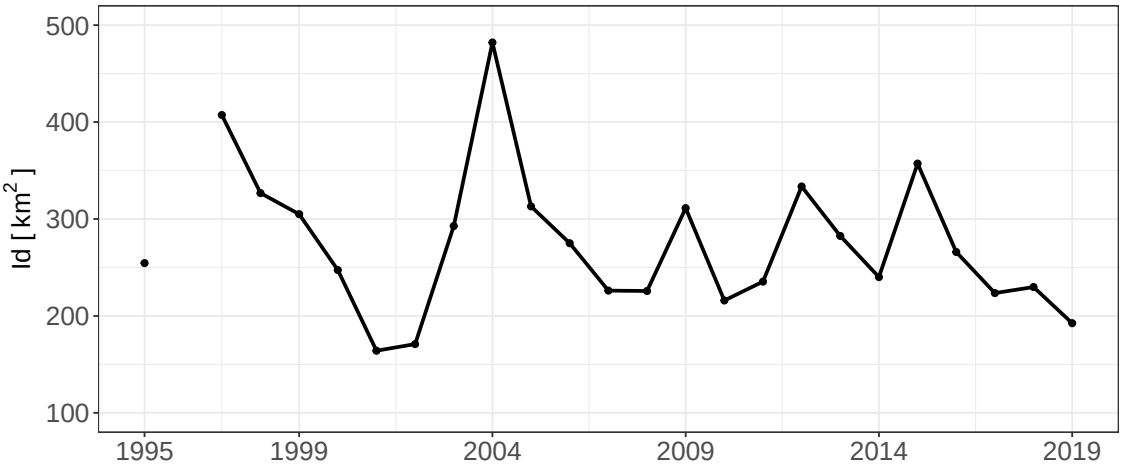

Figure 5.8 – The calculated Id values for year from 1995 to 2019. Note that the year 2006 is a missing year.

Figure 5.8) aggregated to weekly time step and the observed weekly release from CACG registration. In general, the simulated irrigation water demand well correspond to the observed seasonal changes with the peak in summer. The irrigation duration is also well represented. The KGE value between the simulated and observed irrigation water release is 0.63.

However, irrigation demand in autumn during October is underestimated. This is because the simulation only considers the maize irrigation and thus irrigation in autumn for other crops is ignored. For example, in the autumn of year 2018, CACG released water for colza and soybean due to drought events (CACG, 2019). Besides, irrigation in spring during June is slightly underestimated. This is also because the ignorance of other crops (e.g., colza) and the irrigation in spring is normally one round (25-30 mm) if necessary according to the specialist advisor Thierry BAQUE from the Chambre d'Agriculture du Gers. The simulated irrigation water demand in summer is more variant than the observed because the irrigation release is also managed by CACG. For example, in the summer of year 2017 (hot and dry), quota for irrigation is reduced by 10-20% due to the increasing environmental demand.

The simulation results in terms of sowing date, maize growth duration and irrigation duration are presented in Figure 5.10. The boxplots represent the distribution of the simulated values for all the 126 Safran-France grids.

According to the interview with the expertises in the agricultural sector of the Gers department, late or semi-late varieties of maize still dominate the cultivation of maize. The sowing is done at the beginning of April for SB5. However, the simulated sowing date is in the period from 20/April to 15/May, which is about one month later than the real situation. This imperfection is mostly attributed to the predefined configuration in the sowing date simulation, which is the period from 07/April to 31/May. The configuration of sowing date in the ADEAUMIS model is compromised to have a better simulation of irrigation period and peak as presented in Figure 5.9. Besides, the simulated maize growth duration is 130-190 days. According to Arvalis[4], in France, maize completes its

[4]The French arable crop R&D institute (see https://www.arvalis-infos.fr/).

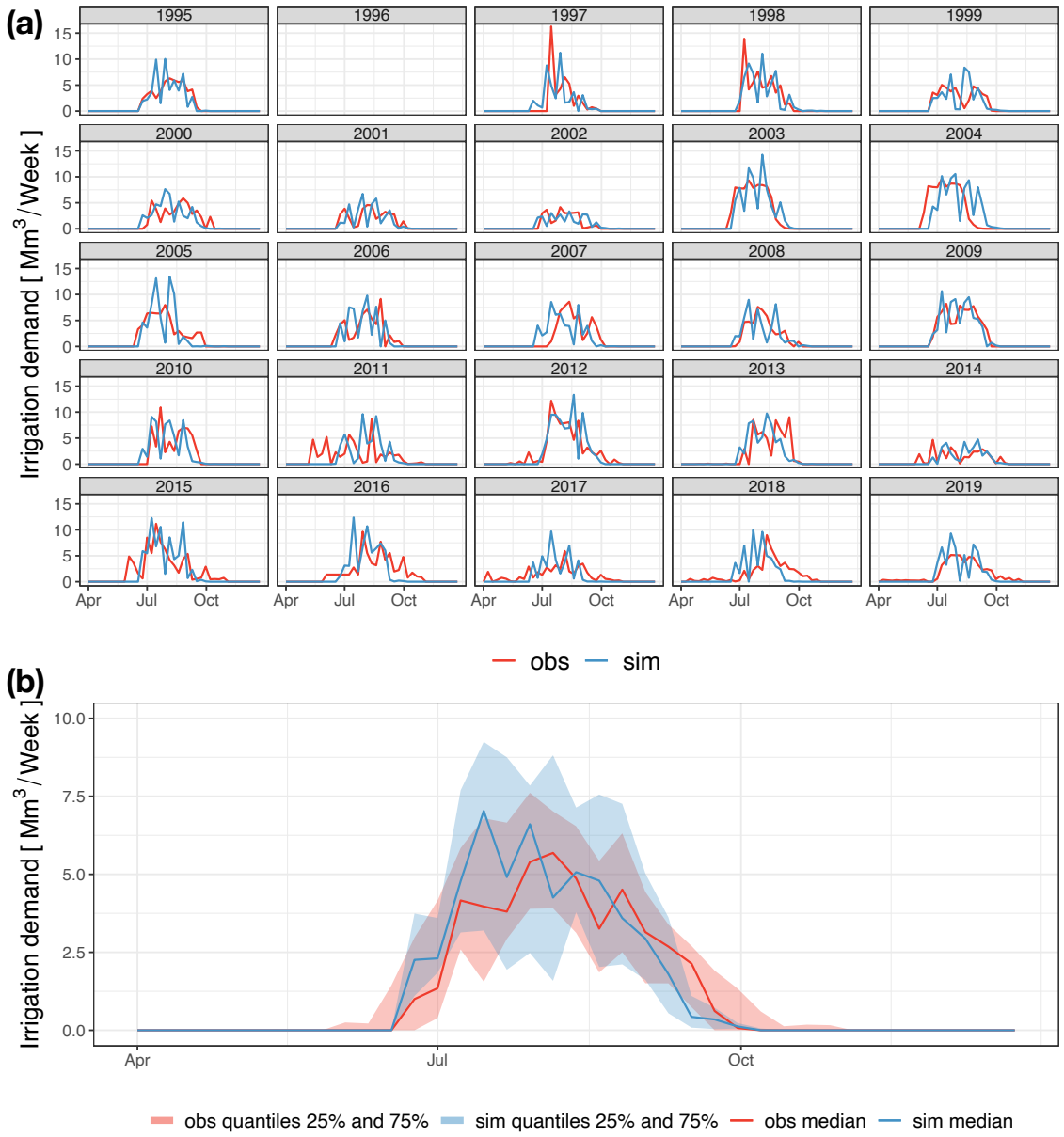

Figure 5.9 – (a) The simulated weekly irrigation water demand compared with the observed CACG registration for each year in 1995-2019; (b) The regime of the simulated weekly irrigation water demand compared with the observed release regime for year 1995-2019.

cycle, from sowing to harvesting, in 4 to 6 months. As such, the simulated duration well corresponds to the realistic situation. The variance of the simulated maize growth duration is due to the spatial and temporal variance of temperature of each Safran-France grid in SB5. The simulated irrigation duration, considered as the duration between the stage of flowering and the stage of 50% grain moisture content, is 60-80 days. As observed, the simulated irrigation duration is homogeneous from 1995-2019. Besides, the simulated three variables (sowing date, maize growth duration, and irrigation duration) share the similar variation.

In summary, maize irrigation activities in SB5 are highly human-induced and variant from year to year. Particularly, important information (i.e., annual maize irrigation area

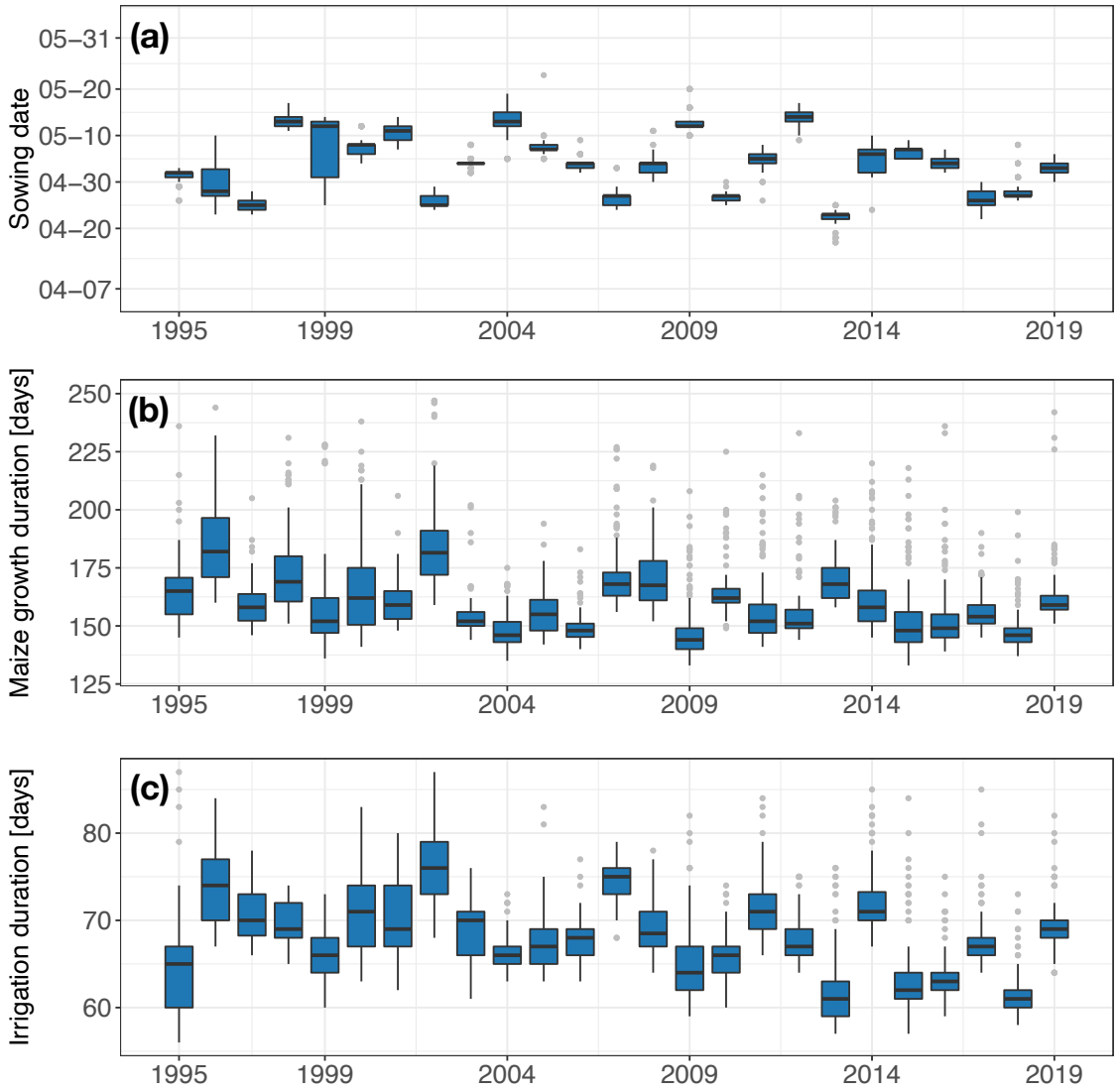

Figure 5.10 – The simulated sowing date (a), maize growth duration (b), and irrigation duration (c) in SB5. Maize growth duration is the time interval between sowing date and the stage of maturity. Irrigation duration is the time interval between the stage of flowering and the stage of 50% grain moisture content. Last irrigation activity in a year is after the stage of 50% grain moisture content.

and irrigation efficiency) remains unknown. In this study, maize irrigation activities are represented by the bio-decisional model ADEAUMIS. In order to link the simulated maize irrigation water demand with the observed water release, a conceptual variable "derived irrigation area" is introduced to fix the annual irrigation water demand. In another word, the simulated annual irrigation water demand and the observed annual irrigation water release are the same. Although there are some imperfections in the simulation results, the maize growth stages are well represented with the simulated growth stages coherent with the realistic maize cropping in France, and weekly irrigation water demand pattern is well simulated with the KGE value of 0.63.

The daily climate variables (PET, P, and T) and maize irrigation surface (here, the "derived irrigation area") are necessary inputs into the calibrated ADEAUMIS model to produce weekly irrigation water demand of SB5 at a year basis (the "derived irrigation

area" can be variant from year to year). In order to investigate the future irrigation water demand, future climate change projections of SB5 and future "derived irrigation area" changes are forced into the calibrated ADEAUMIS model. The results are then used to compare with the simulations forced with current climate conditions and current "derived irrigation area".

From the adaptation point of view, the parameters of calibrated ADEAUMIS model (see Table 5.2) can be changed to represent an adapted irrigation system of SB5. To be more specific, the initial condition (sowing date) is 07/April-31/May can be changed to an earlier sowing calendar to adapt to the future warming conditions. The accumulation of temperature of growth stage can be changed to represent other crops to show that the cropping strategy is changed as an adaptation. To accompany the changes of cropping strategy, the irrigation threshold value (see Table 5.4) should also be changed because different crops have different water demanding. As such, a crop type with less water consumption can be tested as an adaptation. Moreover, the future "derived irrigation area" can also be changed as an adaptation strategy. A lower "derived irrigation area" value can represent a higher irrigation efficiency or a lower irrigation surface.

5.1.6 Water demand for environment from CACG

As mentioned before, CACG manages to maintain a good status of the environment at a daily time step. The historical release for the environment can be calculated based on the formula as follow

$$R^{env}_{obs,t} = R^{tot}_{obs,t} - R^{dri}_{obs,t} - R^{ind}_{obs,t} - R^{irr}_{obs,t} + C_{obs,t} \tag{5.12}$$

where

- $R^{env}_{obs,t}$, is the observed water release for the environment from the CACG reservoirs of day t;
- $R^{tot}_{obs,t}$, the observed total daily water release from the CACG reservoirs as shown in Figure 3.29;
- $R^{dri}_{obs,t}$, the observed annual water release for the drinking water from the CACG reservoirs as shown in Figure 3.27 and then transferred to daily basis;
- $R^{ind}_{obs,t}$, the observed annual water release for the drinking water from the CACG reservoirs as shown in Figure 3.27 and then transferred to daily basis;
- $R^{irr}_{obs,t}$, the observed weekly water release for the irrigation from the CACG reservoirs as shown in Figure 5.9 and then transferred to daily basis;
- $C_{obs,t}$, the observed daily request from the contract of the 48 Mm^3 storage in the SHEM reservoirs of the Aure Valley.

The term $R^{tot}_{obs,t} + C_{obs,t}$ corresponds to the total water release for the four types of water demand in SB5. As such, the calculated water release for the environment is calculated from 01/2013 to 12/2019.

In terms of environmental water demand, there is the DOE requirement (a minimum river discharge) that should be satisfied as shown in Table 3.5 and Figure 3.21. In addition, CACG conducts other two actions to support the environmental quality in SB5. Firstly, CACG releases a flow basis for the environment from the 15 reservoirs. Secondly, CACG extracts water at Sarrancolin via the Neste Canal (Q_{canal}) to feed SB5. Finally, CACG monitors the daily river discharge at the ten control stations near the confluence to the River Garonne as shown in Figure 3.20 to make sure that it is no lower than the DOE requirement. If river flow in SB5 is lower than the DOE value, an extra release from the CACG reservoirs or a higher extraction at Sarrancolin will be conducted to fulfill the difference.

However, there is no specific rule curves to guide the release of flow for the environment. CACG releases water from the 15 reservoirs even though the natural water flow in SB5 is above the DOE value. In this study, we simply assume that the release of the environmental flow relies on the two drivers: the current state of river discharge in SB5 and the current water availability in the 15 CACG reservoirs. Table 5.5 shows the coefficients of determination of the observed water release of the environmental related to natural discharge in SB5 (Q_{nat5}, see equation 3.6), CACG reservoir storage, and both in four seasons. The coefficients of determination are higher when considering both drivers for winter, spring, and autumn seasons. The lower coefficient of determination of both drivers in summer is probably attributed to the biases from the summer irrigation release.

Table 5.5 – Coefficient of determination R^2 between water release of the environmental flow from the CACG reservoirs R^{env}_{obs} and natural discharge in SB5 (or reservoir storage in SB5, or both) for four seasons.

	Natural discharge in SB5 (Q_{nat5})	CACG reservoir storage V^5	Both
Winter	0.23	0.36	0.43
Spring	0.28	0.02	0.28
Summer	0.02	0.30	0.05
Autum	0.20	0.04	0.33

Here, we use the multiple variable quantile regression method to simulate the daily release of the flow basis (β) from the CACG reservoirs for the environment applied to the four seasons. The flow basis is defined as an outflow for the environment when there is no need to satisfy the DOE requirement in SB5. This method is similar to the method of hydropower energy demand and the formulation of this method can be expressed as:

$$\beta = \begin{cases} f(V_t^{CACG}, Q_{5,t}) | R^{env}_{obs,winter} & \text{if } t \text{ in winter} \\ f(V_t^{CACG}, Q_{5,t}) | R^{env}_{obs,spring} & \text{if } t \text{ in spring} \\ f(V_t^{CACG}, Q_{5,t}) | R^{env}_{obs,summer} & \text{if } t \text{ in summer} \\ f(V_t^{CACG}, Q_{5,t}) | R^{env}_{obs,autumn} & \text{if } t \text{ in autumn} \end{cases} \tag{5.13}$$

where V_t^{CACG} is the total water volume of the 15 CACG reservoirs of day t, $Q_{5,t}$ the river runoff in SB5 of day t, and f the linear quantile regression function derived from different seasonal datasets ($R^{env}_{obs,winter}$, $R^{env}_{obs,spring}$, $R^{env}_{obs,summer}$, and $R^{env}_{obs,auntumn}$).

As such, the water demand for the environment in SB5 from the 15 reservoirs can be derived as:

$$D_t^{env} = max\left(DOE_t - Q_{5,t} - (Q_{canal,t} - C_t), \beta\right) \tag{5.14}$$

where D_t^{env} is the environmental demand in SB5 from CACG reservoirs of day t, DOE_t the DOE requirement of day t, $Q_{5,t}$ the river discharge in SB5 of day t, $Q_{canal,t}$ the canal extraction of day t, and C_t the request from the contract of the 48 Mm^3 storage in the SHEM reservoirs. The term $Q_{canal,t} - C_t$ indicates the contribution from Sarrancolin to the environmental water demand in SB5. This contribution to the environment of SB5 will be presented in the next sub-section.

Figure 5.11 shows the regime of the simulated environmental water demand for the CACG reservoirs compared with the observed environmental water release from the CACG reservoirs over the period from 01/2003 to 12/2019. Figure 5.12 shows the ECDF of ten trial simulations of environmental water demand compared with the observed environmental water release from the CACG reservoirs for four seasons over the period from 01/2003 to 12/2019. From the two figures, environmental water demand pattern in winter, spring and autumn is well represented. On the contrary, simulated environmental water demand in summer is not coherent to the observed release, which is attributed to

the low quality of the observed environmental release in summer biased by irrigation water release.

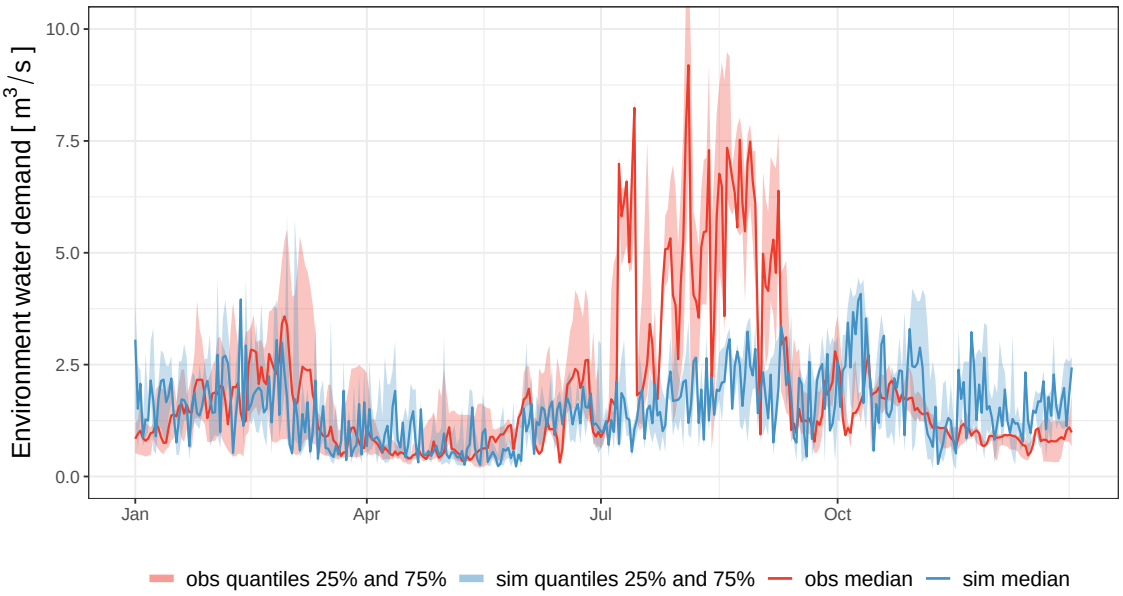

Figure 5.11 – The regime of the simulated daily environmental water demand in SB5 compared with the calculated observed daily water release regime for the environment of SB5 over the period from 01/2003 to 12/2019.

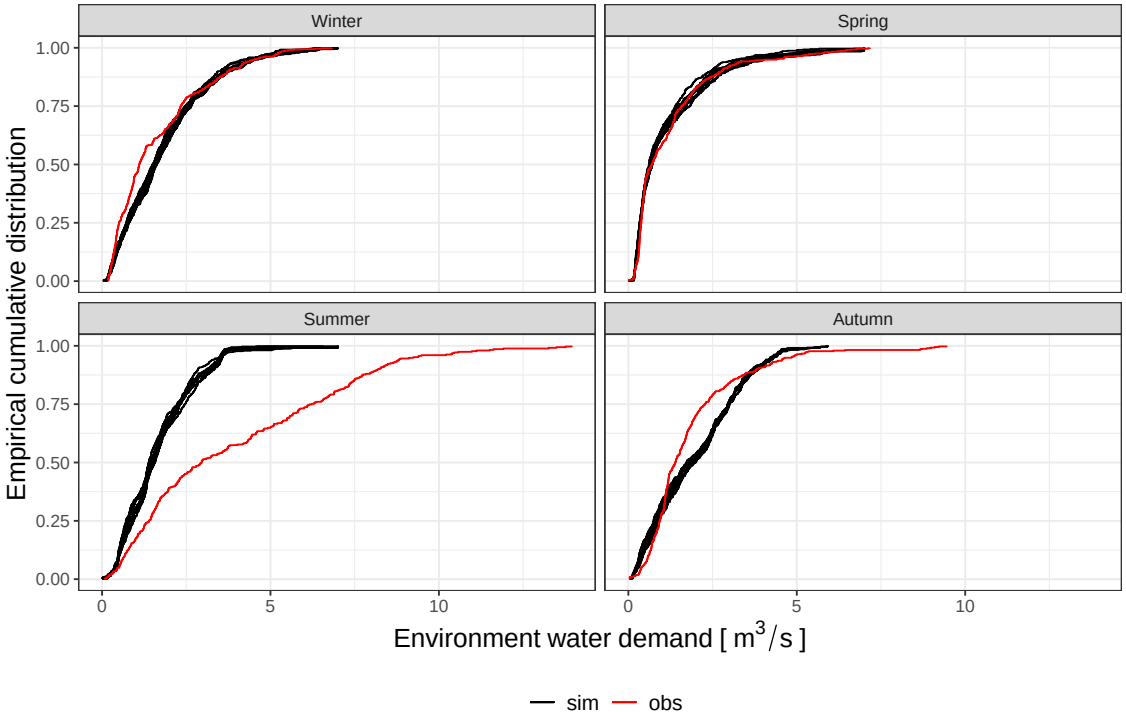

Figure 5.12 – ECDF of the 10 trials of the environmental water demand (simulated with naturalized river discharge Q_{nat5} in SB5, observed canal water extraction, and observed daily request from SHEM reservoirs by CACG) compared with the observed environmental water release from the CACG reservoirs for four seasons over the period from 01/2003 to 12/2019.

5.2 Water management modelling

5.2.1 Introduction

This sub-section explores how to construct water management models in the Neste water system. Since the SHEM and CACG manage water in different ways, water management models for each management component are designed separately. Three management models are presented: the water management model representing SHEM for hydropower production, the water management model representing CACG extracting water at Sarrancolin to feed SB5, and the water management model representing CACG sharing water for the four types of water demand in SB5 (drinking water, industrial use, irrigation, and environmental use).

5.2.2 Water management model of SHEM

Model development

As mentioned before, the reservoirs in the Eget-Louron system, which are single-year and multipurpose, are managed in a joint mode. SHEM makes the management plan for the reservoirs in a deterministic way before the beginning of the management year (typically April to the end of March of the next year). This procedure predicts inflows into the reservoirs, water demand from CACG, and the market electricity prices by the experience of reservoir managers and the tools developed by SHEM. An optimization step is then involved to make a series of decisions about the volume to be allocated at a given time is entailed in this procedure. This optimization is required to make the most use of the available water in the SHEM reservoirs to produce energy for profit while ensuring that various water demand (eflow and CACG demand) and restrictions (e.g., water release capacity, no overflow of the reservoirs, and water transfer capacity) are satisfied. It is considered that water releases are cost-effective when the released volume exceeds the regulatory volume requested by CACG.

In this study, a water management model is developed to reproduce this management mode to manage the Orédon, Oule, Pouchergues, and Caillaouas reservoirs in a coordinated manner. Several simplifications are made in the water management model of SHEM.

- First, the Pouchergues and the Caillaouas reservoirs are aggregated into one reservoir in order to reduce the uncertainties in naturalizing the inflows into the two reservoirs as mentioned in chapter 3. We name it as the Lassoula reservoir.
- Second, we do not include the electricity price model as SHEM does to calculate the "water value" in the reservoirs to guide the release. The market prices are reflected as the balance point in supply and demand, which is out of the scope of the thesis. Instead, the trigger to the hydropower production of SHEM used in this study is the "interest of release" based on the hydropower demand modelling (Hendrickx and Sauquet, 2013). The "interest to release" is relevant to the electricity price: a higher demand in the market normally means a higher market price, and thus a higher interest in producing hyropower for SHEM.
- Third, we transfer the management period from April-March to July-June for two reasons: (1) the Lassoula reservoir has a less variant water volume in July (close the

maximum storage) than water volume in March, which helps to fix the constraint in the optimization procedure; and (2) this transfer facilitates the impact assessment of reservoir refill management.

- Fourth, the maintenance of the turbines in the Eget-Louron hydropower system is not included in the simulation and the hydropower plants can always provide the maximum energy production.

Figure 5.13 shows the simplification of the Eget-Louron hydropower system for the optimization process. In the Eget-Louron system, the hydropower plants that have the highest drop height are those of the Louron system because of the cascade power plants (see Table 3.3). Thus, 1 m^3 of the water in the Louron system produces more energy than that of the Eget system ($K_t^1 < K_t^3$). In the Eget hydropower system, according to SHEM, water in the Oule reservoir is more cost-effective than that in the Orédon reservoir. Although water in the Orédon reservoir is transferred into the Oule reservoir for hydropower production, we introduce a water-energy transition coefficient for the Orédon reservoir K_t^2 that is slightly less than K_t^1 to guide water management ($K_t^2 < K_t^1$). Given that water-energy coefficients have the relation as $K_t^2 < K_t^1 < K_t^3$ for all time steps, they are all considered as constant.

The value of the coefficient K_t^2 is sourced from Table 3.3, which is 1.73. The value of the coefficient K_t^1 is set to be 1.70, a slightly lower value than 1.73. The value of the coefficient K_t^3 is calculated as the mean value of the energy-water coefficient range for the Caillaouas reservoir (water out of the Caiilaouas reservoir for hydropower production will go through the Lassoula-Caillaouas, Tramezaygues, Pont de Prat, and Pont d'Estagnou plants as shown in Table 3.3). Thus, the value of K_t^3 is approximated as 2.05.

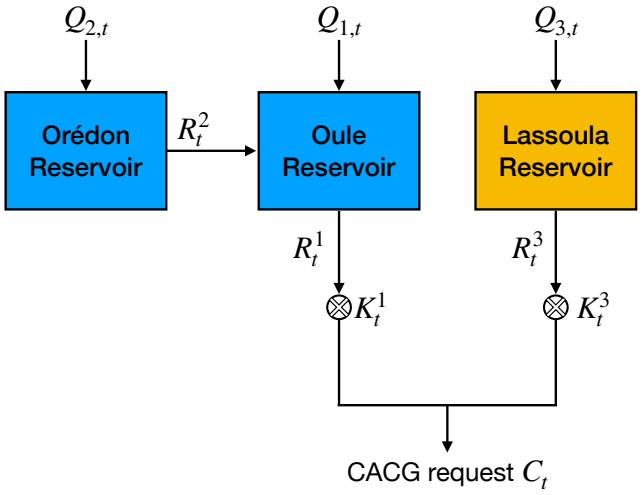

Figure 5.13 – The simplification of the Eget-Louron system for the optimization process. $Q_{1,t}$, $Q_{2,t}$, and $Q_{3,t}$ represents the inflows of day t into the Oule, Orédon, and Lassoula reservoirs, respectively. R_t^1, R_t^2, and R_t^3 represents the outflows of day t from the Oule, Orédon, and Lassoula reservoirs, respectively. K_t^1 and K_t^3 are the water-energy transition coefficient for the Oule and Lassoula reservoirs, respectively.

The water management model is developed based on the rules mentioned above. The time step chosen is daily time step to make the full use of data available and to avoid the

complexity of hourly spot prices in a day. The simulation steps of the management model of SHEM are presented as follow.

1. Stage variables (consecutive days in a management year):
   - t = 1, 2, 3, ..., N
2. Decision variables (water releases from each reservoir for each use at stage t):
   - $R^1_{C,t}$: water release from the Oule reservoir for CACG demand
   - $R^1_{S,t}$: water release from the Oule reservoir for hydropower production
   - $Spil^1_t$: water spills from the Oule reservoir
   - $R^2_{C,t}$: water release from the Orédon reservoir for CACG demand
   - $R^2_{S,t}$: water release from the Orédon reservoir for hydropower production
   - $Spil^2_t$: water spills from the Orédon reservoir
   - $R^3_{C,t}$: water release from the Lassoula reservoir for CACG demand
   - $R^3_{S,t}$: water release from the Lassoula reservoir for hydropower production
   - $Spil^3_t$: water spills from the Lassoula reservoir
3. State variables:
   - ${V_t}^1$: water volume of the Oule reservoir at early stage t
   - ${V_t}^2$: water volume of the Orédon reservoir at early stage t
   - ${V_t}^3$: water volume of the Lassoula reservoir at early stage t
4. State transition functions based on water budget:
   - $V^1_{t+1} = V^1_t + Q_{1,t} + R^2_{C,t} + R^2_{S,t} - R^1_{C,t} - R^1_{S,t} - Spil^1_t - eflow_1$;
   - $V^2_{t+1} = V^2_t + Q_{2,t} - R^2_{C,t} - R^2_{S,t} - Spil^2_t - eflow_2$
   - $V^3_{t+1} = V^3_t + Q_{3,t} - R^3_{C,t} - R^3_{S,t} - Spil^3_t - eflow_3$
5. Target function that is the benefit of water release at stage t:
   - $B_t = R^1_{S,t} \times {K_t}^1 + R^2_{S,t} \times {K_t}^2 + R^3_{S,t} \times {K_t}^3$
6. Objective function:
   - $f_{obj} = max\left(\sum_{t=1}^{t=N} B_t \times P_t\right)$, where P_t is the "interet of release"
   - $P_t = 0.00001 \times D^{ene}_t$, where 0.00001 is the coefficient to transfer hydropower demand to the "interest of release"
7. Constraints:
   - CACG water demand: $C_t = R^1_{C,t} + R^2_{C,t} + R^3_{C,t}$
   - eflow downstream the Oule reservoir $eflow_1$ applied to the state transition function of ${V_t}^1$

- eflow downstream the Orédon reservoir $eflow_2$ applied to the state transition function of V_t^2
- eflow downstream the Lassoula reservoir $eflow_3$ applied to the state transition function of V_t^3
- No overflow of the Oule reservoir: $V_{min}^1 \leqslant {V_t}^1 \leqslant V_{max}^1$
- No overflow of the Orédon reservoir: $V_{min}^2 \leqslant {V_t}^2 \leqslant V_{max}^2$
- No overflow of the Lassoula reservoir: $V_{min}^3 \leqslant {V_t}^3 \leqslant V_{max}^3$
- Water release capacity of the Oule reservoir (water use from the Orédon reservoir is released through the Oule reservoir): $R_{min}^1 \leqslant R_{C,t}^1 + R_{S,t}^1 + R_{C,t}^2 + R_{S,t}^2 \leqslant R_{max}^1$
- Water release capacity of the Orédon reservoir: $R_{min}^2 \leqslant R_{C,t}^2 + R_{S,t}^2 \leqslant R_{max}^2$
- Water release capacity of the Lassoula reservoir: $R_{min}^3 \leqslant R_{C,t}^3 + R_{S,t}^3 \leqslant R_{max}^3$
- Spill water capacity of the Oule reservoir: $Spil_{min}^1 \leqslant Spil_t^1 \leqslant Spil_{max}^1$
- Spill water capacity of the Orédon reservoir: $Spil_{min}^2 \leqslant Spil_t^2 \leqslant Spil_{max}^2$
- Spill water capacity of the Lassoula reservoir: $Spil_{min}^3 \leqslant Spil_t^3 \leqslant Spil_{max}^3$
- Minimum water volume of the Orédon reservoir in winter (water in the Orédon reservoir is transferred to the Oule reservoir for hydropower production in winter): $V_{winter}^2 = V_{min}^2$
- No transfer from the Orédon to Oule reservoir in spring (there is no water transfer in spring for the refill of the Orédon reservoir): $R_{C,spring}^2 + R_{S,spring}^2 = 0$

8. Boundaries (water volume in the reservoirs should achieve the storage target V_{ini} at the end of the management year):

- $V_{t=1}^1 = V_{t=N}^1 = V_{ini}^1$
- $V_{t=1}^2 = V_{t=N}^2 = V_{ini}^2$
- $V_{t=1}^3 = V_{t=N}^3 = V_{ini}^3$

The core of the management model is to maximize the value of objective function. Since the objective function and the constraints are all linear, linear programming method can be applied to solve the optimization problem. The R package "lpSolve"[5], which is a software developed to solve linear programming problems, is used in this study to solve the large linear equations with large linear constraints. The generated results are daily water releases from three reservoirs for each water use. Daily water volume in the three reservoirs can thus be deduced from the step 4 above. Note that the optimization process has no parameters to calibrate and all the parameters (e.g., water-energy coefficients, maximum reservoir storage, and maximum release capacity) are sourced from the current reservoir configurations.

[5] https://github.com/gaborcsardi/lpSolve

Model assessment

In order to assess the performance of the water management model of SHEM, we simulate the reservoir volume for the Oule, Orédon, and Lassoula reservoirs as shown in Figure 5.14. The simulation of water transfer from Orédon to Oule reservoir is illustrated in Figure 5.15. The input data are those of observed energy demand, observed CACG demand, and simulated water inflow over the period from 07/2002 to 06/2014. The reason why simulated flow is used instead of naturalized inflow is that the Orédon reservoir does not have naturalized inflow before 07/2014. The decision variables in the management model are either 0 when there is no interest to release or maximum value when there is a interest to release. The regimes of reservoir volume and water transfer among the Orédon, Oule, and Lassoula reservoirs are calculated with mean, instead of quantiles, so as to reduce variations in performance assessment.

Reservoir refill in spring and reservoir release in summer for CACG demand and winter for hydropower production are well captured for the three reservoirs. Water transfer from the Orédon reservoir to the Oule reservoir also follows the observed water transfer with peaks in summer mainly for CACG demand. The KGE value between simulated and observed water volume of the Oule reservoir is 0.78 (0.55 for the Lassoula reservoir). The KGE value between the simulated and observed water transfer is 0.15 between the Orédon and Oule reservoirs, which shows a lower performance due to the simplification in the simulation process for making decisions (either 0 or the maximum value).

Figure 5.16 also shows the monthly water release for hydropower production in the Eget and Louron power plants. Generally, the simulated water release for hydropower follows the observed trend. However, the simulated water release for the Eget in summer does not correspond with the observed release, which is probably attributed to the registration errors by SHEM (water release for CACG registered as water release for hydropower production). It can also be attributed to the unusual high hydropower production in summer for some years (for example, 2013 and 2014, see Figure 3.18). These years are translated by the management model as high demand in summer and thus hydropower is produced in summer by the Louron system due to higher water-energy coefficient.

In all, water management model of SHEM is developed as an optimization process, which simulates the best water release strategies without considering the various incentives by water managers. Deviations between the simulation results and the observations are attributed to the actual management by SHEM (day by day designing for hydropower production based on hourly energy market prices that is different from optimization strategy at daily basis), inflow hazards, and the uncertainties in the meteorological and economic forecasts. Although some imperfections in the simulation of SHEM management, the model shows a good competence in simulating seasonal water release.

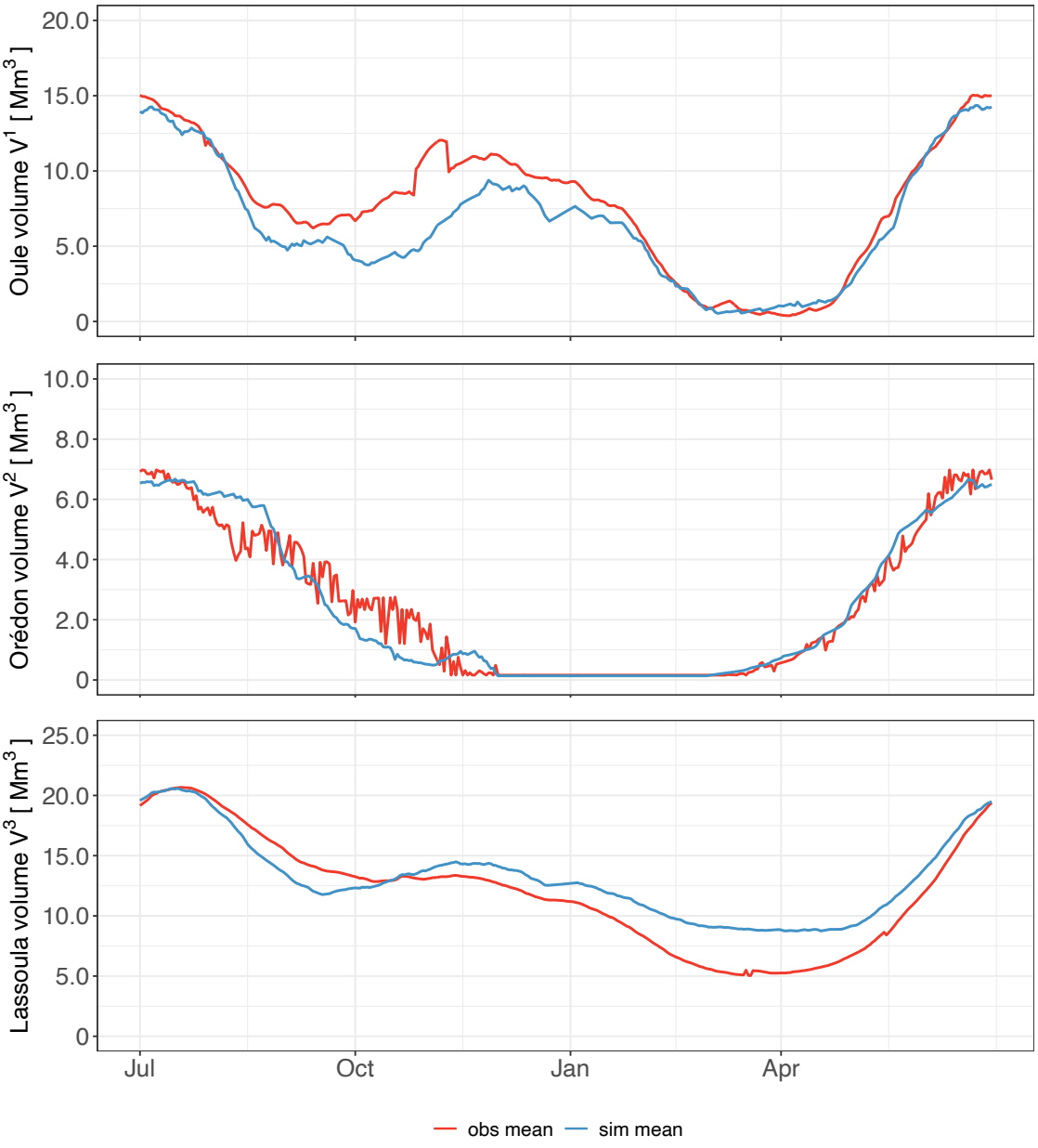

Figure 5.14 – The simulated regimes of water volume in the Oule, Orédon and Lassoula reservoirs compared with the observed water volume regimes over the period from 07/2002 to 06/2014. The observed water volume of the Orédon reservoir is from 07/2014 to 12/2018.

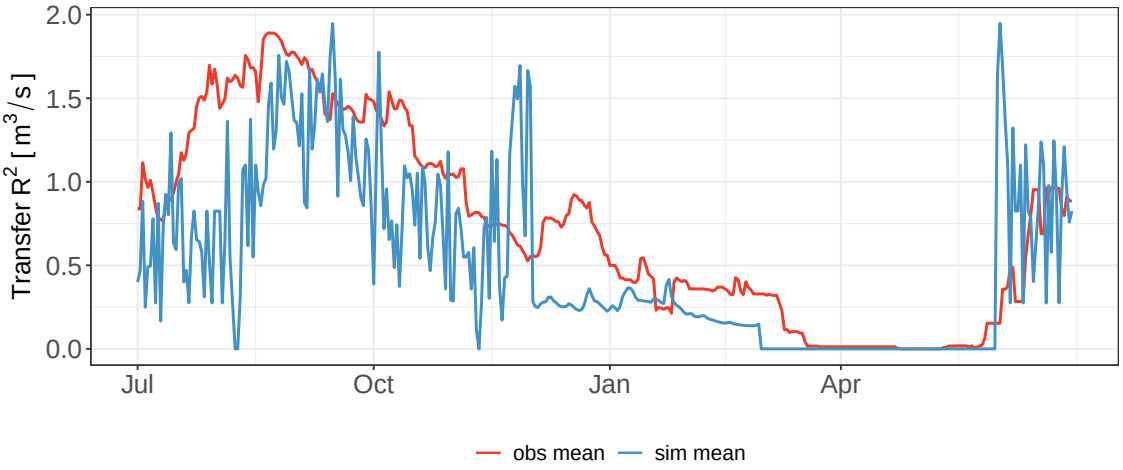

Figure 5.15 – The regime of simulated water transfer from the Orédon to Oule reservoir compared with the observed water transfer regime over the period from 07/2002 to 06/2014.

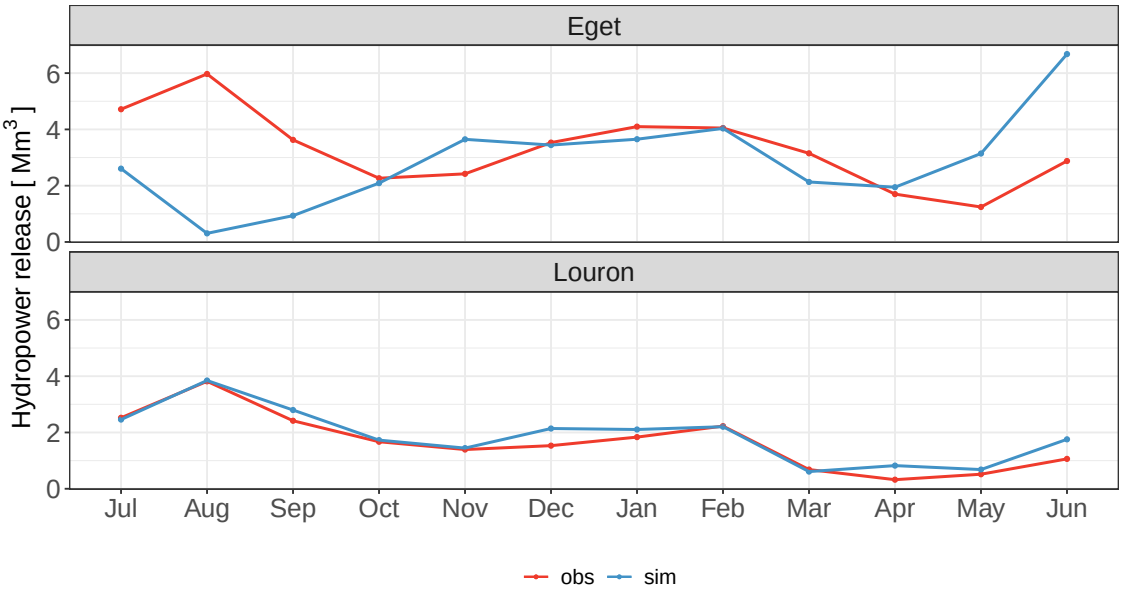

Figure 5.16 – The simulated monthly water release for hydropower production of the Eget-Louron system compared with the observed water release for hydropower.

5.2.3 Water management model of CACG

Water management of CACG is to satisfy the four types of water demand in SB5 (drinking water, industrial, irrigation, and environmental uses). The decisions are made to identify the contribution to water users from the three water sources: (1) water release from the CACG reservoirs (R_t^{tot}); (2) the request from the quota in the SHEM reservoirs (C_t); and (3) water extraction at Sarrancolin if water can be diverted through the Neste Canal based on the DOE requirement ($Q_{canal,t}$). The water sources of C_t and $Q_{canal,t}$ are managed together at Sarrancolin.

Water management at Sarrancolin

As mentioned in the chapter 3, CACG extracts water at Sarrancolin from the Neste River via the Neste Canal to feed SB5 while maintaining the river discharge downstream of Sarrancolin (Q_{infs}) no lower than 4 m^3/s. This DOE requirement at Sarrancolin can be derogated 3 m^3/s for 90 days in case of severe drought events.

The canal extraction managed by CACG has a strong seasonal pattern as Figure 3.28 shows. As such, the simulation of extraction volume can be conducted with seasonal decision trees. The rules are summarized in Table 5.6. From the table, the water volume that can be extracted by the Neste Canal depends on the two variables: water demand in the SB5 and water availability at Sarrancolin.

Table 5.6 – The seasonal extraction rules of the Neste Canal.

	Demand	Extraction rules
Winter	Drinking water, environmental support	1. DOE requirement at Sarrancolin
Spring	Drinking water, environmental support	1. DOE requirement at Sarrancolin; 2. Canal maintenance every 5 years
Summer	Drinking water, environmental support, irrigation	1. DOE requirement at Sarrancolin; 2. CACG releases water first from their reservoirs and then demand water from SHEM; 3. Maximum extraction 14 m^3/s
Autumn	Drinking water, environmental support, irrigation	1. DOE requirement at Sarrancolin; 2. CACG tends to extract 7 m^3/s to fill the reservoirs in SB5

Given that the canal water extraction is limited by the DOE requirement at Sarrancolin, we introduce a potential extraction volume γ_t to represent the extraction volume before the DOE management at Sarrancolin. The actual extraction Q_{canal} can be realized when the DOE requirement at Sarrancolin is maintained.

The quantile regression method is applied to simulate the potential extraction γ_t volume based on the total water demand from SB5. The total water demand of SB5 D_t^{SB5} is expressed in the equation 5.12. The sum of the observed water release from CACG reservoirs and the observed daily request from the contract with the SHEM reservoirs is the total water demand in SB5 ($D_t^{SB5} = R_{obs,t}^{tot} + C_{obs,t}$, $R_{obs,t}^{tot}$ the observed total daily water

release from the CACG reservoirs and $C_{obs,t}$ the observed daily request from the SHEM reservoirs). A model was fitted by season as shown:

$$\gamma_t = \begin{cases} f(D_t^{SB5})|Q_{canal}^{obs,winter} & \text{if } t \text{ in winter} \\ f(D_t^{SB5})|Q_{canal}^{obs,spring} & \text{if } t \text{ in spring} \\ f(D_t^{SB5})|Q_{canal}^{obs,summer} & \text{if } t \text{ in summer} \\ f(D_t^{SB5})|Q_{canal}^{obs,autumn} & \text{if } t \text{ in autumn} \end{cases} \tag{5.15}$$

The process of water extraction by the Neste Canal (Q_{canal}) is illustrated in Figure 5.17. If river discharge at Sarrancolin $Q_{infs,t}$ is lower than 4 m^3/s before the canal extraction, CACG cannot extract water ($Q_{canal} = 0$) and instead request water release from the SHEM reservoirs. The requested water release is $4 - Q_{infs,t}$ that is accounted in the 48 Mm^3 contract. If river discharge at Sarrancolin $Q_{infs,t}$ is larger than 4 m^3/s before the canal extraction, water extraction at Sarrancolin can take place and a potential extraction value is calculated from equation 5.15. If this potential extraction is conducted and the DOE requirement at Sarrancolin can still be maintained, the Neste Canal can extract this potential value γ_t. If not, the process is looped until the DOE requirement at Sarrancolin is maintained.

In order to validate the water extraction model, we simulate the water extraction with observed river flow at Sarrancolin $Q_{infs,t}$ and observed water demand in SB5 D_t^{SB5}. Canal maintenance in spring is not included in the simulation. Figure 5.18 shows the simulation results compared with the observations of the water extraction via the Neste Canal in terms of ECDF and the annual regime. The simulated canal water extraction Q_{canal} well follows the seasonal pattern of observations.

Besides, CACG extracts water volume released by SHEM within the contract of 48 Mm^3 annual quota at Sarrancolin. CACG request to release water from the SHEM reservoirs C_t that is also linked to the total water demand of SB5 D_t^{SB5} as shown in Figure 5.19. A clear linear relationship can be seen and the coefficient of determination R^2 between the two variables is 0.83.

The simulation of the CACG request C_t is also applied with the quantile regression method as formulated as follow.

$$C_t = \begin{cases} f(D_t^{SB5})|C_{obs,winter} & \text{if } t \text{ in winter} \\ 0 & \text{if } t \text{ in months from March to June} \\ f(D_t^{SB5})|C_{obs,summer} & \text{if } t \text{ in summer} \\ f(D_t^{SB5})|C_{obs,autumn} & \text{if } t \text{ in autumn} \end{cases} \tag{5.16}$$

CACG demand is 0 in spring because CACG can not request water from March to 15 June as declared in the chapter 3. In addition, the current water release capacity for SHEM to meet the CACG demand is 10 m^3/s. Figure 5.20 shows the simulation results compared with the observed CACG demand in terms of ECDF and the annual regime. The simulated CACG demand well follows the seasonal pattern of observations.

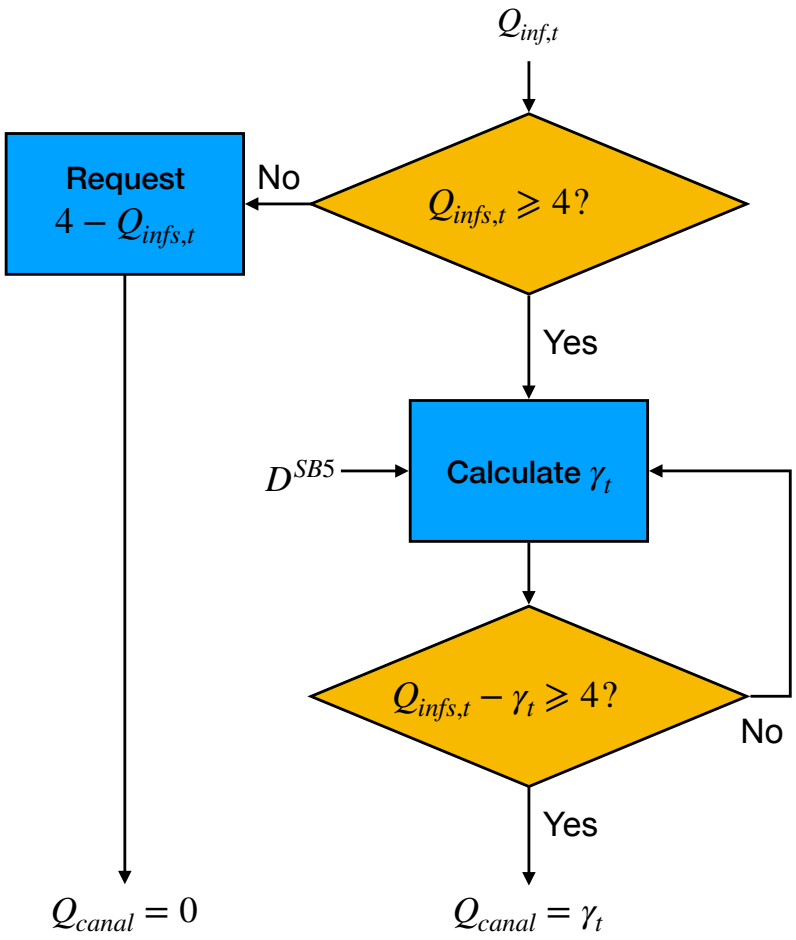

Figure 5.17 – The process of maintaining DOE requirement when extracting water via the Neste Canal at Sarrancolin. $Q_{infs,t}$ and γ_t are river discharge at Sarrancolin and a potential water extraction by the Neste Canal, respectively.

Water management model of CACG reservoirs in SB5

Given the complexity of the Neste water system, CACG applies a real-time management procedure instead of an optimization planning to provide water for the four types of water demand (drinking water, industrial use, irrigation, and environmental support). As such, we apply a parameterization-simulation process to simplify the daily management of the CACG reservoirs. This process calculates the daily water release from the 15 CACG reservoirs based on the natural water inflows in SB5, water extraction from the Neste Canal, and the water demand from the CACG reservoirs. Note that the 15 reservoirs are simplified into one reservoir with the maximum storage of 73.3 Mm^3. The modelling basis can be derived as follows:

$$V_{t+1}^5 = V_t^5 + \alpha_1 \times Q_{5,t} + \alpha_2 \times Q_{canal,t} - \alpha_3 \times D_t^{SB5} \tag{5.17}$$

where V_t^5 is the volume of CACG reservoir storage of day t. Parameters α_1, α_2, and α_3 can be explained as the proportion of diverting natural inflow of SB5 into the CACG reservoirs, the proportion of extracting water volume in the Neste Canal into the CACG reservoirs, and the proportion of releasing water from CACG reservoirs based on the total water demand in SB5.

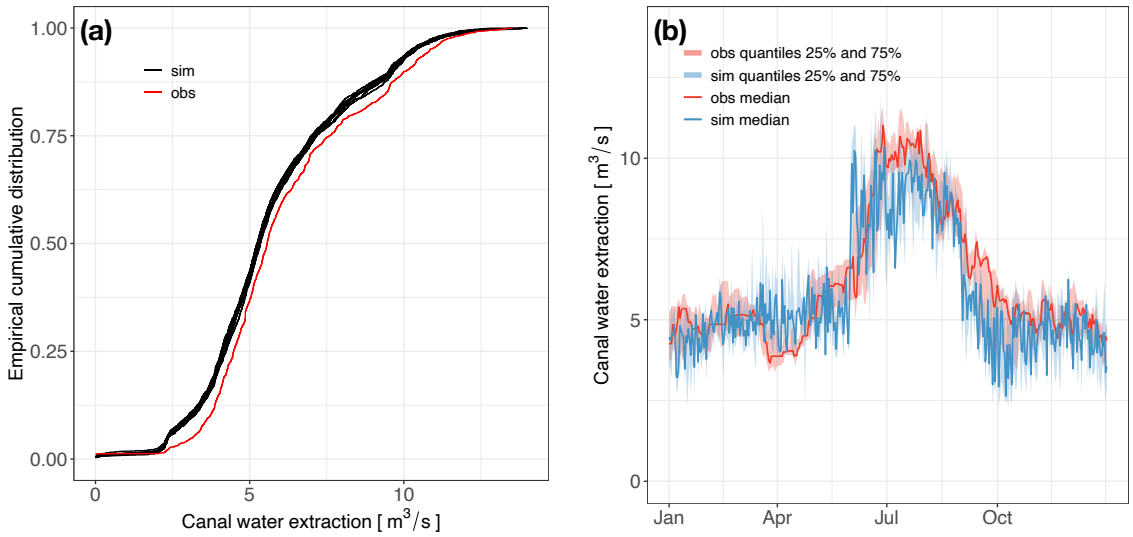

Figure 5.18 – (a) ECDF of the 10 trials of the canal extraction model simulated with the observed river flow at Sarrancolin and the observed water demand in SB5 over the period from 01/2013 to 09/2019 as inputs compared with the observed water extraction from the Neste Canal; (b) The regime of the simulated water extraction from the Neste Canal compared with the regime of the observations over the period from 01/2013 to 09/2019.

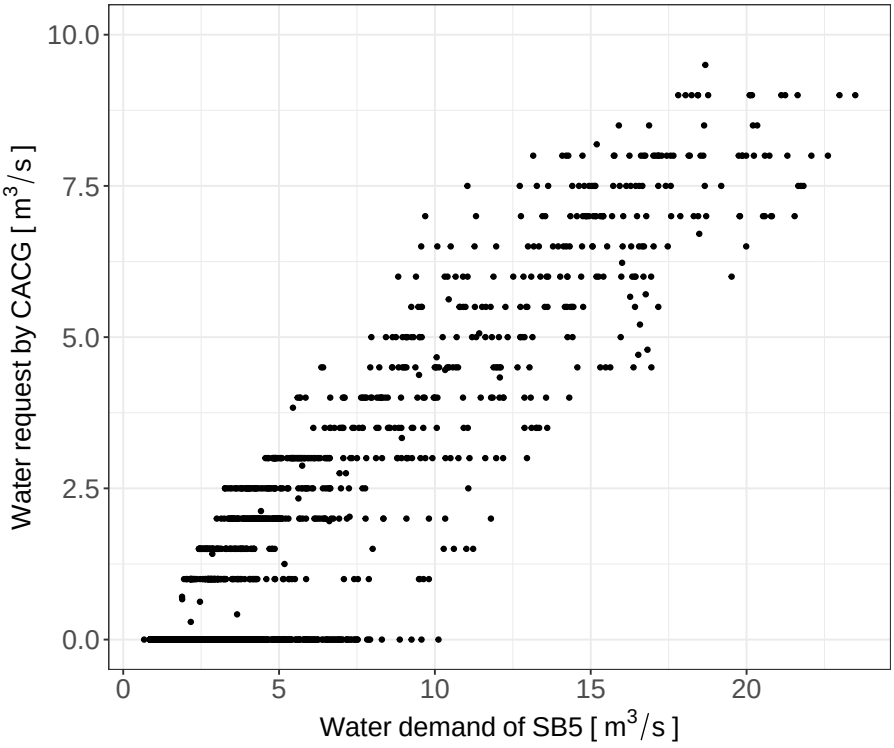

Figure 5.19 – Linear relation between CACG request to release water from the SHEM reservoirs and the total water demand of SB5. The two variables are in the period from 01/2013 to 09/2019.

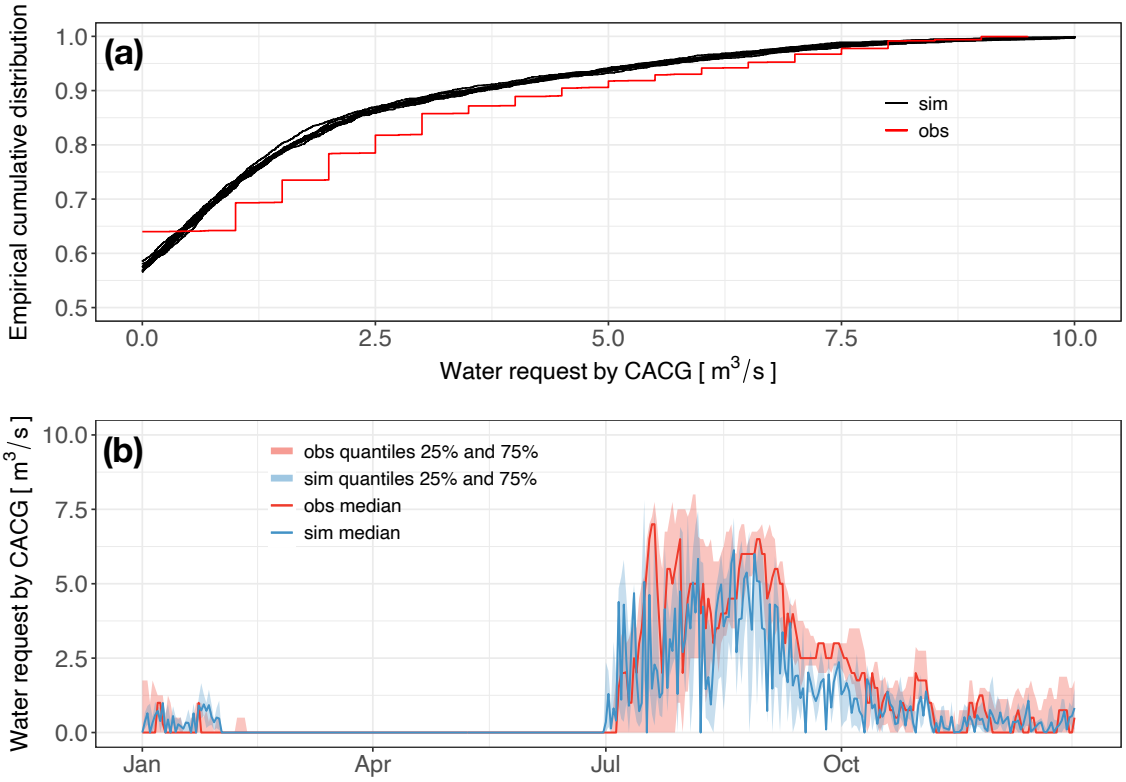

Figure 5.20 – (a) ECDF of the 10 trials of the CACG demand model simulated with the observed water demand in SB5 over the period from 01/2013 to 09/2019 as input compared with the observed CACG demand; (b) The regime of the simulated CACG demand compared with the regime of the observed CACG demand over the period from 01/2013 to 09/2019.

Parameters α_1, α_2, and α_2 are the parameters that need to be calibrated. The ranges of α_1 and α_2 are in [0, 1]. The range of α_3 is in [1, 2] to account for water losses. Here, we apply a global optimization of coefficient of determination R^2 with the Particle Swarm Optimization algorithm (Zambrano-Bigiarini and Rojas, 2013). The calibration period is from 01/2013 to 09/2019 with the naturalized inflow in SB5 (Q_{nat5}), the observed water extraction via the Neste Canal (Q_{canal}), and the observed total water demand in SB5 (D_t^{SB5}) as inputs. The parameters α_1, α_2 and α_3 are thus determined with the optimized R^2 equal to 0.92.

$$\begin{cases} \alpha_1 = 0.273 & (5.18) \\ \alpha_2 = 0.384 & (5.19) \\ \alpha_3 = 1.368 & (5.20) \end{cases}$$

As noted by CACG, in addition to releasing for water demand, around 20% extra water volume of the demand is released from the reservoirs in order to make sure that the consumers can receive at least the water volume that they have demanded. The parameter α_3 larger than 1.2 is reasonable if we account water losses.

Figure 5.21 shows the simulation results and the KGE value is 0.89. The simulated volume of the CACG reservoirs follows the observations, with the maximum storage in spring and minimum storage in autumn. However, the simulated volume of the CACG reservoirs is overestimated during drought period for some wet years. This can be attributed to the actual reservoir refill management by CACG since the canal extractions

are not diverted into the reservoirs when the water storage in the reservoirs and the natural water inflows in SB5 are sufficient for future uses. The extracted water volume is thus diverted to feed the rivers in SB5. We can also observe that the simulated volume of the CACG reservoirs is also overestimated in spring. This is because CACG manages to refill the reservoirs by extracting the natural inflows in SB5 at daily basis with a caution against reservoir overflow. As such, the fixed extraction parameters α_1 and α_2 throughout the year are not capable enough to represent the daily management.

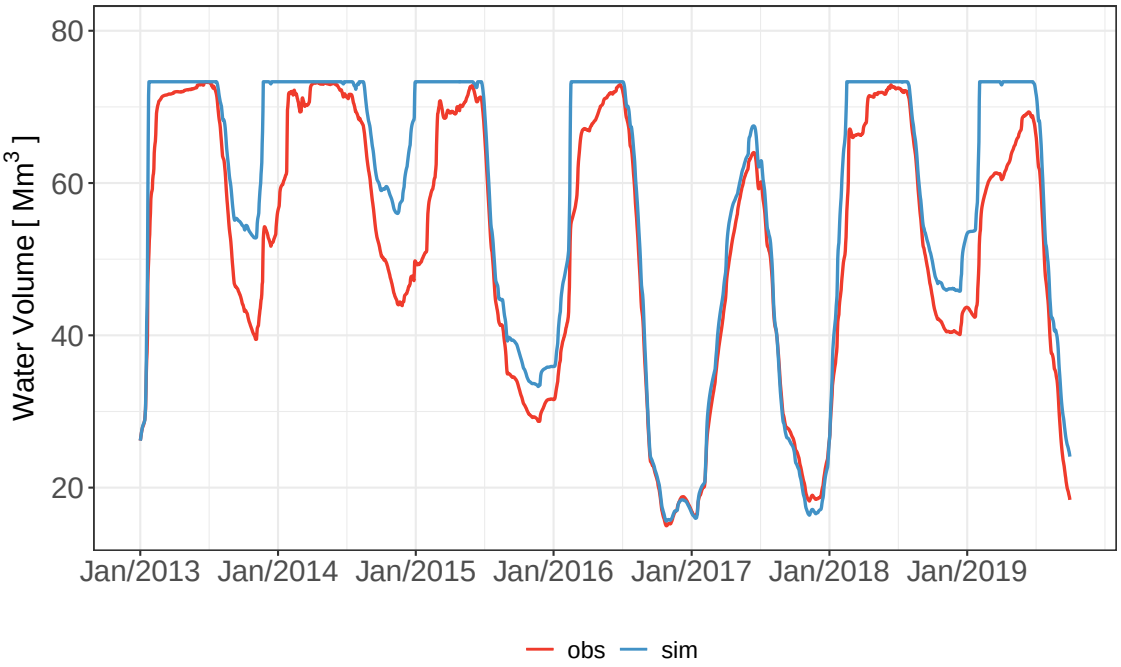

Figure 5.21 – The simulated volume of CACG reservoirs compared with the observed volume of CACG reservoirs over the period from 01/2001 to 09/2019.

There are two limitations in the modelling of water management in SB5: (1) all the steps of the decision making and assimilation processes are not included (e.g., water use quota is applied to water demand when the volume stored in the reservoirs is low); and (2) groundwater abstractions are not considered.

5.3 Summary

This chapter presents the pieces of the water demand and management models developed to represent the water management of the Neste water system. Table 5.7 summarizes the inputs and outputs for each model piece. These models take account of global change drivers as much as possible for the investigation of global change impact in the next chapters. The water management model "CACG management in SB5" will not be used in the next chapters.

Table 5.7 – The summary of the hydrological model, water demand models, and water management models with inputs and outputs.

Type	Model	Input	Output
Natural water resources	GR6J-CEMANEIGE	P, T, and PET	Q and SCA
Water demand	Energy demand	T (HDD)	Demand for hydropower
	Drinking water demand	Population and network efficiency	Demand for drinking water
	Industrial water demand	-	Demand for industrial use
	ADEAUMIS	P, T, PET, and irrigation surface	Demand for irrigation
	Environmental demand	Natural Q in SB5, CACG reservoir storage, and DOE in SB5	Demand for environmental support
Water management	SHEM management	Natural Q in SB1-3, CACG demand, and energy demand	SHEM reservoir releases for different uses
	Influenced Q at Sarrancolin	SHEM reservoir releases and Natural Q in SB4	River discharge at Sarrancolin
	CACG management at Sarrancolin	River discharge at Sarrancolin, total water demand in SB5, and DOE at Sarrancolin	Canal extraction and water volume requested by CACG for SHEM
	CACG management in SB5	Canal extraction, Q5, total water demand in SB5	CACG reservoir releases for different uses

6

Vulnerability assessment

This chapter is a research article submitted to Journal of Hydrology: Regional Studies, entitled "Vulnerability of water resource management to climate change: Application to a Pyrenean valley", and currently under review.

Contents

Abstract **145**

6.1 Introduction **146**

6.2 Study area **149**

6.3 Data and methods **152**

6.3.1 Climatic drivers 152

6.3.2 Naturalized inflow 154

6.3.3 Hydrological modelling 154

6.3.4 The SN framework for water management 155

6.4 Results **159**

6.4.1 Hydrological model performance 159

6.4.2 Water management sensitivity analysis 161

6.4.3 Water management vulnerability assessment 165

6.5 Discussion **169**

6.5.1 The contribution to the Pyrenean studies 169

6.5.2 Potential mitigation and adaptation actions 170

6.5.3 Limitations and future works 170

6.6 Conclusion **172**

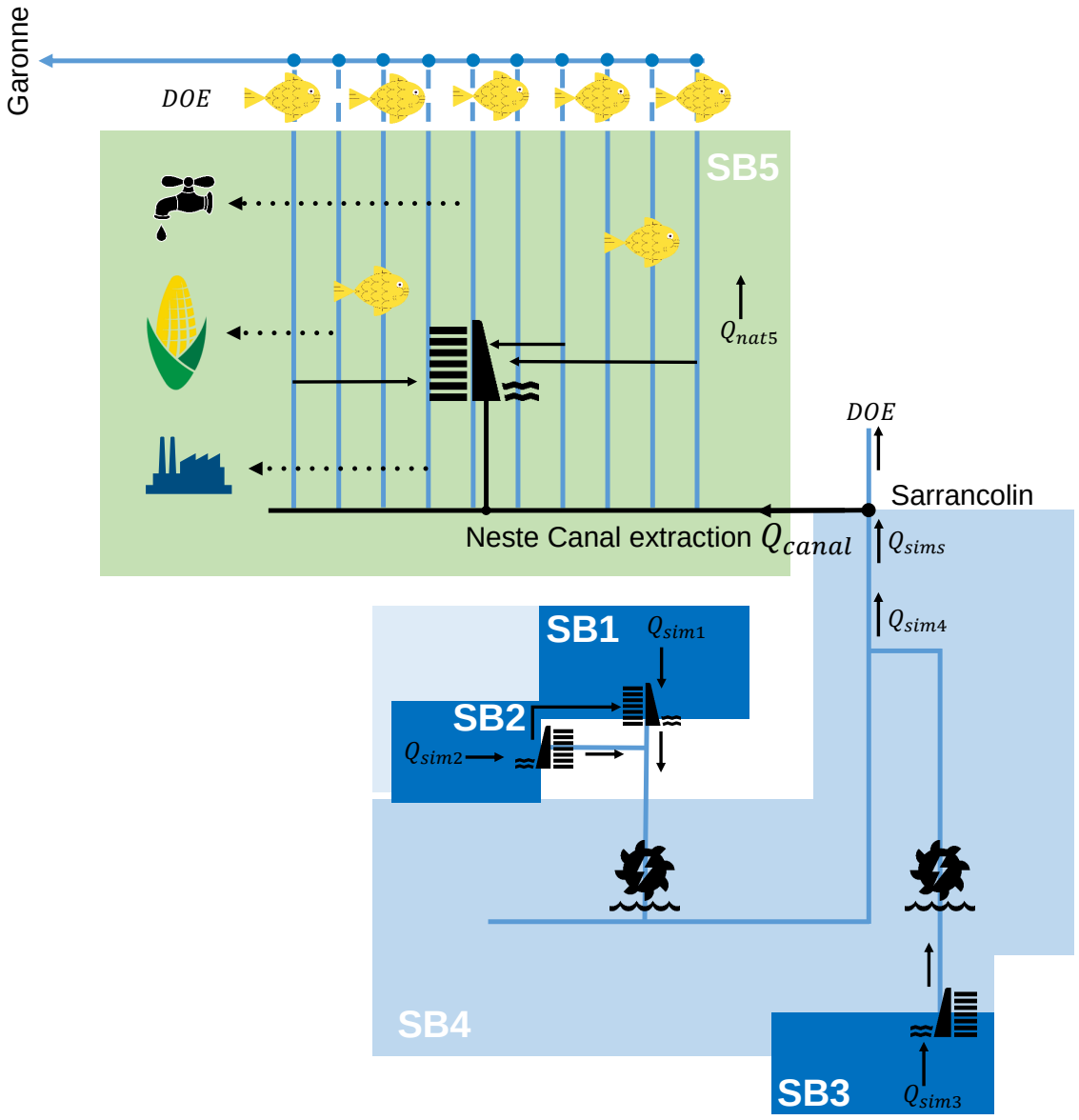

Figure 6.1 – A simplified schema of the Neste water system and this chapter investigates the vulnerability of water management in the Aure Valley (SB1-4) under climate change scenarios with a bottom-up framework.

VULNERABILITY OF WATER RESOURCE MANAGEMENT TO CLIMATE CHANGE: APPLICATION TO A PYRENEAN VALLEY

PENG HUANG[1], ERIC SAUQUET[1], JEAN-PHILIPPE VIDAL[1], NATACHA DARIBA[2]

[1]UR RiverLy, INRAE, Villeurbanne, France
[2]GEM, ENGIE, 34 Boulevard Simon Bolivar, 1000 Brussels, Belgium

Abstract

Study region:
The Aure Valley in the French Pyrenees.

Study focus:
This study applies a bottom-up framework for assessing water management vulnerability in terms of hydropower production, environmental regulations, and reservoir storage management by integrating the sensitivity, the performance metrics, and the exposure of the water system. The hydrological model GR6J-CEMANEIGE is implemented to simulate water resource and the management metrics in the study region. The sensitivity of management metrics to climate change is investigated by comparing simulation results under current climate conditions and those obtained under perturbed climate series. Results are demonstrated with response surfaces, which are overlaid with the predefined thresholds of performance metrics. The thresholds help identifying climate conditions that are critical for water management. Plausible climate change pathways are displayed on the response surfaces to assess the probability of critical conditions.

New hydrological insights for the region:
Results show that annual hydropower production is mostly vulnerable to future drier conditions. Environmental metrics are sensitive to both precipitation and temperature changes while the current policy render the low-flow management less susceptible to risks. Reservoir storage management is found to be extremely sensitive to temperature increase that induces an earlier snowmelt. Although downstream water use is less vulnerable to climate change even under a high greenhouse gases emissions scenario, more intense water competition among stakeholders can be foreseen. Corresponding adaptation actions are proposed to reduce the vulnerability.

6.1 Introduction

Snow-dominated mountains, frequently referred to as natural water towers, provide essential surface water resource that are of great importance for ecosystems and human society water use (Barnett et al., 2005; Immerzeel et al., 2019; Viviroli et al., 2011). Water in these mountains is stored as snowpack or glacier in the cold season and melts in the warm season to naturally sustain low flows. However, climate change significantly impacts the snow accumulation-melting patterns, thus altering hydrological regimes and propagating to water resource management, e.g., hydropower generation, agricultural practices, and respect of environmental rules (e.g., Farinotti et al., 2019; Pepin et al., 2015; Qin et al., 2020a). In particular, the Pyrenees mountain range is an important source of water for regions in Southwestern Europe (e.g., Andorra, France, and Spain) while it is considerably vulnerable to climate change (Amblar-Francés et al., 2020; García-Ruiz et al., 2011; Morán-Tejeda et al., 2017).

The Pyrenees constitute a transition band from Atlantic to Mediterranean climate conditions, which is recognized as a "hotspot" influenced by climate change (e.g., Chauveau et al., 2013; Fayad et al., 2017; Spinoni et al., 2017b; Tuel and Eltahir, 2020). As such, investigating the impact of climate change on Pyrenean water resource and management is a continuous concern.

The most recent climate change study focusing on the Pyrenees (Amblar-Francés et al., 2020) with a high spatial resolution ($5km \times 5km$) indicated a marked warming in the Pyrenees as temperature continues to increase under three Representative Concentration Pathways (RCPs: RCP 4.5, RCP 6.0, and RCP 8.5) while precipitation changes were not clear due to model uncertainty and spatial heterogeneity. Concerning Pyrenean water resource changes, numerous studies have reported a general decrease in terms of snowpack or river flows from in situ observations (e.g., Buendia et al., 2015; López-Moreno et al., 2020; Morán-Tejeda et al., 2012a; Sánchez-Chóliz and Sarasa, 2015) and climate change impact projections (e.g., Dayon et al., 2018; Haro-Monteagudo et al., 2020; López-Moreno et al., 2009, 2011; Morán-Tejeda et al., 2017; Morán-Tejeda et al., 2014). Specifically, snow processes as the dominant factor in the hydrological regimes in the Pyrenees are extremely sensitive to changes in temperature, precipitation, and solar radiation (e.g., Alonso-González et al., 2020; López-Moreno et al., 2008b, 2012). In addition to the major physical drivers (e.g., latitude, elevation, and slope and aspect) that results in different sensitivity of snowpack to warming climate, López-Moreno et al. (2017) further concluded that the Pyrenees is among the most sensitive Mediterranean climate mountains of the world. Water availability in the Pyrenees is thus questioned by climate change.

Increasing efforts have also been made to understand the consequences of changes in hydrological processes on water resource management in the Pyrenees (e.g., Lhuissier et al., 2016). Agricultural irrigation is the leading consumptive use of water in downstream areas, for maize cropping in southern France, and wheat and barley cropping in northern Spain. Irrigation management is threatened by a decreasing water availability and an increasing water demand due to climate change (e.g., Caubel et al., 2018; López-Moreno et al., 2008a, 2014; Majone et al., 2012; Senthilkumar et al., 2015). Haro-Monteagudo et al. (2020) investigated the largest irrigation system of Europe in the Spanish Pyrenees under climate change scenarios and showed that a decrease of available water for summer irrigation. Similar results are found for the Yesa reservoir in the Spanish Pyrenees with reduced water inflow from the upper basin and an earlier spring snow

melt, which accounts for the limited water availability to meet the irrigation demand in summer (López-Moreno et al., 2014). Besides, the increasing water demand that could be attributed to increased crop evapotranspiration by warming climate and enlarged cropland is challenging water management for irrigation (Caubel et al., 2018; López-Moreno et al., 2008a; Majone et al., 2012; Senthilkumar et al., 2015). Regarding hydropower generation, Hendrickx and Sauquet (2013) developed a simplified hydropower reservoir management model based on dynamic programming to simulate dam operations in the Ariège River basin in the French Pyrenees. Results demonstrated that hydropower generation in winter is projected to decrease due to a reduced annual inflow and an earlier snow melt if reservoir operations remain unchanged. The management of other water provisioning services such as drinking water could also be considerably affected with less water yield and more sediment retention in the reservoirs (e.g., Bangash et al., 2013). The flood events in the Pyrenean regions are complex within both meteorological and hydrological processes while climate change is likely to impair flood control as snowmelt contributes to amplifying the flooding duration instead of triggering the events (e.g., García-Ruiz et al., 2011; Morán-Tejeda et al., 2019; Pino et al., 2016). Furthermore, the overall reduced water resource brings about intensive water competition, rendering water management rather challenging in the Pyrenees.

Given the adverse impact of climate change on Pyrenean water resources and water management, adaptation strategies are thus highlighted and a comprehensive assessment under climate change is fundamental to adaptation design. In general, the top-down and bottom-up approaches are two main frameworks to assess water resource and management under climate change. Typically, the top-down approach projects future climate under different emission scenarios by using global climate models (GCMs) whose outputs are downscaled to match regional spatio-temporal scales, and projections are then forced into an integrated water resource system model to compare with current system performance (e.g., Schaefli, 2015; Vidal et al., 2016). However, the top-down approach is reported to cascade uncertainty through the modelling chain and fails to testing more extreme climate change scenarios (Brown and Wilby, 2012b; Wilby and Dessai, 2010). The alternative bottom-up approach shifts attention to assessing the system vulnerability to a wide range of scenarios generated by either parametric or stochastic perturbation of historical climate drivers. This approach is flexible and advantageous in identifying which climatic variables the system is sensitive to (Culley et al., 2016). Several frameworks based on the bottom-up approach have been proposed in the literature, such as "Scenario Neutral" (e.g., Prudhomme et al., 2010; Sauquet et al., 2019), "Decision Scaling" (e.g., Brown et al., 2012; Ray et al., 2020), and "Robust Decision Making" (e.g., Kasprzyk et al., 2013; Lempert et al., 2006). The "Scenario Neutral" (SN) approach distinguishes from the others in leaving decision processes to the decision-maker (Prudhomme et al., 2015). Prudhomme et al. (2010) suggested that the SN approach can be combined with the top-down approach by placing climate change projections at a later stage to inform future risk. This approach has been applied to climate change assessment for natural flow sensitivity analysis (e.g., Guo et al., 2017), drought management (e.g., Prudhomme et al., 2015; Sauquet et al., 2019), and flood risk (e.g., Broderick et al., 2019; Prudhomme et al., 2013a,b).

The main objective of this paper is to present the vulnerability of water management to a changing climate in the Pyrenees, taking the example of the Aure Valley where water resources are mainly used for hydropower generation, downstream water use (irrigation, drinking water, and industrial use), and low-flow support. Based on the literature review

above, the vast majority of studies on Pyrenean water resources and management adopted a top-down approach. This paper constitutes the first bottom-up analysis of water management under climate change in the Pyrenees, which provides complementary insights into water management vulnerability. In addition, a focus is made on changes in snowpack as it is one of the main factor influencing water management in the study area. The paper is organized as follows: section 2 introduces the study area. Section 3 explores the data and methods involved in analyzing water management vulnerability. Results and discussions are given in section 4 and 5, respectively. Conclusions are finally drawn in section 6.

6.2 Study area

Water resources in the Pyrenees plays an important role in addressing the issue of water shortage during summer in the South of France, known as the Gascogne region (see the left-top map in Figure 6.2a). This intensive agriculture region in the Lannemezan plateau does not benefit from mountainous snowmelt because it is separated from the Pyrenees (Leenhardt et al., 2004a,b). An artificial channel (the Neste Canal, not shown in the map) connects the Gascogne region with a Pyrenean valley, the Aure Valley, at Sarrancolin to provide stable water supply. Therefore, the Aure Valley upstream of Sarrancolin is selected as a representative example of complexity with competing water uses.

The Aure Valley is located in the centre of the French Pyrenees. Figure 6.2a shows the topographic characteristics of the Aure Valley, including the four corresponding sub-basins: the sub-basins (SB1-3) upstream the reservoirs (Oule, Orédon, Caillaouas, and Pouchergues) and the intermediate catchment (SB4) between the outlets of the reservoirs and Sarrancolin. The influence of westerly winds, which carry moist air from the Atlantic Ocean, is less effective in the Aure Valley than further west due to the blocking of the massifs (Ingrand, 1961). In addition, southern heat penetrates through the border ridge, particularly affecting the upper valley, and snowmelt dominates spring flows. Table 6.1 summarizes the physiographic and hydro-climatic characteristics for the study area.

The major water use in the valley is hydropower generation (Décamps, 1967). Two main hydroelectricity producers in the valley are the SHEM company[1] that manages the several reservoirs (in orange in Figure 6.2b) of the valley and EDF[2] that manages the westernmost part of the valley (including the Cap de Long, Aubert, and Aumar reservoirs in Figure 6.2b). Natural water flow to the Aure Valley is partly diverted: the westernmost part is transferred outside the valley and is thus not considered in this study. Water in the Oule and Orédon reservoirs generates hydropower in the Eget plant while water in Caillaouas and Pouchergues reservoirs generates hydropower through a cascade of plants, the Louron system, shown in Figure 6.2b. Note that the drainage area upstream the Pouchergues reservoir includes two parts and water in the left part (water intake from the Aygne-Tortes Lake) is transferred into the Pouchergues reservoir in the right part. Besides, water resource in SB4 also contributes to plants downstream Lassoula (e.g., Tramezaygues as shown in Figure 6.2b). The management of the four reservoirs is made on an annual basis: the annual operation process starts from the beginning of April till the end of March of the next year. In addition to hydropower generation, the water system in the valley is oriented to provide at most 48 Mm^3 of water for uses (irrigation, drinking water, industrial use, and ecological flows) in the Gascogne region. The mandatory environmental legislation furthermore requires that the river flow at Sarrancolin where water extraction takes place should be larger than 4 m^3/s. If not maintained, either more water out of the reservoirs in the Aure Valley or less water abstraction at Sarrancolin for downstream use will be conducted.

To simplify the study case, the two hypotheses are: (1) SB4 is seen as near-natural due to the comparatively small regulation storage of the reservoirs in this sub-basin; (2) the Caillaouas and the Pouchergues reservoirs can be considered as a single one because they are jointly managed.

[1] Société Hydro-Electrique du Midi (`www.shem.fr`) is a French electricity producing company, a subsidiary of ENGIE group.

[2] Electricité de France (`www.edf.fr`) is a French electric utility company

Table 6.1 – Physiographic and hydro-climatic (precipitation P, temperature T, and naturalized inflow Q) information of the reservoirs and the sub-basins in the Aure Valley

Reservoir	Dam type	Upstream basin	Hydropower system	Elevation range [m]	Reservoir storage [Mm^3]	Drainage surface [km^2]	Mean annual P [mm]	Mean annual T [°C]	Mean daily Q [m^3/s]
Oule	Gravity	SB1	Eget	1771-2693	16.6	28.4	1581	3.46	1.13
Orédon	Embankment	SB2	Eget	1820-2929	7.27	11.3	1585	3.39	1.18
Caillaouas	Gravity	SB3	Louron	2161-3064	25.4	6.7	1803	1.59	0.47
Poucherges	Gravity	SB3	Louron	2100-3146	0.83	9.9	1590	2.33	0.57
-	-	SB4	-	635-3147	0.002	541.0	1393	5.92	16.31

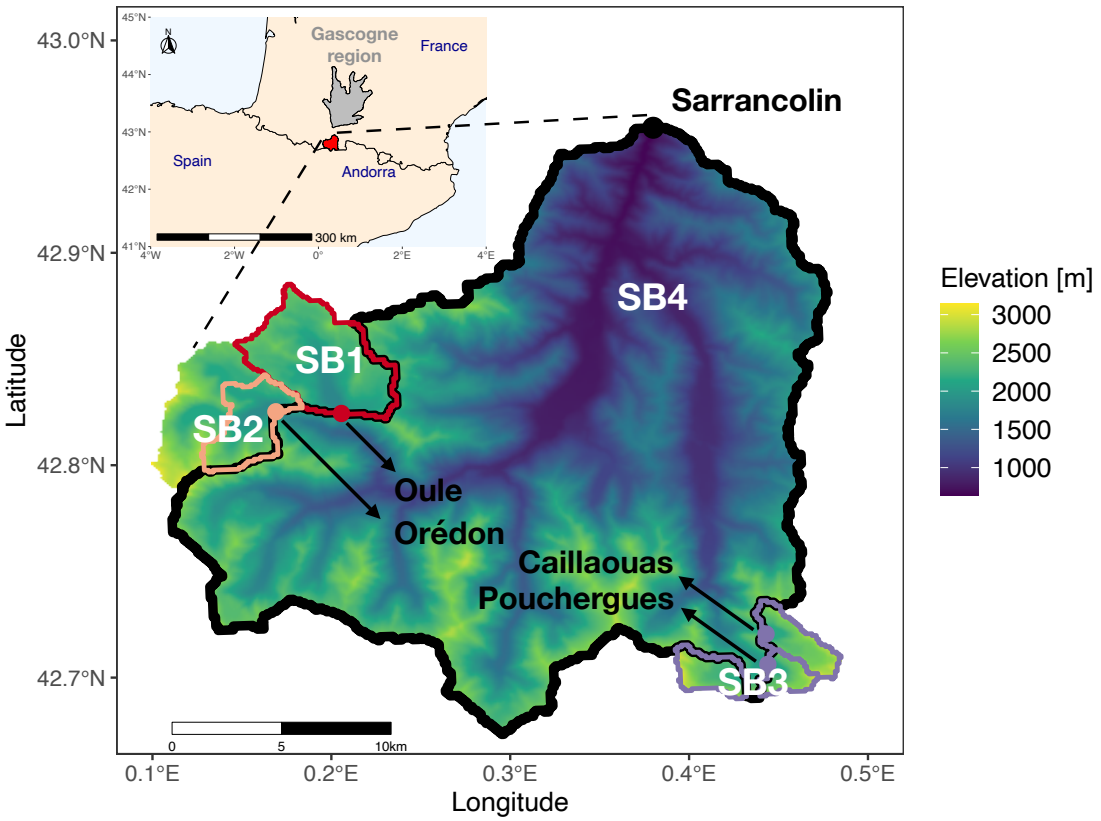

(a)

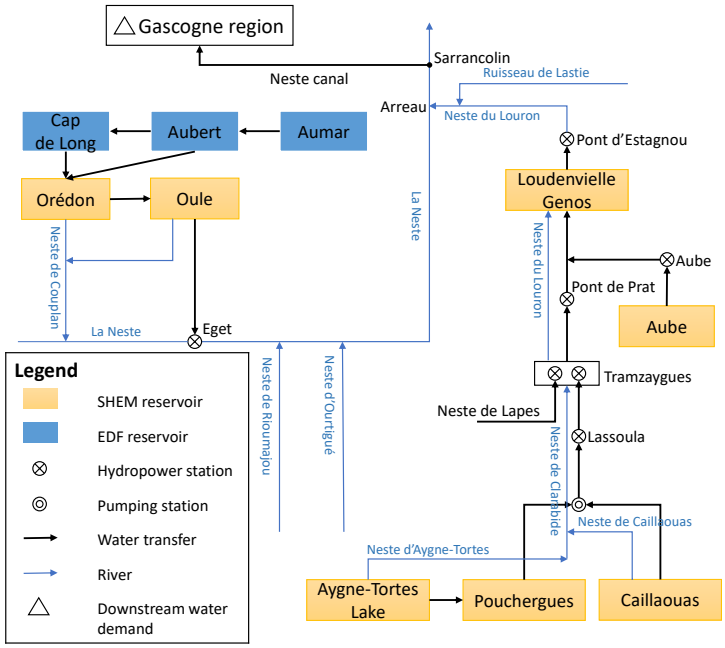

(b)

Figure 6.2 – (a) The topographic map of the Aure Valley with the five sub-basins. (b) The water management system of the Valley.

6.3 Data and methods

The vulnerability assessment of water resource and management in the Pyrenean Aure Valley under climate change is conducted by applying the SN framework (Prudhomme et al., 2010). A schematic flowchart of the overall analytic framework is given in Figure 6.3. The SN framework evaluates vulnerability by comparing plausible climate projections to the predefined thresholds of water management metrics based on the knowledge of system sensitivity to the changes of climatic drivers (Prudhomme et al., 2013a,b). To implement the sensitivity analysis of water management, the responses of the water system's performance indicators are assessed through the spectrum of perturbed climate scenarios generated from the baseline climate. Given this, the water resource system in the Aure Valley is simulated by a rainfall-runoff model. The management metrics with their associated thresholds are designed through participatory meetings among stakeholders (including SHEM) to investigate water management vulnerability. Details of the key steps that involves data, models and the SN framework are provided in the following subsections.

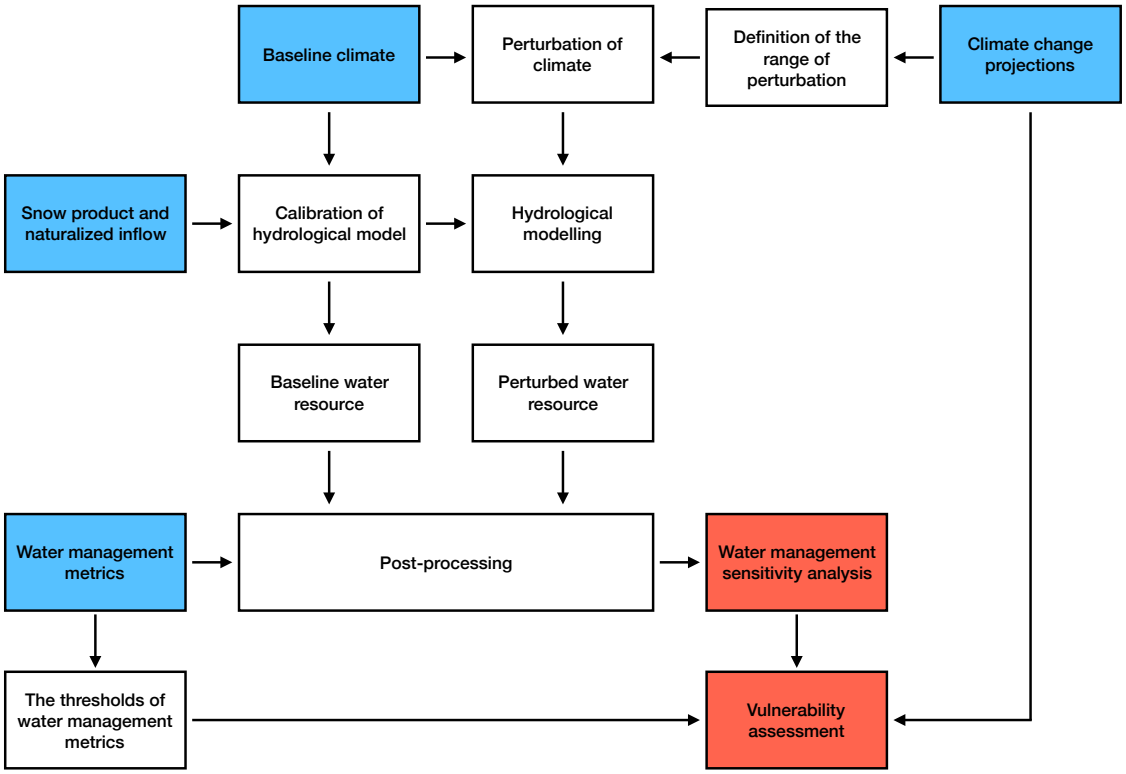

Figure 6.3 – The Scenario Neutral framework is applied to assessing the vulnerability of water management in the study area. The inputs and outputs are labelled in blue and red, respectively.

6.3.1 Climatic drivers

Baseline climate: Safran reanalyses

The near-surface meteorological reanalysis Safran-PIRAGUA that focuses on the Pyrenees is used in this study for driving the hydrological modelling. This dataset is a high resolution ($2.5km \times 2.5km$) surface reanalysis based on the Safran algorithm obtained by

merging the Safran-France reanlysis product (Vidal et al., 2010) and the Safran-Spain reanalysis product (Quintana-Seguí et al., 2016, 2017). It provides daily climate information of air temperature and precipitation. The potential evapotranspiration information is calculated from the Penman-Monteith equation (Allen et al., 1998). Catchment-scale climatic data of the study area is computed with a weighted mean of all cells intersected by the catchment surface. The Safran-PIRAGUA dataset is available from 09/1979 to 08/2014. The Safran-France dataset is also used when the calibration period of hydrological modelling is not overlapped with the SAFRAN-PIRAGUA dataset (see e.g., Table 6.3). The Safran-France dataset is available from 08/1958 to 07/2018.

Snow product: the gap-filled MODIS

MODIS (Moderate Resolution Imaging Spectroradiometer, https://modis.gsfc.nasa.gov/) is an important instrument embedded in the Terra and Aqua satellites to measure the dynamics in Earth's processes, such as snow cover, vegetation index, and land-surface temperature. Daily snow cover products are adopted in this study to calibrate the hydrological model. However, the missing snow cover observations from satellites due to the coverage of clouds make it difficult to acquire a full temporal description on the study area. Gascoin et al. (2015) developed a cloud-free snow cover product in the Pyrenees based on the MODIS products and a gap-filling algorithm. The accuracy of the gap-filled MODIS products was validated against in situ snow observations and Landsat data in the Pyrenees range. The resolution of this gap-filled snow product is consistent with the original MODIS snow product ($0.5km \times 0.5km$). The dynamics of catchment-scale snow cover can thus be computed with a weighted mean of all contributive cells to the catchment surface. Time series of snow cover area (SCA) were derived from the MODIS data over the period from 09/2000 to 04/2018.

Climate change projections

Climate projections considered here originate from a subset of 6 CMIP5 GCMs as shown in Table 6.2 and previously selected for assessing future water resource in Spain run under RCP 4.5 and RCP 8.5 (CEDEX/MAPAMA, 2017). These projections have been previously downscaled with an analogue downscaling method to generate daily total precipitation (Ptot), maximum temperature (Tx), and minimum temperature (Tn) over a $5km \times 5km$ grid for Spain and the Pyrenees within the CLIMPY project (Amblar-Francés et al., 2020; Amblar Francés et al., 2017). The CLIMPY projections have been here further refined in order to match both the higher spatial resolution and the multiple variables of the Safran-PIRAGUA surface reanalysis. To this aim a multi-site and multi-variable analogue resampling method has been set-up following the approach proposed by Clemins et al. (2019). In short, for a target day in a given CLIMPY projection, an analogue date in the 1961-2005 Safran-PIRAGUA surface reanalysis is selected, based on the best possible match of Ptot, Tn, and Tx over the whole Pyrenean mountain range. This analogue resampling is made on monthly anomalies with respect to a baseline climatology, in both Safran-PIRAGUA and CLIMPY projections. For Tn and Tx CLIMPY projections, the baseline climatology is considered as linearly transient from 2006 onwards, in order to find relevant analogue dates even with temperatures higher than any experienced in the Safran-PIRAGUA 1961-2005 archive. All variables from the analogue dates are used as values for the target date considered. Results are therefore daily gridded projections over

the Safran-PIRAGUA grid, with all corresponding variables – including precipitation and temperature required for the hydrological models – for 6 GCMs run under both RCP 4.5 and RCP 8.5 emissions scenarios, for the whole 1961-2100 period. Here, these projections are used to calculate the climate change trajectories under both RCPs for time slices 1980s (1971-1990), 1990s (1981-2000), 2000s (1991-2010), 2010s (2001-2020), 2020s (2011-2030), 2030s (2021-2040), 2040s (2031-2050), 2050s (2041-2060), 2060s (2051-2070), 2070s (2061-2080), 2080s (2071-2090), and 2090s (2081-2100). The benchmark period is from 1979 to 2014 so as to be in line with Safran-PIRAGUA.

Table 6.2 – List of selected CMIP5 GCMs.

Acronym	Institute	Reference
CNRM-CM5	CNRM, France	(Voldoire et al., 2013)
MRI-CGM3	MRI, Japan	(Yukimoto et al., 2012)
MPI-ESM-MR	MPI, Germany	(Giorgetta et al., 2013)
MIROC-ESM	AORI NIES JAMSTEC, Japan	(Watanabe et al., 2011)
inmcm4	INM, Russia	(Volodin et al., 2010)
Bcc-csm1.1	BCC, China	(Wu et al., 2013)

6.3.2 Naturalized inflow

River flow in the Aure Valley is highly influenced due to the intensive developement of hydropower (Décamps, 1967; Ingrand, 1961). A study was conducted by Falgon (2014) to reconstruct natural inflows upstream the reservoirs (SB1-3) in the Aure Valley applying a water balance approach. The principle of this approach is to sum up all exports for water use and to subtract all imports from other basins. Thus, the naturalized inflow in SB4 is the observed river discharge at Sarrancolin minus the observed outflows upstream the reservoirs. The naturalized inflows is at daily time step and the data length is from 01/2001 to 12/2018 for SB1, SB3, and SB4. However, the data length for SB2 is from 07/2014 to 12/2018.

6.3.3 Hydrological modelling

The conceptual lumped rainfall-runoff model GR6J, developed to improve low-flow simulation based on the extensively used GR4J model (Perrin et al., 2003) for French basins, was adopted to simulate the daily inflow into the reservoirs of the water system (Pushpalatha et al., 2011). The GR6J model was largely applied in studies including reconstruction of low-flow events (e.g., Caillouet et al., 2017), climate change projections (e.g., Givati et al., 2019), and streamflow forecasts (e.g., Crochemore et al., 2016). The GR6J model can thus be coupled with a semi-distributed snow-accounting routine CEMANEIGE that exploits snow information for five attitudinal layers of equal area (Valéry et al., 2014a,b). Recent developments have improved the performance of snow cover simulation by using MODIS observations (Riboust et al., 2018). The CEMANEIGE module takes account of the snow accumulation and melting hysteresis between SCA (Snow

Cover Area) and SWE (Snow Water Equivalent), which is the dynamic lag between the two states of snow.

The GR6J hydrological model has six parameters to calibrate while the CEMANEIGE module has four parameters to calibrate. The coupled GR6J-CEMANEIGE model should be calibrated to the two benchmark observations: naturalized inflow and SCA from the gap-filled MODIS product. The calibration process is illustrated as follows. First, a root-square transformation on runoff is chosen to reduce the bias towards high or low flows (Garcia et al., 2017). Second, the KGE criterion was used to assess the model performance (Kling et al., 2012) and its formulation is presented bellow:

$$KGE = 1 - \sqrt{(r-1)^2 + (\beta-1)^2 + (\gamma-1)^2} \tag{6.1}$$

where r is the Pearson correlation coefficient, β the percentage bias, and γ the ratio of the coefficient of variation between simulation and observation. Third, an objective function f that involves the two observations should be optimized and its formulation is presented bellow:

$$\begin{cases} f = a \times KGE(\sqrt{Q}) + \sum_{i=1}^{5} b_i \times KGE(SCA_i) & (6.2) \\ a + \sum_{i=1}^{5} b_i = 1 & (6.3) \end{cases}$$

where a is the weighting coefficient for runoff Q calibration, b_i the weighting coefficient for SCA_i calibration of elevation zone i. We follow here Riboust et al. (2018) who concluded that 75% weighting on runoff with 5% on each elevation zone gives a satisfactory compromise for the overall model performance. The calibrated hydrological model will be run under baseline and perturbed climate over the period from 09/1979 to 08/2014 to simulate water resource conditions in the SN framework as shown in Figure 6.3.

6.3.4 The SN framework for water management

The SN concept

Contrary to the traditional top-down approach, the SN framework investigates water management issues under climate change by underlining the sensitivity of water systems to changes. The vulnerability analysis in the SN framework depends on three concepts: the sensitivity, the exposure, and the performance metric of the water system (Brown et al., 2012; Prudhomme et al., 2013a,b, 2010; Sauquet et al., 2019). Sensitivity is the response of the water system to changes and section 6.3.4 presents how the sensitivity domain is calculated. Exposure is the climatic changes to which the water system could be exposed and section 6.3.1 details the regional climate projections used in this study. The performance metric is the relevant management indicator to characterize the system and its adaptive capacity threshold beyond which the system performs unsatisfactorily or cannot withstand the impact of climate change. Section 6.3.4 presents the performance metrics associated with water management for this study. As such, by understanding the sensitivity and the plausible exposure of the water system, a vulnerability assessment that compares changes to the predefined performance metrics can be provided.

Sensitivity domain

Three steps are involved to produce the sensitivity domain: the generation of perturbed climate scenarios, the response simulation, and the response plotting.

Perturbed climate scenarios can be generated either by parametric methods (e.g., Culley et al., 2016; Sauquet et al., 2019) or stochastic methods (e.g., Guo et al., 2017). Here, the historical climatic data from the Safran-PIRAGUA over the period from 09/1979 to 08/2014 is perturbed by the "delta-change" method based on the single-harmonic function (Prudhomme et al., 2010). The sensitivity domain of the water system to climate change is quantified from the key climatic variables, which are precipitation and temperature.

$$\Delta P(i) = P_0 + A_P \times \cos\left[(i-\phi_P) \times \frac{2\pi}{12}\right] \tag{6.4}$$

$$\Delta T(i) = T_0 + A_T \times \left\{1 - \cos\left[(i-\phi_T) \times \frac{2\pi}{12}\right]\right\} \tag{6.5}$$

where $\Delta P(i)$ and $\Delta T(i)$ are the monthly changes in precipitation and temperature; P_0 and T_0 the mean annual changes in precipitation and temperature; A_P and A_T the semi-amplitude of changes in precipitation and temperature; i the indicator of the month (1 to 12); ϕ_P and ϕ_T phase parameters for changes in precipitation and temperature.

Then, the generated monthly changes in precipitation and temperature are applied to the historical climate dataset Safran-PIRAGUA to generate daily perturbed climatic variables:

$$P^*(d) = P(d) \times \frac{\overline{PM}\big(month(d)\big) + \Delta P\big(month(d)\big)}{\overline{PM}\big(month(d)\big)} \tag{6.6}$$

$$T^*(d) = T(d) + \Delta T\big(month(d)\big) \tag{6.7}$$

where $P^*(d)$ and $T^*(d)$ are the perturbed precipitation and temperature for day d; $P(d)$ and $T(d)$ the baseline of precipitation and temperature for day d; $\overline{PM}(month(d))$ the average monthly baseline precipitation for $month(d)$; $\Delta P(month(d))$ and $\Delta T(month(d))$ the precipitation and temperature changes for $month(d)$.

Since precipitation and temperature are the only variables considered in the sensitivity analysis, changes in potential evapotranspiration is calculated by using the temperature-based formula by Oudin et al. (2005), as follows:

$$PET^*(d) = max\left(PET(d) + \frac{Ra}{28.5} \times \frac{\Delta T\big(month(d)\big)}{100}, 0\right) \tag{6.8}$$

where $PET^*(d)$ is the perturbed PET at day d; $PET(d)$ the baseline of PET at day d; Ra the extra-terrestrial global radiation for the catchment.

The range (P_0 and T_0) and seasonality (A_P and A_T) of perturbation are defined based on the climate change projections from CMIP5 in Western Europe (Terray and Boé, 2013b) and the most recent work of Amblar-Francés et al. (2020). Other parameters applicable to France (ϕ_P and ϕ_T) are given in Sauquet et al. (2019) so that the summer period gets

drier and the winter period gets wetter. These parameters are given as follow:

$$\begin{cases} P_0 = \dfrac{20 \times (j-7)}{3} - 20 & j \text{ in 1 to 15} \\ A_P = \dfrac{20 \times (j-1)}{3} & j \text{ in 1 to 5} \\ T_0 = j - 1 & j \text{ in 1 to 7} \\ A_T = j - 1.5 & j \text{ in 1 to 5} \\ \phi_P = 1 & \text{maximum change in July} \\ \phi_T = 2 & \text{maximum change in August} \end{cases}$$

As such, a set of 75 precipitation and 35 temperature scenarios can be generated (see Figure 6.4), resulting in a total of 2625 precipitation and temperature perturbation combinations used to define the climate sensitivity domain. The color spectrum in Figure 6.4a indicates that annual change of precipitation ranges from -720 to $+400$ mm and the annual change of temperature ranges from -0.5 to $+9.5$ $°C$ in Figure 6.4b. The subsequent step is the response simulation that involves forcing the 2625 scenarios into the calibrated hydrological model to simulate the response of the water system to changes following Figure 6.3. The final step is the response plotting that employs the 2D response surface to illustrate the sensitivity of the water system to changes in precipitation and temperature. To determine the most appropriate axes for the response plotting, regression analysis between response simulation results and seasonal/annual precipitation and temperature changes is applied. The changes with the highest correlation to the response simulation results are the most relevant axes.

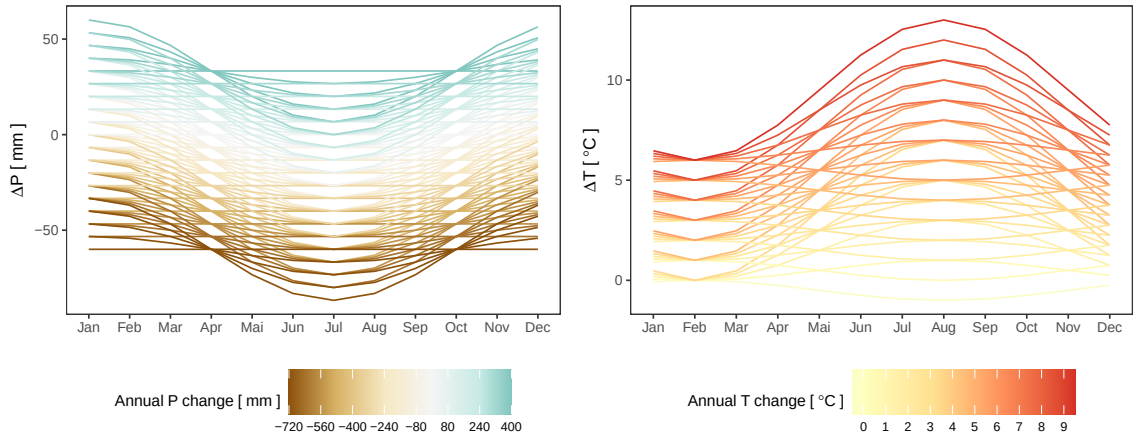

(a) *(b)*

Figure 6.4 – The perturbation of precipitation (P) in (a) and temperature (T) in (b) at monthly time step.

Water management metrics

This section presents the management-relevant metrics that can be characterized by hydrological modelling. In this study, three water management metrics are chosen based on workshops with local stakeholders in terms of hydropower production, ecological flow management, and reservoir refill management:

1. annual inflow volume (QA) for hydropower system production;

2. seasonal failure days to meet the need of mandatory ecological flow (DOE) at Sarrancolin, as well as the timing of failure (tDOE) (the first day of the year when the failure appears);

3. seasonal duration of no snow cover area (NSA) for system Eget and Louron, as well as the timing of no snow cover area (tNSA) (the first day of the year when there is no snow cover).

Water resource in the system Eget and Louron is managed by SHEM for hydropower production. The energy market in France is mostly nuclear-hydropower-mixed: nuclear plants provide base load and hydropower is generated to meet peak demands. The electricity price in the market fluctuates depending on the weather and other external factors such as gas price. Based on the experience of the water managers from SHEM, the Eget system is cost-effective when the annual water inflow into the reservoirs ranges from 28.2 to 41.6 Mm^3 for Eget (21.9 to 28.2 Mm^3 for Lassoula). Besides, there is a water contract for downstream water supply (irrigation, drinking water, and industrial water use) extracted from the four reservoirs with at most 48 Mm^3 each year. According to SHEM, the necessary water volume for SHEM to be cost-effective shows an increasing tendency towards the maximum values. Therefore, we consider the "worst" market scenario, which is 41.6 Mm^3 for the Eget plant and 28.2 Mm^3 for the Lassoula plant, and the highest scenario of downstream water demand, which is 48 Mm^3, as the thresholds for hydropower production in the vulnerability assessment.

The DOE requirement indicates that water flow at Sarrancolin should be larger than 4 m^3/s while this rule can be violated for 90 days over the low-flow period (summer and early autumn months). Thus, the threshold value for DOE is the value of 90 days and those for tDOE are the beginning of low-flow period (July to October).

The metrics of the duration and timing when there is no snow cover in the two systems are essential to reservoir storage management. However, there is no specifically predefined metric for the duration of no snow cover. We used here the concept of time of emergence. Climate conditions under which significant changes in the distribution of mean NSA time series emerge from that of current climate state can be used as the threshold of NSA to imply the necessity of changing reservoir refill strategy. In this study, the Kolmogorov-Smirnov test was conducted to verify whether two time series of mean NSA from one perturbed and the baseline climate scenario are drawn from the same distribution. This test was applied to all perturbed scenarios to determine the climate threshold beyond which significant changes of the distribution of mean NSA appears by rejecting the null hypothesis at 95% significance level. Similar application of the Kolmogorov-Smirnov test to investigate the impact of climate change on water resource can be found in the literature (e.g., Gaetani et al., 2020; Muelchi et al., 2021). In terms of the thresholds of tNSA, the beginning dates of reservoir refill months are used as benchmark values (April to June for the Eget system and April to July for the Lassoula system).

6.4 Results

6.4.1 Hydrological model performance

The hydrological model GR6J-CEMANEIGE was applied to simulate water resource in the water system of the Aure Valley. The outputs, including daily Q and SCA changes, are evaluated with the KGE criterion (Kling et al., 2012) by comparing to naturalized inflow and observed SCA derived from the MODIS images, respectively. Table 6.3 shows the KGE values for the four studied basins and the results indicate that the model performs satisfactorily with all KGE values of Q and SCA above 0.7.

The performance of the GR6J-CEMANEIGE model in reproducing seasonal dynamics is illustrated in Figure 6.5 with simulated discharges compared to naturalized discharges and simulated median SCA patterns compared to observed median SCA patterns. The simulated Q follows the variability of the naturalized inflow and can capture the high peaks and low flow spells. Especially, the recession limbs during summer period are well fitted. However, the hydrological model tends to underestimate spring flow and to overestimate winter flow for SB1-4. Note that the hydrological model has a lower performance for SB2 partly due to the short record of naturalized inflow. The module CEMANEIGE can well reproduce the seasonality of snow cover changes in the five elevation bands (Figure 6.4), as well as the accumulation phase of snow and relatively tardy melting processes. Besides, higher attitudinal elevation band shows longer snow cover duration as expected. However, the snow melting process simulation is less efficient than the snow accumulation process given the simple characteristics of the empirical degree-day model in representing snow thermal state changes (Riboust et al., 2018). SCA variations for SB1-4 are well simulated with a high performance in high elevation bands and a moderate performance in median elevation bands. This can be attributed to the high variability of snow cover in moderate elevation bands which is difficult to represent in the model.

Table 6.3 – GR6J-CEMANEIGE performance (KGE values)

	Calibration						Validation					
	$\sqrt{Q}$	SCA_1	SCA_2	SCA_3	SCA_4	SCA_5	$\sqrt{Q}$	SCA_1	SCA_2	SCA_3	SCA_4	SCA_5
SB1	0.79	0.79	0.91	0.91	0.93	0.93	0.70	0.76	0.89	0.92	0.95	0.94
SB2	0.72	0.80	0.92	0.96	0.95	0.88	-	-	-	-	-	-
SB3	0.83	0.83	0.90	0.92	0.92	0.87	0.84	0.84	0.93	0.93	0.92	0.83
SB4	0.87	0.74	0.74	0.72	0.87	0.92	0.86	0.75	0.75	0.73	0.87	0.92

Notes: The calibration and validation periods for SB1, SB3, and SB4 are 01/2001 - 08/2007 and 09/2007 - 08/2014, respectively. Given the length of naturalized inflow of SB2, only the calibration is conducted from 07/2014 to 07/2018 forced by the Safran-France reanalysis product (Vidal et al., 2010).

Finally, the water management metrics are calculated based on both simulated Q and SCA, and then compared to the observed ones as shown in Table 6.4. The management metrics QA, NSA, and tNSA are calculated for SB1-3 to investigate the accuracy of the model in reproducing hydropower indices and snow changes for reservoir refill. The management metrics DOE and tDOE are computed for the Sarrancolin catchment to show the accuracy of the model in reproducing environmental indices. The simulated natural discharge of the Sarrancolin catchment is the sum of the simulated discharges

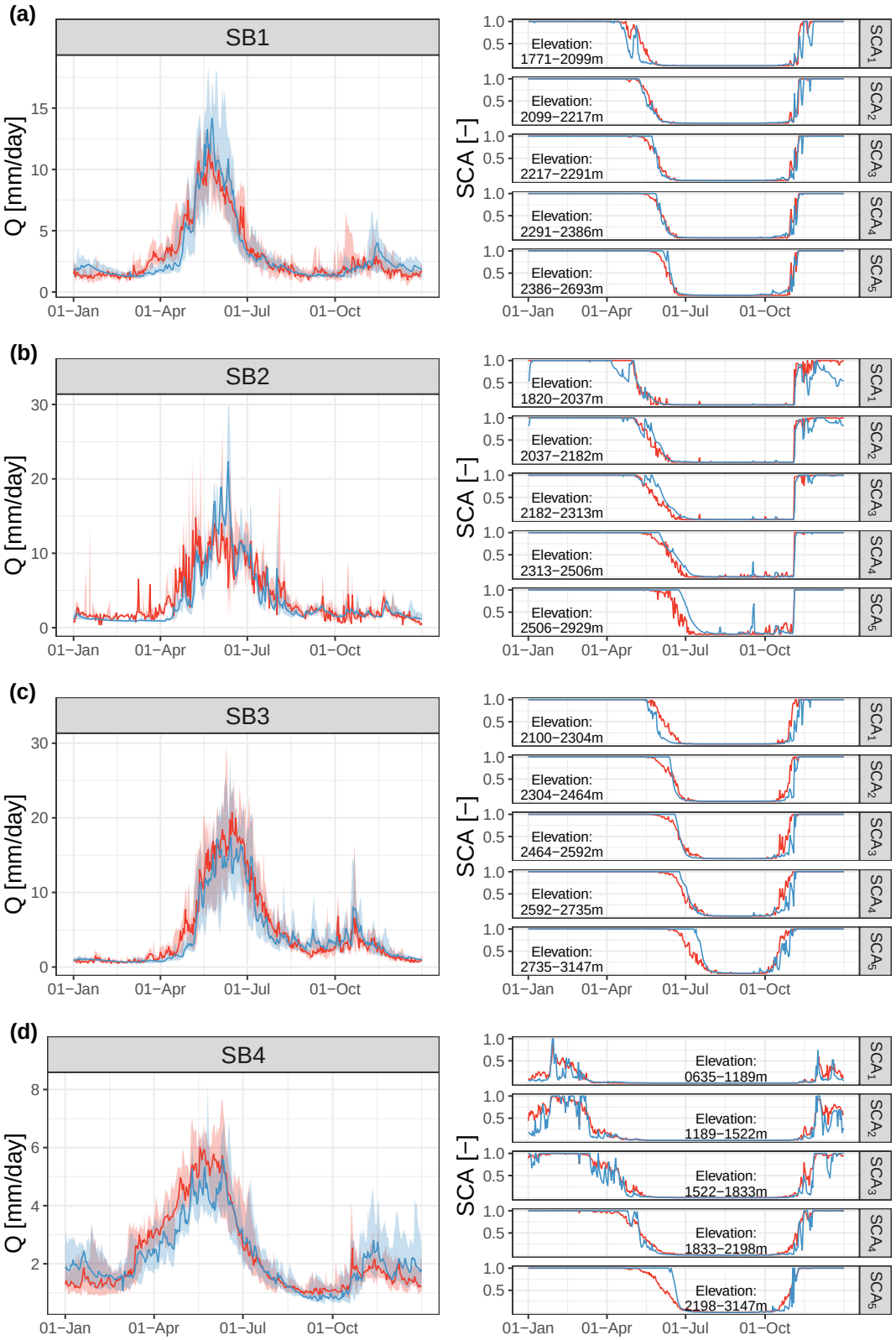

Figure 6.5 – Observed (red) and simulated (blue) median Q (left) and SCA (right) regimes for SB1(a), SB2(b), SB3(c), and SB4(d). The ribbon area in Q regime represents the percentile range of 25% and 75%. The SCA regimes are displayed for the five elevation bands. The observed/simulated period for SB1, SB3, and SB4 is from 01/2001 to 08/2014 while the observed/simulated period for SB2 is from 07/2014 to 07/2018.

of SB1-4. The simulation of management metrics are satisfactory. However, the metric tDOE is less accurate due to model uncertainty while the simulated seasonality is well reproduced. Moreover, management metric simulation of SB2 returns lower performance due to its lower quality of naturalized inflow. Table 6.5 summarizes the reference values of these management metrics for the water systems in the Aure Valley under baseline climate. These values are calculated with the Safran-PIRAGUA dataset over the period from 09/1979 to 08/2014 to represent the current management performance.

6.4.2 Water management sensitivity analysis

Water management metrics (QA, NSA, and tNSA for the Eget and Lassoula systems; DOE and tDOE for the Sarrancolin catchment) are generated through the calibrated GR6J-CEMANEIGE model forced with the total 2625 perturbed climate scenarios as described in section 6.3.4. The calculated 2625 values of each management metric are classified into groups and each group incorporates several perturbed climate scenarios (at least 5) that gather the close precipitation and temperature values. As such, the classified groups can be localized in the response surface space with average precipitation and temperature changes of the scenarios in the groups. The classified groups are symbolized as circles with color gradient indicating the average management metric values and with size indicating the standard deviation (SD) of the scenarios in the groups.

Figure 6.6 displays the 2D response surfaces developed for water management metrics and associated study area. Concerning the mean value changes of the response surfaces, the management metrics degrade when climate conditions are warmer and drier. The values of SD display a patchier pattern for both NSA and tNSA than other metrics. Large values of SD may reveal transition zones of the hydrological regime and high sensitivity to the way changes (see section 6.3.4) are distributed within the year.

The response surfaces of QA for the Eget and Lassoula systems are generated over the whole year period to investigate the annual water volume that is potential for hydropower production. The response surfaces of DOE and tDOE for the Sarrancolin catchment are generated over July to October period when environmental flow management is usually menaced by low water availability and high irrigation water demand downstream. The response surfaces of NSA and tNSA for the Eget and Lassoula systems are generated for December to August period that incorporates the actual reservoir refill management timing from the beginning of April to the end of July. Besides, based on the regression analysis, the most appropriate axes of the response surfaces of NSA and tNSA are winter-spring (December to May) precipitation changes as x axis and spring (March to May) temperature changes as y axis. This also suggests that winter-spring precipitation and spring temperature dominate the snowmelt process.

From Figure 6.6, QA for both Eget and Lassoula systems are both more sensitive to precipitation changes, and QA decreases with the decrease of precipitation. It is also notable that QA of the Eget system is slightly responsive to temperature because the increase in PET associated with temperature increase can compensate the increase in precipitation and thus QA of the Eget system is decreased. In contrast, the Lassoula system does not clearly show this character. This can be explained by the different land cover types of the two hydropower systems: the Eget system that includes SB1 and SB2 is covered with forest and meadow (active evapotranspiration processes) while the Lassoula system that only includes SB3 is covered with bare rocks (no water demand from vegetation). As such, the evapotranspiration is more intensive in the Eget system where vegetation cover

Table 6.4 – The simulation results (sim and sim) of water management metrics by the GR6J-CEMANEIGE model compared with observations (obs) in terms of QA for SB1-3, DOE and tDOE for the Sarrancolin catchment, and NSA and tNSA for SB1-3*

	SB1			SB2			SB3			Sarrancolin		
	obs	sim	sim*	obs	sim	sim*	obs	sim	sim*	obs	sim	sim*
Calculation period	01/2001 to 08/2014	01/2001 to 08/2014	09/1979 to 08/2014	07/2014 to 07/2018	07/2014 to 07/2018	09/1979 to 08/2014	01/2001 to 08/2014	01/2001 to 08/2014	09/1979 to 08/2014	01/2001 to 08/2014	01/2001 to 08/2014	09/1979 to 08/2014
QA [Mm^3]	37.5	37.7	37.1	16.7	15.1	16.2	33.9	30.5	29.7	-	-	-
DOE [days]	-	-	-	-	-	-	-	-	-	0	2.8	2.8
tDOE [date]	-	-	-	-	-	-	-	-	-	-	02/Oct	20/Sep
NSA [days]	64.6	60.2	57.4	47.6	35.7	38.8	28.5	29.4	25.1	-	-	-
tNSA [date]	12/Jun	29/Jun	02/Jul	04/Jul	24/Jul	22/Jul	15/Jul	30/Jul	05/Aug	-	-	-

Notes: The sim results for SB1, SB3, and Sarrancolin catchment are calculated with the Safran-PIRAGUA dataset over the period from 01/2001 to 08/2014 while those for SB2 are calculated with the Safran-France dataset over the period from 07/2014 to 07/2018. The sim* results for SB1-3 and Sarrancolin catchment are calculated with the Safran-PIRAGUA dataset over the period from 09/1979 to 08/2014.

Table 6.5 – The current management reference values for the water systems in the Aure Valley

	Eget	Lassoula	Eget+Lassoula	Sarrancolin
QA [Mm^3]	53.3	29.7	82.9	-
DOE [days]	-	-	-	2.8
tDOE [date]	-	-	-	20/Sep
SCA [days]	46.0	25.1	-	-
tSCA [date]	15/Jul	05/Aug	-	-

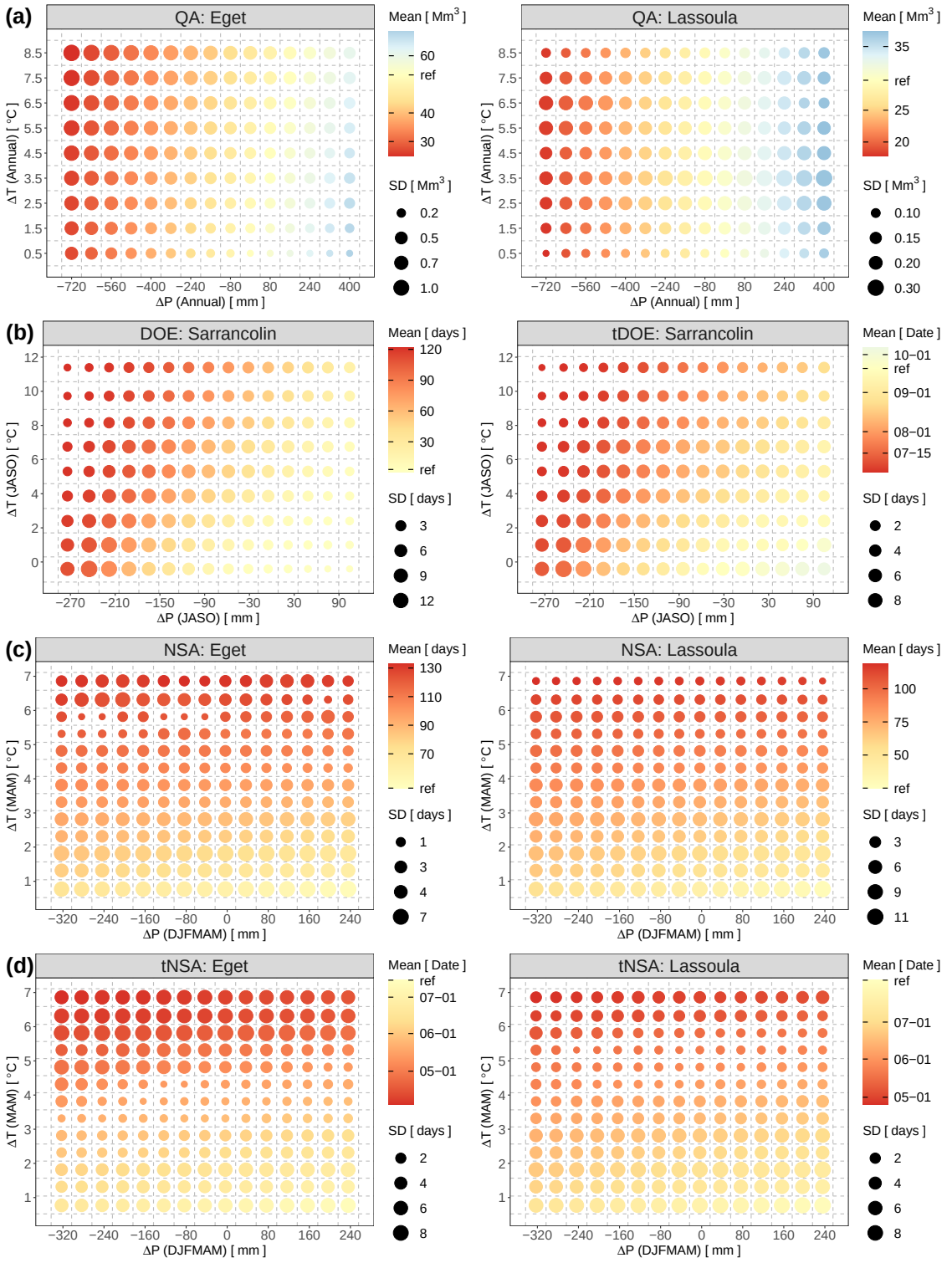

Figure 6.6 – Response surfaces of water management metrics to climate change for QA(a), DOE and tDOE(b), NSA(c), and tNSA(d) with their associated study area. Note the difference in x (precipitation changes) and y (temperature changes) axes with each response surface. The metrics under current climate condition (ref) are also provided (see Table 6.5 for corresponding values).

is developed, which results in a higher temperature sensitivity of QA in the Eget system than the Lassoula system.

Figure 6.6 shows that DOE and its associated tDOE for the Sarrancolin catchment are sensitive to both precipitation and temperature changes in July to October period. DOE becomes longer while tDOE becomes earlier with the increase of temperature and the decrease of precipitation. As the Sarrancolin catchment is covered by vegetation (mainly forest) in the most part, an increase in temperature leads to higher evapotranspiration and thus less water availability during July to October period. The effect of reducing precipitation by around 100 mm for both DOE and tDOE is close to the effect of increasing temperature by around 10 to 12°C.

In regard to NSA and tNSA for the two hydropower systems, the contrasting sensitivity to temperature changes is highlighted in Figure 6.6. The values of NSA becomes longer and tNSA becomes earlier with the increase of temperature. When the increase of temperature is relatively limited (less than 3°C), the precipitation changes in the winter-spring period also has an impact on these metrics. However, when the temperature increase exceeds 3 to 4°C, the impact of precipitation on both NSA and tNSA metrics is no more obvious and changes in these two metrics are predominantly controlled by temperature change. For example, the effect of increasing temperature by 1 to 2°C for the Eget system is close to the effect of reducing precipitation by 300 mm. The high sensitivity of Pyrenean snow to temperature changes is also reported in other studies (e.g., López-Moreno et al., 2008b, 2017, 2012). López-Moreno et al. (2017) explained that the snow state in the Pyrenees is warm and thick, and thus a slight increase in temperature could trigger snowmelt.

6.4.3 Water management vulnerability assessment

Figures 6.7, 6.8, and 6.9 display the vulnerability of water management of the study area under climate change in regard to hydropower production, environmental management, and reservoir refill, respectively. Based on the knowledge of the water management sensitivity to climate change, threshold lines for each management metric that indicate the limit of the water system's satisfactory performance, and climate change pathways that indicate future climate trajectories are overlaid on the sensitivity domain to assess the vulnerability. Climate change trajectories are presented as line-linked squares for the time slices from 1980s to 2090s with the mean climate driver changes as the central points, minimum changes as right-bottom points, and maximum changes as left-top points of the ribbon squares.

Hydropower management in Figure 6.7 is generally more difficult given the future warmer and drier conditions. In the Eget system, the current performance of value 53.3 Mm^3 is not warranted anymore in most cases when annual precipitation decreases by 100 mm. The threshold of 41.6 Mm^3 that is the necessary water volume for hydropower production in the scenario of the lowest energy price in the market could be guaranteed under RCP 4.5. However, the Eget system would not be cost-effective after the middle of the century under RCP 8.5. Compared with the Eget system, the Lassoula system is more vulnerable due to its threshold (28.2 Mm^3) that is relatively close to the reference value (29.7 Mm^3). The Lassoula system would not be cost-effective in most climate change scenarios of two RCPs. As for the total hydropower production of the two systems, the current performance of value 82.9 Mm^3 would not be warranted anymore under two RCPs and the cost-effectiveness of value 69.8 Mm^3 would not be achieved under RCP

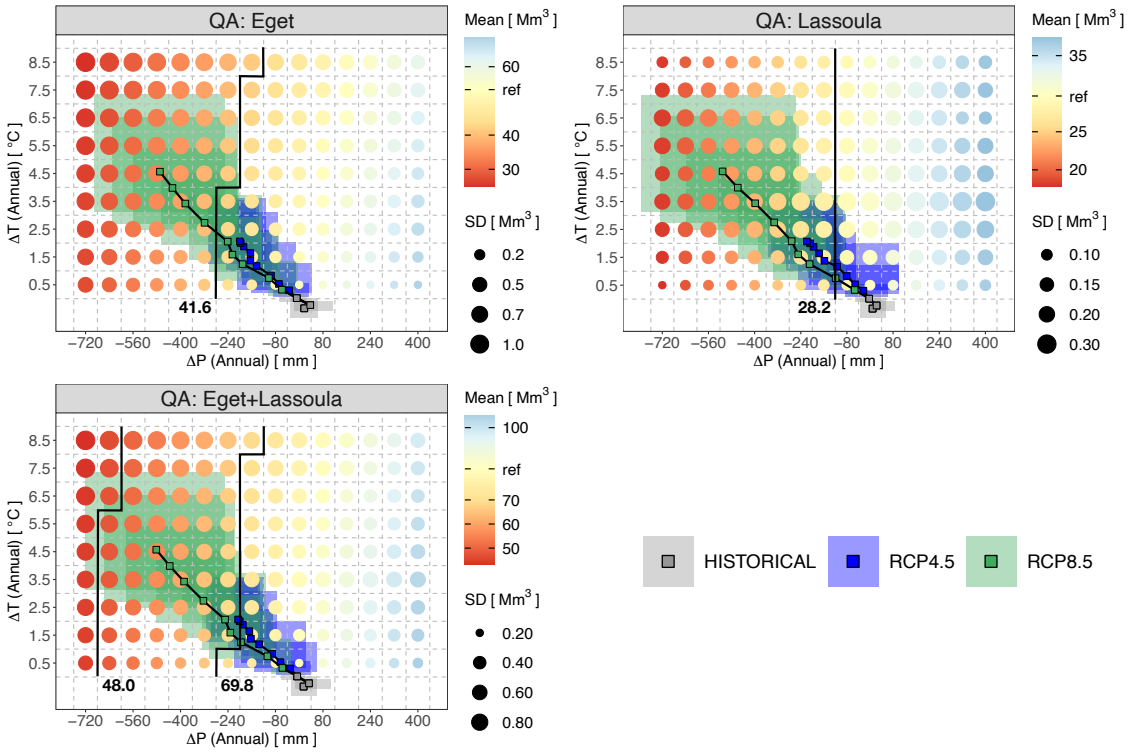

Figure 6.7 – The vulnerability of annual hydropower production under climate change for the Eget and Lassoula systems. The vulnerability is assessed by combining the sensitivity domain of QA, the current hydropower cost-effectiveness thresholds, and the climate change trajectories under RCP 4.5 and 8.5, respectively. The black lines are the isolines that represent the cost-effectiveness thresholds for the management metric QA.

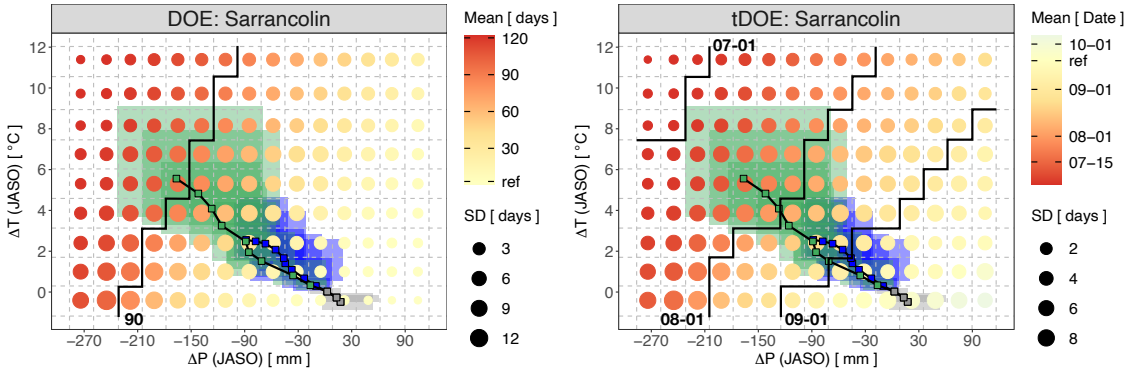

Figure 6.8 – As in figure 6.7 but for the environmental management metrics DOE and tDOE of the Sarrancolin catchment.

8.5. Besides, water demand of the downstream Gascogne region, which is 48 Mm^3 at most, could be guaranteed for most of the climate change scenarios under two RCPs. The demand of 48 Mm^3 could not be meet if considering the conservative attitude of water managers for hydropower, especially in the climate change scenarios under RCP 8.5.

The vulnerability of environmental management metrics DOE and tDOE during July to October period is shown in Figure 6.8. The climate change pathways under RCPs 4.5 and 8.5 are heading towards warmer and drier July to October period. The current

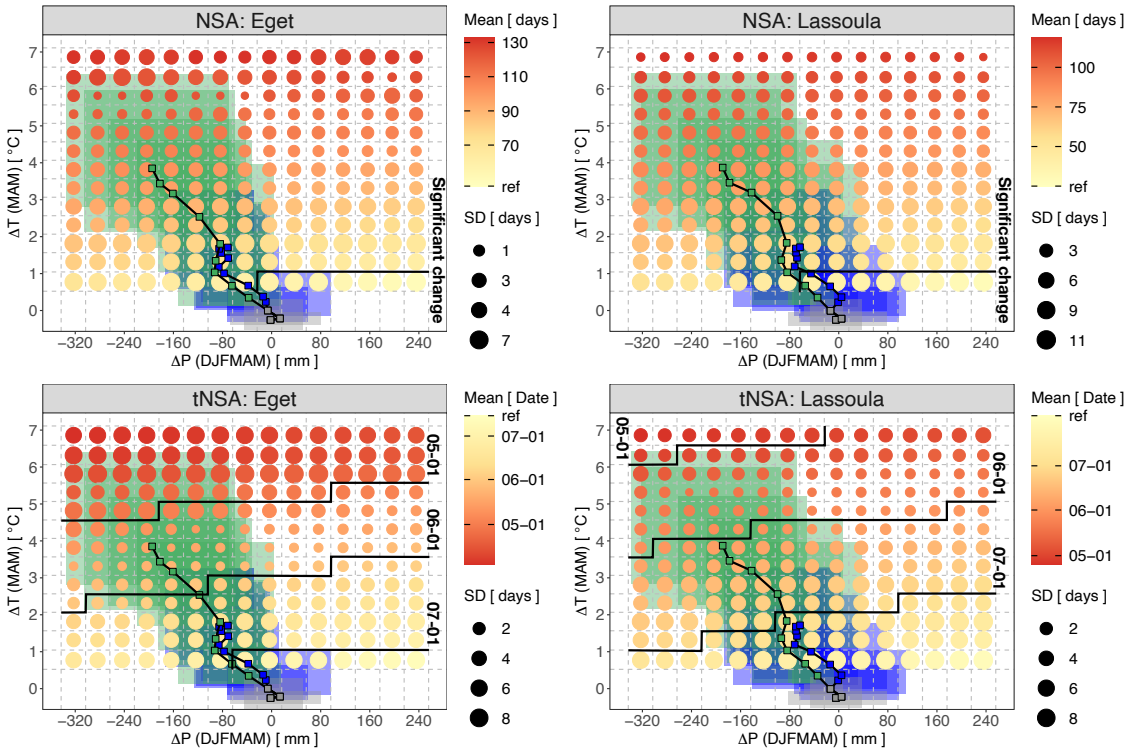

Figure 6.9 – As in figure 6.7 but for the reservoir refill management metrics NSA and tNSA of the Eget and Lassoula systems.

performance for both metrics would not be warranted when July to October precipitation decreases by 50 mm or July to October temperature increases by 3°C. The number of DOE failure days should stay below the 90-day threshold for RCP 4.5 while the threshold could be violated at the end of the century under RCP 8.5. Besides, the timing of DOE failure is earlier under both RCPs with more extreme condition for RCP 8.5. Particularly, at the end of the century under RCP 8.5, the timing of DOE failure date could occur in July when the downstream Gascogne region might demand water for summer irrigation. This causes water competition as either less water abstraction for irrigation or more reservoir release should be conducted to keep river flow at Sarrancolin larger than 4 m^3/s.

NSA and tNSA are shown in Figure 6.9 to assess the vulnerability of the current refill strategy. In the response surface of NSA for the Eget system, the empirical distribution of NSA deviates from the current one when temperature increases by 1°C in spring and precipitation decreases of around 30 mm in the winter-spring period. In the Lassoula system, significant changes appear when temperature increases by 1°C in spring and precipitation decreases of around 60 mm in the winter-spring period. The duration of NSA for both systems for December to August period becomes longer under climate change trajectories of RCP 4.5 and RCP 8.5. The thresholds considered here for both systems cannot withstand most climate change projections, which indicates the high vulnerability of current refill strategy to climate change and thus suggests urgent adaptation actions. Concerning the timing of current refill strategy, the Eget system gets its maximum storage in June and the end of July for the Lassoula system. Note that the difference between the maximum storage date and the no snow cover timing (tNSA) as tNSA is normally later than the maximum storage date. From the two response surfaces of tNSA, tNSA for December to August period will be earlier for both systems. In the worst conditions (RCP

8.5), no more contribution from snow melting could be expected after May and June for Eget and Lassoula, respectively, making the target of a maximum of storage around the current dates uncertain.

6.5 Discussion

6.5.1 The contribution to the Pyrenean studies

This paper implements the first trial of the bottom-up approach, alternative to the traditional top-down approach, for the climate change impact assessment in the Pyrenean region by taking the central Aure Valley as an example. Water management vulnerability in the Valley in terms of hydropower (QA), environmental regulations (DOE and tDOE), and reservoir refill (NSA and tNSA) are investigated by integrating the sensitivity of water management metrics to perturbed climate scenarios, to the predefined thresholds of current management capacity, and to the plausible exposure of future climate change projections. Previous studies applied the top-down approach and demonstrated that climate change could severely impact water resource and management in the Pyrenees by generating discrete "snap-shots" of future time slices for comparison with the current state (e.g., Haro-Monteagudo et al., 2020). However, how the Pyrenean water systems respond to climate change, and at what degree of climate change the performance of water systems shifts from acceptable to unacceptable cannot be fully addressed by the top-down approach. Understanding the response of Pyrenean water systems to changes is critical for water managers to design mitigation and adaptation strategies.

The sensitivity of these three management components is studied for different temporal scales as seasonal meteorological attributes show different importance for management issues. The sensitivity of QA for the selected Eget and Lassoula systems is studied for the whole annual scale. Annual precipitation was found to be a key meteorological driver for QA and consequently for hydropower production. The higher sensitivity to temperature for the Eget system reveals that land cover types in this catchment induces more intensive PET when temperature increases, which then reduces the water availability for hydropower production. Still, annual precipitation changes dominate the hydropower management in the two systems with moderate impact from annual temperature changes. By combining the predefined threshold and plausible climate change pathways, the vulnerability of hydropower can be perceived that the Lassoula system is more vulnerable, highlighting the need for short term actions to reduce vulnerability. Both DOE and tDOE metrics of the Sarrancolin catchment are studied for the July to October period when river flow is low and downstream irrigation demand is intensive. The two metrics are sensitive to both precipitation and temperature changes as the Sarrancolin catchment has a large soil moisture content. Given the warmer and drier tendency of climate change, the current DOE threshold of 90 days is sufficient for most climate change scenarios before the end of the century. It is notable that water competition in this period should be dealt with caution. As for the metrics NSA and tNSA of the two hydropower systems, the study is focused on the December to August period that includes recharge and spring melting processes. A higher sensitivity of both NSA and tNSA to temperature changes is observed, compared to the other metrics. A warmer climate will induce an earlier snowmelt, whatever precipitation changes. More liquid precipitation as a result of temperature increase, instead of solid precipitation, would flash into the reservoirs, which may endanger the reservoir safety and cause water spills and losses for future use. Current reservoir refill strategy should be adapted to climate change.

The sensitivity and vulnerability analyses in the Aure Valley are a powerful visual aid for identifying water management problems. In general, hydropower production and reservoir refill are the most vulnerable management indices among the study area, particu-

larly for the Lassoula system that incorporates the Caillaouas and Pouchergues reservoirs. However, the large storage volume of the Caillaouas reservoir could mitigate the effect of earlier and more flashy inflow. As such, dedicated actions should be implemented to adapt to climate change.

6.5.2 Potential mitigation and adaptation actions

On the premise of the vulnerability assessment of water management in the Aure Valley, mitigation and adaptation actions can be adopted from two sides to reduce climate change risk: water supply and demand sides, jointly and independently. Considering the drier projections in the Aure Valley, increasing reservoir storage is not the best move, let alone the intensive investment and the concern of environment (Maran et al., 2014; Poff et al., 2015; Zarfl et al., 2015). On the contrary, on the water demand side, modernisation of irrigation method (e.g., sprinkler or drip irrigation system), crop promotion for less water requirement, and changes in crop calendars are efficient in adapting to climate change, especially for the Mediterranean area (e.g., Galindo et al., 2018; Harmanny and Malek, 2019; Malek and Verburg, 2017).

The hydropower efficiency in the Eget and Lassoula systems can also be increased to mitigate the loss of hydropower production. Besides, shifting the hydropower production from winter (for heating) to summer (for cooling) to align several water uses (hydropower, irrigation, and environmental regulations) is possible to reduce water competition in the Valley (Pereira-Cardenal et al., 2014). The original refill management that starts from April and ends in July for the two hydropower systems seems too late and too long in the face of warmer climate. As such, reservoir refill strategies might be changed with an earlier start and a flexible duration. Increasing the reservoir spillway capacity should also be considered so as to avoid the extreme high inflow events into the reservoirs that endanger reservoir safety. In particular, given the small storage volume of the Pouchergues reservoir and large storage volume of the Caillaouas reservoir, increasing the capacity of water transfer from the Pouchergues to the Caillaouas reservoir could mitigate water loss from spillway release. However, these changes should be scrutinized with caution as managers might be conservative in changes.

6.5.3 Limitations and future works

This study simplifies the water management processes and thus it is important to acknowledge the limitations that are likely to induce biases in the analysis. Future works focusing on these limitations will help to improve the understanding of water management vulnerability in the study area.

Firstly, uncertainty is partially examined here. The study focuses on climate-related uncertainty, exploring a broad range of climate conditions. The uncertainty of water management metrics to climate change is displayed by the SD values in the response surfaces with larger SD values indicating high dispersion in values for the specified changes. Parts of the uncertainty are due to natural processes that are not perfectly taken into account by the models. For example, the snow melting process simulation is less efficient than the snow accumulation process (see the SCA regimes of Figure 6.5). This results from the choice of the empirical degree-day model CEMANEIGE and the difficulties in representing snow thermal state changes (Riboust et al., 2018). Although the GR6J-CEMANEIGE model has shown satisfying performance, different hydrological models show significant

variations in water resource estimation (e.g., Vidal et al., 2016). Besides, a hydrological model calibrated under current climate may not perform robustly for perturbed climate scenarios due to parameter non-stationarity (e.g., Guo et al., 2017; Westra et al., 2014). These variations would propagate to the sensitivity domain, which may induce biases in the vulnerability assessment (Broderick et al., 2019). Therefore, a multi-model method that involves structurally or conceptually different hydrological models can provide valuable insights in the uncertainty quantification.

Secondly, the term "vulnerability" for water management in this study is not presented as a specially defined index but in a manner of description. Traditionally, vulnerability is used to characterize the performance of water systems in terms of the severity of their failure and the mathematical definition is given in Hashimoto et al. (1982b). Some studies have examined the vulnerability of water management by calculating the water deficit to meet the total demand (e.g., Haro-Monteagudo et al., 2020; Loucks and van Beek, 2017; Sandoval-Solis et al., 2011). Furthermore, vulnerability in the bottom-up framework is derived as "the proportion of exposure simulations that fail below the critical threshold" in Sauquet et al. (2019) (not computed here), or the combination of the three components that includes sensitivity, exposure, and threshold (e.g., Mastrandrea et al., 2010; Prudhomme et al., 2013a,b). In the water management context, the evaluation of management performance is sometimes qualitative (e.g., reservoir refill) and problematic to be simplified as an index. Therefore, vulnerability in this study is given by subjective description with the participation of regional water stakeholders.

Thirdly, downstream water demand is assumed to be the maximum water allocation portion, which is 48 Mm^3 for irrigation, drinking water and industrial use, and to remain constant under all the scenarios investigated. In the historical experience of downstream water demand, the maximal value is actually reached for years 2005 (47 Mm^3), 2006 (48 Mm^3), 2007 (48 Mm^3), and 2011 (48 Mm^3). As such, a possible adaptation strategy may suggest to increase maximum water allocation portion by making new water contracts between SHEM and downstream water uses. Besides, scenarios of land use and water use changes are worth being included in the sensitivity analysis. Previous studies highlighted land use and land cover changes, mostly the forest regeneration due to warming effect in the Pyrenees, could yield less water availability by more intensive PET of vegetation (e.g., Buendia et al., 2015; López-Moreno et al., 2011; Morán-Tejeda et al., 2014; Vicente-Serrano et al., 2019).

Finally, the generation of perturbed climate scenarios is based on the "delta-change" method that parametrically perturbs daily historical climate data with monthly change factors. This method, applied here for reasons of simplicity (straightforward to apply), has well-known limitations (e.g., not suitable for extreme events). However, the delta-change approach was considered relevant to address the vulnerability of a system sensitive to changes in water resources. Alternatives to the parametric method are stochastic methods, such as weather generators (e.g., Culley et al., 2019; Steinschneider et al., 2019). In addition, the climate perturbation is limited to precipitation and temperature in this study. Although precipitation and temperature mean changes are the main drivers in water management, the investigation of other variables, such as PET (Guo et al., 2017), precipitation variability (Poff et al., 2015) and water demand (Foti et al., 2014), could also impact the performance of water systems.

6.6 Conclusion

Water resource and management in the Pyrenees under climate change remains a continuous regional issue. In this study, we illustrated a bottom-up approach to analyze the vulnerability of Pyrenean water management under climate change with an example of the central Aure Valley. To achieve this, we firstly developed a hydrological model GR6J-CEMANEIGE calibrated to the naturalized inflow and observed snow cover derived from satellite images, and the simulation results point to satisfactory water resource and management estimation. The next step is to apply the delta-change method, a parametric method, to perturb historical climate conditions. The current and perturbed climate series are finally forced into the calibrated hydrological model to simulate potential changes of water management metrics for sensitivity analysis. Changes in water management metrics (hydropower production, environmental regulations, and reservoir refill management) are demonstrated by the 2D response surface in answer to precipitation and temperature changes, which is visually practical in identifying the sensitivity of water management to climatic variables. Response surfaces overlaid with performance threshold isolines and plausible climate change pathways are essential for the exploration of key vulnerability.

Our findings confirm the high sensitivity of water management in the Aure Valley to seasonal/annual changes in precipitation and temperature. By integrating the exposure and the performance metrics of water systems in the Aure Valley, the vulnerability of water management under climate change can be assessed. The results in the study can be summarized as follows.

1. Annual hydropower production is mostly dominated by changes in annual precipitation, and secondary by changes in annual temperature. Particularly, the Lassoula hydropower system is vulnerable to future drier climate conditions as the production threshold cannot be maintained under most future climate change projections.

2. The environmental regulations for the Sarrancolin catchment are sensitive to both precipitation and temperature changes in summer and early autumn. Environmental management is less vulnerable to climate change while the timing of environmental water requirement would induce an intensive water competition among irrigation and hydropower.

3. Reservoir refill management is extremely sensitive to changes in temperature for the winter-spring-summer period. The earlier snowmelt induces water loss and reservoir safety issues if the refill strategy remains unchanged.

On the basis of these vulnerability analyses, corresponding adaptation and mitigation actions can be designed to manage climate change risks. Non-structural measures can be suggested, which target the efficient use of water, especially in the irrigation domain. Other actions, such as increasing hydropower plant efficiency and increasing water transfer capacity for more flexible reservoir management could be also appreciated in mitigating hydropower losses. Given the earlier snowmelt, reservoir refill strategy should be correspondingly adjusted accompanied with the increase of spillway capacity for the reservoir safety.

Although there are some limitations, this study demonstrated valuable insights on the impact of climate change on water resource and management by firstly applying a

bottom-up framework in the Pyrenean region. Future works, such as testing other hydrological models with different structure for uncertainty quantification, generating perturbed climate scenarios with more extreme events, testing water management stress to other climate variables or socio-economic changes, could advance the understanding in water management vulnerability. This framework is applicable to other Pyrenean regions for vulnerability assessment and adaptation design under climate change.

7

Impact assessment under global change

This chapter presents the water resources, water demand, and water management changes under global change by applying a top-down analysis.

Contents

7.1 Introduction 177
7.2 Climate change impact on natural water resources 184
7.2.1 The Aure Valley (SB1-4) 184
7.2.2 The Gascogne region (SB5) 191
7.3 Global change impact on water demand 194
7.3.1 Hydropower demand changes 194
7.3.2 Drinking water demand changes 197
7.3.3 Industrial water demand changes 198
7.3.4 Irrigation water demand changes 198
7.3.5 Environmental water demand changes in SB5 201
7.3.6 Summary 202
7.4 Global change impact on water management 206
7.4.1 Water management in the Aure Valley 206
7.4.2 Summary 230

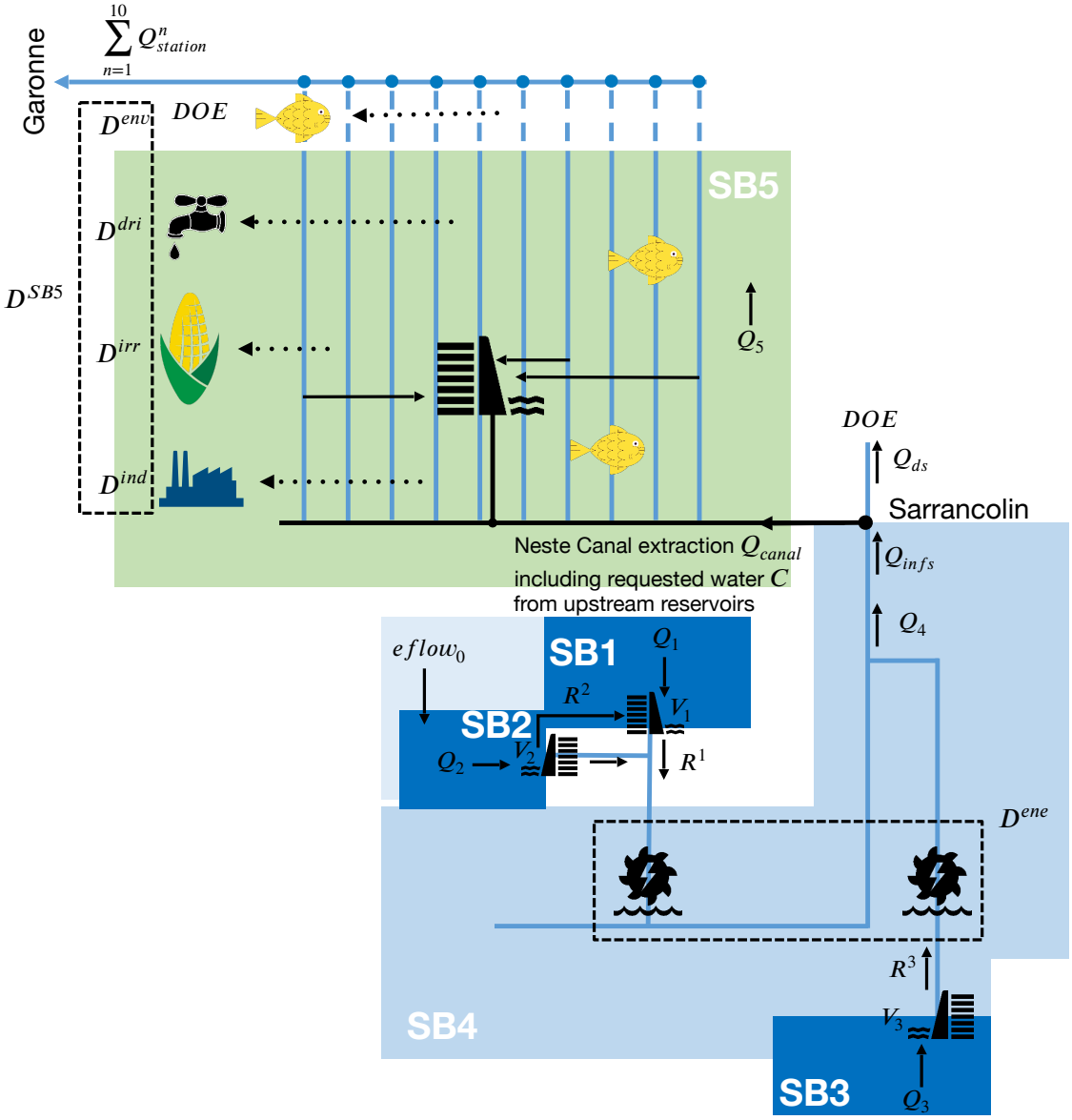

Figure 7.1 – A simplified schema of the Neste water system, and this chapter uses a top-down framework to investigate the natural water resources changes in the Neste water system (SB1-5), the water demand changes in the Neste water system (SB1-5), and the water management changes in the Aure Valley (SB1-4) under global change scenarios.

7.1 Introduction

A top-down approach is implemented in this chapter to analyze the impact of global change. As detailed in chapter 2 (see Figure 2.2a), the top-down approach hinges on the modelling chain that links the global change projections with the impact models (e.g., hydrological models, water demand models, and water management models). Based on the philosophy of the top-down approach, the schema of the Neste water system under global change scenarios is illustrated in Figure 7.2.

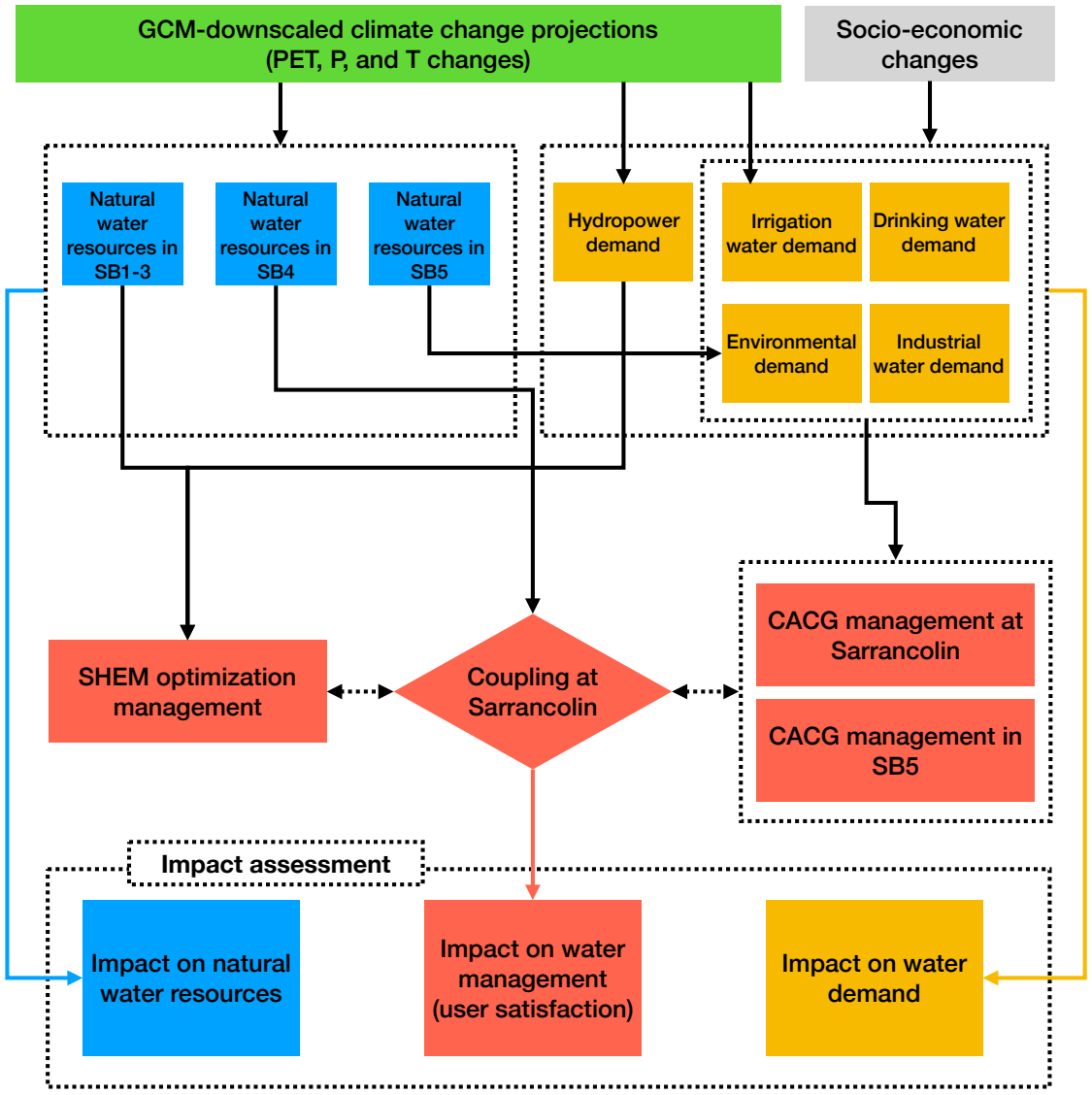

Figure 7.2 – The schema of the modelling chain that represents the Neste water system under global change. Different colors represent different inputs and models: the color green represents climate change projections based on GCMs; the color gray the changes in socio-economic drivers; the color blue the hydrological models in the Neste water system (SB1-5); the color yellow the water demand models; and the color red the water management models by the SHEM and CACG.

From the schema above, the modelling chain representing the Neste water system can be divided into five parts: (1) future climate change projections, (2) future socio-economic

changes, (3) hydrological models simulating the natural water resources of the Neste water system, (4) water demand models simulating the total five water uses (hydropower, drinking water, industrial water, agriculture, and environment uses) in the Neste water system, and (5) water management models simulating the behavior of water managers (SHEM and CACG) on how to satisfy water demand based on natural water availability.

The impact models, including hydrological models, water demand models, and water management models, are summarized in Table 5.7 with inputs and outputs to represent the Neste water system. The inputs into the impact models, including future climate change projections and future socio-economic changes are presented as follows.

Climate change projections in this study are simulated by six GCMs (see Table 3.4) under two RCPs (RCPs 4.5 and 8.5) with the RCP 4.5 representing a moderate GHG concentration and the RCP 8.5 representing a high GHG concentration. The six GCMs and two RCPs provide an ensemble of twelve future climate change projections. Each future climate change projection is simulated from 1961 to 2100 in the CLIMPY project. In the whole temporal length of climate change projections, we divide it into three phases: the near-term over the period from 2021 to 2040, the medium-term over the period from 2041 to 2060, and the long-term over the period from 2081 to 2100 as proposed by IPCC (2021). The outputs of the six GCMs have been downscaled (see chapter 3) to the Neste water system and the downscaled projections are used in this section instead of the direct GCMs outputs. Figures 7.3 and 7.4 show the potential evapotranspiration, temperature and precipitation changes simulated by the 6 GCMs under the RCPs 4.5 and 8.5 for the Aure Valley (SB1-4) and the Gascogne region (SB5).

Air temperature in the historical runs from the GCMs is underestimated by 2 °C in summer when comparing to the Safran-PIRAGUA data for both regions. Besides, precipitation in all seasons is also underestimated in the Aure Valley. The annual precipitation in the Aure Valley is 1438 mm calculated by the Safran-PIRAGUA data as illustrated in Figure 3.4 while the annual precipitation of the historical runs is around 1200 mm as illustrated in Figure 3.12a. A particular underestimation of precipitation by 30 mm/month is found in spring and summer. In the Gascogne region, precipitation in summer is also underestimated when comparing to the Safran-PIRAGUA data. The annual precipitation in the Gascogne region is 786 mm calculated by the Safran-PIRAGUA data as illustrated in Figure 3.4 while the annual precipitation in the historical runs is around 650 mm as illustrated in Figure 3.12a. Besides, there is an underestimation of simulated summer precipitation and an overestimation of simulated autumn precipitation when comparing to the Safran-PIRAGUA data.

Under the scenarios of the two RCPs, the climate in the Aure Valley and the Gascogne region is projected towards warmer and drier conditions with a pronounced warmer and drier summer as shown by Figures 7.3 and 7.4 (see annual changes in Figure 3.12). Air temperature is projected to increase for all seasons. Precipitation changes are variant depending on the GCMs while the projected decreasing trend of precipitation in summer are consistent for all GCMs. Particularly, the RCP 8.5 scenario projects a much more severe warm and dry climate with the maximum increase in summer temperature and the minimum decrease in summer precipitation in the long-term period.

In terms of socio-economic drivers, Table 7.1 summarizes the socio-economic drivers for population, drinking water network efficiency, agricultural activities, environmental regulations and hydropower production behavior in the study area. Except for population growth, other drivers are considered as business as usual conditions (no information about future changes). Furthermore, investigating the impact under these business as usual sce-

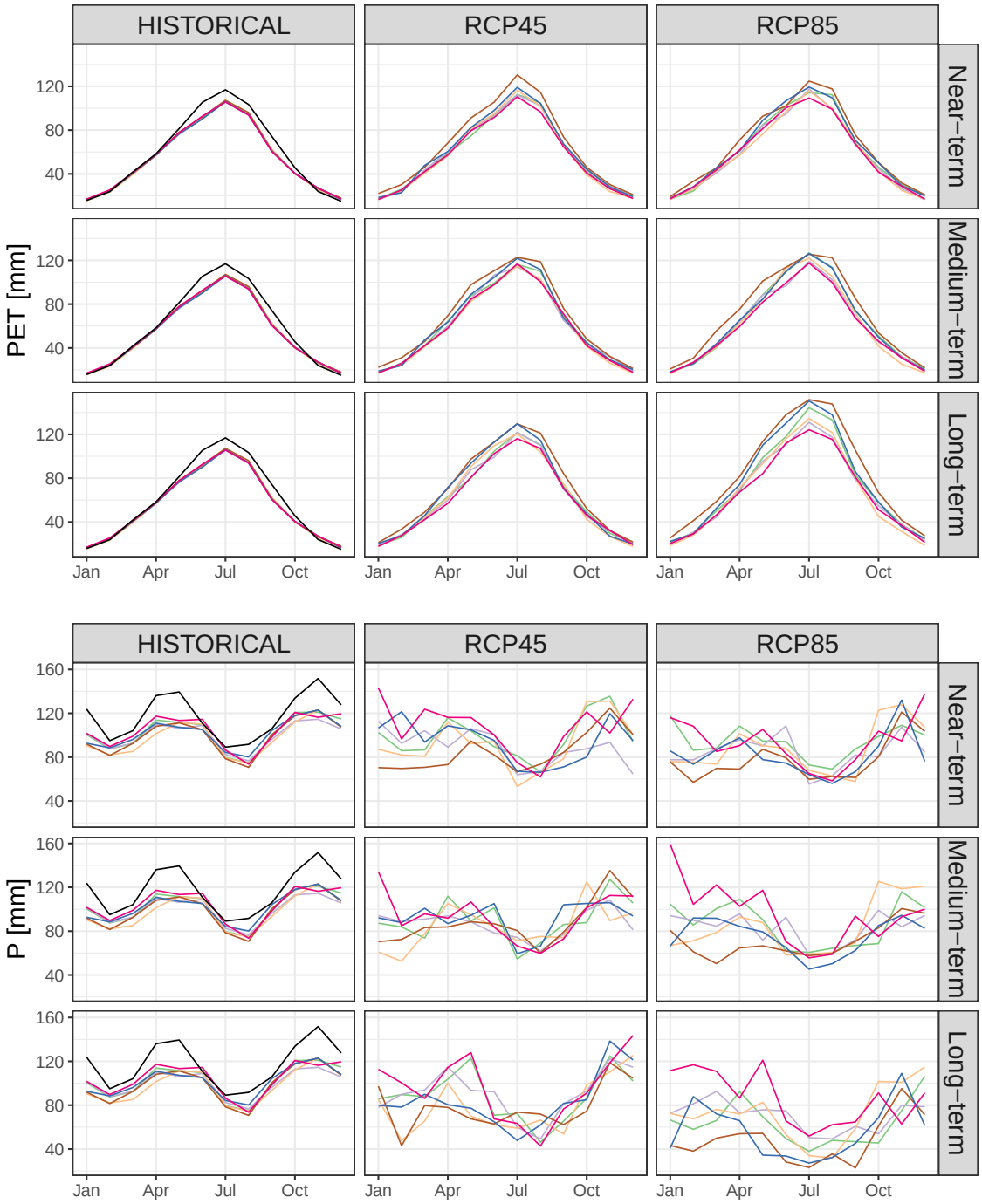

(To be continued)

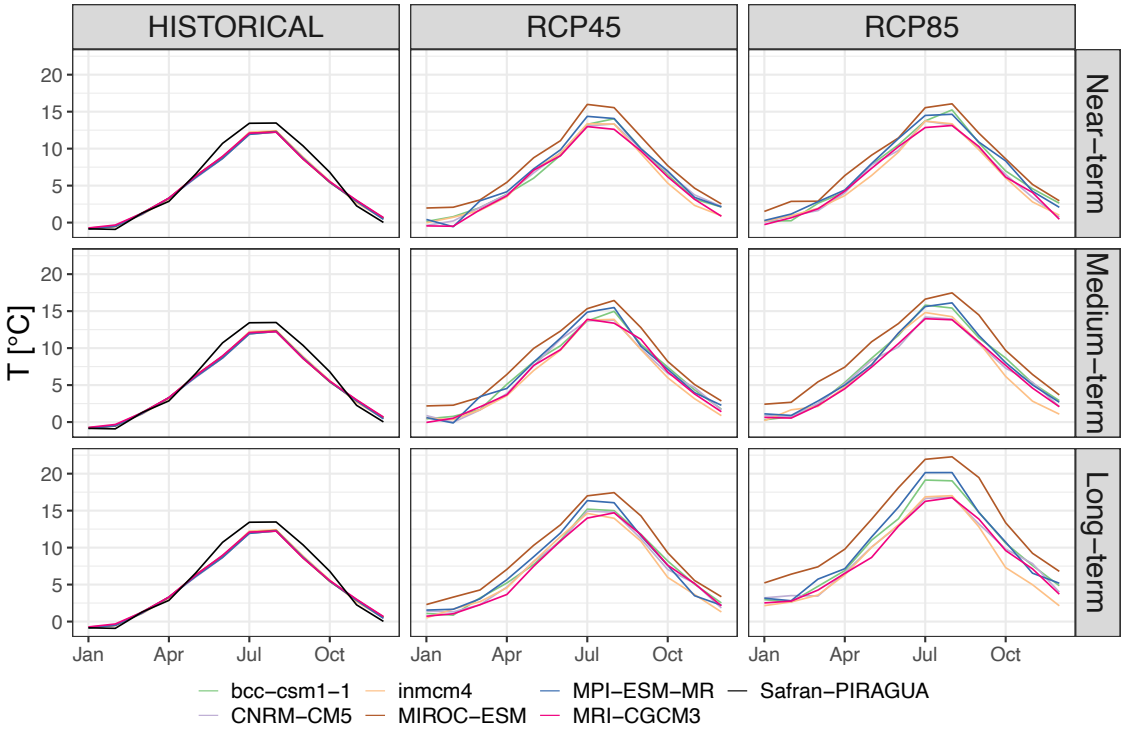

Figure 7.3 – Mean monthly potential evapotranspiration (PET), mean monthly precipitation (T) and mean monthly temperature (T) changes of the Aure Valley under 6 GCMs (bcc-csm1-1, CNRM-CM5, inmcm4, MIROC-ESM, MPI-ESM-MR, MRI-CGCM3) for the near-term (2021-2040), medium-term (2041-2060), and long-term (2081-2100) phases under two RCP scenarios (RCPs 4.8 and 8.5). The changes over historical period (1961-2005) of the 6 GCMs, along with the reanalysis Safran-PIRAGUA (1979-2014), are illustrated to compare with the changes under climate change scenarios. The three sub-figures in the column "HISTORICAL" are identical to visually help the comparison.

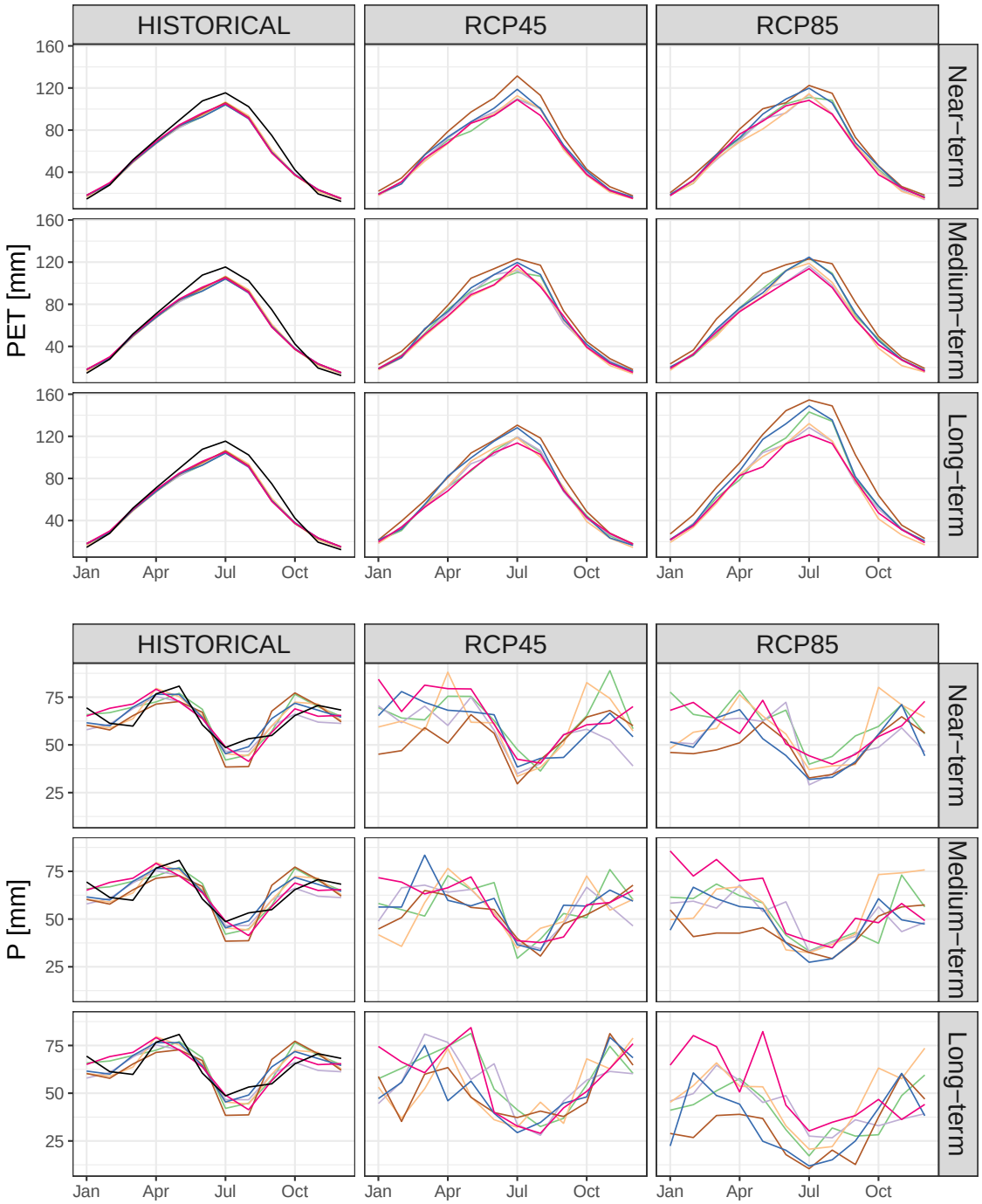

(To be continued)

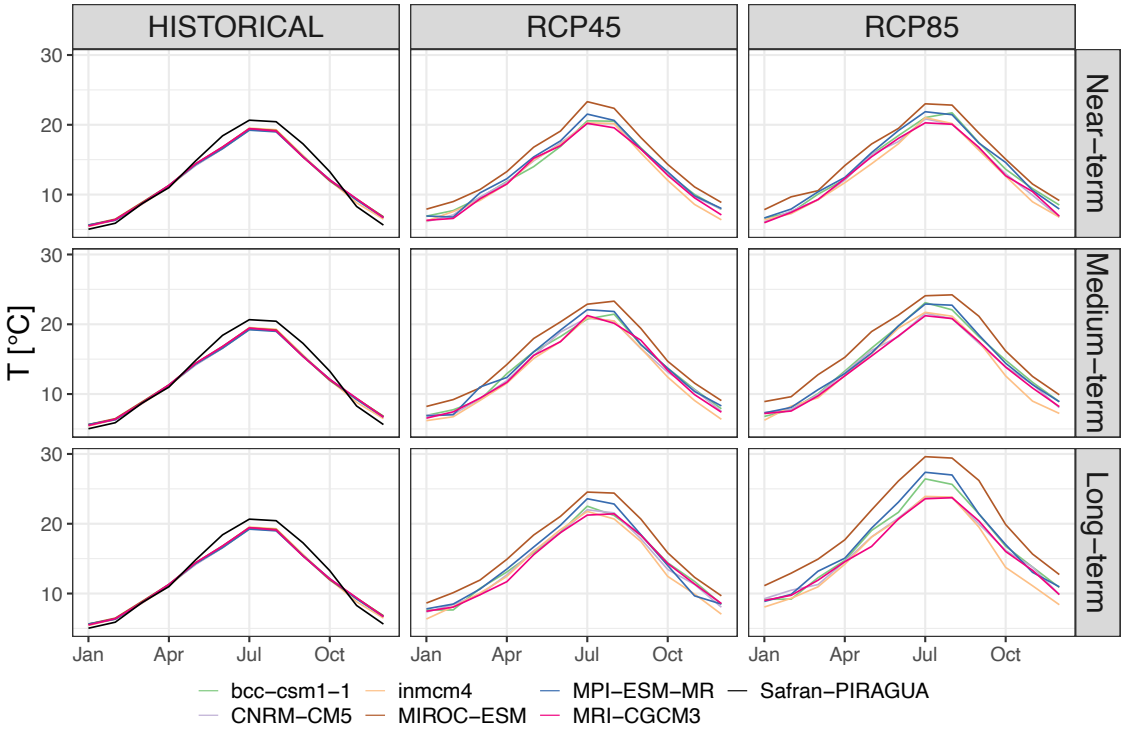

Figure 7.4 – As in Figure 7.3 but for the Gascogne region.

narios gives an overview of which water use is the most plausible to fail in the future, which helps to design adaptation strategies.

The population in the study area is projected by INSEE to increase by 2050 and then remain stable by 2100. Drinking water network efficiency is considered to remain the current 75% efficiency state for the future time. The business as usual condition is considered to represent the future irrigation activities that is the same as the current state with maize (late varieties) as the major irrigation crop and the "derived irrigation area" of 265 km^2 (the mean value from 1995 to 2019, see Figure 5.8). Environmental regulations in terms of the DOE in SB5, the DOE at Sarrancolin, and the eflows out of the hydropower reservoirs in the Aure Valley will also not be changed for the future time (see chapter 3). The hydropower in France is still assumed to provide the peak demand in the energy market in the future like nowadays (same sensitivity to temperature), and the thresholds to trigger the energy demand are still the same with 15 °C for HDD (24 °C for CDD, but not considered in impact assessment of the Neste water system).

Table 7.1 – Socio-economic drivers of the Neste water system in the near-term (2021-2040), medium-term (2041-2060), and long-term (2081-2100).

	Near-term (2021-2040)	Medium-term (2041-2060)	Long-term (2081-2100)
Population	Increase 13430 inhabitants	Increase 6362 inhabitants	Stable as total 216235 inhabitants
Network efficiency	0.75	0.75	0.75
Industrial water use [m^3/s]	0.338	0.338	0.338
Irrigation crop type	Maize (late varieties)	Maize (late varieties)	Maize (late varieties)
Sowing date intervals	07/April-31/May	07/April-31/May	07/April-31/May
Derived irrigation area [km^2]	265	265	265
DOE in SB5 [m^3/s]	5.48 in summer and 6.71 in winter	5.48 in summer and 6.71 in winter	5.48 in summer and 6.71 in winter
DOE at Sarrancolin [m^3/s]	4	4	4
$eflow_1$ [m^3/s]	0.055	0.055	0.055
$eflow_2$ [m^3/s]	0.051	0.051	0.051
$eflow_3$ [m^3/s]	0.025	0.025	0.025
HDD threshold [°C]	15	15	15

7.2 Climate change impact on natural water resources

To recall, the Neste water system is divided into five sub-basins (SB1-5), where the Aure Valley (SB1-4) is snow dominated and the Gascogne region (SB5) is less influenced by snow. The changes of natural water resources in the Aure Valley in terms of discharge (Q) and snow cover area (SCA) are investigated by the calibrated hydrological model GR6J-CEMANEIGE with a consideration of SCA-SWE hysteresis (see Table 4.5) under the six GCMs and the two RCPs. The changes of natural water resources in the Gascogne region in terms of discharge (Q) are investigated by the calibrated GR6J-CEMANEIGE model without a consideration of SCA-SWE hysteresis (see Table 4.5) under the six GCMs and the two RCPs. The changes of natural water resources in the Aure Valley and the Gascogne region are presented as follows.

7.2.1 The Aure Valley (SB1-4)

Figures 7.5, 7.6, 7.7, and 7.8 show the impact of climate change on water resources in terms of median Q regimes and median SCA regimes under the RCPs 4.5 and 8.5 for SB1-4 of the Aure Valley. Note that the SCA series of SB1-4 are the medians of the averaged SCA for the five equi-surface elevation bands. In general, we can observe that Q and SCA simulated under the climate change projections in the historical period for SB1-4 are coherent with the simulations by the reanalysis data Safran-PIRAGUA. The seasonal variations of Q with high-flow peaks in spring and low-flow spells in summer are well represented. However, the high-flow peaks simulated under the climate change projections in the historical period are underestimated compared with the simulation by Safran-PIRAGUA, which could be attributed to the underestimation of simulated precipitation in the historical runs. Besides, in terms of the SCA regimes simulated under the climate change projections in the historical period, the seasonal variations of SCA with full snow cover in winter and no snow cover in summer are well represented when comparing to the simulation by Safran-PIRAGUA. Particularly, the snow melting processes for SB1-4 under historical runs are very close to the simulations by the Safran-PIRAGUA. In contrast, there is an overall overestimation of SCA in autumn during the snow accumulation processes under historical runs, which could be also be attributed to the uncertainties in the CEMANEIGE model and to the seasonal biases of climatic variables simulated by the GCMs.

As for the general future changes of water resources in the Aure Valley, the simulations under climate change conditions indicate an overall decreasing natural flows with earlier flow peaks gradually shifting from late spring to early spring under both RCP scenarios. Besides, SCA changes are more variant in winter than the historical winter depending on future temperature and precipitation changes under both scenarios. The timing of no snow cover gradually shifts from summer to spring, and the period of no snow cover gets longer and longer for both scenarios. In addition, full snow cover cannot be maintained in winter anymore, especially in the long-term under the RCP 8.5. The detailed descriptions of the water resources changes in SB1-4 under the two RCP scenarios are given.

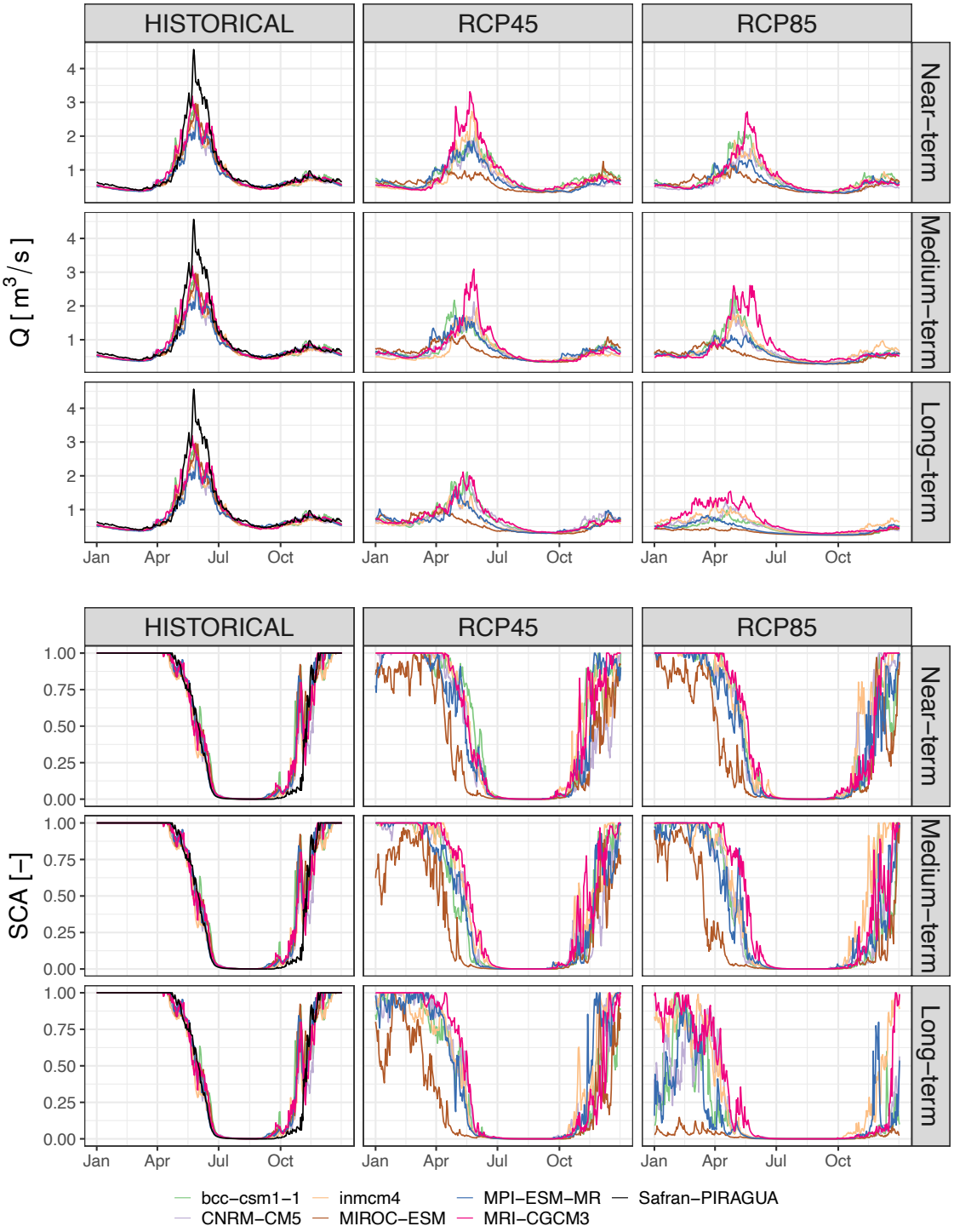

Figure 7.5 – Climate change impact on the median discharge (Q) and median snow cover area (SCA for the averaged 5 elevation bands) of SB1 under 6 GCMs (bcc-csm1-1, CNRM-CM5, inmcm4, MIROC-ESM, MPI-ESM-MR, MRI-CGCM3) for the near-term (2021-2040), medium-term (2041-2060), and long-term (2081-2100) phases under two RCP scenarios (RCPs 4.8 and 8.5). The simulations over historical period (1961-2005) of the 6 GCMs, along with the simulations from Safran-PIRAGUA (1979-2014), are illustrated to compare with the simulations under climate change scenarios. The three sub-figures in the column "HISTORICAL" are identical to visually help the comparison.

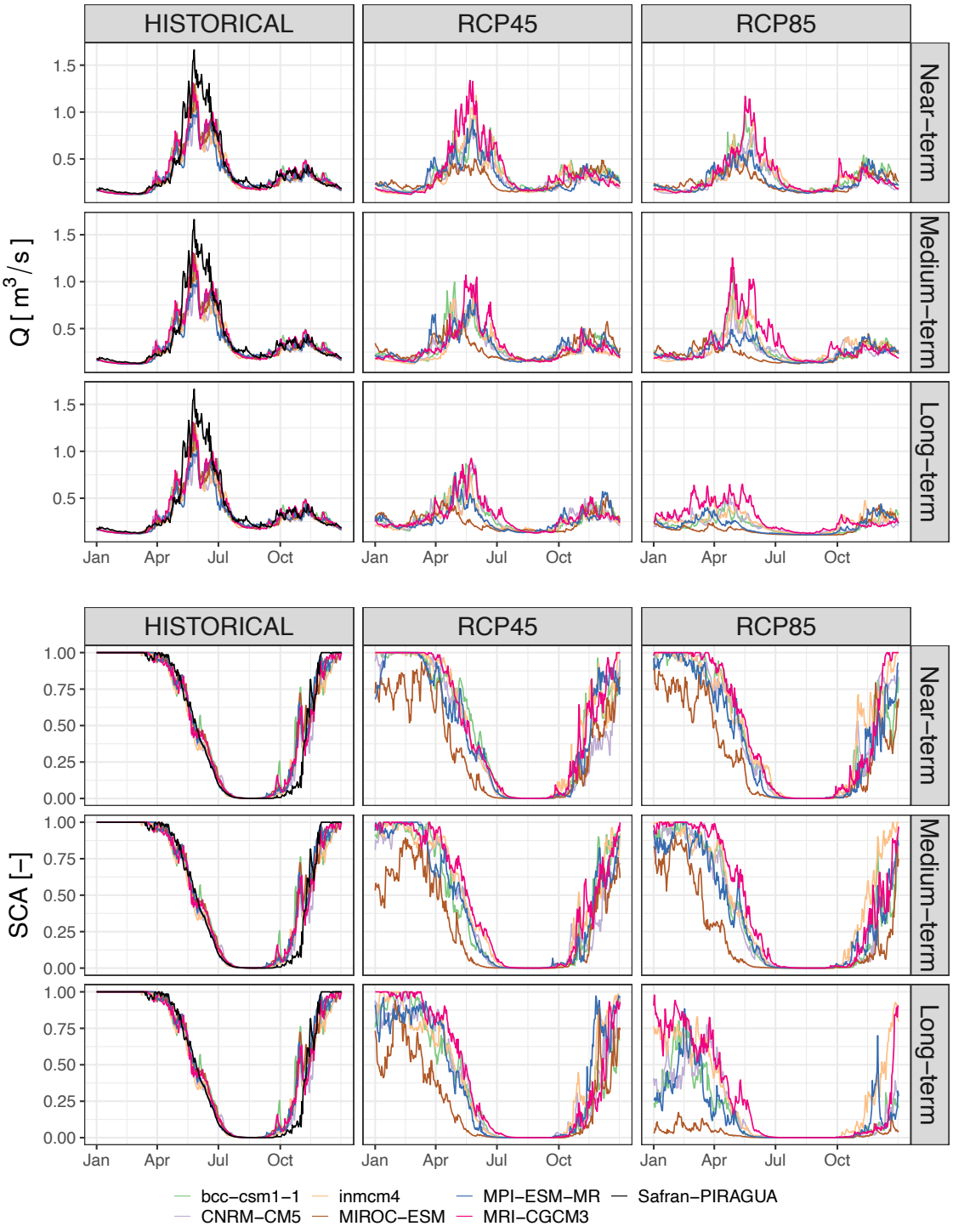

Figure 7.6 – As in Figure 7.5 but for SB2.

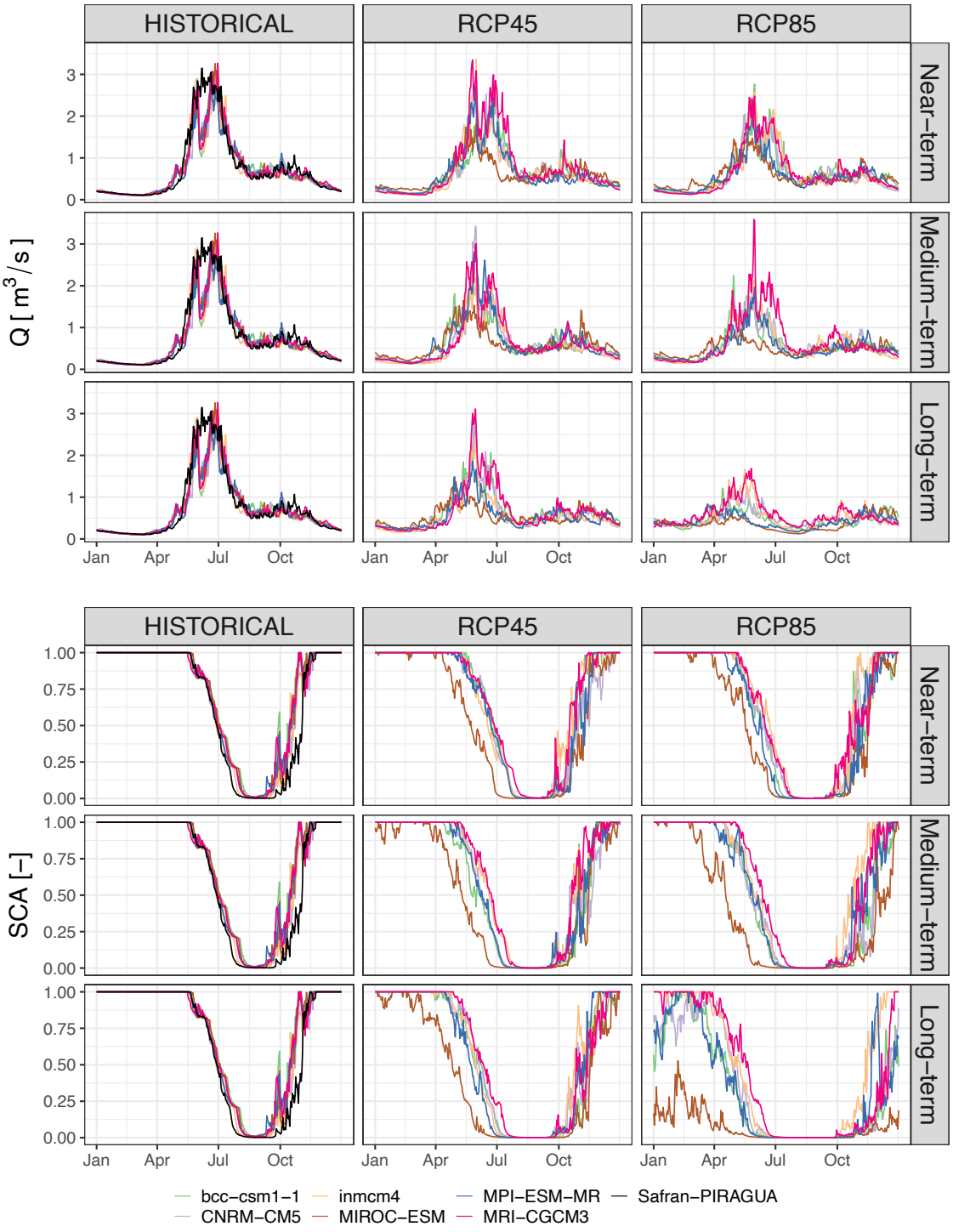

Figure 7.7 – As in Figure 7.5 but for SB3.

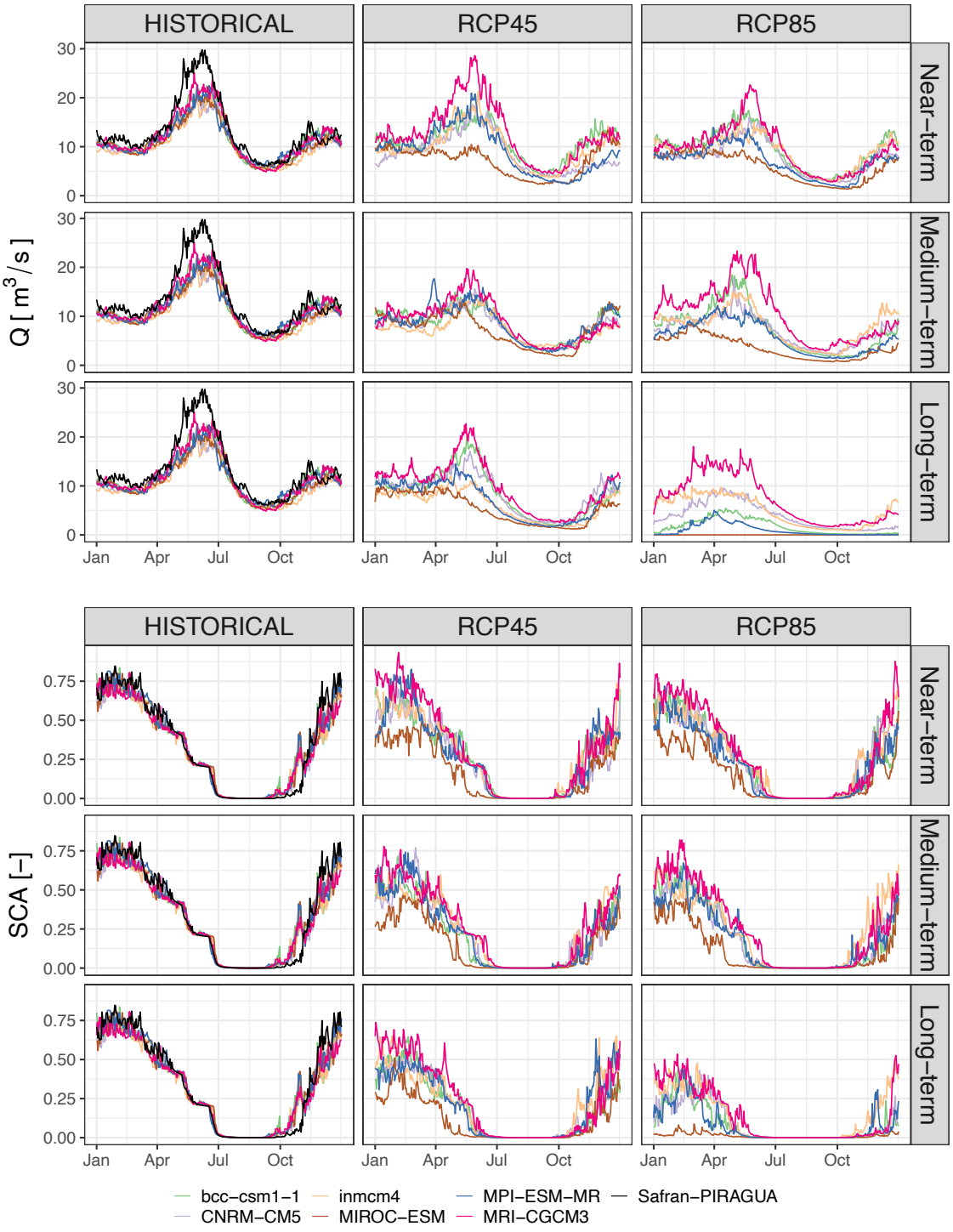

Figure 7.8 – As in Figure 7.5 but for SB4.

SB1 upstream the Oule reservoir

In the historical period The inflows of SB1 feeds the Oule reservoir with an increasing trend starting from April due to snowmelt till the end of June with high-flow peaks. Snow is completely melted in the beginning of July. Since then, there is no snow cover in SB1 and the inflows into the Oule reservoir remain a low state provided by soil water content. The no snow period (low flow spells) ends in the beginning of autumn around September-October when intensive precipitation occurs. SB1 as a typical mountainous basin, temperature lowers to freezing point in autumn and most precipitation is in solid form, which causes the increase of SCA with a slight increase of inflows into the Oule reservoir. Snow fully covers SB1 in the beginning of winter till the spring of the next year. This seasonal pattern remains stable for most historical years as the median Q and SCA regimes are not variant.

Under the RCP 4.5 scenario Under the RCP 4.5 scenario characterized by a modest increase of temperature (particularly in summer) and a modest decrease of precipitation (particularly in summer), the seasonal pattern as shown in the historical simulations alters. With a higher temperature in spring, snow starts to melt earlier, which causes an increase in spring inflows to the Oule reservoir for the near-term, medium-term and long-term compared with historical simulations. The high-flow peaks shift gradually to earlier dates from late spring in the near term to middle spring in the long-term depending on GCMs. The complete melt of snow also advances from the beginning of July to spring months depending on GCMs. It is notable that the spring season is characterized by a decrease in the peak flow, which is attributed to snow losses in winter due to temperature increase and less precipitation in spring for most climate change projections.

The duration of low-flow spells in summer (no snow cover period) is prolonged with lower summer inflows by less precipitation and higher temperature in summer for the three phases. The no snow cover period could last 5 months (May-September) in the long-term for the extremely warm and dry condition simulated by the GCM MIROC-ESM. However, precipitation in autumn (September-October-November) is more variant in climate change projections depending on GCMs (see Figure 7.3). From this point of timing, precipitation is mostly dropped and stored in snow state in SB1 with a late full snow cover (in the middle of winter) for most climate change projections in three phases. However, given the temperature increase in winter, an obvious increase in winter inflows can be observed with a much more variant winter SCA changes for the three phases than the historical period. For example, in the simulations by the GCM MIROC-ESM, SB1 cannot be fully covered by snow in winter due to warmer climate transferring solid precipitation to liquid precipitation and drier climate reducing snow storage capacity, particularly for the long-term period.

Under the RCP 8.5 scenario For the RCP 8.5 characterized by a high increase of temperature (particularly in summer) and a high decrease of precipitation (particularly in summer), the changes in the hydrological regime are more pronounced than those of the RCP 4.5. A much earlier snowmelt than the RCP 4.5 can be observed while the spring inflows into the Oule reservoir can be higher or lower than the RCP 4.5 depending on the climate projections by GCMs. The high-flow peaks shift gradually to earlier dates from late spring in the near term to early spring in the long-term depending on the climate projections by GCMs. As such, the hydrological regime is transferred from the snow-

dominated to the rain-dominated regime for most projections for the medium-term and long-term. The high-flow peaks decrease from the near-term to the long-term due to less snow storage in winter and less precipitation in spring. The low-flow spells could last much longer (from April to October in the long-term for the GCM MIROC-ESM) than the simulations of the RCP 4.5.

Besides, compared with the RCP 4.5, snow cover changes in the RCP 8.5 do not show many distinct differences for the near-term and medium-term. However, in the long-term, SCA in SB1 under the RCP 8.5 is more variant than that in the RCP 4.5 due to the extreme increases of temperature in the RCP 8.5 throughout the year.

Different responses of SB1-4 to climate change

The changes in terms of Q and SCA for SB2-4 are similar to the changes in SB1 under climate change conditions with an earlier snow melt, reduced spring flows, and more severe summer low-flow spells. The detailed descriptions of climate change impact on the SB2-4 will not be repeated.

Instead, different reactions or responses to the warming and drying climate change projections are compared and discussed among SB1-4, in order to link with the vulnerability analysis in chapter 6. The findings in chapter 6 can be summarized as: (1) the annual natural inflows into the reservoirs for SB1-3 are more sensitive (and vulnerable) to precipitation changes than temperature changes; (2) the summer low flows in SB1-4 and are sensitive (and vulnerable) to both summer precipitation and temperature changes; and (3) the duration of no SCA in summer for SB1-3 are extremely sensitive (vulnerable) to winter-spring temperature changes.

SB2 upstream the Orédon reservoir SB2 upstream the Orédon reservoir is located next to SB1 but with a higher elevation. By comparing Figure 7.6 with Figure 7.5, we can observe that the hydrological regimes of SB1 and SB2 are almost identical in both historical and climate change projections, except the difference in the Q magnitude due to different drainage area (larger surface of SB1). The same behavior of Q is probably attributed to the similar soil type (covered with forest and meadow) and slope gradient for SB1 and SB2.

In terms of SCA, in the historical period, snow is completely melted in the end of July for SB2, which is later than that in SB1 (in the beginning of July). No snow duration is shorter in SB2 (around one month of August) than that in SB1 (around two months from July to August). Besides, the duration of snow melt from full snow cover to no snow cover is almost four months for SB2 compared with almost three months for SB1. The duration of snow accumulation from no snow cover to full snow cover is almost three months for SB2 compared with almost two months for SB1. These different snow characteristics are attributed to the higher elevation of SB2 than SB1.

In the RCP 4.5, the more persistent snow characteristics of SB2 than SB1 is observed. For example, we can always observe a shorter duration of no snow cover in SB2 than SB1 in the three phases under the simulations of the RCP 4.5. However, in the RCP 8.5 and particularly in the long-term, this more persistent snow characteristics of SB2 than SB1 seems to fail with the same period of no snow cover in both SB1 and SB2. This is probably because the extreme warming effect offsets the favorable elevation condition for snow storage in SB2.

SB3 upstream the Lassoula reservoir SB3 upstream the Lassoula reservoir is located in the western part of the Aure Valley with a higher elevation than SB1 and SB2. By comparing Figure 7.7 with Figures 7.5 and 7.6, we can observe some differences of the hydrological regime of SB3 from those of SB1-2. In the historical period, the high-flow peaks in SB3 are in early summer, which are later than those of SB1-2 (in late spring). This is due to the higher elevation of SB3 that induces a later snowmelt than SB1-2.

Under climate change conditions, the high-flow peaks in SB3 shift to spring immediately even in the near-term under the RCP 4.5. This response of SB3 with a quicker response to warming than SB1-2 can be attributed to the catchment characteristics of SB3. SB3 is covered with bare rocks and shows a more gradient slope than SB1-3, which induces direct snow melt to the outlet of SB3 without many losses from the evapotranspiration processes. By contrast, SB1-2 is covered with forest and meadow, which induces large losses from evapotranspiration. Thus, Q in SB3 reacts more quickly to warming effect than SB1-2.

Besides, the snow storage in SB3 is more persistent than those in SB1-2 because the higher elevation of SB3 cancels the warming effect to some extend. However, the future drier conditions still reduce the inflows into the Lassoula reservoir.

SB4 By comparing Figure 7.8 with Figures 7.5, 7.6, and 7.7, we can observe that the hydrological regime of SB4 is characterized by high-flow peaks in spring due to snow melt, moderate high flows in winter due to winter precipitation part of which is in liquid form, and low-flow spells in summer in the historical period. The hydrological regime SB4 is thus snow-dominated but rain-influenced, which is different from the completely snow-dominated SB1-3. This is because some parts of SB4 have lower elevation compared with SB1-3 and thus SB4 is hardly full-covered by snow (largest SCA value of 0.75 throughout the year). Under climate change conditions, the hydrological regime of SB4 could be transferred into a rain-dominated one depending on the time leads of future warming effect projected by the GCMs under the RCPs (e.g., the medium-term projected by MIROC-ESM under the RCP 8.5 and the long-term projected by inmcm4 under the RCP 8.5).

SB4 has a forest land cover in most part and the evapotranspiration process is more intensive than SB1-3. This induces more water losses in SB4 under climate change conditions. For example, the extremely warm and dry projections by MIROC-ESM in the long-term of the RCP 8.5 show almost no outflow for SB4, which could be attributed to the double effect of intensive evapotranspiration and less annual precipitation to saturate the soil.

7.2.2 The Gascogne region (SB5)

Figure 7.9 shows the impact of climate change on water resources in terms of median Q regimes under the RCPs 4.5 and 8.5 for SB5. The hydrological regime of SB5 is characterized by rain-dominated regime with high flows in winter-spring period and drought events in summer.

In historical period, the simulations under historical runs are coherent with the simulation by Safran-PIRAGUA. The high-flow peaks are in winter and the low-flow spells are in summer. However, compared with the simulation by Safran-PIRAGUA, the flows in autumn under historical runs are overestimated due to the overestimation of autumn precipitation for some GCMs (for example, bcc-csm1-1). Besides, the low flows in summer

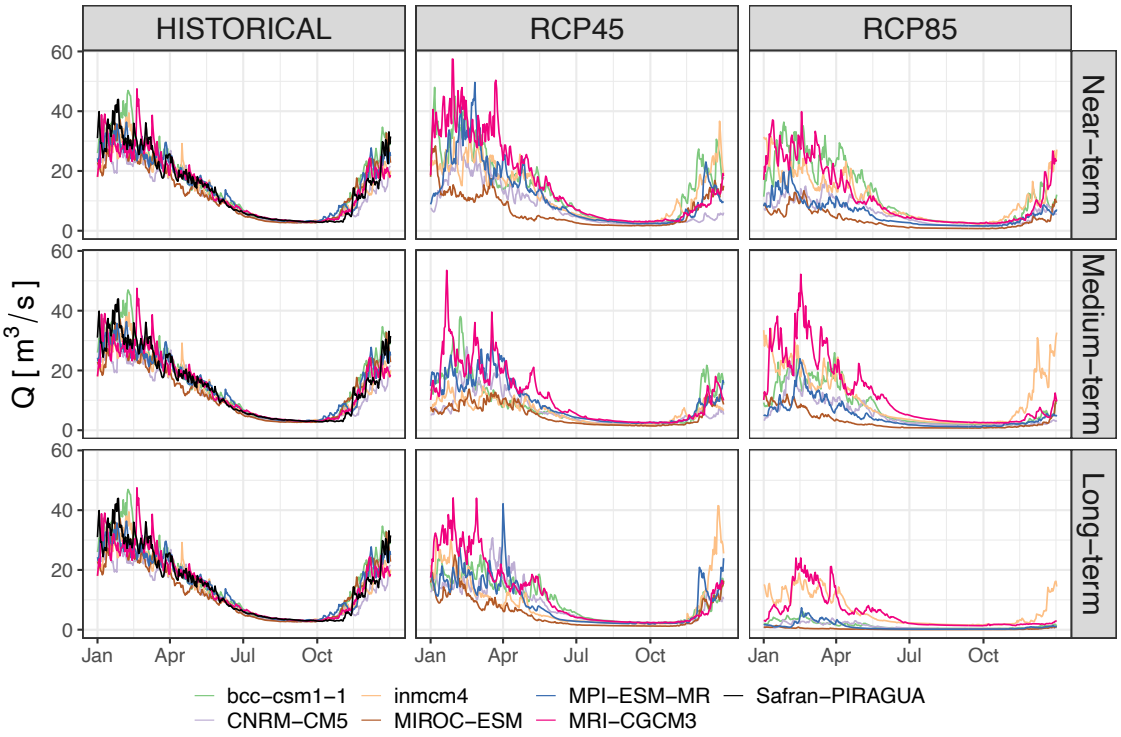

Figure 7.9 – As in Figure 7.5 but for median Q of SB5.

under historical runs are slightly underestimated due to the underestimation of summer precipitation for most GCMs.

The climate change projections in SB5 demonstrate reduced winter flows under the both RCPs 4.5 and 8.5 due to the general decreasing trend of winter precipitation and the increasing trend of winter temperature that induces higher evapotranspiration. Under the RCP 4.5, the simulations of winter-spring flows are variant depending on the downscaled outputs from the GCMs: the minimum flows are simulated by the downscaled outputs from the GCM MIROC-ESM while the maximum flows are simulated by the downscaled outputs from the GCM MRI-CGCM3. The simulated flows in late winter by the outputs from the GCM MRI-CGCM3 are higher than the historical period in the near-term of the RCP 4.5 due to higher winter precipitation projected by this GCM. By contrast, the GCM MIROC-ESM projects less winter precipitation and higher winter temperature than the GCM MRI-CGCM3, which significantly reduces winter flows. In the RCP 8.5, the decrease of winter flows is more severe. The almost no flow state throughout the year is found in the simulations by the downscaled outputs from the GCM MIROC-ESM in the long-term phase under the RCP 8.5.

In summer, climate change projections all simulate a prolonged drought period and reduced summer flows due to the increase of summer temperature and the decrease of summer precipitation for all GCMs projections under the two RCPs. The duration of low-flow spells is variant based on the climate change projections by the GCMs and RCPs, from the August-October period in the near-term simulated by the downscaled outputs from the GCM MRI-CGCM3 under the RCP 4.5 to the almost no flows throughout the year in the long-term simulated by the downscaled outputs from the GCM MIROC-ESM under the RCP 8.5.

Except for the decrease of high flows in winter and pronounced drought effect in

summer, the seasonal shifts in terms of the hydrological regime in SB5 are not observed under climate change conditions. This is because SB5 is rain-dominated that seasonal precipitation decreases and annual temperature increases reduce the magnitude of flows without significant temporal changes.

7.3 Global change impact on water demand

7.3.1 Hydropower demand changes

The general energy demand in the markets is demonstrated by the HDD index that represents the demand for heating and the CDD index that represents the demand for cooling. The higher value of the HDD (or CDD) index, the greater the energy need for heating (or cooling). The value 0 of the two indexes means the lowest energy demand. The HDD and CDD indexes are computed based on mean France temperature, and thus the calculated France temperature in the future (see section 3.2.1) are used to estimate the changes of the two indexes. Analogous to the temperature increase in the Neste water system, the temperature over France is calculated to have an increasing trend throughout the year with the maximum increase in summer and the increasing trend from the near-term to the long-term of the century as illustrated by Figure 3.15. The warming effect is more obvious in the RCP 8.5 than the RCP 4.5.

Annual changes in terms of HDD and CDD indexes are presented. Figure 7.10 shows the number of days when there is energy demand for heating (HDD days) and cooling (CDD days) per year from 1961 to 2100, as simulated by the downscaled outputs from the GCMs under the RCPs 4.5 and 8.5. Under the current climate, the HDD days simulated by the downscaled outputs from the GCMs and by Safran-France are in the range of 250-300 days while the simulated CDD days are in the range of 0-15 days. Thus, the energy demand in the market is largely dominated by heating demand in the historical period.

Under climate change conditions, the structure of energy demand changes. As Figure 7.10 displays, the number of HDD days decreases and the number of CDD days increases from the near-term to the long-term of the century. The magnitudes of the decreasing HDD days and the increasing CDD days are variant depending on the RCP scenarios and the GCM projections. The maximum decrease of HDD days and the maximum increase of CDD days can be found in the simulations by the downscaled outputs from the GCM MIROC-ESM in the long-term under the RCP 8.5. The number of HDD days is decreased to 125-175 days compared to 250-300 days in the historical period. The number of CDD days is increased to 60-110 days compared to 0-15 days in the historical period. Thus, the energy demand structure is shifted with more demand for cooling and less demand for heating given the increasing trend of France temperature.

In addition to the changes in the structure of energy demand, seasonal alterations of energy demand are also noticeable. Figure 7.11 shows the changes of the HDD and CDD regimes over France under climate change conditions for both RCPs 4.5 and 8.5. In the historical period, the energy demand in terms of the HDD and CDD values over France simulated by the downscaled outputs from the GCMs follows the pattern of the simulations by Safran-France reanalysis data. The energy demand in the historical period is mostly for heating in winter. There is scarcely any cooling demand in summer in the historical period.

Under climate change conditions, the HDD values over France decrease in winter, and the duration when HDD=0 is longer and longer in summer from the near-term to the long-term of the century under both RCPs. This indicates that there is lower and lower energy demand for heating in winter in the future and that the duration of the lowest energy demand for heating gets longer and longer. These changes of energy demand for heating are more distinct under the RCP 8.5.

On the contrary, the CDD values over France increase in summer with the longer

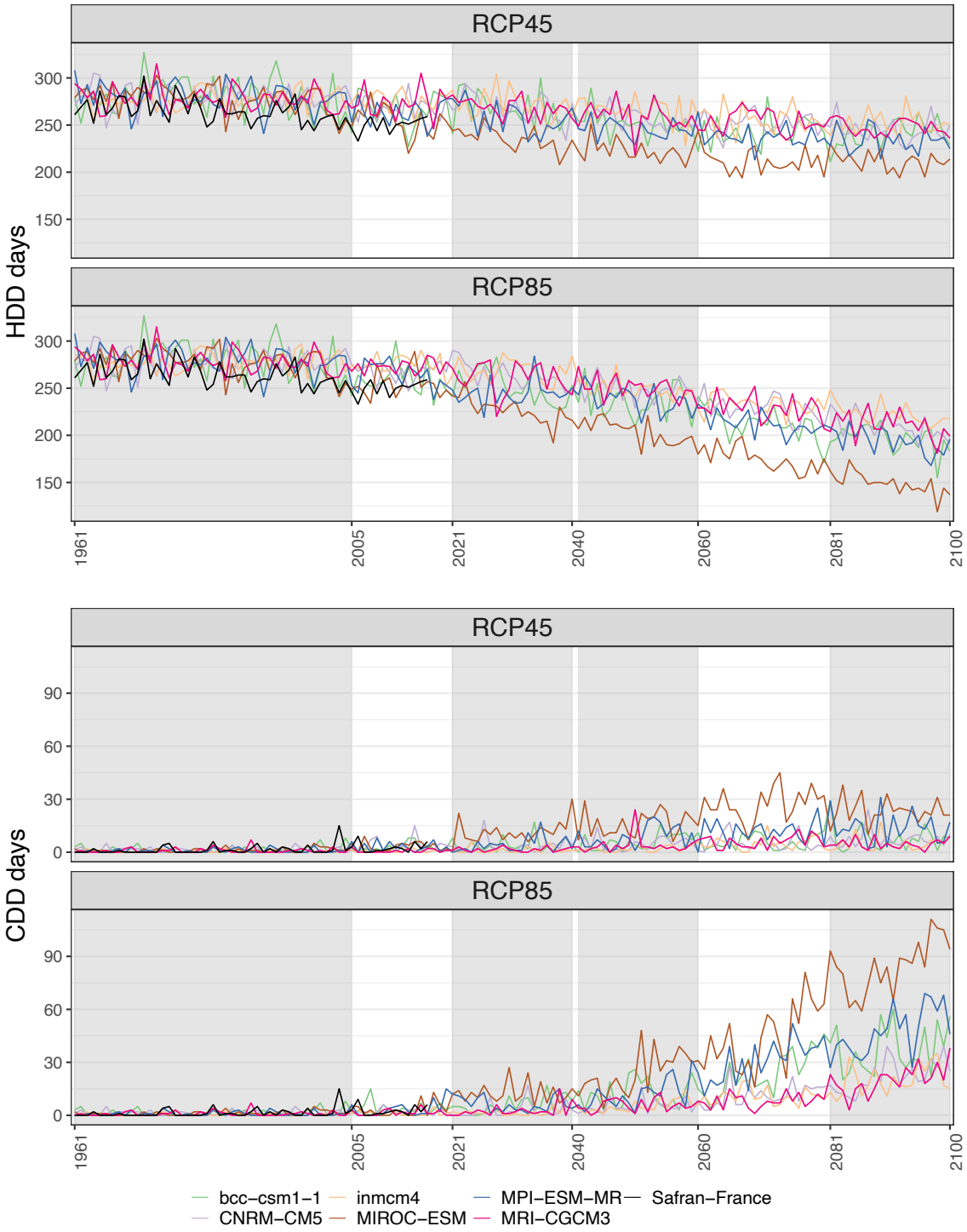

Figure 7.10 – The number of days when there is energy demand for heating in the market within a year (HDD days), and the number of days when there is energy demand for cooling in the market within a year (CDD days) under 6 GCMs (bcc-csm1-1, CNRM-CM5, inmcm4, MIROC-ESM, MPI-ESM-MR, MRI-CGCM3) from 1961 to 2100 for two RCP scenarios (RCPs 4.8 and 8.5). The historical (1961-2005), near-term (2021-2040), medium-term (2041-2060), and long-term (2081-2100) phases are labelled in gray ribbons from left to right. The simulations from Safran-France (1958-2018) are also plotted to compare with the simulations under climate change scenarios.

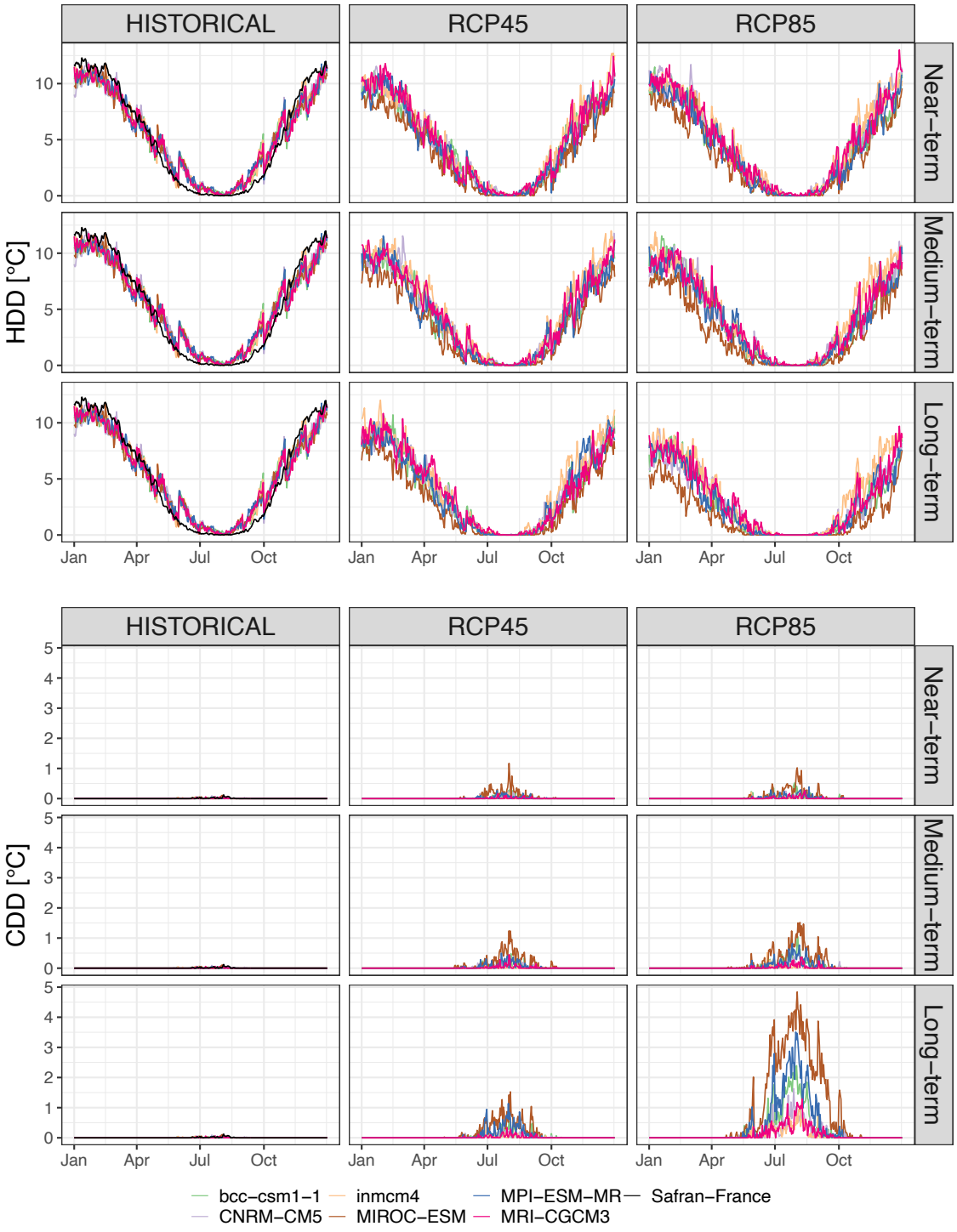

Figure 7.11 – The impact of temperature increase on the mean daily HDD and CDD values under 6 GCMs (bcc-csm1-1, CNRM-CM5, inmcm4, MIROC-ESM, MPI-ESM-MR, MRI-CGCM3) for the near-term (2021-2040), medium-term (2041-2060), and long-term (2081-2100) phases under two RCP scenarios (RCPs 4.8 and 8.5). The simulations over historical period (1961-2005) of the 6 GCMs, along with the simulations from Safran-France (1958-2018), are illustrated to compare with the simulations under climate change scenarios. The three sub-figures in the column "HISTORICAL" are identical to visually help the comparison.

and longer duration when the CDD values are larger than 0 from the near-term to the long-term of the century under both RCPs. This indicates that there is potentially an increasing demand for summer cooling in France in the future and that the duration of summer cooling demand gets longer and longer from the near-term to the long-term of the century. The increasing energy demand and longer demand duration in summer are remarkable in the long-term under the RCP 8.5 scenario.

In summary, the energy demand in France in the future is projected to decrease in winter for heating and to potentially increase in summer for cooling. These demand changes in the energy market can induce changes in hydropower demand for the hydropower producer SHEM. Here, we consider the business as usual scenario that the SHEM produces hydropower only for winter heating since we do not know if the needs for cooling will materialise. The changes in the HDD values over France under climate change conditions are forced into the hydropower demand model of the SHEM to investigate the changes in hydropower demand.

Figure 7.12 shows the seasonal changes of hydropower demand from the markets for the SHEM under climate change conditions. The hydropower demand follows the changes of HDD values with a decrease in hydropower demand throughout the year and a marked decrease in winter compared with the historical period. We also note an increase in the duration in which hydropower demand remains constant in summer. This is attributed to the longer duration when HDD=0 in summer, i.e., the lowest energy demand in the market (the lowest interest for SHEM to produce energy).

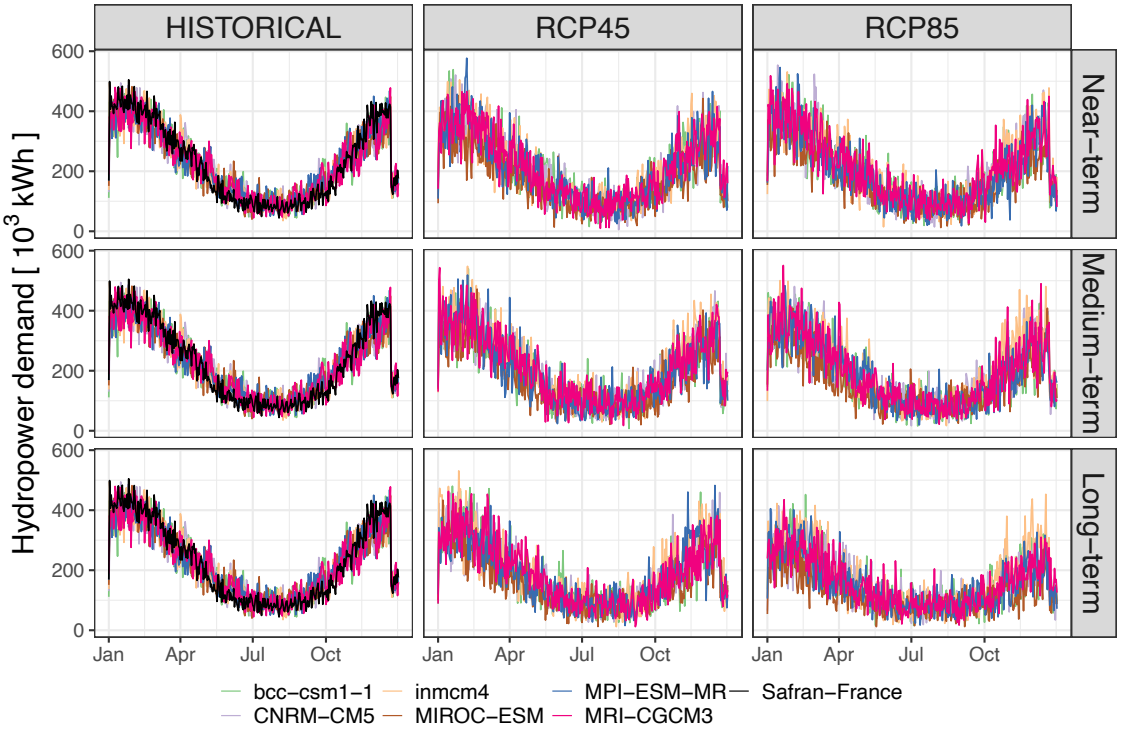

Figure 7.12 – As in Figure 7.11 but for mean daily hydropower demand for the SHEM.

7.3.2 Drinking water demand changes

Drinking water demand is dominated by population growth in the Gascogne region. In this study, drinking water network efficiency is considered to remain the same as the

current situation, which is 75 %. Figure 7.13 shows the changes of daily drinking water demand for each year from 1961 to 2100. The drinking water demand increases from the daily demand value 0.255 m^3/s in 1961 to the daily demand value 0.360 m^3/s in 2050, and remains stable after.

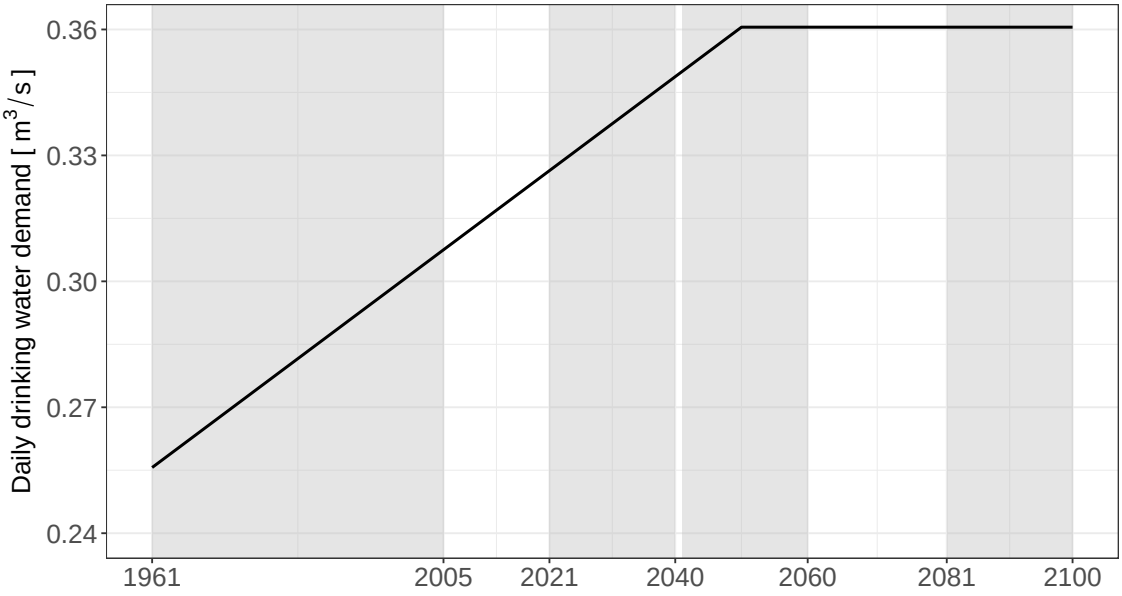

Figure 7.13 – The increase of drinking water demand in the Gascogne region from 1961 to 2100. The historical (1961-2005), near-term (2021-2040), medium-term (2041-2060), and long-term (2081-2100) periods are labelled in gray ribbons from left to right.

7.3.3 Industrial water demand changes

Industrial water demand is always considered as a constant and the daily demand is 0.338 m^3/s throughout the temporal range from 1961 to 2100.

7.3.4 Irrigation water demand changes

Irrigation practices in the Gascogne region in the future is assumed to be the same as the current state. Maize of late maturity varieties is cropped in the period from 07/April to 31/May. The "derived irrigation area" of maize is 265 km^2. As such, these values configure the irrigation water demand model (ADEAUMIS).

The climate change projections under the 6 GCMs and the 2 RCPs in terms of potential evapotranspiration, precipitation, and temperature changes over SB5 are forced into the configured ADEAUMIS model to simulate the irrigation activities (sowing date, maize growth duration, and irrigation duration) and the corresponding irrigation water demand.

Figure 7.14 shows the distribution of sowing dates under climate change conditions. In the historical period, the sowing date simulated by the downscaled outputs from the GCMs is consistent with the simulation by Safran-PIRAGUA. Besides, we can observe that there is no significant change in terms of sowing date under climate change conditions. The sowing date is in the temporal interval 20/April-20/May for all projections, which indicates the similar starting date of maize growth.

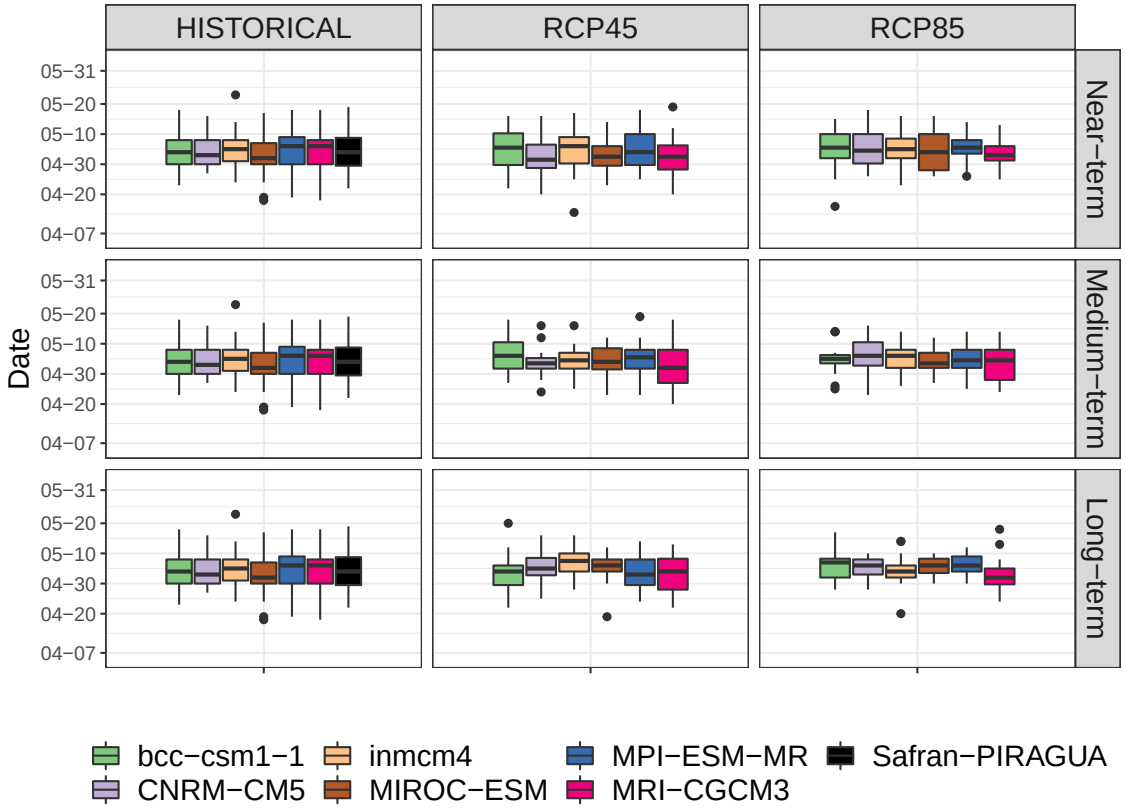

Figure 7.14 – The distribution of sowing date in the 6 GCMs (bcc-csm1-1, CNRM-CM5, inmcm4, MIROC-ESM, MPI-ESM-MR, MRI-CGCM3) for the near-term (2021-2040), medium-term (2041-2060), and long-term (2081-2100) phases under two RCP scenarios (RCPs 4.8 and 8.5). The simulations over historical period (1961-2005) of the 6 GCMs, along with the simulations from Safran-PIRAGUA (1979-2014), are illustrated to compare with the simulations under climate change scenarios. The three sub-figures in the column "HISTORICAL" are identical to visually help the comparison.

Figure 7.15 shows the distribution of maize growth duration and irrigation duration under climate change conditions. The maize growth duration is the number of days needed to develop to the maturity stage from the sowing date. The irrigation duration is the number of days between the stage of 10-12 leaves and the stage of 50% grain moisture content.

In the historical period, the maize growth and irrigation duration are overestimated by the downscaled outputs from the GCMs compared with the simulations by the Safran-PIRAGUA reanlysis data. This is attributed to the underestimation of temperature under historical runs from May to October (see Figure 7.4). Since the temperature in SB5 under historical runs is underestimated, the maize crop needs more days to accumulate the thermal time to complete each growth stage as presented in Table 5.3. Therefore, the maize growth duration is overestimated by 30-50 days in the simulations by the downscaled outputs from the GCMs. Meanwhile, the irrigation duration is also overestimated by 10-20 days in the simulations by the downscaled outputs form the GCMs.

Under climate change conditions, we can observed from Figure 7.15 that there is a general decreasing trend of maize growth duration and irrigation duration under the two RCPs compared with the historical period. This is attributed to the projected temperature

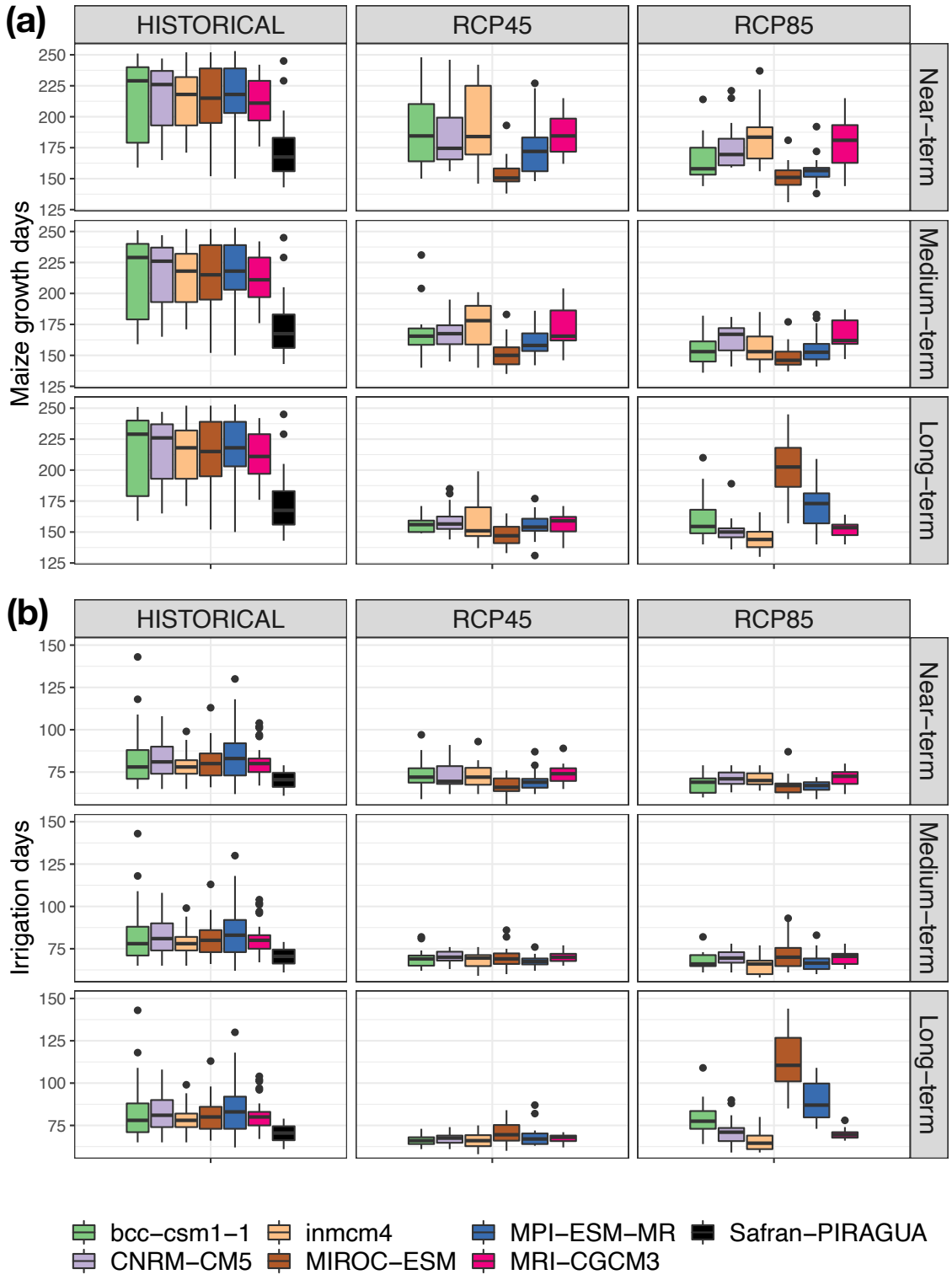

Figure 7.15 – As in Figure 7.14 but for maize growth duration (a) and irrigation duration (b).

increase in the future in SB5 that shortens the maize growth duration due to a quicker thermal time accumulation, and thus a decreased irrigation duration. However, we also note a strange increase of maize growth and irrigation duration in the long-term under the RCP 8.5. The simulated maize growth and irrigation duration by the downscaled outputs from the GCMs (bcc-csm1-1, MIROC-ESM, and MPI-ESM-MR) are generally longer than other simulations under climate change conditions. Particularly, the simulated irrigation duration by the downscaled outputs from the GCMs (MIROC-ESM and MPI-ESM-MR) are even longer than the historical period. This is because these GCMs project extremely high daily temperature, with many days of temperature larger than 27.5 °C, that stops the maize growth in summer. Thus, maize takes more days to the stage of 50% grain moisture content (the end stage of irrigation) and to the stage of maturity (the end stage of growth).

Figure 7.16 shows the regime of daily irrigation water demand under climate change conditions. The results of the ADEAUMIS model in terms of irrigation water demand are generated at weekly time step. The simulations are transferred to daily time step by averaging the results in a week.

In the historical period, the patterns of maize irrigation water demand simulated by the downscaled outputs from the GCMs generally agree with the simulations by the Safran-PIRAGUA data. However, the irrigation peaks in summer are overestimated when comparing to the simulation by Safran-PIRAGUA, which can be attributed to the underestimation of precipitation under historical runs. Besides, the end of irrigation duration simulated by the downscaled outputs from the GCMs is later than that by the Safran-PIRAGUA. The reason is the underestimation of temperature under historical runs as mentioned before.

In the climate change projections, the downscaled outputs from the GCMs mostly project an earlier start of irrigation, a shortened irrigation duration, and a higher irrigation water demand from the near-term to the long-term under the RCP 4.5 and from the near-term to the medium-term under the RCP 8.5. The earlier start of irrigation activities is due to the warmer climate in the future that makes maize go to the stage of 10-12 leaves (the starting point of irrigation) more quickly than the historical period. The shortened irrigation duration is explained before. The higher irrigation water demand is attributed to the projected less summer precipitation and higher summer potential evapotranspiration that makes maize more water demanding. Particularly, in the long-term of the RCP 8.5, the simulations by the downscaed outputs from some GCMS (e.g., MIROC-ESM) show a later end of the irrigation duration due to the more often extremely warming days in summer as explained before.

7.3.5 Environmental water demand changes in SB5

Environmental water release from the CACG reservoirs is mainly used to provide a good ecological status in SB5, particularly the DOE requirement in drought period. Besides, the water extraction from the Neste River via the Neste Canal also contributes to this purpose. Equation 5.14 presents the environmental water demand from the CACG reservoir, which is only the contribution of the CACG reservoirs to the environment. Here, we present the deficit of the natural flows in SB5 to the DOE requirement as the environmental water demand in SB5, calculated as follows:

$$max(DOE_t - Q_{5,t}, \beta) \tag{7.1}$$

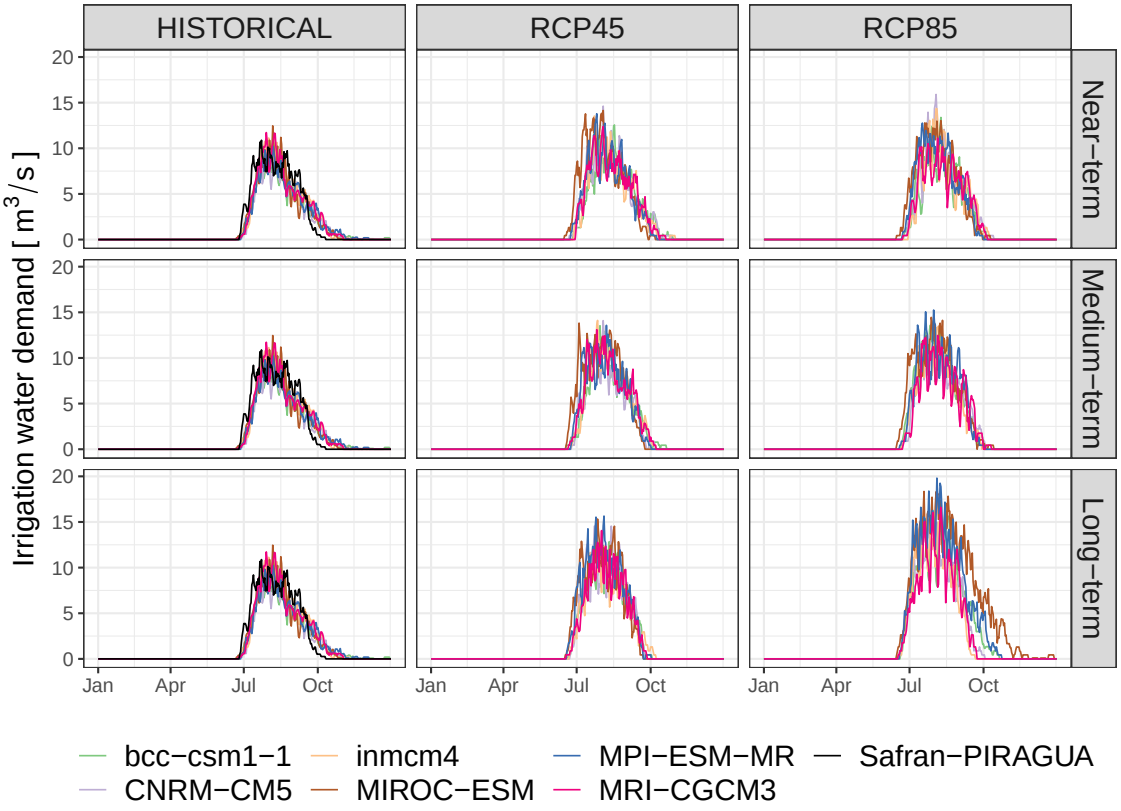

Figure 7.16 – As in Figure 7.14 but for the regime of daily maize irrigation water demand.

Figure 7.17 shows the regime of mean daily environmental water demand under climate change scenarios. In the historical period, the simulations by the downscaled outputs from the GCMs are generally consistent with the simulations by the Safran-PIRAGUA reanlysis data. However, the environmental water demand simulated by the downscaled outputs from the GCMs in the autumn is underestimated compared with the simulation by Safran-PIRAGUA. This is attributed to the overestimation of natural flows in SB5 in autumn that is caused by the higher autumn precipitation projections under historical runs than the Safran-PIRAGUA data.

Under climate change conditions, there is a remarkable increase of environmental water demand in the period when there is DOE requirement (June to March, see Figure 3.21) under the two RCPs compared with the historical period. This is due to the warmer and dryer climate in the future than the historical climate that induces lower natural flows in SB5 and thus higher deficit to the DOE requirement (higher environmental water demand). The environmental water demand under the RCP 8.5 is higher than that under the RCP 4.5.

7.3.6 Summary

The impact of global change on water demand in the Neste water system is summarized as:

1. hydropower demand for heating is projected to decrease throughout the year with the maximum reduction in winter;

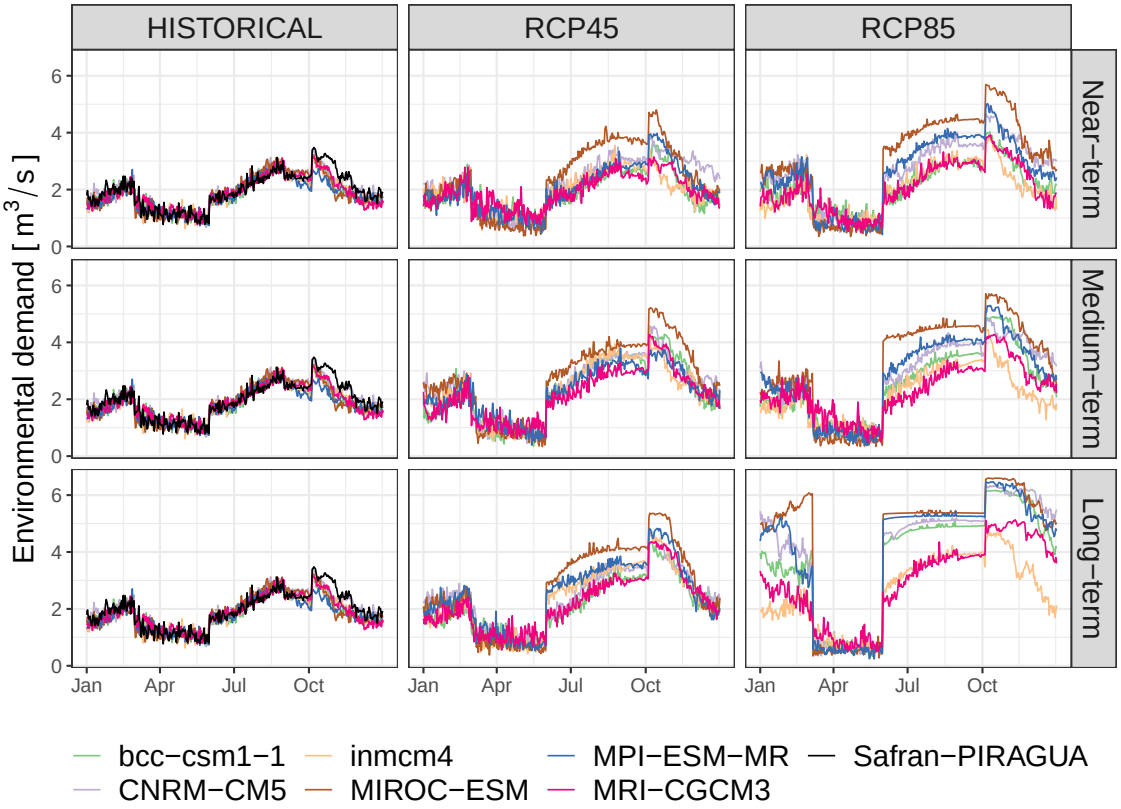

Figure 7.17 – As in Figure 7.14 but for the regime of mean daily environmental water demand in SB5.

2. drinking water demand is projected to increase till the middle of the century and then remain stable till the end of the century;

3. industrial water demand remains constant;

4. irrigation water demand is projected to increase in summer with a general shortened irrigation duration, which indicates a more frequent and higher irrigation water demand;

5. environmental water demand is projected to increase in order to meet the DOE requirement.

Figure 7.18 shows the regime of total water demand in SB5 under climate change scenarios. In terms of the magnitude of water demand, the increase of total water demand is characterized by irrigation water demand in summer and environmental water demand from summer to winter.

Based on the increasing trend of the total water demand in SB5, the CACG should tend to request more water from the SHEM reservoirs to feed SB5 and to meet the DOE requirement at Sarrancolin. Figure 7.19 shows the regime of the CACG request for water release from the SHEM reservoirs under climate change conditions. Figure 7.20 shows the mean annual request for water release from the SHEM reservoirs under climate change conditions.

Note that the two figures only demonstrate the potential how the CACG requests for the water release from the SHEM reservoirs to feed SB5. As we can observe, the tendency

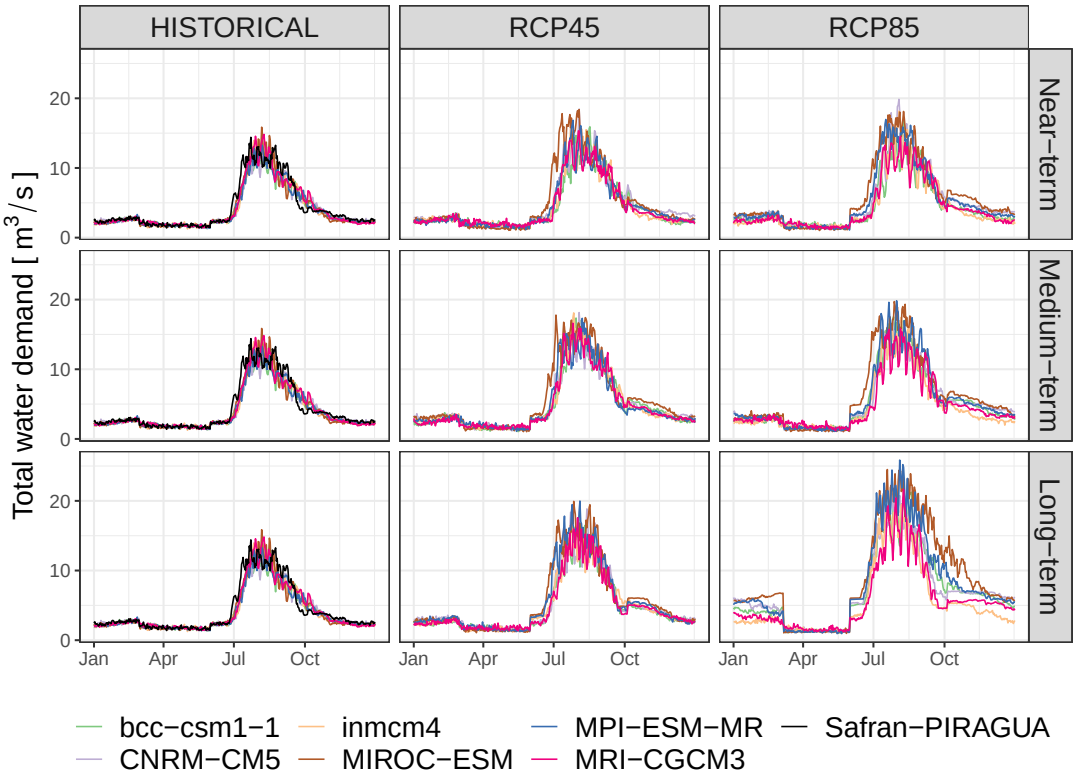

Figure 7.18 – As in Figure 7.14 but for the regime of total water demand in SB5.

of the CACG request follows the total water demand in SB5 with the potential to request more water to feed SB5. Besides, the 48 Mm^3 quota is not sufficient to fully satisfy the CACG request under the climate changes projections, especially in the long-term of the RCP 8.5.

To summarize, there is an increasing water demand in SB5 dominated by irrigation and environmental water demand. The CACG tends to request more water from the SHEM to satisfy the water demand in SB5.

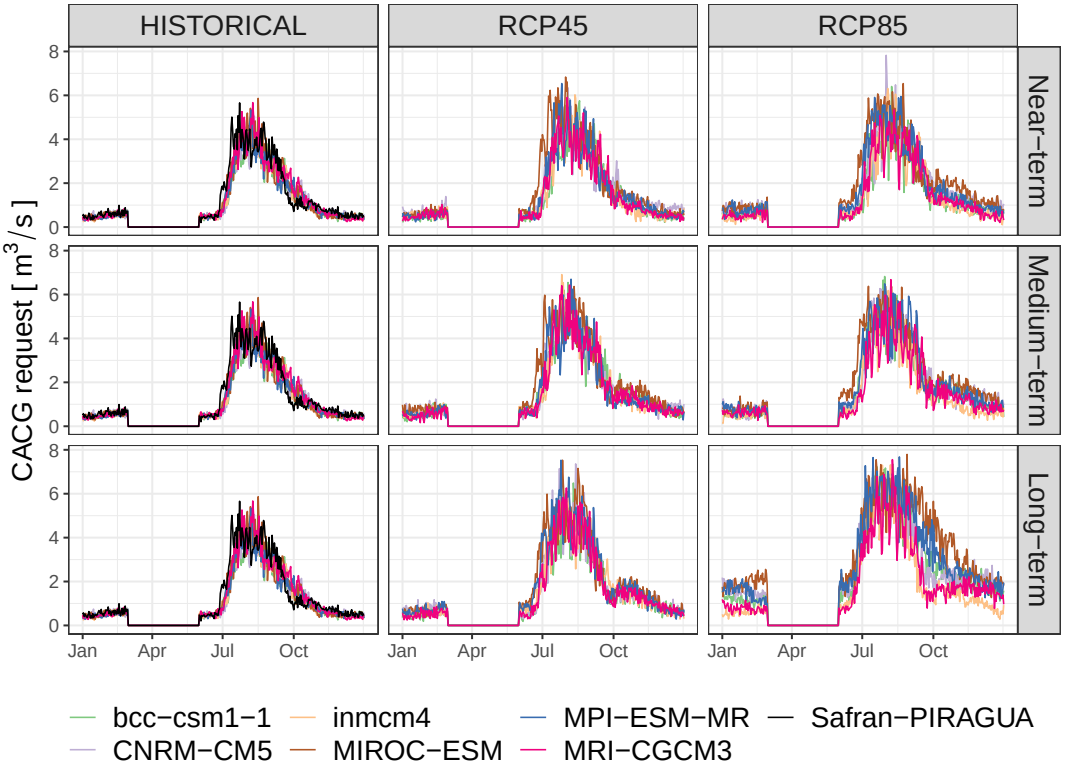

Figure 7.19 – As in Figure 7.14 but for the regime of mean daily CACG request from the SHEM.

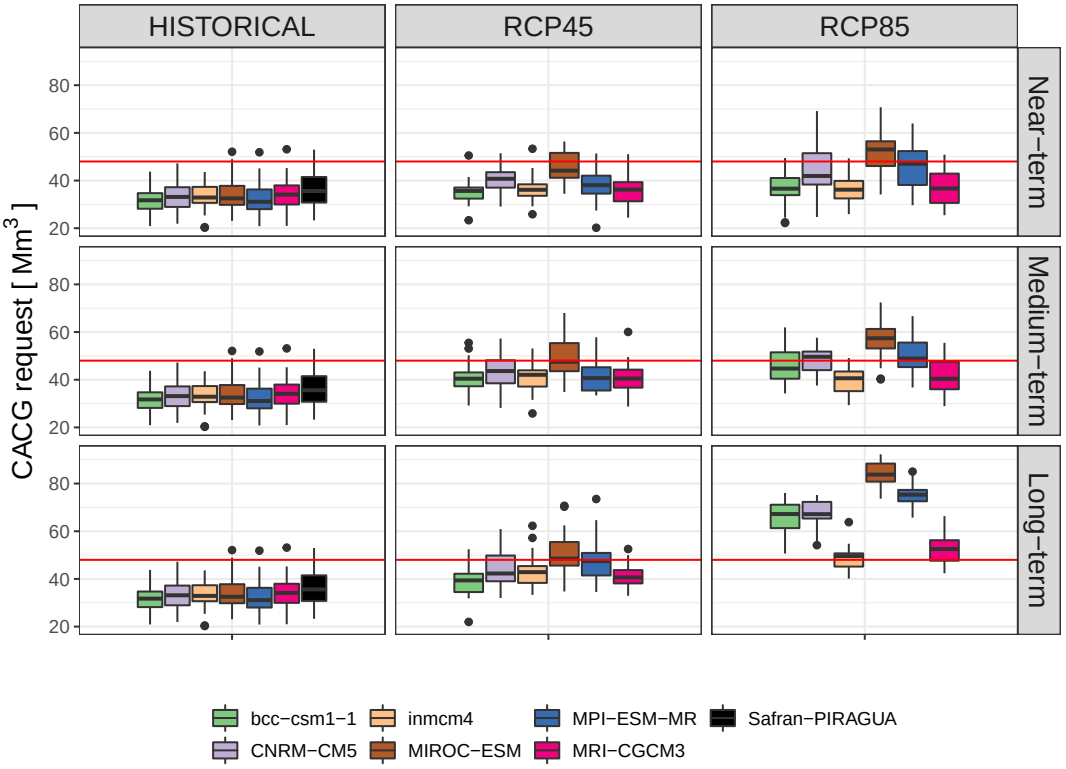

Figure 7.20 – As in Figure 7.14 but for the annual CACG request for the SHEM. The red line is the current limit of the CACG request (48 Mm^3).

7.4 Global change impact on water management

7.4.1 Water management in the Aure Valley

Model coupling

To recall, the Aure Valley (SB1-4) is managed by the SHEM for hydropower production. Besides, the CACG can request a quota of 48 Mm^3 over the period from July to February from the SHEM reservoir storage. At the outlet of the Aure Valley (Sarrancolin), the CACG extracts the water volume requested from the SHEM via the Neste Canal. In addition to the quota of 48 Mm^3, the CACG can also extract the Neste River at Sarrancolin via the Neste Canal to feed the Gascogne region. Whenever the CACG extracts water at Sarrancolin either from the 48 Mm^3 or the Neste River, the CACG should keep the DOE requirement at Sarrancolin, which is the river discharge downstream Sarrancolin should always be maintained no lower than 4 m^3/s.

Therefore, the management in the Aure Valley for water uses is coupled between the SHEM and CACG. In another word, the SHEM management for hydropower depends on the CACG request and in the mean time the CACG management at Sarrancolin is also influenced by the SHEM release. As such, a coupling process should be involved to represent the real management when analyzing the impact of global change on the water management in the Aure Valley as shown in Figure 7.2. Three management models are coupled, which are the SHEM management model, the model that calculating the influenced river flow at Sarrancolin, and the model of the CACG management at Sarrancolin (see Table 5.7).

Since the 48 Mm^3 quota is a binding contract between the CACG and SHEM, the satisfaction of the CACG request should be placed with priority within the SHEM management strategy, so that hydropower production can only be satisfied afterwards. In order to make the coupled model to adapt to global change, particularly the SHEM management model to satisfy the CACG request under global change scenarios, we design four management modes of the SHEM management model as shown in Table 7.2. The four management modes gradually sacrifice the opportunities for hydropower production of the Orédon reservoir and then the reservoir refill targets in the SHEM management model to provide water for the CACG request.

The explanations of the four strategies of management in Table 7.2 are given as follows.

1. The management mode 1 is the management strategy when the natural inflows into the reservoirs and the CACG request allows the SHEM to have water storage in the Oule, Orédon, and Lassoula reservoirs for the optimization of hydropower production. This strategy is the SHEM model configuration developed in chapter 5, which aims at optimizing hydropower production when the CACG demand is satisfied.

2. The management mode 2 is the management strategy that the SHEM reduces the opportunities for hydropower production in order to satisfy the CACG request. In the original SHEM model configuration in chapter 5, a constraint that transfers the water storage in the Orédon reservoir to the Oule reservoir in winter is set to optimize the hydropower production. In this management mode, the constraint of transferring water from the Orédon to the Oule reservoir in winter is deleted to make sure that the Orédon reservoir can achieve the storage target at the end

Table 7.2 – Four management modes of the SHEM management model to satisfy the CACG request under global change

SHEM management	Actions	Model representation
Mode 1	Satisfy both CACG request and hydropower production	1. Consider all the constraints
Mode 2	Satisfy CACG request and reduce hydropower production	1. Consider all the constraints except the water transfer between the Oule and Orédon reservoirs in winter
Mode 3	Satisfy CACG request, reduce hydropower production and lower reservoir storage at the end of the management	1. Consider all the constraints except the water transfer between the Oule and Orédon reservoirs in winter; 2. the storage target V_{ini} decrease by 10%, 20%, ... 100% gradually to satisfy the CACG request for the Oule, Orédon, and Lassoula reservoirs
Mode 4	Fail CACG request and focus on reservoir recovery	1. Consider all the constraints except the CACG request; 2. refill till the storage target V_{ini} reaching 100%, 90% ... 10% of the original level for the Oule, Orédon, and Lassoula reservoirs

of the management. As such, the Orédon reservoir in this management mode is only used to provide water for the CACG request by sacrificing its opportunities of hydropower production in winter. The hydropower production from the Oule and Lassoula reservoir in winter is optimized in this management mode when the CACG request is satisfied.

3. The management mode 3 is the management strategy to deal with the situation when the total water storage in the reservoirs and the natural inflows into the reservoirs are not sufficient to provide water to the CACG request during the request period. This management mode sacrifices not only opportunities for Orédon hydropower production in winter (as described in the management mode 2) but also the reservoir refill targets at the end of the management. This management mode sequentially tests to lower 10%, 20%, ... 100% of the refill targets of the three reservoirs and selects the minimum percentage.

4. The management mode 4 is the management strategy when CACG request cannot be satisfied even by lowering 100% of the refill targets of the Oule, Orédon, and Lassoula reservoirs. This means that the sum of the storage at the beginning the management and the natural inflows into the reservoirs is not sufficient for the CACG request. As such, the CACG demand is failed and the SHEM focuses on the reservoir recovery. This management mode sequentially tests to refill 100%, 90%, ... 10% of the storage targets of the three reservoirs and selects the maximum percentage.

The four management modes are sequentially tested from Mode 1 to Mode 4 under

global change scenarios. If the simulation of one mode fails (for example, the Mode 1), the simulation of the next mode (for example, the Mode 2) is conducted. In this way, the sequential process stops when one mode succeeds and the management simulations by this mode will be exported. The Mode 4 always succeeds because this management mode is designed to encounter the most severe dry conditions in the future. The four sequential management modes from Mode 1 to Mode 4 represent the increasing conservative attitude of the management strategies that can be practiced by SHEM.

The four management modes will be included in the coupled modelling process. Based on the top-down approach illustrated in Figure 7.2, we detail the model coupling process between the SHEM management and the CACG management at Sarrancolin by including the four management modes of SHEM as shown in the Figure 7.21.

Model coupling, which indicates that models are completely linked with bi-directional data transmission, and one-way chain, which is an uncoupled method with data interchange in only one direction, are the two basic forms of conjunctive modeling (Becker and Burzel, 2016). For example, if we take two models that must be conjunctively connected, if the models are coupled, the simulation results of the first model have an influence on the simulation results of the second model, and vice versa. This means that connected models must share information on a time step basis throughout the run time. When two models are uncoupled, the first model's simulation results have an impact on the second, while the second model's simulation results have no feedback effect on the first. In this study, we use the bi-directional iterative coupling approach to represent the coupling process between the SHEM optimization and CACG simulation at Sarrancolin.

The coupling process is presented as follow.

- The coupling process is a loop to gradually search for the results that satisfy the DOE requirement at Sarrancolin. It is based on a management year that starts from July and ends at June to link the optimization of the SHEM management model with the simulation of the CACG management models.

- Firstly, time series of CACG request within a management year is simulated by the CACG management model based on the total water demand in SB5. The simulated time series of request are the initial inputs of the coupling process. The time series of request will be reduced to 48 Mm^3 proportionally if the sum of the CACG request values is larger than 48 Mm^3.

- Secondly, the treated CACG request series, natural inflows of SB1-3, and hydropower demand are forced into the SHEM management model (4 management modes) to simulate the water release from the Oule, Orédon, and Lassoula reservoirs for each water use. Then, the influenced flow of the Neste River at Sarrancolin can be calculted with the simulated release from the SHEM reservoirs and the natural water inflows of SB4.

- Thirdly, the CACG management at Sarrancolin is simulated to generate a new time series of request. Before the management of CACG to satisfy the DOE at Sarrancolin, a boolean test is conducted to check whether the SHEM fails to meet the CACG request. If so, the loop stops and the results are exported, which means that CACG can only extract less water at Sarrancolin to satisfy the DOE requirement. If not, the CACG manages to satisfy the DOE requirement within the 48 Mm^3 quota.

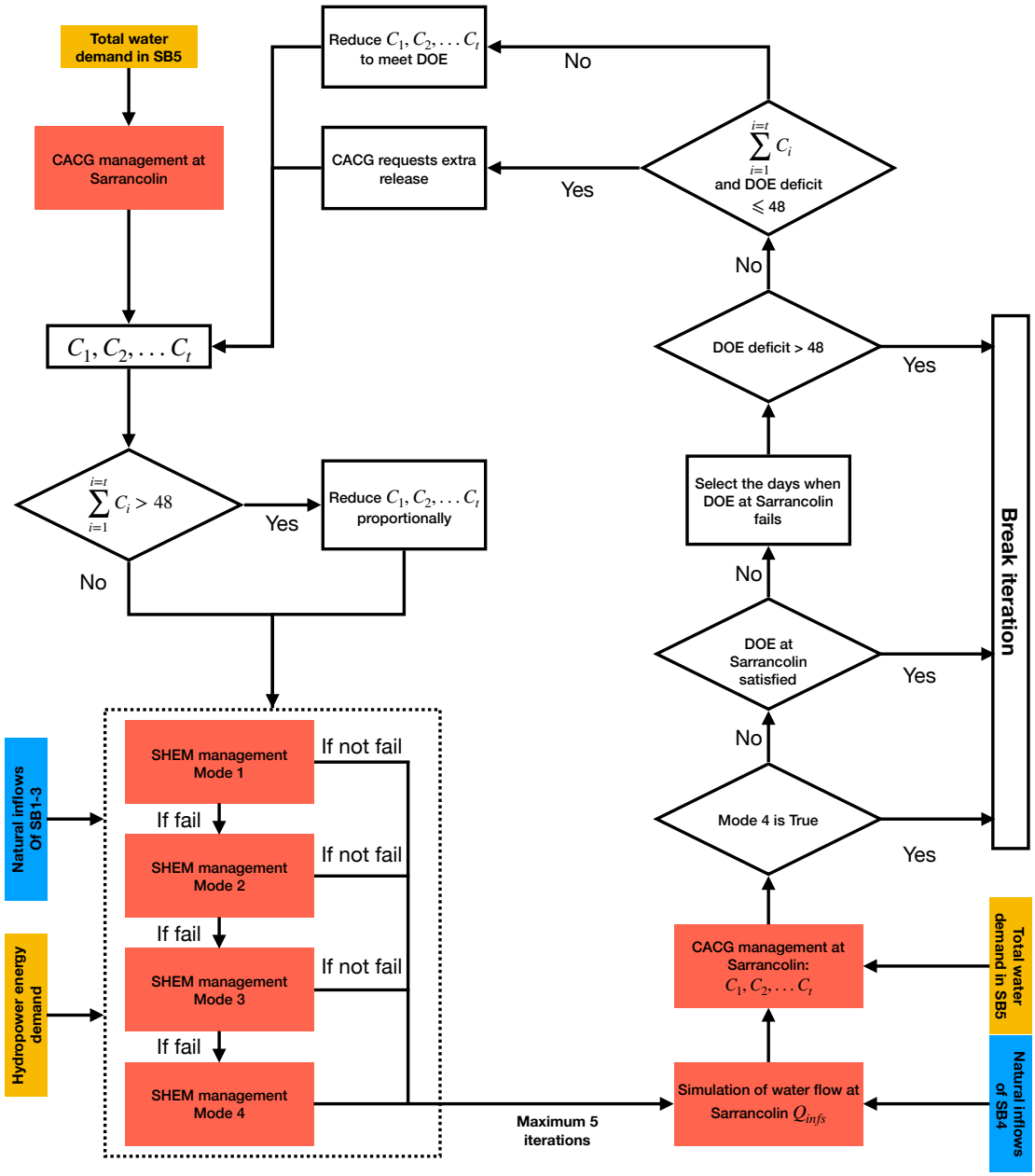

Figure 7.21 – The coupling process to represent the current management of SHEM and CACG at Sarrancolin. The color blue represents the hydrological models associated in the coupling process; the color yellow the water demand; and the color red water management models by SHEM and CACG.

- Fourthly, in the process of satisfying the DOE requirement, the CACG starts with checking whether the DOE requirement is satisfied. If so, the loop stops and the CACG should not request extra water from SHEM due to the principal of saving the storage of the SHEM reservoirs. If not, the CACG proceeds to select the days when there is a DOE deficit at Sarrancolin. If the total DOE deficit is larger than 48 Mm^3, the loop is broken because the DOE deficit is beyond the quota that the CACG can request. If the sum of the total request and the DOE deficit is within the 48 Mm^3 quota, the CACG can request extra release from the reservoirs; if the

sum of the total request and the DOE deficit is out of the 48 Mm^3 quota, the request series are reduced proportionally to fulfill the DOE deficit.

- Finally, the new CACG request time series replace the initial series and go through the loop again as mentioned above. The coupling process is set to have a maximum of 5 iterations to avoid endless loop and computational burden.

Besides, in this study, we consider a completely different management context to compare with the current management in the Aure Valley. The changed management context is that the CACG has the right to request water as much as the CACG wants. In another word, there is no constraint on the volume of water that the CACG can request. The coupling process of the changed management context is illustrated in Figure 7.22.

Figure 7.22 – As in Figure 7.21 but under a different management context that CACG can request as much as the CACG wants.

The simulated natural water resources under climate change scenarios and the simulated water demand under global change scenarios are forced into the two different management contexts. The plausible impacts on the SHEM management and the CACG management at Sarrancolin are presented, respectively.

The impacts on the SHEM management

The impacts of global change in terms of the SHEM management on the reliability of satisfying the CACG demand, the water release for the CACG, the hydropower production, and the reservoir refill target are presented as follows.

Changes in the reliability of SHEM to satisfy the CACG demand Concerning the impact on the SHEM management, we firstly investigate the reliability that the SHEM can satisfy the CACG demand. The opposite to this reliability is the risk that the SHEM fails the CACG request. Based on Hashimoto et al. (1982a,b), the definition of the reliability is the proportion of satisfied occurrences in the total occurrences while the risk is the proportion of failed occurrences in the total occurrences.

By investigating this reliability, the frequency of each management mode used to adapt to the global change scenarios (the changes in natural water resources, the changes in water demand, and the changes in different management context) are calculated in Tables 7.3, 7.4, 7.5, and 7.6. In the tables, the frequency sum of the four management modes under the combination of 1 GCM $\times$ 1 RCP $\times$ 1 management context should be equal to 1. The frequency sum of mode 1-3 is the reliability that the SHEM satisfies the CACG demand while the frequency of mode 4 is the risk that the SHEM fails the contract with the CACG.

The frequencies of the four management modes calculated with the input of Safran-PIRAGUA analysis into the modelling chain in Figure 7.2 is 1, 0, 0, 0, respectively. The underestimation of the frequency of mode 1 by GCMs in the historical period in all RCP and management context scenarios is attributed to the underestimation of precipitation that lows the possibilities for hydropower production. However, the reliability of the CACG demand in the historical period and in the Safran-PIRAGUA data is the same (all equal to 1).

Under the current management context that the CACG can only request 48 Mm^3 from the SHEM (see Tables 7.3 and 7.4), the reliability of CACG demand can be maintained under the RCP 4.5 while there is a slight decrease in the reliability (a slight increase in the frequency of mode 4) under the long-term of the RCP 8.5. Thus, the 48 Mm^3 can be mostly satisfied under both RCPs, which corresponds to the vulnerability assessment in chapter 6.

Under the changed management context that there is no limit on the water volume that the CACG can request from the SHEM (see Tables 7.5 and 7.6), the reliability of CACG demand is challenged because there is an increasing trend of failure (increasing frequency of mode 4) from the near-term to the long-term under both RCPs. Particularly, in the long-term of the RCP 8.5, the GCMs MIROC-ESM and MPI-ESM-MR project a complete failure that the SHEM could not satisfy the CACG request at all. In this case, it is probably because the CACG request is larger than the water resource availability (i.e., no matter how SHEM manages the water resources, the request by CACG will be failed).

Table 7.3 – The utilization frequency of the four management modes in the SHEM management optimization in the 6 GCMs (bcc-csm1-1, CNRM-CM5, inmcm4, MIROC-ESM, MPI-ESM-MR, MRI-CGCM3) for the near-term (2021-2040), medium-term (2041-2060), and long-term (2081-2100) phases under RCP 4.5 and the current management context (CACG can request 48 Mm^3).

RCP 4.5 and current management context					
		Historical (1961-2005)	Near-term (2021-2040)	Medium-term (2041-2060)	Long-term (2081-2100)
Mode 1	bcc-csm1-1	0.78	0.65	0.30	0.50
	CNRM-CM5	0.71	0.50	0.30	0.40
	inmcm4	0.64	0.60	0.25	0.10
	MIROC-ESM	0.64	0.15	0.15	0.00
	MPI-ESM-MR	0.62	0.80	0.55	0.35
	MRI-CGCM3	0.82	0.85	0.70	0.60
Mode 2	bcc-csm1-1	0.22	0.35	0.70	0.50
	CNRM-CM5	0.29	0.50	0.70	0.55
	inmcm4	0.36	0.40	0.75	0.85
	MIROC-ESM	0.36	0.85	0.85	0.95
	MPI-ESM-MR	0.38	0.20	0.45	0.45
	MRI-CGCM3	0.18	0.15	0.30	0.40
Mode 3	bcc-csm1-1	0.00	0.00	0.00	0.00
	CNRM-CM5	0.00	0.00	0.00	0.05
	inmcm4	0.00	0.00	0.00	0.05
	MIROC-ESM	0.00	0.00	0.00	0.05
	MPI-ESM-MR	0.00	0.00	0.00	0.20
	MRI-CGCM3	0.00	0.00	0.00	0.00
Mode 4	bcc-csm1-1	0.00	0.00	0.00	0.00
	CNRM-CM5	0.00	0.00	0.00	0.00
	inmcm4	0.00	0.00	0.00	0.00
	MIROC-ESM	0.00	0.00	0.00	0.00
	MPI-ESM-MR	0.00	0.00	0.00	0.00
	MRI-CGCM3	0.00	0.00	0.00	0.00

The utilization frequency of the management modes 1-4 with Safran-PIRAGUA over the period from 1979-2014 is 1, 0, 0, and 0, respectively.

Table 7.4 – As in Table 7.3 but under RCP 8.5 and the current management context (CACG can request 48 Mm^3).

RCP 8.5 and current management context					
		Historical (1961-2005)	Near-term (2021-2040)	Medium-term (2041-2060)	Long-term (2081-2100)
Mode 1	bcc-csm1-1	0.78	0.50	0.45	0.10
	CNRM-CM5	0.71	0.35	0.30	0.00
	inmcm4	0.64	0.30	0.35	0.10
	MIROC-ESM	0.64	0.00	0.05	0.25
	MPI-ESM-MR	0.62	0.30	0.10	0.05
	MRI-CGCM3	0.82	0.60	0.65	0.25
Mode 2	bcc-csm1-1	0.22	0.50	0.55	0.55
	CNRM-CM5	0.29	0.50	0.70	0.70
	inmcm4	0.36	0.70	0.65	0.75
	MIROC-ESM	0.36	0.85	0.75	0.10
	MPI-ESM-MR	0.38	0.65	0.75	0.35
	MRI-CGCM3	0.18	0.40	0.35	0.75
Mode 3	bcc-csm1-1	0.00	0.00	0.00	0.30
	CNRM-CM5	0.00	0.10	0.00	0.25
	inmcm4	0.00	0.00	0.00	0.15
	MIROC-ESM	0.00	0.10	0.20	0.60
	MPI-ESM-MR	0.00	0.05	0.10	0.50
	MRI-CGCM3	0.00	0.00	0.00	0.00
Mode 4	bcc-csm1-1	0.00	0.00	0.00	0.05
	CNRM-CM5	0.00	0.05	0.00	0.05
	inmcm4	0.00	0.00	0.00	0.00
	MIROC-ESM	0.00	0.05	0.00	0.05
	MPI-ESM-MR	0.00	0.00	0.05	0.10
	MRI-CGCM3	0.00	0.00	0.00	0.00

The utilization frequency of the management modes 1-4 with Safran-PIRAGUA over the period from 1979-2014 is 1, 0, 0, and 0, respectively.

Table 7.5 – As in Table 7.3 but under RCP 4.5 and the changed management context (no limit on CACG request).

RCP 4.5 and changed management context					
		Historical (1961-2005)	Near-term (2021-2040)	Medium-term (2041-2060)	Long-term (2081-2100)
Mode 1	bcc-csm1-1	0.78	0.65	0.30	0.50
	CNRM-CM5	0.71	0.50	0.30	0.40
	inmcm4	0.64	0.50	0.25	0.10
	MIROC-ESM	0.64	0.15	0.05	0.00
	MPI-ESM-MR	0.62	0.75	0.55	0.30
	MRI-CGCM3	0.82	0.85	0.65	0.55
Mode 2	bcc-csm1-1	0.22	0.35	0.70	0.50
	CNRM-CM5	0.29	0.50	0.55	0.45
	inmcm4	0.36	0.35	0.60	0.55
	MIROC-ESM	0.36	0.65	0.55	0.55
	MPI-ESM-MR	0.38	0.20	0.40	0.30
	MRI-CGCM3	0.18	0.15	0.30	0.40
Mode 3	bcc-csm1-1	0.00	0.00	0.00	0.00
	CNRM-CM5	0.00	0.00	0.10	0.10
	inmcm4	0.00	0.05	0.15	0.20
	MIROC-ESM	0.00	0.10	0.20	0.20
	MPI-ESM-MR	0.00	0.00	0.05	0.15
	MRI-CGCM3	0.00	0.00	0.00	0.05
Mode 4	bcc-csm1-1	0.00	0.00	0.00	0.00
	CNRM-CM5	0.00	0.00	0.05	0.05
	inmcm4	0.00	0.10	0.00	0.15
	MIROC-ESM	0.00	0.10	0.20	0.25
	MPI-ESM-MR	0.00	0.05	0.00	0.25
	MRI-CGCM3	0.00	0.00	0.05	0.00

The utilization frequency of the management modes 1-4 with Safran-PIRAGUA over the period from 1979-2014 is 1, 0, 0, and 0, respectively.

Table 7.6 – As in Table 7.3 but under RCP 8.5 and the changed management context (no limit on CACG request).

RCP 8.5 and changed management context					
		Historical (1961-2005)	Near-term (2021-2040)	Medium-term (2041-2060)	Long-term (2081-2100)
Mode 1	bcc-csm1-1	0.78	0.50	0.45	0.05
	CNRM-CM5	0.71	0.35	0.30	0.00
	inmcm4	0.64	0.25	0.35	0.00
	MIROC-ESM	0.64	0.00	0.05	0.00
	MPI-ESM-MR	0.62	0.25	0.15	0.00
	MRI-CGCM3	0.82	0.60	0.65	0.20
Mode 2	bcc-csm1-1	0.22	0.45	0.30	0.00
	CNRM-CM5	0.29	0.40	0.45	0.15
	inmcm4	0.36	0.70	0.55	0.25
	MIROC-ESM	0.36	0.55	0.25	0.00
	MPI-ESM-MR	0.38	0.40	0.40	0.00
	MRI-CGCM3	0.18	0.40	0.25	0.50
Mode 3	bcc-csm1-1	0.00	0.05	0.20	0.15
	CNRM-CM5	0.00	0.05	0.20	0.25
	inmcm4	0.00	0.05	0.10	0.35
	MIROC-ESM	0.00	0.20	0.25	0.00
	MPI-ESM-MR	0.00	0.20	0.25	0.00
	MRI-CGCM3	0.00	0.00	0.00	0.10
Mode 4	bcc-csm1-1	0.00	0.00	0.05	0.80
	CNRM-CM5	0.00	0.20	0.05	0.55
	inmcm4	0.00	0.00	0.00	0.40
	MIROC-ESM	0.00	0.25	0.45	1.00
	MPI-ESM-MR	0.00	0.15	0.20	1.00
	MRI-CGCM3	0.00	0.00	0.10	0.20

The utilization frequency of the management modes 1-4 with Safran-PIRAGUA over the period from 1979-2014 is 1, 0, 0, and 0, respectively.

Changes in the water release for the CACG In addition to the reliability of the SHEM to meet the CACG demand under global change, the changes of the water release for the CACG are presented in Figures 7.23 and 7.24. Figure 7.23 shows the regime of the mean daily water release for the CACG under global change scenarios. Figure 7.24 shows the annual water release for the CACG under global change scenarios.

In the historical period, water release for the CACG simulated by GCMs under both management contexts is consistent with the simulation by Safran-PIRAGUA data. The release for CACG in the historical period is stabilized at around 30-40 Mm^3 per year under both management contexts.

Under the current management context, Figure 7.23 shows that the summer release peaks under both RCPs are slightly larger than the historical period. This is attributed to the increasing demand of SB5 for summer irrigation and environmental demand. Besides, there is an increase of water release for CACG in autumn under both RCPs, which is attributed to the release to meet the DOE requirement at Sarrancolin. However, the summer peaks in the RCP 4.5 are larger than those in the RCP 8.5. This is because of the larger DOE deficit under the RCP 8.5 than the RCP 4.5 that the CACG has to sacrifice the summer release to fulfill the DOE deficit given the limited quota of 48 Mm^3. As we can see, the autumn release under the RCP 8.5 is larger than that under the RCP 4.5. In terms of annual water release illustrated in Figure 7.24, the release for CACG gradually reaches to 48 Mm^3 from the near-term to the long-term under both RCPs. Particularly, in the long-term of the RCP 8.5, the release for CACG is stabilized at 48 Mm^3.

Under the changed management context, the seasonal water release for CACG under the RCP 4.5 in Figure 7.23 is similar to the results of the current management context. However, there is an increasing trend of failure to meet the CACG demand as illustrated in Tables 7.3 and 7.5 because there is no limit on the CACG request in this management context. The failure risk increases to 1 under the RCP 8.5 as illustrated in Tables 7.4 and 7.6. This is because the CACG request large annual water release (see Figure 7.24) that the storage in the SHEM reservoirs can not supply enough water to meet the CACG demand. Due to the high value of failure risk in the long-term under RCP 8.5, the regime in long-term under the RCP 8.5 in Figure 7.23 is lower than other phases.

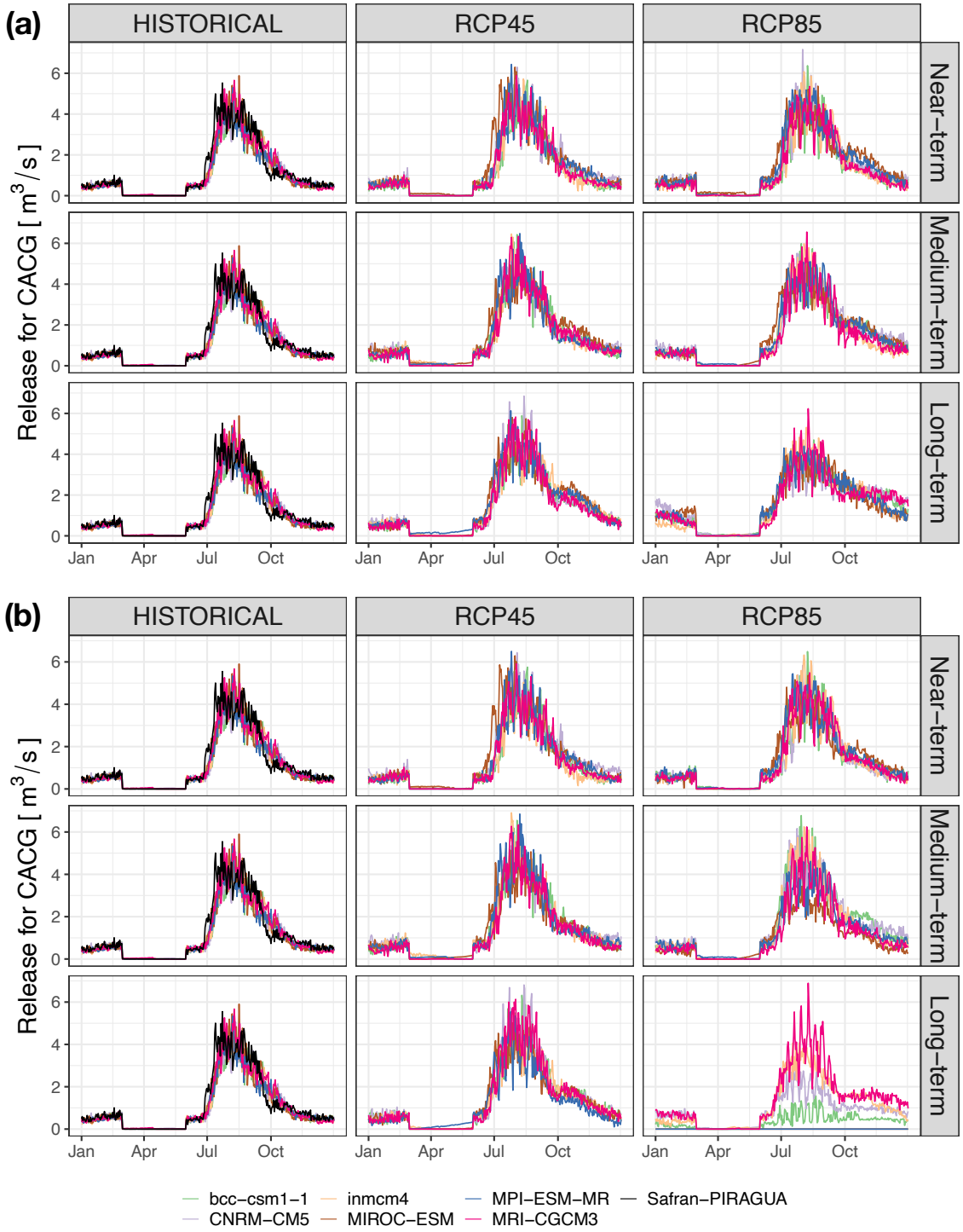

Figure 7.23 – The regime of mean daily water release for CACG under 6 GCMs (bcc-csm1-1, CNRM-CM5, inmcm4, MIROC-ESM, MPI-ESM-MR, MRI-CGCM3) for the near-term (2021-2040), medium-term (2041-2060), and long-term (2081-2100) phases under two RCP scenarios (RCPs 4.8 and 8.5) and the two management contexts ((a) the current management context that the CACG can only request 48 Mm^3; (b) the changed management context that there is no limit on the CACG request). The three sub-figures in the column "HISTORICAL" are identical to visually help the comparison.

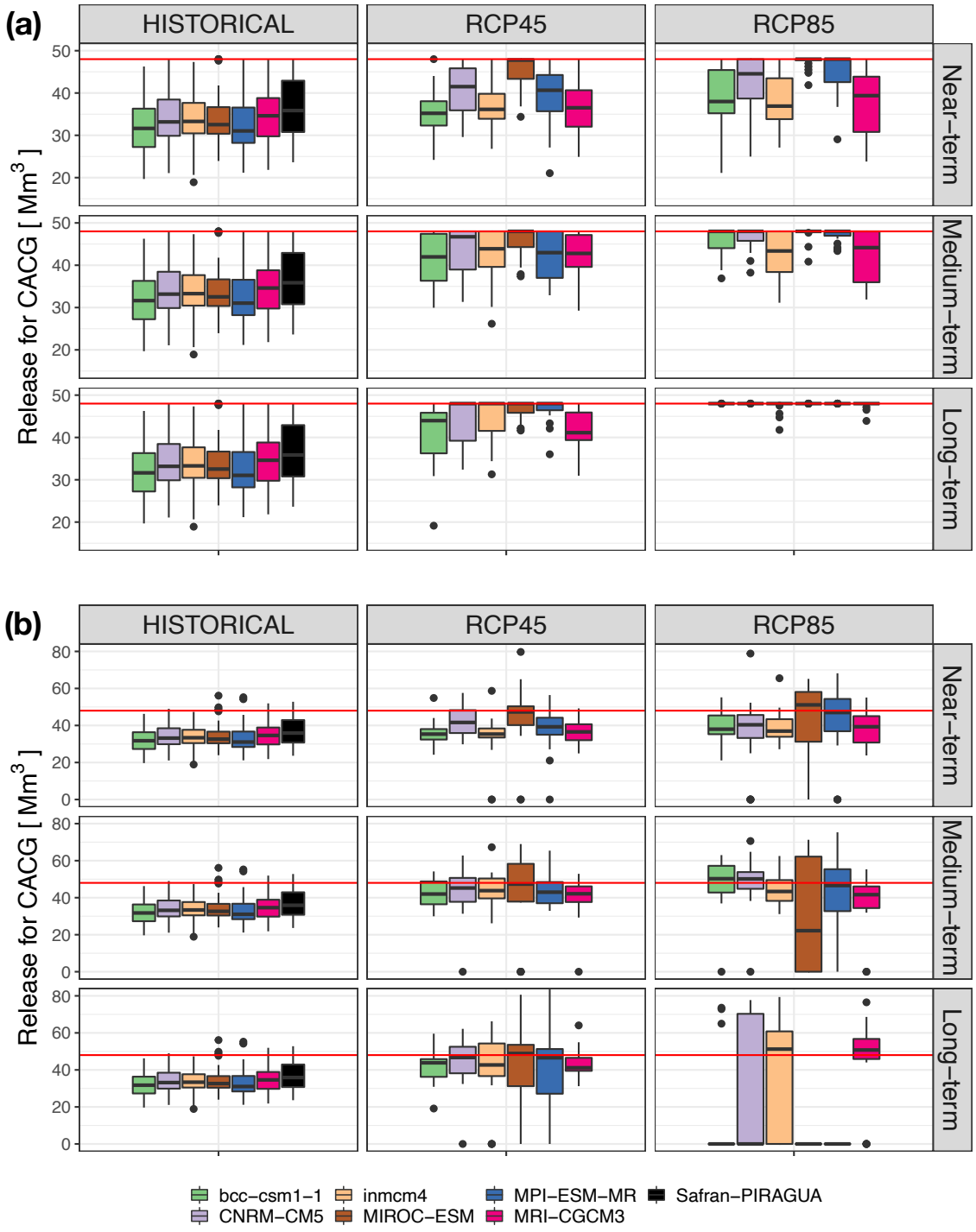

Figure 7.24 – The annual water release for CACG under 6 GCMs (bcc-csm1-1, CNRM-CM5, inmcm4, MIROC-ESM, MPI-ESM-MR, MRI-CGCM3) for the near-term (2021-2040), medium-term (2041-2060), and long-term (2081-2100) phases under two RCP scenarios (RCPs 4.8 and 8.5) and the two management contexts ((a) the current management context that the CACG can only request 48 Mm^3; (b) the changed management context that there is no limit on the CACG request). The three sub-figures in the column "HISTORICAL" are identical to visually help the comparison. The red line is the quota (48 Mm^3) that the CACG can request under the current management context.

Changes in the hydropower production Concerning the impacts of global change on the hydropower production by the SHEM, we employ the cost-effectiveness metric as presented in the chapter 6, the QA metric, to investigate whether the future hydropower production is still profitable for the SHEM. The necessary water volume for SHEM to be cost-effective is 41.6 Mm^3 for the Eget hydropower plant (the Oule and Orédon reservoirs) and 28.2 Mm^3 for the Lassoula reservoir when considering the "worst" energy market scenario for the SHEM. Thus, the threshold that the SHEM can achieve the cost-effectiveness purpose in the "worst" energy market scenario within a management year is 69.8 Mm^3.

Figure 7.25 shows the changes of the annual water release for hydropower production under global change scenarios. In the historical period, the simulations by GCMs are underestimated compared with the simulation by Safran-PIRAGUA due to the underestimation of precipitation by GCMs that reduces the natural inflows into the reservoirs. We note that the current hydropower cost-effectiveness in the "worst" energy market scenario is not achievable in most cases. Under both RCPs and management contexts, the cost-effectiveness of the worst energy market scenario cannot be maintained anymore.

Besides, water release for hydropower production decreases from the near-term to the long-term under both RCPs and the current water management context. This is because the natural inflows into the reservoirs is decreased under climate change scenarios and the CACG request more water within the 48 Mm^3 quota. From the Tables 7.3 and 7.4, we can see that the frequency of management mode 1 decreases from the near-term to the long-term with the increase of the frequency of mode 2 and mode 3, which indicates the less opportunities for hydropower production and more conservative actions to store water for the CACG request.

However, under the changed management context, there is an increase of hydropower production under the RCP 8.5 for some GCMs (e.g., MIROC-ESM, MPI-ESM-MR) compared with the RCP 4.5, which is attributed to the increase of CACG request failure (see Tables 7.5 and 7.6). The SHEM cannot provide the water volume that the CACG requests. The SHEM fails the request and the water volume in the reservoirs are used for hydropower production.

Figure 7.26 shows the regime of mean daily water release for hydropower under global change scenarios. Figure 7.27 shows the number of days that the SHEM releases water for hydropower production. Under both management contexts, the SHEM mostly releases water in winter to optimize the cost-effectiveness. However, there is a decreasing trend of winter peaks for hydropower production from the near-term to the long-term under both RCPs due to the less storage than can be mobilized to produce hydropower. The main reasons are the reduced water inflows under climate change scenarios and the increased CACG demand under global change scenarios. The associated number of days when the SHEM releases water for hydropower production decreases. Note that in the long-term under the RCP 8.5 and the changed management context, there is an increase in hydropower production due to the increasing failure of meeting the CACG demand and thus the water is released for hydropower.

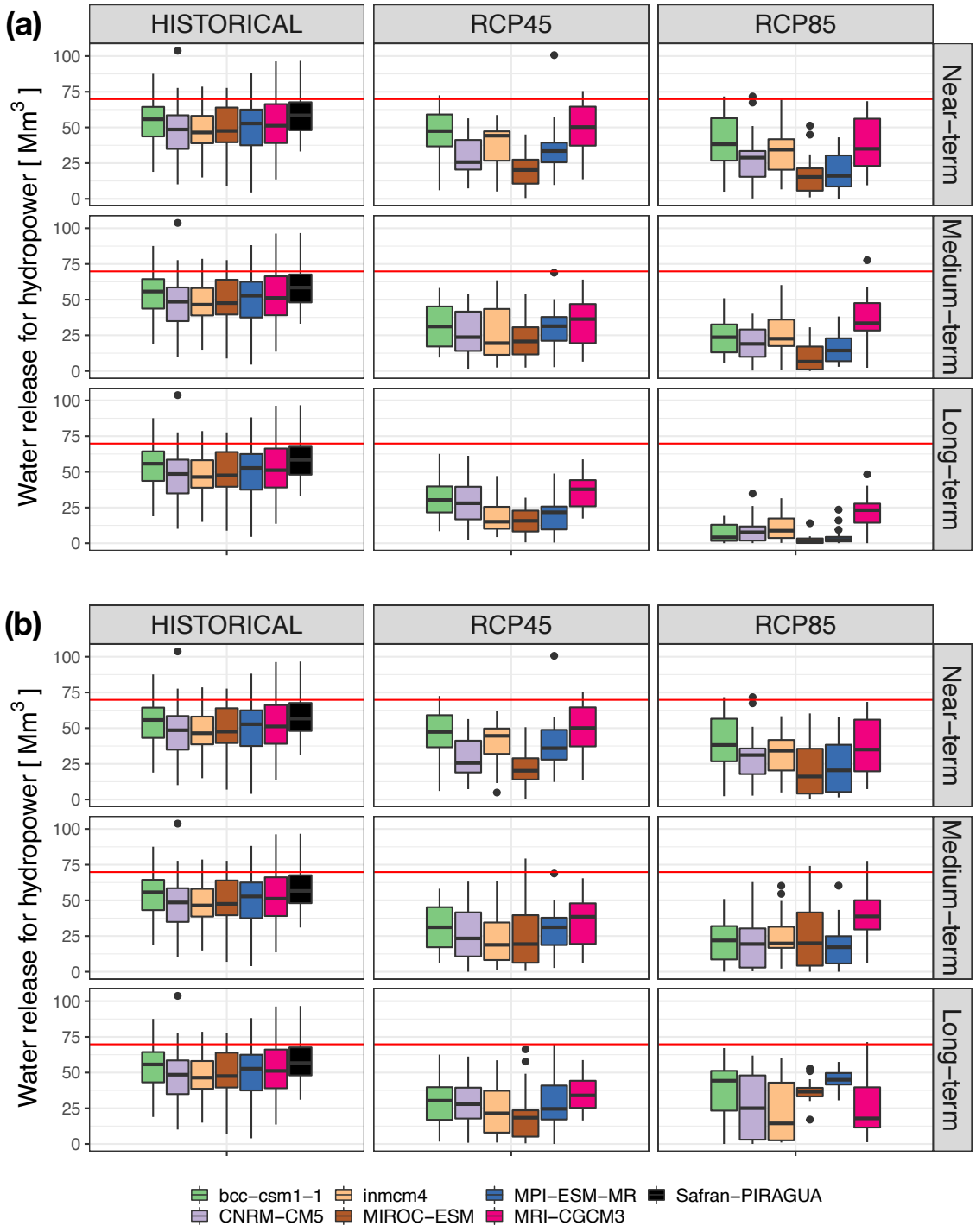

Figure 7.25 – The annual water release for hydropower production by the SHEM under 6 GCMs (bcc-csm1-1, CNRM-CM5, inmcm4, MIROC-ESM, MPI-ESM-MR, MRI-CGCM3) for the near-term (2021-2040), medium-term (2041-2060), and long-term (2081-2100) phases under two RCP scenarios (RCPs 4.8 and 8.5) and the two management contexts ((a) the current management context that the CACG can only request 48 Mm^3; (b) the changed management context that there is no limit on the CACG request). The three sub-figures in the column "HISTORICAL" are identical to visually help the comparison. The red line is the threshold of the cost-effectiveness metric (69.8 Mm^3).

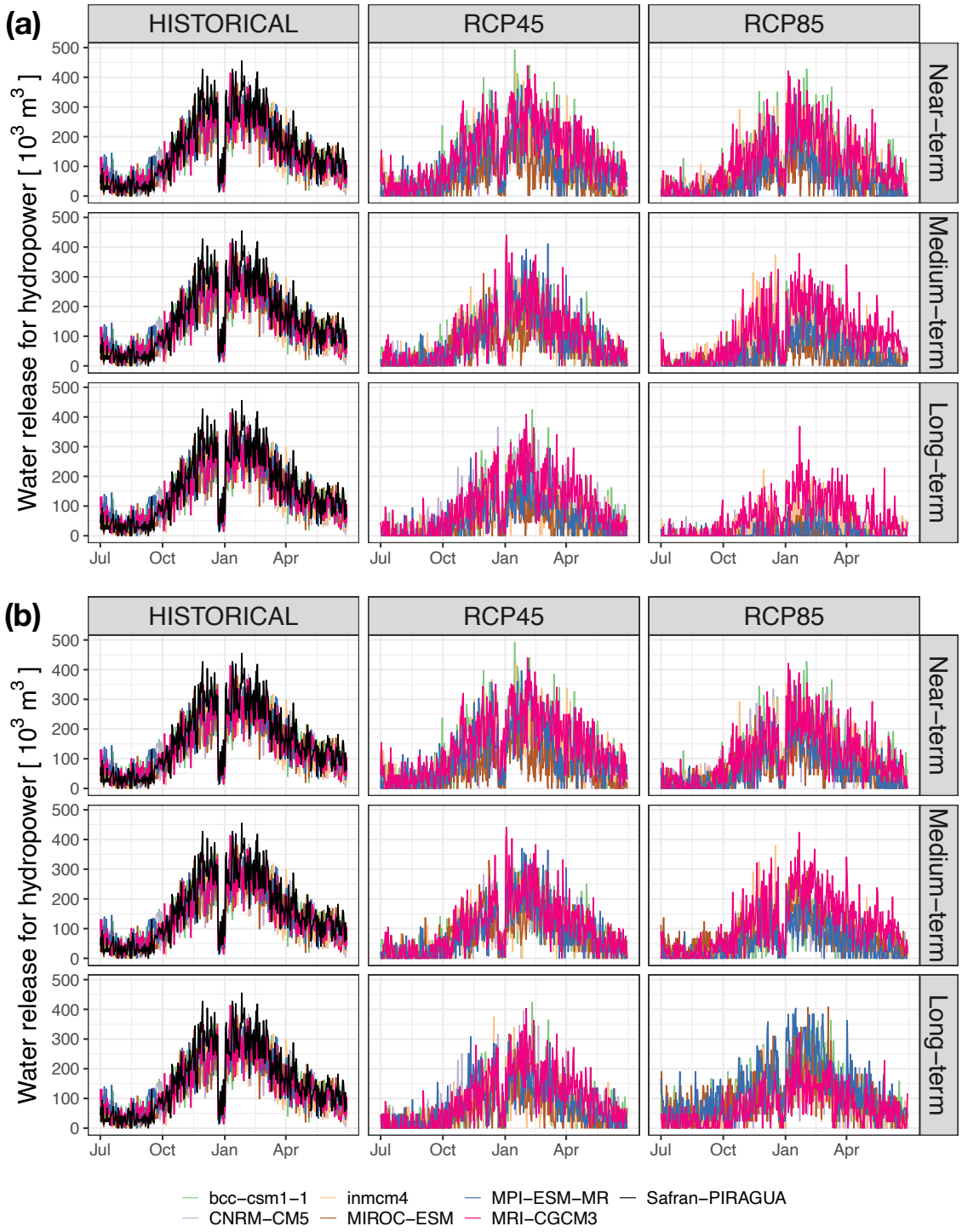

Figure 7.26 – The regime of mean daily water release for hydropower production by the SHEM under 6 GCMs (bcc-csm1-1, CNRM-CM5, inmcm4, MIROC-ESM, MPI-ESM-MR, MRI-CGCM3) for the near-term (2021-2040), medium-term (2041-2060), and long-term (2081-2100) phases under two RCP scenarios (RCPs 4.8 and 8.5) and the two management contexts ((a) the current management context that the CACG can only request 48 Mm^3; (b) the changed management context that there is no limit on the CACG request). The three sub-figures in the column "HISTORICAL" are identical to visually help the comparison.

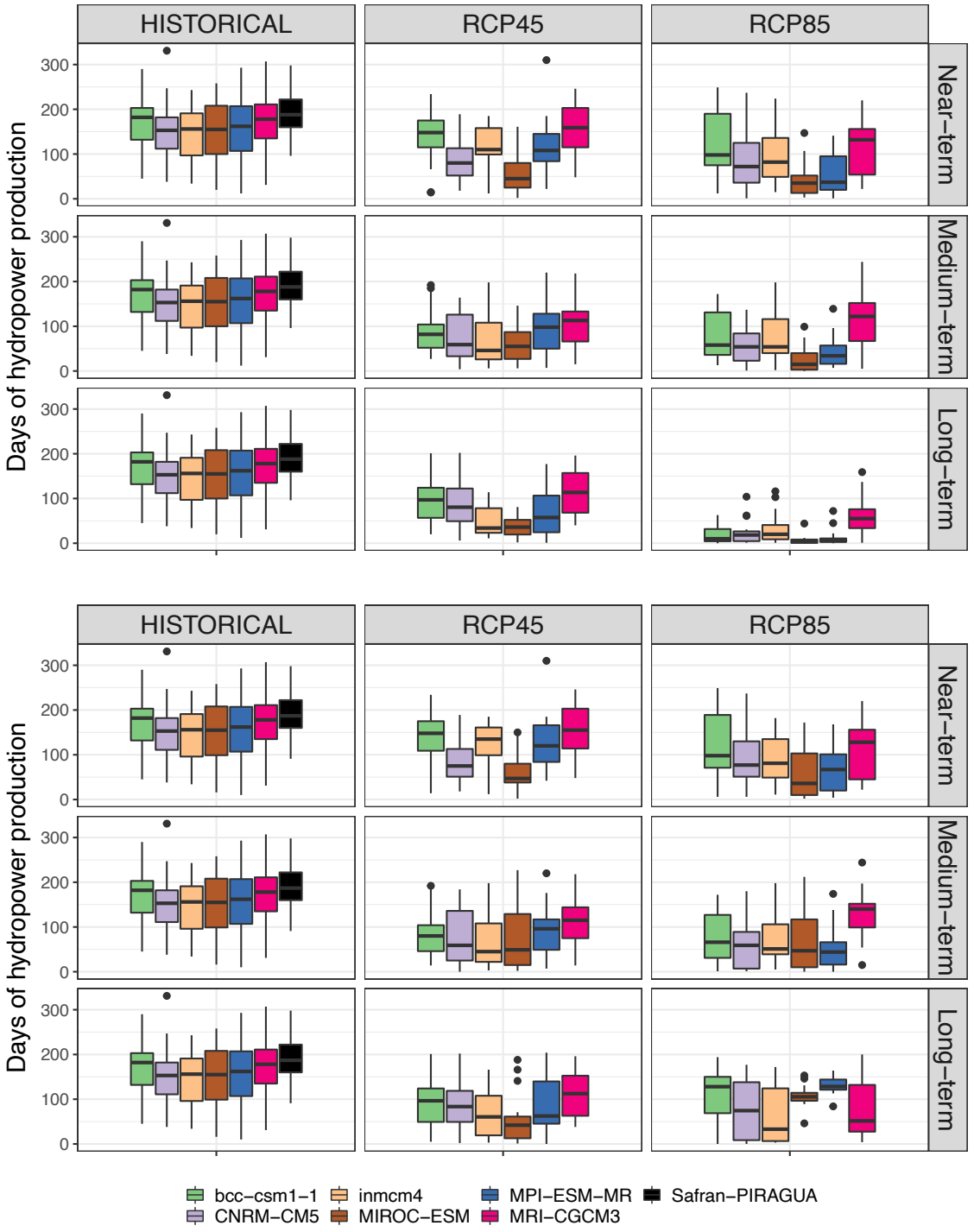

Figure 7.27 – The annual number of days for hydropower production by the SHEM under 6 GCMs (bcc-csm1-1, CNRM-CM5, inmcm4, MIROC-ESM, MPI-ESM-MR, MRI-CGCM3) for the near-term (2021-2040), medium-term (2041-2060), and long-term (2081-2100) phases under two RCP scenarios (RCPs 4.8 and 8.5) and the two management contexts ((a) the current management context that the CACG can only request 48 Mm^3; (b) the changed management context that there is no limit on the CACG request). The three sub-figures in the column "HISTORICAL" are identical to visually help the comparison.

Changes in the reservoir refill target Figures 7.28, 7.29, and 7.30 show the regime of daily mean volume of the Oule, Orédon, and Lassoula reservoir storage under global change scenarios, respectively. The three figures are explained with the Tables 7.3, 7.4, 7.5, and 7.6 to investigate the changes of the refill targets of the three reservoirs and the attitude of the SHEM to release water.

In the historical period, the minimum storage of the reservoirs in spring simulated by GCMs is overestimated, which reflects that the SHEM has to leave a certain volume of water in the reservoir to reach the refill target at the end of management. This means that the underestimated water inflows into the reservoirs (precipitation underestimation by GCMs) are not sufficient to allow a full use reservoir storage for hydropower production. As such, water release for the Orédon reservoir hydropower production are sacrificed in some cases for the reservoir refill at the end of the management as reflected by the underestimation of the frequency of mode 1 in the tables above.

Under both management contexts, in order to adapt to the higher CACG demand and the lower water inflows, the SHEM has to leave much more water in the reservoirs to satisfy the CACG request, instead of releasing water for hydropower production. This conservative attitude of water management induces less opportunities for hydropower production (lower frequency of mode 1, higher frequency of mode 2) so as to reach the refill target at the end of the management. For example, in the near-term and medium term of the RCP 4.5 under both management contexts, the water storage in spring is higher than that of the historical period and the range of the reservoirs (from maximum volume to the minimum volume) reduces. In the some extremely dry conditions (e.g., the GCM MIROC-ESM), the minimum storage is placed in autumn for the Oule and Orédon reservoir because the spring water inflows only are not sufficient to meet the refill target and thus the refill process is prolonged to autumn.

When the natural inflows are much less and the CACG demand are much higher, the refill target of the reservoirs has to be lowered in order to adapt to the difficulty of the reservoir refill target after satisfying the CACG demand and hydropower production (higher frequency of mode 3). For example, in the long-term of the RCP 4.5, the near-term of the RCP 8.5, and the medium-term of the RCP 8.5 under both management contexts, the reservoir refill targets for the three reservoirs are lowered. If lowering reservoir refill target to empty is still insufficient to satisfy the CACG request, the SHEM has to fail the CACG demand. The failure mostly happens in the long-term under the RCP 8.5 and the changed management context as illustrated in Table 7.6. Particularly, the frequency of the mode 4 by the GCMs MIROC-ESM and MPI-ESM-MR is 1 and the behavior of reservoir storage is to store water before the release in winter while keep the 100% of the refill target.

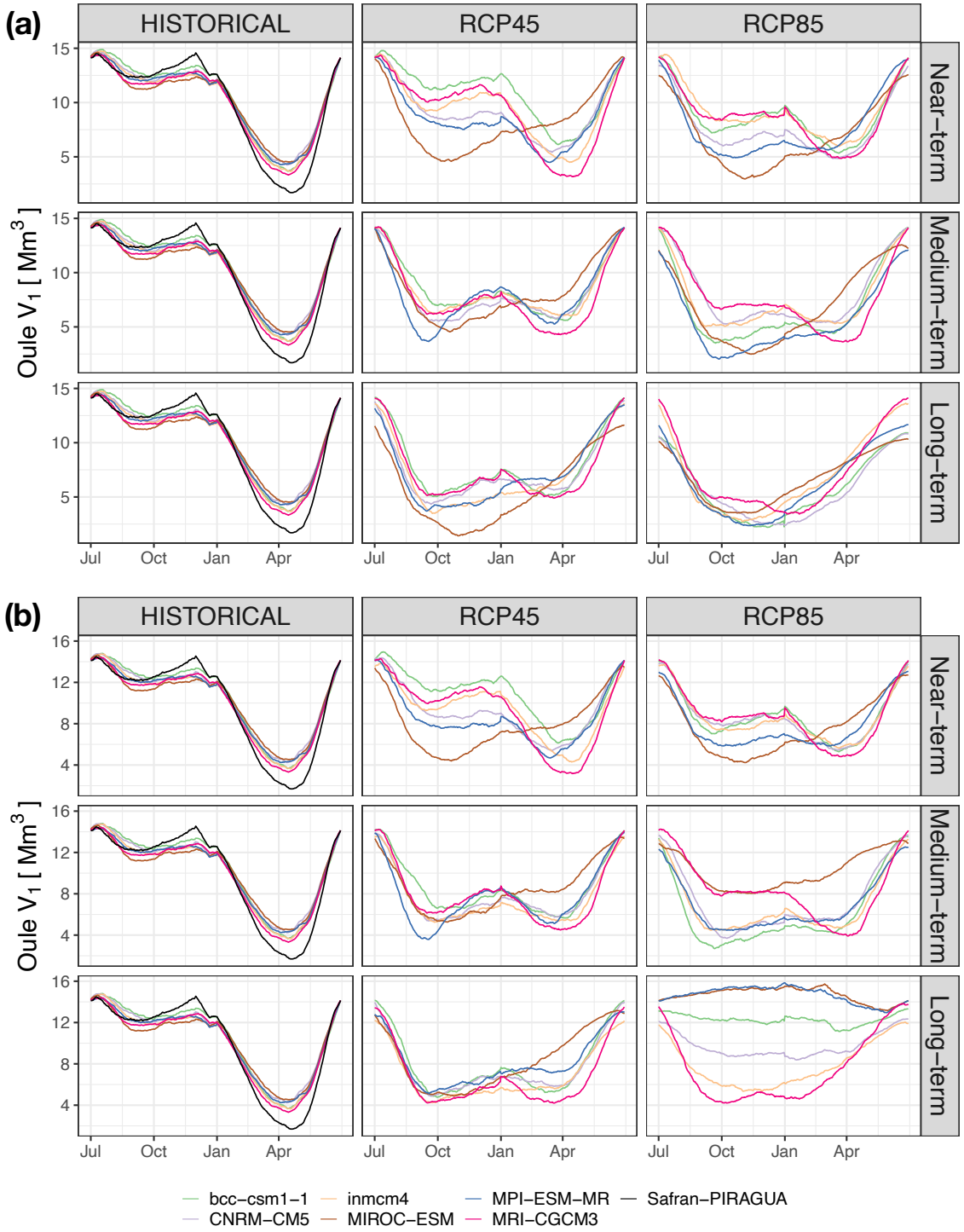

Figure 7.28 – The regime of mean daily volume of the Oule reservoir under 6 GCMs (bcc-csm1-1, CNRM-CM5, inmcm4, MIROC-ESM, MPI-ESM-MR, MRI-CGCM3) for the near-term (2021-2040), medium-term (2041-2060), and long-term (2081-2100) phases under two RCP scenarios (RCPs 4.8 and 8.5) and the two management contexts ((a) the current management context that the CACG can only request 48 Mm^3; (b) the changed management context that there is no limit on the CACG request). The three sub-figures in the column "HISTORICAL" are identical to visually help the comparison.

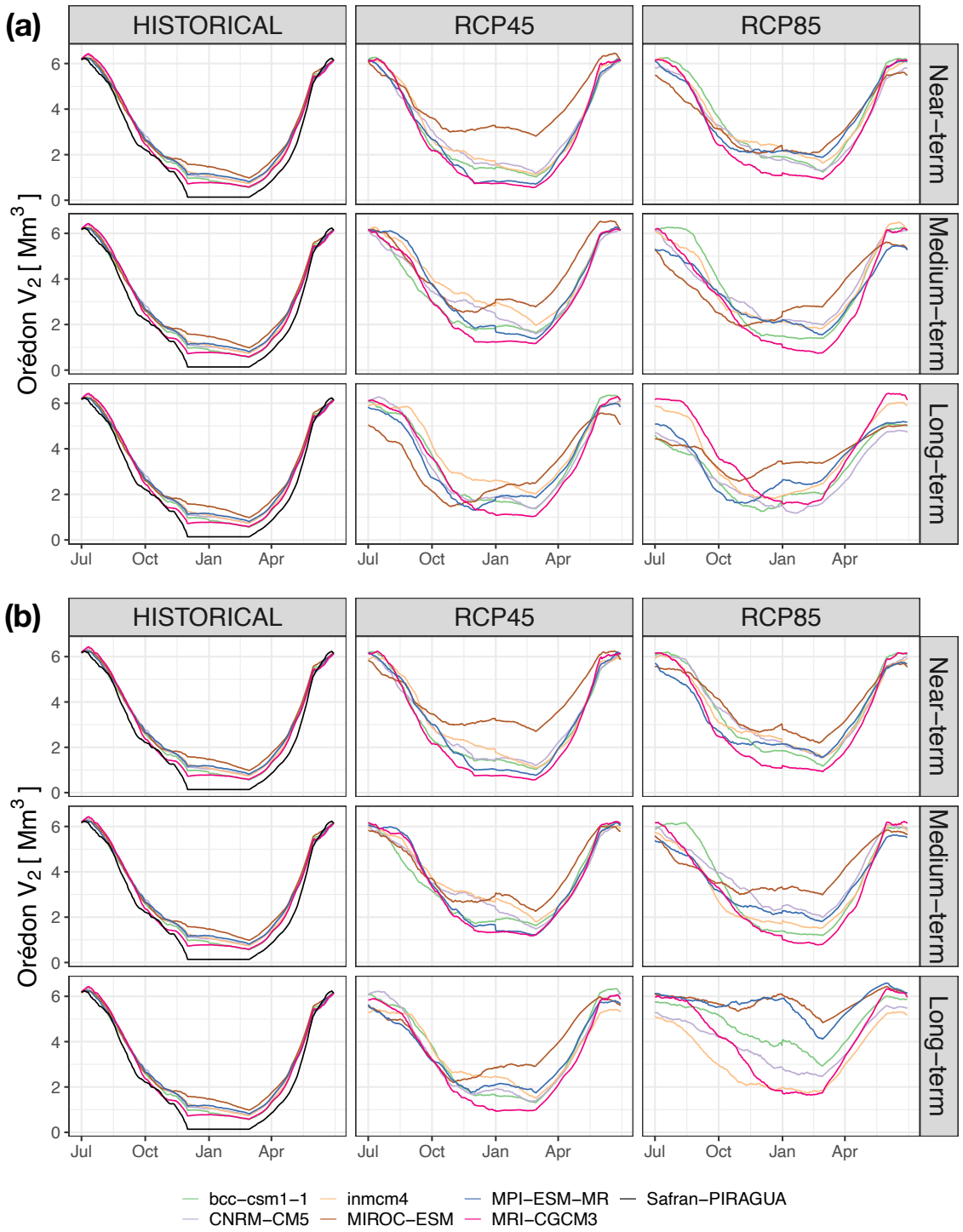

Figure 7.29 – The regime of mean daily volume of the Orédon reservoir under 6 GCMs (bcc-csm1-1, CNRM-CM5, inmcm4, MIROC-ESM, MPI-ESM-MR, MRI-CGCM3) for the near-term (2021-2040), medium-term (2041-2060), and long-term (2081-2100) phases under two RCP scenarios (RCPs 4.8 and 8.5) and the two management contexts ((a) the current management context that the CACG can only request 48 Mm^3; (b) the changed management context that there is no limit on the CACG request). The three sub-figures in the column "HISTORICAL" are identical to visually help the comparison.

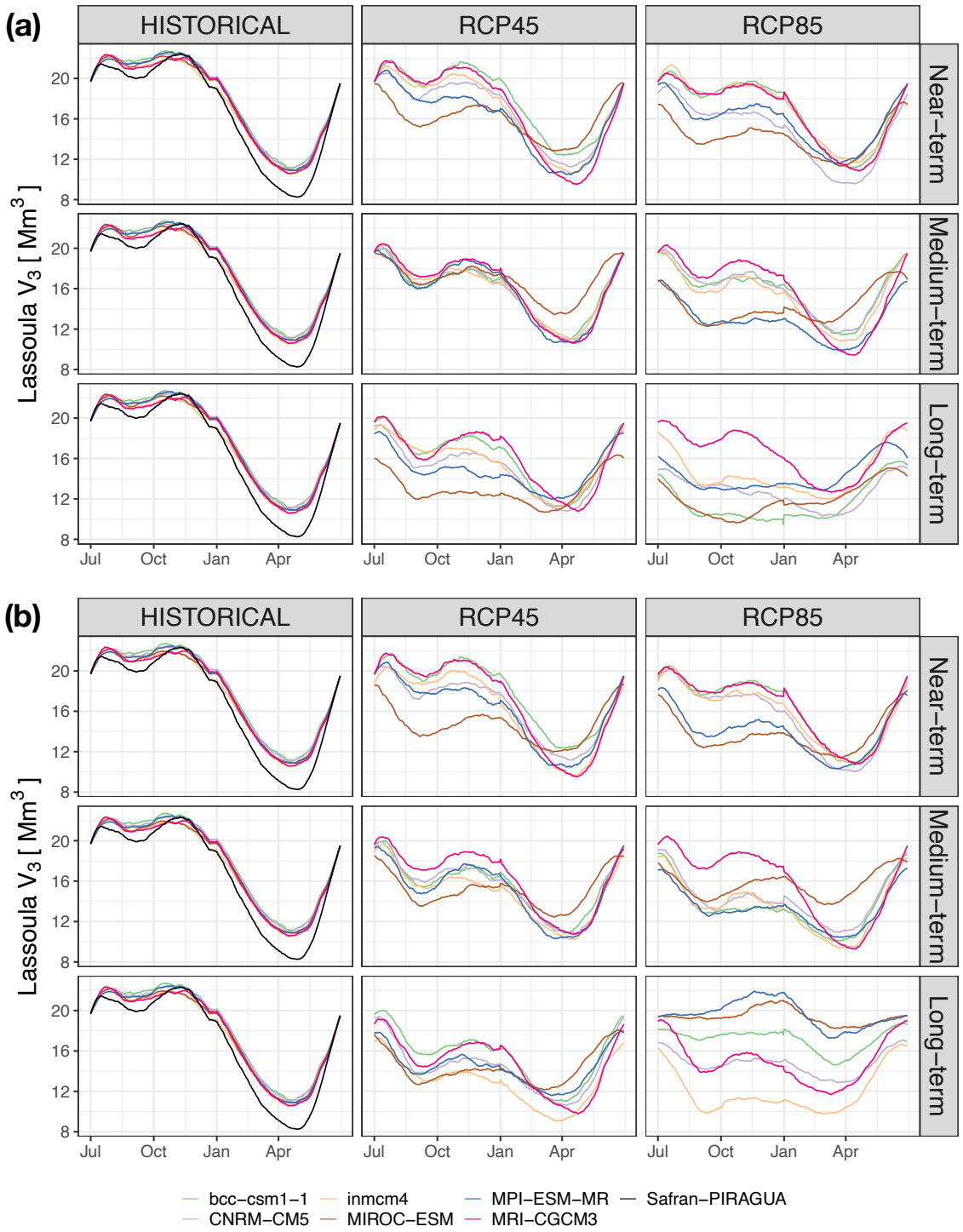

Figure 7.30 – The regime of mean daily volume of the Lassoula reservoir under 6 GCMs (bcc-csm1-1, CNRM-CM5, inmcm4, MIROC-ESM, MPI-ESM-MR, MRI-CGCM3) for the near-term (2021-2040), medium-term (2041-2060), and long-term (2081-2100) phases under two RCP scenarios (RCPs 4.8 and 8.5) and the two management contexts ((a) the current management context that the CACG can only request 48 Mm^3; (b) the changed management context that there is no limit on the CACG request). The three sub-figures in the column "HISTORICAL" are identical to visually help the comparison.

The impacts on the CACG management at Sarrancolin

The management of CACG at Sarrancolin is to extract water via the Neste Canal while maintaining the DOE requirement at Sarrancolin. Figure 7.31 shows the regime of daily influenced river flow at Sarrancolin under global change scenarios. Figure 7.32 shows the regime of daily water extraction by the Neste Canal under global change scenarios.

In the historical period of both management contexts, the simulations by GCMs underestimate the flows peaks at Sarrancolin in spring due to the underestimation of spring precipitation by GCMs when comparing to the simulations by the Safran-PIRAGUA reanalysis data. The DOE requirement at Sarrancolin can always be maintained in drought period (summer and early autumn) and the Neste Canal can thus remain a high level of water extraction during irrigation and environmental demand peaks (summer and autumn) to feed SB5.

Under the RCP 4.5 of both management contexts, the influenced river flow at Sarrancolin is decreased mainly due to less inflows of SB4. The DOE requirement can be satisfied in most cases by the management of CACG. The achievement of the DOE requirement at Sarrancolin is sacrificed by the canal extraction. As shown in Figure 7.32, the canal extraction in summer and early autumn is notably decreased even though the SHEM releases more water for the CACG demand (see Figures 7.23 and 7.24) under these scenarios.

Under the RCP 8.5 of both management contexts, the DOE requirement at Sarrancolin starts to fail in summer in the near-term and the medium term even though the Neste Canal extracts much less than in the RCP 4.5 to compensate for the DOE deficit. Particularly, in the long-term of some GCMs (e.g., bcc-csm-1, MIROC-ESM, and MPI-ESM-MR), the DOE requirement cannot be maintained in drought period and even the most part of the year and the canal can barely extract water to feed SB5.

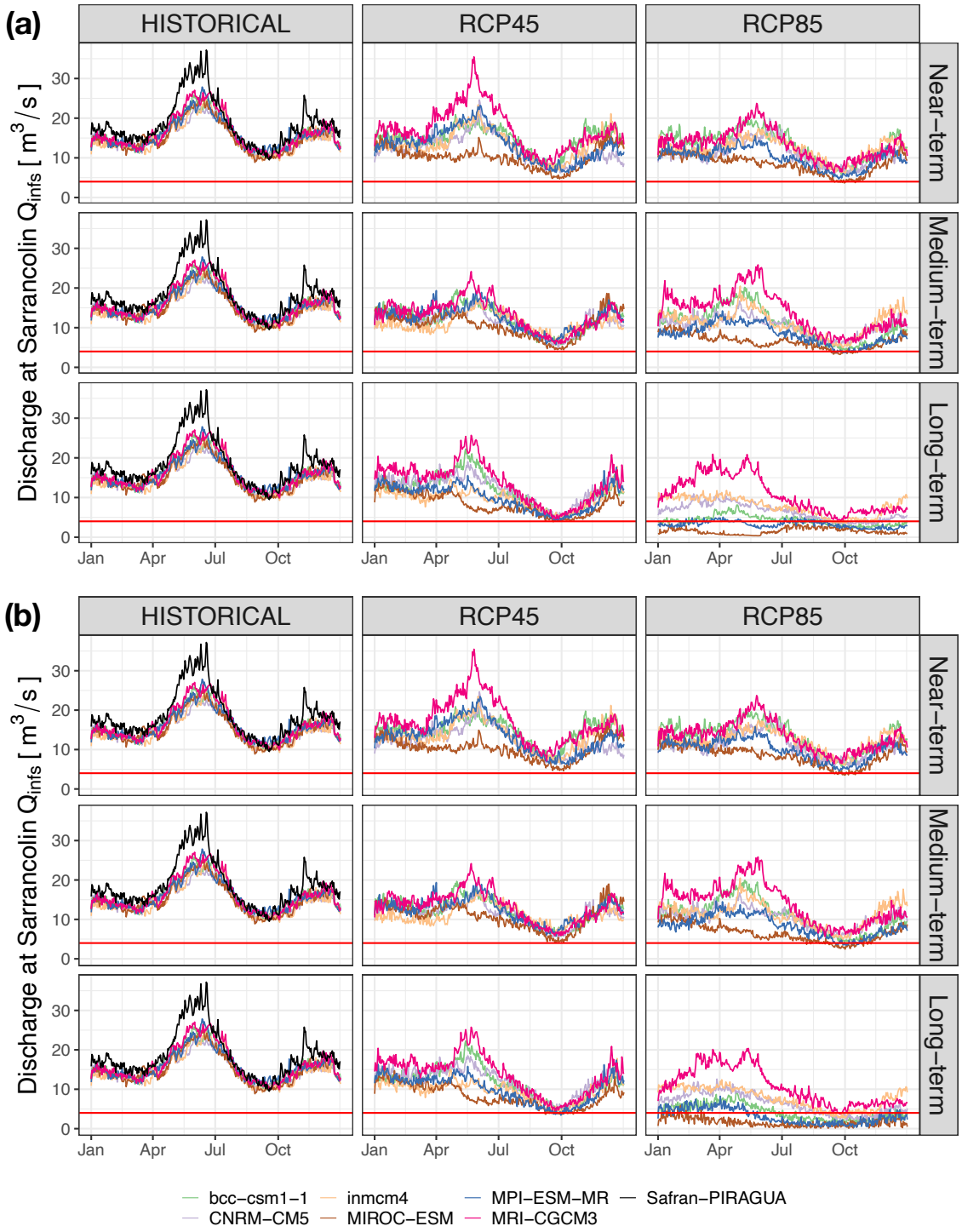

Figure 7.31 – The regime of mean daily influenced river flow at Sarrancolin under 6 GCMs (bcc-csm1-1, CNRM-CM5, inmcm4, MIROC-ESM, MPI-ESM-MR, MRI-CGCM3) for the near-term (2021-2040), medium-term (2041-2060), and long-term (2081-2100) phases under two RCP scenarios (RCPs 4.8 and 8.5) and the two management contexts ((a) the current management context that the CACG can only request 48 Mm^3; (b) the changed management context that there is no limit on the CACG request). The three sub-figures in the column "HISTORICAL" are identical to visually help the comparison. The red line is the DOE requirement at Sarrancolin (4 m^3/s)

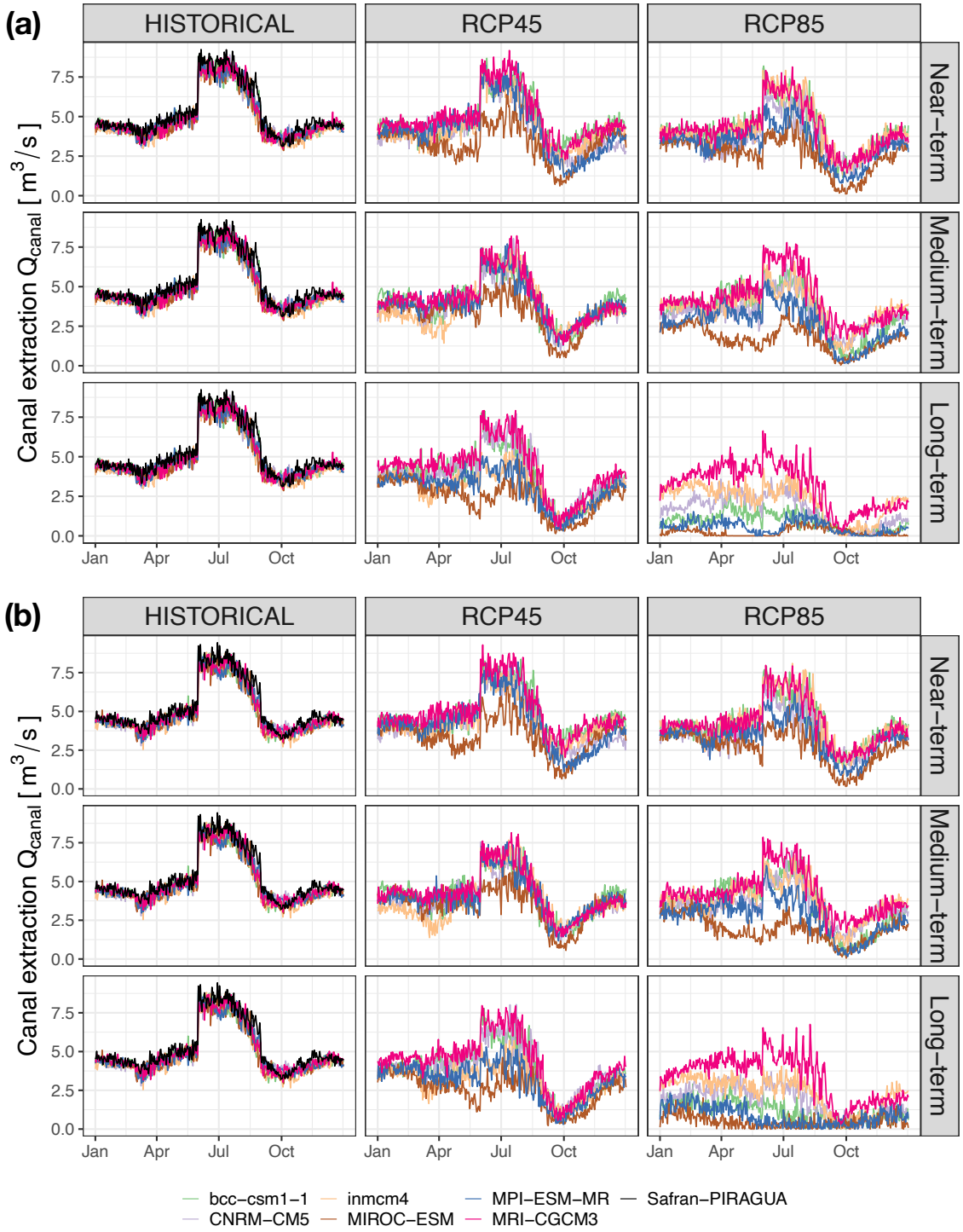

Figure 7.32 – The regime of mean daily canal extraction under 6 GCMs (bcc-csm1-1, CNRM-CM5, inmcm4, MIROC-ESM, MPI-ESM-MR, MRI-CGCM3) for the near-term (2021-2040), medium-term (2041-2060), and long-term (2081-2100) phases under two RCP scenarios (RCPs 4.8 and 8.5) and the two management contexts ((a) the current management context that the CACG can only request 48 Mm^3; (b) the changed management context that there is no limit on the CACG request). The three sub-figures in the column "HISTORICAL" are identical to visually help the comparison.

7.4.2 Summary

In summary, the water management in the Aure Valley under global change scenarios is estimated by the steps: (1) a coupling method that conjunctively links the SHEM optimization and the CACG management models with bi-directional data transmission is developed to represent the current management context (the CACG can request a maximum 48 Mm^3 water from the SHEM); (2) the coupling model is then modified to represent a changed management context to represent a different management context that the CACG can request water from the SHEM as the CACG wants; (3) based on the top-down approach, the projected natural water resources in the Aure Valley under climate change and the projected water demand under global change scenarios are forced into the coupling management models to investigate the impact of global change; and (4) the satisfaction of water use in terms of the SHEM objectives (to meet the CACG demand, to produce hydropower for the cost-effectiveness, and to refill reservoir at the end of management for the use of next year) and the CACG objectives (to satisfy the DOE requirement at Sarrancolin and to extract water at Sarrancolin to feed SB5) are analyzed.

The changes in the satisfaction of the SHEM water management by the reduced natural water resources and the increased CACG water demand are summarized as follows.

- The CACG demand can be mostly satisfied with few failure under both RCPs for the current management context. The changed management context decreases the reliability of satisfying the CACG demand with a notable increase of failure in the long-term of the century. Particularly, in the changed management context, the system cannot be solved since water demand and water availability at the end of the century are unbalanced.

- The hydropower production for the cost-effectiveness purpose can not be maintained anymore under both RCPs and both management contexts.

- The reservoir refill target is the most difficult to achieve under the combination of the RCP 8.5 and the changed management context among all the scenarios considered.

The changes in the satisfaction of the CACG water management at Sarrancolin are summarized as follows.

- The CACG can satisfy the DOE requirement at Sarrancolin in most global change scenarios except the long-term under the RCP 8.5 for both management contexts.

- The water extraction by the Neste Canal shows a decreasing trend due to the lower water availability at Sarrancolin that is limited by the DOE requirement.

The more conservative water management in the Aure Valley that is characterized by less flexibility in producing hydropower under global change scenarios is also found in other studies. Finger et al. (2012) showed that hydropower production in the Swiss Alps could be reduced by about one third till the end of the century due to glacier retreats, earlier snow melt, and more severe summer drought conditions. The management of the hydropower companies in the Swiss Alps that produce maximum energy in winter could be compromised to save more water for summer uses. Besides, similar results are reported the Durance River basin in the French Alps (e.g., François et al., 2014a, 2015), the Iberian Peninsula (e.g., Pereira-Cardenal et al., 2014), and the Ariège River basin in the French

Pyrenees (e.g., Hendrickx and Sauquet, 2013). These examples have several similarities: (1) hydropower management in these regions focuses on providing energy for heating demand in winter; (2) water resources availability in these regions is impacted by climate change with a generally decreased annual inflows and more severe summer drought; and (3) water for summer uses (e.g., irrigation, lake refill for recreation purposes) is mandatory. As such, temporal tradeoffs (definition in chapter 2) in the reservoir management increase significantly, and the reservoir managers have to sacrifice the opportunities for hydropower production to satisfy the summer uses. Given these, adaptation strategies for hydropower management should be prioritized.

8

Conclusion and perspectives

This chapter draws the general conclusion of the thesis and provides complementary perspectives.

Contents

8.1 Conclusion 234
8.2 Perspectives 236

8.1 Conclusion

Understanding the vulnerabilities of water systems to global change has particular significance for adaptation design. Climate change, combined with the acceleration of anthropogenic disturbances, population growth, and restrictions on natural water extraction for environmental purposes continuously challenge the performance of water systems. Investigating water management vulnerabilities, and ultimately developing credible adaptation solutions, necessitate (1) new tools capable of portraying human impact on water resources and (2) innovative frameworks to assess the vulnerability of water management under global change.

This dissertation shows pragmatic approaches (chapters 4 and 5) to evaluate natural water resources, to estimate water demand, and to represent human impact on multipurpose reservoir management by taking the Neste water system in French Pyrenees as an example (chapter 3). The Neste water system is chosen as the study case based on several considerations: (1) the impact of global change on water resources and management is a major concern in the Mediterranean mountainous regions; (2) this complex system allows an exploration of large global change drivers on various water demand (huge efforts have been made to collect and analyze data); (3) the active participation of water managers and stakeholders (e.g., data sharing and discussion) supports the development of modelling chain; (4) the two different water managers that have different management practices but are connected with a binding contract make a good example for the investigation of water management vulnerabilities and water conflicts under global change. The developed modelling chain is applicable to a wide range of global change scenarios and transferable to other case studies as long as the principal controlling factors are known.

Moreover, by scrutinizing the state of the art of the vulnerability assessment frameworks (chapter 2), this dissertation applies the two most widely used frameworks (bottom-up and top-down frameworks) in addressing the vulnerabilities in the Neste water system with the tools developed. The contributions of the bottom-up and top-down frameworks that seeks to identify the water management vulnerabilities in the Neste water system are summarized briefly below.

The bottom-up framework (chapter 6) applied in this dissertation focuses on the sensibility and vulnerability of water management metrics to external disturbances (here, climate change). The sensitivity of water management metrics to climate change is firstly examined to perceive how the water system responds to changes by testing a wide range of plausible climate scenarios perturbed from historical climate records. This sensitivity analysis combined with the exposure, that informs the probability of future climate occurrence, and the threshold, that describes the boundaries of satisfactory management, contributes to answering the questions that interest the water managers the most. How and when the performance of the water system shifts from acceptable to unacceptable? We show that (1) hydropower management is vulnerable to annual precipitation changes, and the cost-effectiveness of hydropower can not be maintained from the middle of the century under the RCP 8.5; (2) environmental management is vulnerable to both precipitation and temperature changes during drought period, and the environmental water target fails at the end of the century under the RCP 8.5; and (3) reservoir refill management is extremely vulnerable to temperature changes, and current reservoir refill strategy is no more suitable from the beginning of the century under the RCP 4.5.

The top-down framework (chapter 7) applied in this dissertation to investigate the water management vulnerabilities is formulated as a modelling chain forced with climate

change projections and socio-economic changes. The modelling chain integrates all the tools developed including water resources model, water demand models, and water management models in an iterative coupling way to represent the water management behaviors in the study area. Particularly, the modelling chain is flexible enough to incorporate different management strategies to adapt to global change and different management contexts. As such, the framework contributes to addressing the question: what is the potential impact and vulnerability in the water management under global change? We show that (1) climate change under both RCPs 4.5 and 8.5 causes a general reduction of natural water resources, including a temporal shift towards earlier but lower flow peaks and a more pronounced drought period (longer and worse than the current climate); (2) water demand changes under global change demonstrate different patterns with decreased hydropower demand in winter for heating (but potentially increased hydropower demand in summer for cooling), increased drinking water demand, increased irrigation water demand in shorter duration, and increased environmental water demand; (3) given the binding water contract and environmental restrictions, water management vulnerability under global change scenarios increases with a more conservative management attitude of hydropower producer and a more intensive water competition among various water uses; (4) hydropower production is the most impacted and vulnerable aspect under global change scenarios that concedes water to reservoir storage and downstream water demand; (5) reservoir storage target is more vulnerable than the satisfaction of downstream water demand because reservoir storage target can be sacrificed to meet the downstream demand; (6) downstream water extraction is limited under global change so as to maintain the environmental requirement.

To conclude, the bottom-up and top-down frameworks offer complimentary insights in evaluating the vulnerability of water management under global change. Insights gleaned from both frameworks give crucial information for practical adaptation objectives. Adaptation strategies may consider: (1) an increase of hydropower efficiency to mitigate hydropower losses; (2) an earlier and more flexible reservoir refill strategy to encounter earlier snowmelt and less inflows; (3) a consideration of hydropower production in summer to align several water uses in summer so as to reduce temporal tradeoffs given the increase for cooling demand in the future; (4) an increase of water transfer capacity among basins to increase water use efficiency; (5) an increase in irrigation water use efficiency by modernizing irrigation method (e.g., drip irrigation system), promoting crops with less water consumption, advancing crop sowing calendars.

8.2 Perspectives

Although the developments achieved in this dissertation have provided a variety of contributions to assess the vulnerability of water management under global change, they have also generated various issues and enabled for the discovery of new difficulties to be handled. The limitations of the dissertation and the associated future research directions are discussed below.

First, the models developed in this dissertation have inevitably certain simplifications. For example, daily time step is coarse to represent hydropower production as energy demand peaks are concentrated upon rush hours in a day in reality. This causes decision variables in the optimization process are antithetical (i.e., either no release or release with daily full capacity). Irrigation activities are simplified to only consider the crop of maize, and the decision rules for maize irrigation are simplified with climatic variables (an overlook of the influence of the soil water content). No detailed information on the water use restrictions in the Gascogne region (i.e., how water quotas are applied to water uses when the water availability is insufficient to total water demand) impedes the thorough investigation on the water use conflicts under global change. Improvements can be made to construct more realistic water demand and management models. Various methods in representing water management are summarized in chapter 2.

Second, the uncertainty related to water resources, water demand, and water management modelling under climate change and global change scenarios is not fully addressed, especially the uncertainty propagation in the modelling chain. The uncertainty in the bottom-up framework has been highlighted and discussed in chapter 6. Further work would be needed to quantify the contributions of the different sources of total uncertainty in the modelling chain of the top-down framework. Several methods of uncertainty quantification are proposed in chapter 2.

Third, from the bottom-up perspective, some limitations in terms of climate perturbation method used in this dissertation (delta-change method) might underestimate the occurrence of extreme climate events. Stochastic methods (e.g., weather generators) can be applied and then compared with the current assessment. In a broader sense, the vulnerability assessment in the bottom-up framework could extend beyond the climate sensitivity analysis. By applying the modelling chain used in the top-down framework, the sensitivity of management metrics to socio-economic drivers (e.g., population growth and irrigation surface) can be further explored.

Finally, efforts should go toward combining the results from bottom-up and top-down frameworks to support efficient adaptation to the challenge of global change. At the local level of the Neste water system, the proposed adaptation strategies can be tested in both frameworks to investigate their effectiveness. Although the top-down framework dominates in the literature for impact assessment and adaptation design, bottom-up framework needs to be given more credit and importance to support adaptation and decision making. Few studies have explored the possibilities of integrating both frameworks (e.g., Brown et al., 2012; Conway et al., 2019; Prudhomme et al., 2010; Sauquet et al., 2019). A robust and generalized adaptation procedure that closely links the scientists, water managers, and stakeholders should be established to efficiently use information provided by both frameworks.

Bibliography

AghaKouchak, A., Chiang, F., Huning, L.S., Love, C.A., Mallakpour, I., Mazdiyasni, O., Moftakhari, H., Papalexiou, S.M., Ragno, E., Sadegh, M., 2020. Climate extremes and compound hazards in a warming world. Annual Review of Earth and Planetary Sciences 48, 519–548. doi:10.1146/annurev-earth-071719-055228.

Ahmadi, M., Haddad, O.B., Loáiciga, H.A., 2014. Adaptive reservoir operation rules under climatic change. Water Resources Management 29, 1247–1266. doi:10.1007/s11269-014-0871-0.

Alam, S., Gebremichael, M., Li, R., Dozier, J., Lettenmaier, D.P., 2019. Climate change impacts on groundwater storage in the Central Valley, California. Climatic Change 157, 387–406. doi:10.1007/s10584-019-02585-5.

Alcamo, J., Flörke, M., Märker, M., 2007. Future long-term changes in global water resources driven by socio-economic and climatic changes. Hydrological Sciences Journal 52, 247–275. doi:10.1623/hysj.52.2.247.

Allen, R.G., Pereira, L.S., Raes, D., Smith, M., 1998. FAO Irrigation and drainage paper No. 56. Rome: Food and Agriculture Organization of the United Nations 56, e156.

Alonso-González, E., López-Moreno, J., Navarro-Serrano, F., Sanmiguel-Vallelado, A., Aznárez-Balta, M., Revuelto, J., Ceballos, A., 2020. Snowpack sensitivity to temperature, precipitation, and solar radiation variability over an elevational gradient in the Iberian mountains. Atmospheric Research 243, 104973. doi:10.1016/j.atmosres.2020.104973.

Amblar-Francés, M.P., Ramos-Calzado, P., Sanchis-Lladó, J., Hernanz-Lázaro, A., Peral-García, M.C., Navascués, B., Dominguez-Alonso, M., Pastor-Saavedra, M.A., Rodríguez-Camino, E., 2020. High resolution climate change projections for the Pyrenees region. Advances in Science and Research 17, 191–208. doi:10.5194/asr-17-191-2020.

Amblar Francés, P., Casado Calle, M.J., Pastor Saavedra, A., Ramos Calzado, P., Rodríguez Camino, E., 2017. Guía de escenarios regionalizados de cambio climático sobre españa a partir de los resultados del IPCC-AR5.

Amundsen, H., Berglund, F., Westskog, H., 2010. Overcoming barriers to climate change adaptation—A question of multilevel governance? Environment and Planning C: Government and Policy 28, 276–289. doi:10.1068/c0941.

Anderson, J., Chung, F., Anderson, M., Brekke, L., Easton, D., Ejeta, M., Peterson, R., Snyder, R., 2007. Progress on incorporating climate change into management of California's water resources. Climatic Change 87, 91–108. doi:10.1007/s10584-007-9353-1.

Andrew, J., Sauquet, E., 2017. Climate change impacts and water management adaptation in two Mediterranean-climate watersheds: Learning from the Durance and Sacramento rivers. Water 9, 126. doi:10.3390/w9020126.

Angelakis, A., Zheng, X., 2015. Evolution of water supply, sanitation, wastewater, and stormwater technologies globally. Water 7, 455–463. doi:10.3390/w7020455.

Anghileri, D., Botter, M., Castelletti, A., Weigt, H., Burlando, P., 2018. A comparative assessment of the impact of climate change and energy policies on Alpine hydropower. Water Resources Research 54, 9144–9161. doi:10.1029/2017wr022289.

Ansar, A., Flyvbjerg, B., Budzier, A., Lunn, D., 2014. Should we build more large dams? The actual costs of hydropower megaproject development. Energy Policy 69, 43–56. doi:10.1016/j.enpol.2013.10.069.

Arheimer, B., Donnelly, C., Lindström, G., 2017. Regulation of snow-fed rivers affects flow regimes more than climate change. Nature Communications 8, 62. doi:10.1038/s41467-017-00092-8.

Arnell, N.W., 2004. Climate change and global water resources: SRES emissions and socio-economic scenarios. Global Environmental Change 14, 31 – 52. doi:https://doi.org/10.1016/j.gloenvcha.2003.10.006.

Arnell, N.W., Gosling, S.N., 2014. The impacts of climate change on river flood risk at the global scale. Climatic Change 134, 387–401. doi:10.1007/s10584-014-1084-5.

Ashofteh, P.S., Bozorg-Haddad, O., Loáiciga, H.A., 2017. Development of adaptive strategies for irrigation water demand management under climate change. Journal of Irrigation and Drainage Engineering 143, 04016077. doi:10.1061/(asce)ir.1943-4774.0001123.

Ashofteh, P.S., Haddad, O.B., Loáiciga, H.A., 2015. Evaluation of climatic-change impacts on multiobjective reservoir operation with multiobjective genetic programming. Journal of Water Resources Planning and Management 141, 04015030. doi:10.1061/(ASCE)WR.1943-5452.0000540.

Ashofteh, P.S., Haddad, O.B., Mariño, M.A., 2013. Climate change impact on reservoir performance indexes in agricultural water supply. Journal of Irrigation and Drainage Engineering 139, 85–97. doi:10.1061/(asce)ir.1943-4774.0000496.

Auffhammer, M., Baylis, P., Hausman, C.H., 2017. Climate change is projected to have severe impacts on the frequency and intensity of peak electricity demand across the United States. Proceedings of the National Academy of Sciences 114, 1886–1891. doi:10.1073/pnas.1613193114.

Bangash, R.F., Passuello, A., Sanchez-Canales, M., Terrado, M., López, A., Elorza, F.J., Ziv, G., Acuña, V., Schuhmacher, M., 2013. Ecosystem services in Mediterranean river basin: Climate change impact on water provisioning and erosion control. Science of The Total Environment 458-460, 246–255. doi:10.1016/j.scitotenv.2013.04.025.

Barnett, T., Adam, J., Lettenmaier, D., 2005. Potential impacts of a warming climate on water availability in snow-dominated regions. Nature 438, 303–309. doi:10.1038/nature04141.

Barnett, T.P., Pierce, D.W., 2009. Sustainable water deliveries from the Colorado River in a changing climate. Proceedings of the National Academy of Sciences 106, 7334–7338. doi:10.1073/pnas.0812762106.

Bates, B., Kundzewicz, Z., Wu, S., Palutikof, J., 2008. Climate change and water. IPCC Secretariat, Geneva.

Becker, B., Burzel, A., 2016. Model Coupling with Open MI Introduction of Basic Concepts. Springer International Publishing, Cham. pp. 279–299. URL: https://doi.org/10.1007/978-3-319-51043-9_11, doi:10.1007/978-3-319-51043-9_11.

Benito, G., Brázdil, R., Herget, J., Machado, M.J., 2015. Quantitative historical hydrology in Europe. Hydrology and Earth System Sciences 19, 3517–3539. doi:10.5194/hess-19-3517-2015.

Berga, L., 2016. The role of hydropower in climate change mitigation and adaptation: A review. Engineering 2, 313–318. doi:10.1016/j.eng.2016.03.004.

Berking, J., Oleson, J.P., Sürmelihindi, G., Maganzani, L., Ronin, M., Schrakamp, I., Gerrard, C., Gutièrrez, A., Isselhorst, S., Schütt, B., Trümper, M., Bouffier, S., Dumas, V., Lenhardt, P., Paillet, J.L., Schomberg, A., 2018. Water management in ancient civilizations. volume 53. Edition Topoi, Berlin. doi:10.17171/3-53.

Bertoni, F., Castelletti, A., Giuliani, M., Reed, P.M., 2019. Discovering dependencies, trade-offs, and robustness in joint dam design and operation: An ex-post assessment of the Kariba dam. Earth's Future 7, 1367–1390. doi:10.1029/2019ef001235.

Bhadoriya, U.P.S., Mishra, A., Singh, R., Chatterjee, C., 2020. Implications of climate change on water storage and filling time of a multipurpose reservoir in India. Journal of Hydrology 590, 125542. doi:10.1016/j.jhydrol.2020.125542.

Biemans, H., Haddeland, I., Kabat, P., Ludwig, F., Hutjes, R.W.A., Heinke, J., von Bloh, W., Gerten, D., 2011. Impact of reservoirs on river discharge and irrigation water supply during the 20th century. Water Resources Research 47, S109–S122. doi:10.1029/2009wr008929.

Biswas, A.K., 2004. Integrated water resources management: A reassessment. Water International 29, 248–256. doi:10.1080/02508060408691775.

Bonjean Stanton, M.C., Dessai, S., Paavola, J., 2016. A systematic review of the impacts of climate variability and change on electricity systems in Europe. Energy 109, 1148–1159. doi:10.1016/j.energy.2016.05.015.

Boretti, A., Rosa, L., 2019. Reassessing the projections of the world water development report. npj Clean Water 2. doi:10.1038/s41545-019-0039-9.

Brekke, L.D., Maurer, E.P., Anderson, J.D., Dettinger, M.D., Townsley, E.S., Harrison, A., Pruitt, T., 2009. Assessing reservoir operations risk under climate change. Water Resources Research 45, W04411. doi:10.1029/2008WR006941.

Brekke, L.D., Miller, N.L., Bashford, K.E., Quinn, N.W.T., Dracup, J.A., 2004. Climate change impacts uncertainty for water resources in the San Joaquin River basin, California. Journal of the American Water Resources Association 40, 149–164. doi:10.1111/j.1752-1688.2004.tb01016.x.

Broderick, C., Murphy, C., Wilby, R.L., Matthews, T., Prudhomme, C., Adamson, M., 2019. Using a scenario-neutral framework to avoid potential maladaptation to future flood risk. Water Resources Research 55, 1079–1104. doi:10.1029/2018wr023623.

Brown, C., 2010. The end of reliability. Journal of Water Resources Planning and Management 136, 143–145. doi:10.1061/(asce)wr.1943-5452.65.

Brown, C., Boltz, F., Freeman, S., Tront, J., Rodriguez, D., 2020. Resilience by design: A deep uncertainty approach for water systems in a changing world. Water Security 9, 100051. doi:10.1016/j.wasec.2019.100051.

Brown, C., Ghile, Y., Laverty, M., Li, K., 2012. Decision scaling: Linking bottom-up vulnerability analysis with climate projections in the water sector. Water Resources Research 48. doi:10.1029/2011wr011212.

Brown, C., Wilby, R.L., 2012a. An alternate approach to assessing climate risks. Eos, Transactions American Geophysical Union 93, 401–402. doi:10.1029/2012eo410001.

Brown, C., Wilby, R.L., 2012b. An alternate approach to assessing climate risks. Eos, Transactions American Geophysical Union 93, 401–402. doi:10.1029/2012eo410001.

Brown, C.M., Lund, J.R., Cai, X., Reed, P.M., Zagona, E.A., Ostfeld, A., Hall, J., Characklis, G.W., Yu, W., Brekke, L., 2015. The future of water resources systems analysis: Toward a scientific framework for sustainable water management. Water Resources Research 51, 6110–6124. doi:10.1002/2015wr017114.

Buendia, C., Batalla, R.J., Sabater, S., Palau, A., Marcé, R., 2015. Runoff trends driven by climate and afforestation in a Pyrenean basin. Land Degradation & Development 27, 823–838. doi:10.1002/ldr.2384.

CACG, 2019. Plan de gestion des étiages de la Neste: Rapport de suivi annuel 2017. Technical Report. Compagnie d'Aménagement des Coteaux de Gascogne. Tarbes.

Cai, W., Borlace, S., Lengaigne, M., van Rensch, P., Collins, M., Vecchi, G., Timmermann, A., Santoso, A., McPhaden, M.J., Wu, L., England, M.H., Wang, G., Guilyardi, E., Jin, F.F., 2014. Increasing frequency of extreme El Niño events due to greenhouse warming. Nature Climate Change 4, 111–116. doi:10.1038/nclimate2100.

Caillouet, L., Vidal, J.P., Sauquet, E., Devers, A., Graff, B., 2017. Ensemble reconstruction of spatio-temporal extreme low-flow events in France since 1871. Hydrology and Earth System Sciences 21, 2923–2951. doi:10.5194/hess-21-2923-2017.

Carruthers, J., 2019. The Anthropocene. South African Journal of Science 115. doi:10.17159/sajs.2019/6428.

Carvalho-Santos, C., Monteiro, A.T., Azevedo, J.C., Honrado, J.P., Nunes, J.P., 2017. Climate change impacts on water resources and reservoir management: Uncertainty and adaptation for a mountain catchment in northeast Portugal. Water Resources Management 31, 3355–3370. doi:10.1007/s11269-017-1672-z.

Castle, S.L., Thomas, B.F., Reager, J.T., Rodell, M., Swenson, S.C., Famiglietti, J.S., 2014. Groundwater depletion during drought threatens future water security of the Colorado River basin. Geophysical Research Letters 41, 5904–5911. doi:10.1002/2014gl061055.

Caubel, J., de Cortazar-Atauri, I.G., Vivant, A., Launay, M., de Noblet-Ducoudré, N., 2018. Assessing future meteorological stresses for grain maize in France. Agricultural Systems 159, 237–247. doi:10.1016/j.agsy.2017.02.010.

CEDEX/MAPAMA, 2017. Evaluación del impacto del cambio climático en los recursos hídricos y sequías en España.

Ceola, S., Montanari, A., Krueger, T., Dyer, F., Kreibich, H., Westerberg, I., Carr, G., Cudennec, C., Elshorbagy, A., Savenije, H., Zaag, P.V.D., Rosbjerg, D., Aksoy, H., Viola, F., Petrucci, G., MacLeod, K., Croke, B., Ganora, D., Hermans, L., Polo, M.J., Xu, Z., Borga, M., Helmschrot, J., Toth, E., Ranzi, R., Castellarin, A., Hurford, A., Brilly, M., Viglione, A., Blöschl, G., Sivapalan, M., Domeneghetti, A., Marinelli, A., Baldassarre, G.D., 2016. Adaptation of water resources systems to changing society and environment: A statement by the International Association of Hydrological Sciences. Hydrological Sciences Journal 61, 2803–2817. doi:10.1080/02626667.2016.1230674.

Chao, B.F., Wu, Y.H., Li, Y.S., 2008. Impact of artificial reservoir water impoundment on global sea level. Science 320, 212–214. doi:10.1126/science.1154580.

Chauveau, M., Chazot, S., Perrin, C., Bourgin, P.Y., Sauquet, E., Vidal, J.P., Rouchy, N., Martin, E., David, J., Norotte, T., Maugis, P., Lacaze, X.D., 2013. Quels impacts des changements climatiques sur les eaux de surface en France à l'horizon 2070 ? La Houille Blanche 99, 5–15. doi:10.1051/lhb/2013027.

Christensen, N.S., Lettenmaier, D.P., 2007. A multimodel ensemble approach to assessment of climate change impacts on the hydrology and water resources of the Colorado River basin. Hydrology and Earth System Sciences 11, 1417–1434. doi:10.5194/hess-11-1417-2007.

Christensen, N.S., Wood, A.W., Voisin, N., Lettenmaier, D.P., Palmer, R.N., 2004. The effects of climate change on the hydrology and water resources of the Colorado River basin. Climatic Change 62, 337–363. doi:10.1023/B:CLIM.0000013684.13621.1f.

Clemins, P.J., Bucini, G., Winter, J.M., Beckage, B., Towler, E., Betts, A., Cummings, R., Chang Queiroz, H., 2019. An analog approach for weather estimation using climate projections and reanalysis data. Journal of Applied Meteorology and Climatology 58, 1763–1777. doi:10.1175/JAMC-D-18-0255.1.

Clow, D.W., 2010. Changes in the timing of snowmelt and streamflow in Colorado: A response to recent warming. Journal of Climate 23, 2293–2306. doi:10.1175/2009jcli2951.1.

Cohen, S.J., Miller, K.A., Hamlet, A.F., Avis, W., 2000. Climate change and resource management in the Columbia River basin. Water International 25, 253–272. doi:10.1080/02508060008686827.

Conway, D., Nicholls, R.J., Brown, S., Tebboth, M.G.L., Adger, W.N., Ahmad, B., Biemans, H., Crick, F., Lutz, A.F., Campos, R.S.D., Said, M., Singh, C., Zaroug, M.A.H., Ludi, E., New, M., Wester, P., 2019. The need for bottom-up assessments of climate risks and adaptation in climate-sensitive regions. Nature Climate Change 9, 503–511. doi:10.1038/s41558-019-0502-0.

Cosgrove, W.J., Loucks, D.P., 2015. Water management: current and future challenges and research directions. Water Resources Research 51, 4823–4839. doi:10.1002/2014wr016869.

Craig, M.T., Cohen, S., Macknick, J., Draxl, C., Guerra, O.J., Sengupta, M., Haupt, S.E., Hodge, B.M., Brancucci, C., 2018. A review of the potential impacts of climate change on bulk power system planning and operations in the United States. Renewable and Sustainable Energy Reviews 98, 255–267. doi:10.1016/j.rser.2018.09.022.

Crochemore, L., Ramos, M.H., Pappenberger, F., 2016. Bias correcting precipitation forecasts to improve the skill of seasonal streamflow forecasts. Hydrology and Earth System Sciences 20, 3601–3618. doi:10.5194/hess-20-3601-2016.

Crutzen, P.J., Stoermer, E.F., 2000. The "Anthropocene. Global Change Newsletter 41, 17.

Culley, S., Bennett, B., Westra, S., Maier, H., 2019. Generating realistic perturbed hydrometeorological time series to inform scenario-neutral climate impact assessments. Journal of Hydrology 576, 111–122. doi:10.1016/j.jhydrol.2019.06.005.

Culley, S., Noble, S., Yates, A., Timbs, M., Westra, S., Maier, H.R., Giuliani, M., Castelletti, A., 2016. A bottom-up approach to identifying the maximum operational adaptive capacity of water resource systems to a changing climate. Water Resources Research 52, 6751–6768. doi:10.1002/2015wr018253.

Dai, A., 2013. Increasing drought under global warming in observations and models. Nature Climate Change 3, 52–58. doi:10.1038/nclimate1633.

Danso, D.K., François, B., Hingray, B., Diedhiou, A., 2021. Assessing hydropower flexibility for integrating solar and wind energy in West Africa using dynamic programming and sensitivity analysis. Illustration with the Akosombo reservoir, Ghana. Journal of Cleaner Production 287, 125559. doi:10.1016/j.jclepro.2020.125559.

Dawadi, S., Ahmad, S., 2012. Changing climatic conditions in the Colorado River basin: Implications for water resources management. Journal of Hydrology 430-431, 127–141. doi:10.1016/j.jhydrol.2012.02.010.

Dayon, G., Boé, J., Martin, É., Gailhard, J., 2018. Impacts of climate change on the hydrological cycle over France and associated uncertainties. Comptes Rendus Geoscience 350, 141–153. doi:10.1016/j.crte.2018.03.001.

Décamps, H., 1967. Écologie des trichoptères de la vallée d'Aure (Hautes-Pyrénées). Annales de Limnologie 3, 399–577. doi:10.1051/limn/1967012.

Dequesne, J., Portela, S., 2019. Observatoire des services publics d'eau et d'assainissement. Technical Report. Office Français de la Biodiversité. France. URL: https://www.services.eaufrance.fr/docs/synthese/rapports/Rapport_Sispea_2019_VF.pdf.

Di Baldassarre, G., Mazzoleni, M., Rusca, M., 2021. The legacy of large dams in the United States. Ambio 50, 1798–1808. doi:10.1007/s13280-021-01533-x.

Di Baldassarre, G., Wanders, N., AghaKouchak, A., Kuil, L., Rangecroft, S., Veldkamp, T.I.E., Garcia, M., van Oel, P.R., Breinl, K., van Loon, A.F., 2018. Water shortages worsened by reservoir effects. Nature Sustainability 1, 617–622. doi:10.1038/s41893-018-0159-0.

Dias, L.F., Aparício, B.A., Nunes, J.P., Morais, I., Fonseca, A.L., Pastor, A.V., Santos, F.D., 2020. Integrating a hydrological model into regional water policies: Co-creation of climate change dynamic adaptive policy pathways for water resources in southern Portugal. Environmental Science & Policy 114, 519–532. doi:10.1016/j.envsci.2020.09.020.

Dittrich, R., Wreford, A., Moran, D., 2016. A survey of decision-making approaches for climate change adaptation: Are robust methods the way forward? Ecological Economics 122, 79–89. doi:10.1016/j.ecolecon.2015.12.006.

Dobson, B., Wagener, T., Pianosi, F., 2019. An argument-driven classification and comparison of reservoir operation optimization methods. Advances in Water Resources 128, 74–86. doi:10.1016/j.advwatres.2019.04.012.

Dono, G., Cortignani, R., Doro, L., Giraldo, L., Ledda, L., Pasqui, M., Roggero, P.P., 2013. An integrated assessment of the impacts of changing climate variability on agricultural productivity and profitability in an irrigated Mediterranean catchment. Water Resources Management 27, 3607–3622. doi:10.1007/s11269-013-0367-3.

Du, S., Scussolini, P., Ward, P.J., Zhang, M., Wen, J., Wang, L., Koks, E., Diaz-Loaiza, A., Gao, J., Ke, Q., Aerts, J.C., 2020. Hard or soft flood adaptation? Advantages of a hybrid strategy for Shanghai. Global Environmental Change 61, 102037. doi:10.1016/j.gloenvcha.2020.102037.

Ehsani, N., Vörösmarty, C.J., Fekete, B.M., Stakhiv, E.Z., 2017. Reservoir operations under climate change: Storage capacity options to mitigate risk. Journal of Hydrology 555, 435–446. doi:10.1016/j.jhydrol.2017.09.008.

Ekström, M., Grose, M.R., Whetton, P.H., 2015. An appraisal of downscaling methods used in climate change research. Wiley Interdisciplinary Reviews: Climate Change 6, 301–319. doi:10.1002/wcc.339.

Ekström, M., Gutmann, E.D., Wilby, R.L., Tye, M.R., Kirono, D.G., 2018. Robustness of hydroclimate metrics for climate change impact research. WIREs Water 5. doi:10.1002/wat2.1288.

Emmanouil, S., Nikolopoulos, E.I., François, B., Brown, C., Anagnostou, E.N., 2021. Evaluating existing water supply reservoirs as small-scale pumped hydroelectric storage options – A case study in Connecticut. Energy 226, 120354. doi:10.1016/j.energy.2021.120354.

Eum, H.I., Simonovic, S.P., 2010. Integrated reservoir management system for adaptation to climate change: The Nakdong River basin in Korea. Water Resources Management 24, 3397–3417. doi:10.1007/s11269-010-9612-1.

Falgon, A., 2014. Reconstitution des apports naturels des groupements d'Eget et du Louron. Technical Report. Compagnie Nationale du Rhône.

Farinotti, D., Round, V., Huss, M., Compagno, L., Zekollari, H., 2019. Large hydropower and water-storage potential in future glacier-free basins. Nature 575, 341–344. doi:10.1038/s41586-019-1740-z.

Fayad, A., Gascoin, S., Faour, G., López-Moreno, J.I., Drapeau, L., Page, M.L., Escadafal, R., 2017. Snow hydrology in Mediterranean mountain regions: A review. Journal of Hydrology 551, 374–396. doi:10.1016/j.jhydrol.2017.05.063.

Fayaed, S.S., El-Shafie, A., Jaafar, O., 2013. Reservoir-system simulation and optimization techniques. Stochastic Environmental Research and Risk Assessment 27, 1751–1772. doi:10.1007/s00477-013-0711-4.

Finger, D., Heinrich, G., Gobiet, A., Bauder, A., 2012. Projections of future water resources and their uncertainty in a glacierized catchment in the Swiss Alps and the subsequent effects on hydropower production during the 21st century. Water Resources Research 48. doi:10.1029/2011WR010733.

Fleck, J., Udall, B., 2021. Managing Colorado River risk. Science 372, 885. doi:10.1126/science.abj5498.

Fletcher, S., Lickley, M., Strzepek, K., 2019. Learning about climate change uncertainty enables flexible water infrastructure planning. Nature Communications 10. doi:10.1038/s41467-019-09677-x.

Fluixá-Sanmartín, J., Altarejos-García, L., Morales-Torres, A., Escuder-Bueno, I., 2018. Review article: Climate change impacts on dam safety. Natural Hazards and Earth System Sciences 18, 2471–2488. doi:10.5194/nhess-18-2471-2018.

Folton, N., Martin, E., Arnaud, P., L'Hermite, P., Tolsa, M., 2019. A 50-year analysis of hydrological trends and processes in a Mediterranean catchment. Hydrology and Earth System Sciences 23, 2699–2714. doi:10.5194/hess-23-2699-2019.

Foti, R., Ramirez, J.A., Brown, T.C., 2014. Response surfaces of vulnerability to climate change: the Colorado River basin, the High Plains, and California. Climatic Change 125, 429–444. doi:10.1007/s10584-014-1178-0.

Fraga-Santiago, P., Gómez-Pazo, A., Pérez-Alberti, A., Montero, P., Pérez, X.L.O., 2019. Trends in the recent evolution of coastal lagoons and lakes in Galicia (NW Iberian Peninsula). Journal of Marine Science and Engineering 7, 272. doi:10.3390/jmse7080272.

François, B., Borga, M., Anquetin, S., Creutin, J.D., Engeland, K., Favre, A.C., Hingray, B., Ramos, M.H., Raynaud, D., Renard, B., Sauquet, E., Sauterleute, J.F., Vidal, J.P., Warland, G., 2014a. Integrating hydropower and intermittent climate-related renewable energies: A call for hydrology. Hydrological Processes 28, 5465–5468. doi:10.1002/hyp.10274.

François, B., Hingray, B., Creutin, J.D., Hendrickx, F., 2015. Estimating water system performance under climate change: Influence of the management strategy modeling. Water Resources Management 29, 4903–4918. doi:10.1007/s11269-015-1097-5.

François, B., Hingray, B., Hendrickx, F., Creutin, J.D., 2014b. Seasonal patterns of water storage as signatures of the climatological equilibrium between resource and demand. Hydrology and Earth System Sciences 18, 3787–3800. doi:10.5194/hess-18-3787-2014.

François, B., Hingray, B., Raynaud, D., Borga, M., Creutin, J., 2016. Increasing climate-related-energy penetration by integrating run-of-the river hydropower to wind/solar mix. Renewable Energy 87, 686–696. doi:10.1016/j.renene.2015.10.064.

François, B., Martino, S., Tøfte, L., Hingray, B., Mo, B., Creutin, J.D., 2017. Effects of increased wind power generation on mid-Norway's energy balance under climate change: A market based approach. Energies 10, 227. doi:10.3390/en10020227.

François, B., Schlef, K., Wi, S., Brown, C., 2019. Design considerations for riverine floods in a changing climate – A review. Journal of Hydrology 574, 557–573. doi:10.1016/j.jhydrol.2019.04.068.

Frei, P., Kotlarski, S., Liniger, M.A., Schär, C., 2018. Future snowfall in the Alps: projections based on the EURO-CORDEX regional climate models. The Cryosphere 12, 1–24. doi:10.5194/tc-12-1-2018.

Gaetani, M., Janicot, S., Vrac, M., Famien, A.M., Sultan, B., 2020. Robust assessment of the time of emergence of precipitation change in West Africa. Scientific Reports 10. doi:10.1038/s41598-020-63782-2.

Galindo, A., Collado-González, J., Griñán, I., Corell, M., Centeno, A., Martín-Palomo, M., Girón, I., Rodríguez, P., Cruz, Z., Memmi, H., Carbonell-Barrachina, A., Hernández, F., Torrecillas, A., Moriana, A., Pérez-López, D., 2018. Deficit irrigation and emerging fruit crops as a strategy to save water in Mediterranean semiarid agrosystems. Agricultural Water Management 202, 311–324. doi:10.1016/j.agwat.2017.08.015.

Garcia, F., Folton, N., Oudin, L., 2017. Which objective function to calibrate rainfall–runoff models for low-flow index simulations? Hydrological Sciences Journal 62, 1149–1166. doi:10.1080/02626667.2017.1308511.

Garcia, M., Ridolfi, E., Baldassarre, G.D., 2020. The interplay between reservoir storage and operating rules under evolving conditions. Journal of Hydrology 590, 125270. doi:10.1016/j.jhydrol.2020.125270.

García-Ruiz, J.M., López-Moreno, J.I., Vicente-Serrano, S.M., Lasanta–Martínez, T., Beguería, S., 2011. Mediterranean water resources in a global change scenario. Earth-Science Reviews 105, 121–139. doi:10.1016/j.earscirev.2011.01.006.

Gascoin, S., Hagolle, O., Huc, M., Jarlan, L., Dejoux, J.F., Szczypta, C., Marti, R., Sánchez, R., 2015. A snow cover climatology for the Pyrenees from MODIS snow products. Hydrology and Earth System Sciences 19, 2337–2351. doi:10.5194/hess-19-2337-2015.

Gaudard, L., Gilli, M., Romerio, F., 2013. Climate change impacts on hydropower management. Water Resources Management 27, 5143–5156. doi:10.1007/s11269-013-0458-1.

Gaudard, L., Romerio, F., 2014. The future of hydropower in Europe: Interconnecting climate, markets and policies. Environmental Science & Policy 37, 172–181. doi:10.1016/j.envsci.2013.09.008.

Gaudard, L., Romerio, F., Valle, F.D., Gorret, R., Maran, S., Ravazzani, G., Stoffel, M., Volonterio, M., 2014. Climate change impacts on hydropower in the Swiss and Italian Alps. Science of The Total Environment 493, 1211–1221. doi:10.1016/j.scitotenv.2013.10.012.

Georgakakos, A.P., Yao, H., Kistenmacher, M., Georgakakos, K.P., Graham, N.E., Cheng, F.Y., Spencer, C., Shamir, E., 2012a. Value of adaptive water resources management in northern California under climatic variability and change: Reservoir management. Journal of Hydrology 412-413, 34–46. doi:10.1016/j.jhydrol.2011.04.038.

Georgakakos, K.P., Graham, N.E., Cheng, F.Y., Spencer, C., Shamir, E., Georgakakos, A.P., Yao, H., Kistenmacher, M., 2012b. Value of adaptive water resources management in northern California under climatic variability and change: Dynamic hydroclimatology. Journal of Hydrology 412-413, 47–65. doi:10.1016/j.jhydrol.2011.04.032.

Gernaat, D.E.H.J., Bogaart, P.W., van Vuuren, D.P., Biemans, H., Niessink, R., 2017. High-resolution assessment of global technical and economic hydropower potential. Nature Energy 2, 821–828. doi:10.1038/s41560-017-0006-y.

Ghile, Y.B., Taner, M.U., Brown, C., Grijsen, J.G., Talbi, A., 2013. Bottom-up climate risk assessment of infrastructure investment in the Niger River basin. Climatic Change 122, 97–110. doi:10.1007/s10584-013-1008-9.

Giorgetta, M.A., Jungclaus, J., Reick, C.H., Legutke, S., Bader, J., Böttinger, M., Brovkin, V., Crueger, T., Esch, M., Fieg, K., Glushak, K., Gayler, V., Haak, H., Hollweg, H.D., Ilyina, T., Kinne, S., Kornblueh, L., Matei, D., Mauritsen, T., Mikolajewicz, U., Mueller, W., Notz, D., Pithan, F., Raddatz, T., Rast, S., Redler, R., Roeckner, E.,

Schmidt, H., Schnur, R., Segschneider, J., Six, K.D., Stockhause, M., Timmreck, C., Wegner, J., Widmann, H., Wieners, K.H., Claussen, M., Marotzke, J., Stevens, B., 2013. Climate and carbon cycle changes from 1850 to 2100 in MPI-ESM simulations for the Coupled Model Intercomparison Project phase 5. Journal of Advances in Modeling Earth Systems 5, 572–597. doi:10.1002/jame.20038.

Giuliani, M., Anghileri, D., Castelletti, A., Vu, P.N., Soncini-Sessa, R., 2016a. Large storage operations under climate change: Expanding uncertainties and evolving trade-offs. Environmental Research Letters 11, 035009. doi:10.1088/1748-9326/11/3/035009.

Giuliani, M., Castelletti, A., 2013. Assessing the value of cooperation and information exchange in large water resources systems by agent-based optimization. Water Resources Research 49, 3912–3926. doi:10.1002/wrcr.20287.

Giuliani, M., Castelletti, A., 2016. Is robustness really robust? How different definitions of robustness impact decision-making under climate change. Climatic Change 135, 409–424. doi:10.1007/s10584-015-1586-9.

Giuliani, M., Castelletti, A., Pianosi, F., Mason, E., Reed, P.M., 2016b. Curses, tradeoffs, and scalable management: Advancing evolutionary multiobjective direct policy search to improve water reservoir operations. Journal of Water Resources Planning and Management 142, 04015050. doi:10.1061/(asce)wr.1943-5452.0000570.

Giuliani, M., Herman, J.D., Castelletti, A., Reed, P., 2014. Many-objective reservoir policy identification and refinement to reduce policy inertia and myopia in water management. Water Resources Research 50, 3355–3377. doi:10.1002/2013wr014700.

Givati, A., Thirel, G., Rosenfeld, D., Paz, D., 2019. Climate change impacts on streamflow at the upper Jordan River based on an ensemble of regional climate models. Journal of Hydrology: Regional Studies 21, 92–109. doi:10.1016/j.ejrh.2018.12.004.

Gleick, P.H., 1993. Water in crisis: A guide to the world's fresh water resources. Oxford University Press, New York, USA.

Gleick, P.H., 2016. Impacts of California's ongoing drought: Hydroelectricity generation. Pacific Institute, California. https://droughtcenter.unl.edu/archive/assessments/Pacific-Hydroelectricity-2015.pdf.

Gobiet, A., Kotlarski, S., Beniston, M., Heinrich, G., Rajczak, J., Stoffel, M., 2014. 21st century climate change in the European Alps—A review. Science of The Total Environment 493, 1138–1151. doi:10.1016/j.scitotenv.2013.07.050.

Golombek, R., Kittelsen, S.A.C., Haddeland, I., 2011. Climate change: Impacts on electricity markets in Western Europe. Climatic Change 113, 357–370. doi:10.1007/s10584-011-0348-6.

Gonzalez, J.M., Olivares, M.A., Medellín-Azuara, J., Moreno, R., 2020. Multipurpose reservoir operation: A multi-scale tradeoff analysis between hydropower generation and irrigated agriculture. Water Resources Management 34, 2837–2849. doi:10.1007/s11269-020-02586-5.

Gorguner, M., Kavvas, M.L., 2020. Modeling impacts of future climate change on reservoir storages and irrigation water demands in a Mediterranean basin. Science of The Total Environment 748, 141246. doi:10.1016/j.scitotenv.2020.141246.

Grafton, R.Q., Chu, H.L., Stewardson, M., Kompas, T., 2011. Optimal dynamic water allocation: Irrigation extractions and environmental tradeoffs in the Murray River, Australia. Water Resources Research 47. doi:10.1029/2010wr009786.

Grafton, R.Q., Williams, J., Perry, C.J., Molle, F., Ringler, C., Steduto, P., Udall, B., Wheeler, S.A., Wang, Y., Garrick, D., Allen, R.G., 2018. The paradox of irrigation efficiency. Science 361, 748–750. doi:10.1126/science.aat9314.

Griffin, D., Anchukaitis, K.J., 2014. How unusual is the 2012-2014 California drought? Geophysical Research Letters 41, 9017–9023. doi:10.1002/2014gl062433.

Groves, D.G., Davis, M., Wilkinson, R., Lempert, R., 2008. Planning for climate change in the Inland Empire: southern California. Water Resources IMPACT 10, 14–17.

Guo, D., Westra, S., Maier, H.R., 2017. Use of a scenario-neutral approach to identify the key hydro-meteorological attributes that impact runoff from a natural catchment. Journal of Hydrology 554, 317–330. doi:10.1016/j.jhydrol.2017.09.021.

Guo, D., Westra, S., Maier, H.R., 2018. An inverse approach to perturb historical rainfall data for scenario-neutral climate impact studies. Journal of Hydrology 556, 877–890. doi:10.1016/j.jhydrol.2016.03.025.

Gupta, H.V., Kling, H., Yilmaz, K.K., Martinez, G.F., 2009. Decomposition of the mean squared error and NSE performance criteria: implications for improving hydrological modelling. Journal of Hydrology 377, 80–91. doi:10.1016/j.jhydrol.2009.08.003.

Haasnoot, M., Kwakkel, J.H., Walker, W.E., ter Maat, J., 2013. Dynamic adaptive policy pathways: A method for crafting robust decisions for a deeply uncertain world. Global Environmental Change 23, 485–498. doi:10.1016/j.gloenvcha.2012.12.006.

Habets, F., Molénat, J., Carluer, N., Douez, O., Leenhardt, D., 2018. The cumulative impacts of small reservoirs on hydrology: A review. Science of The Total Environment 643, 850 – 867. doi:10.1016/j.scitotenv.2018.06.188.

Hadjimichael, A., Gold, D., Hadka, D., Reed, P., 2020. Rhodium: Python library for many-objective robust decision making and exploratory modeling. Journal of Open Research Software 8. doi:10.5334/jors.293.

Hadka, D., Reed, P., 2013. Borg: An auto-adaptive many-objective evolutionary computing framework. Evolutionary Computation 21, 231–259. doi:10.1162/evco_a_00075.

Haguma, D., Leconte, R., Côté, P., Krau, S., Brissette, F., 2014. Optimal hydropower generation under climate change conditions for a northern water resources system. Water Resources Management 28, 4631–4644. doi:10.1007/s11269-014-0763-3.

Haguma, D., Leconte, R., Krau, S., 2017. Hydropower plant adaptation strategies for climate change impacts on hydrological regime. Canadian Journal of Civil Engineering 44, 962–970. doi:10.1139/cjce-2017-0141.

Haguma, D., Leconte, R., Krau, S., Côté, P., Brissette, F., 2015. Water resources optimization method in the context of climate change. Journal of Water Resources Planning and Management 141, 04014051. doi:10.1061/(asce)wr.1943-5452.0000445.

Hallegatte, S., 2009. Strategies to adapt to an uncertain climate change. Global Environmental Change 19, 240–247. doi:10.1016/j.gloenvcha.2008.12.003.

Hamlet, A.F., 2011. Assessing water resources adaptive capacity to climate change impacts in the Pacific Northwest Region of North America. Hydrology and Earth System Sciences 15, 1427–1443. doi:10.5194/hess-15-1427-2011.

Hamlet, A.F., Elsner, M.M., Mauger, G.S., Lee, S.Y., Tohver, I., Norheim, R.A., 2013. An overview of the Columbia Basin Climate Change Scenarios Project: Approach, methods, and summary of key results. Atmosphere-Ocean 51, 392–415. doi:10.1080/07055900.2013.819555.

Hamlet, A.F., Lee, S.Y., Mickelson, K.E.B., Elsner, M.M., 2010. Effects of projected climate change on energy supply and demand in the Pacific Northwest and Washington State. Climatic Change 102, 103–128. doi:10.1007/s10584-010-9857-y.

Hamlet, A.F., Lettenmaier, D.P., 1999. Effects of climate change on hydrology and water resources in the Columbia River basin. Journal of the American Water Resources Association 35, 1597–1623. doi:10.1111/j.1752-1688.1999.tb04240.x.

Hamududu, B., Killingtveit, A., 2012. Assessing climate change impacts on global hydropower. Energies 5, 305–322. doi:10.3390/en5020305.

Hanak, E., Lund, J.R., 2011. Adapting California's water management to climate change. Climatic Change 111, 17–44. doi:10.1007/s10584-011-0241-3.

Hänggi, P., Weingartner, R., 2012. Variations in discharge volumes for hydropower generation in Switzerland. Water Resources Management 26, 1231–1252. doi:10.1007/s11269-011-9956-1.

Hari, V., Rakovec, O., Markonis, Y., Hanel, M., Kumar, R., 2020. Increased future occurrences of the exceptional 2018–2019 Central European drought under global warming. Scientific Reports 10. doi:10.1038/s41598-020-68872-9.

Harmanny, K.S., Malek, Ž., 2019. Adaptations in irrigated agriculture in the Mediterranean region: an overview and spatial analysis of implemented strategies. Regional Environmental Change 19, 1401–1416. doi:10.1007/s10113-019-01494-8.

Haro-Monteagudo, D., Palazón, L., Beguería, S., 2020. Long-term sustainability of large water resource systems under climate change: A cascade modeling approach. Journal of Hydrology 582, 124546. doi:https://doi.org/10.1016/j.jhydrol.2020.124546.

Harris, G.R., Collins, M., Sexton, D.M.H., Murphy, J.M., Booth, B.B.B., 2010. Probabilistic projections for 21st century European climate. Natural Hazards and Earth System Sciences 10, 2009–2020. doi:10.5194/nhess-10-2009-2010.

Hashimoto, T., Loucks, D.P., Stedinger, J.R., 1982a. Robustness of water resources systems. Water Resources Research 18, 21–26. doi:10.1029/wr018i001p00021.

Hashimoto, T., Stedinger, J.R., Loucks, D.P., 1982b. Reliability, resiliency, and vulnerability criteria for water resource system performance evaluation. Water Resources Research 18, 14–20. doi:10.1029/wr018i001p00014.

Hawkins, E., Sutton, R., 2009. The potential to narrow uncertainty in regional climate predictions. Bulletin of the American Meteorological Society 90, 1095–1108. doi:10.1175/2009bams2607.1.

Hawkins, E., Sutton, R., 2010. The potential to narrow uncertainty in projections of regional precipitation change. Climate Dynamics 37, 407–418. doi:10.1007/s00382-010-0810-6.

Hecht, J.S., Lacombe, G., Arias, M.E., Dang, T.D., Piman, T., 2019. Hydropower dams of the Mekong River basin: A review of their hydrological impacts. Journal of Hydrology 568, 285–300. doi:10.1016/j.jhydrol.2018.10.045.

Hendrickx, F., Sauquet, E., 2013. Impact of warming climate on water management for the Ariège River basin (France). Hydrological Sciences Journal 58, 976–993. doi:10.1080/02626667.2013.788790.

Herman, J.D., Quinn, J.D., Steinschneider, S., Giuliani, M., Fletcher, S., 2020. Climate adaptation as a control problem: Review and perspectives on dynamic water resources planning under uncertainty. Water Resources Research 56. doi:10.1029/2019WR025502.

Herman, J.D., Reed, P.M., Zeff, H.B., Characklis, G.W., 2015. How should robustness be defined for water systems planning under change? Journal of Water Resources Planning and Management 141, 04015012. doi:10.1061/(asce)wr.1943-5452.0000509.

Herman, J.D., Zeff, H.B., Reed, P.M., Characklis, G.W., 2014. Beyond optimality: Multistakeholder robustness tradeoffs for regional water portfolio planning under deep uncertainty. Water Resources Research 50, 7692–7713. doi:10.1002/2014wr015338.

Heuvelmans, G., Muys, B., Feyen, J., 2004. Evaluation of hydrological model parameter transferability for simulating the impact of land use on catchment hydrology. Physics and Chemistry of the Earth, Parts A/B/C 29, 739–747. doi:10.1016/j.pce.2004.05.002.

Hipel, K., Ben-Haim, Y., 1999. Decision making in an uncertain world: Information-gap modeling in water resources management. IEEE Transactions on Systems, Man and Cybernetics, Part C (Applications and Reviews) 29, 506–517. doi:10.1109/5326.798765.

Hirabayashi, Y., Mahendran, R., Koirala, S., Konoshima, L., Yamazaki, D., Watanabe, S., Kim, H., Kanae, S., 2013. Global flood risk under climate change. Nature Climate Change 3, 816–821. doi:10.1038/nclimate1911.

Holt, E., 2017. Experts on the past, working in the present: what archaeologists can contribute to current water management. WIREs Water 4. doi:10.1002/wat2.1215.

Huang, Z., Hejazi, M., Tang, Q., Vernon, C.R., Liu, Y., Chen, M., Calvin, K., 2019. Global agricultural green and blue water consumption under future climate and land use changes. Journal of Hydrology 574, 242–256. doi:10.1016/j.jhydrol.2019.04.046.

Huaringa-Alvarez, U.F., Trudel, M., Leconte, R., 2014. Impacts and adaptation to climate change using a reservoir management tool to a northern watershed: Application to Lièvre River watershed, Quebec, Canada. Water Resources Management 28. doi:10.1007/s11269-014-0694-z.

Hui, R., Herman, J., Lund, J., Madani, K., 2018. Adaptive water infrastructure planning for nonstationary hydrology. Advances in Water Resources 118, 83–94. doi:10.1016/j.advwatres.2018.05.009.

ICOLD, 2019. International commission on large dams: World register of dams, Paris, France, 2019. https://www.icold-cigb.org.

Icole, M., 1969. Age et nature de la formation dite «de Lannemezan». Revue géographique des Pyrénées et du Sud-Ouest 40, 157–170. doi:10.3406/rgpso.1969.5019.

Immerzeel, W.W., Lutz, A.F., Andrade, M., Bahl, A., Biemans, H., Bolch, T., Hyde, S., Brumby, S., Davies, B.J., Elmore, A.C., Emmer, A., Feng, M., Fernández, A., Haritashya, U., Kargel, J.S., Koppes, M., Kraaijenbrink, P.D.A., Kulkarni, A.V., Mayewski, P.A., Nepal, S., Pacheco, P., Painter, T.H., Pellicciotti, F., Rajaram, H., Rupper, S., Sinisalo, A., Shrestha, A.B., Viviroli, D., Wada, Y., Xiao, C., Yao, T., Baillie, J.E.M., 2019. Importance and vulnerability of the world's water towers. Nature 577, 364–369. doi:10.1038/s41586-019-1822-y.

Ingrand, R., 1961. L'aménagement hydro-électrique de la vallée d'Aure et ses conséquences géographiques. Revue géographique des Pyrénées et du Sud-Ouest 32, 35–62. doi:10.3406/rgpso.1961.4524.

Insee, 2014. L'emploi départemental et sectoriel en 2014. Institut National de la Statistique et des Études Économiques, Paris.

IPCC, 2014. Climate Change 2014: Synthesis Report. Contribution of Working Groups I, II, III to the Fifth Assessment Report of the Intergovernmental Panel on Climate change [Core Writing Team, R.K. Pachauri and L.A. Meyer (eds.)]. IPCC, Geneva.

IPCC, 2021. Summary for Policymakers. In: Climate Change 2021: The Physical Science Basis. Contribution of Working Group I to the Sixth Assessment Report of the Intergovernmental Panel on Climate Change [MassonDelmotte, V., P. Zhai, A. Pirani, S.L. Connors, C. Péan, S. Berger, N. Caud, Y. Chen, L. Goldfarb, M.I. Gomis, M. Huang, K. Leitzell, E. Lonnoy, J.B.R. Matthews, T.K. Maycock, T. Waterfield, O. Yelekçi, R. Yu, and B. Zhou (eds.)]. Cambridge University Press. In Press.

Jabbari, A.A., Nazemi, A., 2019. Alterations in Canadian hydropower production potential due to continuation of historical trends in climate variables. Resources 8, 163. doi:10.3390/resources8040163.

Jahandideh-Tehrani, M., Bozorg-Haddad, O., Loáiciga, H.A., 2014. Hydropower reservoir management under climate change: The Karoon reservoir system. Water Resources Management 29, 749–770. doi:10.1007/s11269-014-0840-7.

Jamasb, T., Pollitt, M., 2005. Electricity market reform in the European Union: Review of progress toward liberalization & integration. The Energy Journal 26, 11–41. URL: http://www.jstor.org/stable/23297005.

Jeuland, M., Whittington, D., 2014. Water resources planning under climate change: Assessing the robustness of real options for the Blue Nile. Water Resources Research 50, 2086–2107. doi:10.1002/2013wr013705.

Jones, R.N., 2001. An environmental risk assessment/management framework for climate change impact assessments. Natural Hazards 23, 197–230. doi:10.1023/a:1011148019213.

Kaptijn, E., 2017. Learning from ancient water management: Archeology's role in modern-day climate change adaptations. WIREs Water 5. doi:10.1002/wat2.1256.

Kasprzyk, J.R., Nataraj, S., Reed, P.M., Lempert, R.J., 2013. Many objective robust decision making for complex environmental systems undergoing change. Environmental Modelling & Software 42, 55–71. doi:10.1016/j.envsoft.2012.12.007.

Kellner, E., 2021. The controversial debate on the role of water reservoirs in reducing water scarcity. WIREs Water 8. doi:10.1002/wat2.1514.

Kern, J.D., Characklis, G.W., 2017. Evaluating the financial vulnerability of a major electric utility in the Southeastern U.S. to drought under climate change and an evolving generation mix. Environmental Science & Technology 51, 8815–8823. doi:10.1021/acs.est.6b05460.

Kern, J.D., Patino-Echeverri, D., Characklis, G.W., 2014a. The impacts of wind power integration on sub-daily variation in river flows downstream of hydroelectric dams. Environmental Science & Technology 48, 9844–9851. doi:10.1021/es405437h.

Kern, J.D., Patino-Echeverri, D., Characklis, G.W., 2014b. An integrated reservoir-power system model for evaluating the impacts of wind integration on hydropower resources. Renewable Energy 71, 553–562. doi:10.1016/j.renene.2014.06.014.

Kim, D., Eum, H.I., Kaluarachchi, J.J., Chun, J.A., 2019. A sensitivity-based analysis for managing storage capacity of a small agricultural reservoir under drying climate. Agricultural Water Management 213, 410–418. doi:10.1016/j.agwat.2018.10.040.

Kim, S., Tachikawa, Y., Nakakita, E., Takara, K., 2009. Reconsideration of reservoir operations under climate change: Case study with Yagisawa Dam, Japan. Annual Journal of Hydraulic Engineering, JSCE 53, 115–120.

Kingsborough, A., Borgomeo, E., Hall, J.W., 2016. Adaptation pathways in practice: Mapping options and trade-offs for London's water resources. Sustainable Cities and Society 27, 386–397. doi:10.1016/j.scs.2016.08.013.

Kling, H., Fuchs, M., Paulin, M., 2012. Runoff conditions in the upper Danube basin under an ensemble of climate change scenarios. Journal of Hydrology 424-425, 264–277. doi:10.1016/j.jhydrol.2012.01.011.

Koenker, R., Bassett, G., 1978. Regression quantiles. Econometrica 46, 33. doi:10.2307/1913643.

Koenker, R., Machado, J.A.F., 1999. Goodness of fit and related inference processes for quantile regression. Journal of the American Statistical Association 94, 1296–1310. doi:10.1080/01621459.1999.10473882.

Konzmann, M., Gerten, D., Heinke, J., 2013. Climate impacts on global irrigation requirements under 19 GCMs, simulated with a vegetation and hydrology model. Hydrological Sciences Journal 58, 88–105. doi:10.1080/02626667.2013.746495.

Koohafkan, P., Altieri, M.A., 2010. Globally important agricultural heritage systems: A legacy for the future. Food and Agriculture Organization of the United Nations, Rome, Italy.

Koutsoyiannis, D., Zarkadoulas, N., Angelakis, A.N., Tchobanoglous, G., 2008. Urban water management in Ancient Greece: Legacies and lessons. Journal of Water Resources Planning and Management 134, 45–54. doi:10.1061/(asce)0733-9496(2008)134:1(45).

Kummu, M., Guillaume, J.H.A., de Moel, H., Eisner, S., Flörke, M., Porkka, M., Siebert, S., Veldkamp, T.I.E., Ward, P.J., 2016. The world's road to water scarcity: shortage and stress in the 20th century and pathways towards sustainability. Scientific Reports 6. doi:10.1038/srep38495.

Kundzewicz, Z.W., Lugeri, N., Dankers, R., Hirabayashi, Y., Döll, P., Pińskwar, I., Dysarz, T., Hochrainer, S., Matczak, P., 2010. Assessing river flood risk and adaptation in Europe—review of projections for the future. Mitigation and Adaptation Strategies for Global Change 15, 641–656. doi:10.1007/s11027-010-9213-6.

Köplin, N., Schädler, B., Viviroli, D., Weingartner, R., 2012. Relating climate change signals and physiographic catchment properties to clustered hydrological response types. Hydrology and Earth System Sciences 16, 2267–2283. doi:10.5194/hess-16-2267-2012.

Laaha, G., Gauster, T., Tallaksen, L.M., Vidal, J.P., Stahl, K., Prudhomme, C., Heudorfer, B., Vlnas, R., Ionita, M., Lanen, H.A.J.V., Adler, M.J., Caillouet, L., Delus, C., Fendekova, M., Gailliez, S., Hannaford, J., Kingston, D., Loon, A.F.V., Mediero, L., Osuch, M., Romanowicz, R., Sauquet, E., Stagge, J.H., Wong, W.K., 2017. The European 2015 drought from a hydrological perspective. Hydrology and Earth System Sciences 21, 3001–3024. doi:10.5194/hess-21-3001-2017.

Labadie, J., 2004. Optimal operation of multireservoir systems: State-of-the-art review. Journal of Water Resources Planning and Management 130, 93–111. doi:10.1061/(ASCE)0733-9496(2004)130:2(93).

Lecina, S., Isidoro, D., Playán, E., Aragüés, R., 2010. Irrigation modernization and water conservation in Spain: The case of Riegos del Alto Aragón. Agricultural Water Management 97, 1663–1675. doi:10.1016/j.agwat.2010.05.023.

Leenhardt, D., Trouvat, J.L., Gonzalès, G., Pérarnaud, V., Prats, S., Bergez, J.E., 2004a. Estimating irrigation demand for water management on a regional scale I: ADEAUMIS, a simulation platform based on bio-decisional modelling and spatial information. Agricultural Water Management 68, 207–232. doi:10.1016/j.agwat.2004.04.004.

Leenhardt, D., Trouvat, J.L., Gonzalès, G., Pérarnaud, V., Prats, S., Bergez, J.E., 2004b. Estimating irrigation demand for water management on a regional scale II: validation of ADEAUMIS. Agricultural Water Management 68, 233–250. doi:10.1016/j.agwat.2004.04.003.

Lehner, B., Czisch, G., Vassolo, S., 2005. The impact of global change on the hydropower potential of Europe: A model-based analysis. Energy Policy 33, 839–855. doi:10.1016/j.enpol.2003.10.018.

Lempert, R., Nakicenovic, N., Sarewitz, D., Schlesinger, M., 2004. Characterizing climate-change uncertainties for decision-makers. an editorial essay. Climatic Change 65, 1–9. doi:10.1023/b:clim.0000037561.75281.b3.

Lempert, R.J., Groves, D.G., Popper, S.W., Bankes, S.C., 2006. A general, analytic method for generating robust strategies and narrative scenarios. Management Science 52, 514–528. doi:10.1287/mnsc.1050.0472.

Lesk, C., Rowhani, P., Ramankutty, N., 2016. Influence of extreme weather disasters on global crop production. Nature 529, 84–87. doi:10.1038/nature16467.

Lhuissier, L., Lamblin, V., Sauquet, E., Arama, Y., Goulard, F., Strosser, P., 2016. Retour sur l'étude prospective Garonne 2050. La Houille Blanche 102, 30–35. doi:10.1051/lhb/2016057.

Li, D., Long, D., Zhao, J., Lu, H., Hong, Y., 2017. Observed changes in flow regimes in the Mekong River basin. Journal of Hydrology 551, 217–232. doi:10.1016/j.jhydrol.2017.05.061.

Lins, H.F., Cohn, T.A., 2011. Stationarity: Wanted dead or alive? JAWRA Journal of the American Water Resources Association 47, 475–480. doi:10.1111/j.1752-1688.2011.00542.x.

Liu, X., Tang, Q., Voisin, N., Cui, H., 2016. Projected impacts of climate change on hydropower potential in China. Hydrology and Earth System Sciences 20, 3343–3359. doi:10.5194/hess-20-3343-2016.

Loch, A., Wheeler, S., Bjornlund, H., Beecham, S., Edwards, J., Zuo, A., Shanahan, M., 2013. The role of water markets in climate change adaptation. National Climate Change Adaptation Research Facility.

López-Moreno, J., Beniston, M., García-Ruiz, J., 2008a. Environmental change and water management in the Pyrenees: Facts and future perspectives for Mediterranean mountains. Global and Planetary Change 61, 300–312. doi:10.1016/j.gloplacha.2007.10.004.

López-Moreno, J., Goyette, S., Beniston, M., 2009. Impact of climate change on snowpack in the Pyrenees: Horizontal spatial variability and vertical gradients. Journal of Hydrology 374, 384–396. doi:10.1016/j.jhydrol.2009.06.049.

López-Moreno, J., Goyette, S., Beniston, M., Alvera, B., 2008b. Sensitivity of the snow energy balance to climatic changes: prediction of snowpack in the Pyrenees in the 21st century. Climate Research 36, 203–217. doi:10.3354/cr00747.

López-Moreno, J., Zabalza, J., Vicente-Serrano, S., Revuelto, J., Gilaberte, M., Azorin-Molina, C., Morán-Tejeda, E., García-Ruiz, J., Tague, C., 2014. Impact of climate and land use change on water availability and reservoir management: Scenarios in the Upper Aragón River, Spanish Pyrenees. Science of The Total Environment 493, 1222–1231. doi:10.1016/j.scitotenv.2013.09.031.

López-Moreno, J.I., Gascoin, S., Herrero, J., Sproles, E.A., Pons, M., Alonso-González, E., Hanich, L., Boudhar, A., Musselman, K.N., Molotch, N.P., Sickman, J., Pomeroy, J., 2017. Different sensitivities of snowpacks to warming in Mediterranean climate mountain areas. Environmental Research Letters 12, 074006. doi:10.1088/1748-9326/aa70cb.

López-Moreno, J.I., Pomeroy, J.W., Revuelto, J., Vicente-Serrano, S.M., 2012. Response of snow processes to climate change: spatial variability in a small basin in the Spanish Pyrenees. Hydrological Processes 27, 2637–2650. doi:10.1002/hyp.9408.

López-Moreno, J.I., Soubeyroux, J.M., Gascoin, S., Alonso-Gonzalez, E., Durán-Gómez, N., Lafaysse, M., Vernay, M., Carmagnola, C., Morin, S., 2020. Long-term trends (1958–2017) in snow cover duration and depth in the Pyrenees. International Journal of Climatology 40, 6122–6136. doi:10.1002/joc.6571.

López-Moreno, J.I., Vicente-Serrano, S.M., Moran-Tejeda, E., Zabalza, J., Lorenzo-Lacruz, J., García-Ruiz, J.M., 2011. Impact of climate evolution and land use changes on water yield in the Ebro basin. Hydrology and Earth System Sciences 15, 311–322. doi:10.5194/hess-15-311-2011.

Loucks, D.P., van Beek, E., 2017. Water resource systems planning and management: An Overview. Springer International Publishing. doi:10.1007/978-3-319-44234-1.

Ma, T., Sun, S., Fu, G., Hall, J.W., Ni, Y., He, L., Yi, J., Zhao, N., Du, Y., Pei, T., Cheng, W., Song, C., Fang, C., Zhou, C., 2020. Pollution exacerbates China's water scarcity and its regional inequality. Nature Communications 11. doi:10.1038/s41467-020-14532-5.

Madani, K., 2010. Game theory and water resources. Journal of Hydrology 381, 225–238. doi:10.1016/j.jhydrol.2009.11.045.

Madani, K., Lund, J.R., 2009. Estimated impacts of climate warming on California's high-elevation hydropower. Climatic Change 102, 521–538. doi:10.1007/s10584-009-9750-8.

Maier, H., Guillaume, J., van Delden, H., Riddell, G., Haasnoot, M., Kwakkel, J., 2016. An uncertain future, deep uncertainty, scenarios, robustness and adaptation: How do they fit together? Environmental Modelling & Software 81, 154–164. doi:10.1016/j.envsoft.2016.03.014.

Maier, H., Kapelan, Z., Kasprzyk, J., Kollat, J., Matott, L., Cunha, M., Dandy, G., Gibbs, M., Keedwell, E., Marchi, A., Ostfeld, A., Savic, D., Solomatine, D., Vrugt, J., Zecchin, A., Minsker, B., Barbour, E., Kuczera, G., Pasha, F., Castelletti, A., Giuliani, M., Reed, P., 2014. Evolutionary algorithms and other metaheuristics in water resources: Current status, research challenges and future directions. Environmental Modelling & Software 62, 271–299. doi:10.1016/j.envsoft.2014.09.013.

Majone, B., Bovolo, C.I., Bellin, A., Blenkinsop, S., Fowler, H.J., 2012. Modeling the impacts of future climate change on water resources for the Gállego river basin (Spain). Water Resources Research 48. doi:10.1029/2011wr010985.

Majone, B., Villa, F., Deidda, R., Bellin, A., 2016. Impact of climate change and water use policies on hydropower potential in the south-eastern Alpine region. Science of The Total Environment 543, 965–980. doi:10.1016/j.scitotenv.2015.05.009.

Malek, Ž., Verburg, P.H., 2017. Adaptation of land management in the Mediterranean under scenarios of irrigation water use and availability. Mitigation and Adaptation Strategies for Global Change 23, 821–837. doi:10.1007/s11027-017-9761-0.

Maran, S., Volonterio, M., Gaudard, L., 2014. Climate change impacts on hydropower in an Alpine catchment. Environmental Science & Policy 43, 15–25. doi:10.1016/j.envsci.2013.12.001.

Markoff, M.S., Cullen, A.C., 2008. Impact of climate change on Pacific Northwest hydropower. Climatic Change 87, 451–469. doi:10.1007/s10584-007-9306-8.

Mastrandrea, M.D., Heller, N.E., Root, T.L., Schneider, S.H., 2010. Bridging the gap: Linking climate-impacts research with adaptation planning and management. Climatic Change 100, 87–101. doi:10.1007/s10584-010-9827-4.

Maton, L., Leenhardt, D., Goulard, M., Bergez, J.E., 2005. Assessing the irrigation strategies over a wide geographical area from structural data about farming systems. Agricultural Systems 86, 293–311. doi:10.1016/j.agsy.2004.09.010.

McCabe, G.J., Wolock, D.M., 2007. Warming may create substantial water supply shortages in the Colorado River basin. Geophysical Research Letters 34, L22708. doi:10.1029/2007gl031764.

McMillan, H., Montanari, A., Cudennec, C., Savenije, H., Kreibich, H., Krueger, T., Liu, J., Mejia, A., Loon, A.V., Aksoy, H., Baldassarre, G.D., Huang, Y., Mazvimavi, D., Rogger, M., Sivakumar, B., Bibikova, T., Castellarin, A., Chen, Y., Finger, D., Gelfan, A., Hannah, D.M., Hoekstra, A.Y., Li, H., Maskey, S., Mathevet, T., Mijic, A., Acuña, A.P., Polo, M.J., Rosales, V., Smith, P., Viglione, A., Srinivasan, V., Toth, E., van

Nooyen, R., Xia, J., 2016. Panta Rhei 2013–2015: Global perspectives on hydrology, society and change. Hydrological Sciences Journal , 1–18doi:10.1080/02626667.2016.1159308.

Mehta, V.K., Haden, V.R., Joyce, B.A., Purkey, D.R., Jackson, L.E., 2013. Irrigation demand and supply, given projections of climate and land-use change, in Yolo County, California. Agricultural Water Management 117, 70–82. doi:10.1016/j.agwat.2012.10.021.

Mendes, I., Lobo, F., Fernández-Salas, L., López-González, N., Bárcenas, P., Schönfeld, J., Ferreira, Ó., 2015. Multi-proxy evidence of rainfall variability recorded in subaqueous deltaic deposits off the Adra River, southeast Iberian Peninsula. Estuarine, Coastal and Shelf Science 167, 300–312. doi:10.1016/j.ecss.2015.08.005.

Mendoza, G., Jeuken, A., Gilroy, K., Matthews, J.H., Kucharski, J., Stakhiv, E., 2018. Climate risk informed decision analysis (CRIDA) - collaborative water resources planning for an uncertain future. United Nations Educational, Scientific, and Cultural Organization, Paris, France.

Mereu, S., Sušnik, J., Trabucco, A., Daccache, A., Vamvakeridou-Lyroudia, L., Renoldi, S., Virdis, A., Savić, D., Assimacopoulos, D., 2016. Operational resilience of reservoirs to climate change, agricultural demand, and tourism: A case study from Sardinia. Science of The Total Environment 543, 1028–1038. doi:10.1016/j.scitotenv.2015.04.066.

Metzger, J., Kanyama, A.C., Wikman-Svahn, P., Sonnek, K.M., Carstens, C., Wester, M., Wedebrand, C., 2021. The flexibility gamble: Challenges for mainstreaming flexible approaches to climate change adaptation. Journal of Environmental Policy & Planning , 1–16doi:10.1080/1523908x.2021.1893160.

Mideksa, T.K., Kallbekken, S., 2010. The impact of climate change on the electricity market: A review. Energy Policy 38, 3579–3585. doi:10.1016/j.enpol.2010.02.035.

Minville, M., Brissette, F., Krau, S., Leconte, R., 2009. Adaptation to climate change in the management of a Canadian water-resources system exploited for hydropower. Water Resources Management 23, 2965–2986. doi:10.1007/s11269-009-9418-1.

Minville, M., Krau, S., Brissette, F., Leconte, R., 2010. Behaviour and performance of a water resource system in Québec (Canada) under adapted operating policies in a climate change context. Water Resources Management 24, 1333–1352. doi:10.1007/s11269-009-9500-8.

Mithen, S., 2010. The domestication of water: water management in the ancient world and its prehistoric origins in the Jordan Valley. Philosophical Transactions of the Royal Society A: Mathematical, Physical and Engineering Sciences 368, 5249–5274. doi:10.1098/rsta.2010.0191.

Montanari, A., Young, G., Savenije, H., Hughes, D., Wagener, T., Ren, L., Koutsoyiannis, D., Cudennec, C., Toth, E., Grimaldi, S., Blöschl, G., Sivapalan, M., Beven, K.,

Gupta, H., Hipsey, M., Schaefli, B., Arheimer, B., Boegh, E., Schymanski, S., Baldassarre, G.D., Yu, B., Hubert, P., Huang, Y., Schumann, A., Post, D., Srinivasan, V., Harman, C., Thompson, S., Rogger, M., Viglione, A., McMillan, H., Characklis, G., Pang, Z., Belyaev, V., 2013. "Panta Rhei—Everything Flows": Change in hydrology and society—The IAHS Scientific Decade 2013–2022. Hydrological Sciences Journal 58, 1256–1275. doi:10.1080/02626667.2013.809088.

Morán-Tejeda, E., Fassnacht, S.R., Lorenzo-Lacruz, J., López-Moreno, J.I., García, C., Alonso-González, E., Collados-Lara, A.J., 2019. Hydro-meteorological characterization of major floods in Spanish mountain rivers. Water 11, 2641. doi:10.3390/w11122641.

Morán-Tejeda, E., Herrera, S., López-Moreno, J.I., Revuelto, J., Lehmann, A., Beniston, M., 2012a. Evolution and frequency (1970–2007) of combined temperature–precipitation modes in the Spanish mountains and sensitivity of snow cover. Regional Environmental Change 13, 873–885. doi:10.1007/s10113-012-0380-8.

Morán-Tejeda, E., López-Moreno, J.I., Sanmiguel-Vallelado, A., 2017. Changes in Climate, Snow and Water Resources in the Spanish Pyrenees: Observations and Projections in a Warming Climate. Springer International Publishing, Cham. chapter 13. pp. 305–323. doi:10.1007/978-3-319-55982-7-13.

Morán-Tejeda, E., Lorenzo-Lacruz, J., López-Moreno, J.I., Ceballos-Barbancho, A., Zabalza, J., Vicente-Serrano, S.M., 2012b. Reservoir management in the Duero Basin (Spain): Impact on river regimes and the response to environmental change. Water Resources Management 26, 2125–2146. doi:10.1007/s11269-012-0004-6.

Morán-Tejeda, E., Zabalza, J., Rahman, K., Gago-Silva, A., López-Moreno, J.I., Vicente-Serrano, S., Lehmann, A., Tague, C.L., Beniston, M., 2014. Hydrological impacts of climate and land-use changes in a mountain watershed: uncertainty estimation based on model comparison. Ecohydrology 8, 1396–1416. doi:10.1002/eco.1590.

MRC, 2018. The study on sustainable management and development of the Mekong River, including impacts of mainstream hydropower projects. https://www.mrcmekong.org/highlights/the-study-on-sustainable-management-and-development-of-the-mekong-river-including-impacts-of-mainstream-hydropower-projects/.

Muelchi, R., Rössler, O., Schwanbeck, J., Weingartner, R., Martius, O., 2021. River runoff in Switzerland in a changing climate – runoff regime changes and their time of emergence. Hydrology and Earth System Sciences 25, 3071–3086. doi:10.5194/hess-25-3071-2021.

Mulligan, M., van Soesbergen, A., Sáenz, L., 2020. GOODD, a global dataset of more than 38,000 georeferenced dams. Scientific Data 7, 31. doi:10.1038/s41597-020-0362-5.

Nam, W.H., Choi, J.Y., Hong, E.M., 2015. Irrigation vulnerability assessment on agricultural water supply risk for adaptive management of climate change in South Korea. Agricultural Water Management 152, 173–187. doi:10.1016/j.agwat.2015.01.012.

National Research Council, 2011. Global change and extreme hydrology: Testing conventional wisdom. National Academies Press, Washington, D.C. doi:10.17226/13211.

Nazemi, A., Zaerpour, M., Hassanzadeh, E., 2020. Uncertainty in bottom-up vulnerability assessments of water supply systems due to regional streamflow generation under changing conditions. Journal of Water Resources Planning and Management 146, 04019071. doi:10.1061/(asce)wr.1943-5452.0001149.

Nicklow, J., Reed, P., Savic, D., Dessalegne, T., Harrell, L., Chan-Hilton, A., Karamouz, M., Minsker, B., Ostfeld, A., Singh, A., and, E.Z., 2010. State of the art for genetic algorithms and beyond in water resources planning and management. Journal of Water Resources Planning and Management 136, 412–432. doi:10.1061/(asce)wr.1943-5452.0000053.

Nilsson, C., Reidy, C.A., Dynesius, M., Revenga, C., 2005. Fragmentation and flow regulation of the world's large river systems. Science 308, 405–408. doi:10.1126/science.1107887.

Nunes, J.P., Jacinto, R., Keizer, J.J., 2017. Combined impacts of climate and socio-economic scenarios on irrigation water availability for a dry Mediterranean reservoir. Science of The Total Environment 584-585, 219–233. doi:10.1016/j.scitotenv.2017.01.131.

Okkan, U., Kirdemir, U., 2018. Investigation of the behavior of an agricultural-operated dam reservoir under RCP scenarios of AR5-IPCC. Water Resources Management 32, 2847–2866. doi:10.1007/s11269-018-1962-0.

Oni, S., Dillon, P., Metcalfe, R., Futter, M., 2012. Dynamic modelling of the impact of climate change and power flow management options using STELLA: Application to the Steephill Falls Reservoir, Ontario, Canada. Canadian Water Resources Journal 37, 125–148. doi:10.4296/cwrj3702831.

Oudin, L., Hervieu, F., Michel, C., Perrin, C., Andréassian, V., Anctil, F., Loumagne, C., 2005. Which potential evapotranspiration input for a lumped rainfall–runoff model? Journal of Hydrology 303, 290–306. doi:10.1016/j.jhydrol.2004.08.026.

Pagán, B.R., Ashfaq, M., Rastogi, D., Kendall, D.R., Kao, S.C., Naz, B.S., Mei, R., Pal, J.S., 2016. Extreme hydrological changes in the southwestern US drive reductions in water supply to Southern California by mid century. Environmental Research Letters 11, 094026. doi:10.1088/1748-9326/11/9/094026.

Palmer, M.A., Reidy Liermann, C.A., Nilsson, C., Flörke, M., Alcamo, J., Lake, S., Bond, N., 2008. Climate change and the world's river basins: Anticipating management options. Frontiers in Ecology and the Environment 6, 81–89. doi:10.1890/060148.

Park, J.Y., Kim, S.J., 2014. Potential impacts of climate change on the reliability of water and hydropower supply from a multipurpose dam in South Korea. JAWRA Journal of the American Water Resources Association 50, 1273–1288. doi:10.1111/jawr.12190.

Patin, J., 1967. L'évolution morphologique du plateau de Lannemezan. Revue géographique des Pyrénées et du Sud-Ouest 38, 325–337. doi:10.3406/rgpso.1967.4825.

Patsialis, T., Kougias, I., Kazakis, N., Theodossiou, N., Droege, P., 2016. Supporting renewables' penetration in remote areas through the transformation of non-powered dams. Energies 9, 1054. doi:10.3390/en9121054.

Payne, J., Wood, A., Hamlet, A., Palmer, R., Lettenmaier, D., 2004. Mitigating the effects of climate change on the water resources of the Columbia River basin. Climatic Change 62, 233–256. doi:10.1023/B:CLIM.0000013694.18154.d6.

Pepin, N., Bradley, R., Diaz, H., Baraer, M., Cáceres, B., Forsythe, N., Fowler, H., Greenwood, G., Hashmi, M., Liu, X., Miller, J., Ning, L., Ohmura, A., Palazzi, E., Rangwala, I., Schöner, W., Severskiy, I., Shahgedanova, M., Wang, M., Yang, D., 2015. Elevation-dependent warming in mountain regions of the world. Nature Climate Change 5, 424–430. doi:10.1038/nclimate2563.

Pereira-Cardenal, S.J., Madsen, H., Arnbjerg-Nielsen, K., Riegels, N., Jensen, R., Mo, B., Wangensteen, I., Bauer-Gottwein, P., 2014. Assessing climate change impacts on the Iberian power system using a coupled water-power model. Climatic Change 126, 351–364. doi:10.1007/s10584-014-1221-1.

Perrin, C., Michel, C., Andréassian, V., 2003. Improvement of a parsimonious model for streamflow simulation. Journal of Hydrology 279, 275–289. doi:10.1016/s0022-1694(03)00225-7.

Perrone, D., Hornberger, G.M., 2014. Water, food, and energy security: Scrambling for resources or solutions? Wiley Interdisciplinary Reviews: Water 1, 49–68. doi:10.1002/wat2.1004.

Pino, D., Ruiz-Bellet, J.L., Balasch, J.C., Romero-León, L., Tuset, J., Barriendos, M., Mazon, J., Castelltort, X., 2016. Meteorological and hydrological analysis of major floods in NE Iberian Peninsula. Journal of Hydrology 541, 63–89. doi:10.1016/j.jhydrol.2016.02.008.

Poff, N.L., Brown, C.M., Grantham, T.E., Matthews, J.H., Palmer, M.A., Spence, C.M., Wilby, R.L., Haasnoot, M., Mendoza, G.F., Dominique, K.C., Baeza, A., 2015. Sustainable water management under future uncertainty with eco-engineering decision scaling. Nature Climate Change 6, 25–34. doi:10.1038/nclimate2765.

Poff, N.L., Olden, J.D., Merritt, D.M., Pepin, D.M., 2007. Homogenization of regional river dynamics by dams and global biodiversity implications. Proceedings of the National Academy of Sciences 104, 5732–5737. doi:10.1073/pnas.0609812104.

Poff, N.L., Zimmerman, J.K.H., 2010. Ecological responses to altered flow regimes: A literature review to inform the science and management of environmental flows. Freshwater Biology 55, 194–205. doi:10.1111/j.1365-2427.2009.02272.x.

Prudhomme, C., Crooks, S., Kay, A.L., Reynard, N., 2013a. Climate change and river flooding: Part 1 classifying the sensitivity of British catchments. Climatic Change 119, 933–948. doi:10.1007/s10584-013-0748-x.

Prudhomme, C., Kay, A.L., Crooks, S., Reynard, N., 2013b. Climate change and river flooding: Part 2 sensitivity characterisation for British catchments and example vulnerability assessments. Climatic Change 119, 949–964. doi:10.1007/s10584-013-0726-3.

Prudhomme, C., Sauquet, E., Watts, G., 2015. Low flow response surfaces for drought decision support: A case study from the UK. Journal of Extreme Events 02, 1550005. doi:10.1142/s2345737615500050.

Prudhomme, C., Wilby, R., Crooks, S., Kay, A., Reynard, N., 2010. Scenario-neutral approach to climate change impact studies: Application to flood risk. Journal of Hydrology 390, 198–209. doi:10.1016/j.jhydrol.2010.06.043.

Purkey, D.R., Joyce, B., Vicuna, S., Hanemann, M.W., Dale, L.L., Yates, D., Dracup, J.A., 2007. Robust analysis of future climate change impacts on water for agriculture and other sectors: A case study in the Sacramento Valley. Climatic Change 87, S109–S122. doi:10.1007/s10584-007-9375-8.

Pushpalatha, R., Perrin, C., Moine, N.L., Mathevet, T., Andréassian, V., 2011. A downward structural sensitivity analysis of hydrological models to improve low-flow simulation. Journal of Hydrology 411, 66–76. doi:10.1016/j.jhydrol.2011.09.034.

Puspitarini, H.D., François, B., Zaramella, M., Brown, C., Borga, M., 2020. The impact of glacier shrinkage on energy production from hydropower-solar complementarity in Alpine river basins. Science of The Total Environment 719, 137488. doi:10.1016/j.scitotenv.2020.137488.

Qin, P., Xu, H., Liu, M., Xiao, C., Forrest, K.E., Samuelsen, S., Tarroja, B., 2020a. Assessing concurrent effects of climate change on hydropower supply, electricity demand, and greenhouse gas emissions in the Upper Yangtze River basin of China. Applied Energy 279, 115694. doi:10.1016/j.apenergy.2020.115694.

Qin, Y., Abatzoglou, J.T., Siebert, S., Huning, L.S., AghaKouchak, A., Mankin, J.S., Hong, C., Tong, D., Davis, S.J., Mueller, N.D., 2020b. Agricultural risks from changing snowmelt. Nature Climate Change 10, 459–465. doi:10.1038/s41558-020-0746-8.

Quinn, J.D., Reed, P.M., Giuliani, M., Castelletti, A., 2017. Rival framings: A framework for discovering how problem formulation uncertainties shape risk management trade-offs in water resources systems. Water Resources Research 53, 7208–7233. doi:10.1002/2017wr020524.

Quinn, J.D., Reed, P.M., Giuliani, M., Castelletti, A., Oyler, J.W., Nicholas, R.E., 2018. Exploring how changing monsoonal dynamics and human pressures challenge multireservoir management for flood protection, hydropower production, and agricultural water supply. Water Resources Research 54, 4638–4662. doi:10.1029/2018wr022743.

Quintana-Seguí, P., Peral, C., Turco, M., Llasat, M., Martin, E., 2016. Meteorological analysis systems in North-East Spain: Validation of SAFRAN and SPAN. Journal of Environmental Informatics 27, 116–130. doi:10.3808/jei.201600335.

Quintana-Seguí, P., Turco, M., Herrera, S., Miguez-Macho, G., 2017. Validation of a new SAFRAN-based gridded precipitation product for Spain and comparisons to Spain02 and ERA-Interim. Hydrology and Earth System Sciences 21, 2187–2201. doi:10.5194/hess-21-2187-2017.

Rajagopalan, B., Nowak, K., Prairie, J., Hoerling, M., Harding, B., Barsugli, J., Ray, A., Udall, B., 2009. Water supply risk on the Colorado River: Can management mitigate? Water Resources Research 45, W08201. doi:10.1029/2008wr007652.

Rajagopalan, K., Chinnayakanahalli, K.J., Stockle, C.O., Nelson, R.L., Kruger, C.E., Brady, M.P., Malek, K., Dinesh, S.T., Barber, M.E., Hamlet, A.F., Yorgey, G.G., Adam, J.C., 2018. Impacts of near-term climate change on irrigation demands and crop yields in the Columbia River basin. Water Resources Research 54, 2152–2182. doi:10.1002/2017wr020954.

Raje, D., Mujumdar, P., 2010. Reservoir performance under uncertainty in hydrologic impacts of climate change. Advances in Water Resources 33, 312–326. doi:10.1016/j.advwatres.2009.12.008.

Rani, D., Moreira, M.M., 2009. Simulation–optimization modeling: A survey and potential application in reservoir systems operation. Water Resources Management 24, 1107–1138. doi:10.1007/s11269-009-9488-0.

Ray, P., Wi, S., Schwarz, A., Correa, M., He, M., Brown, C., 2020. Vulnerability and risk: Climate change and water supply from California's Central Valley water system. Climatic Change 161, 177–199. doi:10.1007/s10584-020-02655-z.

Ray, P.A., Bonzanigo, L., Wi, S., Yang, Y.C.E., Karki, P., García, L.E., Rodriguez, D.J., Brown, C.M., 2018. Multidimensional stress test for hydropower investments facing climate, geophysical and financial uncertainty. Global Environmental Change 48, 168–181. doi:10.1016/j.gloenvcha.2017.11.013.

Reclamation, 2016. SECURE Water Act Section 9503(c) - Reclamation Climate Change and Water: Prepared for the United States Congress. Technical Report. U.S. Department of the Interior Bureau of Reclamation. Denver, CO: Bureau of Reclamation, Policy and Administration.

Reclamation, 2021. Water Reliability in the West - 2021 SECURE Water Act Report: Prepared for the United States Congress. Technical Report. U.S. Department of the Interior Bureau of Reclamation. Denver, CO: Bureau of Reclamation, Water Resources and Planning Office.

Reed, P., Hadka, D., Herman, J., Kasprzyk, J., Kollat, J., 2013. Evolutionary multiobjective optimization in water resources: The past, present, and future. Advances in Water Resources 51, 438–456. doi:10.1016/j.advwatres.2012.01.005.

Rehana, S., Mujumdar, P.P., 2012. Regional impacts of climate change on irrigation water demands. Hydrological Processes 27, 2918–2933. doi:10.1002/hyp.9379.

Renöfält, B.M., Jansson, R., Nilsson, C., 2010. Effects of hydropower generation and opportunities for environmental flow management in Swedish riverine ecosystems. Freshwater Biology 55, 49–67. doi:10.1111/j.1365-2427.2009.02241.x.

Riboust, P., Thirel, G., Moine, N.L., Ribstein, P., 2018. Revisiting a simple degree-day model for integrating satellite data: Implementation of SWE-SCA hystereses. Journal of Hydrology and Hydromechanics 67, 70–81. doi:10.2478/johh-2018-0004.

Ritchie, H., 2017. Water use and stress. Our World in Data Https://ourworldindata.org/water-use-stress.

Ritchie, H., Roser, M., 2014. Natural disasters. Our World in Data https://ourworldindata.org/natural-disasters.

Rocha, J., Carvalho-Santos, C., Diogo, P., Beça, P., Keizer, J.J., Nunes, J.P., 2020. Impacts of climate change on reservoir water availability, quality and irrigation needs in a water scarce Mediterranean region (southern Portugal). Science of The Total Environment 736, 139477. doi:10.1016/j.scitotenv.2020.139477.

Ronco, P., Zennaro, F., Torresan, S., Critto, A., Santini, M., Trabucco, A., Zollo, A., Galluccio, G., Marcomini, A., 2017. A risk assessment framework for irrigated agriculture under climate change. Advances in Water Resources 110, 562–578. doi:10.1016/j.advwatres.2017.08.003.

Ruddiman, W.F., 2018. Three flaws in defining a formal 'Anthropocene'. Progress in Physical Geography: Earth and Environment 42, 451–461. doi:10.1177/0309133318783142.

Sánchez-Chóliz, J., Sarasa, C., 2015. River flows in the Ebro basin: A century of evolution, 1913–2013. Water 7, 3072–3082. doi:10.3390/w7063072.

Sandoval-Solis, S., McKinney, D.C., Loucks, D.P., 2011. Sustainability index for water resources planning and management. Journal of Water Resources Planning and Management 137, 381–390. doi:10.1061/(asce)wr.1943-5452.0000134.

Santos, L., Thirel, G., Perrin, C., 2018. Technical note: pitfalls in using log-transformed flows within the KGE criterion. Hydrology and Earth System Sciences 22, 4583–4591. doi:10.5194/hess-22-4583-2018.

Sauquet, E., Richard, B., Devers, A., Prudhomme, C., 2019. Water restrictions under climate change: A Rhône–Mediterranean perspective combining bottom-up and top-down approaches. Hydrology and Earth System Sciences 23, 3683–3710. doi:10.5194/hess-23-3683-2019.

Savelsberg, J., Schillinger, M., Schlecht, I., Weigt, H., 2018. The impact of climate change on Swiss hydropower. Sustainability 10, 2541. doi:10.3390/su10072541.

Schaefli, B., 2015. Projecting hydropower production under future climates: A guide for decision-makers and modelers to interpret and design climate change impact assessments. Wiley Interdisciplinary Reviews: Water 2, 271–289. doi:10.1002/wat2.1083.

Schaefli, B., Hingray, B., Musy, A., 2007. Climate change and hydropower production in the Swiss Alps: Quantification of potential impacts and related modelling uncertainties. Hydrology and Earth System Sciences 11, 1191–1205. doi:10.5194/hess-11-1191-2007.

Schittekatte, T., Reif, V., Meeus, L., 2021. Welcoming new entrants into European electricity markets. Energies 14, 4051. doi:10.3390/en14134051.

Schlef, K.E., Steinschneider, S., Brown, C.M., 2018. Spatiotemporal impacts of climate and demand on water supply in the Apalachicola-Chattahoochee-Flint basin. Journal of Water Resources Planning and Management 144, 05017020. doi:10.1061/(asce)wr.1943-5452.0000865.

Senthilkumar, K., Bergez, J.E., Leenhardt, D., 2015. Can farmers use maize earliness choice and sowing dates to cope with future water scarcity? a modelling approach applied to south-western france. Agricultural Water Management 152, 125–134. doi:10.1016/j.agwat.2015.01.004.

Seung-Hwan, Y., Jin-Yong, C., Sang-Hyun, L., Yun-Gyeong, O., Koun, Y.D., 2013. Climate change impacts on water storage requirements of an agricultural reservoir considering changes in land use and rice growing season in Korea. Agricultural Water Management 117, 43–54. doi:10.1016/j.agwat.2012.10.023.

Shrestha, B., Cochrane, T.A., Caruso, B.S., Arias, M.E., 2017. Land use change uncertainty impacts on streamflow and sediment projections in areas undergoing rapid development: A case study in the Mekong basin. Land Degradation & Development 29, 835–848. doi:10.1002/ldr.2831.

Singh, R., Wagener, T., Crane, R., Mann, M.E., Ning, L., 2014. A vulnerability driven approach to identify adverse climate and land use change combinations for critical hydrologic indicator thresholds: Application to a watershed in Pennsylvania, USA. Water Resources Research 50, 3409–3427. doi:10.1002/2013wr014988.

Sivapalan, M., Blöschl, G., 2015. Time scale interactions and the coevolution of humans and water. Water Resources Research 51, 6988–7022. doi:10.1002/2015wr017896.

Smiatek, G., Kunstmann, H., Senatore, A., 2016. EURO-CORDEX regional climate model analysis for the Greater Alpine Region: Performance and expected future change. Journal of Geophysical Research: Atmospheres 121, 7710–7728. doi:10.1002/2015jd024727.

Sovacool, B.K., 2011. Hard and soft paths for climate change adaptation. Climate Policy 11, 1177–1183. doi:10.1080/14693062.2011.579315.

Spinoni, J., Vogt, J., Barbosa, P., 2014. European degree-day climatologies and trends for the period 1951-2011. International Journal of Climatology 35, 25–36. doi:10.1002/joc.3959.

Spinoni, J., Vogt, J.V., Barbosa, P., Dosio, A., McCormick, N., Bigano, A., Füssel, H.M., 2017a. Changes of heating and cooling degree-days in Europe from 1981 to 2100. International Journal of Climatology 38, 191–208. doi:10.1002/joc.5362.

Spinoni, J., Vogt, J.V., Naumann, G., Barbosa, P., Dosio, A., 2017b. Will drought events become more frequent and severe in Europe? International Journal of Climatology 38, 1718–1736. doi:10.1002/joc.5291.

Stainforth, D.A., Downing, T.E., Washington, R., Lopez, A., New, M., 2007. Issues in the interpretation of climate model ensembles to inform decisions. Philosophical Transactions of the Royal Society A: Mathematical, Physical and Engineering Sciences 365, 2163–2177. doi:10.1098/rsta.2007.2073.

Stanton, M.C.B., Dessai, S., Paavola, J., 2016. A systematic review of the impacts of climate variability and change on electricity systems in Europe. Energy 109, 1148–1159. doi:10.1016/j.energy.2016.05.015.

Steffen, W., Broadgate, W., Deutsch, L., Gaffney, O., Ludwig, C., 2015a. The trajectory of the Anthropocene: The great acceleration. The Anthropocene Review 2, 81–98. doi:10.1177/2053019614564785.

Steffen, W., Richardson, K., Rockström, J., Cornell, S.E., Fetzer, I., Bennett, E.M., Biggs, R., Carpenter, S.R., de Vries, W., de Wit, C.A., Folke, C., Gerten, D., Heinke, J., Mace, G.M., Persson, L.M., Ramanathan, V., Reyers, B., Sörlin, S., 2015b. Planetary boundaries: guiding human development on a changing planet. Science 347. doi:10.1126/science.1259855.

Steinschneider, S., Brown, C., 2012. Dynamic reservoir management with real-option risk hedging as a robust adaptation to nonstationary climate. Water Resources Research 48. doi:10.1029/2011wr011540.

Steinschneider, S., Brown, C., 2013. A semiparametric multivariate, multisite weather generator with low-frequency variability for use in climate risk assessments. Water Resources Research 49, 7205–7220. doi:10.1002/wrcr.20528.

Steinschneider, S., McCrary, R., Wi, S., Mulligan, K., Mearns, L.O., Brown, C., 2015. Expanded decision-scaling framework to select robust long-term water-system plans under gydroclimatic uncertainties. Journal of Water Resources Planning and Management 141, 04015023. doi:10.1061/(asce)wr.1943-5452.0000536.

Steinschneider, S., Ray, P., Rahat, S.H., Kucharski, J., 2019. A weather-regime-based stochastic weather generator for climate vulnerability assessments of water systems in the western United States. Water Resources Research 55, 6923–6945. doi:10.1029/2018wr024446.

Stöckle, C.O., Nelson, R.L., Higgins, S., Brunner, J., Grove, G., Boydston, R., Whiting, M., Kruger, C., 2010. Assessment of climate change impact on Eastern Washington agriculture. Climatic Change 102, 77–102. doi:10.1007/s10584-010-9851-4.

Su, Y., Kern, J.D., Characklis, G.W., 2017. The impact of wind power growth and hydrological uncertainty on financial losses from oversupply events in hydropower-dominated systems. Applied Energy 194, 172–183. doi:10.1016/j.apenergy.2017.02.067.

Suen, J.P., 2010. Determining the ecological flow regime for existing reservoir operation. Water Resources Management 25, 817–835. doi:10.1007/s11269-010-9728-3.

Swain, D.L., Tsiang, M., Haugen, M., Singh, D., Charland, A., Rajaratnam, B., Diffenbaugh, N.S., 2014. The extraordinary California drought of 2013/2014: Character,

context, and the role of climate change. Bulletin of the American Meteorological Society 95, S3–S7.

Tabari, H., 2020. Climate change impact on flood and extreme precipitation increases with water availability. Scientific Reports 10. doi:10.1038/s41598-020-70816-2.

Tanaka, S., Zhu, T., Lund, J., Howitt, R., Jenkins, M., Pulido, M., Tauber, M., Ritzema, R., Ferreira, I., 2006. Climate warming and water management adaptation for California climatic change. Climatic Change 76, 361–387. doi:10.1007/s10584-006-9079-5.

Taner, M.Ü., Ray, P., Brown, C., 2017. Robustness-based evaluation of hydropower infrastructure design under climate change. Climate Risk Management 18, 34–50. doi:10.1016/j.crm.2017.08.002.

Tang, F.H.M., Lenzen, M., McBratney, A., Maggi, F., 2021. Risk of pesticide pollution at the global scale. Nature Geoscience 14, 206–210. doi:10.1038/s41561-021-00712-5.

Tapiador, F.J., Navarro, A., Moreno, R., Sánchez, J.L., García-Ortega, E., 2020. Regional climate models: 30 years of dynamical downscaling. Atmospheric Research 235, 104785. doi:10.1016/j.atmosres.2019.104785.

Terray, L., Boé, J., 2013a. Quantifying 21st-century France climate change and related uncertainties. Comptes Rendus Geoscience 345, 136–149. doi:10.1016/j.crte.2013.02.003.

Terray, L., Boé, J., 2013b. Quantifying 21st-century France climate change and related uncertainties. Comptes Rendus Geoscience 345, 136–149. doi:10.1016/j.crte.2013.02.003.

Teyssier, F., 2006. Les consommations d'eau pour irrgation en Midi-Pyrénées. Technical Report. Direction régional de l'agriculture et de la forêt de Midi-Pyrénées.

Tilmant, A., Goor, Q., Pinte, D., 2009. Agricultural-to-hydropower water transfers: Sharing water and benefits in hydropower-irrigation systems. Hydrology and Earth System Sciences 13, 1091–1101. doi:10.5194/hess-13-1091-2009.

Tilmant, A., Pina, J., Salman, M., Casarotto, C., Ledbi, F., Pek, E., 2020. Probabilistic trade-off assessment between competing and vulnerable water users – the case of the senegal river basin. Journal of Hydrology 587, 124915. doi:10.1016/j.jhydrol.2020.124915.

Tramblay, Y., Llasat, M.C., Randin, C., Coppola, E., 2020. Climate change impacts on water resources in the Mediterranean. Regional Environmental Change 20. doi:10.1007/s10113-020-01665-y.

Trenberth, K.E., Dai, A., van der Schrier, G., Jones, P.D., Barichivich, J., Briffa, K.R., Sheffield, J., 2013. Global warming and changes in drought. Nature Climate Change 4, 17–22. doi:10.1038/nclimate2067.

Tuel, A., Eltahir, E.A.B., 2020. Why is the Mediterranean a climate change hot spot? Journal of Climate 33, 5829–5843. doi:10.1175/jcli-d-19-0910.1.

Turner, S.W., Hejazi, M., Kim, S.H., Clarke, L., Edmonds, J., 2017a. Climate impacts on hydropower and consequences for global electricity supply investment needs. Energy 141, 2081–2090. doi:10.1016/j.energy.2017.11.089.

Turner, S.W., Ng, J.Y., Galelli, S., 2017b. Examining global electricity supply vulnerability to climate change using a high-fidelity hydropower dam model. Science of The Total Environment 590-591, 663–675. doi:10.1016/j.scitotenv.2017.03.022.

Turner, S.W.D., Marlow, D., Ekström, M., Rhodes, B.G., Kularathna, U., Jeffrey, P.J., 2014. Linking climate projections to performance: A yield-based decision scaling assessment of a large urban water resources system. Water Resources Research 50, 3553–3567. doi:10.1002/2013wr015156.

Turner, S.W.D., Voisin, N., 2022. Simulation of hydropower at subcontinental to global scales: a state-of-the-art review. Environmental Research Letters 17, 023002. doi:10.1088/1748-9326/ac4e38.

Turner, S.W.D., Voisin, N., Fazio, J., Hua, D., Jourabchi, M., 2019. Compound climate events transform electrical power shortfall risk in the Pacific Northwest. Nature Communications 10. doi:10.1038/s41467-018-07894-4.

Udall, B., Overpeck, J., 2017. The twenty-first century Colorado River hot drought and implications for the future. Water Resources Research 53, 2404–2418. doi:10.1002/2016wr019638.

Valéry, A., Andréassian, V., Perrin, C., 2014a. 'as simple as possible but not simpler': What is useful in a temperature-based snow-accounting routine? part 1 – comparison of six snow accounting routines on 380 catchments. Journal of Hydrology 517, 1166–1175. doi:10.1016/j.jhydrol.2014.04.059.

Valéry, A., Andréassian, V., Perrin, C., 2014b. 'as simple as possible but not simpler': What is useful in a temperature-based snow-accounting routine? part 2 – sensitivity analysis of the cemaneige snow accounting routine on 380 catchments. Journal of Hydrology 517, 1176–1187. doi:10.1016/j.jhydrol.2014.04.058.

Van Dijk, A.I.J.M., Beck, H.E., Crosbie, R.S., de Jeu, R.A.M., Liu, Y.Y., Podger, G.M., Timbal, B., Viney, N.R., 2013. The Millennium Drought in southeast Australia (2001-2009): Natural and human causes and implications for water resources, ecosystems, economy, and society. Water Resources Research 49, 1040–1057. doi:10.1002/wrcr.20123.

Van Loon, A.F., Gleeson, T., Clark, J., Dijk, A.I.J.M.V., Stahl, K., Hannaford, J., Baldassarre, G.D., Teuling, A.J., Tallaksen, L.M., Uijlenhoet, R., Hannah, D.M., Sheffield, J., Svoboda, M., Verbeiren, B., Wagener, T., Rangecroft, S., Wanders, N., Lanen, H.A.J.V., 2016. Drought in the Anthropocene. Nature Geoscience 9, 89–91. doi:10.1038/ngeo2646.

Van Vliet, M., Van Beek, L., Eisner, S., Flörke, M., Wada, Y., Bierkens, M., 2016a. Multi-model assessment of global hydropower and cooling water discharge potential under climate change. Global Environmental Change 40, 156–170. doi:10.1016/j.gloenvcha.2016.07.007.

Van Vliet, M.T.H., Wiberg, D., Leduc, S., Riahi, K., 2016b. Power-generation system vulnerability and adaptation to changes in climate and water resources. Nature Climate Change 6, 375–380. doi:10.1038/nclimate2903.

Vano, J.A., 2020. Implications of losing snowpack. Nature Climate Change 10, 388–390. doi:10.1038/s41558-020-0769-1.

Vano, J.A., Nijssen, B., Lettenmaier, D.P., 2015. Seasonal hydrologic responses to climate change in the Pacific Northwest. Water Resources Research 51, 1959–1976. doi:10.1002/2014wr015909.

Vano, J.A., Scott, M.J., Voisin, N., Stöckle, C.O., Hamlet, A.F., Mickelson, K.E.B., Elsner, M.M., Lettenmaier, D.P., 2010. Climate change impacts on water management and irrigated agriculture in the Yakima River basin, Washington, USA. Climatic Change 102, 287–317. doi:10.1007/s10584-010-9856-z.

Vano, J.A., Udall, B., Cayan, D.R., Overpeck, J.T., Brekke, L.D., Das, T., Hartmann, H.C., Hidalgo, H.G., Hoerling, M., McCabe, G.J., Morino, K., Webb, R.S., Werner, K., Lettenmaier, D.P., 2014. Understanding uncertainties in future Colorado River streamflow. Bulletin of the American Meteorological Society 95, 59–78. doi:10.1175/bams-d-12-00228.1.

VanRheenen, N.T., Wood, A.W., Palmer, R.N., Lettenmaier, D.P., 2004. Potential implications of PCM climate change scenarios for Sacramento–San Joaquin River basin hydrology and water resources. Climatic Change 62, 257–281. doi:10.1023/B:CLIM.0000013686.97342.55.

Varela-Ortega, C., Blanco-Gutiérrez, I., Esteve, P., Bharwani, S., Fronzek, S., Downing, T.E., 2014. How can irrigated agriculture adapt to climate change? Insights from the Guadiana Basin in Spain. Regional Environmental Change 16, 59–70. doi:10.1007/s10113-014-0720-y.

Vicente-Serrano, S.M., Peña-Gallardo, M., Hannaford, J., Murphy, C., Lorenzo-Lacruz, J., Dominguez-Castro, F., López-Moreno, J.I., Beguería, S., Noguera, I., Harrigan, S., Vidal, J.P., 2019. Climate, irrigation, and land cover change explain streamflow trends in countries bordering the Northeast Atlantic. Geophysical Research Letters 46, 10821–10833. doi:10.1029/2019gl084084.

Vicuna, S., Leonardson, R., Hanemann, M.W., Dale, L.L., Dracup, J.A., 2008. Climate change impacts on high elevation hydropower generation in California's Sierra Nevada: A case study in the Upper American River. Climatic Change 87, S123–S137. doi:10.1007/s10584-007-9365-x.

Vicuna, S., Maurer, E.P., Joyce, B., Dracup, J.A., Purkey, D., 2007. The sensitivity of California water resources to climate change scenarios. Journal of the American Water Resources Association 43, 482–498. doi:10.1111/j.1752-1688.2007.00038.x.

Vicuña, S., McPhee, J., Garreaud, R.D., 2012. Agriculture vulnerability to climate change in a snowmelt-driven basin in semiarid Chile. Journal of Water Resources Planning and Management 138, 431–441. doi:10.1061/(asce)wr.1943-5452.0000202.

Vidal, J.P., Hingray, B., Magand, C., Sauquet, E., Ducharne, A., 2016. Hierarchy of climate and hydrological uncertainties in transient low-flow projections. Hydrology and Earth System Sciences 20, 3651–3672. doi:10.5194/hess-20-3651-2016.

Vidal, J.P., Martin, E., Franchistéguy, L., Baillon, M., Soubeyroux, J.M., 2010. A 50-year high-resolution atmospheric reanalysis over France with the Safran system. International Journal of Climatology 30, 1627–1644. doi:10.1002/joc.2003.

Vidal, J.P., Martin, E., Kitova, N., Najac, J., Soubeyroux, J.M., 2012. Evolution of spatio-temporal drought characteristics: Validation, projections and effect of adaptation scenarios. Hydrology and Earth System Sciences 16, 2935–2955. doi:10.5194/hess-16-2935-2012.

Viviroli, D., Archer, D.R., Buytaert, W., Fowler, H.J., Greenwood, G.B., Hamlet, A.F., Huang, Y., Koboltschnig, G., Litaor, M.I., López-Moreno, J.I., Lorentz, S., Schädler, B., Schreier, H., Schwaiger, K., Vuille, M., Woods, R., 2011. Climate change and mountain water resources: Overview and recommendations for research, management and policy. Hydrology and Earth System Sciences 15, 471–504. doi:10.5194/hess-15-471-2011.

Vogel, R.M., Yaindl, C., Walter, M., 2011. Nonstationarity: Flood magnification and recurrence reduction factors in the United States. JAWRA Journal of the American Water Resources Association 47, 464–474. doi:10.1111/j.1752-1688.2011.00541.x.

Voldoire, A., Sanchez-Gomez, E., Salas y Mélia, D., Decharme, B., Cassou, C., Sénési, S., Valcke, S., Beau, I., Alias, A., Chevallier, M., Déqué, M., Deshayes, J., Douville, H., Fernandez, E., Madec, G., Maisonnave, E., Moine, M.P., Planton, S., Saint-Martin, D., Szopa, S., Tyteca, S., Alkama, R., Belamari, S., Braun, A., Coquart, L., Chauvin, F., 2013. The CNRM-CM5.1 global climate model: description and basic evaluation. Climate Dynamics 40, 2091–2121. doi:10.1007/s00382-011-1259-y.

Volodin, E.M., Dianskii, N.A., Gusev, A.V., 2010. Simulating present-day climate with the INMCM4.0 coupled model of the atmospheric and oceanic general circulations. Izvestia Atmospheric and Oceanic Physics 46, 414–431. doi:10.1134/S000143381004002X.

Vormoor, K., Rössler, O., Bürger, G., Bronstert, A., Weingartner, R., 2017. When timing matters-considering changing temporal structures in runoff response surfaces. Climatic Change 142, 213–226. doi:10.1007/s10584-017-1940-1.

Vörösmarty, C.J., Green, P., Salisbury, J., Lammers, R.B., 2000. Global water resources: Vulnerability from climate change and population growth. Science 289, 284–288. doi:10.1126/science.289.5477.284.

Vörösmarty, C.J., McIntyre, P.B., Gessner, M.O., Dudgeon, D., Prusevich, A., Green, P., Glidden, S., Bunn, S.E., Sullivan, C.A., Liermann, C.R., Davies, P.M., 2010. Global threats to human water security and river biodiversity. Nature 467, 555–561. doi:10.1038/nature09440.

Wada, Y., Flörke, M., Hanasaki, N., Eisner, S., Fischer, G., Tramberend, S., Satoh, Y., van Vliet, M.T.H., Yillia, P., Ringler, C., Burek, P., Wiberg, D., 2016. Modeling

global water use for the 21st century: the Water Futures and Solutions (WFaS) initiative and its approaches. Geoscientific Model Development 9, 175–222. doi:10.5194/gmd-9-175-2016.

Wada, Y., Wisser, D., Eisner, S., Flörke, M., Gerten, D., Haddeland, I., Hanasaki, N., Masaki, Y., Portmann, F.T., Stacke, T., Tessler, Z., Schewe, J., 2013. Multimodel projections and uncertainties of irrigation water demand under climate change. Geophysical Research Letters 40, 4626–4632. doi:10.1002/grl.50686.

Wagner, B., Hauer, C., Habersack, H., 2019. Current hydropower developments in Europe. Current Opinion in Environmental Sustainability 37, 41–49. doi:10.1016/j.cosust.2019.06.002.

Wagner, T., Themeßl, M., Schüppel, A., Gobiet, A., Stigler, H., Birk, S., 2016. Impacts of climate change on stream flow and hydro power generation in the Alpine region. Environmental Earth Sciences 76. doi:10.1007/s12665-016-6318-6.

Walker, W.E., Haasnoot, M., Kwakkel, J.H., 2013. Adapt or perish: A review of planning approaches for adaptation under deep uncertainty. Sustainability 5, 955–979. doi:10.3390/su5030955.

Walsh, C.L., Blenkinsop, S., Fowler, H.J., Burton, A., Dawson, R.J., Glenis, V., Manning, L.J., Jahanshahi, G., Kilsby, C.G., 2016. Adaptation of water resource systems to an uncertain future. Hydrology and Earth System Sciences 20, 1869–1884. doi:10.5194/hess-20-1869-2016.

Wang, X., Mei, Y., Kong, Y., Lin, Y., Wang, H., 2017. Improved multi-objective model and analysis of the coordinated operation of a hydro-wind-photovoltaic system. Energy 134, 813–839. doi:10.1016/j.energy.2017.06.047.

Wasti, A., Ray, P., Wi, S., Folch, C., Ubierna, M., Karki, P., 2022. Climate change and the hydropower sector: A global review. WIREs Climate Change doi:10.1002/wcc.757.

Watanabe, S., Hajima, T., Sudo, K., Nagashima, T., Takemura, T., Okajima, H., Nozawa, T., Kawase, H., Abe, M., Yokohata, T., Ise, T., Sato, H., Kato, E., Takata, K., Emori, S., Kawamiya, M., 2011. MIROC-ESM 2010: model description and basic results of CMIP5-20c3m experiments. Geoscientific Model Development 4, 845–872. doi:10.5194/gmd-4-845-2011.

Weiß, M., 2011. Future water availability in selected European catchments: A probabilistic assessment of seasonal flows under the IPCC A1B emission scenario using response surfaces. Natural Hazards and Earth System Sciences 11, 2163–2171. doi:10.5194/nhess-11-2163-2011.

Westra, S., Thyer, M., Leonard, M., Kavetski, D., Lambert, M., 2014. A strategy for diagnosing and interpreting hydrological model nonstationarity. Water Resources Research 50, 5090–5113. doi:10.1002/2013wr014719.

Whateley, S., Steinschneider, S., Brown, C., 2014. A climate change range-based method for estimating robustness for water resources supply. Water Resources Research 50, 8944–8961. doi:10.1002/2014wr015956.

Whateley, S., Steinschneider, S., Brown, C., 2016. Selecting stochastic climate realizations to efficiently explore a wide range of climate risk to water resource systems. Journal of Water Resources Planning and Management 142, 06016002. doi:10.1061/(asce)wr.1943-5452.0000631.

WHO, 2007. Risk reduction and emergency preparedness: WHO six-year strategy for the health sector and community capacity development. WHO, Geneva, Switzerland.

Wilby, R.L., Dessai, S., 2010. Robust adaptation to climate change. Weather 65, 180–185. doi:10.1002/wea.543.

Wilby, R.L., Wigley, T.M.L., 1997. Downscaling general circulation model output: A review of methods and limitations. Progress in Physical Geography: Earth and Environment 21, 530–548. doi:10.1177/030913339702100403.

World Commission on Dams, 2000. Dams and Development: A New Framework for Decision-making: the Report of the World Commission on Dams. Earthscan, London.

World Energy Council, 2013. World Energy Resources 2013, Survey Summary. Technical Report. World Energy Council. London.

Wu, T., Li, W., Ji, J., Xin, X., Li, L., Wang, Z., Zhang, Y., Li, J., Zhang, F., Wei, M., Shi, X., Wu, F., Zhang, L., Chu, M., Jie, W., Liu, Y., Wang, F., Liu, X., Li, Q., Dong, M., Liang, X., Gao, Y., Zhang, J., 2013. Global carbon budgets simulated by the Beijing Climate Center Climate System Model for the last century. Journal of Geophysical Research: Atmospheres 118, 4326–4347. doi:10.1002/jgrd.50320.

Yalew, S.G., van Vliet, M.T.H., Gernaat, D.E.H.J., Ludwig, F., Miara, A., Park, C., Byers, E., Cian, E.D., Piontek, F., Iyer, G., Mouratiadou, I., Glynn, J., Hejazi, M., Dessens, O., Rochedo, P., Pietzcker, R., Schaeffer, R., Fujimori, S., Dasgupta, S., Mima, S., da Silva, S.R.S., Chaturvedi, V., Vautard, R., van Vuuren, D.P., 2020. Impacts of climate change on energy systems in global and regional scenarios. Nature Energy 5, 794–802. doi:10.1038/s41560-020-0664-z.

Yin, X.A., Yang, Z.F., Petts, G.E., 2011. Reservoir operating rules to sustain environmental flows in regulated rivers. Water Resources Research 47. doi:10.1029/2010wr009991.

Yoshikawa, S., Cho, J., Yamada, H.G., Hanasaki, N., Kanae, S., 2014. An assessment of global net irrigation water requirements from various water supply sources to sustain irrigation: Rivers and reservoirs (1960–2050). Hydrology and Earth System Sciences 18, 4289–4310. doi:10.5194/hess-18-4289-2014.

Yu, C., Huang, X., Chen, H., Godfray, H.C.J., Wright, J.S., Hall, J.W., Gong, P., Ni, S., Qiao, S., Huang, G., Xiao, Y., Zhang, J., Feng, Z., Ju, X., Ciais, P., Stenseth, N.C., Hessen, D.O., Sun, Z., Yu, L., Cai, W., Fu, H., Huang, X., Zhang, C., Liu, H., Taylor, J., 2019. Managing nitrogen to restore water quality in china. Nature 567, 516–520. doi:10.1038/s41586-019-1001-1.

Yukimoto, S., Adachi, Y., Hosaka, M., Sakami, T., Yoshimura, H., Hirabara, M., Tanaka, T.Y., Shindo, E., Tsujino, H., Deushi, M., Mizuta, R., Yabu, S., Obata, A., Nakano,

H., Koshiro, T., Ose, T., Kitoh, A., 2012. A new global climate model of the Meteorological Research Institute: MRI-CGCM3 —model description and basic performance—. Journal of the Meteorological Society of Japan. Ser. II 90A, 23–64. doi:10.2151/jmsj.2012-A02.

Zalasiewicz, J., Waters, C.N., Head, M.J., Poirier, C., Summerhayes, C.P., Leinfelder, R., Grinevald, J., Steffen, W., Syvitski, J., Haff, P., McNeill, J.R., Wagreich, M., Fairchild, I.J., Richter, D.D., Vidas, D., Williams, M., Barnosky, A.D., Cearreta, A., 2019. A formal Anthropocene is compatible with but distinct from its diachronous anthropogenic counterparts: a response to W.F. Ruddiman's 'three flaws in defining a formal Anthropocene'. Progress in Physical Geography: Earth and Environment 43, 319–333. doi:10.1177/0309133319832607.

Zambrano-Bigiarini, M., Rojas, R., 2013. A model-independent Particle Swarm Optimisation software for model calibration. Environmental Modelling & Software 43, 5–25. doi:10.1016/j.envsoft.2013.01.004.

Zandvoort, M., Campos, I.S., Vizinho, A., Penha-Lopes, G., Lorencová, E.K., van der Brugge, R., van der Vlist, M.J., van den Brink, A., Jeuken, A.B., 2017. Adaptation pathways in planning for uncertain climate change: Applications in Portugal, the Czech Republic and the Netherlands. Environmental Science & Policy 78, 18–26. doi:10.1016/j.envsci.2017.08.017.

Zarfl, C., Lumsdon, A.E., Berlekamp, J., Tydecks, L., Tockner, K., 2015. A global boom in hydropower dam construction. Aquatic Sciences 77, 161–170. doi:10.1007/s00027-014-0377-0.

Zeff, H.B., Herman, J.D., Reed, P.M., Characklis, G.W., 2016. Cooperative drought adaptation: Integrating infrastructure development, conservation, and water transfers into adaptive policy pathways. Water Resources Research 52, 7327–7346. doi:10.1002/2016wr018771.

Zemp, M., Huss, M., Thibert, E., Eckert, N., McNabb, R., Huber, J., Barandun, M., Machguth, H., Nussbaumer, S.U., Gärtner-Roer, I., Thomson, L., Paul, F., Maussion, F., Kutuzov, S., Cogley, J.G., 2019. Global glacier mass changes and their contributions to sea-level rise from 1961 to 2016. Nature 568, 382–386. doi:10.1038/s41586-019-1071-0.

Zeng, R., Cai, X., Ringler, C., Zhu, T., 2017. Hydropower versus irrigation—an analysis of global patterns. Environmental Research Letters 12, 034006. doi:10.1088/1748-9326/aa5f3f.

Zhang, X., Cai, X., 2013. Climate change impacts on global agricultural water deficit. Geophysical Research Letters 40, 1111–1117. doi:10.1002/grl.50279.

Zhang, X., Li, H.Y., Deng, Z.D., Ringler, C., Gao, Y., Hejazi, M.I., Leung, L.R., 2018. Impacts of climate change, policy and water—energy—food nexus on hydropower development. Renewable Energy 116, 827–834. doi:10.1016/j.renene.2017.10.030.

Zhou, Q., Hanasaki, N., Fujimori, S., Masaki, Y., Hijioka, Y., 2018. Economic consequences of global climate change and mitigation on future hydropower generation. Climatic Change 147, 77–90. doi:10.1007/s10584-017-2131-9.

Zhou, T., Nijssen, B., Gao, H., Lettenmaier, D.P., 2016. The contribution of reservoirs to global land surface water storage variations. Journal of Hydrometeorology 17, 309–325. doi:10.1175/JHM-D-15-0002.1.

Zhou, Y., Hejazi, M., Smith, S., Edmonds, J., Li, H., Clarke, L., Calvin, K., Thomson, A., 2015. A comprehensive view of global potential for hydro-generated electricity. Energy & Environmental Science 8, 2622–2633. doi:10.1039/c5ee00888c.

A

Sensitivity analysis between Safran reanalyses and the two sets of the hydrological model GR6J-CEMANEIGE

This Appendix presents the performance between the two sets of hydrological models forced with the two different Safran reanlyses so as to choose a better model set and a better input data.

A.1 Model validation

Since two input reanalysis data (Safran-France and Safran-PIRAGUA) and two sets of models (8-parameter-GR6J-CEMANEIGE and 10-parameter-GR6J-CEMANEIGE models) are available, a test to choose a better model set and a more relevant meteorological input can also be implemented in the model validation based on the evaluation of KGE criteria. From the data summary Table 3.6, a common time period for all the data source is from year 2001 to 08/2014. This almost 14-year period is divided in half for model calibration and model validation, separately. Input data and observations from year 2001 to 08/2007 are used to calibrate model. The rest years from 09/2007 to 08/2014 are used to validate model. The process can also be turned around for a fulfill evaluation, 09/2007 - 08/2014 for model calibration and 2001-08/2007 for model calibration. In each evaluation, the beginning two years are chosen to "warm-up" the model.

Two different inputs data and two different model sets forms four different combinations, which are Safran-France data with the 8-parameter model, Safran-PIRAGUA data with the 8-parameter model, Safran-France data with the 10-parameter model, Safran-PIRAGUA data with the 10-parameter model. Both study cases, SB1 upstream the Oule reservoir and SB3 upstream the Lassoula reservoir (the sum of the Pouchergues and Caillaouas reservoirs), are investigated.

A.1.1 A better model set

In order to choose a better model set, tests of the 8-parameter-GR6J-CEMANEIGE model and the 10-parameter-GR6J-CEMANEIGE model for the input data Safran-France are conducted. The tests are also applied on the Safran-PIRAGUA data to check if the situation remains the same. Figure A.1 shows the performance of two sets of models with the same input SAFRAN on discharge Q and 5 elevation bands SCA1-5 for SB1 and SB3.

From Figure A.1, the model set 10-parameter-GR6J-CEMANEIGE shows a significantly better SCA performance and the discharge Q degrades slightly than the model set 8-parameter-GR6J-CEMANEIGE for the two cases and two different calibration-validation procedure. The degradation of Q is due to the calibration process where the 10-parameter-GR6J-CEMANEIGE model sacrifices 25% in the objective function to make up to SCA. This degree of decrease in Q performance is rather acceptable, not to mention the huge increase in SCA performance.

If the two sets of models are forced with the Safran-PIRAGUA data, the results remains identical and the KGE results are presented in Figure A.2. As such, no matter which source of input, the 10-parameter-GR6J-CEMANEIGE model gives an overall better simulation performance. The use of two parameters to describe SCA-SWE hysteresis are robust and efficient in the two cases.

A.1.2 A better forcing data

Since the 10-parameter-GR6J-CEMANEIGE model shows a better performance, it is also necessary to choose which reanalysis data as input, Safran-France or Safran-PIRAGUA. The two input data are based on the same calculation algorithm but they have different size of resolution, 8 km for Safran-France and 2.5 km for Safran-PIRAGUA. They are forced in the 10-parameter-GR6J-CEMANEIGE model and Figure A.3 shows the KGE criterion results.

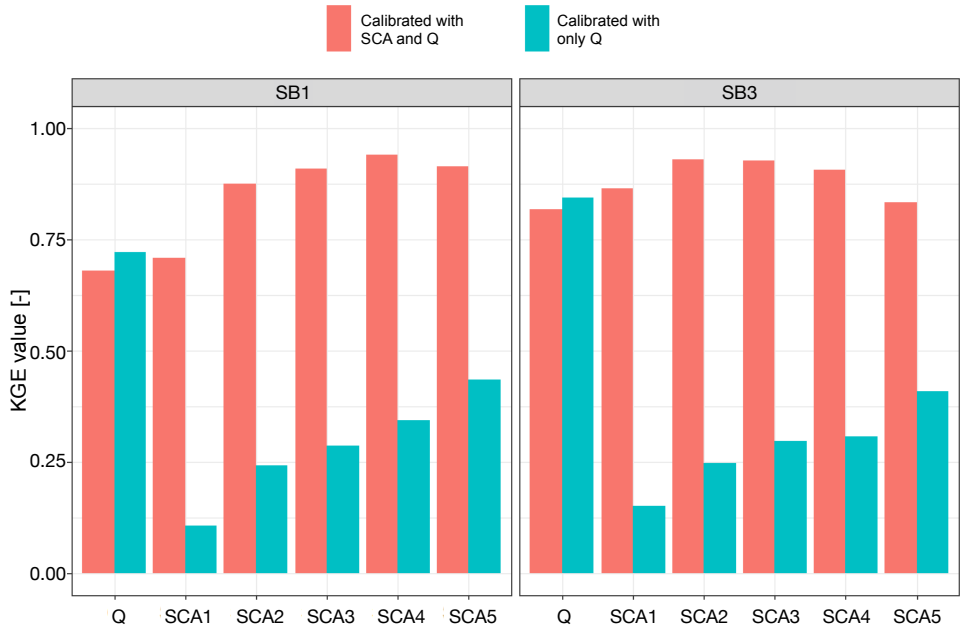

(a) Calibration 2001-2007 and validation 2007-2014

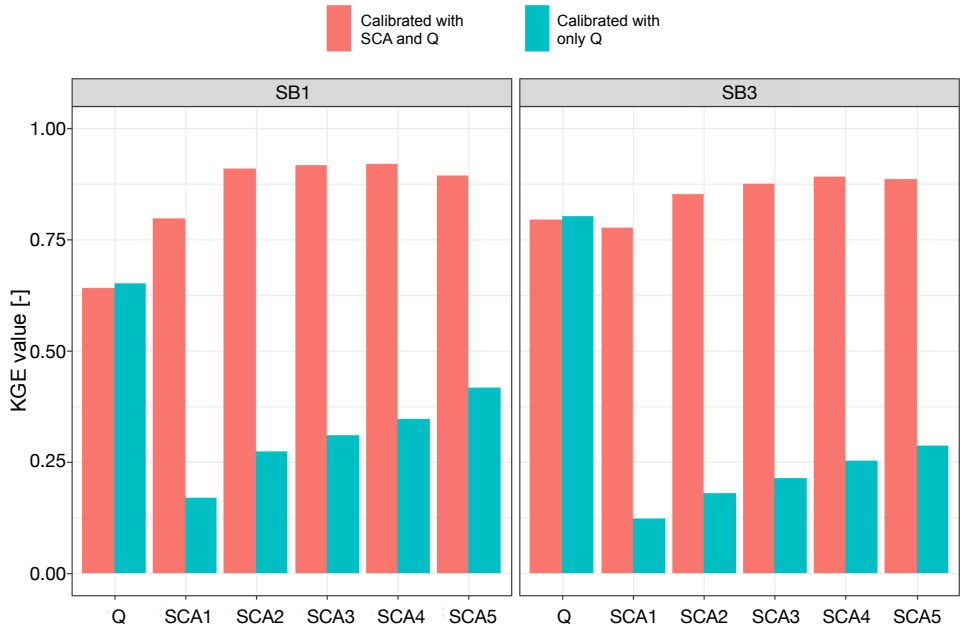

(b) Calibration 2007-2014 and validation 2001-2007

Figure A.1 – KGE criterion results on two model sets with the Safran-France input data are presented on two different calibration-validation procedure A.1a and A.1b: the 10-parameter model set (with a consideration of SCA-SWE hysteresis) are histograms labeled "calibrated with snow and Q" and the 8-parameter model set (without a consideration of SCA-SWE hysteresis) are labeled "calibrated with only Q".

From Figure A.3, the KGE criterion results of the tests have no distinct difference due to the same origin of the two data. However, the Safran-PIRAGUA data shows a slight better performance. Although the Safran-PIRAGUA data has a higher resolution, the better performance of the Safran-PIRAGUA data in this model set can not be arbi-

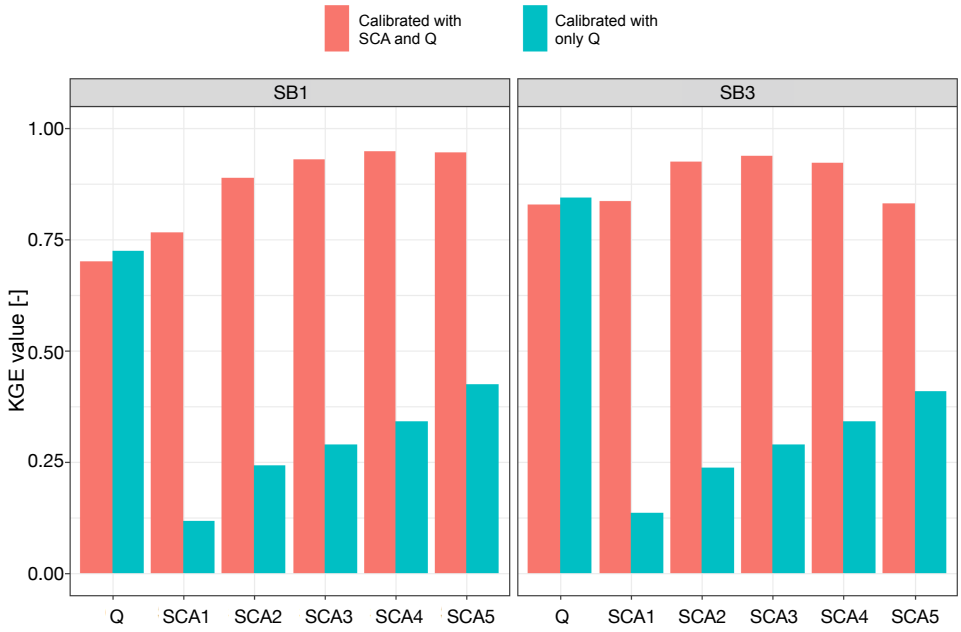

(a) Calibration 2001-2007 and validation 2007-2014

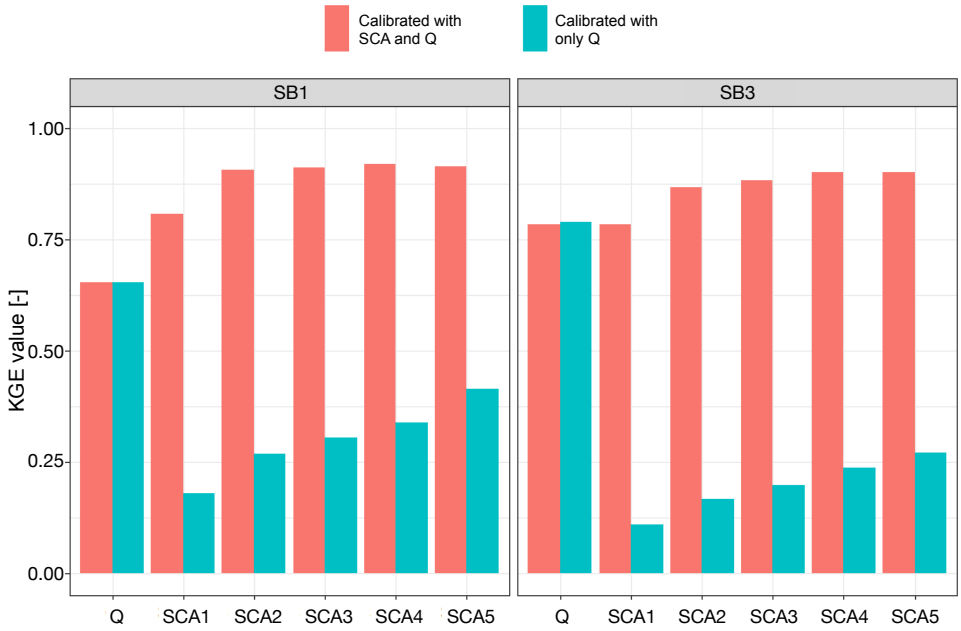

(b) Calibration 2007-2014 and validation 2001-2007

Figure A.2 – KGE criterion results on two model sets with the Safran-PIRAGUA input data are presented on two different calibration-validation procedure A.1a and A.1b: the 10-parameter model set (with a consideration of SCA-SWE hysteresis) are histograms labeled "calibrated with snow and Q" and the 8-parameter model set (without a consideration of SCA-SWE hysteresis) are labeled "calibrated with only Q".

trarily attributed to its higher resolution. If the Safran-PIRAGUA data still shows a better performance in the 8-parameter-GR6J-CEMANEIGE model, it is probably the case. However, in Figure A.4, Safran-France data shows an overall better performance than Safran-PIRAGUA in the 8-parameter-GR6J-CEMANEIGE model.

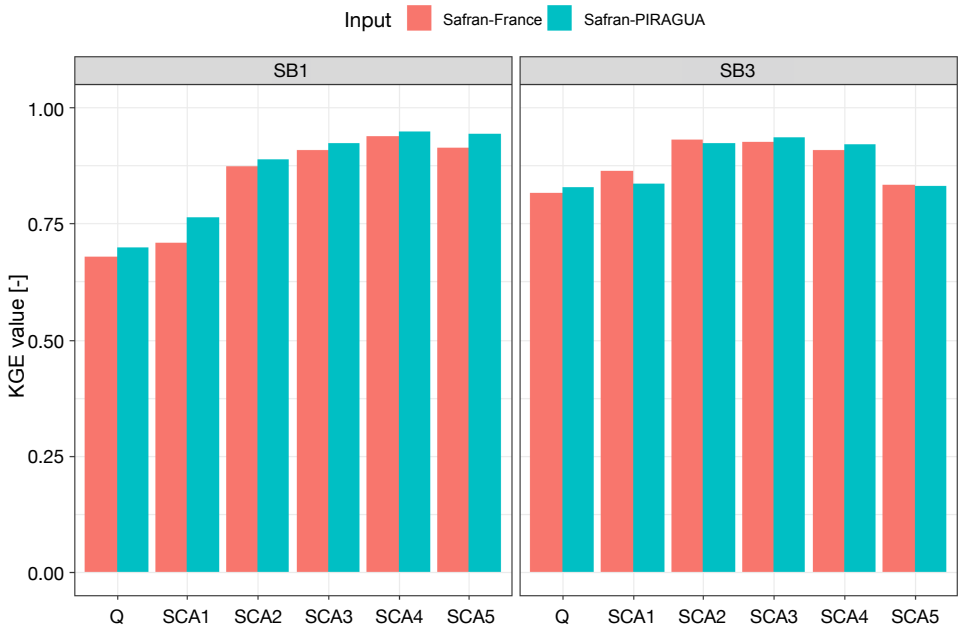

(a) Calibration 2001-2007 and validation 2007-2014

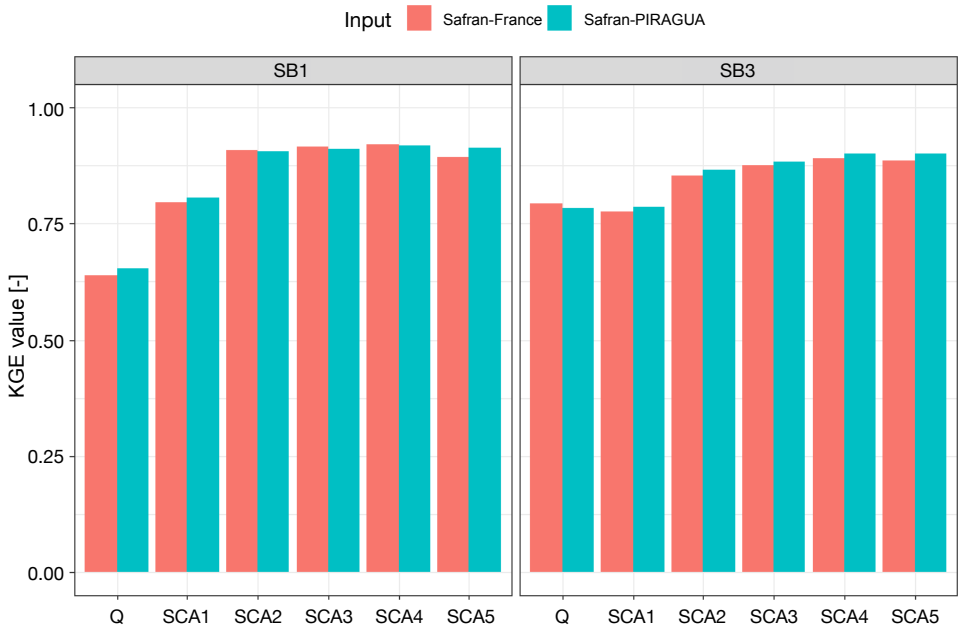

(b) Calibration 2007-2014 and validation 2001-2007

Figure A.3 – KGE criterion results on the 10-parameter-GR6J-CEMANEIGE model with two different input data Safran-France and Safran-PIRAGUA.

The reason of this behavior is highly related to the implementation of the SCA-SWE hysteresis. The snow model CEMANEIGE is semi-distributed, dividing the simulation catchment into 5 equal-surface elevation layers. And the use of SCA-SWE hysteresis based on MODIS observations (resolution 0.5 km) makes the snow model more efficient in representing snow content. As the input of the snow model is temperature and precipitation which are highly variable in mountainous area, the finer Safran-PIRAGUA data can better describe input information than Safran-France and thus this semi-distributed snow

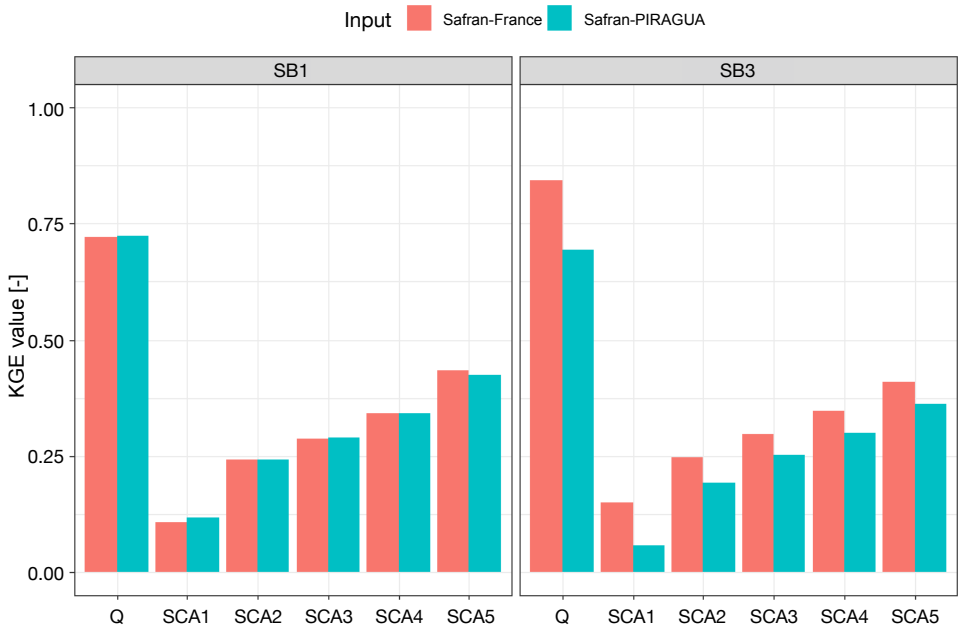

(a) Calibration 2001-2007 and validation 2007-2014

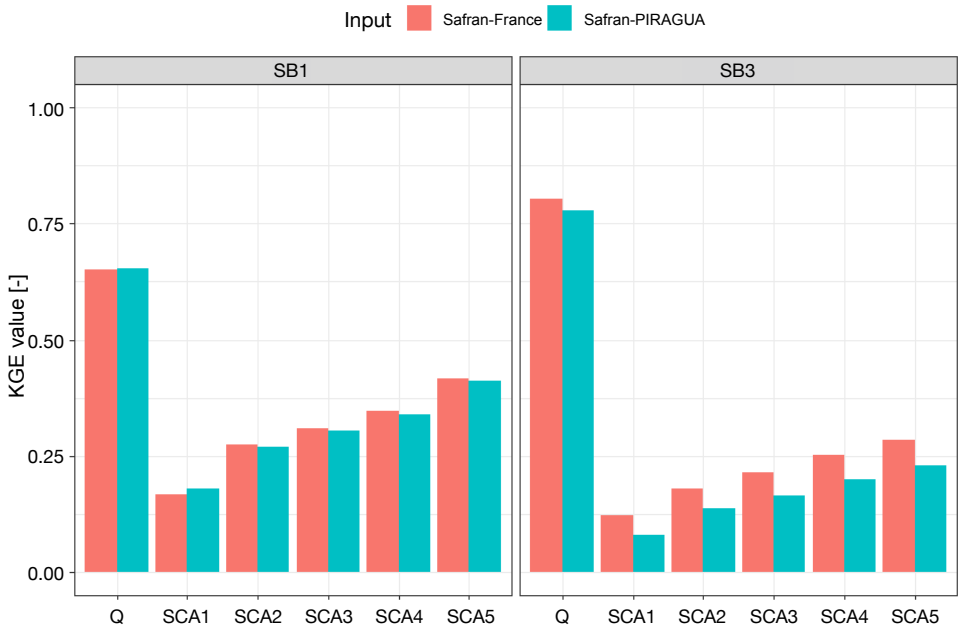

(b) Calibration 2007-2014 and validation 2001-2007

Figure A.4 – KGE criterion results on the 8-parameter-GR6J-CEMANEIGE model with two different input data Safran-France and Safran-PIRAGUA.

model can improve the snow simulation. Globally, the 10-parameter-GR6J-CEMANEIGE model combined with the Safran-PIRAGUA as input gains a better simulation results. This combination of model and forcing data is employed to construct the water resources model.

Representation of a multipurpose reservoir system and vulnerability of water management under global change

Application to the Neste water system

Résumé

La compréhension de la vulnérabilité de la gestion de l'eau dans le contexte du changement global est la condition préalable à la conception de mesures d'adaptation. Une évaluation complète de la vulnérabilité des modes de gestion de l'eau aux changements futurs repose sur de nouveaux outils capables de représenter l'impact humain sur les ressources en eau et sur des cadres innovants capables de générer de nouvelles idées pour informer la conception de l'adaptation. Par conséquent, cette thèse vise à (1) développer et améliorer des modèles pour représenter les ressources en eau, la demande en eau et la gestion de l'eau de manière intégrée ; (2) appliquer un cadre bottom-up "scenario-neutral" et un cadre top-down "scenario-led" pour identifier et étudier la vulnérabilité et l'impact plausibles dans le cadre du changement global. Ces développements et applications ont concerné le système Neste dans les Pyrénées françaises.

Mots-clés : Gestion de l'eau, vulnérabilité, impact, système d'eau, réservoir, changement global, changement climatique, cadre bottom-up, cadre top-down, hydroélectricité, irrigation, environnement

Abstract

Understanding the vulnerability of water management under global change is the premise for designing adaptation actions. A comprehensive assessment of current water management vulnerability to future changes hinges on new tools that are able to represent human impact on water resources and innovative frameworks that are able to generate new insights to inform adaptation designing. Therefore, this dissertation sets out to (1) develop and improve models to represent water resources, water demand, and water management in an integrated hydrological modelling framework; (2) apply a "scenario-neutral" bottom-up framework and a "scenario-led" top-down framework to identify and investigate plausible vulnerability and impact under global change. These developments and applications are demonstrated by taking the Neste water system in French Pyrenees as a case study.

Keywords : Water management, vulnerability, impact, water system, reservoir, global change, climate change, bottom-up framework, top-down framework, hydropower, irrigation, environment